# IMPACT OF AASHTO LRFD SPECIFICATIONS ON THE DESIGN OF PRECAST, PRETENSIONED U-BEAM BRIDGES

A Thesis

by

MOHSIN ADNAN

Submitted to the Office of Graduate Studies of
Texas A&M University
in partial fulfillment of the requirements for the degree of

MASTER OF SCIENCE

December 2005

Major Subject: Civil Engineering

# IMPACT OF AASHTO LRFD SPECIFICATIONS ON THE DESIGN OF PRECAST, PRETENSIONED U-BEAM BRIDGES

A Thesis

by

MOHSIN ADNAN

Submitted to the Office of Graduate Studies of
Texas A&M University
in partial fulfillment of the requirements for the degree of

MASTER OF SCIENCE

Approved by:

| | |
|---|---|
| Co-Chairs of Committee, | Mary Beth D. Hueste |
| | Peter B. Keating |
| Committee Member, | Terry Kohutek |
| Head of Department, | David V. Rosowsky |

December 2005

Major Subject: Civil Engineering

# ABSTRACT

Impact of AASHTO LRFD Specifications on the Design of Precast, Pretensioned U-Beam Bridges. (December 2005)

Mohsin Adnan, B.S., NWFP University of Engineering and Technology

Co-Chairs of Advisory Committee: Dr. Mary Beth D. Hueste
Dr. Peter B. Keating

Texas Department of Transportation (TxDOT) is currently designing its highway bridge structures using the *AASHTO Standard Specifications for Highway Bridges*, and it is expected that TxDOT will make transition to the use of the *AASHTO LRFD Bridge Design Specifications* before 2007. The objectives of this portion of the study are to evaluate the current LRFD Specifications to assess the calibration of the code with respect to typical Texas U54 bridge girders, to perform a critical review of the major changes when transitioning to LRFD design, and to recommend guidelines to assist TxDOT in implementing the LRFD Specifications. This study focused only on the service and ultimate limit states and additional limit states were not evaluated.

The available literature was reviewed to document the background research relevant to the development of the LRFD Specifications, such that it can aid in meeting the research objectives. Two detailed design examples, for Texas U54 beams using the LRFD and Standard Specifications, were developed as a reference for TxDOT bridge design engineers. A parametric study was conducted for Texas U54 beams to perform an in-depth analysis of the differences between designs using both specifications. Major parameters considered in the parametric study included span length, girder spacing, strand diameter and skew angle. Based on the parametric study supplemented by the literature review, several conclusions were drawn and recommendations were made. The most crucial design issues were significantly restrictive debonding percentages and the limitations of approximate method of load distribution.

The current LRFD provisions of debonding percentage of 25 percent per section and 40 percent per row will pose serious restrictions on the design of Texas U54 bridges. This will limit the span capability for the designs incorporating normal strength concretes. Based on previous research and successful past practice by TxDOT, it was recommended that up to 75% of the strands may be debonded, if certain conditions are met.

The provisions given in the LRFD Specifications for the approximate load distribution are subject to certain limitations of span length, edge distance parameter ($d_e$) and number of beams. If these limitations are violated, the actual load distribution should be determined by refined analysis methods. During the parametric study, several of these limitations were found to be restrictive for typical Texas U54 beam bridges. Two cases with span lengths of 140 ft. and 150 ft., and a 60 degree skew were investigated by grillage analysis method.

# DEDICATION

I dedicate this thesis to my grandfather Saeed Ahmed Khan, my parents Nuzhat Mufti and Ahmed Zia Babar and my wife Zubia Naji.

# ACKNOWLEDGMENTS

My utmost gratitude is to Almighty God, who has been very kind to me during all these years.

It is a pleasure to thank many who made this thesis possible. Firstly, I would like to gratefully acknowledge the guidance and support that I received from my advisor, Dr. Mary Beth D. Hueste. I could not have imagined having a better advisor and mentor for my M.S., and without her common-sense, knowledge and perceptiveness I would never have finished. I appreciate the contribution of Dr. Peter Keating and Dr. Terry Kohutek for their helpful review of this document. I am grateful to my father-in-law Dr. Ahmed Riaz Naji as he has been a continual source of guidance and support during my M.S.

I wish to acknowledge the Texas Department of Transportation (TxDOT) who funded this research through the Texas Transportation Institute. I also wish to acknowledge the financial support provided by the Department of Civil Engineering at Texas A&M University. I greatly benefited from very many technical discussions with Mr. Mohammad Safiudin Adil, a graduate student at Texas A&M University.

Finally, and most importantly, I am forever indebted to my parents Nuzhat Mufti and Ahmed Zia Babar, and my wife Zubia Naji for their understanding, endless patience, encouragement and love when it was most required. I am also grateful to Tashfeen, Farhan and Hassan for their love and support.

# TABLE OF CONTENTS

Page

# LIST OF FIGURES

Page

Page

Page

# LIST OF TABLES

Page

Page

Page

Page

# 1. INTRODUCTION

## 1.1 BACKGROUND AND PROBLEM STATEMENT

Until the mid-1990s, the design of bridges in the United States was governed by the *AASHTO Standard Specifications for Highway Bridges* (AASHTO 1992). To ensure a more consistent level of reliability among bridge designs, research was directed towards developing an alternate design philosophy. As a result, the *AASHTO Load and Resistance Factor Design (LRFD) Bridge Design Specifications* were introduced in 1994 (AASHTO 1994). The LRFD Specifications are based on reliability theory and include significant changes for the design of highway bridges. The latest edition of the Standard Specifications (AASHTO 2002) will not be updated again, and the Federal Highway Administration (FHWA) has established a mandatory goal of designing all new bridge structures according to the LRFD Specifications no later than 2007.

Until 1970, the AASHTO Standard Specifications were based on the working stress design (WSD) philosophy, alternatively named allowable stress design (ASD). In ASD, the allowable stresses are considered to be a fraction of a given structural member's load carrying capacity and the calculated design stresses are restricted to be less than or equal to those allowable stresses. The possibility of several loads acting simultaneously on the structure is specified through different load combinations, but variation in likelihood of those load combinations and loads themselves is not recognized in ASD. In the early 1970s, a new design philosophy, load factor design (LFD), was introduced to take into account the variability of loads by using different multipliers for dead, live, wind and other loads to a limited extent (i.e., statistical variability of design parameters was not taken into account). As a result, the ASD and LFD requirements, as specified in the AASHTO Standard Specifications (AASHTO

---

This thesis follows the style of ASCE *Journal of Structural Engineering*.

1992, AASHTO 2002), do not provide for a consistent and uniform safety level for various groups of bridges (Nowak 1995).

AASHTO's National Cooperative Highway Research Program (NCHRP) Project 12-33 was initiated in July of 1988 to develop the new AASHTO LRFD Specifications and Commentary (AASHTO 1998). The project included the development of load models, resistance models and a reliability analysis procedure for a wide variety of typical bridges in the United States. To calibrate this code, a reliability index related to the probability of exceeding a particular limit state was used as a measure of structural safety. About 200 representative bridges were chosen from various geographical regions of the United States based on current and future trends in bridge designs, rather than choosing from existing bridges only. Reliability indices were calculated using an iterative procedure for these bridges, which were designed according to the Standard Specifications (AASHTO 1992). In order to ensure an adequate level of reliability for calibration of the LRFD Specifications, the performance of all the representative bridges was evaluated and a corresponding target reliability index was chosen to provide a minimum, consistent and uniform safety margin for all structures. The load and resistance factors were then calculated so that the structural reliability is close to the target reliability index (Nowak 1995).

This study is part of the Texas Department of Transportation (TxDOT) project 0-4751 "Impact of AASHTO LRFD Specifications on Design of Texas Bridges." TxDOT is currently designing its highway bridge structures using the Standard Specifications, and it is expected that TxDOT will make transition to the use of the LRFD Specifications before 2007. It is crucial to assess the impact of the LRFD Specifications on the TxDOT bridge design practice because of the significant differences in the design philosophies of the Standard and LRFD Specifications.

## 1.2 OBJECTIVES AND SCOPE

The major objectives of the study described in this thesis are (1) to evaluate the impact of the current LRFD on the design of typical Texas precast, pretensioned U54 bridge girders, (2) to perform a critical review of the major changes when transitioning from current TxDOT practices to LRFD based design, and (3) to recommend guidelines to assist TxDOT in implementing the LRFD Specifications.

The scope of this study is limited to precast, prestressed Texas U54 beams. Detailed design examples were developed and a parametric study was carried out only for interior beams. The provisions in TxDOT Bridge Design Manual are based on previous research and experience, and these provisions address the needs that are typical for Texas bridges. So, in general TxDOT's past practices, as outlined in their Bridge Design Manual (TxDOT 2001, are considered in this study when possible. For example, although the modular ratio is usually less than unity in bridge design practice because of beam elastic modulus being greater than the deck slab elastic modulus, it is considered to be unity for the service limit state design, based on TxDOT practice. The actual value of the modular ratio was used for all other limit states in this study. Only the most recent editions of the AASHTO LRFD and Standard Specifications (AASHTO 2002, 2004) are considered in this study.

## 1.3 RESEARCH METHODOLGY

The following five major tasks were performed to achieve the aforementioned objectives.

### 1.3.1 Task1: Literature Review and Current State of Practice

Review and synthesis of available literature was performed to document the research relevant to the development of the AASHTO LRFD Specifications. The work that has been conducted to evaluate different aspects of the specifications are also documented. This review of literature and current state of practice thoroughly covers the significant changes in the LRFD Specifications with respect to design concerns. For example, several issues including the effect of diaphragms and edge-stiffening elements, continuity, and skew on live load distribution factors were either not considered in the original study by Zokaie et al. (1991) or were deemed by the bridge design community as significant enough to be reevaluated. Therefore many studies were initiated to address these issues and to evaluate the live load distribution criteria adopted by the LRFD Specifications. Certain Departments of Transportation (DOTs) such as Illinois (IDOT), California (Caltrans) and Tennessee (TDOT), sponsored research geared towards either simplifying and revamping the live load distribution criteria to suit their typical bridge construction practices or to justify their previous practices of live load distribution (Tobias et al. 2004, Song et al. 2003, Huo et al. 2004). In general, various aspects in the development of the LRFD Specifications such as the theory of structural reliability, load and resistance models, and adaptation of a new live load model (HL-93) are covered as a part of this task. In addition, this review includes issues relevant to precast, pretensioned concrete Texas U beam bridges, such as debonding of prestressing strands and live load distribution factors.

### 1.3.2 Task 2: Develop Detailed Design Examples

Two detailed design examples were developed to illustrate the application of the *AASHTO Standard Specifications for Highway Bridges, 17th edition* (2002) and *AASHTO LRFD Bridge Design Specifications, 3rd edition* (2004), for typical precast, pretensioned Texas U54 beam bridges. The purpose of these design examples is to show

the differences in the two design approaches and to enable a more thorough comparison of the two design specifications.

HL93 and HS20-44 live load models were used for designs according to the LRFD and Standard Specifications, respectively, and the live load distribution factors were calculated according to the procedures described in each specification. Prestress losses were calculated by an iterative procedure to match TxDOT current practices (TxDOT 2004), while using the respective equations given in each specification. This iterative procedure results in optimized initial and final concrete strength values. Based on TxDOT practice (TxDOT 2001), the modular ratio between beam and slab concrete will be considered as unity for the service limit state design, in which the number of strands and optimum values of initial and final concrete strengths are determined. All the limits states and load combinations are considered applicable to the design of typical bridge structures in the state of Texas as prescribed by both specifications except the extreme event limit state in the LRFD Specifications because extreme events like ice pressure do not occur in Texas, TxDOT does not design for earthquakes, and stream current rarely controls the design (TxDOT 2001). Moreover, TxDOT's debonding provisions are followed throughout the study and the debonding requirement will be evaluated at several sections as per the methodology of the TxDOT prestressed girder design software PSTRS14 (TxDOT 2004). Maximum camber in the bridge girders is determined by the hyperbolic functions method (Sinno 1968). PSTRS14 (TxDOT 2004), which was recently updated for LRFD design, is used to check the detailed design by the Standard and LRFD Specifications to ensure consistency with TxDOT practices.

### 1.3.3 Task 3: Conduct Parametric Study

A parametric study was conducted to perform an in-depth analysis of the differences between designs using the current Standard and LRFD Specifications (AASHTO 2002, 2004). The focus of this study was on the bridge types that were of most interest to TxDOT for future bridge structures. Appropriate parameters were

selected based on collaboration of the research team and TxDOT. Because a great number of variations were possible, spreadsheet programs and a MatLAB program were developed and used to expedite the design calculations for a particular set of parameters. The entire parametric study was carried out for interior beams to be consistent with TxDOT current practices.

Any automated calculation process facilitated by a computer program, such as a spreadsheet or MatLAB solution, is prone to errors and inaccuracies. To ensure that the entire design process was error free, the spreadsheet and MatLAB results were checked against the detailed design examples and the TxDOT design software PSTRS14 (TxDOT 2004). Different design trends were determined and compared, graphically and in tabular format, for both specifications. In addition, the parametric study was helpful for determining the most critical and controlling limit states for the design of different types of bridges.

### 1.3.4 Task 4: Identify Important Design Issues

The parametric study, supplemented by the literature review, was used to identify needs for revising the design criteria for pretensioned concrete Texas U beams. Areas that necessitate additional study include the validation of AASHTO LRFD live load distribution factors formulas (especially for wider girder spacings and span lengths longer than 140 ft.) and the LRFD debonding provisions.

The debonding provisions of the LRFD Specifications are fairly restrictive. The LRFD Specifications limit the debonding of strands to 25% per section and 40% per row, whereas the TxDOT Bridge Design Manual guidelines (TxDOT 2001) allow debonding of strands up to 75% per row per section. The new LRFD debonding provisions restrict the span capability of Texas U54 girders. Further investigation into the basis for the LRFD debonding limits was conducted as part of this study.

### 1.3.5 Task 5: Provide Guidelines for Revised Design Criteria

It becomes mandatory to apply refined analysis procedures recommended by the LRFD Specifications in a case when any particular bridge design parameter violates the limitations set by the LRFD Specifications for the use of its provisions. This typically occurs when a particular bridge geometry is outside the allowable range for the use of the LRFD live load distribution factor formulas and/or uniform distribution of permanent dead loads. Refined analysis techniques as allowed by the LRFD Specifications, such as grillage analysis, was employed to validate the existing distribution factors beyond the limitations set by the specifications. Following the review of the research for the current and LRFD debonding limits, recommendations were made regarding appropriate limits for future designs.

A grillage analogy model was developed for Texas U54 beams to study the validity of the LRFD live load distribution factor formulas beyond the span length limit. The grillage analogy is a simplified analysis procedure in which the bridge superstructure system is represented by transverse and longitudinal grid members. Careful evaluation of grid member properties and support conditions is an essential step. Two cases were evaluated through grillage analysis method to determine the applicability of the LRFD live load distribution factors. These cases were selected because for 8.5 ft. spacing and 60 degree skew, possible design span lengths were found to be more than 140 ft., which is the limit for live load distribution factors formulas to be valid for spread box beams.

## 1.4 ORGANIZATION OF THESIS

This thesis is organized in the following manner. Section 2 provides the literature review regarding code calibration and reliability theory, development of live load models and live load distribution factors, debonding provisions, and refined analysis procedures used in the study. In Section 3 the issues regarding selection of parameters

and analysis and design procedures for the parametric study are discussed. Section 4 gives a detailed account of the parametric study results. Section 5 provides information on the details of the selection and application of grillage analogy method and presents a detailed discussion on the assumptions and bridge superstructure modeling procedure. Finally, Section 6 gives a summary, conclusions and recommendations for future research. Additional information such as detailed results of the parametric study, complete detailed design examples, and results of the grillage analysis are presented in the appendices. Throughout this study, whenever applicable, the notations have been kept consistent with the LRFD and Standard Specifications (AASHTO 2004, 2002).

# 2. LITERATURE REVIEW

## 2.1 INTRODUCTION

This section consists of a review and synthesis of the available literature to document the research relevant to the development of the *AASHTO LRFD Bridge Design Specifications*. This review of literature and the current state of practice is intended to thoroughly cover the significant changes in the LRFD Specifications with respect to design concerns. For example, several issues including the effect of diaphragms and edge-stiffening elements, continuity, and skew. on live load distribution were either not considered in the original study by Zokaie et al. (1991) or were deemed by the bridge design community as significant enough to be reevaluated. Therefore, many studies were initiated to address these issues and to evaluate the live load distribution criteria adopted by the LRFD Specifications.

A comparison of the LRFD and Standard Specifications is also provided. In general, various aspects in the development of the state-of-the-art LRFD Specifications such as the theory of structural reliability and load and resistance models, including the adaptation of a new live load (HL-93), are discussed. More specifically, literature review is carried out with special emphasis on the issues relevant to precast, pretensioned concrete Texas U beam bridges, such as debonding of prestressing strands and live load distribution factors.

## 2.2 AASHTO STANDARD AND LRFD SPECIFICATIONS

Until 1970, the AASHTO Standard Specifications were based on working stress design (WSD) philosophy, alternatively named allowable stress design (ASD). In ASD,

the allowable stresses are considered to be a fraction of a given structural member's load carrying capacity and the calculated design stresses are restricted to be less than or equal to those allowable stresses. The possibility of several loads acting simultaneously on the structure is specified through different load combinations, but variation in likelihood of those load combinations and loads themselves is not recognized in ASD. In the early 1970s, a new design philosophy, load factor design (LFD), was introduced to take into account the variability of loads by using different multipliers for dead, live, wind and other loads to a limited extent. However, the statistical variability of the design parameters was not taken into account. As a result, the ASD and LFD requirements, as specified in the AASHTO Standard Specifications (AASHTO 1992, AASHTO 2002), do not provide for a consistent and uniform safety level for various groups of bridges (Nowak 1995).

AASHTO's National Cooperative Highway Research Program (NCHRP) Project 12-33 was initiated in 1988 to develop the new AASHTO LRFD Specifications and Commentary. The project included the development of load models, resistance models and a reliability analysis procedure for a wide variety of typical bridges in the United States. To calibrate this code, a reliability index related to the probability of exceeding a particular limit state was used as a measure of structural performance.

### 2.2.1 Significant Changes

Designs according to the LRFD Specifications will not necessarily be lighter, heavier, weaker or stronger in comparison with designs per the Standard Specifications. Rather, more uniform reliability for bridge structures will result. To facilitate the understanding and application of the design provisions, a parallel commentary is provided in the LRFD Specifications. This feature is not present in the Standard Specifications. The LRFD Specifications explicitly allow the use of refined methods of analysis in conjunction with the code provisions. Hueste and Cuadros (2003), Richard and Nielson (2002), and Mertz and Kulicki (1996) discuss the significant changes in the

AASHTO LRFD Specifications as compared to the AASHTO Standard Specifications. Some significant differences between the two code specifications are outlined below.

#### *2.2.1.1 Limit States and Load Combinations*

The way in which the LRFD and Standard Specifications (AASHTO 2004, 2002) address several limit states is fundamentally the same, but the LRFD Specifications explicitly groups the design criteria in four different limit state categories: (1) service, (2) strength, (3) fatigue and fracture, and (4) extreme event limit states. The serviceability limit states ensure that the stress, deformation and crack width in a bridge structure are within acceptable limits for its intended service life. The purpose of strength limit states is to ensure that under a statistically significant load combination during the entire design life, the bridge structure will have enough strength and stability to maintain the overall structural integrity, although it may experience some degree of damage and distress. The crack growth, during the design life of the bridge structure, under the action of repetitive loads can lead to fracture. The fatigue and fracture limit state is intended to limit such crack growth. The extreme event limit state relates to the structural survival of a bridge during a major earthquake or flood, or when collided by a vessel, vehicle, or ice flow, possibly under scoured conditions. These limit states are considered to be unique occurrences whose return period may be significantly greater than the design life of the bridge.

In general, new load factors are introduced to ensure that a minimum target safety level is achieved in the strength design of all bridges. The limit states in the LRFD Specifications are categorized with the intention of ensuring that all the limit states are equally important. The serviceability limit state is further divided into Service I and Service III for the design of prestressed concrete bridge girders, where Service I addresses compression stresses, while Service III addresses tensile stresses with a specific objective of crack control. Table 2.1 compares serviceability and strength limit states in the LRFD and Standard Specifications (AASHTO 2004, 2002).

**Table 2.1 Comparison of Serviceability and Strength Limit States**

| Standard Specifications | LRFD Specifications |
|---|---|
| *Service:*<br>$Q = 1.0(D) + 1.0(L + I)$<br>*Strength:*<br>$Q = 1.3\left[1.0(D) + 1.67(L + I)\right]$ | *Service I:*<br>$Q = 1.0(D) + 1.0(L + I)$<br>*Service III:*<br>$Q = 1.0(D) + 0.8(L + I)$<br>*Strength I:*<br>$Q = 1.0\left[1.25(DC) + 1.5(DW) + 1.75(L + I)\right]$<br>$Q = 1.0\left[0.9(DC) + 0.65(DW) + 1.75(L + I)\right]$ |

where:

$DC$ = Dead load of structural components and non-structural attachments
$DW$ = Dead load of wearing surface and utilities
$D$ = Dead load of all components
$L$ = Vehicular live load
$I$ = Vehicular dynamic load allowance

### *2.2.1.2 Load and Resistance Factors*

In the Standard Specifications, pretensioned concrete bridge girders are designed to satisfy the ASD and LFD philosophies. To satisfy ASD, the pretensioned concrete bridge girders must stay within allowable initial flexural stress limits at release, as well as final flexural stress limits at service load conditions. To satisfy LFD, the ultimate flexural and shear capacity of the section is checked. The Standard Specifications give several load combination groups and requires that the structure be able to resist the load combination in each applicable load group corresponding to ASD and LFD. The general design equation is of the following form,

$$\phi R_n \geq Group(N) = \gamma \sum \left[\beta_i L_i\right] \tag{2.1}$$

where:

$\phi$ = Resistance factor

$R_n$ = Nominal resistance
$N$ = Group number
$\gamma$ = Load factor
$\beta_i$ = Coefficient that varies with the type of load and depends on the load group and design method
$L_i$ = Force effect

In the AASHTO LRFD Specifications, the load and resistance factors are chosen more systematically based on reliability theory and on the statistical variation of the load and resistance. Moreover, additional factors are introduced in the general design equation that take into account consideration of ductility, redundancy, and operational importance. The general design equation that is required to be satisfied for all limit states is as follows.

$$\phi R_n \geq Q = \sum \left[ \eta_i \gamma_i Q_i \right] \tag{2.2}$$

where:

$\gamma_i$ = Statistical load factor applied to the force effects
$Q_i$ = Force effect
$\eta_i$ = $\eta_D \, \eta_R \, \eta_I$ is the load modification factor
$\eta_D$ = Ductility factor
$\eta_R$ = Redundancy factor
$\eta_I$ = Operational importance factor

*2.2.1.3 Live Load Model*

The live load model specified in the current Standard Specifications (AASHTO 2002) is the maximum effect of each of the following as separate loadings: (1) HS20-44 truck load, and (2) HS20-44 lane load. The live load model used in the Standard Specifications did not prove adequate because its accuracy varied with the span length (Kulicki 1994). The live load model in the LRFD Specifications, HL-93, consists of the superposition of the design truck load HS20-44 or the design tandem load with the design lane load, whichever produces the maximum effect. This new live load model

more accurately represents the truck traffic on national highways and was developed to give a consistent margin of safety for a wide range of spans (Kulicki 1994).

#### *2.2.1.4 Live Load Distribution Factors and Skew Effect*

Major changes have occurred in the way live load distribution factors (DFs) are calculated in the LRFD Specifications. A variety of formulas depending upon the location (interior or exterior) of the girder, type of resistance (bending moment, shear force or fatigue), and type of bridge superstructure have been specified. To make live load DFs more accurate for a wider range of bridge geometries and types, additional parameters such as bridge type, span length, girder depth, girder location, transverse and longitudinal stiffness, and skew were taken into account. The bridge type corresponding to the TxDOT U54 beam comes under the category of type 'c', which is concrete deck on concrete spread box beams. The live load DF formulas for precast, prestressed box beams are given in Table 2.2. Application of the LRFD live load DF formula is only valid within certain limitations, as noted in Eq. 2.3. In addition, some general restrictions such as span curvature to be lesser than 12 degrees and girders to be parallel and prismatic are also imposed on the use of these formulas. In general, LRFD live load DFs are found to give a more accurate estimate of load distribution as compared to the lever rule or the DFs in the Standard Specifications.

The Standard Specifications live load DF formulas are of the form $S/D$, where, $S$ is the girder spacing and $D$ is 11 for prestressed concrete girders and TxDOT Bridge Design Manual (TxDOT 2001) also recommends the same value for TxDOT U54 beams.

These Standard Specifications formulas were found to give valid results for typical bridge geometries (i.e., girder spacing of 6 ft. and span length of 60 ft.), but lose accuracy when the bridge parameters are varied (Zokaie 2000).

**Table 2.2 LRFD Live Load Distribution Factors for Concrete Deck on Concrete Spread Box Beams**

| Category | Distribution Factor Formulas | Range of Applicability |
|---|---|---|
| **Live Load Distribution per Lane for Moment in Interior Beams** | One Design Lane Loaded:<br>$\left(\frac{S}{3.0}\right)^{0.35}\left(\frac{Sd}{12.0L^2}\right)^{0.25}$<br>Two or More Design Lanes Loaded:<br>$\left(\frac{S}{6.3}\right)^{0.6}\left(\frac{Sd}{12.0L^2}\right)^{0.125}$ | $6.0 \le S \le 18.0$<br>$20 \le L \le 140$<br>$18 \le d \le 65$<br>$N_b \ge 3$ |
| | Use Lever Rule | $S > 18.0$ |
| **Live Load Distribution per Lane for Moment in Exterior Longitudinal Beams** | One Design Lane Loaded:<br>Lever Rule<br>Two or More Design Lanes Loaded:<br>$g = e \times g_{\text{int}erior}$<br>$e = 0.97 + \frac{d_e}{28.5}$ | $0 \le d_e \le 4.5$<br>$6.0 \le S \le 18.0$ |
| | Use Lever Rule | $S > 18.0$ |
| **Live Load Distribution per Lane for Shear in Interior Beams** | One Design Lane Loaded:<br>$\left(\frac{S}{10}\right)^{0.6}\left(\frac{d}{12.0L}\right)^{0.1}$<br>Two or More Design Lanes Loaded:<br>$\left(\frac{S}{7.4}\right)^{0.8}\left(\frac{d}{12.0L}\right)^{0.1}$ | $6.0 \le S \le 18.0$<br>$20 \le L \le 140$<br>$18 \le d \le 65$<br>$N_b \ge 3$ |
| | Use Lever Rule | $S > 18.0$ |
| **Live Load Distribution per Lane for Shear in Exterior Beams** | One Design Lane Loaded:<br>Lever Rule<br>Two or More Design Lanes Loaded:<br>$g = e \times g_{\text{int}erior}$<br>$e = 0.8 + \frac{d_e}{10}$ | $0 \le d_e \le 4.5$ |
| | Use Lever Rule | $S > 18.0$ |

where:

$S$ = Beam spacing, ft.
$L$ = Span length, ft.
$d$ = Girder depth, in.
$N_b$ = Number of beams.

$d_e$ = Distance from the exterior web of exterior beam to the interior edge of curb or traffic barrier, in.

For the Standard Specifications (AASHTO 2002), the live load DF formula for interior girders consisting of a concrete deck on spread box beams (similar to Texas U54 beams), originally developed by Mortarjemi and Vanhorn (1969), is as follows.

$$DFM_{\text{int}erior} = \frac{2N_L}{N_B} + k\frac{S}{L} \tag{2.3}$$

where:

$N_L$ = Number of design traffic lanes
$N_B$ = Number of beams ($4 \le N_B \le 10$)
$S$ = Beam spacing, ft. ($6.57 \le N_B \le 11.0$)
$L$ = Span length, ft.
$k$ = $0.07W - N_L(0.10N_L - 0.26) - 0.2N_B - 0.12$
$W$ = Roadway width between curbs, ft. ($32 \le W \le 66$)

The LRFD Specifications provide skew correction factors for the live load DFs to account for the resulting reduction in bending moment in all girders and increase in the shear force in exterior girders. These correction factors can significantly affect the final design. The effects due to transverse and longitudinal stiffness, skew, curved alignment and continuity are ignored in the Standard Specifications.

#### *2.2.1.5 Dynamic Load Allowance Factor*

The dynamic load allowance (*IM*) is an increment to be applied to the static lane load to account for wheel load impact from moving vehicles. The LRFD Specifications give a dynamic load allowance factor for all limit states as 33%, except 15% for the fatigue and fracture limit state and 75% for design of deck joints. The Standard Specification uses the following formula to calculate the impact factor, *I*.

$$I = \frac{50}{L + 125} \leq 30\% \tag{2.4}$$

where:

$L$ = Span length, ft.

The new *IM* factor can substantially increase the live load moments for LRFD designs as compared to designs based on the Standard Specifications, especially for longer spans (e.g. a 48.5% increase for a 100 ft. span and a 75% increase for a 140 ft. span).

#### *2.2.1.6 Allowable Stress Limits*

The LRFD Specifications (AASHTO 2004) give the allowable stress limits in units of *ksi* as compared to *psi* in the Standard Specifications and thus, the coefficients are different. Moreover, the tensile stress limit at initial loading stage at transfer has slightly increased from $7.5\sqrt{f'_{ci}(psi)}$ in the Standard Specifications to $7.59\sqrt{f'_{ci}(psi)}$ in the LRFD Specifications. The compressive stress limit at intermediate loading stage at service has increased from $0.40 f'_c$ in the Standard Specifications to $0.45 f'_c$ in the LRFD Specifications. For the compressive stress at the final loading stage at service, the LRFD Specifications has introduced a multiplier as a reduction factor to account for the fact that the unconfined concrete of the compression sides of the box girders are expected to creep to failure at a stress far lower than the nominal strength of the concrete.

#### *2.2.1.7 Effective Flange Width*

The provisions for determining the effective flange width are the same in both specifications except that in the LRFD Specifications commentary it is mentioned that for open boxes, such as Texas U54 beams, the effective flange width of each web should

be determined as though each web was an individual supporting element. The Standard Specifications do not mention any guideline to determine the effective flange width for open box beams.

*2.2.1.8 Transfer Length, Development Length, and Debonding*

The transfer length of prestressing strands is determined as $50d_b$ in the Standard Specifications as compared to the LRFD Specifications where the transfer length is increased to $60d_b$. The development length is determined by Eq. 2.5 in the Standard Specifications and by Eq. 2.6 in the LRFD Specifications. The Standard Specifications in Art. 9.28.3 require the development length, calculated by the Eq. 2.5, to be doubled when tension at service load is allowed in the precompressed tensile zone for the region where one or more strands are debonded.

$$l_d = \left( f_{su}^* - \frac{2}{3} f_{se} \right) D \tag{2.5}$$

$$l_d = \kappa \left( f_{ps} - \frac{2}{3} f_{pe} \right) d_b \tag{2.6}$$

where:

$f_{su}^*$ or $f_{ps}$ = Average stress in prestressing steel for the ultimate conditions, ksi
$f_{se}$ or $f_{pe}$ = Effective stress in prestressing steel after all losses, ksi
$\kappa$ = Modification factor taken as 1.6 for precast, prestressed beams
D or $d_b$ = Diameter of prestressing strands, in.

The Standard Specifications do not give any limit on the debonding percentage. The LRFD Specifications in Article 5.11.4.3 limit the debonding of strands to 40% per horizontal row and 25% per section. Debonding termination is allowed at any section, if and only if, it is done for less than 40% of the total debonded strands or 4 strands, whichever is greater. The LRFD Specifications in Commentary 5.11.4.3, however, allow

the consideration of successful past practices regarding debonding and further instruct to perform a thorough investigation of shear resistance of the sections in the debonded regions. The Standard Specifications do not specify any limit on the allowable debonding length of the debonded strands. The LRFD Specifications allow the strands to be debonded to any length as long as the total resistance developed at any section satisfies all the limit states.

### *2.2.1.9 Initial and Final Relaxation Losses*

The LRFD Specifications recommend new equations for the calculation of the initial and final relaxation losses. The equations for relaxation losses in low relaxation strands are given in Table 2.3.

**Table 2.3 Comparison of Relaxation Loss Equations in the LRFD and Standard Specifications**

| **Standard Specifications** | **LRFD Specifications** |
|---|---|
| *Final Relaxation Loss:*<br>$CR_S = \left[5000 - 0.10\,ES - 0.05(SH + CR_C)\right]$ | *Initial Relaxation Loss:*<br>$\Delta f_{pR1} = \frac{\log(24.0 \times t)}{40.0}\left[\frac{f_{pj}}{f_{py}} - 0.55\right] f_{pj}$<br><br>*Final Relaxation Loss:*<br>$\Delta f_{pR2} = 30\%\left[20.0 - 0.4\,\Delta f_{pES} - 0.2\left(\Delta f_{pSR} + \Delta f_{pCR}\right)\right]$ |

where:

$SH$, $\Delta f_{pSR}$ = Loss of prestress due to concrete shrinkage, ksi
$EC$, $\Delta f_{pES}$ = Loss of prestress due to elastic shortening, ksi
$CR_C$, $\Delta f_{pCR}$ = Loss of prestress due to creep of concrete, ksi
$CR_S$, $\Delta f_{pR2}$ = Loss of prestress due to final relaxation of prestressing steel, ksi
$\Delta f_{pR1}$ = Loss of prestress due to initial relaxation of prestressing steel, ksi
$f_{pj}$ = Initial stress in the tendon at the end of stressing operation, ksi
$f_y$ = Specified yield strength of prestressing steel, ksi

$t$ = Time estimated in days from stressing to transfer, days

*2.2.1.10 Shear Design*

The design for transverse shear in the LRFD Specifications is based on the Modified Compression Field Theory (MCFT), in which the angle of diagonal compressive stress is considered to be a variable and is determined in an iterative way. On the contrary, the transverse shear design in the Standard Specifications consider the diagonal compressive stress angle as constant at 45 degrees. This change is significant for prestressed concrete members because the angle of inclination of the diagonal compressive stress is typically 20 degrees to 40 degrees due to the effect of the prestressing force. Moreover, in MCFT the critical section for shear design is determined in an iterative process, whereas in the Standard Specifications the critical section is constant at a pre-determined section corresponding to the 45 degree angle assumed for the diagonal compressive stress. The MCFT method is a rational method that is based on equilibrium, compatibility and constitutive relationships. It is a unified method applicable to both prestressed and non-prestressed concrete members. It also accounts for the tension in the longitudinal reinforcement due to shear and the stress transfer across the cracks.

The interface shear design in the LRFD Specifications is based on shear friction theory and is significantly different from that of the Standard Specifications. This method assumes a discontinuity along the shear plane and the relative displacement is considered to be resisted by cohesion and friction, maintained by the shear friction reinforcement crossing the crack.

## 2.3 CODE CALIBRATION AND APPLICATION OF RELIABILITY THEORY

### 2.3.1 Introduction

The main parts of Standard Specifications (AASHTO 2002) were written about 60 years ago and there have been many changes and adjustments at different times which have resulted in gaps and inconsistencies (Nowak 1995). Moreover, the Standard Specifications (AASHTO 2002) do not provide for a consistent and uniform safety level for various groups of bridges. Therefore, in order to overcome these shortcomings rewriting the specifications based on the state-of-the-art knowledge about various branches of bridge engineering was required. Lately, a new generation of bridge design specifications, based on structural reliability theory, have been developed such as the OHBDC (Ontario Highway Bridge Design Code), the AASHTO LRFD, and the Eurocode.

The major tool in the development of the LRFD Specifications (AASHTO 2004) is a reliability analysis procedure that employs probability of failure to maximize the structural safety within the economic constraints. In order to design structures to a predefined target reliability level and to provide a consistent margin of safety for a variety of bridge structure types, the theory of probability and statistics is applied to derive the load and resistance factors. The greater the safety margin, the lesser is the risk of failure of the structural system. But a higher safety level will also cause the cost of initial investment in terms of design and construction to increase. On the contrary, the probability of failure decreases with a higher safety level. Thus, selection of the desired level of safety margin is a trade off between economy and safety.

### 2.3.2 Calibration Procedure

The calibration procedure was developed by Nowak et al (1987) and is described in Nowak (1995; 1999). The LRFD Specifications (AASHTO 2004) is calibrated in such a way so as to provide the same target safety level as that of previous satisfactory performances of bridges (Nowak 1999). The major steps in the calibration procedure of AASHTO LRFD specifications were selection of representative bridges and establishment of statistical database for load and resistance parameters, development of load and resistance models, calculation of reliability indices for selected bridges, selection of target reliability index and calculation of load and resistance factors (Nowak 1995). These steps are briefly outlined in the following.

About 200 representative bridges were chosen from various geographical regions of the United States based on current and future trends in bridge designs instead of choosing very old bridges. Reliability indices were calculated using an iterative procedure for these bridges, which were designed according to the Standard Specifications (AASHTO 1992). To ensure an adequate level of reliability for calibration of the LRFD Specifications, the performance of all representative bridges was evaluated and a corresponding target reliability index was chosen to provide a minimum, consistent and uniform safety margin for all structures. The load and resistance factors for the LRFD Specifications were calculated so that the resulting designs have a reliability index close to the target value (Nowak 1995).

### 2.3.3 Probabilistic Load Models

Load components can include dead load, live load (static and dynamic), environmental forces (wind, earthquake, temperature, water pressure, ice pressure), and special forces (collision forces, emergency braking) (Nowak 1995). These load components are further divided into subcomponents. The load models are developed using the available statistical data, surveys and other observations. Load components are

treated as normal random variables and their variation is described by the cumulative distribution function (CDF), mean value or bias factor (ratio of mean to nominal) and coefficient of variation (ratio of standard deviation to mean). The relationship among various load parameters is described in terms of the coefficients of correlation. Several load combinations were also considered in the reliability analysis.

The self weight of permanent structural or non-structural components under the action of gravity forces is termed as dead load. Due to the difference in variation between subcomponents, the dead load was further categorized into weight of factory made elements, cast-in-place concrete members, wearing surface and miscellaneous items (e.g. railing, luminaries) (Nowak 1999; Nowak and Szerszen 1996). Bias factors (ratio of mean to nominal value) were taken as used in Nowak (1999), while the coefficient of variations (ratio of standard deviation to mean value) were taken as recommended by Ellingwood et al. (1980). The thickness of the asphalt surface was modeled on the basis of statistical data available from Ontario Ministry of Transportation (MTO) and reported by Nowak and Zhou (1985). The average thickness of asphalt is 3.5 in. which needs to be verified for the United States.

**Table 2.4 Statistical Parameters of Dead Load (Nowak and Szerszen 1996)**

| COMPONENT | BIAS FACTOR | COEFFICIENT OF VARIATION |
|---|---|---|
| **Factory made members, D1** | 1.03 | 0.08 |
| **Cast-in-place members, D2** | 1.05 | 0.10 |
| **Asphalt, D3** | 3.5 in. | 0.25 |
| **Miscellaneous, D4** | 1.03-1.05 | 0.08-0.10 |

### 2.3.4 Probabilistic Resistance Models

In order to be able to quantify the safety reserve for resistance by reliability theory, accurate prediction of load carrying capacity of structural components is of paramount importance.

#### *2.3.4.1 Development of Probabilistic Resistance Models*

The bridge capacity is dependant upon the resistance of its components and connections. The resistance of a component, R, is assumed to be a lognormal random variable that is primarily dependant on material strength, and dimensions. Uncertainty in this case is caused by three major factors namely, material properties M, fabrication (dimensions) factor F, and analysis approximations factor P. Material uncertainty is caused by the variation in strength of material, modulus of elasticity, cracking stress, and chemical composition, whereas fabrication uncertainty is the result of variations in geometry, dimensions, and section modulus, and analysis uncertainty exists due to approximation in the methods of analysis, and idealized stress strain distribution models (Nowak et al. 1994). Material and fabrication uncertainties are combined by Nowak et al (1994) into one single variable *MF*. The statistical parameters for professional factor *P* are taken from the available literature (Nowak et al 1994). The statistical parameters for mechanical properties of concrete and prestressing steel were taken from available test data (Ellingwood et al 1980) for use in the simulations.

The statistical parameters such as bias factor (ratio of mean to nominal) and coefficient of variation (ratio of standard deviation to mean) are at the heart of the reliability methods used. In the absence of extensive experimental database, Monte Carlo simulation technique was used to calculate these parameters for bending and shear capacity. Flexural capacity of prestressed concrete AASHTO type girders is established by the strain incremental approach and moment-curvature relationships were developed

and the shear capacity of concrete components is calculated by the modified compression field theory (Nowak 1995).

The resistance of a component, $R$, is computed as

$$R = R_n MFP \tag{2.7}$$

The mean value of $R$ is calculated as

$$m_R = R_n m_M m_F m_P \tag{2.8}$$

where the $m_R$, $m_M$, $m_F$, and $m_P$ are the means of $R$, $M$, $F$ and $P$ respectively. The coefficient of variation of $R$, ($V_R$), may be approximated as

$$V_R \approx \sqrt{V_M^2 + V_F^2 + V_P^2} \tag{2.9}$$

The final calculated statistical parameters for resistance of prestressed concrete bridges are shown in Table 2.5.

**Table 2.5 Statistical Parameters for Resistance of Prestressed Concrete Bridges (Nowak et al. 1994)**

| Limit State | *FM* | | *P* | | *R* | |
|---|---|---|---|---|---|---|
| | **Bias** | **COV** | **Bias** | **COV** | **Bias** | **COV** |
| **Moment** | 1.04 | 0.04 | 1.01 | 0.06 | 1.05 | 0.075 |
| **Shear** | 1.07 | 0.08 | 1.075 | 0.1 | 1.15 | 0.13 |

### 2.3.5 Reliability Analysis of Prestressed Concrete Girder Bridges

As resistance is a product of parameters $M$, $F$, and $P$, therefore, Nowak (1995) assumed that the cumulative distribution function (CDF) of $R$ is lognormal. The CDF of the load is treated as a normal distribution function because $Q$ is a sum of the components of dead, live and dynamic load.

If $R - Q > 0$, then the structure fails. Probability of failure, $P_F$, can be defined as

$$P_F = Prob(R - Q < 0) \tag{2.10}$$

Very often structural safety is related to the limit states. Generally, a limit state function can be a function of many variables (e.g. material properties, structural geometry and dimensions, analysis techniques etc.), which makes the direct calculation of $P_F$ very complex. Therefore, it becomes very convenient to measure the structural safety in terms of a reliability index. The reliability index, $\beta$, defined as a function of $P_F$,

$$\beta = -\Phi^{-1}(P_F) \tag{2.11}$$

where:

$\Phi^{-1}$ = Inverse standard normal distribution function

As an example, a normal random variable having a reliability index of 3.5 is said to have a probability of failure of 0.0233%.

For the cases where the $R$ and $Q$ are best treated using dissimilar distribution functions, iterative methods such as the Rackwitz-Fiessler can be used to determine the value of $\beta$ (Nowak 1999; Rackwitz and Fiessler 1978). Reliability indices are also calculated for bridges designed according to AASHTO Standard specifications, which gives a considerable variation in $\beta$ values. Nowak (1999) assumed that safety level corresponding to 60 ft. span, 6 ft. spacing and simple span moment is considered acceptable. Therefore, target reliability index was set equal to 3.5 which is the average $\beta$ value considering all the girder types for the aforementioned span and spacing. In general, it can be different for different consideration scenarios depending upon the acceptability level of the consequences of potential failure and the cost of increasing safety. The calculated load and resistance factors provide a consistent and uniform reliability of design, as depicted in the Figures 2.1 and 2.2.

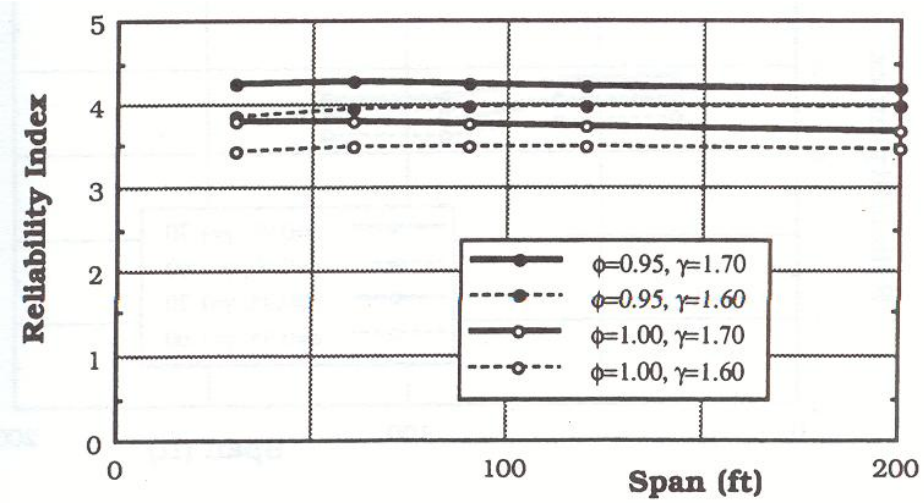


**Figure 2.1 Reliability Indices for LRFD Code, Simple Span Moments in Prestressed Concrete Girders (Nowak 1999).**

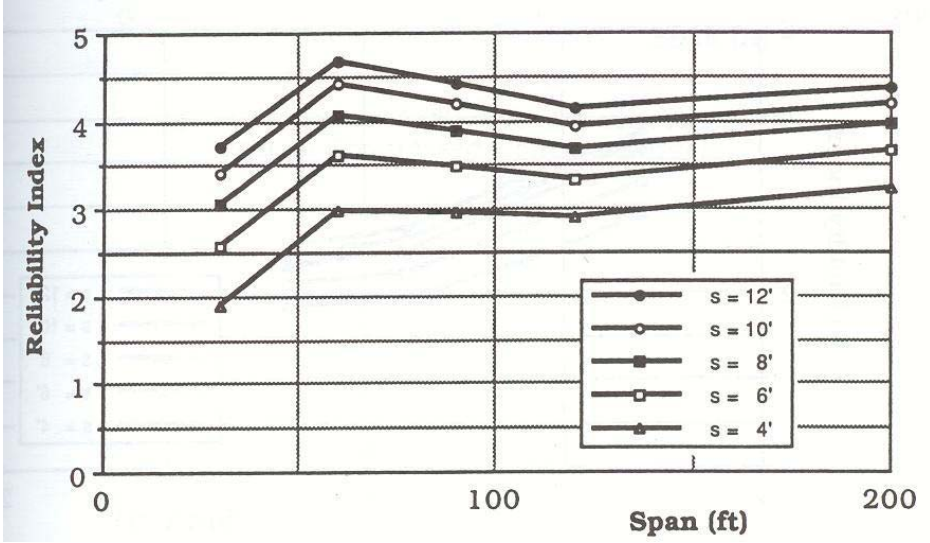


**Figure 2.2 Reliability Indices for AASHTO Standard (1992), Simple Span Moments in Prestressed Concrete Girders (Nowak 1999).**

Nowak and Saraf (1996) designed each structural component to satisfy ultimate limit state, serviceability limit state and fatigue limit state. Ultimate limit state was considered to be reached upon loss of flexural strength, shear strength, stability or onset of rupture et cetera. Serviceability limit state was assumed to be related to cracking, deflection and vibration. Design of a wide range of prestressed concrete girders revealed

that instead of ultimate limit state, serviceability limit state (allowable tension stress at the final stage) always governed. For serviceability limit state the $\beta$ value is 1.0 for tension stress limit and 3.0 for compression stress limit, whereas, for ultimate limit state the $\beta$ value is 3.5. Lower $\beta$ values for serviceability limit state indicate the lesser severity of consequences as compared to ultimate limit states. Nowak (1999) have clearly stated that bridges designed according to their proposed load and resistance factors have reliability index greater than 3.5 and the same value has been proposed by Nowak and Saraf (1996).

### 2.3.6 Future Trends and Challenges

Perhaps the most important issue facing code writers as well as researchers and engineers involved in safety evaluation of new and existing bridges is that of the selection of target reliability levels. Currently, only strength limit state is calibrated, other limit states such as service, fatigue and fracture and extreme event limit states need to be calibrated based on the structural reliability theory. In general, future research will be geared towards resolving the issues like time dependent reliability models, deterioration models and bridge reliability, bridge load and resistance reliability models, nonlinear reliability analysis of bridge structures, reliability of a bridge as a link in transportation network systems and lifetime reliability.

## 2.4 DEVELOPMENT OF VEHICULAR LIVE LOAD MODEL

Kulicki (1994) discusses the development of the vehicular live load model, HL93, adopted by the AASHTO LRFD Specifications. This study considered twenty two representative vehicles from a report released by National Transportation Research Board. This report reviewed the vehicles configurations allowed by various states as

exceptions to the allowable weight limits. The bending moment ratio (i.e. ratio between exclusion vehicle and 1989 AASHTO live load moments) varied from 0.9 to 1.8 with respect to various spans, which called for a new live load model that can represent the exclusion vehicles adequately. Therefore, five candidate notional loads were selected for the development of a new live load model for the AASHTO LRFD Specifications:

(1) A single vehicle weighing a total of 57 tons with a fixed wheel base, axle spacing and weights,
(2) A design family, HL93, consisting of a combination of a design tandem or design HS-20 truck with a uniform load of 0.64 kips per running foot of the lane,
(3) HS25 truck load followed and preceded by a uniform load of 0.48 kips per running foot of the lane, with the uniformly distributed load broken for the HS vehicle,
(4) A family of three loads consisting of a tandem, a four-axle single unit, with a tridem rear combination, and a 3-S-3 axle configuration taken together with a uniform load, preceding and following that axle grouping, and
(5) An equivalent uniform load in kips per foot of the lane required to produce the same force effect as that produced by the envelope of the exclusion vehicles.

The equivalent uniform load option was eliminated due to the possibility of a complex equation required to represent such a load. A comparison of four remaining possible live load models was performed for various combinations of moments and shears in simply supported beams and continuous beams. The HL93 live load model proved to be the best combination to represent the exclusion vehicles. Moreover, the results showed that this live load model was independent of the span length and a single live load factor will suffice to represent all the force effects.

## 2.5 VEHICULAR LIVE LOAD DISTRIBUTION FACTORS

### 2.5.1 Introduction

The lateral distribution of vehicular live load has a significant impact in quantification of the demand on highway bridges. Determination of accurate lateral distribution of live load to the bridge girders is a complex issue that has been the topic of research over the past several decades. Many approximate methods with varying levels of accuracy have been proposed and verified based on analytical studies, field and laboratory testing (Zellin et al. 1973, Sanders and Elleby 1970, Motarjemi and Vanhorn 1969, Scordelis 1966, Arya et al. 1960 et cetera). Zokaie et al. (1991) has not only documented various proposed formulas as a result of these past researches but also compared their levels of accuracy. In general, bridge design community has been using the empirical relations for live load distribution as recommended by AASHTO Standard Specifications (AASHTO 1989), with only minor changes since 1931, and recent additions to these specifications have included improved load distribution factors for particular types of superstructures based on tests and/or mathematical analyses (Zokaie et al. 1991).

In 1994, AASHTO LRFD Specifications (AASHTO 1994) introduced a comprehensive set of live load DF formulas that resulted from the NCHRP 12-26 project, entitled “Distribution of Live Loads on Highway Bridges” (Zokaie 2000). Although these formulas are also approximate but they consistently give conservative results, with a better accuracy, for a wide range of bridge types and bridge geometric parameters when compared to the other formulas available in the literature (Zokaie et al. 1991). Despite the universal agreement about the superiority of LRFD Specifications (AASHTO 2004) live load DFs over Standard Specifications (AASHTO 2002) live load DFs, the former still lack in accuracy. Primarily due to overlooking various structural and non-structural components of a typical bridge as noticed by Chen and Aswad (1996), Barr et al. (2001), and Eamon and Nowak (2002) among others.

### 2.5.2 Development of AASHTO LRFD Live Load Distribution Factor Formulas

The current AASHTO LRFD live load DF formulas are the result of study by Zokaie et al. (1991). The procedures followed by this study are comprehensively summarized in the following.

#### *2.5.2.1 History and Objectives*

In 1994, AASHTO LRFD Specifications (AASHTO 1994) introduced a comprehensive set of live load distribution factor formulas (LLDF) that resulted from the NCHRP 12-26 project, entitled "Distribution of Live Loads on Highway Bridges" (Zokaie 2000). The NCHRP 12-26 project was initiated in 1985 to improve the accuracy of the S/D formulas of the Standard Specifications and to develop comprehensive specifications for distribution of wheel loads on highway bridges (Zokaie 2000; Zokaie et al. 1991). The resulting recommendations out of this project were adopted by AASHTO as the guide specifications for lateral distribution of vehicular live loads on highway bridges (Guide 1994). With the advent of the first edition of the LRFD Specifications (AASHTO 1994), the formulas that were developed for the Standard Specifications (AASHTO 1996) needed to be modified to take into account the changes in vehicular live load model and multiple presence factors (Zokaie 2000). Thus, the formulas were recalibrated and incorporated in the LRFD Specifications (AASHTO 1994).

The objectives of this project were to evaluate the available methods for live load distribution, develop additional formulas to improve the accuracy of existing methods, and to provide guidelines for the selection of most efficient refined analysis methods.

*2.5.2.2 Procedure*

Several hundred bridges were selected from the National Bridge Inventory File (NBIF) to create a representative database of all the bridges in the United States (Zokaie 2000). The focus of this project was on typical bridge types such as beam-slab bridges, box girder bridges, slab bridges, multi-box beam bridges, and spread box beam bridges. The database basically included the details required to build the analytical model of a particular bridge required to carry out a finite-element or grillage analysis of bridge superstructure. In particular, several parameters such as bridge type, span length, edge to edge width, curb to curb width, skew angle, number of girders, girder depth, slab thickness, overhang, year built, girder moment of inertia, girder area, and girder eccentricity (distance between the centroids of the girder and the slab) were extracted from the bridge plans obtained from various state departments of transportations. Among other bridge types, the database included 55 spread box beam bridges. The statistical analysis of the database parameters was performed with the help of histograms and scattergrams plots to identify the range and variation of each parameter, and the degree of correlation among several parameters. According to Zokaie (2000), the parameters were by and large not found to be correlated to each other.

For each bridge type three different levels of analyses were considered. The most accurate level of analysis, Level Three, included the detailed 3D modeling of the bridge superstructure and finite element modeling was recommended for this level of accuracy. Level Two included graphical methods, nomographs, influence surfaces, or simplified computer programs. Grillage analysis method, which has the comparable level of accuracy, was considered to be in Level Two analysis category. Level One analysis methods include the empirical formulas developed as the result of experimental or analytical studies, which generate approximate results and are simple in their application. To identify the most accurate available computer program for a particular bridge type, test data from field and laboratory experiments was compiled and analytical models developed in the Level Three computer programs. Analytical models were

analyzed and results were compared with experimental results. The programs that produced the most accurate results were identified for particular bridge types and considered as the basis for the evaluation of Level Two and Level One methods.

Parametric sensitivity study was performed to identify the important parameters that affect the lateral distribution of live loads. A finite element model was developed using the mean values of all the parameters except the one under consideration, which was varied from minimum to maximum in order to recognize its affects on the distribution factors under HS20 truck loading. After examining the results, span length, girder spacing and beam depth were considered key parameters for spread box beams. Since the HS20 truck gage length is constant at 6ft. so it was not considered in sensitivity study but it may have a considerable affect on LLDFs if varied. Smaller gage width will result in larger distribution factors and larger gage width will result in smaller distribution factors. Although, this study is based on AASHTO HS family of trucks, but a limited parametric study conducted in this research showed that truck weight and axle configuration does not significantly affect the live load distribution.

According to Zokaie (2000) the development of AASHTO LRFD LLDF simplified formulas is based on certain assumptions. It was assumed that there was no correlation between parameters considered to be included in the formula. It was also assumed that the effect of each parameter can be modeled by an exponential function of the form $ax^b$, where $x$ is the value of the given parameter and constants $a$ and $b$ are determined to represent the degree of variation of the distribution factor. For the selected set of key parameters for a particular bridge type the following general form of the exponential formulas was devised.

$$g = (a)(S)^{b1}(L)^{b2}(d)^{b3}(.....)^{b4} \tag{2.12}$$

where:

$a$ = Scale factor

$g$ = Distribution factor

$S$, $L$, $d$ = Selected parameters

*b1*, *b2*, *b3*, *b4* = Exponents of each parameter

The exponents of each parameter are selected to make the exponential curve fit the simulated variation between the particular parameter and distribution factor. Different values of distribution factor *g* were calculated for different values of a particular parameter in the formula, say *S*, while keeping all other parameters same as of the average bridge and the resulting formulas will be,

$$\begin{aligned} g_1 &= (a)(S_1)^{b1}(L)^{b2}(d)^{b3}(.....)^{b4} \\ g_2 &= (a)(S_2)^{b1}(L)^{b2}(d)^{b3}(.....)^{b4} \\ &\quad . \quad . \quad . \quad . \quad . \quad . \\ &\quad . \quad . \quad . \quad . \quad . \quad . \\ g_n &= (a)(S_n)^{b1}(L)^{b2}(d)^{b3}(.....)^{b4} \end{aligned} \tag{2.13}$$

For the first two equations, we have,

$$\left(\frac{g_1}{g_2}\right) = \left(\frac{S_1}{S_2}\right)^{b1} \tag{2.14}$$

$$\text{Or} \quad b1 = \frac{\ln\left(\frac{g_1}{g_2}\right)}{\ln\left(\frac{S_1}{S_2}\right)} \tag{2.15}$$

So for *n* number of equations we will get (*n*-1) different *b1* values. If all *b1* values are generally close to each other, then an exponential curve based on the average of all *b1* values was used to model the variation in the distribution factors. The value of scale factor *a* was determined from the average bridge by the following equation,

$$a = \frac{g_{avg}}{\left(\left(S_{avg}\right)^{b1}\left(L_{avg}\right)^{b2}\left(d_{avg}\right)^{b3}\left(.....\right)^{b4}\right)} \qquad (2.16)$$

This entire procedure was repeated for all other parameters in the similar manner.

The process of development of simplified formulas was based on certain assumptions and parameters which did not affect the load distribution in a significant way were ignored altogether. In order to gain confidence in the accuracy of the developed formulas and to compare their relative accuracy level with other proposed formulas, their verification and evaluation was a very important step. Therefore, the bridges in the database were analyzed by a Level Three accurate method, best suited to a particular class of bridges as determined earlier. Mean, minimum, maximum and standard deviations were determined and compared for all the formulas and the accurate method. A low standard deviation was considered to be indicative of relatively higher accuracy level for a particular formula. The trends in the accuracy of the formula with respect to the Level Three accurate method were analyzed with the help of statistical data so obtained. For the optimization of the accuracy level of the developed formulas it was made sure that standard deviation is minimized and kept lower than that obtained from the AASHTO Standard formulas and to make formulas as simple as possible while maintaining the desired level of accuracy.

Once these base formulas (i.e., formulas for flexure and shear, for single and multiple lanes loading, in the interior girders) were established, several extensions of the formulas for continuity, skew effects and exterior girder were investigated. Correction factors were calculated to take into account the effect of these additional issues. Those correction factors were scale factors for base formulas to adjust the calculation.

#### *2.5.2.3 Limitations*

The AASHTO LRFD Specifications formulas were calibrated against a database of real bridges. This database was characterized by particular ranges of span lengths, girder spacings, girder depths and over-hang widths etc. Although these formulas produce results that are generally within 5% of the results of finite element deck analysis results and are most accurate when applied to bridges within the scope of the calibration database (Zokaie 2000). The effects of edge stiffening elements were ignored in this study. Some special cases where these formulas were recommended to be applied by using engineering judgment are non-prismatic girders, varying skew and span lengths in continuous bridges, different girder spacings, varying girder widths, large curvatures etc.

### 2.5.3 Various Subsequent Researches

In order to determine the suitability and applicability of the new proposed formulas to their particular cases, several departments of transportations and independent researchers carried different studies. Certain departments of transportation (DOTs) such as Illinois (IDOT), California (Caltrans) and Tennessee (TDOT), sponsored researches geared towards either simplifying and revamping the live load distribution criteria to suit their typical bridge construction practices or to justify their previous practices of live load distribution (Tobias et al. 2004, Song et al. 2003, Huo et al. 2004). Part of the recommendations made in the researches discussed below is separately summarized in section 2.5.5. and are not discussed in this section to avoid repetition.

#### *2.5.3.1 Song et al. (2003)*

Song et al. (2003) found that the limitations such as constant deck width, parallel beams with approximately equal stiffness, span length-to-width ratio to be greater than

2.5 and angular change of less than $12^{o}$ in plan for a torsionally stiff closed section, on the use of the LRFD (AASHTO 1998) live load distribution factor formulas place severe restrictions on the routine designs of bridges in California, as box-girder bridges outside of these limits are frequently constructed. They performed the grillage analysis for multicellular box girder typical California bridges with aspect ratio from 0.93 to 3.28, with angular change in curvature from $5.7^{o}$ to $34.4^{o}$ and with nonparallel girders or a non-prismatic cross section. They concluded that in general these formulas can be used for the box girder bridges within the parametric scope considered in this study. The plan aspect ratio limit was concluded to be unwarranted because as the plan aspect ratio becomes smaller than the limit 2.5, the general trend indicates that the LRFD Specifications formula becomes increasingly conservative. Furthermore, it was found that the distribution factor from the refined analysis does not vary significantly with the different radii of curvature or angular change between the bents. The authors finally conclude that because of the small set of bridges used in this study, results presented should not be construed to imply an overall conservatism of the LRFD formulas; further study of the limits with a more extensive parameter range is warranted.

#### *2.5.3.2 Huo et al. (2004)*

Huo et al. (2004) carefully examined Henry's method which is a simplified live load distribution method used by Tennessee Department of Transportation since 1963 and proposed a modifications to the original method. They introduced the method as simple and flexible in application which can treat both interior and exterior beams in a bridge and which requires only basic bridge information, such as the width of the bridge, the number of traffic lanes, and the number of beams. It was concluded that results of Henry's method were in reasonable agreement with the values from the LRFD Specifications (AASHTO 1998) method, the Standard Specifications (AASHTO 1996) method, and the finite element analysis (ANSYS 5.7). Effects of four key parameters

such as span length, beam spacing, slab thickness, and beam stiffness were documented and for all those parameters the Henry's method was found to be in very good agreement with the other two methods of the LRFD and the Standard Specifications. Particularly, the LRFD Specifications method was found to have a better correlation with Henry's method.

#### *2.5.3.3 Kocsis (2004)*

Kocsis (2004) evaluated the AASHTO Standard specifications line loads (curbs, sidewalks, barriers and railings) and live load distribution factors. The author discussed the computer program SECAN (Semi-continuum Method of Analysis for Bridges) and made suggestions for obtaining more accurate distribution factors for line loads, AASHTO live loads, and non-AASHTO live loads. The author raised the question as to how the line loads should be accurately distributed to bridge girders. He further made his point that wearing surface, being spread over almost the entire deck, can be distributed equally to all girders but for curbs, sidewalks, barriers, and railings, it would be expected that the girder nearest the load should take the largest portion of the load. For a particular case of a 175 ft simple span five steel girder bridge with a total weight of sidewalk and railing to be 635 lb/ft, he showed that AASHTO Standard uniform distribution of sidewalk and railing yielded 254 lb/ft per girder as compared to analysis performed by the computer program SECAN which yielded the actual load taken by the exterior girder to be 632 lb/ft. His calculations showed that the actual share of the sidewalk and railing loads carried by the outer girders is substantially more than that by the AASHTO method of dividing the load equally among all the girders. Moreover, he recommends the use of SECAN for line load distribution factors and the use of AASHTO (Guide 1994) formulas for live load distribution.

*2.5.3.4 Tobias et al. (2004)*

The study conducted by Tobias et al. (2004) targeted the typical bridges in Illinois bridge inventory such as concrete deck-on-steel stringer construction and concrete deck-on-precast prestressed I-beams. Moreover, they considered simply supported and continuous bridges, which had span lengths ranging between 20ft to 120ft with 10ft increments. The transverse beam spacing varied from 3.5ft to 10ft with 0.5ft increments. The continuous structures had two spans of equal lengths. The stringers of beams were of constant depths and section moduli throughout each span. The studied structures were designed efficiently i.e., the ratios of actual section moduli to required were all close to unity. No curved or skewed structures were included in the study and interior beams were assumed to govern the design. Only the factored design moments and shears were compared because of the dissimilar nature of the two design philosophies (LFD and LRFD). For all considered simple spans and continuous spans, LRFD design moments ranged between 22% larger to 7% smaller than those computed using LFD. For mid-range span (50-90ft) with common Illinios transverse spacings (5.5-7.5ft) the average increase in design moment over LFD was 3 to 4%. LRFD design shears ranged between 41% larger to 3% smaller. For mid-range span (50-90ft) with common Illinios transverse spacings (5.5-7.5ft) the average increase in design shears over LFD was 24 to 15% with average of about 20%. In general, the disparity between predicted shears using LRFD and LFD was found to be more profound for shear than for moment. The authors described the pile analogy method provision for calculation of live load distribution factor for exterior beam in bridges with diaphragms or cross-frames to be very conservative approach. The ratio of longitudinal to transverse stiffness parameter ($K_g/Lt^3$) in the live load distribution factor formula is said to have insignificant affect on the final calculation of bending moment or shear and was set equal to 1.10 for prestressed I-beam shapes and 1.15 for standard Illinois bulb-tee shapes. They recommended that the exterior beam overhang cantilever span will be such that the interior beam governs primary superstructure design in Illinois for typical bridges and

that these bridges be design for two or more lane loading except for fatigue and stud design where single lane loading should be checked.

#### *2.5.3.5 Chen and Aswad (1996, 1997)*

Chen and Aswad (1996; 1997) reviewed the LRFD live load distribution formulas for modern prestressed concrete I-girder and spread box girder bridges with larger span-to-depth ratios and compared LRFD's results with those obtained by finite element analysis method. They pointed out certain shortcomings in the methodology followed by Zokaie et al. (1991). The "average bridge" and the database of bridges was not the representative of the future bridges which are characterized by larger span-to-depth ratios and higher concrete strengths. As an example, they said that Zokaie et al. (1991) considered the average bridge span length to be 65.5 ft., which was well below the expected average span of future bridges and thus, a more rigorous analysis is required to take into account this increase in average span. The effect of diaphragms was not considered in the original study; therefore, the rigid diaphragm model required by interim LRFD (AASHTO 1994) provision in section 4.6.2.2.2d produces over-conservative results. They showed that for spread box girders the finite element analysis method produced smaller distribution factors by 6 to 12% for both interior and exterior girders. But, in the two cases where the aforementioned LRFD (AASHTO 1994) provision of rigid diaphragm model was controlling, the LRFD (AASHTO 1994) distribution factors were very conservative by 30% for the cases considered (e.g. 0.785 and 0.9 by LRFD (AASHTO 1994) as compared to 0.548 and 0.661 by FEA). This assumption of rigid diaphragm model for exterior girders is no longer applicable to spread box beams in the latest LRFD Specifications (AASHTO 2004). They also summarized the conclusions of Lehigh reports on Spread-box beams (Lin and Vanhorn 1968; Guilford and Vanhorn 1968; Vanhorn 1969): The deflections of the girders directly under the truck load were only slightly reduced by the use of mid-span diaphragms, the structural function and usefulness of mid-span diaphragms was found to

be questionable, and the center-to-center spacing of girders was a reasonably accurate estimate of the effective flange width for the composite girder.

#### *2.5.3.6 Eamon and Nowak (2002)*

Eamon and Nowak (2002) studied the effects of edge-stiffening elements such as barriers, and sidewalks, and other secondary elements such as diaphragms on the resistance and load distribution characteristics of composite steel and prestressed concrete bridge girders. They found that steel girder bridges tend to benefit more from secondary elements in terms of load distribution than general stiffer prestressed concrete bridge girders. For the finite element analysis in the elastic range, they found that diaphragms reduce the maximum girder moment by up to 13% (4% on average), barriers up to 32% (10% on average), sidewalks up to 35% (20% on average), combinations of barriers and sidewalks from 9% to 34%, combinations of barriers and diaphragms from 11% to 25%, and combinations of barriers, sidewalks, and diaphragms from 17% to 42%. In general for the elastic finite element analysis case, neglecting barrier and diaphragms together lead to discrepancies ranging from 10% to 35%, while if we neglect barrier, sidewalk, and diaphragm then the discrepancies ranged from 25% to 55%. Finally, they concluded that in the elastic range, secondary elements affect the longitudinal and transverse position, and magnitude of maximum girder moment and can results in 10% to 40% decrease in girder distribution factor for typical cases. Similarly, for inelastic finite element analysis case, girder distribution factors can undergo an additional decrease of 5% to 20%. Moreover, they observed that ignoring the secondary elements affect can produce varying levels of reliability for the girder bridges designed as per LRFD Specifications (AASHTO 1998).

#### *2.5.3.7 Khaloo and Mirzabozorg (2003)*

Khaloo and Mirzabozorg (2003) conducted a study to assess the effect of skew and internal diaphragms on the live load distribution characteristics of simply supported bridges consisting of five I-section concrete girders and confirmed that the Standard Specifications (AASHTO 1996) approach produces very conservative results when compared with the load distribution factors obtained by finite element analysis. The scope of their study was defined by the key parameters of girder spacings (1.8, 2.4, 2.7 m), span lengths (25, 30, 35 m), skew angles (0, 30, 45, 60 degrees), and different arrangements and spacings of internal diaphragms. They considered three different arrangements for internal diaphragms: In the first system, there were no internal diaphragms considered, in the second system internal transverse diaphragms at one third of span length parallel to the supporting lines of the deck are considered, in the third system internal transverse diaphragms are considered to be perpendicular to the longitudinal girders with two different diaphragm spacing patterns followed (i.e. one spacing pattern followed the Standard Specifications (AASHTO 1996) and in the other diaphragm were considered to spaced at 5m center to center). All of their models contained two end diaphragms and the distance of the exterior girder from the edges of the deck was constant at 1m. The authors proposed some modifications in relations originally proposed by Khaleel and Itani (1990), for the load distribution factor calculations for decks with internal diaphragms perpendicular to the longitudinal girders. Those relations lower the conservatism in the load distribution factors provided by the Standard Specifications (AASHTO 1996). The authors concluded that the arrangement of internal diaphragms has a great effect on the load distribution pattern. They showed that even in bridges with zero skew without internal diaphragms, the load distribution factors of the aforementioned Standard Specifications are very conservative. And this difference between the Standard Specifications and finite element analysis increases with the increment in skew angle, especially in decks with internal diaphragms perpendicular to the longitudinal girders.

#### *2.5.3.8 Barr et al. (2001)*

Barr et al. (2001) studied the effects of lifts (haunches), intermediate and end diaphragms, continuity, skew angle and load type (truck and lane) on the live load distribution in a continuous high-performance prestressed concrete girder bridge, designed by Washington Department of Transportation (WSDOT). The bridge had five W74MG girders and was skewed at $40^{o}$ with three span lengths 24.4 m, 41.7 m and 24.4 m. A finely meshed (6000 nodes) finite element model was evaluated with the results of field measurements of the bridge and the discrepancy in the maximum moments in each girder in the analytical model as compared to the actual field measurements was found to be within 6%, with the results by analytical model always on the conservative side. In their study, the difference between a rigorous finite element model, which most closely represented the actual bridge, and the LRFD Specifications (AASHTO 1998) was up to 28%. While for the finite element model most similar to that considered in developing the LRFD live load distribution factor method (i.e. without lifts, diaphragms, and continuity), the LRFD Specifications (AASHTO 1998) distribution factors were only 6% higher which matches the 5% value anticipated by Zokaie et al. (1991). It was observed in their study that the presence of lifts and end diaphragms were the major factors to significantly reduce the distribution factor values. They concluded that in comparison to code values for distribution factor, the live load distribution factor by finite element method would, if used, either reduce the required concrete release strength by 6.9 MPa or could allow for increasing the live load by 39%.

### 2.5.4 Effect of Various Parameters

#### *2.5.4.1 Effect of Edge Stiffening Elements*

Based on a limited sensitivity study Chen and Aswad (1996) found that exterior girder could carry more than 50% of parapet and/or noise wall loads and that the number

of girders was a dominant variable for the case of these loads. Eamon and Nowak (2002) found that barriers and sidewalks or their combinations are more effective for closely spaced girders and longer spans. They also found that steel girder bridges tend to benefit more from edge stiffening elements in terms of load distribution than generally stiffer prestressed concrete bridge girders. They observed that the addition of the edge-stiffening elements tends to shift the location of maximum moment away from the edge and closer to the center girder and for bridges with longer spans and fewer girders, the edge-stiffening elements have least affect on the maximum moment position. Eamon and Nowak (2002) also found that barriers decrease all girders deflections but this decrease is more for exterior girders as compared to interior ones. Moreover, they noticed that the large shifts in the neutral axis upwards at the edges of the bridge are indicative of the effectiveness of the addition of sidewalk and barrier or their combination. They also found that edge stiffening element effect is dependant upon bridge geometry (i.e. span length, bridge width and girder spacing), stiffness of secondary elements relative to that of girders or deck slab, and sidewalk width. Kocsis (2004) made his point that wearing surface, being spread over almost the entire deck, can be distributed equally to all girders but for curbs, sidewalks, barriers, and railings, it would be expected that the girder nearest the load should take the largest portion of the load.

#### *2.5.4.2 Effect of Diaphragms*

Eamon and Nowak (2002) found that diaphragms tend to make the girder deflections uniform among interior and exterior girders and that the addition of stiffer midspan diaphragms shift the longitudinal position of maximum moment away from midspan closer to the second truck axle and that stiffer girders are not as much affected by this longitudinal shift as more flexible ones. They observed that diaphragms have a little effect on the shifting the neutral axis of the bridge superstructure. Khaloo and Mirzabozorg (2003) concluded that in order to achieve the maximum efficiency for the presence of internal diaphragms, they should be placed perpendicular to the longitudinal

girders, and the load distribution is negligibly affected by the spacing between internal diaphragms that are perpendicular to the longitudinal girders. As per findings of Barr et al. (2001), the end diaphragms affect the load distribution significantly in comparison to intermediate diaphragms. They found that at high skew angles ($\geq 30^o$) the intermediate diaphragms were slightly beneficial, while introducing the end diaphragms decreased the distribution factors and this effect increased with increasing skew (e.g. for exterior girders, the decrease was up to 6% for zero skew to 23% for $60^o$ skew angle).

#### *2.5.4.3 Effect of Skew Angle*

Khaloo and Mirzabozorg (2003) found the skew angle to be the most influential factor on the load distribution and the load distribution factor is always less in the case of skewed bridges as compared to those of no skew. They observed that comparing the results of finite element analysis with those of the Standard Specifications (AASHTO 1996), the load distribution decreases by 24% and 26.5% for exterior and interior girders respectively, for a skew angle of $60^o$, but for skew angles less than $30^o$ this reduction is insignificant (with the Standard Specifications always conservative). They further observed that for all the girders, the effect of skew angle on the load distribution factor decreases when span length increases. According to the findings of Barr et al. (2001), generally interior girders were more affected by skew than were exterior girders.

#### *2.5.4.4 Effect of Lifts*

According to Barr et al. (2001), the lift slightly increases the composite girder stiffness and at the same time, it significantly increases the transverse bending stiffness of the deck by adding to the effective depth of the deck slab. This change makes the live load distribution more uniform and a lower live load distribution factor due to increased transverse to longitudinal stiffness, especially at the higher skew angles. In their

investigation of the effects of lifts they found that the addition of lifts reduced the distribution factors by 17% for exterior girders and 11% for interior girders.

#### *2.5.4.5 Effect of Continuity*

Barr et al. (2001) found that in their model the exterior girders in a continuous span model faced higher distribution factors as compared to simply supported model and their findings complement the results by Zokaie et al. (1991). They further maintained that continuity decreased the distribution factor for a low skew angle and increased the distribution factor only for skews greater than $40^{o}$.

#### *2.5.4.6 Effect of Miscellaneous Other Parameters*

Barr et al. (2001) observed that the type of a particular loading does affect the distribution of load, as the lane load distribution factor was found by the to be 10% lower than the truck load distribution. They further referred to the findings of Stanton (1992) that the uniform loads are better distributed among adjacent members in precast concrete floors than are concentrated loads.

## 2.6 DEBONDING OF PRESTRESSING STRANDS

### 2.6.1 General Background

The purpose of the partial debonding of the strands, also known as blanketing or jacketing, is to decrease the applied prestressing force to the end regions of the beam by preventing bond between some of the strands and the concrete. Debonding is used to control the excessive tensile stresses that occur in the top fibers of the end regions of the

beam due to large amount of prestressing force in the bottom flange, immediately after the transfer of prestress and before the application of externally applied loads. Debonding is an alternative to harping of strands where the stresses in the extreme fiber at the end regions are brought within allowable limits by varying the strand eccentricity at the ends of the beam. Harping of strands can be dangerous to workers, relatively expensive, and difficult to achieve, especially in the case of a beam with inclined webs such as Texas U-beams.

The adequate anchorage of reinforcement is crucial to the integrity of all reinforced and prestressed concrete structures. The anchorage behavior of fully bonded strands can be significantly different than that of partially debonded strands. Based on past experimental research studies, the LRFD and the Standard Specifications (AASHTO 2004, 2002) and TxDOT Bridge Design Manual (TxDOT 2001) have recommended different guidelines regarding debonding of strands.

The Standard Specifications (AASHTO 2002) require doubling the development length when the strands are partially debonded. The LRFD Specifications, among other restrictions related to strand debonding, limit the debonding percentage of strands to 40% per row and 25% per section. When these LRFD Specifications are compared to the limits of 75% per row per section in TxDOT Bridge Design Manual (TxDOT 2001), they can be very restrictive and can seriously limit the span capability. The reason for such a restrictive debonding percentages is stated in the LRFD C 5.11.4.3 as the reduction in shear capacity of a beam section due to reduction in horizontal prestressing force and increase in the requirement of development length when strands are debonded.

### 2.6.2 Debonding Requirements

The provisions of the Standard and LRFD Specifications (AASHTO 2002, 2004) and TxDOT Bridge Design Manual are discussed in the following.

#### *2.6.2.1 Debonding Percentage Limit*

The Standard Specifications do not give any limit on the debonding percentage. The LRFD Specifications in Article 5.11.4.3 limit the debonding percentage of strands to 40% per horizontal row and 25% per section. Debonding termination is allowed at any section, if and only if, it is done for less than 40% of the total debonded strands or 4 strands, whichever is greater. The LRFD Specifications in Commentary 5.11.4.3, however, allow the consideration of successful past practices regarding debonding and further instruct to perform a thorough investigation of shear resistance of the sections in the debonded regions. The LRFD Specifications refer to the conclusions drawn in research by Shahawy et al. (1993) and Shahawy and Batchelor (1992) that shear resistance is primarily influenced by the anchored strength of the strands in the end zones of the prestressed concrete beams. The TxDOT Bridge Design Manual allows the debonding of strands as long as it satisfy the limit of 75% per row per section.

#### *2.6.2.2 Debonding Length*

The Standard Specifications do not specify any limit on the allowable debonding length of the debonded strands. The LRFD Specifications allow the strands to be debonded to any length as long as the total resistance developed at any section satisfies all the limit states. The TxDOT Bridge Design Manual specifies the maximum of debonding length as the lesser of the following:

1. Half-span length minus the maximum development length as specified in the Standard Specifications (AASHTO 1996) Art. 9.28.
2. 0.2 times the span length, or
3. 15 ft.

### *2.6.2.3 Development Length for Debonded Strands*

The Standard Specifications in Art. 9.28.3 require the development length, calculated by the Eq. 2.21, to be doubled when tension at service load is allowed in the precompressed tensile zone for the region where one or more strands are debonded. The $\left(f_{pe}/3\right)d_b$ is the transfer length and $\left(f_{ps}-f_{pe}\right)d_b$ is the flexural bond length.

$$l_d=\left(f_{ps}-\frac{2}{3}f_{pe}\right)d_b=\left(\frac{f_{pe}}{3}\right)d_b+\left(f_{ps}-f_{pe}\right)d_b \tag{2.17}$$

The LRFD Specifications mention a general expression of development length in Art. 5.11.4.2 for bonded and debonded strands which is given as follows

$$l_d\geq\kappa\left(f_{ps}-\frac{2}{3}f_{pe}\right)d_b \tag{2.18}$$

where:

$l_d$ = Development length, in.
$d_b$ = Strand diameter, in.
$\kappa$ = 1.6 for bonded strands and 2.0 for debonded strands in cases where tension exists in the precompressed tensile zones, ksi
$f_{pe}$ = Effective prestress prior to the application of the load, ksi
$f_{ps}$ = Average stress in prestressed strands at the time for which the nominal resistance of the member is required, ksi

### *2.6.2.4 Transfer Length*

The Standard Specifications recommend a transfer length of $0.5d_b$, while the LRFD Specifications recommend a transfer length of $0.6d_b$ in Art. 9.20.2.4 and Art. 5.11.4.1, respectively.

### 2.6.3 Research on Debonding

#### *2.6.3.1 General*

Almost all the research studies, regarding the comparison of behavior of beams with debonded strands to those beams with fully bonded strands, also study the transfer and development length. In the following, only those results of various research studies are summarized which are related to the effect of debonding of strands in prestressed beams with special emphasis on the past researches that considered the effect of debonding on the shear capacity of the beam.

#### *2.6.3.2 Barnes, Burns and Kreger (1999)*

The objective of the research was to measure the development and transfer length for 0.6 in. diameter prestressing strands, placed with center to center spacing of 2 in. More specifically, this study was conducted to study the effect of concrete strength, surface conditions of the strands, and debonding of strands on the anchorage behavior of pretensioned concrete flexural members.

A total of 36 AASHTO TYPE I (TxDOT Type A) I-beams were tested. These beams were designed to satisfy ACI 318-99 and the Standard Specifications (AASHTO 1996) allowable stress limits and to represent the worst case behavior by achieving the ultimate strand elongation values of at least 3.5 percent. A cast-in-place deck slab was added to the beams to provide a large compressive top flange and its size was determined by strain compatibility analysis so as to ensure the total elongation of 3.5 percent in the bottom row of strands at flexural failure. Beams of span lengths 40 ft. were used for fully bonded strands series and beams of span lengths of 54 ft. were used for debonded strands series. Concrete with final strength ranging from 5 to 15 ksi and initial strength ranging from 4 to 9 ksi was used in the beams. Strands were debonded

with percentages of 50%, 60% and 75%. The debonding patterns were selected with a purpose of violating several of the LRFD Art. 5.11.4.3 (AASHTO 1998). For example, all the specimens were debonded with percentages exceeding 25% per section and 40% per row limit, in a few specimens the debonded strands were not symmetrically distributed, and in several specimens the exterior strands in horizontal rows were debonded. The shear reinforcement was provided on the basis of conservative estimate of expected shear force which was in excess of TxDOT standard design practice for AASHTO Type I beams. The shear reinforcement provided satisfied the provisions of the LRFD and the Standard Specifications (1998, 1996).

The results of experiments, performed to evaluate the strand transfer length, showed that the use of staggered debonding of strands can effectively reduce the intensity of concrete stresses in the end regions of beams. The experiments, performed to evaluate the development length required to prevent the general bond slip failure, showed that development length shows an increasing trend with increasing number of debonded strands and the debonding length. The location of the transfer length in relation to the load effects is influenced by the debonded length of the strands. Moreover, the cracking resistance of each transfer length region was determined by the amount and configuration of debonding. It was observed by the researchers that the presence and opening of a crack within or closer to the transfer length of strands than approximately $20d_b$ initiated the general bond slip in every group of strands in the debonded specimens. When the cracks are prevented to occur within the transfer length or adjacent to the transfer length and the strands are embedded for a length greater than or equal to the development length of fully bonded strands, no general bond slip should occur and this observation is true for the cases where 75% of strands were debonded. The researchers concluded, “Up to 75% of strands may be debonded as long as cracking is prevented in or near the transfer length and the ACI and the AASHTO (1998) rules for terminating the tensile reinforcement are applied to the bonded length of prestressing strands”.

All the specimen failed in pure flexural, flexural with slip and bond failure mechanisms. The influence of horizontal web reinforcement was explored to a very limited extent as a part of this study. Where present, the horizontal web reinforcement slightly improved the performance and reduced the crack width. The authors concluded that due to the presence of excess shear reinforcement, the specimens could not exhibit premature shear failure due to loss of bond and the horizontal reinforcement did not get a chance to yield significant improvements in strength.

#### *2.6.3.3 Shahawy et al. (1993)*

The main objective of this study was to develop design formulas for transfer and development length. However, it was intended to establish the shear design criteria so that optimal use of web shear reinforcement and debonding of strands can be assured for prestressed concrete beams. Moreover, it was also intended to study the effects of debonding of prestressing strands on the shear strength of beams, to evaluate the effect of prestressed compressive action on the overall behavior of the beams and to determine the minimum fatigue load below which fatigue need not be considered.

The experimental program was performed with 33 AASHTO Type II prestressed concrete girders. The primary variables considered for the scope of this study were debonding percentage, web shear reinforcement ratio, beam end details and size of the strands. The initial length, initial ultimate flexural strength, initial concrete compressive strength at transfer and 28 day final concrete compressive strength of all the girders was constant at 41 ft., 2100 kip-ft., 4 ksi, and 6 ksi respectively. This study considered 270 ksi, low relaxation strands with diameters of 0.5 in. and 0.5 in. special with maximum debonding length of 5.5 ft., and strands with 0.6 in. diameters with maximum debonding length of 4.5 ft. The choice of debonding percentages was limited to zero, 25% or 50%. The amount of shear reinforcement varied from minimum shear reinforcement required to the three times of what is required by the Standard Specifications (AASHTO 1992)

for the design dead and live loads. The results of the part of the study related to the debonding of strands were also published in PCI Journal (Shahawy et al. 1992).

All the girders tested in this program, failed beyond their ultimate design moment, $M_u$, and ultimate shear, $V_u$, with the exception of the girders that were under-designed for shear (ranging from zero to half of the nominal shear capacity required by the AASHTO Standard Specifications, 1992). The researchers did not make any recommendation regarding the limits for critical percentage of debonding. Only four of the specimens with strand diameter of 0.6 in., that have 25 percent and 50 percent debonded strands, and where the nominal shear reinforcement was provided as per the Standard Specifications (AASHTO 1992) underwent shear and bond failure.

#### *2.6.3.4 Abdalla, Ramirez and Lee (1993)*

The main objective of this experimental research was to study and compare the flexural and shear behavior of simply supported pretensioned beams with debonded and fully bonded strands. Adequacy of strand anchorage, and ACI (1989) and AASHTO (1992) provisions regarding development length of prestressing strands were also investigated.

Five specimen sets consisting of two beams each, one beam with strands debonded and other one with fully bonded strands, were tested to failure under a single monotonic concentrated load. Four specimen sets consisted of AASHTO Type I girders and one of the specimen consisted of Indiana State Type box girders. All the beams were casted with a deck slab on top. Except for one of the beam specimen set, which had the span length of 24 ft., all the beams had 17.5 ft. span. This experiment considered both stress-relieved and low relaxation Grade 270, uncoated seven-wire 0.5 in. diameter strands. The final and initial concrete compressive strength for the beam was 6000 and 4000 psi, respectively. Non-prestressed reinforcement, used in the beams and deck slab, consisted of standard deformed Grade 60 #6 bars, while the stirrup reinforcement consisted of deformed Grade 60 #3 double legged bars spaced at 4 in. center to center.

All the debonding scheme was symmetrical with exterior strand on each side of every specimen always debonded except for the box beam. Debonding percentages were either 50% or 67% and it was ensured that debonded strands lie in a region where shear failure was likely to occur. It is also mentioned that all the beams were designed to ensure that shear failure would not occur. Therefore, none of the beams reached the predicted shear capacity.

It was concluded that based on ACI/AASHTO debonding of strands reduces the flexure-shear cracking capacity of the pretentioned beams when compared with those beams with fully bonded strands only. Though the failure loads were lower in the beams with debonded strands as compared to failure loads of beams with fully bonded strands, yet the deflections were relatively larger in the beams with debonded strands. Moreover, it was observed that flexure-shear cracking occurred at the debonding points. The researchers concluded that by increasing the debonding percentage, the degree of conservatism reduced, so the recommendation was made to limit the debonding to 67% of the strands in a section while the limit on debonding percentage of strands in a row was not considered necessary and staggering of the debonding was recommended to reduce the stress concentration.

#### *2.6.3.5 Bruce W. Russell and Ned H. Burns (1993)*

This research project has two specific objectives: 1) to determine the transfer length and the development length of both 0.5 in. and 0.6 in. prestressing strands and 2) to develop design guidelines for the use of debonded strands in pretensioned concrete.

Altogether, 10 tests were performed on 6 specimens. Each beam contained eight 0.5 in. strands four of which were debonded. Four beams were 40 ft. in length with the debonded length equal to 78 in. The other two beams were 27 ft.–6 in. in length with a debonded length equal to 36 in. All of the beams possessed identical cross sections similar to AASHTO I-beams. Shear reinforcement was spaced at 6 in. for all specimens without any variation. No special confining steel or anchorage details were provided on

the debonded strands. Debonding of strands was symmetrically distributed in the cross section with debonding percentages of 50% or lesser when the strand cut off was staggered.

The variables considered in the study were 1) the length of debonding as either 36 in. or 78 in., 2) type of debonding cutoff as either staggered or concurrent, and 3) embedment length as either 84 in. or 150 in. Debonded lengths were selected in order to test embedment lengths between 1.0 and 2.0 times the basic development length given in AASHTO equation 9-32. The embedment lengths were chosen for each test so that the results from the complete test series would span the probable failure modes. It is noteworthy that percentage of debonding and shear reinforcement is not considered as a variable.

In all the tests it was clearly shown that cracking was the primary source of bond or anchorage failure, not vice versa. The entire test program was aimed at validating the prediction model which states, “If cracks propagate through the anchorage zone of a strand, or immediately next to the transfer zone, then failure of the strand anchorage is imminent”. This prediction model successfully corroborated test results for pretensioned beams with debonded strands as well as beams where all of the strands are fully bonded to the end of the member. Some exceptions to this model have been noticed, where the strands have slipped very small distances prior to flexural failure, without anchorage failure. The tests have shown that beams with staggered debonding performed better than beams with concurrent debonding.

The recommendations related to debonded strands are summarized here. Debonded strands should be staggered. Termination points should be evenly distributed throughout the debond/transfer zone. Debonding should be terminated as gravity moments reduce stresses from pretensioning to within the allowable stresses. No more than 33% of the strands should be debonded and at least 6% of the total prestressing force should be included in the top flange of the pretensioned beam. It was found that by using two top strands into the design of pretensioned girders, the number and the length of debonded strands can be significantly reduced. It was concluded that the flexural and

web-shear cracking in the transfer zone region caused the slip of debonded strands and consequently, the bond failure. Whereas, the bond failure did not take place where there was no crack in the debond/transfer zone region.

#### *2.6.3.6 D. Krishnamurthy (1971)*

The primary objective of this study was to investigate the effect of debonding of strands on the shear behavior of pretensioned concrete I-beams. All the beams were 2.9 meters long with effective span length (i.e. the distance between the supports) of 2.75 meters and loaded with two point loading and had constant shear span of 0.5 meters. The debonding length was also constant at 0.6 meters. Moreover, prestressing force at the mid-section of beams, shear span to depth ratio and the concrete strength were kept constant for all the specimens.

All the beams tested failed in shear with a diagonal crack developing in the shear span region and the failure was quite sudden without any warning. It was observed that shear resistance of the section increased by increasing the number of debonded strands in the upper flange and it decreased when the number of debonded strands was increased in the bottom flange of the beam. Debonding percentages used in different specimens were selected to as 25%, 50% per row and 12.5%, 25%, 37.5%, 50% per section. In all the beams where debonding of strands was employed, the diagonal crack initiated at the support and extended to quite near the load point and the horizontal distance between the support and the load point is the shear span. No recommendation was made for the allowable debonding percentages.

#### *2.6.3.7 Summary*

Krishnamurthy (1971) observed that shear resistance of the section increased by increasing the number of debonded strands in the upper flange and it decreased when the number of debonded strands was increased in the bottom flange of the beam. All the aforementioned studies in this section recommended the use of staggered debonded strand pattern and confirmed the fact that the beam can fail due to loss of anchorage, before reaching its ultimate capacities, if the cracks propagate through the transfer length region. Abadalla et al. (1993) recommended to debond the strands to no more than 67%, while Barnes et al. (1999) recommended 75% of strands can be debonded provided the cracks are prevented to propagate through the transfer length region and the AASHTO (1998) rules for terminating the tensile reinforcement are followed. The study by Shahawy et al. (1993) showed that some beam specimens, where strand debonding was done, did fail in shear.

Based on input from TxDOT engineers, it became evident that the TxDOT Bridge Design Manual (TxDOT 2001) limits of maximum percentage of debonded strands and maximum debonded length were developed by Leroy Crawford and Mary Rou Ralls, when box beams were being added to PSTRS14.

## 2.7 REFINED ANALYSIS

### 2.7.1 General

Bridge superstructure analysis is the fundamental step in the design process of any bridge structure. Generally, a bridge superstructure is structurally continuous in two dimensions of the plane of the deck slab and the resulting distribution of the applied load into shear, flexural and torsional stresses in two dimensions is considerably more complex as compared to those in one-dimensional continuous beams. A close form

solution of the mathematical model, that describes the structural behavior of a bridge superstructure, is seldom possible. Several approximate methods of analysis have evolved. Depending upon the objectives of analysis, several simplified or refined analysis procedures such as grillage analogy, finite strip, orthotropic plate, folded plate, finite difference, finite element, and series or harmonic methods have been used to analyze the bridge superstructures subjected to various loading conditions. The LRFD Specifications (AASHTO 2004) explicitly allow the use of aforementioned analysis methods and all those methods which satisfy the requirements of equilibrium, and compatibility, and utilize constitutive relationships for the structural materials.

Transverse distribution of the vehicular live load to individual bridge girders has been studied for many years. The AASHTO LRFD Specifications provide simplified live load distribution factor formulas, which were developed by Zokaie et al. (1991) based on more detailed analysis methods such as grillage analogy and finite element method. Puckett (2001) analyzed all of the 352 bridges in the original bridge database, used by Zokaie et al. (1991), by finite strip method and validated the accuracy of these formulas for interior beams. Several other research endeavors have independently studied the validity and accuracy of the AASHTO LRFD simplified live load distribution factor formulas and in general, all of them have used either finite element method or grillage analogy method towards that objective. In this section, the application of grillage analogy and finite element method are reviewed in the context of lateral distribution of vehicular live loads.

### 2.7.2 Grillage Analogy Method

Before the advent of finite element analysis method, perhaps, the grillage analogy method has been the most popular method for bridge deck analysis because it is easily comprehensible, computationally efficient and produces reliably accurate results. According to Hambly and Pennells (1975) and Hambly (1991), the grillage analogy method has been applied to several types of slab bridges (e.g. composite voided and

composite solid, solid and voided), slab-on-girder and box girder bridges (e.g. twin cell, multiple cell with vertical and sloping webs, spread box), and moreover, skew, curvature, continuity, edge stiffening, deep haunches over supports, isolated supports and varying section properties can also be modeled without difficulty (Hambly and Pennells 1975, Jaeger and Bakht 1982).

The grillage analogy is a simplified analysis procedure in which the bridge superstructure system is represented by transverse and longitudinal grid members and the longitudinal and transverse force systems interact at the nodal points. The bending and torsional stiffness characteristics of the bridge superstructure are distributed uniformly among the grillage members. The longitudinal stiffnesses are distributed to the members in longitudinal direction and transverse stiffnesses are distributed to the members in the transverse direction. Hambly (1991) puts the fundamental principle of grillage analogy method very concisely as:

> Ideally the beam stiffnesses should be such that when prototype slab [bridge] and equivalent grillage are subjected to identical loads, the two structures should deflect identically and the moments, shear forces and torsions in any grillage beam should equal the resultants of stresses on the cross-section of the part of the slab [bridge] the beam represents.

The closeness of the response of analytical grillage model to that of actual structure depends upon the degree of appreciation of the structural behavior exercised by the design engineer. Although there are no fixed rules to determine the appropriate arrangement and cross sectional properties, and support conditions of the grillage members, yet based on the past experience, successful implementation and engineering judgment many researchers have given valuable guidelines for the application of grillage analogy method to different bridge types. Among those Hambly (1991), Bakht and Jaeger (1985), O'Brien and Keogh (1999), Cusens and Pama (1975), Hambly and Pennells (1975), Cheung et al. (1982), Jaeger and Bakht (1982) and Zokaie et al. (1991)

are worth mentioning. More recently, Song et al. (2003), Schwarz et al. (2001), and Aswad (1994) successfully used grillage analogy method for analysis of prestressed concrete girder bridges. In particular, Schwarz et al. (2001) has compared the response results from grillage analogy model to those of experimental evaluation of a number of bridges and concluded that the numerical grillage model prediction of transverse distribution of live loads closely agree with those of experimentally measured results of actual bridges.

Generally, a cellular bridge deck is continuous in three dimensions and is characterized by smooth progression of the stresses along the length, breadth and thickness of the entire superstructure. On the contrary, the stresses in the grillage tend to change abruptly and are centered on the nodal locations as is shown in Figure 2.3. A particular response force systems develops in a box girder bridge under the action of applied loads. This force system, as shown in Figure 2.4, includes (b) longitudinal bending stresses and longitudinal bending shear flow, (c) transverse bending stresses, (d) torsional stresses and (e) distortional action due to interaction of torsion and transverse shear. Grillage modeling of a cellular bridge decks can be done by shear flexible grillage. In shear flexible grillage the transverse members are given a reduced shear area, so that they can experience a shear distortion equal to the actual transverse distortion of the cells in the bridge deck. It is very crucial to incorporate the effects of shear lag, actual position of neutral axis, equivalent shear area, and bending and torsional stiffnesses. Due to high level of interaction between bending and torsion at the skew supports, the torsional stiffness should be carefully calculated. Eby et al. (1973) discuss comprehensively, various theoretical and approximate approaches to evaluate the St. Venant's torsional stiffness constant for the non-circular cross sections. The poisson effect is not so significant and is generally neglected in a grillage analysis but it can be included when desired (Jaeger and Bakht 1982). These guidelines and the grillage modeling approach followed in this research study are covered in detail in Section 5.

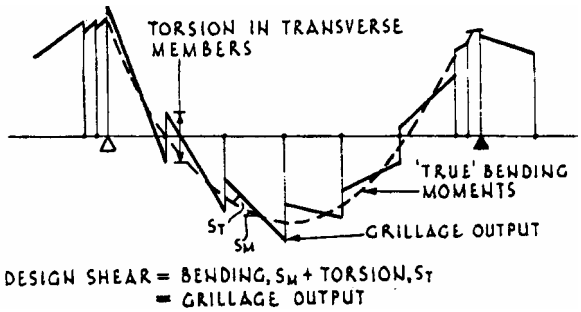


**Figure 2.3 Grillage Bending Moment Diagram for Longitudinal Member (Hambly and Pennells 1975).**

Zokaie et al. (1991) summarized the advantages of grillage analogy method in comparison to other simplified methods of analysis in their final comment as:

> Also grillage analysis presents a good alternative to other simplified bridge deck analysis methods, and will generally produce more accurate results. Grillage analogy may be used to model most common bridge types and each bridge type requires special modeling techniques. Guidelines for modeling these bridge types along with sample problems illustrating their application are given in Appendix G. A major advantage of plane grid analysis is that shear and moment values for girders are directly obtained and integration of stresses is not needed. Loads normally need to be applied at nodal points, and it is recommended that simple beam distribution be used to distribute wheel loads to individual nodes. If the model is generated according to Appendix G recommendations and the loads are placed in their correct locations, the results will be close to those of detailed finite element analysis.

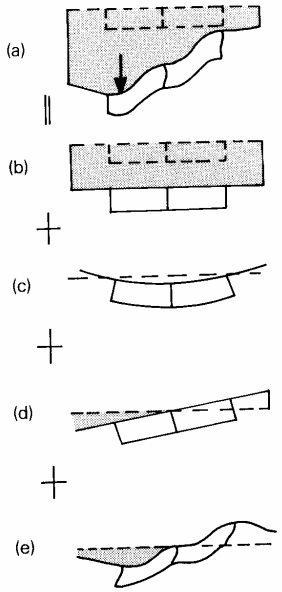


**Figure 2.4 Principle Modes of Deformation (a)Total, (b) Longitudinal Bending, (c) Transverse Bending, (d) Torsion, (e) Distortion (Hambly 1991).**

### 2.7.3 Finite Element Analysis

Finite element method (FEM) is the most versatile analysis technique available at present in which a complicated structure is analyzed by dividing the continuum into a number of small finite elements, which are connected at discrete nodal joints. This method of analysis is relatively computationally expensive, requires greater analysis time, and modeling and post processing of output data is often times very cumbersome. Adequate theoretical and working knowledge of FEM and classical structural mechanics is a pre-requisite for any sound finite element analysis. Finite element analysis has been used in many research studies to evaluate the live load distribution characteristics of all types of bridge superstructures. Zokaie et al. (1991), Schwarz et al. (2001), Barr et al. (2001), Khaloo and Mirzabozorg (2003), Chen and Aswad (1996), and Eamon and Nowak (2002) have evaluated the load distribution characteristics of prestressed I-girder bridge superstructures. Song et al. (2004) have used FEM to calibrate the grillage analogy model. Chen et al. (1996) has applied FEM to analyze the spread box girder

bridges. While Zokaie et al. (1991) has analyzed multicellular and spread box girder bridges with FEM. General guidelines for the application of FEM to the analysis of bridge superstructures have been recommended by the LRFD Specifications (AASHTO 2004) and several research studies in the past. Those guidelines and other relevant information is summarized in the following paragraphs.

#### *2.7.3.1 Type of Analysis*

Almost all the research studies analyzed the prestressed bridge superstructures by linear and elastic analysis (i.e. small deflection theory and elastic and homogeneous material). Eamon and Nowak (2002) applied the FEM to analyze the structure in both elastic and inelastic range.

#### *2.7.3.2 Element Aspect Ratio*

The LRFD Specification allow the maximum aspect ratio of 5.0 for finite element analysis. Chen et al. (1996) and Barr et al. (2001) have maintained the ratio of length to width of shell elements at 2 or lesser.

#### *2.7.3.3 Mesh Refinement*

Eamon and Nowak (2002) have used a simplified and a detailed FEM model in their study. The simplified model contained 2,900 to 9,300 nodes, 1,700 to 6,200 elements, and 8,500 to 30,000 degrees of freedom. While the detailed FEM model contained 20,000 to 39,000 nodes, 12,000 to 22,000 elements, and 62,000 to 120,000 degrees of freedom. Barr et al. (2001) used 6,000 nodes to model the deck slab and the entire model comprised of 12,000 nodes. It is of particular interest that Eamon and

Nowak (2002) had a finer mesh at the midspan region as compared to the quarter or end span regions.

#### *2.7.3.4 Selection of Element Type*

**Plate or Shell Elements**

Zokaie et al. (1991) has used eight node quadrilateral plate elements, with four integration points to model the spread box prestressed girder bridges. They further recommended for the plate elements to have at least five degrees of freedom (DOF) per node (i.e. 3 displacements and two in-plane bending rotations). The quadratic element shape functions were used to accurately model the parabolic variation of the shear stressed in the girder web. According to O'Brien and Keogh (1999), the transverse distortional behavior that makes cellular bridge decks different from other forms and this distortional behavior is affected by deck depth, the stiffness of individual webs and flanges (i.e. slenderness ratio) and the extent of transverse bracing (i.e. diaphragms) to the cells. They further assert that the use of the plate element will not only allow modeling the distortional action, but also it takes into account the varying neutral axis depth (if not properly accounted for, neutral axis depth varies when bridge girders are modeled with beam finite elements or in the grillage analogy model).

Hambly (1991) recommends that a three dimensional plate model of a cellular bridge deck must have six DOF at each node (i.e. 3 displacements, 2 in-plane bending rotations, and 1 out-of-plane bending rotations). A comment of particular interest in relation to the use of plate elements made by Hambly (1991) is.

> At every intersection of plates lying in different planes there is an interaction between the in-plane forces of one plate and the out-of-plane forces of the other, and vice versa. For this reason it is essential to use finite element which can distort under plane stress as well as plate bending.

Barr et al. (2001) use shell element to model the deck slab, diaphragms and the haunch. Chen and Aswad (1996) use the shell element to model the deck slab. Khaloo and Mirzabozorg (2003) use 4 noded shell element with 6 DOF per node.

**Beam Elements**

A beam element is a typical 3D line element with six DOF per node. Beam elements are used to model diaphragms, bridge girders (such as I-sections or box sections), and rigid links (used to model the eccentricity of girder centroid to deck slab centroid). Eamon and Nowak (2002) and Khaloo and Mirzobozorg (2003) have used beam elements to model girder and diaphragms in their simplified finite element model. Chen and Aswad (1996), Zokaie et al (1991) and Barr et al. (2001) used beam elements to model the bridge girders and rigid links.

**Solid Elements**

Hambly (1991) notes that solid elements are seldom used to model the bridge decks because generally these structures correspond to the thin plate behavior. Eamon and Nowak (2002) demonstrated successful implementation of a eight node hexahedron solid element, with three DOF (i.e. 3 displacements) at each node, to model a prestressed I girder bridge. These solid elements were used to model the deck slab, and girder webs and flanges in their detailed finite element model. It is also worth noting that the mesh density was finer than that used on their simplified model.

#### *2.7.3.5 Relative Mutual Eccentricity of Beam and Deck Slab*

The LRFD Specifications (AASHTO 2004) recommend maintaining the relative vertical distances between the elements representing beam and slab of the actual bridge. The LRFD Specifications also allow to place the longitudinal or transverse beam elements at the mid-thickness of plate elements, only when the equivalent element properties account for the eccentricity. Eamon and Nowak (2002) have demonstrated

that using the equivalent element properties method to account for the girder slab eccentricity also yields acceptable results. Chen and Aswad (1996), Barr et al. (2001), Zokaie (2000) and Khaloo and Mirzabozorg (2003) have represented the eccentricity by using rigid link elements (beam elements with very high stiffness).

#### *2.7.3.6 Post-Processing of Results*

The finite element methods almost always outputs results in the form of stresses at the integration points. Zokaie et al. (1991) caution about any program showing the stresses at the nodes because those stresses at the nodal locations are produced by some form of extrapolation and that the extrapolated results can be unreliable and the results should only be used with extreme care. They recommend that the stress output at the integration points should be integrated over the plate width to obtain the force results. Further details of calculating the bending moment and shear forces for a bridge girder can be found in their report. Chen and Aswad (1996) discuss a simplified method to calculate the composite girder moments by using the moment formula from simple beam theory as given below in Eq. 2.19.

$$M_c = S_{bc} f_b \tag{2.19}$$

where:

$M_c$ = Composite Girder Moment, k-ft.
$S_{bc}$ = Composite section modulus at the bottom fiber, in.$^3$
$f_b$ = Stress at the centerline of the bottom girder flange, ksi

# 3. DESCRIPTION OF PARAMETRIC STUDY AND ANALYSIS PROCEDURES

## 3.1 GENERAL

A parametric study was conducted as a part of this research project to evaluate the impact of the LRFD Specifications (AASHTO 2004) on the design of typical Texas bridges. The main objective of the parametric study was to carry out the design process according to the LRFD and Standard Specifications and compare their results with respect to the effects of various combinations of span length, girder spacing, strand diameter, and skew angle. The primary focus of the study was to evaluate the service and ultimate strength limit states. While the ultimate limit state is evaluated for both shear and flexure, the service limit state is evaluated for flexure and deflection. In general, all the limits states and load combinations are considered applicable to the design of typical bridge structures in the state of Texas as prescribed by both specifications. The exception is the extreme event limit state in the LRFD Specifications, because extreme events like ice pressure do not occur in Texas, TxDOT does not design for earthquakes, and stream current rarely controls the design (TxDOT 2001). Moreover, wind load or loads due to vehicle collision were not considered in this study. The subtasks that were performed for the parametric study are as follows.

1. Develop a MatLAB program to automate the iterative analysis and design process.
2. To ensure that the entire design process is error free, the spreadsheet solution is verified against the hand calculated detailed design examples and the TxDOT design software PSTRS14 (TxDOT 2004).
3. Define the analysis and design assumptions.
4. Define the design variables for the parametric study.

5. Perform the parametric study for the entire range and different combinations of the aforementioned design variables.
6. Compile the results in graphical and tabular format so that designs using the LRFD and Standard Specifications can be compared.

This section describes the typical bridge geometry and girder cross-section considered, design variables and design parameters, analysis and design assumptions and methodology, and the detailed design examples.

## 3.2 BRIDGE GEOMETRY AND GIRDER SECTION

A typical bridge cross-section is shown in Figure 3.1. The scope of this study is restricted to precast, prestressed Texas U54 beam bridges as the longitudinal structural members. A T501 traffic barrier is used as recommended in the Standard Drawings prepared by the TxDOT Bridge Design Manual (TxDOT 2001). Although the actual bottom width of a T501 rail is 1 ft. 5 in., the nominal face of the rail is selected to be 1 ft. per TxDOT's recommendation. The asphalt wearing surface is considered to be 1.5 in. thick.

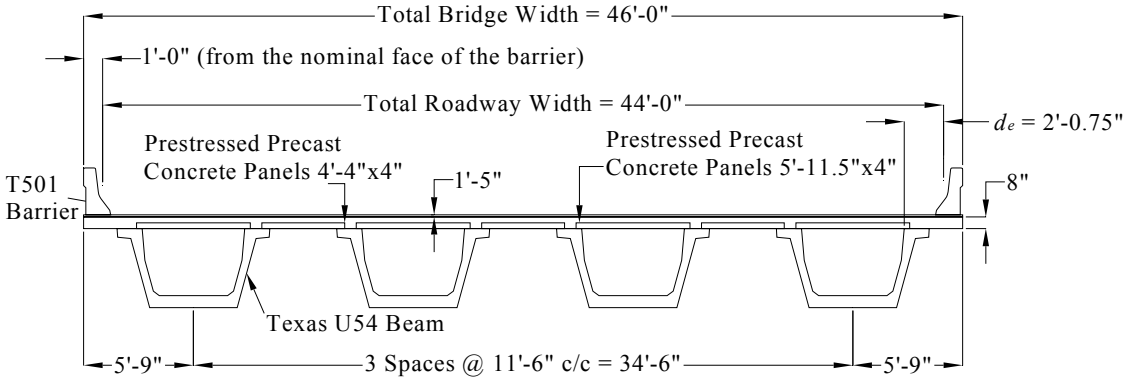


**Figure 3.1 Typical Girder Bridge Cross Section.**

The development of the precast, prestressed Texas U beam, which is an open-top trapezoidal section, began in the late 1980s (Ralls 1993). The main purpose of

developing U beams was not to replace the widely used AASHTO Type IV and Texas Type C beams, but, rather to provide an aesthetically pleasing, efficient cross-section that is economically more viable with ease of construction (TxDOT 2001). Two U beam sections, U40 and U54, were developed for use as prestressed concrete bridge girders, where 40 and 54 signify the non-composite depth in inches of the two girders respectively. Figure 3.2 shows the U54 beam cross-section and a pre-determined pattern for the arrangement of strands. The major section dimensions are outlined in Table 3.1. According to Appendix A in the TxDOT Bridge Design Manual (TxDOT 2001), for a normal strength concrete, 0.5 in. strand diameter, and miscellaneous other design constraints as mentioned in the manual, a maximum span length of 130 ft. is achievable for a maximum girder spacing of 9.75 ft. for Texas U54 beam bridges.

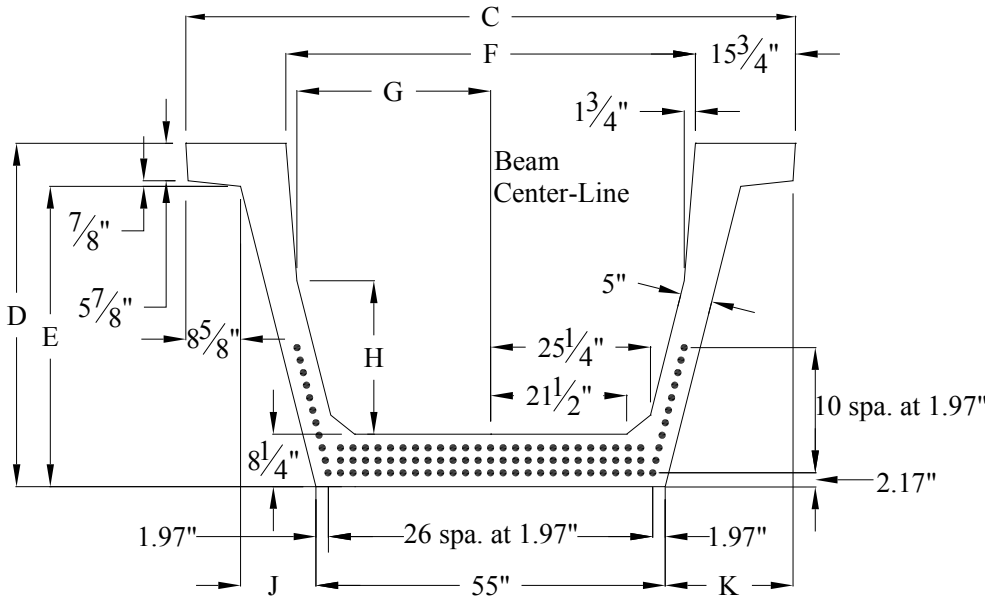


**Figure 3.2 Typical Section Geometry and Strand Pattern of Texas U54 Beam (Adapted from TxDOT 2001).**

**Table 3.1 Section Properties of Texas U54 Beams (Adapted from TxDOT 2001)**

| C | D | E | F | G | H | J | K | $Y_t$ | $Y_b$ | Area | $I$ | Weight |
|---|---|---|---|---|---|---|---|---|---|---|---|---|
| in. | in. | in. | in. | in. | in. | in. | in. | in. | in. | $in.^2$ | $in.^4$ | plf |
| 96 | 54 | 47.25 | 64.5 | 30.5 | 24.125 | 11.875 | 20.5 | 31.58 | 22.36 | 1120 | 403,020 | 1,167 |

## 3.3 DESIGN PARAMETERS

The selected design variables for the overall parametric study of Texas U54 beam bridges are shown in Table 3.2. Various design parameters that were kept constant for a particular specification are outlined in Table 3.3. The values of relative humidity and asphalt wearing surface thickness are based on suggestions from TxDOT engineers and are considered to be appropriate for the state of Texas.

**Table 3.2 Proposed Parameters for Parametric Study**

| **Parameter** | **Description / Selected Values** |
|---|---|
| Design Codes | AASHTO Standard Specifications, 17th Edition (2002)<br>AASHTO LRFD Specifications, 3rd Edition (2004) |
| Girder Spacing (ft.) | 8'-6", 10'-0", 11'-6", 14'-0" and 16'-8" |
| Spans | 90 ft. to maximum span at 10 ft. intervals |
| Strand Diameter (in.) | 0.5 and 0.6 |
| Concrete Strength at Release, $f'_{ci}$ | varied from 4000 to 6750 psi for design with optimum number of strands |
| Concrete Strength at Service, $f'_c$ | varied from 5000 to 8500 psi for design with optimum number of strands<br>($f'_c$ may be increased up to 8750 psi for optimization on longer spans) |
| Skew Angle (degrees) | 0, 15, 30 and 60 |
| Total Bridge Width | For 10 ft. and 14 ft. spacings: 42 ft.<br>For 8.5 ft., 11.5 ft., 16.67 ft. spacings: 46 ft. |
| Humidity | 60% |

**Table 3.3 Additional Design Parameters**

| Category | Description | Proposed Value |
|---|---|---|
| Prestressing Strands | Ultimate Tensile Strength, $f_{pu}$ | 270 ksi – low relaxation |
| | Yield Strength, $f_{py}$ | $0.9 f_{pu}$ |
| | Stress limit before transfer, $f_{pi}$ | $f_{pi} \geq 0.75 f_{pu}$ |
| | Stress limit at service, $f_{pe}$ | $f_{pe} \geq 0.8 f_{py}$ (LRFD) |
| | Modulus of Elasticity, $E_p$ | 28500 ksi (LRFD)<br>28000 ksi (Standard) |
| Concrete-Precast | Unit weight, $w_c$ | 150 pcf |
| | Modulus of Elasticity, $E_{pc}$ | $33 w_c^{1.5} \sqrt{f_c'}$ ( $f_c'$ precast) |
| Concrete-CIP Deck Slab | Slab Thickness, $t_s$ | 8 in. |
| | Unit weight, $w_c$ | 150 pcf |
| | Modulus of Elasticity, $E_{cip}$ | $33\ w_c^{1.5}\ \sqrt{f'_c}$ ( $f_c'$ CIP Deck Slab) |
| | Specified Compressive Strength, $f_c'$ | 4000 psi |
| Other | Relative Humidity | 60% |
| | Non-Composite Dead Loads | 1.5 in. asphalt wearing surface $(w_{ws} = 140$ pcf$)$<br>Two interior diaphragms of 3 kips each, located at 10 ft. on either side of the beam midspan |
| | Composite Dead Loads | T501 type rails (326 plf) |
| | Debonding Length & Percentage | L ≤100 ft.: the lesser of 0.2 L or 15 ft.<br>100 ft. < L <120 ft.: 0.15 L<br>L ≥ 120 ft.: 18 ft.<br>No more than 75% of strands debonded per row per section |

Span lengths, as given in Table 3.2, are considered to be the distances between faces of the abutment backwalls or center-lines of the interior bents. Overall beam length is the actual end to end length of the beam, which is calculated by subtracting 6 in. from the total span length. Design span length is the center-to-center distance between between the bridge bearing pads which is calculated by subtracting 19 in. from the total span length. Beam end details are shown in the Figure 3.3.

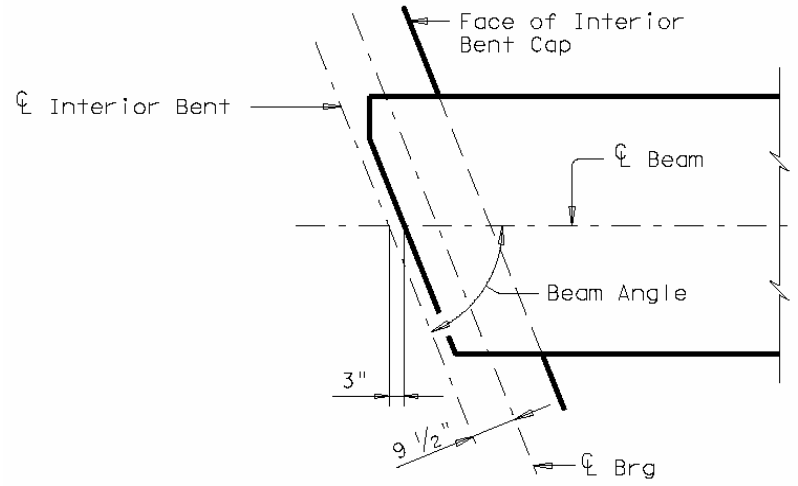


**Figure 3.3 Beam End Detail for Texas U54 Beams (TxDOT 2001).**

## 3.4 DETAILED DESIGN EXAMPLES

Two detailed design examples were developed to illustrate the application of the *AASHTO Standard Specifications for Highway Bridges,* 17th edition (2002) and *AASHTO LRFD Bridge Design Specifications,* 3rd edition (2004), for typical precast, pretensioned Texas U54 beam bridges. The purpose of these design examples is to show the differences in the two design specifications and to enable a more thorough comparison of LRFD versus Standard designs. Moreover, these detailed design examples are intended to serve as a reference guide for bridge design engineers to assist them in transitioning from the AASHTO Standard Specifications to the AASHTO LRFD Specifications. Complete detailed design examples are given in Appendix B.

The detailed design examples developed follow the same procedures for load and response calculations, prestress loss calculations, and limit state design as described in this section. Based on TxDOT's feedback, the following parameters were decided upon for these detailed design examples: span length = 110 ft., girder spacing = 11 ft. 6 in., strand diameter = 0.5 in., deck thickness = 8 in., wearing surface thickness = 1.5 in.,

skew = $0^{o}$ and relative humidity = 60 %. The cross section of the bridge used to develop detailed design examples is shown in Fig 3.1.

## 3.5 VERIFICATION OF DESIGN APPROACH

Spreadsheets and MatLAB programs were developed for automating the entire design procedure, and thus, the parametric study. The verification of design approach was an essential step to ensure its accuracy and that the design and analysis approach results are consistent with TxDOT's standard practices. For this purpose, the results of two case studies for the spreadsheet solution, with all the parameters consistent with those of detailed design examples, were compared with those of TxDOT's design software, PSTRS14 (TxDOT 2004). In general, for all the design variables (except for shear and camber), the difference in results was very insignificant (between 0 to 3.9 percent). This check confirms the consistency between PSTRS14 (TxDOT 2004), and the parametric study results generated by the MatLAB program developed for this study.

For the service limit state design, the MatLAB results of the detailed design example matches those of PSTRS14 with very insignificant differences. In Table 3.4, a difference up to 5.9 percent can be noticed for the top and bottom fiber stress calculation at transfer. This is due to the difference in the top fiber section modulus values and the number of debonded strands in the end zone, respectively. Large differences in the camber calculations are observed, which may be due to the fact that PSTRS14 uses a single step hyperbolic functions method, whereas, a multi step approach is used in the detailed design example and parametric study. In Table 3.5, a difference of 26 percent in transverse shear stirrup spacing is observed. This difference may be because PSTRS14 calculates the spacing according to the AASHTO Standard Specifications 1989 edition (AASHTO 1989) while this detailed design example, all the calculations were performed according to the AASHTO Standard Specifications 2002 edition (AASHTO 2002).

**Table 3.4 Comparison of Detailed Example Design for LRFD Specifications (PSTRS14 vs. MatLAB)**

| Design Parameters | | PSTRS14 | MatLAB | Difference (%) |
|---|---|---|---|---|
| Prestress Losses (%) | Initial | 8.41 | 8.40 | 0.1 |
| | Final | 22.85 | 22.84 | 0.0 |
| Required Concrete Strengths (psi) | $f'_{ci}$ | 4,944 | 4,944 | 0.0 |
| | $f'_c$ | 5,586 | 5,582 | 0.1 |
| At Transfer (ends) (psi) | Top | -506 | -533 | -5.4 |
| | Bottom | 1,828 | 1,936 | -5.9 |
| At Service (midspan) (psi) | Top | 2,860 | 2,856 | 0.1 |
| | Bottom | -384 | -383 | 0.3 |
| Number of Strands | | 64 | 64 | 0 |
| Number of Debonded Strands | | (20+10)[1] | (20+8)[1] | 2 |
| $M_u$ (kip–ft.) | | 9,082 | 9,077 | -0.1 |
| $\phi M_n$ (kip–ft.) | | 11,888 | 12,028 | -1.2 |
| Ultimate Horizontal Shear Stress @ critical section (psi) | | 143.3 | 143.9 | 0.0 |
| Transverse Shear Stirrup (#4 bar) Spacing (in.) | | 10.3 | 10.0 | 2.9 |
| Maximum Camber (ft.) | | 0.281 | 0.350 | -24.6 |

1. Number of debonded strands in bottom row and second row, respectively.

**Table 3.5 Comparison of Detailed Example Design for Standard Specifications (PSTRS14 vs. MatLAB)**

| Design Parameters | | PSTRS14 | MatLAB | Difference (%) |
|---|---|---|---|---|
| Prestress Losses (%) | Initial | 8.00 | 8.01 | -0.1 |
| | Final | 22.32 | 22.32 | 0.0 |
| Required Concrete Strengths (psi) | $f'_{ci}$ | 5,140 | 5,140 | 0.0 |
| | $f'_c$ | 6,223 | 6,225 | 0.0 |
| At Transfer (ends) (psi) | Top | -530 | -526 | 0.8 |
| | Bottom | 1,938 | 1,935 | 0.2 |
| At Service (midspan) (psi) | Top | -402 | -397 | 1.2 |
| | Bottom | 2,810 | 2,805 | 0.2 |
| Number of Strands | | 66 | 66 | 0 |
| Number of Debonded Strands | | (20+10)[1] | (20+10)[1] | 0 |
| $M_u$ (kip–ft.) | | 9,801 | 9,780 | 0.3 |
| $\phi M_n$ (kip–ft.) | | 12,086 | 12,118 | -0.3 |
| Transverse Shear Stirrup (#4 bar) Spacing (in.) | | 8.8 | 6.5 | 26.1 |
| Maximum Camber (ft.) | | 0.295 | 0.340 | -15.3 |

1. Number of debonded strands in bottom row and second row, respectively.

## 3.6 DESIGN LOADS AND DISTRIBUTION

### 3.6.1 General

This section discusses the design loads that include the permanent dead loads and vehicular live loads for both the specifications. The summary of all the formulas used to determine shear forces and bending moments due to dead and live loads is also presented. The approximate method of load distribution in the LRFD Specifications is discussed along with their limitations.

### 3.6.2 Dead Load and Superimposed Dead Loads

Within the scope of this study, the self-weight of the Texas U54 girder, deck slab, and diaphragms come into the category of dead loads. The self-weight of the wearing surface and T501 rail loads are treated as superimposed dead loads. The deck slab dead load is calculated based on the tributary width, which is equal to the center-to-center spacing of the beams. Based on the TxDOT Bridge Design Manual (TxDOT 2001), two-thirds of the rail dead load is distributed to the exterior beam and one-third of the rail dead load is distributed to the adjacent interior beam. The two interior diaphragms of the Texas U54 beam are considered to be a 3 kip load each with a maximum average thickness of 13 in. Each of the interior diaphragms are considered to be located as close as 10 ft. from midspan of the beam. The wearing surface superimposed dead load is calculated by considering the dimensions of the design span length and the total roadway width, where the total roadway width is the width of the bridge deck between the nominal faces of the bridge as shown in the Figure 3.1. The unit weights for the cast-in-place (CIP) concrete, precast concrete, and asphalt materials are provided in Table 3.3.

The superimposed dead loads are distributed equally among all the girders for the designs according to the Standard Specifications (AASHTO 2002). The LRFD

Specifications also allow the uniform distribution of all permanent dead loads to all the girders provided the following criteria provided in LRFD Art. 4.6.2.2 are met.

1. Width of the deck is constant.
2. Unless otherwise specified, the number of beams is not less than four.
3. Beams are parallel and have approximately the same stiffness.
4. Unless otherwise specified, the roadway part of the overhang, $d_e$, does not exceed 3.0 ft.
5. Curvature in plan is less than the limit specified in LRFD Art. 4.6.1.2.
6. Cross-section is consistent with one of the cross-sections shown in LRFD Table 4.6.2.2.1-1.

If the bridge geometry is not consistent with the provisions of the LRFD Art. 4.6.2.2, the LRFD Specifications (AASHTO 2004) require the determination of the permanent dead load distribution based on refined analysis methods.

### 3.6.3 Live Loads

According to the LRFD Art. 3.6.1.2 (AASHTO 2004) the live load model, known as HL93, was considered for this study. The HL93 load model consists of both of the following combinations.

1. Design truck and design lane load
2. Design tandem and design lane load

The live load effects on a bridge structure are calculated based on the load combination that produces the maximum response in the structure. The design tandem load consists of a pair of 25 kip axles spaced 4 ft. apart and is subjected to a dynamic load allowance. The design tandem load consists of 0.64 klf uniformly distributed in the longitudinal direction and is not subjected to a dynamic load allowance. In general, the load combination consisting of design tandem and design lane load governs for spans less than 40 ft. The design truck for the HL93 load model is shown in the Figure 3.4. The

design lane load for the HL93 load model is 640 lb/ft. in the longitudinal direction and uniformly distributed over a 10 ft. width.

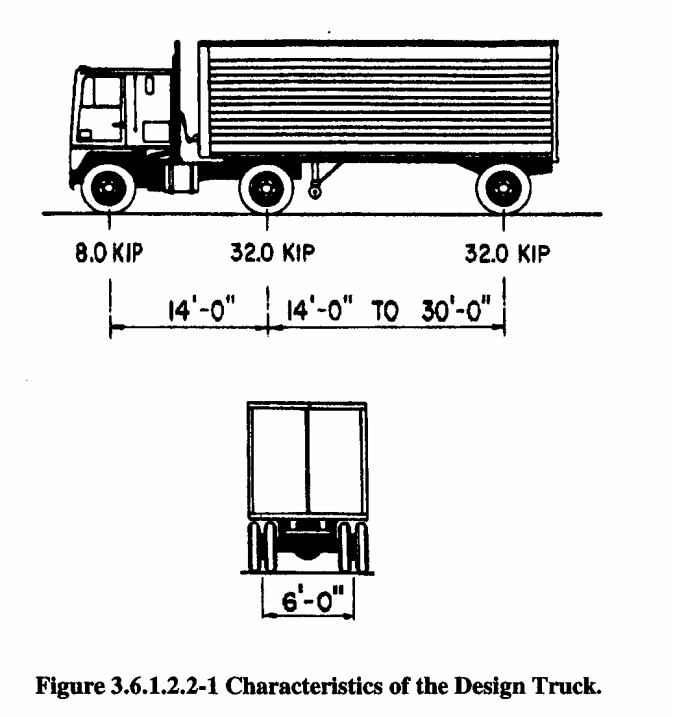


**Figure 3.6.1.2.2-1 Characteristics of the Design Truck.**

**Figure 3.4 HL93 Design Truck (AASHTO 2004).**

According to Standard Art. 3.7 (AASHTO 2002), the live load model designated as HS20-44 was considered for this study. The HS20-44 consists of a design truck or a design lane loading, as shown in Figures 3.5 and 3.6. The live load effects on a bridge structure are calculated based on the design truck or design lane load, whichever produces the maximum response in the structure. Note that the HS20-44 design truck is equivalent to the design truck used for the HL-93 live load model.

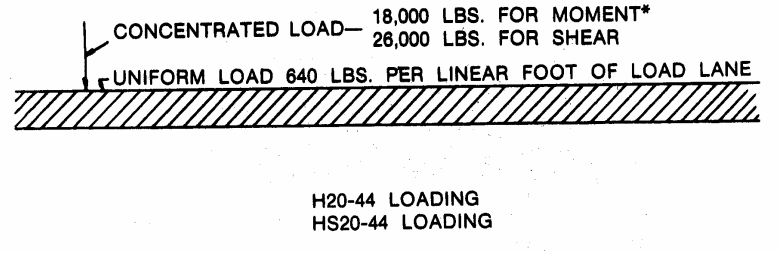


**Figure 3.5 HS20-44 Design Lane Load (AASHTO 2002).**

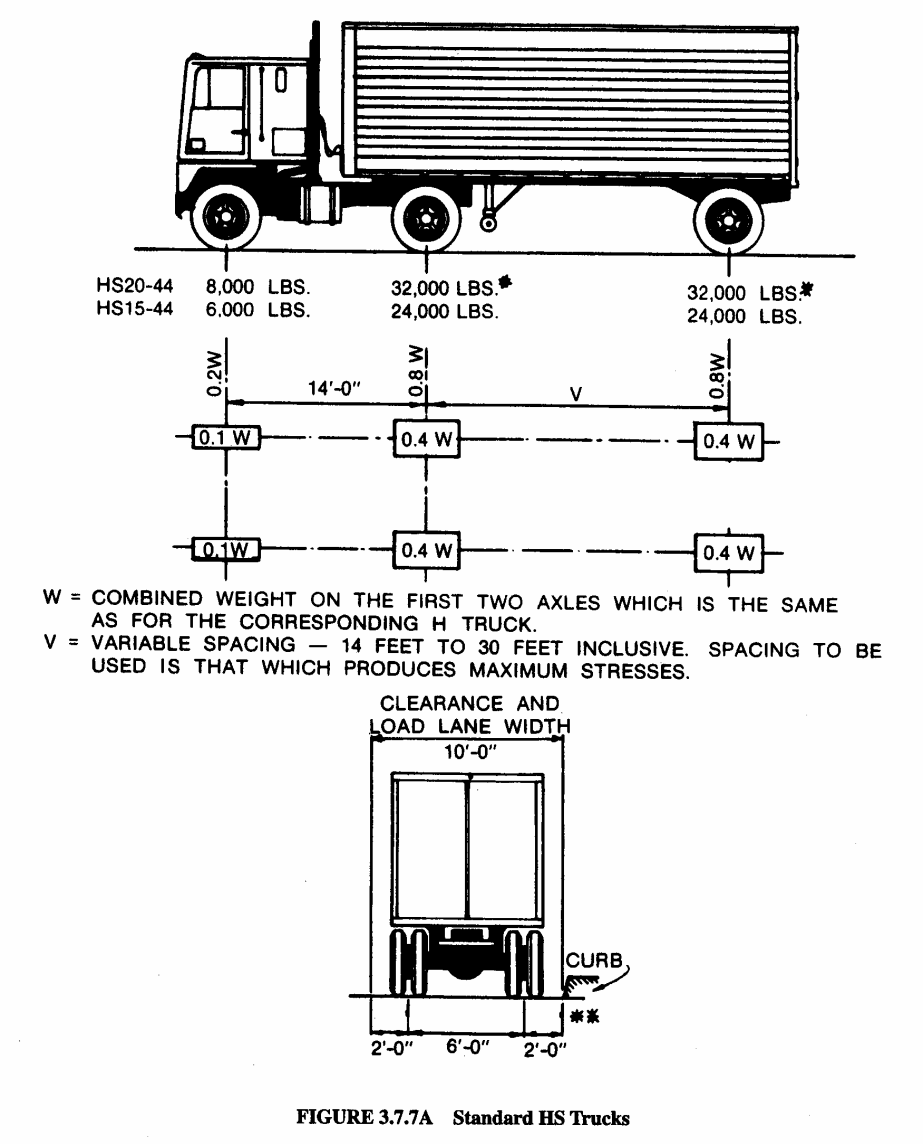


**FIGURE 3.7.7A Standard HS Trucks**

**Figure 3.6 HS20-44 Design Truck Load (AASHTO 2002).**

### 3.6.4 Shear Force and Bending Moment due to Permanent Dead Loads

The bending moment ($M$) and shear force ($V$) due to dead loads and super-imposed dead loads at any section along the span are calculated using the following formulas.

$$M = 0.5wx\,(L - x) \tag{3.1}$$

$$V = w\,(0.5L - x) \tag{3.2}$$

where,

$x$ = Distance from left support to the section being considered (ft.)

$L$ = Design span length (ft.)

### 3.6.5 Shear Force and Bending Moment due to Vehicular Live Loads

Table 3.6 summarizes formulas to calculate the shear forces and bending moments in a simply supported beam which corresponds to the support conditions used for this study and typical TxDOT bridges. The applicable live load model is noted for each formula. Figure 3.7 provides the corresponding load placement schemes.

**Table 3.6 Formulas for Different Live Load Placement Schemes in Figure 3.7 (Adapted from *PCI Bridge Design Manual*).**

| Applicability | Load Placement Scheme (Figure 3.7) | *x/L* | Formulas | Min | | Max |
|---|---|---|---|---|---|---|
| | | | | ***x*, (ft.)** | ***L*, (ft.)** | ***L*, ft.** |
| Design Truck as per HL93 or HS20-44 | (a) Moment @ *x* | 0 – 0.333 | $\frac{72(x)\left[(L-x)-9.33\right]}{L}$ | 0 | 28 | - |
| | (a) Shear @ *x* | 0.333 – 0.5 | $\frac{72(x)\left[(L-x)-4.67\right]}{L}-112$ | 14 | 28 | - |
| | (b) Moment @ *x* | 0 – 0.5 | $\frac{72\left[(L-x)-4.67\right]}{L}-8$ | 14 | 28 | 42 |
| | (b) Shear @ *x* | 0 – 0.5 | $\frac{72\left[(L-x)-9.33\right]}{L}$ | 0 | 14 | - |
| Design Lane as per HL93 | (c) Moment @ *x* | 0 – 0.5 | $\frac{0.64(x)(L-x)}{2}$ | - | - | - |
| | (d) Shear @ *x* | 0 – 0.5 | $\frac{0.64}{2L}(L-x)^2$ | - | - | - |
| Design Tandem as per HL93 | (e) Moment @ *x* | 0 – 0.5 | $50(x)\left(\frac{L-x-2}{L}\right)$ | - | - | - |
| | (e) Shear @ *x* | 0 – 0.5 | $50\left(\frac{L-x-2}{L}\right)$ | - | - | - |

The bending moments and shear forces due to HS20-44 design truck load are calculated from load placement schemes (a) and (b) shown in Figure 3.7 and the respective formulas as shown in Table 3.6. The undistributed bending moments and shear forces due to HS20-44 design lane load are calculated using the following formulas.

Maximum undistributed bending moment,

$$M(x)=\frac{P(x)(L\ -\ x)}{L}\ +\ 0.5(w)(x)(L-x) \tag{3.3}$$

Maximum undistributed shear force,

$$V(x)=\frac{Q(L\ -\ x)}{L}\ +\ (w)(\frac{L}{2}\ -\ x) \tag{3.4}$$

where,

$P$ = Concentrated load for moment = 18 kips

$Q$ = Concentrated load for shear = 26 kips

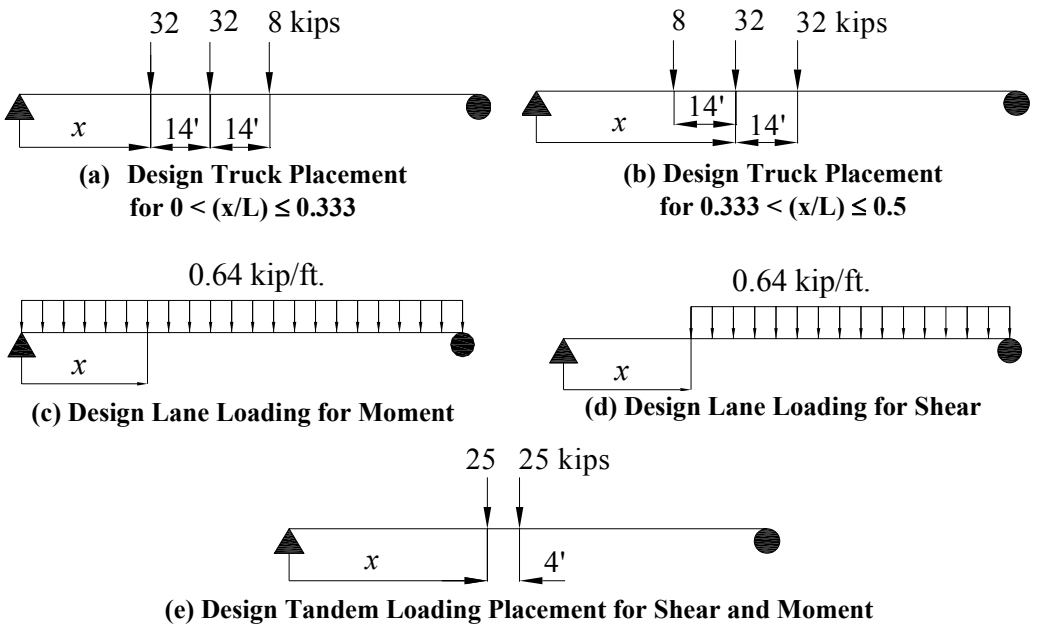


**Figure 3.7 Placement of Design Live Loads for a Simply Supported Beam.**

### 3.6.6 Vehicular Live Load Distribution Factor

#### *3.6.6.1 Limitations and Formula*

The LRFD Specifications (AASHTO 2004) provide formulas for the calculation of live load distribution factors (DFs), which are summarized in the Table 3.7. These formulas are valid within their range of applicability. The general limitations on the use of all LRFD live load DF formulas, as stated in the LRFD Art. 4.6.2.2, are same as discussed in Section 3.6.2.

**Table 3.7 LRFD Live Load DFs for Concrete Deck on Concrete Spread Box Beams (Adapted from AASHTO 2004)**

| Category | Distribution Factor Formulas | Range of Applicability |
|---|---|---|
| Live Load Distribution per Lane for Moment in Interior Beams | One Design Lane Loaded:<br>$\left(\frac{S}{3.0}\right)^{0.35}\left(\frac{Sd}{12.0L^2}\right)^{0.25}$<br>Two or More Design Lanes Loaded:<br>$\left(\frac{S}{6.3}\right)^{0.6}\left(\frac{Sd}{12.0L^2}\right)^{0.125}$ | $6.0 \le S \le 18.0$<br>$20 \le L \le 140$<br>$18 \le d \le 65$<br>$N_b \ge 3$ |
| | Use Lever Rule | $S > 18.0$ |
| Live Load Distribution per Lane for Moment in Exterior Longitudinal Beams | One Design Lane Loaded:<br>Lever Rule<br>Two or More Design Lanes Loaded:<br>$g = e \times g_{\text{int}erior}$<br>$e = 0.97 + \frac{d_e}{28.5}$ | $0 \le d_e \le 4.5$<br>$6.0 \le S \le 18.0$ |
| | Use Lever Rule | $S > 18.0$ |
| Live Load Distribution per Lane for Shear in Interior Beams | One Design Lane Loaded:<br>$\left(\frac{S}{10}\right)^{0.6}\left(\frac{d}{12.0L}\right)^{0.1}$<br>Two or More Design Lanes Loaded:<br>$\left(\frac{S}{7.4}\right)^{0.8}\left(\frac{d}{12.0L}\right)^{0.1}$ | $6.0 \le S \le 18.0$<br>$20 \le L \le 140$<br>$18 \le d \le 65$<br>$N_b \ge 3$ |
| | Use Lever Rule | $S > 18.0$ |
| Live Load Distribution per Lane for Shear in Exterior Beams | One Design Lane Loaded:<br>Lever Rule<br>Two or More Design Lanes Loaded:<br>$g = e \times g_{\text{int}erior}$<br>$e = 0.8 + \frac{d_e}{10}$ | $0 \le d_e \le 4.5$ |
| | Use Lever Rule | $S > 18.0$ |

### *3.6.6.2 Edge Distance Parameter*

The edge distance parameter, $d_e$, takes into account the closeness of a truck wheel line to the exterior girder. The edge girder is more sensitive to the truck wheel line placement than any other factor, as reported by Zokaie (2000). The LRFD Specifications define $d_e$ as the distance from the exterior web of exterior beam to the interior edge of curb or traffic barrier. The value of $d_e$ is important because it limits the use of the LRFD live load DF formulas and it is also used to determine the correction factor to determine the live load distribution for the exterior girder.

For calculating $d_e$ for inclined webs, as in the case of Texas U54 beam, the LRFD Specifications and the research references (Zokaie 1991, 2000) do not provide guidance to calculate the exact value of $d_e$. Thus, in this study the $d_e$ value is considered to be the average distance between the curb and exterior inclined web of the U54 beam, as shown in the Figure 3.8.

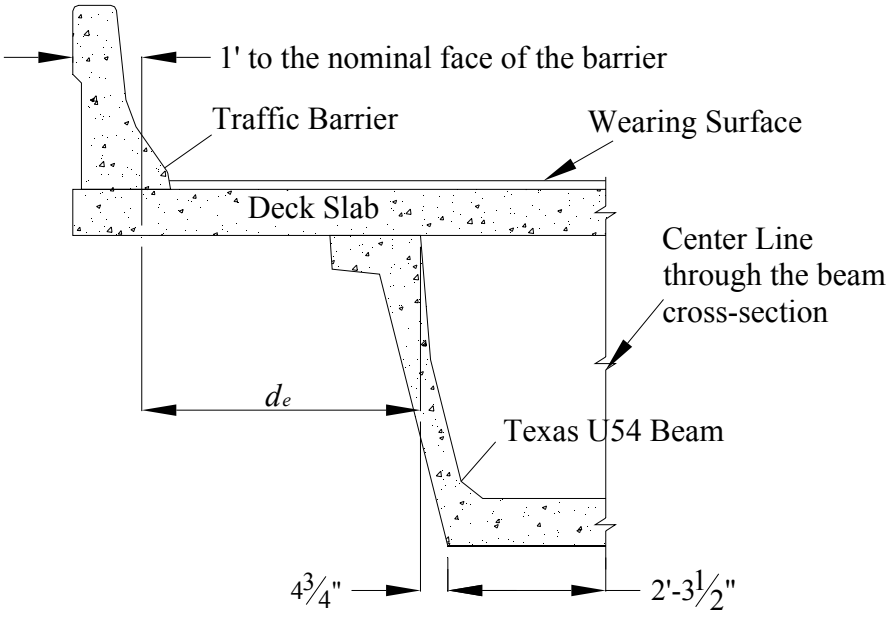


**Figure 3.8 Definition of $d_e$ (for This Study).**

*3.6.6.3 Applicability of LRFD Load Distribution Rules*

Initially, the total roadway width (TRW) was considered to be constant of 46 ft., as compared to the values stated in Table 3.1. For this value of TRW, certain spacings used for the parametric study of precast, prestressed Texas U54 beams were found to violate the LRFD Specifications provisions for applicability of live load DFs and uniform distribution of permanent dead loads. The spacings and summary of the parameters in violation are stated in Table 3.8.

**Table 3.8 Spacings – Reasons of Invalidation**

| Spacings | LRFD Restrictions Violated | LRFD Restrictions |
|---|---|---|
| 10 ft. | Actual $d_e$ = 4.31 ft. | $0 < d_e \leq 3$ ft.[2] |
| 14 ft. | Actual $d_e$ = 5.31 ft.<br><br>Actual $N_b = 3$ | $0 < d_e \leq 3$ ft.[2]<br>$0 < d_e \leq 4.5$ ft.[1]<br>$N_b \geq 4$ [2] |
| 16.67 ft. | Actual $N_b = 3$ | $N_b \geq 4$ [2] |

1 This restriction is related to the LRFD Live Load Distribution Factor formulas as given in Table 3.3.
2 This restriction is related to the general set of limitations as described in Section 3.6.2.

Among other restrictions, the LRFD Specifications allow for uniform distribution of permanent dead loads (such as rail, sidewalks, and wearing surface) if $N_b \geq 4$, where $N_b$ is the number of beams in a bridge cross-section. Kocsis (2004) shows that, in general, a larger portion of the rail and sidewalk load is taken by exterior girders for cases when $N_b < 4$. The implication of distributing the dead load of railing and sidewalk uniformly among all the beams for the case where $N_b = 3$ is that the exterior girder may be designed unconservatively, if the same design is used for the exterior and interior girders. The justification of using the spacings with $N_b = 3$, is that as per TxDOT standard practices (TxDOT 2001), two-thirds of the railing load is distributed to the exterior girder and one-third is distributed to the interior girder.

According to the TxDOT Bridge Design Manual (TxDOT 2001) the standard bridge overhang is 6 ft. 9 in. for Texas U beams. Overhang is defined as the distance

between the centerline of the exterior U54 beam to the edge of deck slab. For the 10 ft. and 14 ft. spacings, the overhang is restricted to 6 ft. 9 in., rather than the value determined for a 46 ft. TRW. Referring to Figure 3.8, $d_e$ is calculated to be 3 ft. 0.75 in., which is reasonably close to the limiting value of $d_e \leq 3$ ft. The resulting TRW is 42 ft. for these spacings, as noted in Table 3.1.

## 3.7 ANALYSIS AND DESIGN PROCEDURE

### 3.7.1 General

This section discusses the analysis and design procedures adopted for this study based on the provisions of the LRFD and Standard Specifications. The approach and corresponding equations are presented for flexural design for service and strength limit states, transverse and interface shear design, calculation of prestress loss, and calculation of deflection and camber. The assumptions and approach in the calculating the effective flange width are discussed in detail, as the Standard Specifications do not give any specific guidelines for the calculation of effective flange width for open box sections, such as the Texas U54 beam. The TxDOT Bridge Design Software, PSTRS14 (TxDOT 2004), calculates the prestress losses, concrete strengths at release and service, number of bonded and debonded strands in an iterative procedure. This procedure is also outlined in this section.

### 3.7.2 Effective Flange Width

Composite section properties of the Texas U54 composite section are calculated based on the effective flange width of the deck slab associated with each girder section. According to Hambly (1991), “The effective flange width is the width of a hypothetical

flange that compresses uniformly across its width by the same amount as the loaded edge of the real flange under the same edge shear forces."

The Standard Specifications do not give any specific guidelines regarding the calculation of the effective flange width for open box sections, such as the Texas U54 beam. So, for both the LRFD and Standard Specifications, each web of the Texas U54 beam is considered an individual supporting element according to the LRFD Specifications commentary C4.6.2.6.1. Each supporting element is then considered to be similar to a wide flanged I-beam. After making this assumption, the provisions for the effective flange width in the Standard Art. 9.8.3 (AASHTO 2002) and LRFD Art. 4.6.2.6.1 (AASHTO 2004) are applied to the individual webs of the Texas U54 beam.

The procedure in the Standard Specifications is to first calculate the effective web width of the precast, prestressed beam, and then the effective flange width is calculated. For a composite prestressed concrete beam where slabs or flanges are assumed to act integrally with the precast beams, the effective web width of the precast beam is taken as lesser of

1. Six times the maximum thickness of the flange (excluding fillets) on each side of the web plus the web and fillets, or
2. The total width of the top flange.

For a composite prestressed concrete beam the effective flange width of the precast beam is taken as lesser of the following three values:

1. One-fourth of the girder span length,
2. Six times the thickness of the slab on each side of the effective web width plus the effective web width (as determined in steps shown above), or
3. One-half the clear distance on each side of the effective web width plus the effective web width.

The LRFD Specifications treat the interior and exterior beams differently to calculate the effective flange width. This section discusses the effective flange width for interior beams only, because only interior beams are considered in the parametric study.

In LRFD Specifications, the effective flange width for the interior beams is taken as the least of:

1. One-quarter of the effective span length; and
2. 12 times the average depth of the slab, plus the greater of the web thickness or one-half the width of the top flange of the girder; or
3. The average spacing of adjacent beams.

### 3.7.3 Flexural Design for Service Limit State

#### *3.7.3.1 General*

The service limit state design of prestressed concrete load carrying members typically governs the flexural design. The LRFD and Standard Specifications (AASHTO 2004, 2002) provide allowable compressive and tensile stress limits for three loading stages. This section describes the equations that are used to compute the compressive and tensile stresses caused due to the applied loading for both specifications. These stresses are used in the design to ensure that the allowable stress limits are not exceeded for the service limit states. These equations are derived on the basis of simple statical analysis of prestressed concrete bridge girder, using the uncracked section properties and assuming the beam to be homogeneous and elastic. The sign convention used for tension is negative and for compression is positive in this section. Furthermore, the LRFD Specifications specifies various subcategories of service limit states and only SERVICE-I and SERVICE-III are found to be relevant to the scope of this study. Compression in prestressed concrete is evaluated through the SERVICE-I limit state and tension in the prestressed concrete superstructures is evaluated through the SERVICE-III limit state with the objective of crack control. The difference, pertaining to this study, between these two limit states is that SERVICE-I uses a load factor of 1.0 for all permanent dead loads and live load plus impact, while SERVICE-III uses a load factor of 1.0 for all permanent dead loads and a load factor of 0.8 for live load plus impact.

### *3.7.3.2 Initial Loading Stage at Transfer*

In the initial loading stage, the initial prestressing force is applied to the non-composite Texas U54 beam section. The initial prestressing force is calculated based on initial prestress losses that occur during and immediately after transfer of prestress. The top and bottom fiber stresses are calculated as follows.

$$f_t = \frac{P_{si}}{A} - \frac{P_{si}\, e_c}{S_t} + \frac{M_g}{S_t} \tag{3.5}$$

$$f_b = \frac{P_{si}}{A} + \frac{P_{si}\, e_c}{S_b} - \frac{M_g}{S_b} \tag{3.6}$$

where:

$A$ = Total area of non-composite precast section (in.$^2$)

$S_b$ = Section modulus referenced to the extreme bottom fiber of the non-composite precast beam (in.$^3$)

$S_t$ = Section modulus referenced to the extreme top fiber of the non-composite precast beam (in.$^3$)

$e_c$ = Eccentricity of the prestressing tendons from the centroid of non-composite precast section (in.)

$f_b$ = Concrete stress at the bottom fiber of the beam (ksi)

$f_t$ = Concrete stress at the top fiber of the beam (ksi)

$M_g$ = Unfactored bending moment due to beam self-weight (k-ft.)

$P_{si}$ = Effective pretension force after initial losses (kips)

### *3.7.3.3 Intermediate Loading Stage at Service*

At the intermediate loading stage, the effective prestressing force is evaluated for the composite beam section. Composite action develops after the cast-in-place (CIP)

concrete slab is hardened. The effective prestressing force is calculated based on final prestress losses, which include initial losses and all time-dependent losses. Permanent dead loads due to the girder, CIP concrete slab, and diaphragm are considered to act on the non-composite beam section. Permanent dead loads placed after the CIP slab, such as rail loads, and wearing surface loads are considered to be acting on the composite beam section, as for unshored construction.

$$f_t = \frac{P_{se}}{A} - \frac{P_{se}\, e_c}{S_t} + \frac{M_g + M_s + M_{dia}}{S_t} + \frac{M_b + M_{ws}}{S_{tg}} \qquad (3.7)$$

$$f_b = \frac{P_{se}}{A} + \frac{P_{se}\, e_c}{S_b} - \frac{M_g + M_s + M_{dia}}{S_b} - \frac{M_b + M_{ws}}{S_{bc}} \qquad (3.8)$$

where:

$P_{se}$ = Effective pretension force after all losses (kips)

$S_{bc}$ = Composite section modulus referenced to extreme bottom fiber of the precast beam (in.$^3$)

$S_{tg}$ = Composite section modulus referenced to top fiber of the precast beam (in.$^3$)

$M_S$ = Unfactored bending moment due to CIP deck slab self weight (k-ft.)

$M_{dia}$ = Unfactored bending moment due to diaphragm self weight (k-ft.)

$M_b$ = Unfactored bending moment due to barrier self weight (k-ft.)

$M_{ws}$ = Unfactored bending moment due to wearing surface self weight (k-ft.)

#### *3.7.3.4 Final Loading Stage at Service*

In the final loading stage, the effective prestressing force along with total permanent dead loads, live loads and impact loads are acting on the composite beam section. The effective prestressing force is calculated based on total prestress losses,

which include initial losses and all time-dependent losses. For the SERVICE-III limit state in the LRFD Specifications, only 80% of the total live load and impact load should be considered in Equation 3.10 for checking the tensile stresses in the bottom fiber of the beam. Equation 3.11 should be used for checking the tensile stresses in the bottom fiber of the beam using the Standard Specifications, where a factor of 1.0 is used with the total live load and impact load.

$$f_t = \frac{P_{se}}{A} - \frac{P_{se}\, e_c}{S_t} + \frac{M_g + M_s + M_{dia}}{S_t} + \frac{M_b + M_{ws} + M_{LT} + M_{LL}}{S_{tg}} \tag{3.9}$$

$$f_b = \frac{P_{se}}{A} + \frac{P_{se}\, e_c}{S_b} - \frac{M_g + M_s + M_{dia}}{S_b} - \frac{M_b + M_{ws} + 0.8(M_{LT} + M_{LL})}{S_{bc}} \tag{3.10}$$

$$f_b = \frac{P_{se}}{A} + \frac{P_{se}\, e_c}{S_b} - \frac{M_g + M_s + M_{dia}}{S_b} - \frac{M_b + M_{ws} + 1.0(M_{LT} + M_{LL})}{S_{bc}} \tag{3.11}$$

where:

$M_{LT}$ = Unfactored bending moment due to truck load and impact.

$M_{LL}$ = Unfactored bending moment due to lane load.

### *3.7.3.5 Additional Check of Compressive Stresses at Service*

An additional check evaluates the compressive stress in the prestressed section due to the live loads and one-half the sum of effective prestress and permanent dead loads. The compressive stress at the top fiber at the service stage is found by the following equation.

$$f_t = \frac{(M_{LT} + M_{LL})}{S_{tg}} + 0.5\left( \frac{P_{se}}{A} - \frac{P_{se}\, e_c}{S_t} + \frac{M_g + M_b + M_{dia}}{S_t} + \frac{M_b + M_{ws}}{S_{tg}} \right) \tag{3.12}$$

### 3.7.4 Allowable Stress Limits for Service Limit States

This section summarizes the allowable compressive and tensile stress limits in the LRFD and Standard Specifications (AASHTO 2004, 2002). Table 3.9 provides these limits for each load stage. The LRFD Specification give a different coefficient for allowable stress limits for compressive stress at intermediate loading stage at service and at final loading stage at service. The allowable stress limits are also slightly different for tensile stresses at initial loading stage at transfer.

**Table 3.9 Allowable Stress Limits for the LRFD and Standard Specifications**

| Stage of Loading | Type of Stress | Allowable Stress Limits | | |
|---|---|---|---|---|
| | | LRFD | | Standard |
| | | $f_c'$ or $f_{ci}'$ (ksi) | $f_c'$ or $f_{ci}'$ (psi) | $f_c'$ or $f_{ci}'$ (psi) |
| Initial Loading Stage at Transfer | Compressive | $0.6f_{ci}'$ | $0.6f_{ci}'$ | $0.6f_{ci}'$ |
| | Tensile | $0.24\sqrt{f_{ci}'}$ [1] | $7.59\sqrt{f_{ci}'}$ [1] | $7.5\sqrt{f_{ci}'}$ [2] |
| Intermediate Loading Stage at Service | Compressive | $0.45f_c'$ | $0.45f_c'$ | $0.4f_c'$ |
| | Tensile | $0.19\sqrt{f_c'}$ | $6\sqrt{f_c'}$ | $6\sqrt{f_c'}$ |
| Final Loading Stage at Service | Compressive | $0.6\phi_\omega f_c'$ | $0.6\phi_\omega f_c'$ | $0.6f_c'$ |
| | Additional Compressive Check | $0.4f_c'$ | $0.4f_c'$ | $0.4f_c'$ |
| | Tensile | $0.19\sqrt{f_c'}$ | $6\sqrt{f_c'}$ | $6\sqrt{f_c'}$ |

Notes:

1 AASHTO LRFD Specifications allow this larger tensile stress limit when additional bonded reinforcement is provided to resist the total tensile force in the concrete when the tensile stress exceeds $0.0948\sqrt{f_{ci}'}$, or 0.2 ksi, whichever is smaller.

2 AASHTO Standard Specifications allow this larger tensile stress limit when additional bonded reinforcement is provided to resist the total tensile force in the concrete when the tensile stress exceeds $3\sqrt{f_{ci}'}$, or 200 psi, whichever is smaller.

The LRFD Specifications introduces a reduction factor, $\phi_\omega$, for the compressive stress limit at the final load stage to account for the fact that the unconfined concrete of the compression sides of the box girders are expected to creep to failure at a stress far lower than the nominal strength of the concrete. This reduction factor is taken equal to

1.0 when the web or flange slenderness ratio, calculated according to the LRFD Art. 5.7.4.7.1, is less than or equal to 15. When either the web or flange slenderness ratio is greater than 15, the provisions of the LRFD Art. 5.7.4.7.2 are used to calculate the value for the reduction factor, $\phi_\omega$. For a trapezoidal box section such as composite Texas U54 beam, which has variable thickness across the flanges and webs, the LRFD Specification outlines a general guideline to determine the approximate slenderness ratios for webs and flanges. Figure 3.9 shows various choices for web and flange lengths and thicknesses for Texas U54 beam. The slenderness ratio for any web or flange portion of Texas U54 beam is less than 15, which gives the value of the reduction factor, $\phi_\omega$ equal to 1.0. The maximum slenderness ratio of 9.2 occurs in the webs of the U54 beam.

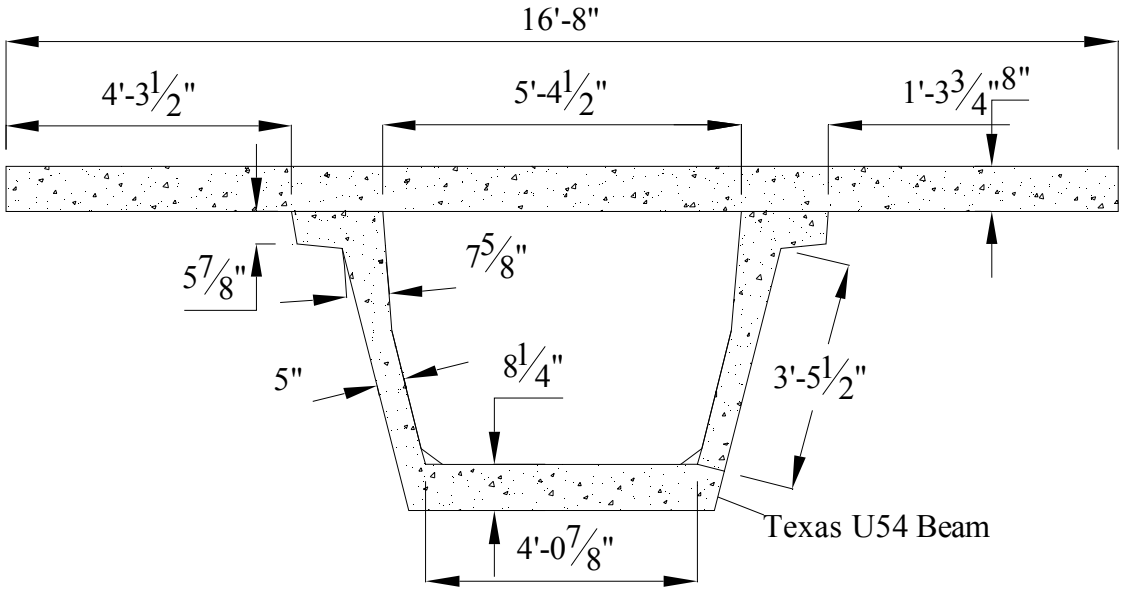


**Figure 3.9 Various Choices for Web and Flange Lengths, and Thicknesses for Texas U54 Beam to Calculate the Reduction Factor, $\phi_\omega$.**

### 3.7.5 Initial Estimate of Required Number of Prestressing Strands

To make an initial estimate of required number of prestressing strands, first the tensile stress at the extreme fiber of the beam is calculated for service conditions.

Assuming a 20 percent final prestress loss and a reasonable guess (i.e. 2 inches in this study) of eccentricity of the strand group from the bottom fiber, the required number of strands can be calculated by Equations 3.10 and 3.11 for the LRFD and Standard Specifications, respectively. From this the actual eccentricity and bottom fiber stress is recalculated, and compared with the required bottom fiber stress. Further iterations are performed as necessary.

### 3.7.6 Partial Debonding of Prestressing Strands

To be consistent with TxDOT design procedures, the debonding of strands is carried out in accordance with the procedure followed in the TxDOT bridge design software PSTRS14 (TxDOT 2004). The Standard Specifications do not give any recommendation for limitations on debonding of strands. Whereas, the LRFD Specifications give explicit guidelines for limitations on debonding of strands. The debonding procedure, followed for both the LRFD and Standard designs, is described in the following paragraph.

Two strands are debonded at a time at each section located at uniform increments of 3 ft. along the span length, beginning at the end of the girder. The debonding is started at the end of the girder because, due to relatively higher initial stresses at the end, a greater number of strands are required to be debonded. The debonding requirement, in terms of number of strands, reduces as the section moves away from the end of the girder. To make the most efficient use of debonding, due to greater eccentricities in the lower rows, the debonding at each section begins at the bottom most row and goes up. Debonding at a particular section will continue until the initial stresses are within the allowable stress limits or until a debonding limit is reached. When the debonding limit is reached, the initial concrete strength is increased and the design cycles to convergence.

As per *TxDOT Bridge Design Manual* (TxDOT 2001) and AASHTO LRFD Art. 5.11.4.3, the limits of debonding for partially debonded strands are described as follows:

1. Maximum percentage of debonded strands per row
    - *TxDOT Bridge Design Manual* (TxDOT 2001) recommends a maximum percentage of debonded strands per row should not exceed 75%.
    - AASHTO LRFD recommends a maximum percentage of debonded strands per row should not exceed 40%.
2. Maximum percentage of debonded strands per section
    - *TxDOT Bridge Design Manual* (TxDOT 2001) recommends a maximum percentage of debonded strands per section should not exceed 75%.
    - AASHTO LRFD recommends a maximum percentage of debonded strands per section should not exceed 25%.
3. LRFD Specifications recommend that not more than 40% of the debonded strands or four strands, whichever is greater, shall have debonding terminated at any section.
4. Maximum length of debonding
    - According to *TxDOT Bridge Design Manual* (TxDOT 2001), the maximum debonding length chosen to be lesser of the following:
        - 15 ft.
        - 0.2 times the span length, or
        - half the span length minus the maximum development length as specified in AASHTO LRFD Art. 5.11.4.2 and Art. 5.11.4.3 for the LRFD designs and as specified in the 1996 AASHTO Standard Specifications for Highway Bridges, Section 9.28 for the Standard designs.
    - An additional requirement for the LRFD designs was followed, which states that the length of debonding of any strand shall be such that all limit states are satisfied with the consideration of total developed resistance at any section being investigated.

5. An additional requirement for the LRFD designs was followed, which states:
    - Debonded strands shall be symmetrically distributed about the center line of the member.
    - Debonded lengths of pairs of strands that are symmetrically positioned about the centerline of the member shall be equal.
    - Exterior strands in each horizontal row shall be fully bonded.

### 3.7.7 Calculation of Prestress Losses

#### *3.7.7.1 General*

The prestress losses were calculated following the typical TxDOT practices for design of prestressed concrete girders. This approach is used in the TxDOT design software PSTRS14 (TxDOT 2004). The TxDOT procedure for prestress losses is described below:

1. The minimum required number of strands is initially selected for a particular span length and girder spacing.
2. The concrete strengths at service and at release are first assumed to be 5000 psi and 4000 psi, respectively.
3. An estimate of the initial prestress loss is made, and the initial prestress force is calculated.
4. The refined prestress losses are then calculated, based on the equations described in this section, both for the LRFD and Standard Specifications.
5. The actual initial prestress losses are calculated by the equations described in this section and compared with the initial estimate made in Step 3.
6. This process in Step 3 through 5 is repeated until the assumed and actual initial prestress loss are reasonably close to each other.
7. The optimized values of concrete strength at service is calculated by comparing the actual stresses calculated by Equations 3.10 through 3.12

with the allowable stress limits as given in Table 3.7. The required concrete strength at transfer is typically very high and strands are debonded such that this very high requirement of concrete strength at transfer is lowered to a value calculated at a section beyond which strands can not be debonded (due to the debonding length limitation). The debonding of strands is described in Section 3.7.6.

8. The process in Step 3 through 7 is repeated until the assumed concrete strength at transfer and initial prestress loss values converge.

### *3.7.7.2 Total Loss of Prestress*

According to the LRFD Specifications (AASHTO 2004), in pretensioned members that are constructed and prestressed in a single stage, relative to the stress immediately before transfer, the total prestress loss is determined by the following equation.

$$\Delta f_{pT} = \Delta f_{pES} + \Delta f_{pSR} + \Delta f_{pCR} + \Delta f_{pR1} + \Delta f_{pR2} \tag{3.13}$$

where:

$\Delta f_{pT}$ = Total prestress loss

$\Delta f_{pES}$ = Loss of prestress due to elastic shortening

$\Delta f_{pSR}$ = Loss of prestress due to concrete shrinkage

$\Delta f_{pCR}$ = Loss of prestress due to creep of concrete

$\Delta f_{pR1}$ = Loss of prestress due to relaxation of prestressing steel at transfer

$\Delta f_{pR2}$ = Loss of prestress due to relaxation of prestressing steel after transfer

According to the Standard Specifications (AASHTO 2002), for pretensioned members the total prestress losses may be determined as follows.

$$\Delta f_s = SH + ES + CR_C + CR_S \quad (3.14)$$

where:

$\Delta f_s$ = Total prestress losses

$SH$ = Loss of prestress due to concrete shrinkage

$EC$ = Loss of prestress due to elastic shortening

$CR_C$ = Loss of prestress due to creep of concrete

$CR_S$ = Loss of prestress due to relaxation of prestressing steel

*3.7.7.3 Immediate Losses*

**Elastic Shortening Loss**

According to the LRFD Specifications (AASHTO 2004), the elastic shortening loss in the pretensioned members, $\Delta f_{ES}$, is determined as follows.

$$\Delta f_{pES} = \frac{E_p}{E_{ci}} f_{cgp} \quad (3.15)$$

where:

$f_{cgp}$ = Sum of the concrete stresses at the center of gravity of the prestressing tendons due to prestressing force and the self-weight of the member at the section of maximum moment (ksi)

$$f_{cgp} = \frac{P_{si}}{A} + \frac{P_{si} e_c^2}{I} - \frac{(M_g) e_c}{I} \quad (3.16)$$

$P_{si}$ = Pretension force after allowing for the initial losses (kips)

$E_p$ = Modulus of elasticity of prestressing steel (ksi)

$E_{ci}$ = Modulus of elasticity of concrete at transfer (ksi)

$I$ = Moment of inertia of the non-composite U54 Section (in.$^4$)

$A$ = Cross-sectional area of the non-composite U54 Section (in.$^2$)

$e_c$ = Eccentricity of the prestressing strands from the centroid of the non-composite U54 Section (in.)

According to the Standard Specifications (AASHTO 2002), the elastic shortening loss in the pretensioned members, *ES,* is determined as follows.

$$ES = \frac{E_s}{E_{ci}} f_{cir} \tag{3.17}$$

where:

$E_s$ = Modulus of elasticity of prestressing steel (ksi)

$f_{cir}$ = Average concrete stress at the center of gravity of the prestressing steel due to pretensioning force and self-weight of beam immediately after transfer (use Equation 3.16) (ksi)

**Initial Relaxation Loss Before Transfer**

According to the LRFD Specifications (AASHTO 2004), the initial relaxation loss in prestressing steel, initially stressed in excess of $0.5 f_{pu}$, is calculated as follows.

$$\Delta f_{pR1} = \frac{\log(24.0 \times t)}{40.0} \left[ \frac{f_{pj}}{f_{py}} - 0.55 \right] f_{pj} \tag{3.18}$$

where:

$\Delta f_{pR1}$ = Specified yield strength of prestressing steel (ksi)

$f_{pj}$ = Initial stress in the tendon at the end of stressing, as per LRFD Commentary C.5.9.5.4.4, $f_{pj}$ is assumed to be $0.8 f_{pu}$ (ksi)

$f_y$ = Specified yield strength of prestressing steel (ksi)

$t$ = Time estimated in days from stressing to transfer, assumed 1 day for this study (days)

The Standard Specifications (AASHTO 2002) do not give any expression to account for initial relaxation loss before transfer. In order to match the TxDOT Bridge Design Manual (TxDOT 2001) procedure, the initial relaxation loss is taken to be equal to half of the total relaxation loss computed by the Standard Specifications.

*3.7.7.4 Time-Dependent Losses*

**Shrinkage**

The LRFD Specifications (AASHTO 2004) give the following expression to determine the shrinkage loss, $\Delta f_{pSR}$, for prestressing steel.

$$\Delta f_{pSR} = 17.0 - 0.15\,H \tag{3.19}$$

According to the Standard Specifications (AASHTO 2002), the shrinkage loss, *SH*, for prestressing steel is calculated by the following expression.

$$SH = 17000 - 150\,RH \tag{3.20}$$

where:

$RH, H$ = Relative humidity, taken as 60 percent for this study

**Final Relaxation Loss After Transfer**

According to the LRFD Specifications (AASHTO 2004), the total relaxation loss, $\Delta f_{pR2}$, in the prestressing steel is calculated as follows.

$$\Delta f_{pR2} = 30\%\left[20.0 - 0.4\,\Delta f_{pES} - 0.2\left(\Delta f_{pSR} + \Delta f_{pCR}\right)\right] \tag{3.21}$$

The Standard Specifications (AASHTO 2002) use the following expression to calculate the total relaxation loss, $CR_S$, in the prestressing steel.

$$CR_S = \left[5000 - 0.10\,ES - 0.05\left(SH + CR_C\right)\right] \tag{3.22}$$

**Creep**

According to the LRFD Specifications (AASHTO 2004), the loss in prestressing steel due to concrete creep is calculated as follows.

$$\Delta f_{pCR} = 12 f_{cgp} - 7\Delta f_{cdp} \quad (3.23)$$

where:

$\Delta f_{cdp}$ = Change in the concrete stress at center of gravity of prestressing steel due to permanent loads, with the exception of the load acting at the time the prestressing force is applied. Values of $\Delta f_{cdp}$ are calculated at the same section or at sections for which $f_{cgp}$ is calculated.

$$\Delta f_{cdp} = \frac{(M_{slab} + M_{dia})e_c}{I} + \frac{(M_b + M_{ws})(y_{bc} - y_{bs})}{I_c} \quad (3.24)$$

where:

$y_{bs}$ = Distance from center of gravity of the prestressing strands at midspan to the bottom of the beam (in.)

$y_{bc}$ = Distance from center of gravity of the composite girder cross-section at midspan to the bottom of the beam (in.)

$I$ = Moment of inertia of the composite U54 Section (in.$^4$)

$M_{slab}$ = Unfactored bending moment due to self-weight of the deck slab (k-ft.)

$M_{dia}$ = Unfactored bending moment due to diaphragm self-weight (k-ft.)

$M_b$ = Unfactored bending moment due to barrier self-weight (k-ft.)

$M_{ws}$ = Unfactored bending moment due to wearing surface self-weight (k-ft.)

The Standard Specifications (AASHTO 2002) use the following expression to calculate the creep loss, *CR*, in prestressing steel.

$$CR_C = 12 f_{cir} - 7 f_{cds} \quad (3.25)$$

where:

$f_{cds}$ = Concrete stress at the center of gravity of the prestressing steel due to all dead loads except the dead load present at the time the pretensioning force is applied (calculated the same way as $\Delta f_{cdp}$)

### 3.7.8 Flexural Design for Strength Limit State

The Standard and LRFD Specifications both give equations for calculating the nominal flexural strength for the cases of rectangular section behavior and flanged or T-section behavior. The significant differences and similarities are summarized as follows.

1. Both specifications give different equations (STD Eq. 9-17, LRFD Eq. 5.7.3.1.1-1) to calculate the average stress in the prestressing steel, $f_{ps}$, at ultimate.
2. Both specifications give equations to calculate the nominal flexural strength for T-section behavior. However, they cannot be readily applied to a composite section, because these equations do not differentiate between difference between the concrete strength of the deck slab and the concrete strength of the precast girder cross-section.
3. As per LRFD C5.7.3.2.2 (AASHTO 2004), there is an inconsistency in the Standard Specifications equations for T-sections, which becomes evident when, at first, a rectangular section behavior is assumed and it is found that $c > h_f$, while $a = \beta_1 c < h_f$. When $c$ is recalculated using the expressions for T-section behavior, it can come out to be smaller than $h_f$ or even negative. In order to overcome this deficiency, $\beta_1$ is included in the LRFD equations for calculating the nominal flexural strength for the case of T-section behavior.

As a part of this study, three equations were derived to calculate the nominal flexural strength of the Texas U54 beam were derived based on the conditions of equilibrium and strain compatibility. One of the equations is for the case when the neutral axis falls within the deck slab and other two equations are for the case when neutral axis falls within the depth of Texas U54 beam. These three locations of the neutral axis are shown in Figure 3.10. In order to overcome the inconsistency, as described above, $\beta_1$ is included in the equations according to the LRFD C5.7.3.2.2. Moreover, the same equations are used for both the Standard and LRFD Specifications.

To calculate the average stress in prestressing steel, $f_{ps}$, the Equations 3.26 and 3.27 are used for the Standard and LRFD Specifications respectively.

$$f_{ps} = f_{pu}\left[1-\left(\frac{k}{\beta_1}\right)\left(p\frac{f_{pu}}{f'_{cAVG}}\right)\right] \tag{3.26}$$

$$f_{ps} = f_{pu}\left(1-k\frac{c}{d_p}\right) \tag{3.27}$$

where:

$f_{ps}$ = Average stress in prestressing steel at nominal bending resistance (ksi)

$f_{pu}$ = Specified tensile strength of the prestressing steel (ksi)

$f'_{cAVG}$ = Specified compressive strength of the concrete at 28 days (ksi)

= $f'_{cs}$, when neutral axis falls within the thickness of deck slab

= $\frac{f'_{cs}+f'_{cb}}{2}$, when neutral axis falls within the depth of Texas U54 beam

$f'_{cs}$ = Specified compressive strength of the deck slab concrete at 28 days (ksi)

$f'_{cb}$ = Specified compressive strength of the beam concrete at 28 days (ksi)

$k$ = 0.28 for low relaxation strands [LRFD Table C5.7.3.1.1-1]

$c$ = Distance between the neutral axis (Case 1) and the extreme compression fiber (in.)

$d_p$ = Distance from the extreme compression fiber to the centroid of the prestressing tendons (in.)

$\beta_1$ = Stress block factor (taken as 0.85 for $f'_c \le 4.0$ ksi ; for $4.0 \text{ ksi} < f'_c \le 8.0$ ksi , $\beta_1$ shall be reduced at a rate of 0.05 for each 1.0 ksi and shall not be taken less than 0.65)

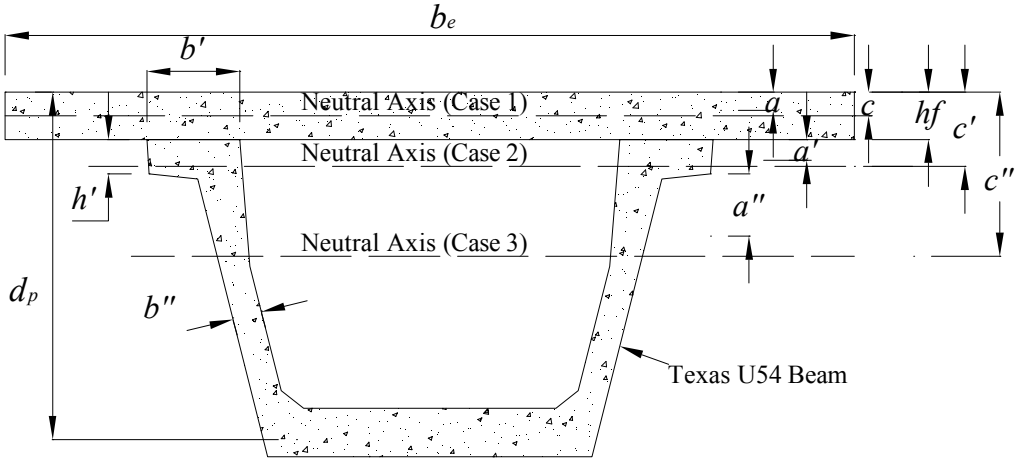


**Figure 3.10 Neutral Axis Location.**

*3.7.8.1 Rectangular Section Behavior (Case 1)*

Rectangular section behavior occurs when the neutral axis falls within the thickness of the deck slab. The reduced nominal moment strength of Texas U54 beams can be found using the following equations.

$$c = \frac{A_{ps} f_{ps}}{0.85 f'_{cs} b_e \beta_{1s} + \frac{k}{d_p} A_{ps} f_{ps}} \tag{3.28}$$

$$\phi M_n = \phi \left[ A_{ps} f_{ps} \left( d_p - \frac{a}{2} \right) \right] \tag{3.29}$$

where:

$\beta_{1s}$ = Stress block factor, $\beta_1$, for the deck slab based on $f'_{cs}$

$b_e$ = Effective flange width (in.)

$\phi$ = Resistance factor = 1.0 for flexural limit state for prestressed members

$A_{ps}$ = Area of prestressing tendons (in$^2$)

$M_n$ = Nominal moment strength at ultimate conditions (k – in.)

$a$ = Depth of the equivalent stress block = $c\,\beta_{1s}$ (in.)

*3.7.8.2 Flanged- Section Behavior*

T-section behavior occurs when the neutral axis falls within the depth of the precast U54 beam section. Due to the difference in the concrete compressive strengths at the interface of the CIP deck slab and the precast U54 beam, a stress discontinuity is introduced which is accounted by considering different equivalent stress blocks for the deck slab and the U54 beam. The LRFD Specifications in Art. 5.7.2.2 and C5.7.2.2 recommends three different ways to account for the stress block factor, $\beta_1$, which bears a different value for the deck slab than the U54 beam because of their different concrete compressive strengths. In this study, the stress block factor for slab, $\beta_{1s}$, is calculated corresponding to $f'_{cs}$ and the stress block factor for U54 beam, $\beta_{1b}$, is calculated corresponding to $f'_{cb}$.

**Neutral Axis Falls within the U54 Flanges (Case 2)**

When the neutral axis lies within the U54 beam flange thickness, $h'$, the following equations are used to calculate the nominal flexural strength at the ultimate conditions. This situation corresponds to Case 2 as shown in the Figure 3.10.

$$c' = \frac{\left[ A_{ps} f_{ps} - 0.85 h_f \left( f'_{cs} b_e \overline{\beta}_{1s} - f'_{cb} b' \frac{\beta_{1b}}{\beta_{1s}} \right) \right]}{0.85 f'_{cb} b' \beta_{1b} + \frac{k}{d_p} A_{ps} f_{ps}} \tag{3.30}$$

$$\phi M_n = \phi \left[ A_{ps} f_{ps} \left( d_p - \left( h_f + \frac{a'}{2} \right) \right) + 0.85 f'_{cs} b_e \overline{\beta}_{1s} \left( \frac{h_f + a'}{2} \right) \right] \tag{3.31}$$

where:

$c'$ = Distance between the neutral axis (Case 2) and the extreme compression fiber (in.)

$\beta_{1b}$ = Stress block factor, $\beta_1$, for the U54 section based on $f'_{cb}$

$\bar{\beta}_{1s}$ = Same value as $\beta_{1s}$. The bar on top of $\beta$ signifies that the term $\bar{\beta}_{1s}$ is included in the original equation derived based on principles of equilibrium and strain compatibility to account for the inconsistency as per LRFD C5.7.3.2.2.

$b'$ = Effective flange width (in.)

$h_f$ = Flange thickness (in.)

$a'$ = Depth of the equivalent stress block of the compression area in the U54 beam flanges only = $\left(c - \frac{h_f}{\beta_{1s}}\right)\beta_{1b}$ (in.)

**Neutral Axis Falls within the U54 Beam Web (Case 3)**

When the neutral axis lies within the U54 beam web, the following equations are developed to calculate the nominal flexural strength at the ultimate conditions. This situation corresponds to Case 3 as shown in the Figure 3.10.

$$c'' = \frac{\left[A_{ps}f_{ps} - \left[0.85h_f\left(f'_{cs}b_e\bar{\beta}_{1s} - f'_{cb}b'\frac{\beta_{1b}}{\beta_{1s}}\right) + 0.85f'_{cb}h'\left(b'\bar{\beta}_{1b} - b''\frac{\beta_{1b}}{\beta_{1s}}\right)\right]\right]}{0.85f'_{cb}b''\beta_{1b} + \frac{k}{d_p}A_{ps}f_{ps}} \quad (3.32)$$

$$\phi M_n = \phi\left[A_{ps}f_{ps}\left(d_p - \left(h_f + h' + \frac{a''}{2}\right)\right) + 0.85f'_{cs}b_e\bar{\beta}_{1s}\left(\frac{h_f + a''}{2} + h'\right) + 0.85f'_{cb}b'\bar{\beta}_{1b}\left(\frac{h' + a''}{2}\right)\right] \quad (3.33)$$

where:

$c''$ = Distance between the neutral axis (Case 3) and the extreme compression fiber (in.)

$b''$ = Combined width of the webs of the U54 section (in.)

$\bar{\beta}_{1b}$ = Same value as $\beta_{1b}$. The bar on top of $\beta$ signifies that the term $\bar{\beta}_{1b}$ is included in the original equation derived based on principle of equilibrium and strain compatibility to account for the inconsistency as per LRFD C5.7.3.2.2.

$h'$ = U54 flange thickness (in.)

$a''$ = Depth of the equivalent stress block of the compression area in the U54 beam web only = $\left( c - \frac{h_f}{\beta_{1s}} - \frac{h'}{\beta_{1b}} \right) \beta_{1b}$ (in.)

### 3.7.9 Transverse Shear Design

#### *3.7.9.1 Standard Specifications Method*

The Standard Specifications require that the members subject to shear to be designed such that the following condition is fulfilled.

$$V_u \leq \phi(V_c + V_s) \tag{3.34}$$

where:

$V_u$ = Factored shear force at the section considered (kips)

$V_c$ = Nominal shear strength provided by concrete (kips)

$V_s$ = Nominal shear strength provided by web reinforcement (kips)

$\phi$ = Strength reduction factor = 0.90 for prestressed concrete members

The critical section for shear is located at a distance $h_c/2$ from the face of the support, where $h_c$ is the total height of the composite section. The concrete contribution, $V_c$, is taken as the force required to produce shear cracking. The Standard Specification requires the $V_c$ to be the lesser of $V_{cw}$ or $V_{ci}$, which are the shear forces that produce web-shear cracking and flexural-shear cracking, respectively. $V_{ci}$ is calculated by Equation 3.35 as follows.

$$V_{ci} = 0.6\sqrt{f_c'}b'd + V_d + \frac{V_i M_{cr}}{M_{\max}} \leq 1.7\sqrt{f_c'}\, b'd \tag{3.35}$$

where:

$b'$ = Web width of a flanged member (in.)

$f_c'$ = Compressive strength of beam concrete at 28 days ( psi)

$M_{max}$ = Maximum factored moment at the section due to externally applied loads

= $M_u - M_d$ = (k-ft.)

$M_u$ = Factored bending moment at the section (k-ft.)

$M_d$ = Bending moment at the section due to unfactored dead load (k-ft.)

$V_i$ = Factored shear force at the section due to externally applied loads occurring simultaneously with $M_{max}$ (kips)

= $V_{mu}$ - $V_d$

$V_d$ = Shear force due to total dead loads at section considered (kips)

$V_{mu}$ = Factored shear force occurring simultaneously with $M_u$, conservatively taken as maximum shear force at the section (kips)

$M_{cr}$ = Moment causing flexural cracking of section due to externally applied loads (k-ft.)

= $(6\sqrt{f_c'} + f_{pe} - f_d)\, S_{bc}$

$f_d$ = Stress due to unfactored dead load, at extreme fiber of section where tensile stress is caused by externally applied loads (ksi)

$$= \left[ \frac{M_g + M_S}{S_b} + \frac{M_{SDL}}{S_{bc}} \right]$$

$f_{pe}$ = Compressive stress in concrete due to effective pretension forces at extreme fiber of section where tensile stress is caused by externally applied loads (i.e. bottom of the beam in this study)

$$f_{pe} = \frac{P_{se}}{A} + \frac{P_{se}\, e}{S_b}$$

$e$ = Eccentricity of the strands at $h_c/2$

$d$ = Distance from extreme compressive fiber to centroid of pretensioned reinforcement, but not less than $0.8h_c$ (in.)

$V_{cw}$ is calculated by the following expression.

$$V_{cw} = (3.5\ \sqrt{f_c'} + 0.3\, f_{pc})\, b'd\ + V_p \tag{3.36}$$

where:

$f_{pc}$ = Compressive stress in concrete at centroid of cross-section (since the centroid of the composite section does not lie within the flange of the cross-section) resisting externally applied loads. For a non-composite section

$$\frac{P_{se}}{A} - \frac{P_{se}\, e(y_{bc} - y_b)}{I} + \frac{M_D(y_{bc} - y_b)}{I}$$

$M_D$ = Moment due to unfactored non-composite dead loads (k-ft.)

$y_b$ = Distance from center of gravity of the non-composite U54 beam to the bottom fiber of the beam (in.)

$y_{bc}$ = Distance from center of gravity of the composite girder cross-section at midspan to the bottom of the beam (in.)

$I$ = Moment of inertia of the composite U54 Section (in.$^4$)

$A$ = Cross-sectional area of the non-composite U54 Section (in.$^2$)

$e$ = Eccentricity of the prestressing strands from the centroid of the composite U54 Section (in.)

After calculating the governing value for $V_c$, $V_s$ can be calculated from Equation 3.34. The amount of web reinforcement can then be computed using Equation 3.37.

$$A_v = \frac{V_s\, s}{f_y\, d} \tag{3.37}$$

where:

$A_v$ = Area of web reinforcement (in.$^2$)

$S$ = Longitudinal spacing of the web reinforcement (in.)

$f_y$ = Yield strength of the non-prestressed conventional web reinforcement (ksi).

Over-reinforcement of the web, which can lead to brittle web-crushing shear failure, is prevented by requiring $V_s$ to be less than or equal to $8\sqrt{f_c'}b'd$ . The minimum reinforcement is calculated by the following relation.

$$A_{v-min} = \frac{50\ b'\ s}{f_y} \tag{3.38}$$

The Standard Specifications require the maximum spacing of the web reinforcement not to exceed 0.75 $h_c$ or 24 in. If $V_s > 4\sqrt{f_c'}\ b'\ d$ , then the maximum spacing limits shall be reduced by one-half to 0.375 $h_c$ or 12 in.

### *3.7.9.2 LRFD Specifications Method*

The LRFD Specifications (AASHTO 2004) design for shear based on Modified Compression Field Theory (MCFT). This method is based on the variable angle truss model in which the inclination of the diagonal compression field is allowed to vary. In contrast, this angle of inclination remains constant at 45˚ in the approach used in the Standard Specifications. In prestressed concrete members this angle of inclination typically varies between 20˚ to 40˚ (PCI 2003).

Transverse shear reinforcement is provided when:

$$V_u < 0.5\ \phi\ (V_c + V_p) \tag{3.39}$$

where:

$V_u$ = Factored shear force at the section considered

$V_c$ = Nominal shear strength provided by concrete

$V_p$ = Component of prestressing force in direction of the shear force (kips)

$\phi$ = Strength reduction factor = 0.90 for prestressed concrete members

The critical section near the supports is the greater of $0.5d_v\cot\theta$ or $d_v$ for the case of uniformly distributed loads.

where:

$d_v$ = Effective shear depth

= Distance between resultants of tensile and compressive forces, ($d_e$ - $a$/2), but not less than the greater of (0.9$d_e$) or (0.72$h$)

$\theta$ = Angle of inclination of diagonal compressive stresses (slope of compression field)

Shear design using MCFT is an iterative process that begins with assuming a value for $\theta$. Taking the advantage of precompression and using a lower value for $\theta$ will help the iterative procedure to converge faster for prestressed members. The contribution of the concrete to the nominal shear resistance is given by Equation 3.40.

$$V_c = 0.0316\beta\sqrt{f_c'(ksi)}b_v d_v \tag{3.40}$$

where:

$\beta$ = Factor indicating ability of diagonally cracked concrete to transmit tension

$b_v$ = Effective web width taken as the minimum web width within the depth $d_v$ (in.)

To design the member for shear, the factored shear force due to applied loads at the critical section under investigation is first determined. The factored shear stress, $v_u$, is calculated using the following relation.

$$v_u = \frac{V_u - \phi V_p}{\phi b_v d_v} \tag{3.41}$$

The quantity $v_u / f_c'$ is then computed, and value of $\theta$ is assumed. The strain in the reinforcement on the flexural tension side is calculated using Equation 3.42, which is for cases where the section contains at least the minimum transverse reinforcement.

$$\varepsilon_x = \frac{\frac{M_u}{d_v} + 0.5N_u + 0.5(V_u - V_p)\cot\theta - A_{ps}f_{po}}{2(E_s A_s + E_p A_{ps})} \le 0.001 \tag{3.42}$$

If Equation 3.42 yields a negative value, then, Equation 3.43 should be used given as below.

$$\varepsilon_x = \frac{\frac{M_u}{d_v} + 0.5N_u + 0.5(V_u - V_p)\cot\theta - A_{ps}f_{po}}{2(E_cA_c + E_sA_s + E_pA_{ps})} \tag{3.43}$$

where:

$V_u$ = Factored shear force at the critical section, taken as positive quantity (kips)

$M_u$ = Factored moment, taken as positive quantity (k-in.)
$\geq V_u d_v$ (kip-in.)

$V_p$ = Component of the effective prestressing force in the direction of the applied shear (no harped strands are used for Texas U54 beams)

$N_u$ = Applied factored normal force at the specified section

$A_c$ = Area of the concrete on the flexural tension side below $h/2$ (in.$^2$)

$f_{po}$ = Parameter taken as modulus of elasticity of prestressing tendons multiplied by the locked-in difference in strain between the prestressing tendons and the surrounding concrete which is approximately equal to $0.7 f_{pu}$ (ksi)

In this study, the parameter, $f_{po}$, was calculated by using the following expression.

$$f_{po} = f_{pe} + f_{pc}\left(\frac{E_{ps}}{E_c}\right) \tag{3.44}$$

where:

$f_{pc}$ = Compressive stress in concrete after all prestress losses have occurred either at the centroid of the cross-section resisting live load or at the junction of the web and flange when the centroid lies in the flange (ksi). In a composite section, it is the resultant compressive stress at the centroid of the composite section or at the junction of the web and flange when the centroid lies within the flange, that results from both

prestress and the bending moments resisted by the precast member acting alone (ksi).

$$= \frac{P_{se}}{A_n} - \frac{P_{se} ec \left( y_{bc} - y_b \right)}{I} + \frac{\left( M_g + M_{slab} \right)\left( y_{bc} - y_b \right)}{I}$$

where,

$M_g$ = Moment due to girder self-weight (k-ft.)

$M_{slab}$ = Moment due to self-weight of the deck slab (k-ft.)

$y_b$ = Distance from center of gravity of the non-composite U54 beam to the bottom fiber of the beam (in.)

$y_{bc}$ = Distance from center of gravity of the composite girder cross-section at midspan to the bottom of the beam (in.)

$I$ = Moment of inertia of the composite U54 Section (in.$^4$)

$A_n$ = Cross-sectional area of the non-composite U54 Section (in.$^2$)

$e_c$ = Eccentricity of the prestressing strands from the centroid of the composite U54 Section (in.)

The LRFD Specifications Table 5.8.3.4.2-1 is then entered with the values of $v_u / f_c'$ and $\varepsilon_x$. The value of $\theta$ corresponding to $v_u / f_c'$ and $\varepsilon_x$ is compared to the assumed value of $\theta$. If the values match, $V_c$ is calculated using Equation 3.40 with the value of $\beta$ from the table. If the values do not match, the value of $\theta$ taken from the table is used for another iteration.

After $V_c$ has been computed, $V_s$ is determined as the lesser of the following expressions.

$$\frac{V_u}{\phi} \le (V_c + V_s + V_p) \tag{3.45}$$

$$V_n = 0.25 f_c' b_v d_v + V_p \tag{3.46}$$

The area of the transverse shear reinforcement is computed using the expression given below.

$$V_s = \frac{A_v f_y d_v (\cot\theta + \cot\alpha)\sin\alpha}{s} \tag{3.47}$$

where:

$s$ = Spacing of stirrups, (in.)

$\alpha$ = Angle of inclination of transverse reinforcement to the longitudinal axis

$V_s$ = The nominal shear strength provided by web reinforcement (kips)

The spacing of the transverse reinforcement will not exceed the maximum permitted spacing, $s_{max}$, calculated as follows.

If $v_u < 0.125 f_c'$ then;

$s_{\max} = 0.8 d_v \le 24.0$ in.

If $v_u \ge 0.125 f_c'$ then;

$s_{\max} = 0.4 d_v \le 12.0$ in.

Shear force causes tension in the longitudinal reinforcement. For a given shear, this tension becomes larger as θ becomes smaller and as $V_c$ becomes larger. In regions of high shear stresses (i.e. at the critical section), the development and amount of the longitudinal (flexural) reinforcement is also checked by satisfying the Equation 3.48.

$$A_s f_y + A_{ps} f_{ps} \ge \frac{M_u}{d_v \phi_f} + 0.5\frac{N_u}{\phi_c} + \left(\frac{V_u}{\phi_v} + 0.5V_s - V_p\right)\cot\theta \tag{3.48}$$

where:

$N_u$ = Factored axial force, taken as positive if tensile and negative if compressive (kips)

$\phi_f$, $\phi_v$, $\phi_c$ = Resistance factors for moment, shear and axial resistance = 1.0, 0.9 and 1.0, respectively.

### 3.7.10 Interface Shear Design

*3.7.10.1 Standard Specifications Method*

The Standard Specifications do not identify the location of the critical section for interface shear design. In this study, it was assumed to be the same location as the critical section for transverse shear. Composite sections are designed for horizontal shear at the interface between the precast beam and deck using the following expression.

$$V_u \leq \phi V_{nh} \tag{3.49}$$

where:

$V_{nh}$ = Nominal horizontal shear strength (kips)

$V_u$ = Factored vertical shear force acting at the section, (kips)

$\phi$ = Strength reduction factor = 0.90 for prestressed concrete beams

When the contact surface is roughened, or when minimum ties are used, the nominal horizontal shear force, $V_{nh}$ (in lbs.), is found as follows.

$$V_{nh} = 80 b_v d \tag{3.50}$$

where:

$b_v$ = Width of cross-section at the contact surface being investigated for horizontal shear (in.)

$d$ = Distance from extreme compressive fiber to the centroid of pretensioning force (in.)

When the contact surface is roughened, and when minimum ties are used, the nominal horizontal shear force, $V_{nh}$ (in lbs.), is computed by the following expression.

$$V_{nh} = 350 b_v d \tag{3.51}$$

The minimum required number of stirrups for horizontal shear are determined by Equation (3.52).

$$A_{vh} = 50 \frac{b_v s}{f_y} \tag{3.52}$$

where:

$A_{vh}$ = Horizontal shear reinforcement area (in.$^2$)

$s$ = Maximum spacing not to exceed 4 times the least web width of the support element, nor 24 in. (in.)

$f_y$ = Yield stress of non-prestressed conventional reinforcement (in.)

*3.7.10.2 LRFD Specifications Method*

The LRFD Specifications (AASHTO 2004) specify a method for interface shear design based on the shear-friction theory. This method assumes a discontinuity along the shear plane and the relative displacement is considered to be resisted by cohesion and friction, maintained by the shear friction reinforcement crossing the crack.

According to the guidance given by the LRFD Specifications for computing the factored horizontal shear.

$$V_h = \frac{V_u}{d_e} \tag{3.53}$$

where:

$V_h$ = Horizontal shear per unit length of girder (kips)

$V_u$ = Factored vertical shear (kips)

$d_e$ = Distance between the centroid of the steel in the tension side of the beam to the center of the compression block in the deck ($d_e$ - $a/2$) at ultimate conditions (in.)

The LRFD Specifications do not identify the location of the critical section. For this study, it was assumed to be the same location as the critical section for vertical shear. The required nominal shear resistance is calculated by Equation 3.54.

$$V_n = \frac{V_h}{\phi} \tag{3.54}$$

The nominal shear resistance as calculated by Equation 3.54 shall not be greater than the lesser of the following.

$$V_n \le 0.2 f_c' A_{cv} \tag{3.55}$$

$$V_n \le 0.8 A_{cv} \tag{3.56}$$

The nominal shear resistance of the interface surface is:

$$V_n = cA_{cv} + \mu\left[A_{vf} f_y + P_c\right] \tag{3.57}$$

where:

$c$ = Cohesion factor

$\mu$ = Friction factor

$A_{cv}$ = Area of concrete engaged in shear transfer (in.$^2$)

$A_{vf}$ = Area of shear reinforcement crossing the shear plane n(in.$^2$)

$P_c$ = Permanent net compressive force normal to the shear plane (kips)

$f_y$ = Shear reinforcement yield strength (ksi)

In this study it was assumed that concrete is placed against clean, hardened concrete and free of laitance, but not an intentionally roughened surface. The

corresponding values of cohesion and friction factors as given by the LRFD Specifications are $c$ = 0.075 ksi and $\mu = 0.6\lambda$, where $\lambda$ = 1.0 for normal weight concrete.

### 3.7.11 Deflection and Camber Calculations

#### *3.7.11.1 General*

This section describes the procedures to calculate the camber and deflections due to dead loads. The deflections due to live loads are not calculated in this study as they are not a design factor for TxDOT bridges. Camber is calculated based on the Hyperbolic Functions Methods (Sinno 1968).

#### *3.7.11.2 Dead Load Deflection*

Dead load deflections for a simply supported beam are calculated by application of the classical structural analysis methods. The following relations were used to compute the dead load deflections.

$$\Delta_b = \frac{5w_g L^4}{384E_{ci}I} \tag{3.58}$$

$$\Delta_s = \frac{5w_g L^4}{384E_{ci}I} \tag{3.59}$$

$$\Delta_{dia} = \frac{P_{dia} b}{24E_c I}\left(3L^2 - 4b^2\right) \tag{3.60}$$

$$\Delta_{rail} = \frac{5w_{rail} L^4}{384E_c I_c} \tag{3.61}$$

$$\Delta_{ws} = \frac{5w_{ws}L^4}{384E_cI_c} \tag{3.62}$$

where:

$\Delta_b$ = Dead load deflection due to girder self weight (in.)

$\Delta_s$ = Dead load deflection due to the deck slab (in.)

$\Delta_{dia}$ = Dead load deflection due to diaphragm (in.)

$\Delta_{rail}$ = Dead load deflection due to rail (in.)

$\Delta_{ws}$ = Dead load deflection due to wearing surface (in.)

$w_b$ = Uniformly distributed load due to the girder self-weight (k/in.)

$w_s$ = Uniformly distributed load due to the deck slab (k/in.)

$P_{dia}$ = Concentrated load due to the interior diaphragms (kips)

$w_{rail}$ = Uniformly distributed load due to the rail (k/in.)

$w_{ws}$ = Uniformly distributed load due to the wearing surface (k/in.)

$E_{ci}$ = Modulus of elasticity of concrete at transfer (ksi)

$E_c$ = Modulus of elasticity of concrete at service (ksi)

$L$ = Span Length (in.)

$I_c$ = Moment of inertia of the composite section (in.$^4$)

$I$ = Moment of inertia of the non-composite precast section (in.$^4$)

### *3.7.11.3 Camber*

Camber in prestressed concrete bridge beams is the upward elastic deflection due to the eccentric prestressed force only. Camber is a time-dependent phenonmenon and its growth with the concrete creep is known to reach as high as 100 percent of the initial camber in normal weight concrete (Sinno 1968). Prestress loss is due to the relaxation in the elastic strain of the steel which is caused by elastic shortening, shrinkage, and creep

strains of concrete. This study uses the Hyperbolic Functions Methods, developed by Sinno (1968), to be consistent with the camber calculations of PSTRS14 (TxDOT 2004). The calculated camber values in this study were found to match closely with the results of PSTRS14. This method for calculating camber is simple and practical. Though it does not reflect the actual complexity of the camber phenomenon, it has produced good results that match the experimental evidence (Sinno 1968). The step-by-step procedure used in this study to calculate camber in precast, prestressed girder at time, *t*, is summarized below.

**Step 1:**

The initial prestressing force immediately after release is evaluated by the following relation.

$$P = \frac{P_{si}}{\left(1 + \frac{A_{ps}E_{ps}}{AE_c} + \frac{e_c^2 A_{ps}E_{ps}}{E_c I}\right)} + \frac{M_g e_c A_{ps}E_{ps}}{E_c I\left(1 + \frac{A_{ps}E_{ps}}{AE_c} + \frac{e_c^2 A_{ps}E_{ps}}{E_c I}\right)} \tag{3.63}$$

where:

$P$ = Initial prestressing force immediately after release (kips)

$P_{si}$ = Anchor force in the prestressing steel (kips)

$A_{ps}$ = Area of the total number of prestressing strands (in.$^2$)

$A$ = Area of the precast section (in.$^2$)

$e_c$ = Eccentricity of the prestressing strand group from the neutral axis (in.)

$E_{ps}$ = Modulus of elasticity of the prestressing steel (ksi)

**Step 2:**

The initial prestress loss, $\underline{PL_i}$, is calculated as a dimensionless quantity as follows.

$$PL_i = \frac{P_{si} - P}{P_{si}} \tag{3.64}$$

**Step 3:**

The concrete stress at the steel level, $f_{ci}^{s}$, is calculated immediately after release by the following expression.

$$f_{ci}^{s} = P\left(\frac{1}{A} + \frac{e_c^2}{I}\right) - \frac{M_g e_c}{I} \tag{3.65}$$

**Step 4:**

The total strain due to creep and shrinkage is calculated by assuming constant sustained stress.

$$\varepsilon_{c1}^{s} = \varepsilon_{cr}^{\infty} f_{ci}^{s} + \varepsilon_{sh}^{\infty} \tag{3.66}$$

where:

$\varepsilon_{cr}^{\infty}$ = Total creep in concrete at time $t$ (days)

$$= \left[\frac{340t}{5.0+t}\right] \times 10^{-6}\ in/in.$$

$\varepsilon_{sh}^{\infty}$ = Total shrinkage in concrete at time $t$ (days)

$$= \left[\frac{175t}{4.0+t}\right] \times 10^{-6}\ in/in.$$

$\varepsilon_{c1}^{s}$ = Total strain at the prestressing steel level (in./in.)

$t$ = Total time in days at which camber is desired to be evaluated. Based on the experimental evidence in the work by Sinno (1968), camber is predicted at 280$^{th}$ day.

**Step 5:**

The total strain at the prestressing level, $\varepsilon_{c2}^{s}$, is adjusted by subtracting the concrete elastic strain rebound.

$$\varepsilon_{c2}^{s} = \varepsilon_{c1}^{s} - \varepsilon_{c1}^{s} \frac{E_{ps} A_{ps}}{E_c}\left(\frac{1}{A} + \frac{e_c^2}{I}\right) \tag{3.67}$$

**Step 6:**

The change in the concrete stress at the prestressing steel level, $\Delta f_c^{s}$, is computed.

$$\Delta f_c^s = \varepsilon_{c2}^s E_{ps} A_{ps} \left( \frac{1}{A} + \frac{e_c^2}{I} \right) \tag{3.68}$$

**Step 7:**

The total strain at the prestressing level, $\varepsilon_{c1}^s$ , is corrected.

$$\varepsilon_{c4}^s = \varepsilon_{cr}^\infty \left( f_{ci}^s - \frac{\Delta f_c^s}{2} \right) + \varepsilon_{sh}^\infty \tag{3.69}$$

**Step 8:**

Step 5 is repeated again and using the corrected value for the total strain which is $\varepsilon_{c4}^s$ ,

$$\varepsilon_{c5}^s = \varepsilon_{c4}^s - \varepsilon_{c4}^s \frac{E_{ps} A_{ps}}{E_c} \left( \frac{1}{A} + \frac{e_c^2}{I} \right) \tag{3.70}$$

**Step 9:**

The ultimate time-dependent prestress loss, $PL^\infty$, is calculated.

$$PL^\infty = \frac{\varepsilon_{c5}^s E_{ps} A_{ps}}{P_{si}} \tag{3.71}$$

**Step 10:**

The time (days) at which the time-dependent prestress loss is equal to half its ultimate value, $N_{PL}$ , is calculated.

$$N_{PL} = \frac{\left[ 5\varepsilon_{cr}^\infty \left( f_{ci}^s - \frac{\Delta f_c^s}{2} \right) + 4\varepsilon_{sh}^\infty \right]}{\varepsilon_{c4}^s} \tag{3.72}$$

**Step 11:**

The total prestress loss at time (*t), PL,* is calculated as follows,

$$PL = \frac{PL^\infty t}{N_{PL} + t} + PL_i \tag{3.73}$$

**Step 12:**

Finally the total camber at any time, *t*, is calculated by the following expression,

$$C_t = C_i \frac{\left[\varepsilon_{cr}^{\infty}\left(f_{ci}^{s} - \frac{\Delta f_c^s}{2}\right) + \varepsilon_e\right]}{\varepsilon_e}\left(1 - PL^{\infty}\right) \tag{3.74}$$

where:

$C_i$ = Initial camber immediately after the release of the prestressing force (in.)

$C_t$ = Total camber at any time, $t$ (in.)

$\varepsilon_e$ = Elastic strain in concrete at steel level immediately after release of the prestressing force = $\frac{f_{ci}^{s}}{E_c}$ (in./in.)

# 4. PARAMETRIC STUDY RESULTS

## 4.1 INTRODUCTION

A parametric study composed of a number of designs was conducted as the part of this research study. Only bridge superstructures with Texas U54 precast prestressed concrete bridge girders were considered for this portion of study. The main objective was to investigate the effect of the provisions in the LRFD Specifications as compared to designs following the Standard Specifications. The results obtained for designs based on both the Standard and LRFD Specifications were validated using TxDOT's bridge design software PSTRS14 (TxDOT 2004). Various design output quantities such as distribution factors (DFs), live load moment and shear, factored moment and shear, transverse and horizontal shear reinforcement area required, nominal moment capacity, concrete strengths, prestress losses, maximum span capability, number of strands required, camber, and debonding requirements were compared. A summary of the design parameters is given in Table 4.1, and additional details are provided in Section 3.

**Table 4.1 Summary of Design Parameters**

| Parameter | Description / Selected Values |
|---|---|
| Girder Spacing (ft.) | 8'-6", 10'-0", 11'-6", 14'-0" and 16'-8" |
| Spans | 90 ft. to maximum span at 10 ft. intervals |
| Strand Diameter (in.) | 0.5 and 0.6 |
| Concrete Strength at Release, $f'_{ci}$ | Varied from 4000 to 6750 psi for design with optimum number of strands |
| Concrete Strength at Service, $f'_{c}$ | Varied from 5000 to 8750 psi for design with optimum number of strands |
| Skew Angle (degrees) | 0, 15, 30 and 60 |

For the parametric study, the span lengths were increased from 90 ft. to the maximum possible span length at 10 ft. intervals. For the purpose of the discussion of results, the spans are categorized as "short spans," "long spans," and "maximum spans." A short span is considered to be in the range of 90 to 100 ft. length, and a long span is considered to be greater than 100 ft. up to, but not including, the maximum span length. The maximum span length is the length beyond which a particular limit state (e.g. service limit state) is exceeded or a particular set of parameters (e.g. $f'_{ci}$) reach their maximum value. The percent difference was calculated by the following equation.

$$\text{Diff. ( percent)} = \left( \frac{\lambda_{LRFD} - \lambda_{STD}}{\lambda_{STD}} \right) \times 100 \tag{4.1}$$

where, $\lambda_{LRFD}$ and $\lambda_{STD}$ are the design values of interest based on the LRFD and Standard Specifications, respectively. Therefore, a negative difference indicates a decrease in the design value based on the LRFD Specifications with respect to the design value based on the Standard Specifications. The focus of this research was on the interior girders, so all the results that are presented in this section relate to the interior girder calculations unless otherwise specified. The provisions for flexural service limit state design, and flexural ultimate limit state design, transverse and interface shear designs are evaluated in the parametric study.

The detailed design information for every case studied is available in the tables and graphs provided in Appendix A. Based on these results, the following sections summarize the findings with the help of tables and graphs that illustrate the overall trends.

## 4.2 LIVE LOAD MOMENTS AND SHEARS

### 4.2.1 General

The Standard Specifications specify the live load as the maximum effect produced by either HS20-44 design truck load or a design lane load. The LRFD Specifications specify a different live load model HL-93, which is the maximum effect produced by the combination of a design truck load or design tandem load with the design lane load. The formulas for load distribution and impact factors provided by the Standard Specifications differ significantly from those provided by the LRFD Specifications. The impact factors as given in the Standard Specifications vary with the span length and are applicable to both the truck and lane loading; whereas the LRFD Specifications requires the impact factor, which is constant at 33 percent, to be applicable to only the design truck and design tandem loads.

The live load moments are calculated at the midspan location, whereas the live load shears are calculated at the critical section locations. The live load distribution factors and undistributed and distributed live load moments and shears are calculated for each case and the comparisons between the Standard and LRFD Specifications are presented below.

### 4.2.2 Live Load Distribution Factors

Tables 4.2 and 4.3 and Figure 4.1 show differences in the live load DFs calculated by the two specifications. Detailed results for all skews are given in Appendix A. The results in Table 4.3 are based on the live load DFs that were calculated without applying the skew correction factor. In general, the live load DFs, without applying the skew correction factor, calculated by the LRFD Specifications decrease in the range of 0.217 to 0.619 (23.8 to 40.8 percent). More specifically, for the spacings of 10 ft. and

11.5 ft. this decrease ranges from 0.217 to 0.36 (23.8 to 34.5 percent), while for the spacings of 8.5 ft., 14 ft. and 16.67 ft. it decreases by 0.284 to 0.619 (31.6 to 40.8 percent). The strand diameter does not affect the calculation of the live load DFs.

The skew correction factors for skew angles of 0, 15, 30 and 60 degree are 1, 0.983, 0.906 and 0.617. These skew correction factors, when applied to the live load DFs, do not change them significantly for skew angles up to 30 degree but, they do change them significantly for skew angle of 60 degree. Figure 4.1 shows the live load DFs, calculated by taking into account the skew correction factor, for all the spacings. The summary of results of live load DFs for moment for all the skew angles is outlined in Table 4.2. It can be seen that for skew angles of 0, 15 and 30 degree, the live load DFs decreases in the range of 0.217 to 0.703 (23.8 to 46.4 percent), while for the skew angle of 60 degree this decrease ranges from 0.52 to 0.962 (57.8 to 63.5 percent).

The skew does not affect shear live load DFs for the interior beams. Table 4.3 outlines the summary of results for shear live load DFs. In general, it increases by 0.036 (3.9 percent) and decreases by 0.156 (10.3 percent). Shear live load DFs for both specifications are drawn in Figure 4.2. For the spacings of 10 ft. and 11.5 ft. the difference is negligible, but for the spacings of 8.5 ft., 14 ft. and 16.67 ft. the Standard Specification's live load DFs for shear are relatively larger.

The live load DFs calculated in the Standard Specifications are larger than those calculated in the LRFD Specifications, but for moment live load DFs, when compared to shear live load DFs, this difference is more pronounced as can be seen in Figures 4.1 and 4.3.

**Table 4.2 Comparison of Moment Distribution Factors for U54 Interior Beams**

| Spacing (ft.) | Span (ft.) | All Skews | Skew = 0 | | Skew = 15 | | Skew = 30 | | Skew = 60 | |
|---|---|---|---|---|---|---|---|---|---|---|
| | | DF | DF | % Diff. w.r.t STD | DF | % Diff. w.r.t STD | DF | % Diff. w.r.t STD | DF | % Diff. w.r.t STD |
| | | STD | LRFD | | LRFD | | LRFD | | LRFD | |
| 8.50 | 90 | 0.900 | 0.616 | -31.6 | 0.605 | -32.8 | 0.557 | -38.1 | 0.380 | -57.8 |
| | 100 | | 0.599 | -33.4 | 0.589 | -34.5 | 0.543 | -39.7 | 0.370 | -58.9 |
| | 110 | | 0.585 | -35.0 | 0.575 | -36.1 | 0.530 | -41.1 | 0.361 | -59.9 |
| | 120 | | 0.572 | -36.4 | 0.562 | -37.5 | 0.518 | -42.4 | 0.353 | -60.8 |
| | 130 | | 0.561 | -37.7 | 0.551 | -38.8 | 0.508 | -43.6 | 0.346 | -61.6 |
| | 140 | | 0.550 | -38.9 | 0.541 | -39.9 | 0.498 | -44.6 | 0.340 | -62.3 |
| 10.00 | 90 | 0.909 | 0.692 | -23.8 | 0.681 | -25.1 | 0.627 | -31.0 | 0.427 | -53.0 |
| | 100 | | 0.674 | -25.8 | 0.663 | -27.1 | 0.611 | -32.8 | 0.416 | -54.2 |
| | 110 | | 0.658 | -27.6 | 0.647 | -28.8 | 0.596 | -34.4 | 0.406 | -55.3 |
| | 120 | | 0.644 | -29.2 | 0.633 | -30.4 | 0.583 | -35.9 | 0.397 | -56.3 |
| | 130 | | 0.631 | -30.6 | 0.620 | -31.8 | 0.571 | -37.2 | 0.389 | -57.2 |
| | 140 | | 0.619 | -31.9 | 0.609 | -33.1 | 0.561 | -38.3 | 0.382 | -58.0 |
| 11.50 | 90 | 1.046 | 0.766 | -26.7 | 0.753 | -27.9 | 0.694 | -33.6 | 0.473 | -54.8 |
| | 100 | | 0.746 | -28.6 | 0.733 | -29.9 | 0.676 | -35.4 | 0.460 | -56.0 |
| | 110 | | 0.728 | -30.3 | 0.716 | -31.5 | 0.660 | -36.9 | 0.449 | -57.0 |
| | 120 | | 0.712 | -31.9 | 0.700 | -33.0 | 0.645 | -38.3 | 0.440 | -58.0 |
| | 130 | | 0.698 | -33.2 | 0.686 | -34.4 | 0.632 | -39.5 | 0.431 | -58.8 |
| | 140 | | 0.685 | -34.5 | 0.673 | -35.6 | 0.620 | -40.7 | 0.423 | -59.6 |
| 14.00 | 90 | 1.273 | 0.884 | -30.6 | 0.869 | -31.7 | 0.800 | -37.1 | 0.545 | -57.2 |
| | 100 | | 0.860 | -32.4 | 0.846 | -33.5 | 0.779 | -38.8 | 0.531 | -58.3 |
| | 110 | | 0.840 | -34.0 | 0.826 | -35.1 | 0.761 | -40.2 | 0.518 | -59.3 |
| | 120 | | 0.822 | -35.4 | 0.808 | -36.5 | 0.744 | -41.5 | 0.507 | -60.2 |
| | 130 | | 0.805 | -36.7 | 0.791 | -37.8 | 0.729 | -42.7 | 0.497 | -61.0 |
| | 140 | | 0.790 | -37.9 | 0.777 | -39.0 | 0.716 | -43.8 | 0.487 | -61.7 |
| 16.67 | 90 | 1.516 | 1.003 | -33.8 | 0.986 | -34.9 | 0.908 | -40.1 | 0.619 | -59.2 |
| | 100 | | 0.977 | -35.6 | 0.960 | -36.7 | 0.884 | -41.6 | 0.603 | -60.2 |
| | 110 | | 0.953 | -37.1 | 0.937 | -38.2 | 0.863 | -43.0 | 0.588 | -61.2 |
| | 120 | | 0.932 | -38.5 | 0.917 | -39.5 | 0.844 | -44.3 | 0.575 | -62.0 |
| | 130 | | 0.914 | -39.7 | 0.898 | -40.7 | 0.827 | -45.4 | 0.564 | -62.8 |
| | 140 | | 0.897 | -40.8 | 0.881 | -41.8 | 0.812 | -46.4 | 0.553 | -63.5 |

**Table 4.3 Comparison of Live Load Distribution Factors**

| Spacing (ft.) | Span (ft.) | Moment DF | | %diff. w.r.t STD | Shear DF | | %diff. w.r.t STD |
|---|---|---|---|---|---|---|---|
| | | LRFD | STD | | LRFD | STD | |
| 8.50 | 90 | 0.616 | 0.900 | -31.6 | 0.830 | 0.900 | -7.8 |
| | 100 | 0.599 | | -33.4 | 0.821 | | -8.8 |
| | 110 | 0.585 | | -35.0 | 0.813 | | -9.7 |
| | 120 | 0.572 | | -36.4 | 0.806 | | -10.5 |
| | 130 | 0.561 | | -37.7 | 0.799 | | -11.2 |
| | 140 | 0.550 | | -38.9 | 0.793 | | -11.9 |
| 10.00 | 90 | 0.692 | 0.909 | -23.8 | 0.945 | 0.909 | 3.9 |
| | 100 | 0.674 | | -25.8 | 0.935 | | 2.8 |
| | 110 | 0.658 | | -27.6 | 0.926 | | 1.8 |
| | 120 | 0.644 | | -29.2 | 0.917 | | 0.9 |
| | 130 | 0.631 | | -30.6 | 0.910 | | 0.1 |
| | 140 | 0.619 | | -31.9 | 0.903 | | -0.6 |
| 11.50 | 90 | 0.766 | 1.046 | -26.7 | 1.056 | 1.046 | 1.0 |
| | 100 | 0.746 | | -28.6 | 1.045 | | 0.0 |
| | 110 | 0.728 | | -30.3 | 1.035 | | -1.0 |
| | 120 | 0.712 | | -31.9 | 1.026 | | -1.9 |
| | 130 | 0.698 | | -33.2 | 1.018 | | -2.7 |
| | 140 | 0.685 | | -34.5 | 1.010 | | -3.4 |
| 14.00 | 90 | 0.884 | 1.273 | -30.6 | 1.237 | 1.273 | -2.8 |
| | 100 | 0.860 | | -32.4 | 1.223 | | -3.9 |
| | 110 | 0.840 | | -34.0 | 1.212 | | -4.8 |
| | 120 | 0.822 | | -35.4 | 1.201 | | -5.6 |
| | 130 | 0.805 | | -36.7 | 1.191 | | -6.4 |
| | 140 | 0.790 | | -37.9 | 1.182 | | -7.1 |
| 16.67 | 90 | 1.003 | 1.516 | -33.8 | 1.422 | 1.516 | -6.2 |
| | 100 | 0.977 | | -35.6 | 1.407 | | -7.2 |
| | 110 | 0.953 | | -37.1 | 1.393 | | -8.1 |
| | 120 | 0.932 | | -38.5 | 1.381 | | -8.9 |
| | 130 | 0.914 | | -39.7 | 1.370 | | -9.6 |
| | 140 | 0.897 | | -40.8 | 1.360 | | -10.3 |

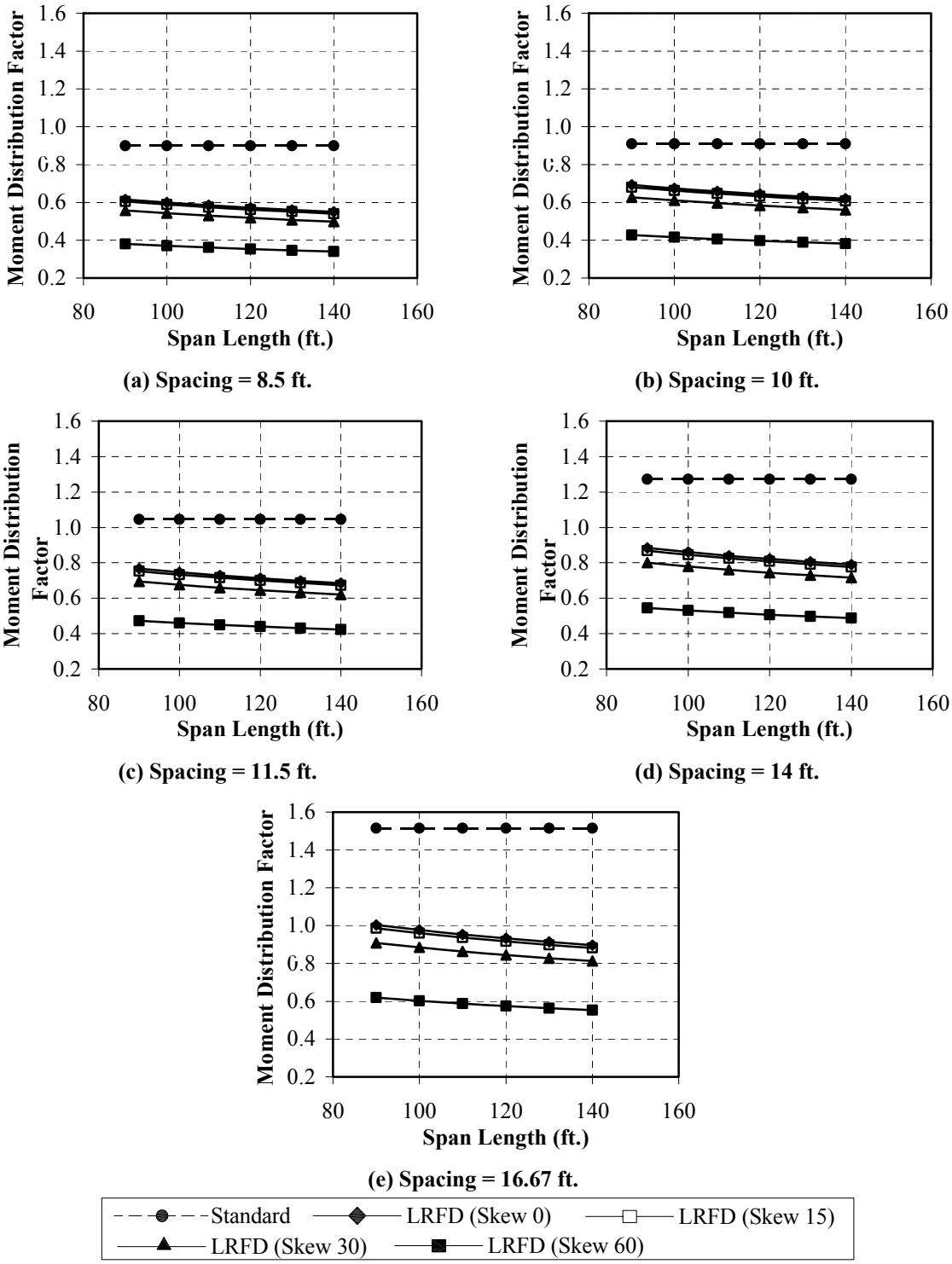


**Figure 4.1 Comparison of Live Load Distribution Factor for Moment.**

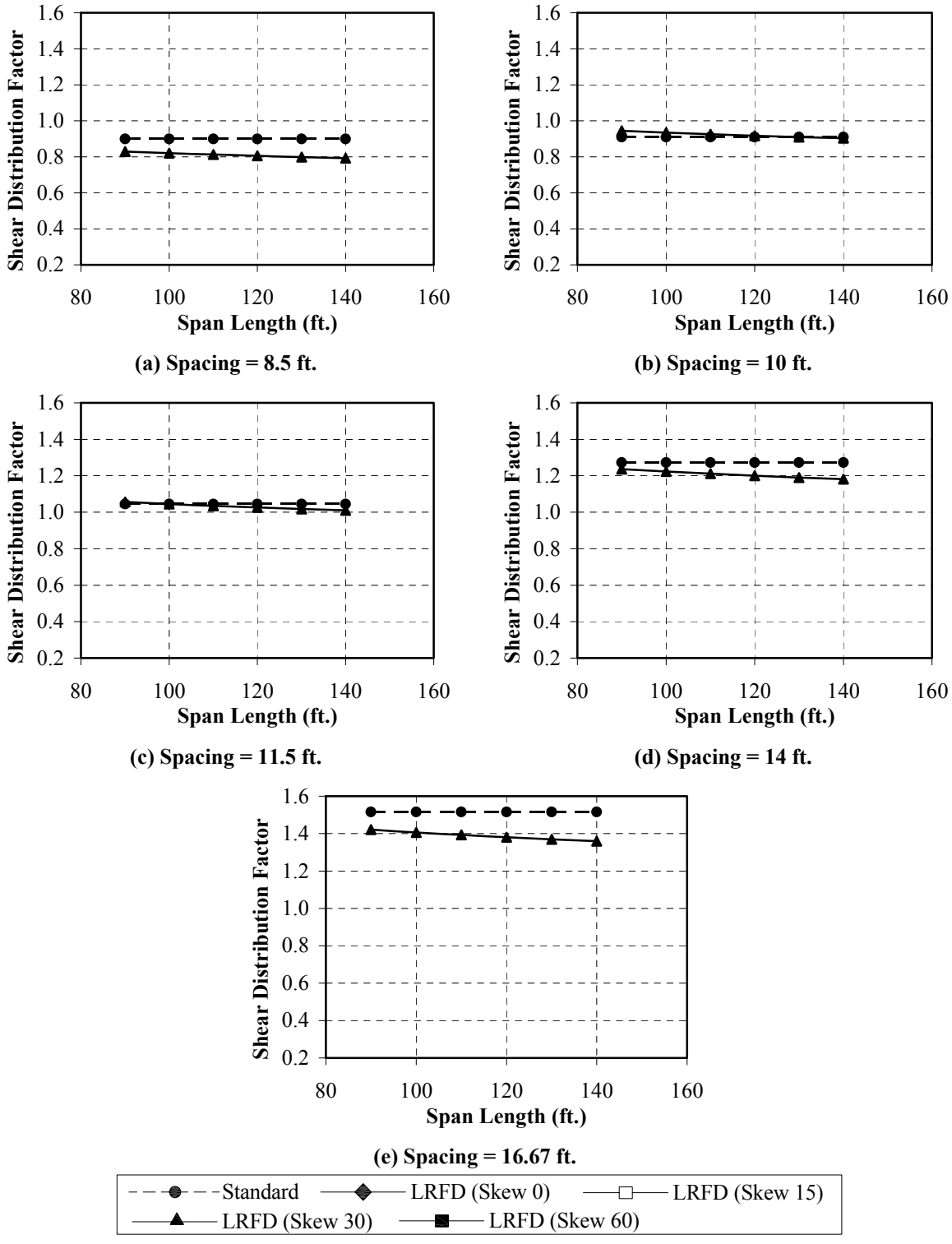


**Figure 4.2 Comparison of Live Load Distribution Factor for Shear.**

### 4.2.3 Undistributed Live Load Moment and Shear

#### *4.2.3.1 Undistributed Live Load Moment*

For simply supported bridge superstructures, the undistributed live load moment is calculated by placing the vehicular live load on a simply supported beam, such that a maximum response affect can be obtained. The LRFD Specifications has introduced a new live load model, HL93, which is heavier than its predecessor, HS20-44, as used in the Standard Specifications. The undistributed live load moment solely depends on the bridge span length and position of the live load. The LRFD Specifications give larger estimate of undistributed live load moment as shown in Figure 4.3, when compared to that of the Standard Specifications. When undistributed live load moment is calculated by LRFD Specifications, it increases from 778.6 k-ft to 1884.5 k-ft (47.1 to 70.8 percent) relative to the Standard Specifications.

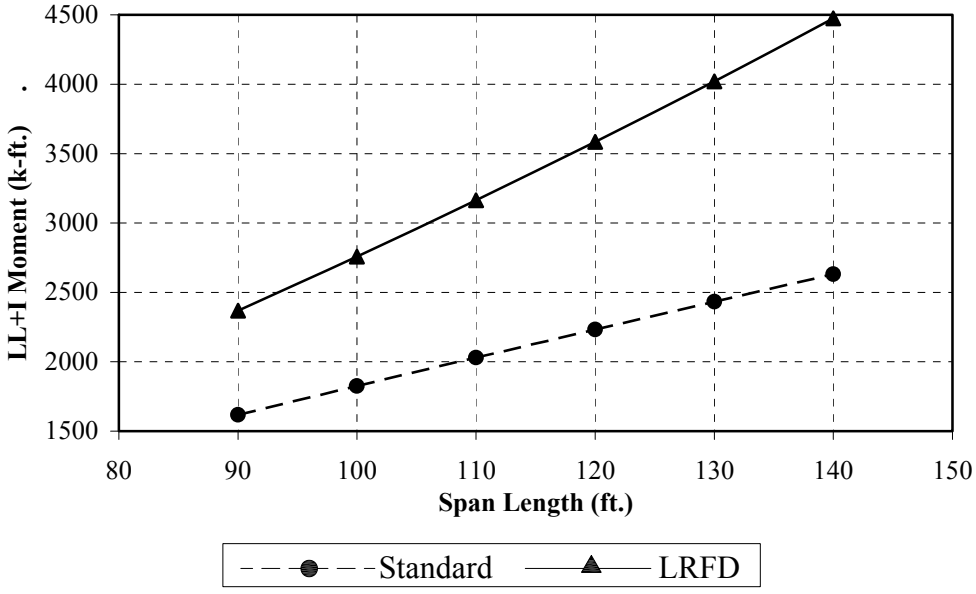


**Figure 4.3 Comparison of Undistributed Live Load Moment.**

The truck plus lane load combination as compared to tandem plus lane load combination in HL93 live load model and the truck load as compared to the lane load in

HS20-44 live load model always controls for the span range considered in this study. The detailed results are outlined in Appendix A.

#### *4.2.3.2 Undistributed Live Load Shear and Critical Section Location*

**Critical Section for Shear**

The critical section for shear varies significantly from the Standard to the LRFD Specifications. For the Standard Specifications the critical section is constant and is located at a distance $h/2$ (where $h$ is the total height of the composite girder section) from the end of the beam, where in the LRFD Specifications the critical section is calculated by an iterative procedure. For all the bridges considered in this study, the critical section in Standard Specifications is 2.583 ft. from the end of the beam, where in the LRFD Specifications the critical section location varies from 5.03 ft. to 6.04 ft. from the end of the beam for both the strand diameters of 0.5 in. and 0.6 in. The strand diameter has a very insignificant affect on the overall range of the critical section location. In general, the critical section location reduces with the increasing spacing, and for a particular spacing the critical section location is largest for short and long spans, and smallest for the medium spans considered in this study.

**Undistributed Live Load Shear**

Figure 4.4 shows the plots for undistributed live load shear force for the actual critical section location and actual possible span lengths for a particular spacing and the detailed results are outlined in Appendix A. When the LRFD Specifications results are viewed in isolation, the variation in the undistributed live load shear force due to skew angle and the spacing is negligible, as can be seen in Figure 4.4 that the shear force plot for all the skew angles is superimposed on each other and similarly the undistributed live load shear force values change very insignificantly due to change in spacings. This negligible change in the LRFD Specifications results due to varying skew and spacing can be explained by the fact that the critical section at which the undistributed shear is

calculated is changing in the range of 5.03 ft. to 6.04 ft for the set of bridge superstructures considered in this study. The undistributed shear force calculated in the LRFD Specifications increases by 27 kips to 43.5 kips (35 to 55.6 percent) relative to the Standard Specifications.

### 4.2.4 Distributed Live Load Moment and Shear

#### *4.2.4.1 Distributed Live Load Moment*

A distributed live load moment results when an undistributed live load moment is multiplied with the corresponding distribution factor and skew correction factors and distributed to an individual bridge girder. Figure 4.5 and Table 4.4 shows the range of difference in distributed live load shear for the LRFD relative to the Standard Specifications and for the spacing 16.67 ft. the Standard Specifications give a slightly larger estimate. For the skew angles of 0 and 15 degree, the distributed live load moment comparison follows a similar trend and the LRFD moment increases up to 386.6 k-ft (16 percent) and decreases up to 117.5 k-ft (4.7 percent) relative to that of the Standard moment. For the 30 degree skew angle, the distributed live load moment increases up to 121.8 k-ft (5 percent) and decreases up to 358.3 k-ft (12.2 percent). For the 60 degree skew angle, the distributed live load moment decreases in the range of 467.7 to 1526.3 k-ft (28.4 to 40.2 percent).

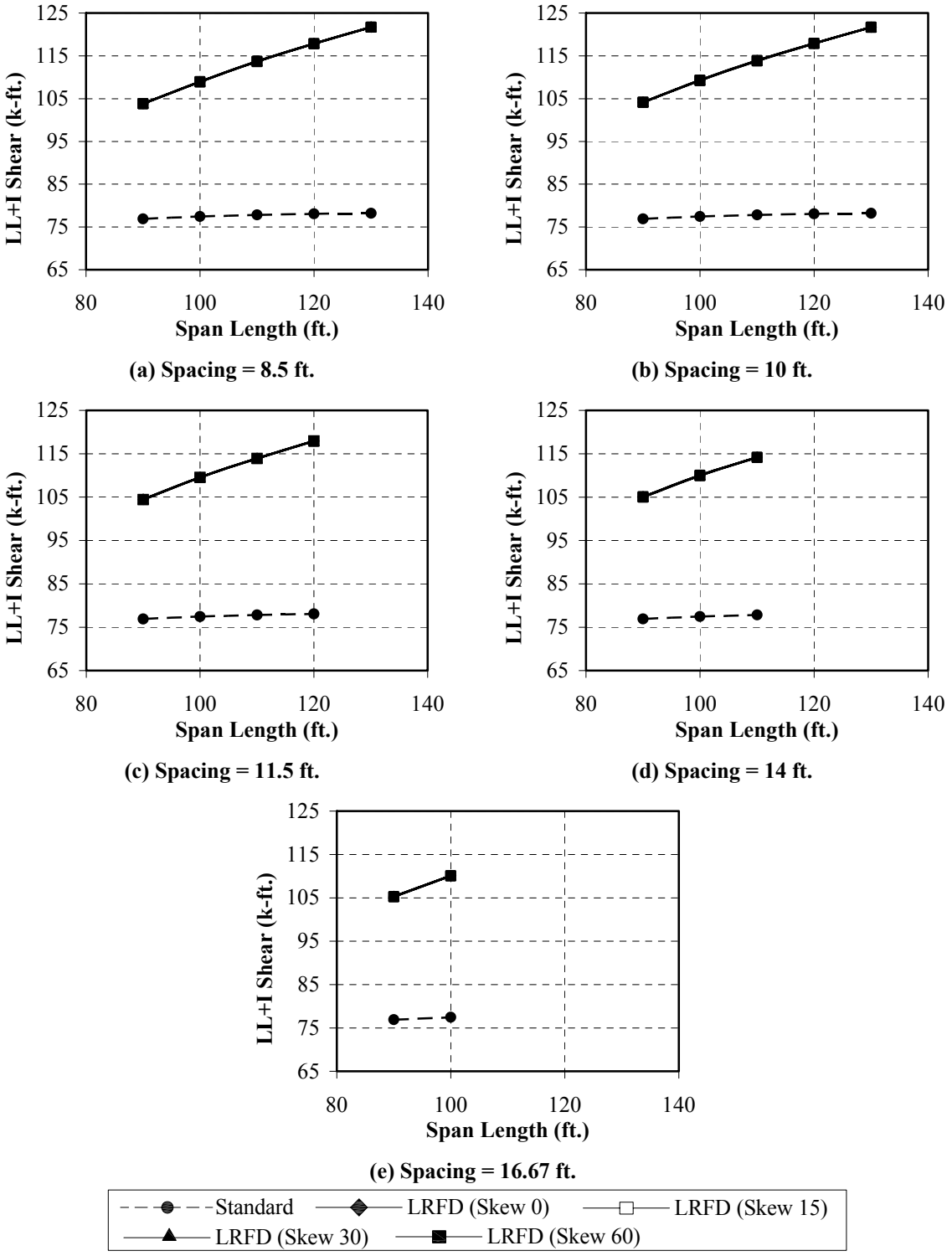


**Figure 4.4 Comparison of Undistributed Live Load Shear Force at Critical Section.**

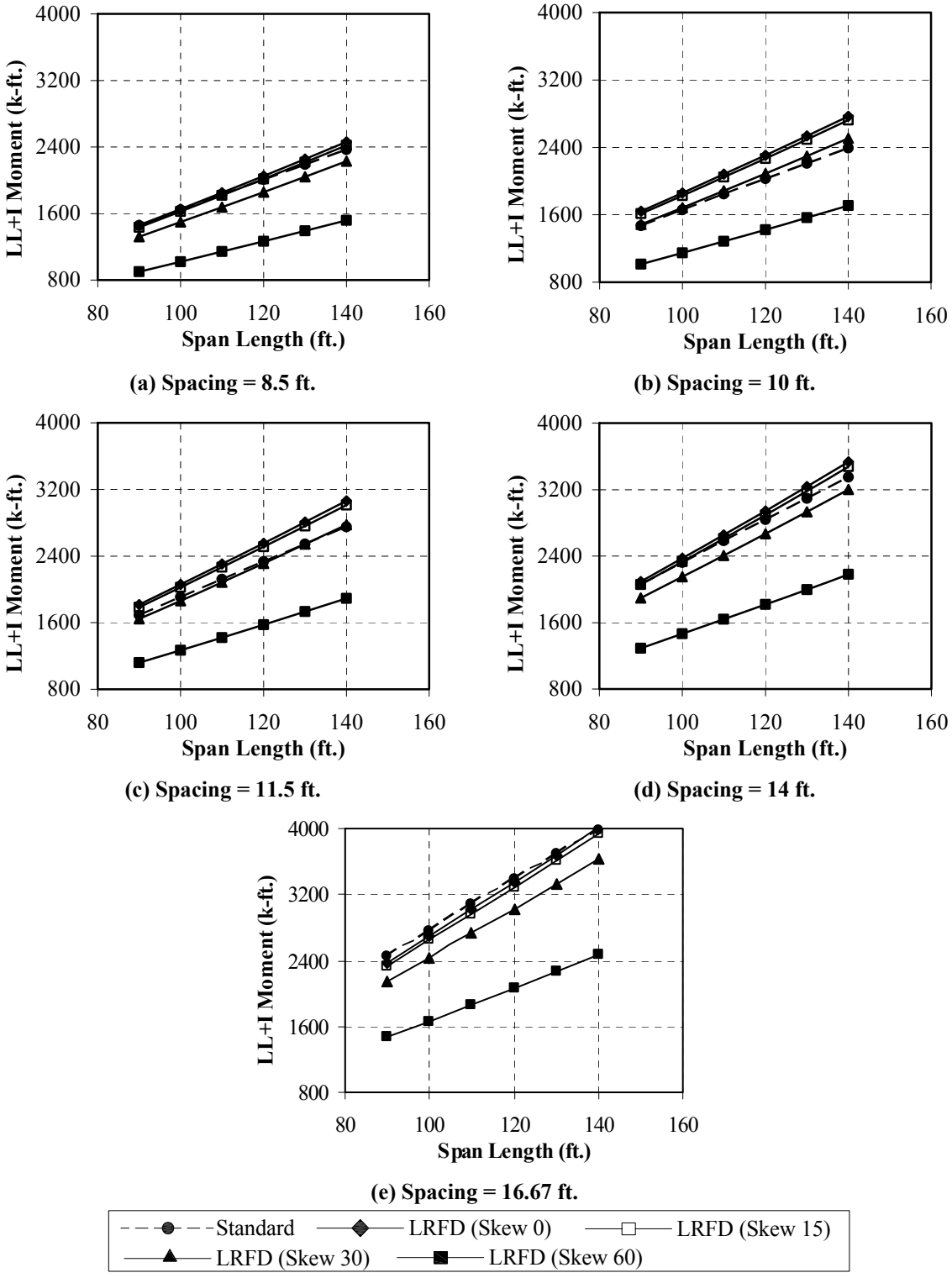


**Figure 4.5 Comparison of Distributed Live Load Moment.**

**Table 4.4 Comparison of Distributed Live Load Moments**

| Spacing (ft.) | Span (ft.) | All Skews | Skew = 0 | | Skew = 15 | | Skew = 30 | | Skew = 60 | |
|---|---|---|---|---|---|---|---|---|---|---|
| | | Moment (k-ft) | Moment (k-ft) | % Diff. w.r.t STD | Moment (k-ft) | % Diff. w.r.t STD | Moment (k-ft) | % Diff. w.r.t STD | Moment (k-ft) | % Diff. w.r.t STD |
| | | STD | LRFD | | LRFD | | LRFD | | LRFD | |
| 8.50 | 90 | 1486.3 | 1489.1 | 0.2 | 1463.8 | -1.5 | 1348.6 | -9.3 | 918.8 | -38.2 |
| | 100 | 1671.9 | 1684.0 | 0.7 | 1655.4 | -1.0 | 1525.2 | -8.8 | 1039.0 | -37.9 |
| | 110 | 1855.4 | 1881.8 | 1.4 | 1849.8 | -0.3 | 1704.3 | -8.1 | 1161.0 | -37.4 |
| | 120 | 2037.2 | 2082.8 | 2.2 | 2047.4 | 0.5 | 1886.3 | -7.4 | 1285.0 | -36.9 |
| | 130 | 2217.4 | 2287.1 | 3.1 | 2248.3 | 1.4 | 2071.4 | -6.6 | 1411.1 | -36.4 |
| | 140 | 2396.2 | 2495.0 | 4.1 | 2452.6 | 2.4 | 2259.6 | -5.7 | 1539.4 | -35.8 |
| 10.00 | 90 | 1501.3 | 1675.3 | 11.6 | 1646.9 | 9.7 | 1517.3 | 1.1 | 1033.7 | -31.2 |
| | 100 | 1688.8 | 1894.6 | 12.2 | 1862.4 | 10.3 | 1715.9 | 1.6 | 1168.9 | -30.8 |
| | 110 | 1874.1 | 2117.1 | 13.0 | 2081.2 | 11.0 | 1917.4 | 2.3 | 1306.2 | -30.3 |
| | 120 | 2057.8 | 2343.2 | 13.9 | 2303.4 | 11.9 | 2122.2 | 3.1 | 1445.7 | -29.7 |
| | 130 | 2239.8 | 2573.1 | 14.9 | 2529.4 | 12.9 | 2330.4 | 4.0 | 1587.6 | -29.1 |
| | 140 | 2420.5 | 2807.0 | 16.0 | 2759.3 | 14.0 | 2542.2 | 5.0 | 1731.9 | -28.4 |
| 11.50 | 90 | 1726.5 | 1854.0 | 7.4 | 1822.5 | 5.6 | 1679.1 | -2.7 | 1143.9 | -33.7 |
| | 100 | 1942.1 | 2096.6 | 8.0 | 2061.0 | 6.1 | 1898.8 | -2.2 | 1293.6 | -33.4 |
| | 110 | 2155.3 | 2342.9 | 8.7 | 2303.1 | 6.9 | 2121.9 | -1.5 | 1445.5 | -32.9 |
| | 120 | 2366.4 | 2593.1 | 9.6 | 2549.0 | 7.7 | 2348.5 | -0.8 | 1599.9 | -32.4 |
| | 130 | 2575.8 | 2847.5 | 10.5 | 2799.1 | 8.7 | 2578.9 | 0.1 | 1756.9 | -31.8 |
| | 140 | 2783.5 | 3106.3 | 11.6 | 3053.6 | 9.7 | 2813.3 | 1.1 | 1916.6 | -31.1 |
| 14.00 | 90 | 2101.9 | 2138.2 | 1.7 | 2101.9 | 0.0 | 1936.5 | -7.9 | 1319.2 | -37.2 |
| | 100 | 2364.3 | 2418.0 | 2.3 | 2377.0 | 0.5 | 2189.9 | -7.4 | 1491.9 | -36.9 |
| | 110 | 2623.8 | 2702.0 | 3.0 | 2656.1 | 1.2 | 2447.1 | -6.7 | 1667.1 | -36.5 |
| | 120 | 2880.9 | 2990.6 | 3.8 | 2939.8 | 2.0 | 2708.4 | -6.0 | 1845.1 | -36.0 |
| | 130 | 3135.7 | 3284.0 | 4.7 | 3228.2 | 2.9 | 2974.2 | -5.2 | 2026.2 | -35.4 |
| | 140 | 3388.6 | 3582.5 | 5.7 | 3521.6 | 3.9 | 3244.5 | -4.3 | 2210.4 | -34.8 |
| 16.67 | 90 | 2502.7 | 2426.6 | -3.0 | 2385.4 | -4.7 | 2197.7 | -12.2 | 1497.2 | -40.2 |
| | 100 | 2815.2 | 2744.2 | -2.5 | 2697.6 | -4.2 | 2485.4 | -11.7 | 1693.2 | -39.9 |
| | 110 | 3124.2 | 3066.5 | -1.8 | 3014.5 | -3.5 | 2777.3 | -11.1 | 1892.0 | -39.4 |
| | 120 | 3430.3 | 3394.0 | -1.1 | 3336.4 | -2.7 | 3073.8 | -10.4 | 2094.1 | -39.0 |
| | 130 | 3733.7 | 3727.0 | -0.2 | 3663.7 | -1.9 | 3375.4 | -9.6 | 2299.5 | -38.4 |
| | 140 | 4034.9 | 4065.8 | 0.8 | 3996.7 | -0.9 | 3682.3 | -8.7 | 2508.6 | -37.8 |

#### *4.2.4.2 Distributed Live Load Shear*

Table 4.5 shows the maximum and minimum range of difference in distributed live load shear for the LRFD relative to the Standard Specifications. As mentioned earlier that the LRFD Specifications provide the skew correction factor for shear only for the exterior girders, while this study focuses on the interior girders. Therefore, as it is evident from Table 4.5 and Figure 4.6 that skew does not affect the shear force in the girders. Moreover, the live load shear forces are also found to be insensitive to the strand diameter. In Figure 4.6, the distributed live load shear force is calculated at the critical section location for each specification and is plotted for the actual possible span lengths. The distributed live load shear, as calculated in the LRFD Specifications, increases by 16.9 to 39.6 kips (24.5 to 55.7 percent) for all the spacings considered.

**Table 4.5 Range of Difference in Distributed Live Load Shear for LRFD Relative to Standard Specifications**

| Girder Spacing (ft.) | Difference (kips) | Difference (%) |
|---|---|---|
| 8.50 | 26.9 to 16.9 | 38.2 to 24.5 |
| 10.00 | 39.6 to 28.5 | 55.7 to 40.8 |
| 11.50 | 39.4 to 29.9 | 48.3 to 37.3 |
| 14.00 | 39.3 to 32.1 | 39.7 to 32.8 |
| 16.67 | up to 37.6 | up to 32 |

### 4.2.5 Comparison of Undistributed Dynamic Load Moment and Shear

The LRFD Specifications recommend the use of 33 percent of the total undistributed live load as the dynamic load, while the Standard Specifications give a relation to calculate the dynamic load allowance factor (known as impact factor in the Standard Specifications), which is then multiplied with the total undistributed live load to get the dynamic load. The impact factor in the Standard Specifications ranges from 23.3 percent to 18.9 percent as compared to 33 percent in the LRFD Specifications as shown in Table 4.6 and Figure 4.7.

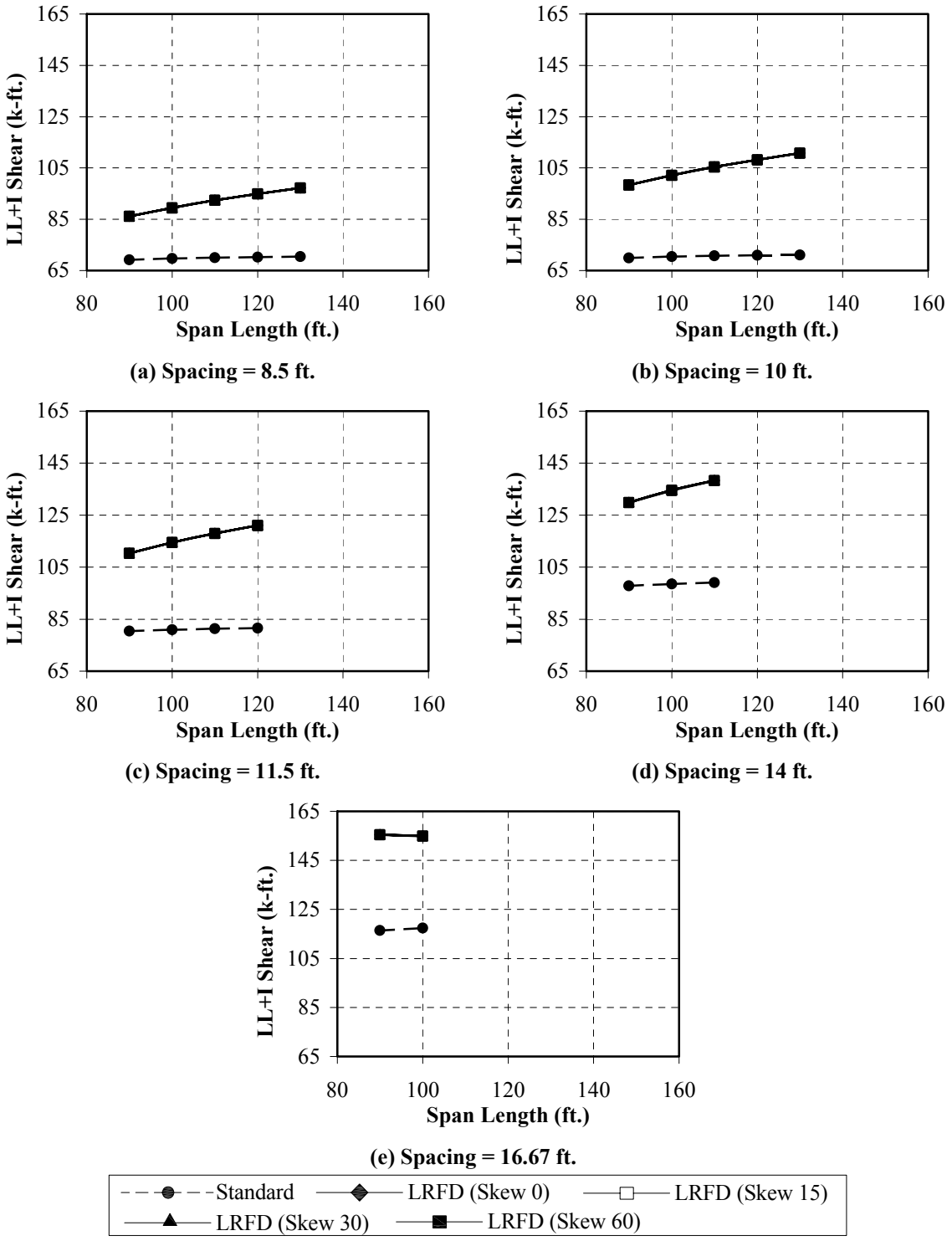


**Figure 4.6 Comparison of Distributed Live Load Shear Force at Critical Section.**

There is a significant increase in the dynamic load moment from 310 to 125.5 k-ft. (73.9 to 40.8 percent) and dynamic load shear force also increases in the range of 8.0 to 5.1 kips (62.1 to 34.9 percent). A trend in the change in dynamic load shear with respect to the span length can be observed in Figure 4.8. For the LRFD Specifications the dynamic load shear increases with respect to the span length, while for the Standard Specifications the dynamic load shear decreases with respect to the span length. The reason for this trend is that the impact factor in the Standard Specifications decreases with the span length as compared to the LRFD Specifications where it is constant.

**Table 4.6 Range of Difference in Undistributed Dynamic Load Moment and Shear for LRFD Relative to Standard Specifications**

| Girder Spacing (ft.) | Shear | | Moment | |
|---|---|---|---|---|
| | Difference (kips) | Difference (%) | Difference (kips) | Difference (%) |
| 8.50 | 8.0 to 5.1 | 62.1 to 34.9 | 310.0 to 125.5 | 73.9 to 40.8 |
| 10.00 | | | | |
| 11.50 | 7.4 to 5.2 | 55.6 to 35.6 | | |
| 14.00 | 6.8 to 5.3 | 49.5 to 36.3 | | |
| 16.67 | 6.1 to 5.3 | 43.1 to 36.3 | | |

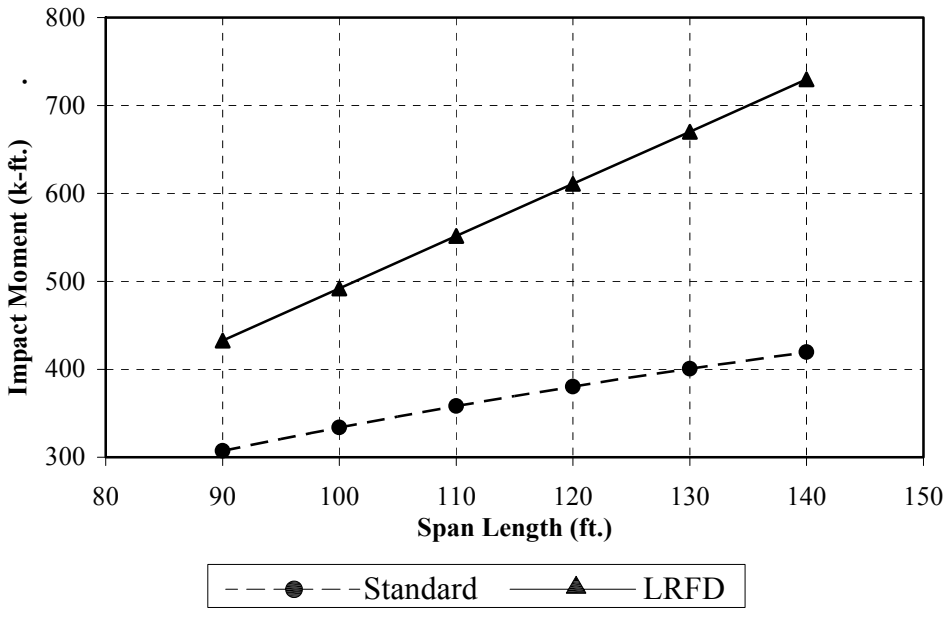


**Figure 4.7 Comparison of Undistributed Dynamic Load Moment at Midspan.**

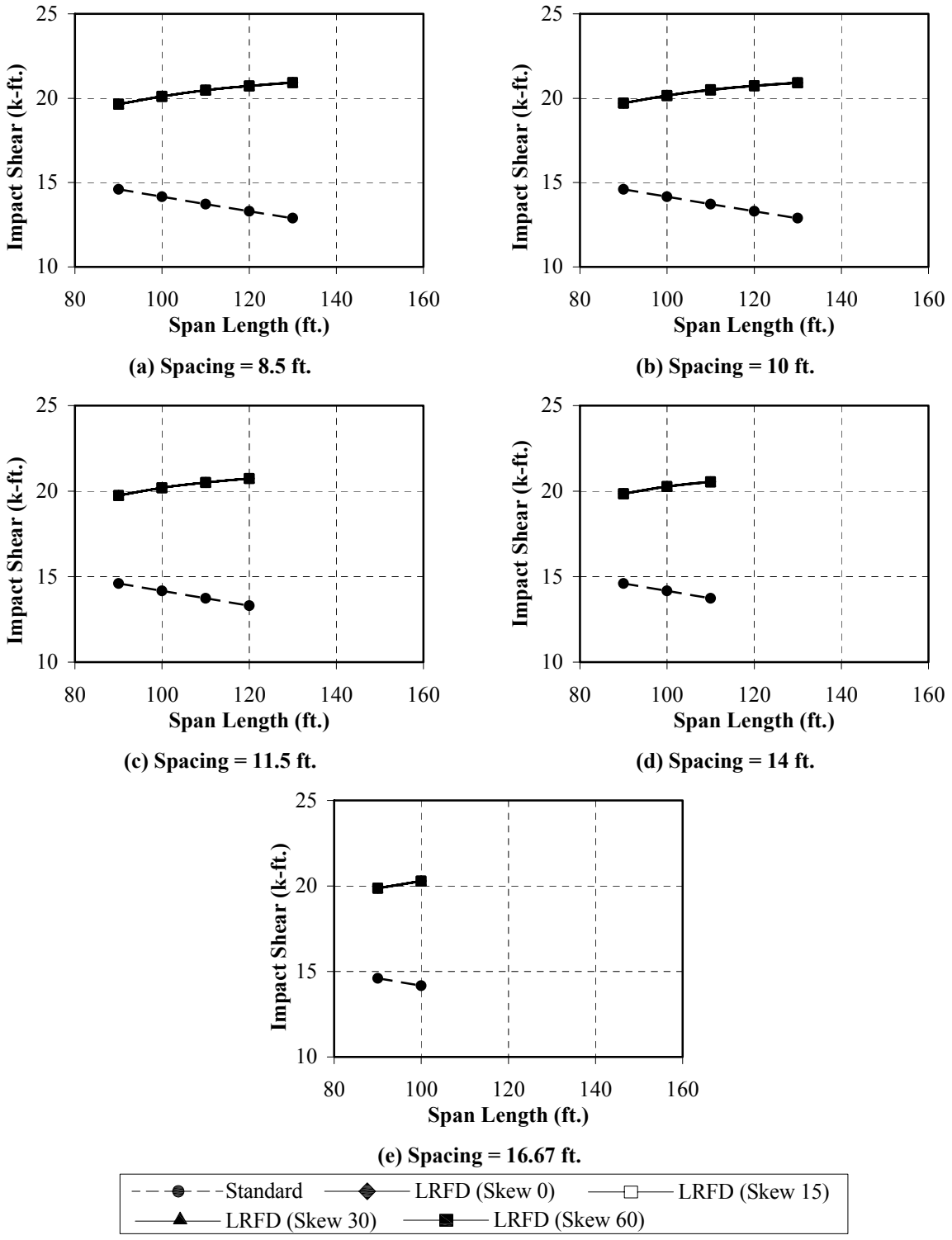


**Figure 4.8 Comparison of Undistributed Dynamic Load Shear Force at Critical Section.**

## 4.3 SERVICE LOAD DESIGN

### 4.3.1 General

The impact of the AASHTO LRFD Specifications on the service load design for flexure is discussed in this section. The effect on the maximum span length capability, required number of strands, initial and final prestress losses, and the required concrete strengths at service and at release is presented in graphical and tabular format. In general, the designs based on the LRFD were able to achieve a higher span length with lesser number of strands, lesser prestress losses, and lower concrete strengths. A decrease in the live load moments and a different live load factor in service limit is the reason for such a trend.

### 4.3.2 Maximum Span Lengths

Tables 4.7 and 4.8 show the comparison of possible maximum span lengths for the LRFD and the Standard Specifications for the skew angles of 0, 15, 30 and 60 degree, and for 0.5 and 0.6 in. diameter strands, respectively. The required number of strands is also mentioned for each design case. In these tables, when only the comparison for 0 degree skew is considered, it is obvious that sometimes for equal number of strands and sometimes for lesser number of strands, the LRFD Specifications designs can span slightly longer, ranging from 1.5 to 7.5 ft. The plots in Figure 4.9 show that for larger spacings the difference of maximum span lengths between the LRFD and the Standard Specifications increase.

Table 4.9 shows the range of maximum differences in maximum span lengths for the LRFD and the Standard Specifications, for both of 0.5 in. and 0.6 in. diameter strands. If the skew correction is taken into consideration and the comparison for maximum span length is made between the two specifications, then, based on Table 4.9

and Figure 4.9, it can be said that the overall increase in span capability ranges from 1.5 to 18.5 ft. (1.1 to 18.8 percent) and the maximum span length increases with the increase in the skew.

Some of the maximum span lengths are greater than 140 ft., which is one of the limits for the use of the LRFD Specifications live load distribution factor formulas. There are only two such cases, both for 8.5 ft. spacing and 60 degree skew, for strand diameters 0.5 and 0.6 in. For the purpose of parametric study, this LRFD live load distribution factor limit is neglected and the distribution factor for moment and shear is calculated using the same formulas. The distribution factor for these two cases will be checked by performing refined analysis in section 5.

**Table 4.7 Maximum Differences in Maximum Span Lengths of LRFD Designs Relative to Standard Designs**

| Girder Spacing (ft.) | Strand Diameter = 0.5 in. | | Strand Diameter = 0.6 in. | |
|---|---|---|---|---|
| | Skew (degrees) | | Skew (degrees) | |
| | 0, 15, 30 | 60 | 0, 15, 30 | 60 |
| 8.5 | 1.5 ft. to 3.5 ft. | 10 ft. | 2 ft. to 4 ft. | 10 ft. |
| | (1.1% to 2.6%) | 7.4% | (1.5% to 3%) | 7.4% |
| 10.0 | 0.5 ft. to 3 ft. | 9 ft. | 0 ft. to 1.5 ft. | 8.0 ft. |
| | (0.4% to 2.3%) | 6.9% | (0% to 1.2%) | 6.2% |
| 11.5 | 1.5 ft. to 3.5 ft. | 10.0 ft. | 0 ft. to 2 ft. | 9 ft. |
| | (1.2% to 2.8%) | 8.1% | (0% to 1.6%) | 7.3% |
| 14.0 | 2.5 ft. to 5 ft. | 10.5 ft. | 3.5 ft. to 5 ft. | 11.5 ft. |
| | (2.2% to 4.4%) | 9.3% | (3.1% to 4.5%) | 10.3% |
| 16.7 | 4.5 ft. to 6.5 ft. | 12.5 ft. | 7.5 ft. to 11.5 ft. | 18.5 ft. |
| | (4.3% to 6.2%) | 12.0% | (7.6% to 11.7%) | 18.8% |

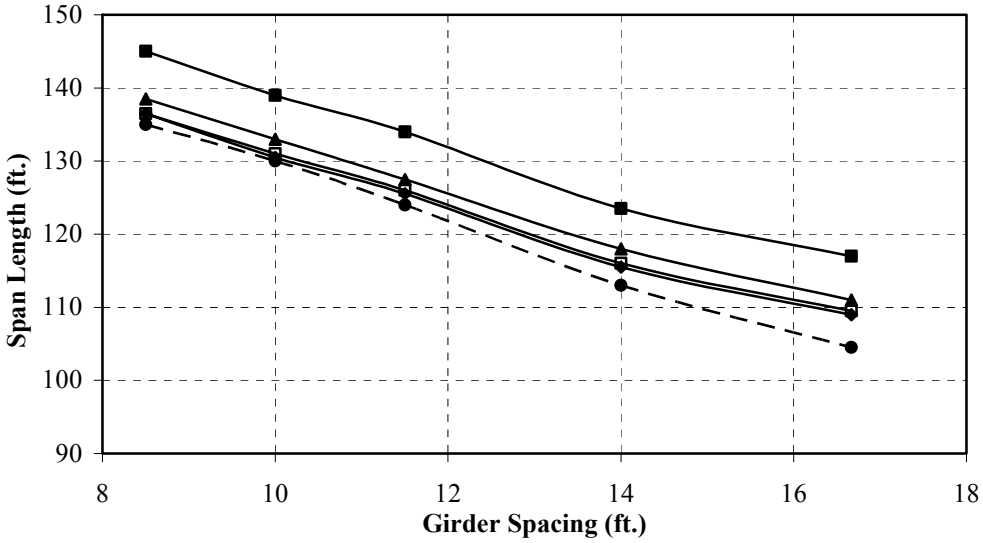


**(a) Strand Diameter = 0.5 in.**

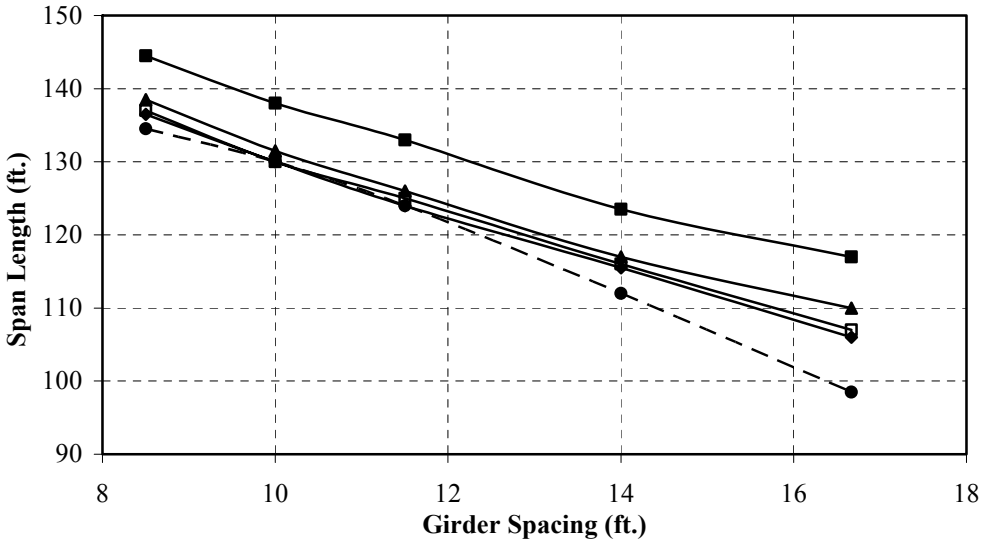


**(b) Strand Diameter = 0.6 in.**


**Figure 4.9 Maximum Span Length versus Girder Spacing for U54 Beam.**

**Table 4.8 Comparison of Maximum Span Lengths (Strand Diameter = 0.5 in.)**

| Skew | Girder Spacing (ft.) | Standard | | LRFD | | Span Diff. w.r.t. STD ft. (%) |
|---|---|---|---|---|---|---|
| | | Max. Span (ft.) | No. Strands | Max. Span (ft.) | No. Strands | |
| 0 | 8.5 | 135.0 | 89 | 136.5 | 89 | 1.5 (1.1) |
| | 10.0 | 130.0 | 87 | 130.5 | 89 | 0.5 (0.4) |
| | 11.5 | 124.0 | 87 | 125.5 | 89 | 1.5 (1.2) |
| | 14.0 | 113.0 | 87 | 115.5 | 87 | 2.5 (2.2) |
| | 16.7 | 104.5 | 85 | 109.0 | 87 | 4.5 (4.3) |
| 15 | 8.5 | 135.0 | 89 | 136.5 | 89 | 1.5 (1.1) |
| | 10.0 | 130.0 | 87 | 131.0 | 89 | 1.0 (0.8) |
| | 11.5 | 124.0 | 87 | 126.0 | 89 | 2.0 (1.6) |
| | 14.0 | 113.0 | 87 | 116.0 | 87 | 3.0 (2.7) |
| | 16.7 | 104.5 | 85 | 109.5 | 87 | 5.0 (4.8) |
| 30 | 8.5 | 135.0 | 89 | 138.5 | 89 | 3.5 (2.6) |
| | 10.0 | 130.0 | 87 | 133.0 | 91 | 3.0 (2.3) |
| | 11.5 | 124.0 | 87 | 127.5 | 89 | 3.5 (2.8) |
| | 14.0 | 113.0 | 87 | 118.0 | 89 | 5.0 (4.4) |
| | 16.7 | 104.5 | 85 | 111.0 | 87 | 6.5 (6.2) |
| 60 | 8.5 | 135.0 | 89 | 145.0 | 89 | 10.0 (7.4) |
| | 10.0 | 130.0 | 87 | 139.0 | 89 | 9.0 (6.9) |
| | 11.5 | 124.0 | 87 | 134.0 | 89 | 10.0 (8.1) |
| | 14.0 | 113.0 | 87 | 123.5 | 87 | 10.5 (9.3) |
| | 16.7 | 104.5 | 85 | 117.0 | 87 | 12.5 (12.0) |

**Table 4.9 Comparison of Maximum Span Lengths (Strand Diameter = 0.6 in.)**

| Skew | Girder Spacing (ft.) | Standard | | LRFD | | Span Diff. w.r.t. STD ft. (%) |
|---|---|---|---|---|---|---|
| | | Max. Span (ft.) | No. Strands | Max. Span (ft.) | No. Strands | |
| 0 | 8.5 | 134.5 | 60 | 136.5 | 60 | 2.0 (1.5) |
| | 10.0 | 130.0 | 60 | 130.0 | 60 | 0.0 (0.0) |
| | 11.5 | 124.0 | 60 | 124.0 | 60 | 0.0 (0.0) |
| | 14.0 | 112.0 | 58 | 115.5 | 60 | 3.5 (3.1) |
| | 16.7 | 98.5 | 51 | 106.0 | 56 | 7.5 (7.6) |
| 15 | 8.5 | 134.5 | 60 | 137.0 | 60 | 2.5 (1.9) |
| | 10.0 | 130.0 | 60 | 130.0 | 60 | 0.0 (0.0) |
| | 11.5 | 124.0 | 60 | 125.0 | 60 | 1.0 (0.8) |
| | 14.0 | 112.0 | 58 | 116.0 | 60 | 4.0 (3.6) |
| | 16.7 | 98.5 | 51 | 107.0 | 56 | 8.5 (8.6) |
| 30 | 8.5 | 134.5 | 60 | 138.5 | 60 | 4.0 (3.0) |
| | 10.0 | 130.0 | 60 | 131.5 | 60 | 1.5 (1.2) |
| | 11.5 | 124.0 | 60 | 126.0 | 60 | 2.0 (1.6) |
| | 14.0 | 112.0 | 58 | 117.0 | 60 | 5.0 (4.5) |
| | 16.7 | 98.5 | 51 | 110.0 | 58 | 11.5 (11.7) |
| 60 | 8.5 | 134.5 | 60 | 144.5 | 60 | 10.0 (7.4) |
| | 10.0 | 130.0 | 60 | 138.0 | 60 | 8.0 (6.2) |
| | 11.5 | 124.0 | 60 | 133.0 | 60 | 9.0 (7.3) |
| | 14.0 | 112.0 | 58 | 123.5 | 60 | 11.5 (10.3) |
| | 16.7 | 98.5 | 51 | 117.0 | 60 | 18.5 (18.8) |

### 4.3.3 Number of Strands

Tables 4.10 through 4.14 show the differences in the number of strands required for span lengths from 90 ft. to the maximum spans designed under the LRFD and the Standard Specifications for 0.5 in. diameter strands and for 0.6 in. diameter strands the similar tables are shown in Appendix A. Each table shows the designs for different girder spacing. The difference in the number of strands for maximum spans is not reported since the number of strands for different spans cannot be compared.

The general trend is that the LRFD designs required fewer numbers of strands than for the designs based on the Standard Specifications. The number of strands for LRFD designs decreases with the increase in spacing, span or skew angle relative to the designs based on the Standard Specifications. For the skew angles of 0, 15 and 30 degree and for girder spacings less than or equal to 11.5 ft., the LRFD designs required between one to 6 fewer strands and for girder spacings greater than 11.5 ft., the LRFD designs required between one to 10 fewer strands relative to the designs based on the Standard Specifications. There is significant drop in the number of strands required by the LRFD designs relative to those of the Standard designs for the 60 degree skew and the reason for this is that the flexural demand reduces significantly in this case. For the 60 degree skew and for girder spacings less than or equal to 11.5 ft., the LRFD designs required between 4 to 14 fewer strands and for girder spacings greater than 11.5 ft., the LRFD designs required between 12 to 18 fewer strands relative to the designs based on the Standard Specifications.

The effect of the 0.8 live load reduction factor included in the LRFD Service III limit state compared to the 1.0 live load reduction factor in the Standard Specifications should result in a reduction of strands required for the same load requirements. Although, the LRFD Specifications provide for a heavier live load but the final distributed moment is less than that of the Standard Specifications, as explained in Section 4.2.4.

**Table 4.10 Comparison of Number of Strands**
**(Strand Diameter = 0.5 in., Girder Spacing = 8.5 ft.)**

| Skew | Standard | | LRFD | | Difference in No. of Strands |
|---|---|---|---|---|---|
| | Span Length (ft.) | No. of Strands | Span Length (ft.) | No. of Strands | |
| 0 | 90 | 35 | 90 | 31 | -4 |
| | 100 | 43 | 100 | 41 | -2 |
| | 110 | 53 | 110 | 51 | -2 |
| | 120 | 66 | 120 | 64 | -2 |
| | 130 | 80 | 130 | 78 | -2 |
| | 135 | 89 | 136.5 | 89 | - |
| 15 | 90 | 35 | 90 | 31 | -4 |
| | 100 | 43 | 100 | 41 | -2 |
| | 110 | 53 | 110 | 51 | -2 |
| | 120 | 66 | 120 | 62 | -4 |
| | 130 | 80 | 130 | 78 | -2 |
| | 135 | 89 | 136.5 | 89 | - |
| 30 | 90 | 35 | 90 | 31 | -4 |
| | 100 | 43 | 100 | 39 | -4 |
| | 110 | 53 | 110 | 49 | -4 |
| | 120 | 66 | 120 | 60 | -6 |
| | 130 | 80 | 130 | 76 | -4 |
| | 135 | 89 | 138.5 | 89 | - |
| 60 | 90 | 35 | 90 | 27 | -8 |
| | 100 | 43 | 100 | 35 | -8 |
| | 110 | 53 | 110 | 45 | -8 |
| | 120 | 66 | 120 | 54 | -12 |
| | 130 | 80 | 130 | 66 | -14 |
| | 135 | 89 | 140 | 80 | - |
| | - | - | 145 | 89 | - |

**Table 4.11 Comparison of Number of Strands**
**(Strand Diameter = 0.5 in., Girder Spacing = 10 ft.)**

| Skew | Standard | | LRFD | | Difference in No. of Strands |
|---|---|---|---|---|---|
| | Span Length (ft.) | No. of Strands | Span Length (ft.) | No. of Strands | |
| 0 | 90 | 37 | 90 | 35 | -2 |
| | 100 | 47 | 100 | 47 | 0 |
| | 110 | 58 | 110 | 58 | 0 |
| | 120 | 72 | 120 | 72 | 0 |
| | 130 | 87 | 130 | 87 | 0 |
| | - | - | 130.5 | 89 | - |
| 15 | 90 | 37 | 90 | 35 | -2 |
| | 100 | 47 | 100 | 45 | -2 |
| | 110 | 58 | 110 | 58 | 0 |
| | 120 | 72 | 120 | 70 | -2 |
| | 130 | 87 | 130 | 87 | 0 |
| | - | - | 131 | 89 | - |
| 30 | 90 | 37 | 90 | 35 | -2 |
| | 100 | 47 | 100 | 45 | -2 |
| | 110 | 58 | 110 | 56 | -2 |
| | 120 | 72 | 120 | 68 | -4 |
| | 130 | 87 | 130 | 85 | -2 |
| | - | - | 133 | 91 | - |
| 60 | 90 | 37 | 90 | 31 | -6 |
| | 100 | 47 | 100 | 39 | -8 |
| | 110 | 58 | 110 | 49 | -9 |
| | 120 | 72 | 120 | 60 | -12 |
| | 130 | 87 | 130 | 74 | -13 |
| | - | - | 139 | 89 | - |

**Table 4.12 Comparison of Number of Strands**
**(Strand Diameter = 0.5 in., Girder Spacing = 11.5 ft.)**

| Skew | Standard | | LRFD | | Difference in No. of Strands |
|---|---|---|---|---|---|
| | Span Length (ft.) | No. of Strands | Span Length (ft.) | No. of Strands | |
| 0 | 90 | 41 | 90 | 39 | -2 |
| | 100 | 53 | 100 | 51 | -2 |
| | 110 | 66 | 110 | 64 | -2 |
| | 120 | 80 | 120 | 78 | -2 |
| | 124 | 87 | 125.5 | 89 | - |
| 15 | 90 | 41 | 90 | 39 | -2 |
| | 100 | 53 | 100 | 51 | -2 |
| | 110 | 66 | 110 | 62 | -4 |
| | 120 | 80 | 120 | 78 | -2 |
| | 124 | 87 | 126 | 89 | - |
| 30 | 90 | 41 | 90 | 37 | -4 |
| | 100 | 53 | 100 | 49 | -4 |
| | 110 | 66 | 110 | 60 | -6 |
| | 120 | 80 | 120 | 76 | -4 |
| | 124 | 87 | 127.5 | 89 | - |
| 60 | 90 | 41 | 90 | 33 | -8 |
| | 100 | 53 | 100 | 43 | -10 |
| | 110 | 66 | 110 | 53 | -13 |
| | 120 | 80 | 120 | 66 | -14 |
| | 124 | 87 | 130 | 83 | -4 |
| | - | - | 134 | 89 | - |

**Table 4.13 Comparison of Number of Strands**
**(Strand Diameter = 0.5 in., Girder Spacing = 14 ft.)**

| Skew | Standard | | LRFD | | Difference in No. of Strands |
|---|---|---|---|---|---|
| | Span Length (ft.) | No. of Strands | Span Length (ft.) | No. of Strands | |
| 0 | 90 | 51 | 90 | 51 | 0 |
| | 100 | 64 | 100 | 60 | -4 |
| | 110 | 81 | 110 | 76 | -5 |
| | 113 | 87 | 115.5 | 87 | - |
| 15 | 90 | 51 | 90 | 49 | -2 |
| | 100 | 64 | 100 | 60 | -4 |
| | 110 | 81 | 110 | 76 | -5 |
| | 113 | 87 | 116 | 87 | - |
| 30 | 90 | 51 | 90 | 45 | -6 |
| | 100 | 64 | 100 | 58 | -6 |
| | 110 | 81 | 110 | 74 | -7 |
| | 113 | 87 | 118 | 89 | - |
| 60 | 90 | 51 | 90 | 39 | -12 |
| | 100 | 64 | 100 | 51 | -13 |
| | 110 | 81 | 110 | 64 | -17 |
| | 113 | 87 | 120 | 81 | - |
| | - | - | 123.5 | 87 | - |

**Table 4.14 Comparison of Number of Strands**
**(Strand Diameter = 0.5 in., Girder Spacing = 16.67 ft.)**

| Skew | Standard | | LRFD | | Difference in No. of Strands |
|---|---|---|---|---|---|
| | Span Length (ft.) | No. of Strands | Span Length (ft.) | No. of Strands | |
| 0 | 100 | 76 | 100 | 70 | -6 |
| | 104.5 | 85 | 109 | 87 | - |
| 15 | 100 | 76 | 100 | 68 | -8 |
| | 104.5 | 85 | 109.5 | 87 | - |
| 30 | 100 | 76 | 100 | 66 | -10 |
| | 104.5 | 85 | 110 | 85 | - |
| | - | - | 111 | 87 | - |
| 60 | 100 | 76 | 100 | 58 | -18 |
| | 104.5 | 85 | 110 | 74 | - |
| | - | - | 117 | 87 | - |

### 4.3.4 Concrete Strengths Required at Release and at Service

#### *4.3.4.1 Concrete Strength at Release*

Figure 4.10 and Table 4.15 show the summary of comparison of concrete strengths at release ($f'_{ci}$), required for all the design cases considered in this study, for the LRFD and the Standard Specifications for strand diameter 0.5 in. The figure and table for the summary of comparison for strand diameter 0.6 in. are not shown in this section, because the trends were not different than those of strand diameter 0.5 in., and can be found in Appendix A.

**Table 4.15 Comparison of Initial Concrete Strength (Strand Diameter = 0.5 in.)**

| Spacing (ft.) | Span (ft.) | All Skews | Skew = 0 | | Skew = 15 | | Skew = 30 | | Skew = 60 | |
|---|---|---|---|---|---|---|---|---|---|---|
| | | $f'_{ci}$ (psi) | $f'_{ci}$ (psi) | % Diff. w.r.t STD | $f'_{ci}$ (psi) | % Diff. w.r.t STD | $f'_{ci}$ (psi) | % Diff. w.r.t STD | $f'_{ci}$ (psi) | % Diff. w.r.t STD |
| | | STD | LRFD | | LRFD | | LRFD | | LRFD | |
| 8.50 | 90 | 4000 | 4000 | 0.0 | 4000 | 0.0 | 4000 | 0.0 | 4000 | 0.0 |
| | 100 | 4000 | 4000 | 0.0 | 4000 | 0.0 | 4000 | 0.0 | 4000 | 0.0 |
| | 110 | 4080 | 4000 | -2.0 | 4000 | -2.0 | 4000 | -2.0 | 4000 | -2.0 |
| | 120 | 5072 | 4879 | -3.8 | 4719 | -7.0 | 4559 | -10.1 | 4077 | -19.6 |
| | 130 | 6132 | 5929 | -3.3 | 5929 | -3.3 | 5771 | -5.9 | 4977 | -18.8 |
| 10.00 | 90 | 4000 | 4000 | 0.0 | 4000 | 0.0 | 4000 | 0.0 | 4000 | 0.0 |
| | 100 | 4000 | 4000 | 0.0 | 4000 | 0.0 | 4000 | 0.0 | 4000 | 0.0 |
| | 110 | 4491 | 4464 | -0.6 | 4464 | -0.6 | 4303 | -4.2 | 4000 | -10.9 |
| | 120 | 5555 | 5514 | -0.7 | 5356 | -3.6 | 5197 | -6.4 | 4559 | -17.9 |
| | 130 | 6653 | 6598 | -0.8 | 6598 | -0.8 | 6460 | -2.9 | 5613 | -15.6 |
| 11.50 | 90 | 4000 | 4000 | 0.0 | 4000 | 0.0 | 4000 | 0.0 | 4000 | 0.0 |
| | 100 | 4152 | 4000 | -3.7 | 4000 | -3.7 | 4000 | -3.7 | 4000 | -3.7 |
| | 110 | 5140 | 4944 | -3.8 | 4784 | -6.9 | 4624 | -10.0 | 4058 | -21.1 |
| | 120 | 6196 | 5988 | -3.4 | 5988 | -3.4 | 5830 | -5.9 | 5038 | -18.7 |
| 14.00 | 90 | 4055 | 4029 | -0.6 | 4000 | -1.4 | 4000 | -1.4 | 4000 | -1.4 |
| | 100 | 5050 | 4693 | -7.1 | 4693 | -7.1 | 4533 | -10.2 | 4000 | -20.8 |
| | 110 | 6342 | 5894 | -7.1 | 5894 | -7.1 | 5736 | -9.6 | 4943 | -22.1 |
| 16.67 | 90 | 4498 | 4200 | -6.6 | 4200 | -6.6 | 4029 | -10.4 | 4000 | -11.1 |
| | 100 | 6013 | 5488 | -8.7 | 5329 | -11.4 | 5171 | -14.0 | 4533 | -24.6 |

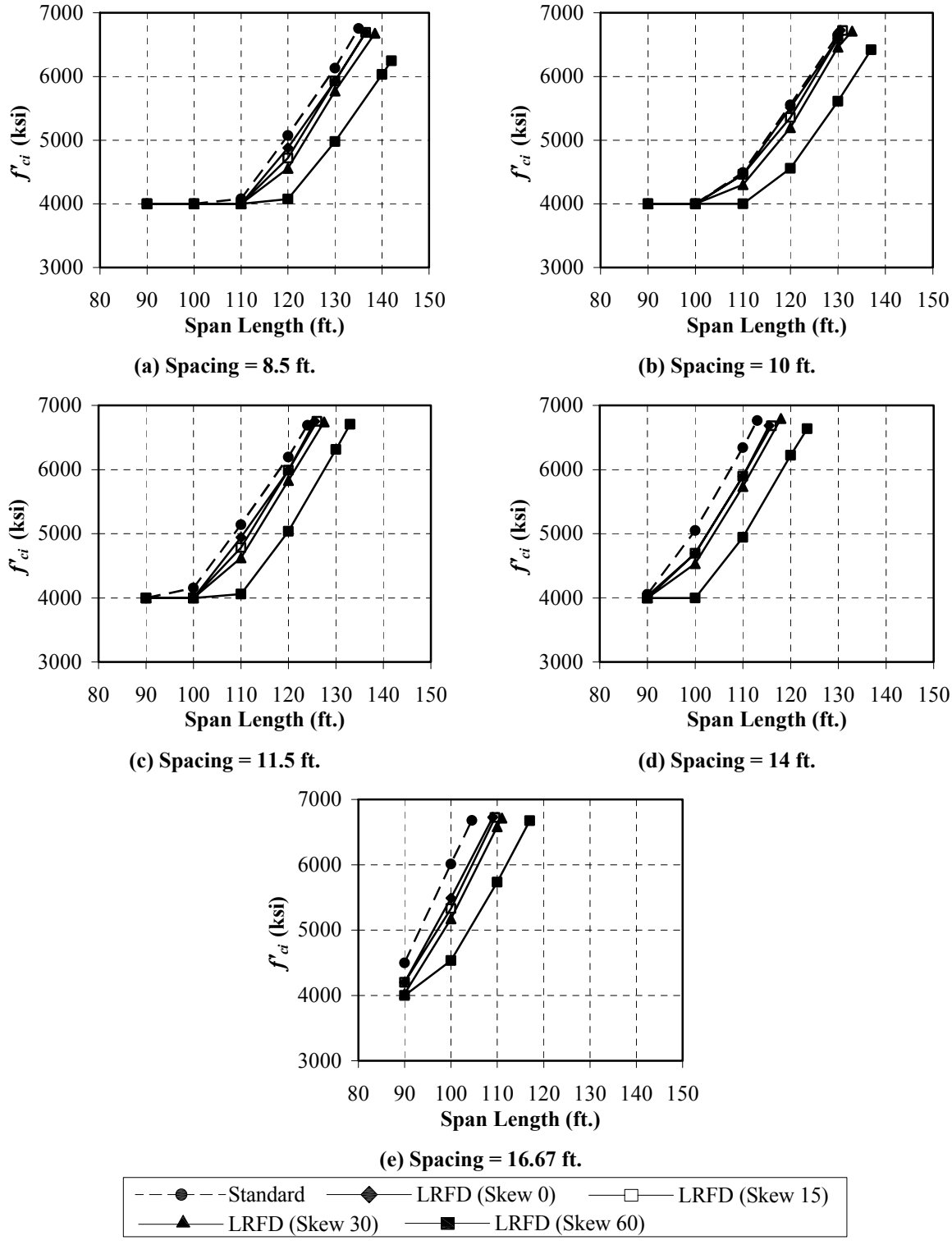


**Figure 4.10 Comparison of Initial Concrete Strength (Strand Diameter 0.5 in.).**

In general, relative to the Standard Specifications, the range of difference in $f'_{ci}$ decreases with the increase in spacing and span length. The designs based on the Standard Specifications give a larger estimate of $f'_{ci}$ as compared to those based on the LRFD Specifications and this difference increases with the increasing skew, as shown in Figure 4.10. For the 0, 15 and 30 degree skew, the difference in $f'_{ci}$ decreases in the range of 0 to 842 ksi (0 to 14 percent) and for 60 degree skew, the difference in $f'_{ci}$ decreases in the range of 0 to 1480 ksi (0 to 24.6 percent).

#### *4.3.4.2 Concrete Strength at Service*

Figure 4.11 and Table 4.16 show the summary of comparison of concrete strength at service ($f'_c$), required for all the design cases considered in this study, for the LRFD and the Standard Specifications for strand diameter 0.5 in. The figure and table for the summary of comparison for strand diameter 0.6 in. is not shown in this section, because the trends were not different than those of strand diameter 0.5 in., but can be found in Appendix A. Moreover, the detailed comparison of each design case is also included in the Appendix A.

In general, relative to the Standard Specifications, the decrease in range of difference in $f'_c$, with the increase in spacing and span length, remain more or less constant. The designs based on the Standard Specifications give a larger estimate of $f'_c$ as compared to those based on the LRFD Specifications and the skew angle does not affect the $f'_c$ value significantly, as shown in Figure 4.11. For the skew angles of 0, 15, 30 degree, the difference in $f'_c$ decreases in the range of 0 to 928 ksi (0 to 10.8 percent) and for 60 degree skew, the difference in $f'_c$ decreases in the range of 0 to 837 ksi (0 to 9.8 percent).

**Table 4.16 Comparison of Final Concrete Strengths Required for LRFD Relative to Standard Specifications (Strand Diameter = 0.5 in.)**

| Spacing (ft.) | Span (ft.) | All Skews | Skew = 0 | | Skew = 15 | | Skew = 30 | | Skew = 60 | |
|---|---|---|---|---|---|---|---|---|---|---|
| | | $f'_c$ (psi) | $f'_c$ (psi) | % Diff. w.r.t STD | $f'_c$ (psi) | % Diff. w.r.t STD | $f'_c$ (psi) | % Diff. w.r.t STD | $f'_c$ (psi) | % Diff. w.r.t STD |
| | | STD | LRFD | | LRFD | | LRFD | | LRFD | |
| 8.50 | 90 | 5000 | 5000 | 0.0 | 5000 | 0.0 | 5000 | 0.0 | 5000 | 0.0 |
| | 100 | 5000 | 5000 | 0.0 | 5000 | 0.0 | 5000 | 0.0 | 5000 | 0.0 |
| | 110 | 5431 | 5000 | -7.9 | 5000 | -7.9 | 5000 | -7.9 | 5000 | -7.9 |
| | 120 | 6598 | 5919 | -10.3 | 5945 | -9.9 | 5970 | -9.5 | 6049 | -8.3 |
| | 130 | 7893 | 7129 | -9.7 | 7129 | -9.7 | 7151 | -9.4 | 7211 | -8.6 |
| 10.00 | 90 | 5000 | 5000 | 0.0 | 5000 | 0.0 | 5000 | 0.0 | 5000 | 0.0 |
| | 100 | 5000 | 5000 | 0.0 | 5000 | 0.0 | 5000 | 0.0 | 5000 | 0.0 |
| | 110 | 5852 | 5231 | -10.6 | 5231 | -10.6 | 5257 | -10.2 | 5391 | -7.9 |
| | 120 | 7117 | 6358 | -10.7 | 6381 | -10.3 | 6405 | -10.0 | 6505 | -8.6 |
| | 130 | 8580 | 7660 | -10.7 | 7660 | -10.7 | 7652 | -10.8 | 7743 | -9.8 |
| 11.50 | 90 | 5000 | 5000 | 0.0 | 5000 | 0.0 | 5000 | 0.0 | 5000 | 0.0 |
| | 100 | 5000 | 5000 | 0.0 | 5000 | 0.0 | 5000 | 0.0 | 5000 | 0.0 |
| | 110 | 6223 | 5586 | -10.2 | 5611 | -9.8 | 5636 | -9.4 | 5736 | -7.8 |
| | 120 | 7593 | 6804 | -10.4 | 6804 | -10.4 | 6826 | -10.1 | 6944 | -8.5 |
| 14.00 | 90 | 5000 | 5000 | 0.0 | 5000 | 0.0 | 5000 | 0.0 | 5000 | 0.0 |
| | 100 | 5560 | 5022 | -9.7 | 5022 | -9.7 | 5047 | -9.2 | 5165 | -7.1 |
| | 110 | 6916 | 6233 | -9.9 | 6233 | -9.9 | 6255 | -9.6 | 6374 | -7.8 |
| 16.67 | 90 | 5000 | 5000 | 0.0 | 5000 | 0.0 | 5000 | 0.0 | 5000 | 0.0 |
| | 100 | 6119 | 5537 | -9.5 | 5560 | -9.1 | 5584 | -8.7 | 5684 | -7.1 |

### 4.3.5 Initial and Final Prestress Losses

#### *4.3.5.1 Initial Prestress Loss*

Figure 4.12 and Table 4.17 show the summary of comparison of initial prestress losses, required for all the design cases considered in this study, for the LRFD and the Standard Specifications for strand diameter 0.5 in. The figure and the detailed comparison of each design case for strand diameter 0.6 in. are not shown in this section,

because the trends were not different than those of strand diameter 0.5 in., and can be found in Appendix A.

**Table 4.17 Comparison of Initial Prestress Loss for LRFD Relative to Standard Specifications (Strand Diameter = 0.5 in.)**

| Spacing (ft.) | Span (ft.) | All Skews | Skew = 0 | | Skew = 15 | | Skew = 30 | | Skew = 60 | |
|---|---|---|---|---|---|---|---|---|---|---|
| | | TIL (ksi) | TIL (ksi) | % Diff. w.r.t STD | TIL (ksi) | % Diff. w.r.t STD | TIL (ksi) | % Diff. w.r.t STD | TIL (ksi) | % Diff. w.r.t STD |
| | | STD | LRFD | | LRFD | | LRFD | | LRFD | |
| 8.50 | 90 | 10.6 | 9.7 | -8.7 | 9.7 | -8.7 | 9.7 | -8.7 | 8.2 | -22.6 |
| | 100 | 12.2 | 12.2 | -0.2 | 12.2 | -0.2 | 11.5 | -6.0 | 10.1 | -17.8 |
| | 110 | 14.2 | 14.4 | 1.9 | 14.4 | 1.9 | 13.8 | -2.9 | 12.4 | -12.5 |
| | 120 | 15.3 | 16.0 | 4.4 | 15.6 | 2.1 | 15.3 | -0.3 | 14.1 | -8.0 |
| | 130 | 16.4 | 17.3 | 5.4 | 17.3 | 5.4 | 16.9 | 3.4 | 15.2 | -7.0 |
| 10.00 | 90 | 11.5 | 12.1 | 5.2 | 12.1 | 5.2 | 11.0 | -4.2 | 9.9 | -14.0 |
| | 100 | 13.7 | 14.5 | 5.7 | 14.5 | 5.7 | 13.5 | -1.4 | 11.5 | -15.9 |
| | 110 | 15.3 | 16.3 | 6.5 | 16.3 | 6.5 | 15.7 | 2.8 | 14.2 | -6.8 |
| | 120 | 16.2 | 17.3 | 7.0 | 17.3 | 7.0 | 16.8 | 3.9 | 15.7 | -2.8 |
| | 130 | 17.4 | 18.8 | 7.7 | 18.8 | 7.7 | 18.3 | 5.4 | 16.7 | -3.9 |
| 11.50 | 90 | 12.6 | 12.6 | 0.0 | 12.6 | 0.0 | 11.9 | -5.5 | 10.4 | -17.0 |
| | 100 | 15.1 | 15.6 | 3.2 | 15.6 | 3.2 | 14.9 | -1.4 | 12.9 | -14.8 |
| | 110 | 16.2 | 17.0 | 5.0 | 16.7 | 2.9 | 16.3 | 0.8 | 15.0 | -7.3 |
| | 120 | 17.2 | 18.2 | 5.9 | 18.2 | 5.9 | 17.9 | 4.2 | 16.3 | -5.1 |
| 14.00 | 90 | 15.6 | 16.6 | 6.5 | 16.0 | 2.5 | 16.0 | 2.5 | 12.6 | -19.4 |
| | 100 | 16.7 | 17.3 | 3.4 | 17.3 | 3.4 | 14.6 | -12.5 | 15.6 | -6.7 |
| | 110 | 18.1 | 18.9 | 3.9 | 18.9 | 3.9 | 18.6 | 2.3 | 17.0 | -6.2 |
| 16.67 | 90 | 17.5 | 17.0 | -2.9 | 17.0 | -2.9 | 16.6 | -5.1 | 14.6 | -16.6 |
| | 100 | 18.3 | 18.8 | 3.2 | 18.5 | 1.6 | 18.2 | -0.1 | 17.0 | -7.0 |

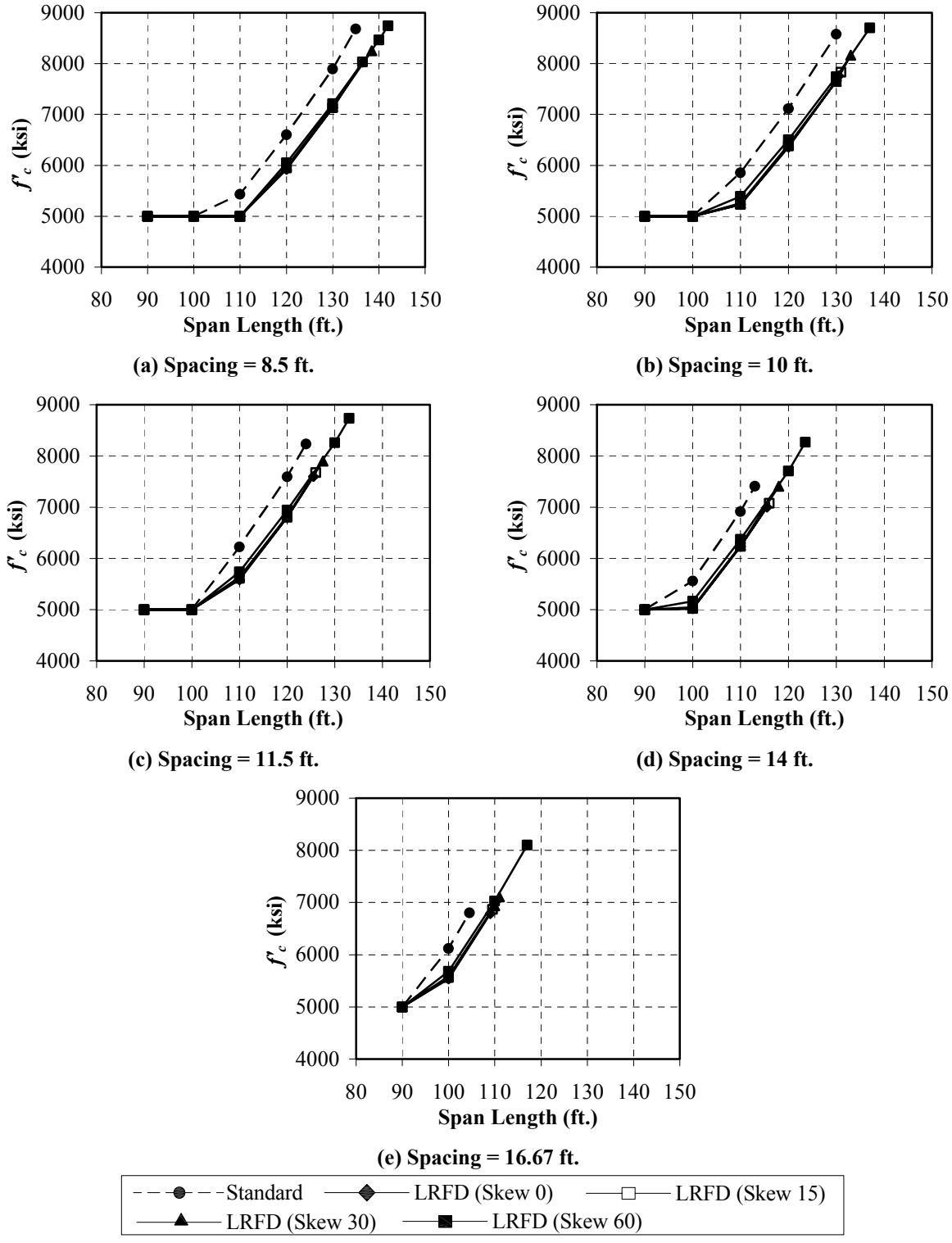


**Figure 4.11 Comparison of Final Concrete Strength (Strand Diameter 0.5 in.).**

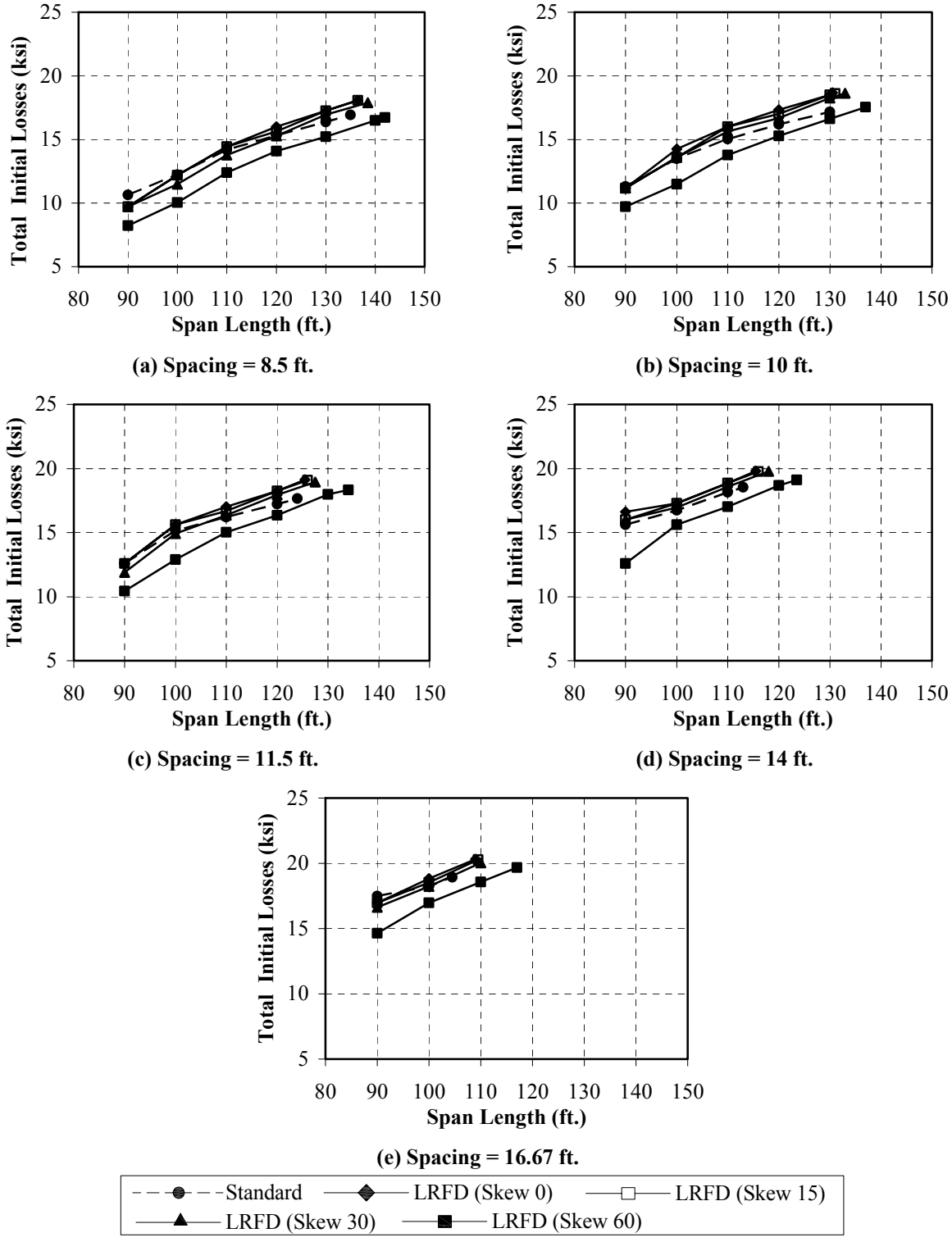


**Figure 4.12 Comparison of Initial Prestress Loss (Strand Diameter 0.5 in.).**

In general, relative to the Standard Specifications, the decrease in initial prestress losses, with the increase in spacing and span length, remain more or less constant. Considering the skew angles of 0, 15, 30 degree, generally the designs based on the Standard Specifications give a slightly lower estimate of initial losses as compared to those based on the LRFD Specifications and the 60 degree skew increases this difference significantly, as shown in Figure 4.12. For the skew angles of 0, 15, 30 degree, the difference in the initial losses vary in the range of 1.3 to -2.1 ksi (7.7 to -12.5 percent) and for 60 degree skew, the difference in the initial losses decrease in the range of -1.2 to -3.0 ksi (-7.0 to -19.4 percent) relative to the Standard Specifications.

**Prestress Loss due to Elastic Shortening of Concrete**

The loss of prestress due to elastic shortening of the prestressing strands is dependent on the elastic modulus of the prestressing strands, the elastic modulus of the concrete at release, and the total prestressing force at release. The modulus of elasticity of the prestressing strands is specified by the Standard Specifications as 28,000 ksi, while the LRFD Specifications specify this value to be 28,500 ksi. The elastic modulus of the concrete at release depends on the concrete strength at release based on the prediction formulas given in the specifications. As discussed in Section 4.3.4.1, the LRFD Specifications give a lower estimate of the concrete strength at release.

In general, relative to the designs based on the Standard Specifications, the elastic shortening loss decreases in the designs based the LRFD Specifications. For the skew angles of 0, 15, 30 degree, the difference in the initial losses vary in the range of 0.2 to -1.3 ksi (1.2 to –13.3 percent) and for 60 degree skew, the difference in the elastic shortening losses decrease in the range of -1.5 to -2.5 ksi (-9.9 to -29.7 percent) relative to the Standard Specifications. These differences can be attributed to the combined effect of all the parameters discussed above. The effect of lower concrete strengths and higher value of modulus of elasticity of prestressing strands in the LRFD Specifications should results in higher value of elastic modulus of prestressing strands. On the contrary, the decrease in the live load moments, thereby decreases the number of prestressing strands

which as a consequence decreases the stress in the concrete. A comparison of predicted elastic shortening (ES) losses for 0.5 in. diameter strands is presented in Table 4.18. A similar comparison for 0.6 in. diameter strands is presented in Appendix A.

**Table 4.18 Comparison of Elastic Shortening Loss for LRFD Relative to Standard Specifications (Strand Diameter = 0.5 in.)**

| Spacing (ft.) | Span (ft.) | All Skews | Skew = 0 | | Skew = 15 | | Skew = 30 | | Skew = 60 | |
|---|---|---|---|---|---|---|---|---|---|---|
| | | ES (ksi) STD | ES (ksi) LRFD | % Diff. w.r.t STD | ES (ksi) LRFD | % Diff. w.r.t STD | ES (ksi) LRFD | % Diff. w.r.t STD | ES (ksi) LRFD | % Diff. w.r.t STD |
| 8.5 | 90 | 8.3 | 7.7 | -7.3 | 7.7 | -7.3 | 7.7 | -7.3 | 5.9 | -29.7 |
| | 100 | 10.8 | 10.2 | -5.2 | 10.2 | -5.2 | 9.5 | -11.8 | 8.1 | -25.0 |
| | 110 | 13.1 | 12.5 | -4.8 | 12.5 | -4.8 | 12.5 | -4.8 | 10.4 | -20.5 |
| | 120 | 14.2 | 14.0 | -1.2 | 14.0 | -1.2 | 13.7 | -3.7 | 12.1 | -14.6 |
| | 130 | 15.4 | 15.3 | -0.8 | 14.9 | -2.9 | 14.6 | -5.0 | 13.2 | -14.0 |
| 10 | 90 | 9.8 | 9.2 | -5.9 | 9.2 | -5.9 | 8.5 | -13.3 | 7.7 | -20.7 |
| | 100 | 12.1 | 11.6 | -4.5 | 11.6 | -4.5 | 11.6 | -4.5 | 9.5 | -21.7 |
| | 110 | 13.8 | 14.0 | 1.3 | 14.0 | 1.3 | 13.6 | -1.3 | 11.8 | -14.7 |
| | 120 | 15.1 | 15.3 | 1.2 | 15.0 | -0.9 | 14.7 | -3.0 | 13.7 | -9.9 |
| | 130 | 16.3 | 16.5 | 1.2 | 16.5 | 1.2 | 16.0 | -2.0 | 14.6 | -10.4 |
| 11.5 | 90 | 11.2 | 10.6 | -5.0 | 10.6 | -5.0 | 9.9 | -11.3 | 8.5 | -24.1 |
| | 100 | 13.9 | 13.6 | -2.1 | 13.0 | -6.9 | 13.0 | -6.9 | 10.9 | -21.7 |
| | 110 | 15.2 | 15.0 | -0.9 | 15.0 | -0.9 | 14.7 | -3.0 | 13.1 | -13.8 |
| | 120 | 16.3 | 16.3 | -0.6 | 16.3 | -0.6 | 16.0 | -2.4 | 14.4 | -12.2 |
| 14 | 90 | 13.9 | 13.3 | -3.7 | 13.3 | -3.7 | 12.7 | -8.6 | 10.6 | -23.6 |
| | 100 | 15.7 | 15.3 | -2.7 | 15.3 | -2.7 | 15.0 | -4.8 | 13.6 | -13.4 |
| | 110 | 17.2 | 16.9 | -2.0 | 16.9 | -2.0 | 16.6 | -3.7 | 15.0 | -12.7 |
| 16.67 | 90 | 15.6 | 15.0 | -4.1 | 15.0 | -4.1 | 14.6 | -6.4 | 12.7 | -19.1 |
| | 100 | 17.5 | 16.8 | -3.6 | 16.5 | -5.2 | 16.2 | -6.9 | 15.0 | -14.2 |

**Prestress Loss due to Initial Steel Relaxation**

The loss in prestress due to the initial relaxation of steel is specified by the LRFD Specifications to be a function of time, jacking stress and the yield stress of the prestressing strands. The time for release of prestress is taken as 12 hours in this study. This provides a constant estimate of initial steel relaxation loss of 1.975 ksi for the

designs based on the LRFD Specifications and is not affected by skew, strand diameter or span length as can be observed in Table 4.19. The Standard Specifications do not specify a particular formula to evaluate the initial relaxation loss. Based on the TxDOT Bridge Design Manual (TxDOT 2001) recommendation, the initial relaxation loss is taken as half of the total estimated relaxation loss.

**Table 4.19 Comparison of Initial Relaxation Loss for LRFD Relative to Standard Specifications (Strand Diameter = 0.5 in.)**

| Spacing (ft.) | Span (ft.) | All Skews | All Skews | |
|---|---|---|---|---|
| | | IRL (ksi) | IRL (ksi) | % Diff. w.r.t STD |
| | | STD | LRFD | |
| 8.5 | 90 | 1.65 | 1.97 | 19.3 |
| | 100 | 1.46 | 1.97 | 35.4 |
| | 110 | 1.26 | 1.97 | 56.5 |
| | 120 | 1.13 | 1.97 | 75.2 |
| | 130 | 0.97 | 1.97 | 104.1 |
| | 135 | 0.87 | 1.97 | 126.9 |
| 10 | 90 | 1.54 | 1.97 | 28.0 |
| | 100 | 1.35 | 1.97 | 45.9 |
| | 110 | 1.20 | 1.97 | 65.0 |
| | 120 | 1.03 | 1.97 | 92.0 |
| | 130 | 0.87 | 1.97 | 127.2 |
| 11.5 | 90 | 1.43 | 1.97 | 38.1 |
| | 100 | 1.20 | 1.97 | 64.8 |
| | 110 | 1.04 | 1.97 | 89.3 |
| | 120 | 0.89 | 1.97 | 122.4 |
| | 124 | 0.81 | 1.97 | 142.8 |
| 14 | 90 | 1.22 | 1.97 | 62.3 |
| | 100 | 1.00 | 1.97 | 97.0 |
| | 110 | 0.81 | 1.97 | 144.1 |
| | 113 | 0.72 | 1.97 | 173.0 |
| 16.67 | 90 | 1.03 | 1.97 | 92.0 |
| | 100 | 0.79 | 1.97 | 150.0 |
| | 104.5 | 0.68 | 1.97 | 190.7 |

While the percentage differences are significant, the actual magnitude of the maximum difference on initial relaxation losses are only slightly more than 1.0 ksi. It was observed that the prestress loss due to initial steel relaxation, calculated in accordance with the LRFD Specifications, yields a greater estimate than the Standard Specifications. For the designs based on the LRFD Specifications, the difference in the elastic shortening losses decrease in the range of 0.32 to 1.3 ksi (19.3 to 190.7 percent) relative to the Standard Specifications. A comparison of predicted initial relaxation losses (IRL) for 0.5 in. diameter strands is presented in Table 4.19. A similar comparison for 0.6 in. diameter strands is presented in Appendix A.

#### *4.3.5.2 Final Prestress Loss*

Figure 4.13 and Table 4.20 show the summary of comparison of final prestress losses, required for all the design cases considered in this study, for the LRFD and the Standard Specifications for strand diameter 0.5 in. For strand diameter of 0.6 in., the detailed comparison of each design case along with figures is included in the Appendix A.

In general, the decrease in final prestress losses (TFL) relative to the Standard Specifications, with the increase in spacing and span length, remain more or less constant. Except for 14 ft. and 16.67 ft. spacings, for the skew angles of 0 and 15 degree, the designs based on the Standard Specifications give a slightly lower estimate of final losses as compared to those based on the LRFD Specifications and the difference increases with the increasing skew, as shown in Figure 4.13. For the 0, 15 and 30 degree skew, the difference in the final losses vary in the range of 2.5 to -3.9 ksi (6.9 to -7.5 percent) and for 60 degree skew, the difference in the final losses decrease in the range of -2.6 to -9.0 ksi (-8.2 to -17.9 percent) relative to the Standard Specifications.

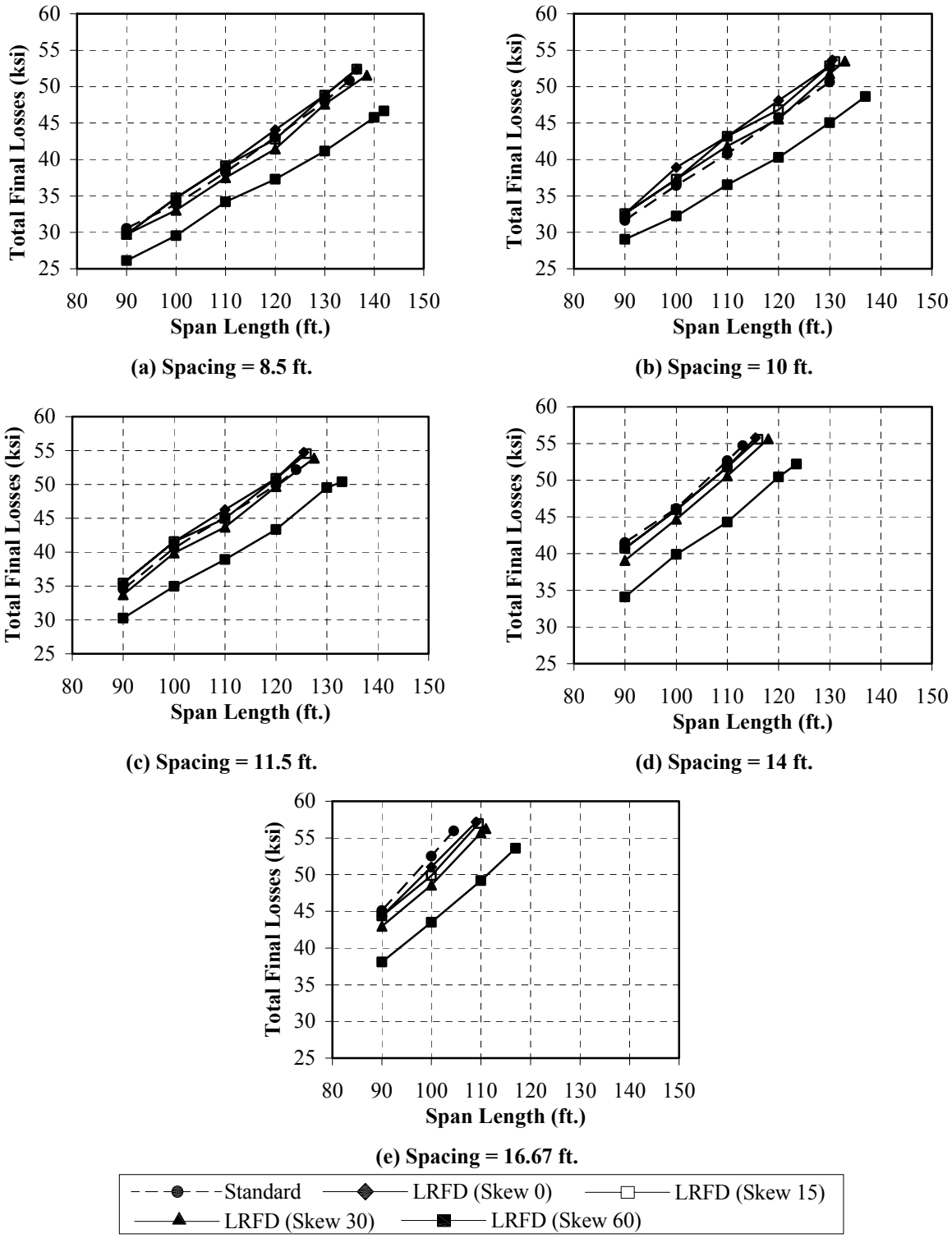


**Figure 4.13 Comparison of Final Prestress Loss (Strand Diameter 0.5 in.).**

**Table 4.20 Comparison of Final Prestress Loss for LRFD Relative to Standard Specifications (Strand Diameter = 0.5 in.)**

| Spacing (ft.) | Span (ft.) | All Skews | Skew = 0 | | Skew = 15 | | Skew = 30 | | Skew = 60 | |
|---|---|---|---|---|---|---|---|---|---|---|
| | | TFL (ksi) | TFL (ksi) | % Diff. w.r.t | TFL (ksi) | % Diff. w.r.t | TFL (ksi) | % Diff. w.r.t | TFL (ksi) | % Diff. w.r.t |
| | | STD | LRFD | STD | LRFD | STD | LRFD | STD | LRFD | STD |
| 8.50 | 90 | 30.5 | 29.7 | -2.7 | 29.7 | -2.7 | 29.7 | -2.7 | 26.1 | -14.5 |
| | 100 | 33.8 | 34.7 | 2.8 | 34.7 | 2.8 | 33.0 | -2.3 | 29.5 | -12.6 |
| | 110 | 38.2 | 39.1 | 2.4 | 39.1 | 2.4 | 37.5 | -1.9 | 34.2 | -10.5 |
| | 120 | 43.0 | 44.1 | 2.4 | 42.8 | -0.6 | 41.4 | -3.7 | 37.3 | -13.3 |
| | 130 | 47.9 | 48.8 | 1.9 | 48.8 | 1.9 | 47.6 | -0.7 | 41.1 | -14.1 |
| 10.00 | 90 | 31.6 | 32.6 | 3.0 | 32.6 | 3.0 | 32.6 | 3.0 | 29.0 | -8.2 |
| | 100 | 36.4 | 38.9 | 6.9 | 37.3 | 2.4 | 37.3 | 2.4 | 32.2 | -11.5 |
| | 110 | 40.7 | 43.2 | 6.0 | 43.2 | 6.0 | 41.8 | 2.7 | 36.5 | -10.3 |
| | 120 | 45.8 | 48.1 | 5.1 | 46.8 | 2.3 | 45.6 | -0.4 | 40.3 | -11.9 |
| | 130 | 50.6 | 52.9 | 4.4 | 52.9 | 4.4 | 51.8 | 2.3 | 45.1 | -11.0 |
| 11.50 | 90 | 34.5 | 35.4 | 2.6 | 35.4 | 2.6 | 33.7 | -2.3 | 30.3 | -12.4 |
| | 100 | 40.6 | 41.5 | 2.3 | 41.5 | 2.3 | 39.9 | -1.7 | 35.0 | -13.9 |
| | 110 | 45.2 | 46.3 | 2.4 | 45.0 | -0.5 | 43.7 | -3.4 | 38.9 | -13.9 |
| | 120 | 49.9 | 50.9 | 2.1 | 50.9 | 2.1 | 49.7 | -0.4 | 43.3 | -13.2 |
| 14.00 | 90 | 41.5 | 40.7 | -1.9 | 40.7 | -1.9 | 39.1 | -5.9 | 34.1 | -17.9 |
| | 100 | 46.1 | 46.0 | -0.4 | 46.0 | -0.4 | 44.7 | -3.2 | 39.9 | -13.6 |
| | 110 | 52.7 | 51.8 | -1.6 | 51.8 | -1.6 | 50.6 | -4.0 | 44.3 | -15.9 |
| 16.67 | 90 | 45.1 | 44.4 | -1.7 | 44.4 | -1.7 | 43.0 | -4.7 | 38.1 | -15.5 |
| | 100 | 52.5 | 51.1 | -2.8 | 49.9 | -5.1 | 48.6 | -7.5 | 43.5 | -17.2 |

**Prestress Loss due to Shrinkage of Concrete**

The LRFD and Standard Specifications prescribe the loss of prestress due to shrinkage of concrete as a function of relative humidity. For a relative humidity of 60%, the prestress loss due to shrinkage was found to be 8 ksi for both the Standard and LRFD Specifications for all the cases.

**Prestress Loss due to Steel Relaxation at Service**

The prestress loss due to steel relaxation (CRs) at service is the combination of loss due to initial relaxation and final relaxation of steel. The Standard and LRFD

Specifications specify empirical formulas to estimate the loss due to steel relaxation at service. The formulas given in the two specifications are similar in form with only slight difference in the coefficients. The steel relaxation depends upon the effects due to elastic shortening, creep of concrete and shrinkage. Table 4.21 provides a comparison of estimated prestress loss due to steel relaxation for 0.5 in. diameter strands in the parametric study. For strand diameter of 0.6 in., the detailed comparison of each design case is included in the Appendix A.

**Table 4.21 Comparison of Steel Relaxation Loss for LRFD Relative to Standard Specifications (Strand Diameter = 0.5 in.)**

| Spacing (ft.) | Span (ft.) | All Skews | Skew = 0 | | Skew = 15 | | Skew = 30 | | Skew = 60 | |
|---|---|---|---|---|---|---|---|---|---|---|
| | | CRs (ksi) | CRs (ksi) | % Diff. w.r.t STD | CRs (ksi) | % Diff. w.r.t STD | CRs (ksi) | % Diff. w.r.t STD | CRs (ksi) | % Diff. w.r.t STD |
| | | STD | LRFD | | LRFD | | LRFD | | LRFD | |
| 8.5 | 90 | 3.31 | 4.12 | 24.5 | 4.12 | 24.5 | 4.12 | 24.5 | 4.53 | 36.8 |
| | 100 | 2.92 | 3.64 | 24.9 | 3.64 | 24.9 | 3.80 | 30.1 | 4.11 | 40.9 |
| | 110 | 2.52 | 3.21 | 27.4 | 3.21 | 27.4 | 3.21 | 27.4 | 3.66 | 45.1 |
| | 120 | 2.25 | 2.80 | 24.3 | 2.80 | 24.3 | 2.91 | 29.0 | 3.35 | 48.8 |
| | 130 | 1.93 | 2.42 | 24.9 | 2.52 | 30.1 | 2.62 | 35.4 | 3.04 | 57.1 |
| 10 | 90 | 3.09 | 3.85 | 24.7 | 3.85 | 24.7 | 4.00 | 29.8 | 4.16 | 34.9 |
| | 100 | 2.71 | 3.39 | 25.2 | 3.39 | 25.2 | 3.39 | 25.2 | 3.85 | 42.0 |
| | 110 | 2.39 | 2.86 | 19.5 | 2.86 | 19.5 | 2.97 | 24.1 | 3.42 | 43.1 |
| | 120 | 2.06 | 2.46 | 19.7 | 2.56 | 24.6 | 2.66 | 29.6 | 2.98 | 44.9 |
| | 130 | 1.74 | 2.08 | 19.9 | 2.08 | 19.9 | 2.26 | 30.0 | 2.70 | 55.5 |
| 11.5 | 90 | 2.86 | 3.57 | 24.9 | 3.57 | 24.9 | 3.73 | 30.3 | 4.04 | 41.2 |
| | 100 | 2.40 | 2.99 | 24.7 | 3.13 | 30.8 | 3.13 | 30.8 | 3.58 | 49.6 |
| | 110 | 2.09 | 2.60 | 24.5 | 2.60 | 24.5 | 2.70 | 29.4 | 3.19 | 52.9 |
| | 120 | 1.78 | 2.22 | 25.2 | 2.22 | 25.2 | 2.32 | 30.7 | 2.83 | 59.3 |
| 14 | 90 | 2.43 | 3.06 | 25.6 | 3.06 | 25.6 | 3.21 | 31.7 | 3.66 | 50.3 |
| | 100 | 2.01 | 2.60 | 29.6 | 2.60 | 29.6 | 2.70 | 34.7 | 3.09 | 54.3 |
| | 110 | 1.62 | 2.13 | 31.5 | 2.13 | 31.5 | 2.22 | 37.5 | 2.72 | 68.3 |
| 16.67 | 90 | 2.06 | 2.72 | 32.2 | 2.72 | 32.2 | 2.83 | 37.7 | 3.27 | 58.9 |
| | 100 | 1.58 | 2.18 | 37.7 | 2.27 | 43.9 | 2.37 | 50.1 | 2.78 | 75.8 |

The estimate of prestress loss due to steel relaxation at service provided by the LRFD Specifications is found to be larger as compared to the Standard Specifications,

although the maximum difference is less than 2.0 ksi. For 0.5 in. diameter stands and the skew angles of 0, 15 and 30 degree, the percent increase for the designs based on the LRFD Specifications is in the range of 0.47 to 0.79 ksi (19.5 to 50.1 percent). For 0.5 in. diameter stands and the skew angle of 60 degree, the percent increase for the designs based on the LRFD Specifications is in the range of 1.08 to 1.2 ksi (34.9 to 75.8 percent). This difference increases with the skew angle, span length and girder spacing.

**Prestress Loss due to Creep of Concrete**

The Standard and LRFD Specifications specify similar expressions for estimating the prestress loss due to creep of concrete. The loss due to creep depends on the concrete stress at the center of gravity (c.g.) of the prestressing strands due to dead loads before and after prestressing. Table 4.22 provides a comparison of estimated prestress loss due

**Table 4.22 Comparison of Creep Loss for LRFD Relative to Standard Specifications (Strand Diameter = 0.5 in.)**

| Spacing (ft.) | Span (ft.) | All Skews | Skew = 0 | | Skew = 15 | | Skew = 30 | | Skew = 60 | |
|---|---|---|---|---|---|---|---|---|---|---|
| | | CRc (ksi) STD | CRc (ksi) LRFD | % Diff. w.r.t STD | CRc (ksi) LRFD | % Diff. w.r.t STD | CRc (ksi) LRFD | % Diff. w.r.t STD | CRc (ksi) LRFD | % Diff. w.r.t STD |
| 8.5 | 90 | 9.11 | 7.87 | -13.6 | 7.87 | -13.6 | 7.87 | -13.6 | 4.79 | -47.5 |
| 8.5 | 100 | 12.13 | 10.90 | -10.2 | 10.90 | -10.2 | 9.74 | -19.7 | 7.39 | -39.1 |
| 8.5 | 110 | 15.33 | 13.48 | -12.0 | 13.48 | -12.0 | 13.48 | -12.0 | 10.11 | -34.0 |
| 8.5 | 120 | 18.56 | 17.28 | -6.9 | 17.28 | -6.9 | 16.21 | -12.6 | 11.87 | -36.1 |
| 8.5 | 130 | 22.53 | 21.19 | -5.9 | 20.15 | -10.5 | 19.11 | -15.2 | 14.87 | -34.0 |
| 10 | 90 | 10.78 | 9.54 | -11.5 | 9.54 | -11.5 | 8.36 | -22.4 | 7.16 | -33.5 |
| 10 | 100 | 13.56 | 12.32 | -9.2 | 12.32 | -9.2 | 12.32 | -9.2 | 8.88 | -34.5 |
| 10 | 110 | 16.49 | 16.30 | -1.1 | 16.30 | -1.1 | 15.23 | -7.6 | 11.34 | -31.2 |
| 10 | 120 | 20.57 | 20.31 | -1.3 | 19.26 | -6.4 | 18.21 | -11.5 | 15.01 | -27.0 |
| 10 | 130 | 24.60 | 24.25 | -1.4 | 24.25 | -1.4 | 22.35 | -9.1 | 17.72 | -28.0 |
| 11.5 | 90 | 12.51 | 11.27 | -9.9 | 11.27 | -9.9 | 10.12 | -19.1 | 7.76 | -37.9 |
| 11.5 | 100 | 16.23 | 14.93 | -8.0 | 13.83 | -14.8 | 13.83 | -14.8 | 10.46 | -35.5 |
| 11.5 | 110 | 19.94 | 18.64 | -6.5 | 18.64 | -6.5 | 17.59 | -11.8 | 12.70 | -36.3 |
| 11.5 | 120 | 23.78 | 22.43 | -5.7 | 22.43 | -5.7 | 21.39 | -10.0 | 16.14 | -32.1 |
| 14 | 90 | 15.59 | 14.34 | -8.0 | 14.34 | -8.0 | 13.23 | -15.2 | 9.82 | -37.0 |
| 14 | 100 | 20.42 | 18.07 | -11.5 | 18.07 | -11.5 | 17.01 | -16.7 | 13.16 | -35.5 |
| 14 | 110 | 25.21 | 22.81 | -9.5 | 22.81 | -9.5 | 21.78 | -13.6 | 16.54 | -34.4 |
| 16.67 | 90 | 19.55 | 16.65 | -14.8 | 16.65 | -14.8 | 15.51 | -20.6 | 12.19 | -37.6 |
| 16.67 | 100 | 25.48 | 22.06 | -13.4 | 21.02 | -17.5 | 19.98 | -21.6 | 15.75 | -38.2 |

to creep of concrete for 0.5 in. diameter strands in the parametric study. For strand diameter of 0.6 in., the detailed comparison of each design case is included in the Appendix A.

The estimate of prestress loss due to creep of concrete provided by the LRFD Specifications is found to be smaller as compared to the Standard Specifications. For 0.5 in. diameter stands and the skew angles of 0, 15 and 30 degree, the decrease for the designs based on the LRFD Specifications is in the range of 0.18 to 5.5 ksi. For 0.5 in. diameter stands and the skew angle of 60 degree, the decrease for the designs based on the LRFD Specifications is in the range of 3.62 to 9.74 ksi. This difference increases with the skew angle, span length and girder spacing.

## 4.4 ULTIMATE LIMIT STATE DESIGN

### 4.4.1 General

The impact of the LRFD Specifications on the requirements for the flexural strength limit state design, shear strength limit state design, camber and debonding of prestressing strands is discussed in the following section. The decrease in the live load and live load factor, the required concrete strength at service, and the number of strands as determined in the service limit state, decreases the factored design moments and nominal design moments. The reinforcement limits are also different in the LRFD Specifications. However, for all the design cases, the girder sections were found to be under reinforced.

The LRFD Specifications employ a different methodology for the transverse and interface shear design as compared to that of the Standard Specifications. This change in the design procedures significantly impact the shear design results. In general, factored shear by the LRFD Specifications slightly increases with respect to those of the Standard Specifications. The interface shear reinforcement area requirement by the LRFD

Specifications increases by a very large amount relative to the Standard Specifications, while the transverse shear reinforcement are decreases in the designs based on the LRFD Specifications.

### 4.4.2 Factored Design Moment and Shear

#### *4.4.2.1 Factored Design Moment*

Table 4.23 and Figure 4.14 show the differences in factored design moments of the designs based on the LRFD relative to those of the Standards Specifications and the detailed results are reported in the Appendix A. It can be observed in the plot in Figure 4.14 that the factored design moments based on the Standard Specifications are always larger relative to those of the LRFD Specifications and the difference increases as the skew increases. In general, this difference also increases with the increase in the girder spacings, however, the difference between the factored design moments by the two specifications does not vary with the varying span length for a particular spacing. The maximum differences in the factored design moments are reported in Table 4.23. For the skew angles of 0, 15 and 30 degree, the factored design moment of the LRFD designs decreases relative to the Standard designs in the range of 401 to 1880 k-ft. (4.4 to 16.5 percent) and for the skew angle of60 degree, it decreases in the range of 1503 to 3239 k-ft. (19.1 to 28.4 percent). The strand diameter has no affect on the calculation of factored design moment.

**Table 4.23 Comparison of Factored Design Moment**

| Spacing (ft.) | Span (ft.) | All Skews | Skew = 0 | | Skew = 15 | | Skew = 30 | | Skew = 60 | |
|---|---|---|---|---|---|---|---|---|---|---|
| | | Moment (k-ft) | Moment (k-ft) | % Diff. | Moment (k-ft) | % Diff. | Moment (k-ft) | % Diff. | Moment (k-ft) | % Diff. |
| | | STD | LRFD | w.r.t STD | LRFD | w.r.t STD | LRFD | w.r.t STD | LRFD | w.r.t STD |
| 8.50 | 90.0 | 6197 | 5511 | -11.1 | 5466 | -11.8 | 5266 | -15.0 | 4530 | -26.9 |
| | 100.0 | 7310 | 6541 | -10.5 | 6492 | -11.2 | 6270 | -14.2 | 5433 | -25.7 |
| | 110.0 | 8493 | 7653 | -9.9 | 7597 | -10.5 | 7348 | -13.5 | 6410 | -24.5 |
| | 120.0 | 9746 | 8839 | -9.3 | 8776 | -10.0 | 8500 | -12.8 | 7463 | -23.4 |
| | 130.0 | 11070 | 10108 | -8.7 | 10038 | -9.3 | 9735 | -12.1 | 8594 | -22.4 |
| 10.00 | 90.0 | 6468 | 6067 | -6.2 | 6021 | -6.9 | 5797 | -10.4 | 4965 | -23.2 |
| | 100.0 | 7642 | 7201 | -5.8 | 7147 | -6.5 | 6896 | -9.8 | 5953 | -22.1 |
| | 110.0 | 8892 | 8418 | -5.3 | 8357 | -6.0 | 8074 | -9.2 | 7020 | -21.1 |
| | 120.0 | 10219 | 9721 | -4.9 | 9652 | -5.5 | 9338 | -8.6 | 8170 | -20.1 |
| | 130.0 | 11623 | 11107 | -4.4 | 11029 | -5.1 | 10684 | -8.1 | 9402 | -19.1 |
| 11.50 | 90.0 | 7155 | 6559 | -8.3 | 6505 | -9.1 | 6259 | -12.5 | 5340 | -25.4 |
| | 100.0 | 8438 | 7777 | -7.8 | 7714 | -8.6 | 7438 | -11.9 | 6393 | -24.2 |
| | 110.0 | 9801 | 9082 | -7.3 | 9016 | -8.0 | 8705 | -11.2 | 7536 | -23.1 |
| | 120.0 | 11245 | 10478 | -6.8 | 10403 | -7.5 | 10057 | -10.6 | 8770 | -22.0 |
| 14.00 | 90.0 | 8466 | 7564 | -10.7 | 7481 | -11.6 | 7231 | -14.6 | 6171 | -27.1 |
| | 100.0 | 9975 | 8987 | -9.9 | 8890 | -10.9 | 8551 | -14.3 | 7395 | -25.9 |
| | 110.0 | 11578 | 10502 | -9.3 | 10392 | -10.2 | 10059 | -13.1 | 8717 | -24.7 |
| 16.67 | 90.0 | 9661 | 8391 | -13.1 | 8320 | -13.9 | 7999 | -17.2 | 6798 | -29.6 |
| | 100.0 | 11387 | 9957 | -12.6 | 9874 | -13.3 | 9507 | -16.5 | 8148 | -28.4 |

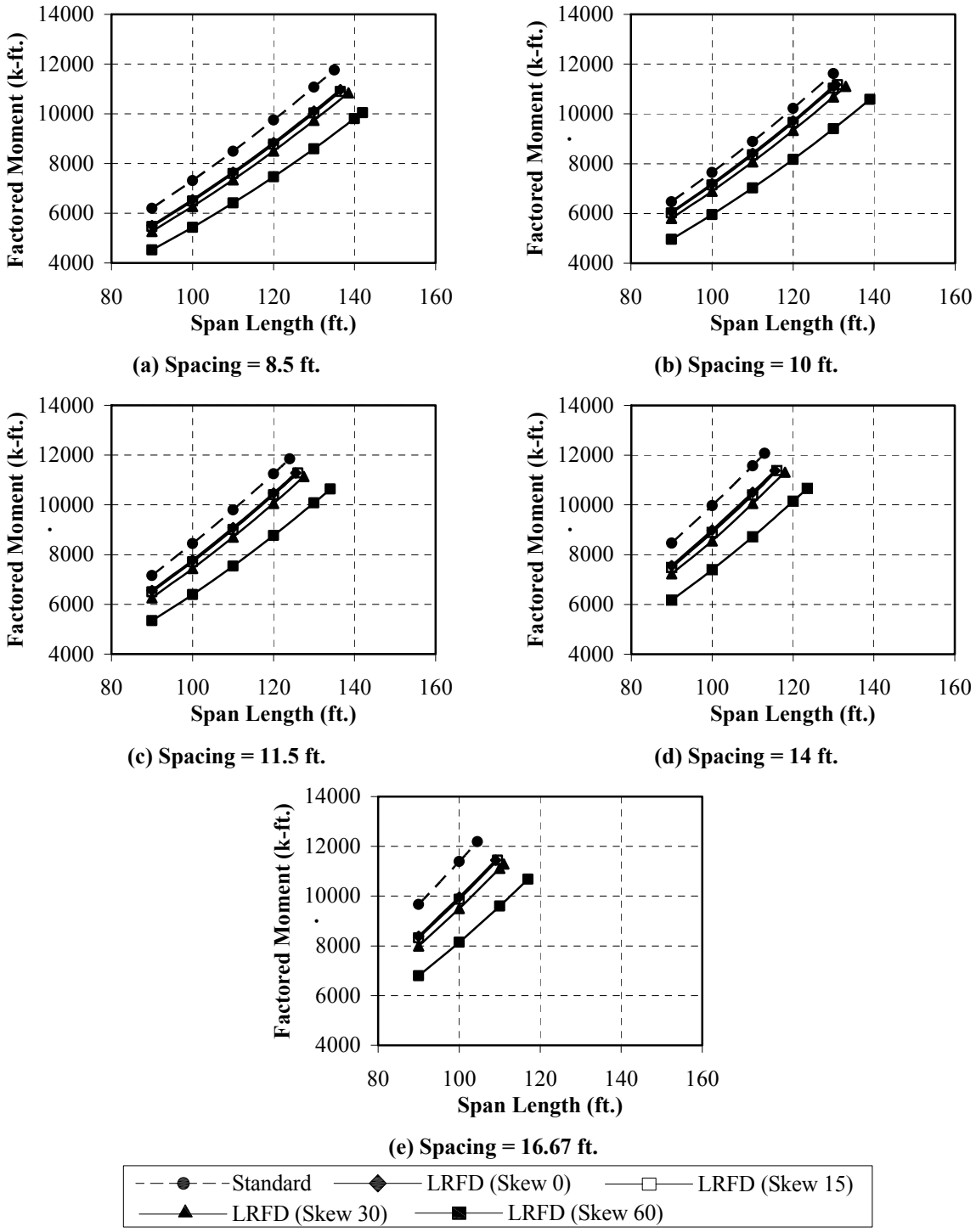


**Figure 4.14 Comparison of Factored Design Moment.**

#### *4.4.2.2 Factored Design Shear at Respective Critical Section Location*

Table 4.24 and Figure 4.15 shows the comparison of factored design shear for the LRFD designs relative to those of the Standard Specifications for a strand diameter 0.5 in. and the detailed results for both the strand diameters are reported in the Appendix A. The factored design shear values are calculated at the critical section locations, which are calculated based on the provisions of each specifications. Except for the lower spans of the girder spacings 8.5 ft. and 16.67 ft., the factored design shears for the LRFD Specifications increase with respect to that of the Standard Specification. Since only the interior girders were considered for the purpose of this parametric study, therefore, skew has a very insignificant affect on the factored design shear as can be seen in the Figure 4.15. The same trend is observed for the designs for strand diameter 0.6 in.

### 4.4.3 Nominal Moment Capacity

Tables 4.25, and Figures 4.16 and 4.17 show the comparison of nominal moment capacity for the LRFD designs relative to those of the Standard Specifications for a strand diameter 0.5 in. and 0.6 in., respectively. For skew angle of $0^{\circ}$, the nominal moment capacity values calculated for designs based on the Standard Specifications are more conservative when compared to those of the designs based on the LRFD Specifications. And the results for the Standard Specifications become more conservative for higher skew angles, as can be noticed in Figures 4.15 and 4.16. In general, the degree of conservatism increases with the increasing girder spacing, while the increasing span length has a very insignificant affect on this comparison. For the skew angles of 0, 15 and 30 degree, the nominal moment capacity for the LRFD designs varies relative to the Standard designs in the range of 447 to -1576 k-ft. (2.9 to -13.3 percent) and for the skew angle of 60 degree, it decreases in the range of -728 to -2953k-ft. (-4.7 to -22.9 percent).

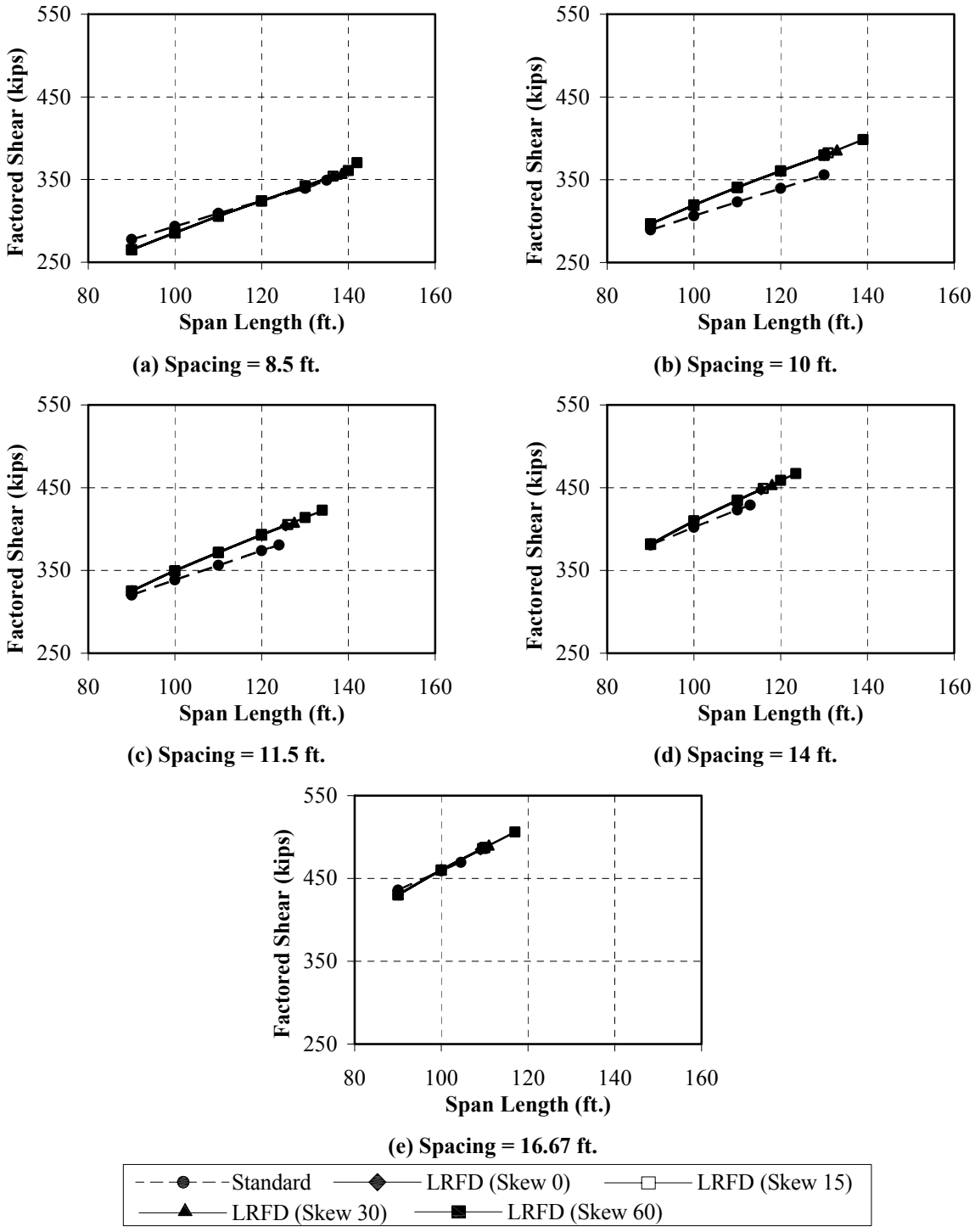


**Figure 4.15 Comparison of Factored Design Shear at Respective Critical Section Location (Strand Diameter 0.5 in.).**

**Table 4.24 Comparison of Factored Design Shear at Respective Critical Section Location (Strand Diameter 0.5 in.)**

| Spacing (ft.) | Span (ft.) | All Skews | Skew = 0 | | Skew = 15 | | Skew = 30 | | Skew = 60 | |
|---|---|---|---|---|---|---|---|---|---|---|
| | | Shear (k-ft) | Shear (k-ft) | % Diff. | Shear (k-ft) | % Diff. | Shear (k-ft) | % Diff. | Shear (k-ft) | % Diff. |
| | | STD | LRFD | w.r.t STD | LRFD | w.r.t STD | LRFD | w.r.t STD | LRFD | w.r.t STD |
| 8.50 | 90.0 | 277 | 265 | -4.5 | 265 | -4.5 | 265 | -4.5 | 265 | -4.5 |
| | 100.0 | 293 | 286 | -2.6 | 286 | -2.6 | 286 | -2.7 | 286 | -2.7 |
| | 110.0 | 309 | 306 | -1.0 | 306 | -1.0 | 306 | -1.0 | 306 | -1.1 |
| | 120.0 | 324 | 324 | 0.0 | 324 | 0.0 | 324 | 0.0 | 324 | 0.0 |
| | 130.0 | 339 | 342 | 0.8 | 342 | 0.8 | 342 | 0.8 | 342 | 0.8 |
| 10.00 | 90.0 | 289 | 297 | 2.5 | 297 | 2.5 | 296 | 2.5 | 296 | 2.5 |
| | 100.0 | 306 | 319 | 4.3 | 319 | 4.2 | 319 | 4.2 | 319 | 4.2 |
| | 110.0 | 323 | 341 | 5.5 | 341 | 5.5 | 341 | 5.4 | 340 | 5.3 |
| | 120.0 | 340 | 360 | 6.1 | 361 | 6.2 | 361 | 6.2 | 361 | 6.2 |
| | 130.0 | 356 | 380 | 6.7 | 380 | 6.7 | 380 | 6.7 | 380 | 6.7 |
| 11.50 | 90.0 | 320 | 325 | 1.6 | 325 | 1.6 | 325 | 1.6 | 325 | 1.5 |
| | 100.0 | 338 | 350 | 3.3 | 350 | 3.3 | 350 | 3.3 | 349 | 3.3 |
| | 110.0 | 356 | 372 | 4.4 | 372 | 4.4 | 372 | 4.4 | 372 | 4.4 |
| | 120.0 | 374 | 393 | 5.2 | 393 | 5.2 | 393 | 5.1 | 393 | 5.2 |
| 14.00 | 90.0 | 381 | 382 | 0.3 | 382 | 0.3 | 382 | 0.2 | 382 | 0.2 |
| | 100.0 | 402 | 410 | 1.9 | 410 | 1.9 | 410 | 1.9 | 409 | 1.8 |
| | 110.0 | 423 | 435 | 2.8 | 435 | 2.8 | 435 | 2.8 | 435 | 2.7 |
| 16.67 | 90.0 | 436 | 430 | -1.2 | 430 | -1.2 | 430 | -1.2 | 430 | -1.3 |
| | 100.0 | 459 | 460 | 0.3 | 460 | 0.2 | 460 | 0.2 | 460 | 0.2 |

### 4.4.4 Camber

Table 4.26 and Figures 4.18 show the comparison of the camber for the LRFD designs relative to those of the Standard Specifications for a strand diameter 0.5 in. and the comparison for strand diameter 0.6 in. are reported in Appendix A. For skew angle of 0 degree, the camber calculated for designs based on the Standard Specifications are more conservative when compared to those of the designs based on the LRFD Specifications. And the results for the Standard Specifications become more

conservative for higher skew angles, as can be noticed in Figures 4.18. In general, the degree of conservatism increases with the increasing girder spacing, while the increasing span length has a very insignificant affect on this comparison. For the skew angle of 0, 15 and 30 degree and for 0.5 in. strand diameter, the nominal moment capacity for the LRFD designs varies relative to the Standard designs in the range of 0.024 to -0.023 ft. (6.2 to -22.5 percent) and for the skew angle of 60 degree, it decreases in the range of -0.022 to -0.128 ft. (-5.2 to -45.1 percent).

**Table 4.25 Comparison of Nominal Moment Capacity (Strand Diameter 0.5 in.)**

| Spacing (ft.) | Span (ft.) | All Skews | Skew = 0 | | Skew = 15 | | Skew = 30 | | Skew = 60 | |
|---|---|---|---|---|---|---|---|---|---|---|
| | | Mn (k-ft) | Mn (k-ft) | % Diff. w.r.t STD | Mn (k-ft) | % Diff. w.r.t STD | Mn (k-ft) | % Diff. w.r.t STD | Mn (k-ft) | % Diff. w.r.t STD |
| | | STD | LRFD | | LRFD | | LRFD | | LRFD | |
| 8.50 | 90.0 | 6707 | 6043 | -9.9 | 6043 | -9.9 | 6043 | -9.9 | 5322 | -20.7 |
| | 100.0 | 8077 | 7805 | -3.4 | 7805 | -3.4 | 7457 | -7.7 | 6755 | -16.4 |
| | 110.0 | 9729 | 9506 | -2.3 | 9506 | -2.3 | 9171 | -5.7 | 8492 | -12.7 |
| | 120.0 | 11699 | 11608 | -0.8 | 11313 | -3.3 | 11013 | -5.9 | 10005 | -14.5 |
| | 130.0 | 13690 | 13624 | -0.5 | 13624 | -0.5 | 13354 | -2.5 | 11943 | -12.8 |
| 10.00 | 90.0 | 7127 | 6814 | -4.4 | 6814 | -4.4 | 6814 | -4.4 | 6090 | -14.6 |
| | 100.0 | 8862 | 8936 | 0.8 | 8587 | -3.1 | 8587 | -3.1 | 7529 | -15.0 |
| | 110.0 | 10677 | 10789 | 1.0 | 10789 | 1.0 | 10465 | -2.0 | 9282 | -13.1 |
| | 120.0 | 12830 | 13076 | 1.9 | 12777 | -0.4 | 12380 | -3.5 | 11111 | -13.4 |
| | 130.0 | 14965 | 15203 | 1.6 | 15203 | 1.6 | 14955 | -0.1 | 13415 | -10.4 |
| 11.50 | 90.0 | 7894 | 7583 | -3.9 | 7583 | -3.9 | 7221 | -8.5 | 6492 | -17.8 |
| | 100.0 | 9984 | 9717 | -2.7 | 9717 | -2.7 | 9365 | -6.2 | 8301 | -16.9 |
| | 110.0 | 12086 | 11888 | -1.6 | 11562 | -4.3 | 11234 | -7.0 | 10066 | -16.7 |
| | 120.0 | 14250 | 14123 | -0.9 | 14123 | -0.9 | 13809 | -3.1 | 12212 | -14.3 |
| 14.00 | 90.0 | 9763 | 9825 | 0.6 | 9466 | -3.0 | 8743 | -10.4 | 7648 | -21.7 |
| | 100.0 | 11958 | 11382 | -4.8 | 11382 | -4.8 | 11043 | -7.7 | 9825 | -17.8 |
| | 110.0 | 14697 | 14042 | -4.5 | 14042 | -4.5 | 13714 | -6.7 | 12056 | -18.0 |
| 16.67 | 90.0 | 11422 | 10271 | -10.1 | 10271 | -10.1 | 9907 | -13.3 | 8807 | -22.9 |
| | 100.0 | 14100 | 13204 | -6.4 | 12864 | -8.8 | 12524 | -11.2 | 11147 | -20.9 |

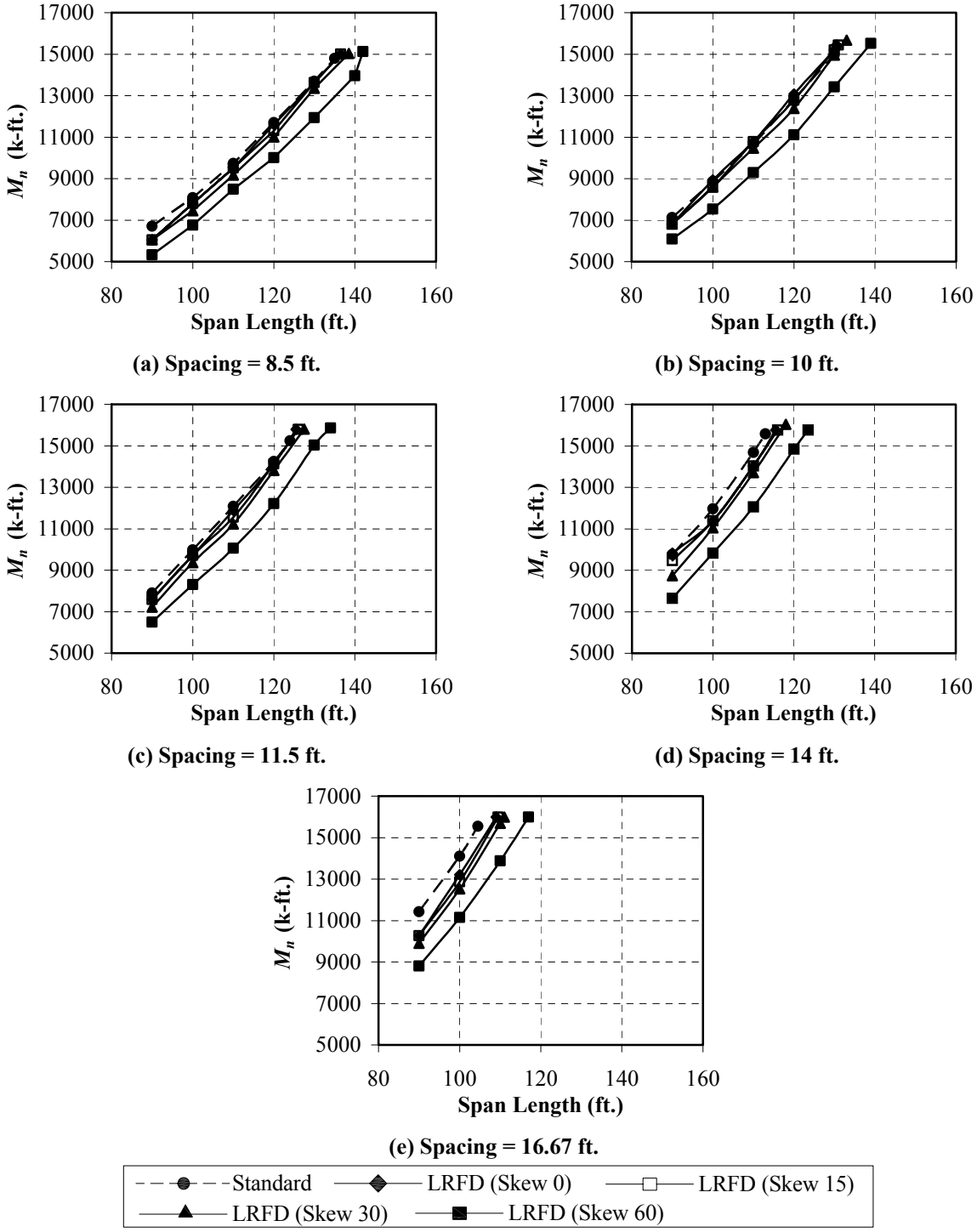


**Figure 4.16 Comparison of Nominal Moment Resistance (Strand Diameter 0.5 in.).**

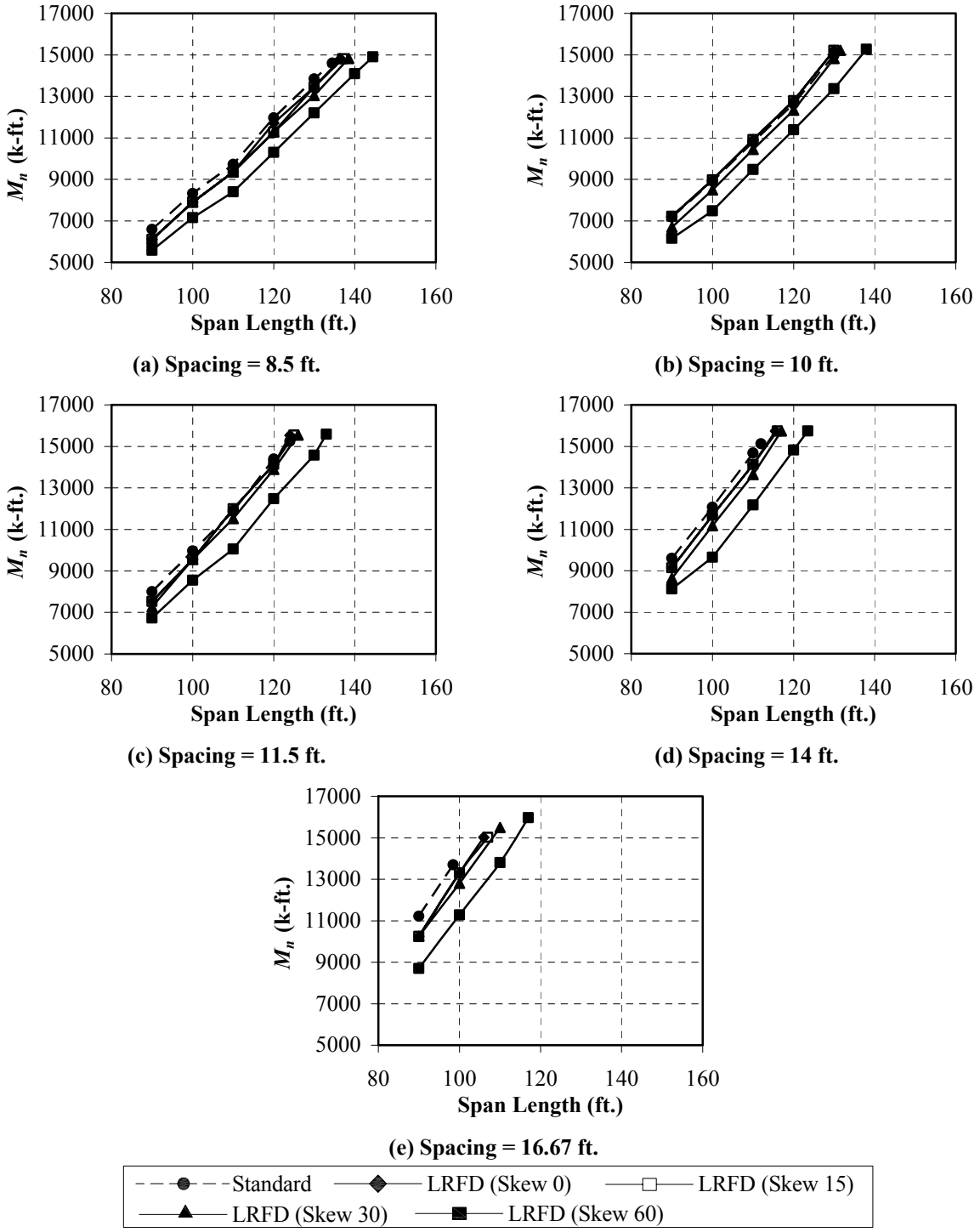


**Figure 4.17 Comparison of Nominal Moment Resistance (Strand Diameter 0.6 in.).**

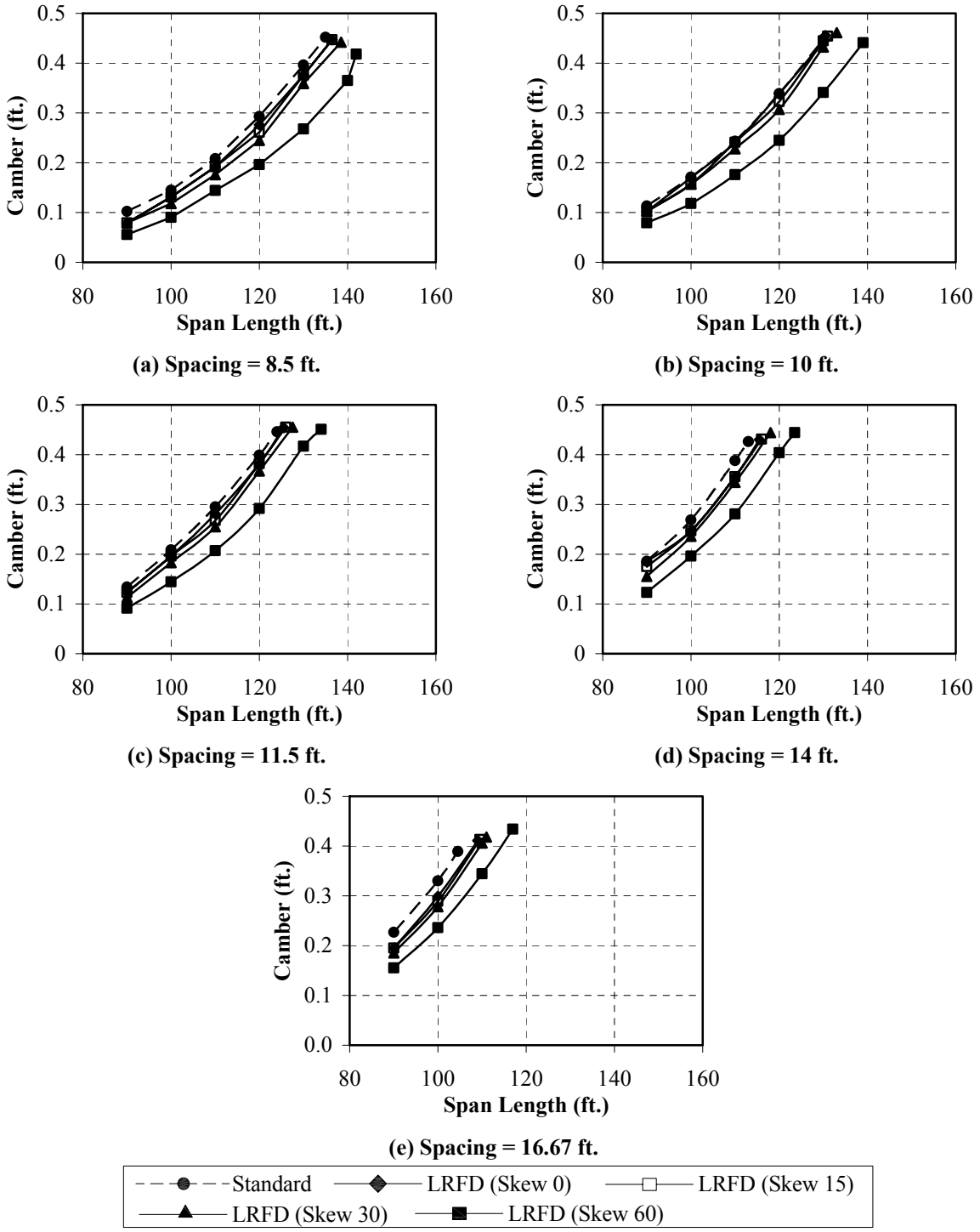


**Figure 4.18 Comparison of Camber (Strand Diameter 0.5 in.).**

**Table 4.26 Comparison of Camber (Strand Diameter 0.5 in.)**

| Spacing (ft.) | Span (ft.) | All Skews | Skew = 0 | | Skew = 15 | | Skew = 30 | | Skew = 60 | |
|---|---|---|---|---|---|---|---|---|---|---|
| | | Camber (ft.) | Camber (ft.) | % Diff. w.r.t STD | Camber (ft.) | % Diff. w.r.t STD | Camber (ft.) | % Diff. w.r.t STD | Camber (ft.) | % Diff. w.r.t STD |
| | | STD | LRFD | | LRFD | | LRFD | | LRFD | |
| 8.50 | 90.0 | 0.102 | 0.079 | -22.5 | 0.079 | -22.5 | 0.079 | -22.5 | 0.056 | -45.1 |
| | 100.0 | 0.145 | 0.131 | -9.7 | 0.131 | -9.7 | 0.118 | -18.6 | 0.09 | -37.9 |
| | 110.0 | 0.208 | 0.192 | -7.7 | 0.192 | -7.7 | 0.176 | -15.4 | 0.144 | -30.8 |
| | 120.0 | 0.293 | 0.276 | -5.8 | 0.261 | -10.9 | 0.245 | -16.4 | 0.196 | -33.1 |
| | 130.0 | 0.396 | 0.376 | -5.1 | 0.376 | -5.1 | 0.359 | -9.3 | 0.268 | -32.3 |
| 10.00 | 90.0 | 0.113 | 0.102 | -9.7 | 0.102 | -9.7 | 0.102 | -9.7 | 0.079 | -30.1 |
| | 100.0 | 0.171 | 0.17 | -0.6 | 0.157 | -8.2 | 0.157 | -8.2 | 0.118 | -31.0 |
| | 110.0 | 0.243 | 0.241 | -0.8 | 0.241 | -0.8 | 0.228 | -6.2 | 0.176 | -27.6 |
| | 120.0 | 0.339 | 0.338 | -0.3 | 0.323 | -4.7 | 0.307 | -9.4 | 0.245 | -27.7 |
| | 130.0 | 0.447 | 0.445 | -0.4 | 0.445 | -0.4 | 0.432 | -3.4 | 0.341 | -23.7 |
| 11.50 | 90.0 | 0.134 | 0.123 | -8.2 | 0.123 | -8.2 | 0.113 | -15.7 | 0.091 | -32.1 |
| | 100.0 | 0.209 | 0.196 | -6.2 | 0.196 | -6.2 | 0.183 | -12.4 | 0.144 | -31.1 |
| | 110.0 | 0.340 | 0.350 | -0.1 | 0.268 | -9.2 | 0.255 | -13.6 | 0.207 | -29.8 |
| | 120.0 | 0.399 | 0.382 | -4.3 | 0.382 | -4.3 | 0.367 | -8.0 | 0.292 | -26.8 |
| 14.00 | 90.0 | 0.186 | 0.185 | -0.5 | 0.175 | -5.9 | 0.155 | -16.7 | 0.123 | -33.9 |
| | 100.0 | 0.269 | 0.247 | -8.2 | 0.247 | -8.2 | 0.236 | -12.3 | 0.196 | -27.1 |
| | 110.0 | 0.388 | 0.356 | -8.2 | 0.356 | -8.2 | 0.344 | -11.3 | 0.281 | -27.6 |
| 16.67 | 90.0 | 0.227 | 0.195 | -14.1 | 0.195 | -14.1 | 0.185 | -18.5 | 0.155 | -31.7 |
| | 100.0 | 0.33 | 0.299 | -9.4 | 0.289 | -12.4 | 0.278 | -15.8 | 0.236 | -28.5 |

### 4.4.5 Shear Design

#### *4.4.5.1 Transverse Shear Reinforcement Area*

Table 4.27 and Figure 4.19 show the comparison of the transverse shear reinforcement area ($A_v$) for the LRFD designs relative to those of the Standard Specifications and the detailed results are reported in Appendix A. For all skews and both strand diameters, the $A_v$ calculated for designs based on the Standard Specifications

are more conservative when compared to those of the designs based on the LRFD Specifications. In general, the degree of conservatism increases with the increasing girder spacing, while the increasing span length has a very insignificant affect on this comparison, as can be noticed in Figure 4.19. Based on the summary of detailed results, as reported in Table 4.27, for the all skews and for 0.5 in. and 0.6 in. strand diameter, the $A_v$ for the LRFD designs decreases relative to the Standard designs in the range of 0.19 to 0.47 $in^2$ (30.1 to 46.6 percent).

**Table 4.27 Comparison of Transverse Shear Reinforcement Area (Strand Diameter 0.5 in.)**

| Spacing (ft.) | Span (ft.) | All Skews | Skew = 0 | | Skew = 15 | | Skew = 30 | | Skew = 60 | |
|---|---|---|---|---|---|---|---|---|---|---|
| | | $A_v$ ($in^2$) STD | $A_v$ ($in^2$) LRFD | % Diff. w.r.t STD | $A_v$ ($in^2$) LRFD | % Diff. w.r.t STD | $A_v$ ($in^2$) LRFD | % Diff. w.r.t STD | $A_v$ ($in^2$) LRFD | % Diff. w.r.t STD |
| 8.5 | 90 | 0.42 | 0.23 | -45.4 | 0.23 | -45.4 | 0.23 | -45.6 | 0.23 | -46.6 |
| | 100 | 0.47 | 0.28 | -39.8 | 0.28 | -39.9 | 0.28 | -40.6 | 0.27 | -41.5 |
| | 110 | 0.50 | 0.33 | -33.3 | 0.33 | -33.3 | 0.33 | -33.5 | 0.32 | -35.2 |
| | 120 | 0.48 | 0.33 | -30.7 | 0.33 | -30.7 | 0.33 | -31.1 | 0.32 | -33.4 |
| | 130 | 0.46 | 0.32 | -30.3 | 0.32 | -30.5 | 0.32 | -30.8 | 0.31 | -33.7 |
| 10 | 90 | 0.48 | 0.30 | -37.8 | 0.30 | -37.8 | 0.29 | -38.5 | 0.29 | -39.0 |
| | 100 | 0.53 | 0.36 | -33.3 | 0.36 | -33.4 | 0.35 | -33.5 | 0.35 | -34.9 |
| | 110 | 0.55 | 0.40 | -26.3 | 0.40 | -26.4 | 0.40 | -27.4 | 0.38 | -30.1 |
| | 120 | 0.54 | 0.39 | -27.1 | 0.39 | -27.3 | 0.39 | -27.6 | 0.38 | -29.3 |
| | 130 | 0.52 | 0.38 | -26.1 | 0.38 | -26.2 | 0.38 | -26.5 | 0.37 | -28.3 |
| 11.5 | 90 | 0.61 | 0.36 | -40.2 | 0.36 | -40.3 | 0.36 | -40.3 | 0.35 | -41.7 |
| | 100 | 0.67 | 0.43 | -36.0 | 0.43 | -35.9 | 0.43 | -36.0 | 0.42 | -37.1 |
| | 110 | 0.66 | 0.45 | -32.2 | 0.45 | -32.2 | 0.45 | -32.5 | 0.44 | -34.5 |
| | 120 | 0.66 | 0.44 | -32.7 | 0.44 | -32.8 | 0.44 | -33.5 | 0.43 | -35.1 |
| 14 | 90 | 0.85 | 0.50 | -41.5 | 0.50 | -41.5 | 0.50 | -41.5 | 0.49 | -42.9 |
| | 100 | 0.90 | 0.57 | -36.3 | 0.57 | -36.3 | 0.57 | -36.7 | 0.55 | -38.7 |
| | 110 | 0.91 | 0.57 | -37.9 | 0.57 | -38.0 | 0.56 | -38.6 | 0.54 | -40.3 |
| 16.67 | 90 | 1.08 | 0.62 | -42.5 | 0.62 | -42.5 | 0.62 | -42.5 | 0.61 | -43.3 |
| | 100 | 1.11 | 0.67 | -40.2 | 0.66 | -40.6 | 0.66 | -40.9 | 0.64 | -42.3 |

#### *4.4.5.2 Interface Shear Reinforcement Area*

Table 4.28 and Figure 4.20 show the comparison of the interface shear reinforcement area ($A_{vh}$) for the LRFD designs relative to those of the Standard Specifications and the detailed results are reported in Appendix A. For all skews and both strand diameters, the $A_{vh}$ calculated for designs based on the LRFD Specifications are more conservative when compared to those of the designs based on the Standard Specifications. In general, the degree of conservatism increases with the increasing girder spacing and the span length, as can be noticed in Figure 4.20. Based on the summary of detailed results, as reported in Table 4.21, for the all skews and for 0.5 in. and 0.6 in. strand diameter, the $A_{vh}$ for the LRFD designs increases relative to the Standard designs in the range of 0.47 to 1.39 $in^2$ (148 to 443 percent).

**Table 4.28 Comparison of Interface Shear Reinforcement Area (Strand Diameter 0.5 in.)**

| Spacing (ft.) | Span (ft.) | All Skews | Skew = 0 | | Skew = 15 | | Skew = 30 | | Skew = 60 | |
|---|---|---|---|---|---|---|---|---|---|---|
| | | $A_{vh}$ ($in^2$) | $A_{vh}$ ($in^2$) | % Diff. w.r.t STD | $A_{vh}$ ($in^2$) | % Diff. w.r.t STD | $A_{vh}$ ($in^2$) | % Diff. w.r.t STD | $A_{vh}$ ($in^2$) | % Diff. w.r.t STD |
| | | STD | LRFD | | LRFD | | LRFD | | LRFD | |
| 8.50 | 90.0 | 0.315 | 0.79 | 150.7 | 0.79 | 150.4 | 0.79 | 150.4 | 0.78 | 147.5 |
| | 100.0 | | 0.86 | 172.2 | 0.86 | 172.1 | 0.85 | 170.9 | 0.85 | 168.4 |
| | 110.0 | | 0.92 | 192.1 | 0.92 | 192.1 | 0.92 | 192.0 | 0.91 | 188.6 |
| | 120.0 | | 0.98 | 211.1 | 0.98 | 211.1 | 0.98 | 209.8 | 0.96 | 204.1 |
| | 130.0 | | 1.04 | 229.7 | 1.04 | 228.7 | 1.03 | 227.6 | 1.01 | 222.0 |
| 10.00 | 90.0 | | 0.94 | 199.8 | 0.94 | 199.8 | 0.94 | 198.4 | 0.94 | 197.0 |
| | 100.0 | | 1.02 | 223.1 | 1.02 | 223.1 | 1.02 | 223.1 | 1.01 | 219.5 |
| | 110.0 | | 1.09 | 246.6 | 1.09 | 246.6 | 1.09 | 244.9 | 1.07 | 240.2 |
| | 120.0 | | 1.16 | 267.3 | 1.15 | 266.1 | 1.15 | 264.9 | 1.14 | 260.7 |
| | 130.0 | | 1.22 | 288.8 | 1.22 | 288.8 | 1.21 | 285.7 | 1.20 | 280.4 |
| 11.50 | 90.0 | | 1.08 | 243.3 | 1.08 | 243.2 | 1.08 | 242.1 | 1.07 | 239.1 |
| | 100.0 | | 1.16 | 268.9 | 1.16 | 268.0 | 1.16 | 267.9 | 1.15 | 264.5 |
| | 110.0 | | 1.24 | 293.0 | 1.24 | 293.0 | 1.23 | 291.6 | 1.21 | 284.9 |
| | 120.0 | | 1.31 | 314.5 | 1.31 | 314.5 | 1.30 | 313.1 | 1.28 | 307.0 |
| 14.00 | 90.0 | | 1.37 | 333.5 | 1.37 | 333.5 | 1.36 | 332.5 | 1.35 | 328.4 |
| | 100.0 | | 1.47 | 365.7 | 1.47 | 365.7 | 1.46 | 364.0 | 1.44 | 358.4 |
| | 110.0 | | 1.56 | 393.7 | 1.56 | 393.7 | 1.55 | 392.2 | 1.53 | 385.0 |
| 16.67 | 90.0 | | 1.59 | 406.0 | 1.59 | 406.0 | 1.59 | 405.0 | 1.58 | 401.5 |
| | 100.0 | | 1.71 | 442.2 | 1.70 | 440.6 | 1.70 | 439.1 | 1.68 | 432.4 |

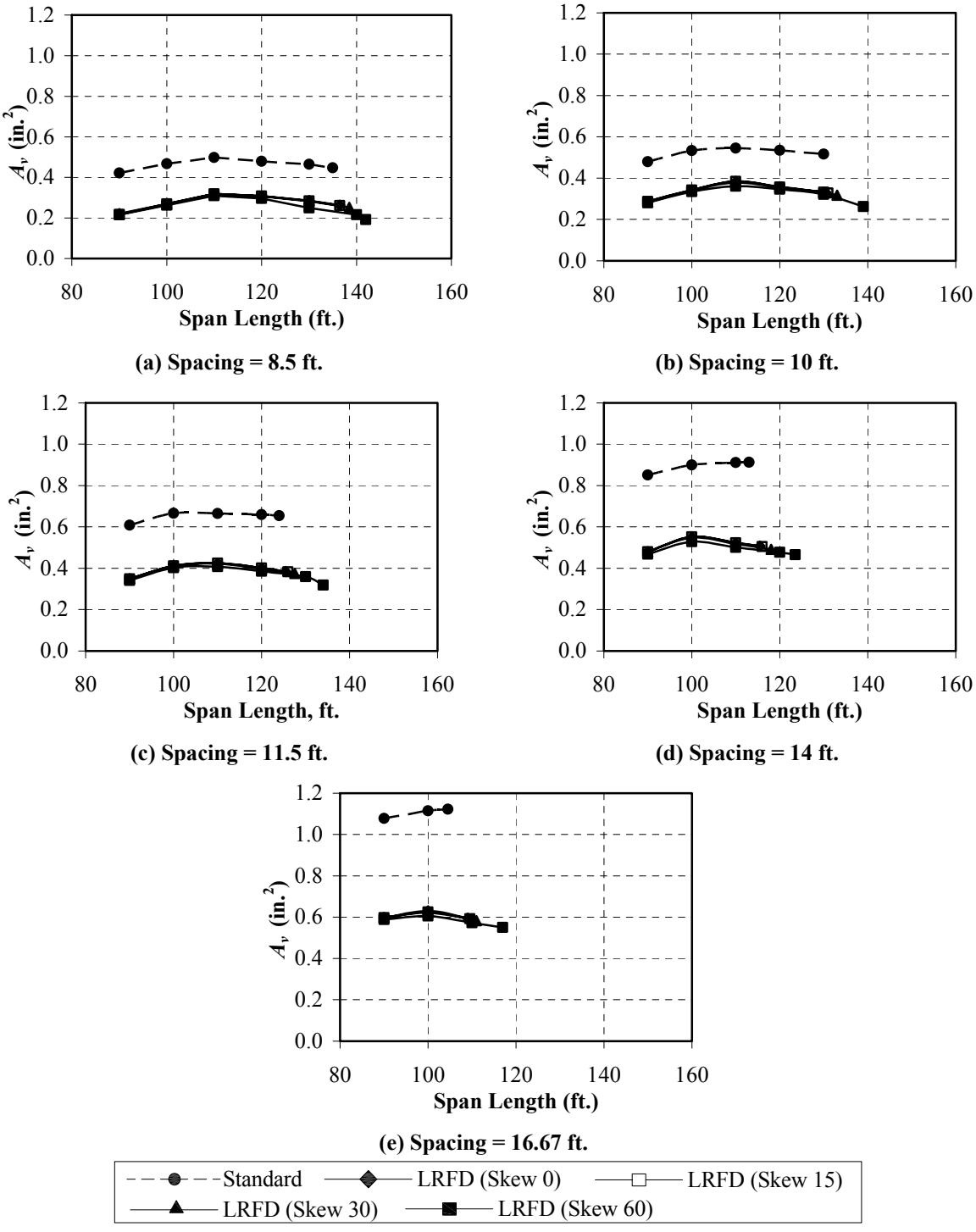


**Figure 4.19 Comparison of Transverse Shear Reinforcement Area (Strand Diameter 0.5 in.).**

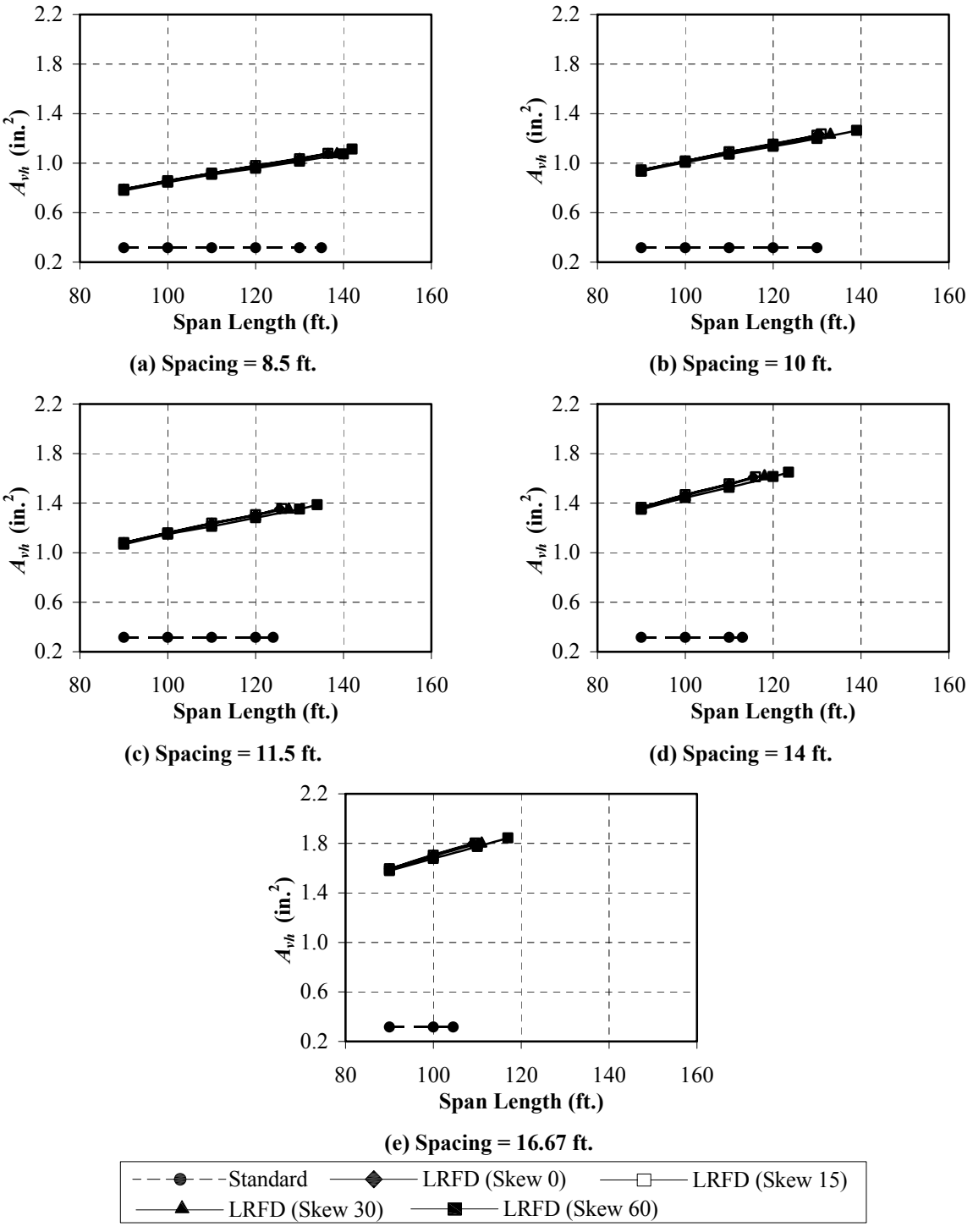


**Figure 4.20 Comparison of Interface Shear Reinforcement Area (Strand Diameter 0.5 in.).**

# 5. GRILLAGE ANALYSIS

## 5.1 INTRODUCTION

The approximate method of load distribution in the LRFD Specifications is convenient and gives conservative results, but it comes with certain limitations. The most restrictive limitations with respect to the typical Texas U54 beam bridges include the limitation on span length, number of beams, edge distance parameter, and girder spacing. It becomes mandatory to apply refined analysis procedures recommended by the LRFD Specifications in a case where these or other limitations are violated by any particular bridge design parameter. The limitations are there because these formulas were developed based on a database of bridges that fell within these limitations. Therefore, it is possible that beyond these limitations, the LRFD live load distribution factor (DF) formulas will continue to give conservative estimates for load distribution.

In the parametric study it was found that the span length limit for use of the LRFD live load DFs is violated for certain cases. In general, the refined analysis methods are time consuming and require expertise and experience to use them. The grillage analysis method is one such refined analysis method that can be used to analyze bridge superstructures. This section discusses the development of the equivalent grillage model of a typical Texas U54 beam bridge. Moreover, the results of the grillage analysis method and the results of the LRFD live load DF formulas are compared for the cases evaluated.

A three step procedure is followed to ensure that the grillage model developed represents the real bridge as correctly as possible. In the first step, a finite element modeling technique is verified against actual field measured results. In the second step, a correct grillage model is developed and calibrated against a finite element model. And in

the third step, the developed grillage model is used to evaluate the LRFD live load DF formulas. All steps and associated procedures are discussed in the following sections.

## 5.2 PROBLEM STATEMENT

The use of the LRFD live load distribution factor formulas is limited to spans no longer than 140 ft. The parametric study indicated that this limitation is slightly violated for the 8.5 ft. girder spacing with a 60 degree skew (corresponding maximum span = 144 ft.). The two cases noted in Table 5.1 are investigated using grillage analysis to determine the applicability of the LRFD live load distribution factor for spread box beams spanning up to 150 ft.

**Table 5.1 Parameters for Refined Analysis**

| Span (ft.) | Spacing (ft.) | Skew (degrees) |
|---|---|---|
| 140 | 8.5 | 60 |
| 150 | 8.5 | 60 |

## 5.3 VERIFICATION OF FINITE ELEMENT ANALYSIS

### 5.3.1 General

The Finite Element (FE) analysis results in this section are verified for their accuracy by comparing them with the results from field testing of an actual bridge. The purpose of this verification process is to ensure that the FE model adequately represents the actual bridge structure and that the results obtained by FE analysis are close to those measured experimentally on an actual bridge. This FE model will then be used in the selection and calibration of the grillage model used in this study.

### 5.3.2 Description of Bridge Used for Verification

Derhersville bridge in Pennsylvania, over Little Schuylkill River, was selected as for the verification of the FE analysis. It is a three span simply supported spread box girder prestressed bridge with 0 degree skew as shown in Figures C.1 and C.2 in Appendix C. The length of the test span was 61.5 ft. with a total roadway width of 30 ft. The specified minimum thickness of the bridge deck was 7.5 in. The bridge was supported by five prestressed spread box girders. The girder spacing and dimensions of girders, safety curb and parapet are shown in Figure C.2. Cast-in-place concrete diaphragms, 10 in. in thickness, are located between beams at the ends of the span and at the midspan. The joint between the slab and the curb was a construction joint with a raked finish and the verticle reinforcement for the curb section extended through the joint into the slab (Douglas and Vanhorn 1966).

Douglas and Vanhorn (1966) investigated the lateral distribution of static loads on Derhersville bridge by loading it with vehicular live loads and determined the response quantities such as bending moments and deflections at sections M and N shown in the elevation view of the bridge in Figure C.1.

### 5.3.3 Finite Element Model

A three dimensional FE model was developed for the test span of Derhersville bridge. A commercial FE analysis software, ANSYS version 8.0, was used for the analysis. Based on the analyses conducted by Chen and Aswad (1996) for spread box girders, two elements from ANSYS element library, such as BEAM44 and SHELL63, were found to be appropriate for this study. The spread box beams were modeled with a BEAM44 element and the deck slab was modeled with a SHELL63 element. The

parapet and curb were modeled with a BEAM44 element. The eccentricity of the centroids of the spread box girders, and curb and parapet was modeled by a rigid link element by assuming a 100 percent composite action of these elements with the deck slab. The mesh was generated with all the nodes spaced at 6 in. from the adjacent nodes. The total count of nodes in the mesh representing the deck was 7564 and the beam elements were meshed into 124 nodes. The total number of nodes in the entire model was 8432. The idealized FE model is superimposed on the actual bridge section in Figure 5.1. The truck axle load as shown in Figure C.3 (Appendix C) is statically distributed to the closest nodes. Hinge support was considered at one end of the bridge and a roller support was considered at the other end of the bridge.

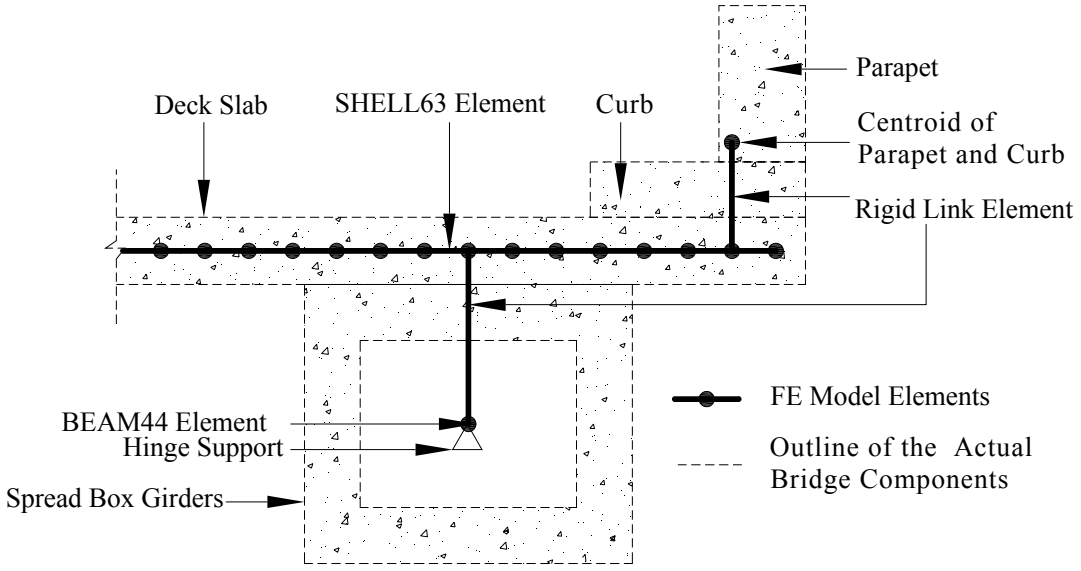


**Figure 5.1 Illustration of the Finite Element Model Used for Verification.**

BEAM44 element is a uniaxial element with tension, compression, torsion, and bending capabilities, while SHELL63 element has bending and membrane capabilities. Both the elements are three dimensional elements with six degree of freedoms at each node (i.e. translation in nodal x, y, and z directions and rotations about nodal x, y, and z directions).

### 5.3.4 Comparison of Results (FE analysis vs Actual Field Measurements)

Figure C.2 (Appendix C) shows the location of seven loading lanes on the roadway. These lanes are selected such that the truck centerline closely corresponds to the girder centerline or to a line midway between girder centerlines. For the purpose of comparison only the results for the two cases of loading lanes are shown in this study: (1) Lane 4 loaded, (2) Lanes 1 and 4 loaded. The results are presented in Figure 5.2 and Tables 5.2 and 5.3.

**Table 5.2 Comparison of Experimental Results with Respect to Finite Element Analysis Results (Lanes 1 and 4 Loaded)**

| Girder Location (See Figure C.2) | Experimental Results (k - ft.) | FEA (k - ft.) | Diff. w.r.t. Experimental Results (%) |
|---|---|---|---|
| A | 477.12 | 280.00 | 41 |
| B | 373.03 | 339.63 | 9 |
| C | 273.76 | 295.60 | -8 |

Note: The comparison is made between respective bending moment values at section M as shown in Figure C.1.

**Table 5.3 Comparison of Experimental Results with Respect to Finite Element Analysis Results (Lane 4 Loaded)**

| Girder Location (See Figure C.2) | Experimental Results (k - ft.) | FEA (k - ft.) | Diff. w.r.t. Experimental Results (%) |
|---|---|---|---|
| A | 144.01 | 108.51 | 25 |
| B | 158.50 | 162.68 | -3 |
| C | 178.35 | 210.93 | -18 |
| D | 135.48 | 162.68 | -20 |
| E | 131.96 | 108.51 | 18 |

Note: The comparison is made between respective bending moment values at section M as shown in Figure C.1.

For interior girder C the moment value of the FE analysis is 8 and 18 percent higher than that of the moment values determined experimentally, while for the exterior girder A this difference is 41 and 25 percent lesser than that of the values determined experimentally.

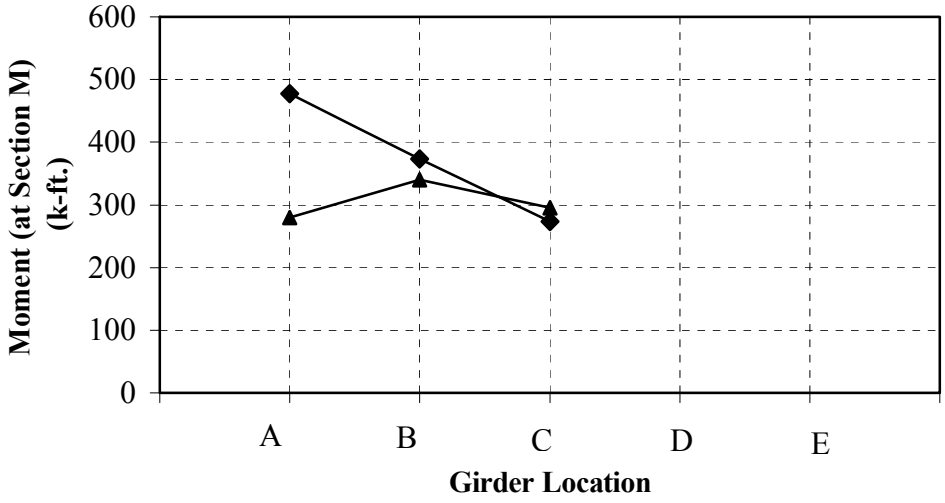


**(a) Lanes 1 and 4 Loaded**

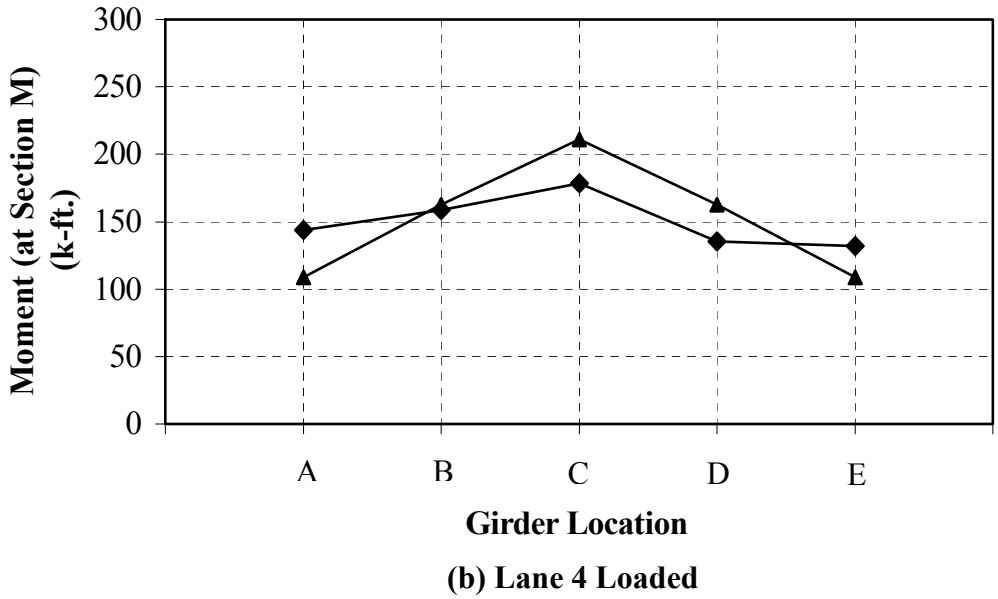


**(b) Lane 4 Loaded**

**Figure 5.2 Comparison of Experimental Results vs. FEA Results.**

## 5.4 CALIBRATION OF GRILLAGE MODEL

### 5.4.1 General

The grillage analogy method is an approximate method of analysis in which a bridge superstructure is modeled as equivalent grillage of rigidly connected beams at discrete nodes. The geometry and properties of the network of grillage beams, support conditions and application of loads should be such that if the real bridge superstructure and the equivalent grillage are subjected to the same deflections and rotations at the grillage nodes, the resulting force response in both the structures should be equivalent. This section discusses the approach and results of calibration of the grillage model with respect to the results of the FE analysis. The grillage model developed in this section is used to analyze the two cases described in Section 5.2. The FE model of the U54 girder bridge shown in Figure 3.1 (Section 3) is developed based on the modeling approach discussed in Section 5.3.3.

### 5.4.2 Grillage Models

The development of the grillage model is discussed in detail in Section 5.5 and is not repeated here and only the differences are highlighted in this section. The calibration procedure was performed for a U54 girder bridge with 110 ft. span length and 8.5 ft. girder spacing with five U54 girders. Two grillage models were selected: (1) one longitudinal grillage member representing each web of a U54 girder and is shown in Figure 5.3, (2) one longitudinal grillage member representing a U54 girder and is shown in Figure 5.4. Both of these models included the supports with the torsional restraint and

edge longitudinal members. Moreover, the transverse grillage members that coincided with the end and intermediate diaphragm locations were assigned the section properties corresponding to the end and intermediate diaphragms as described in Section 5.5. The transverse grillage members were spaced at 5 ft. center-to-center. The distance between the two longitudinal members, representing a U54 girder, was taken to be 65 in. for Grillage Model No. 1 as shown in Figure 5.5. For Grillage Model No. 2 the distance between adjacent longitudinal members was 102 in., corresponding to the girder spacing.

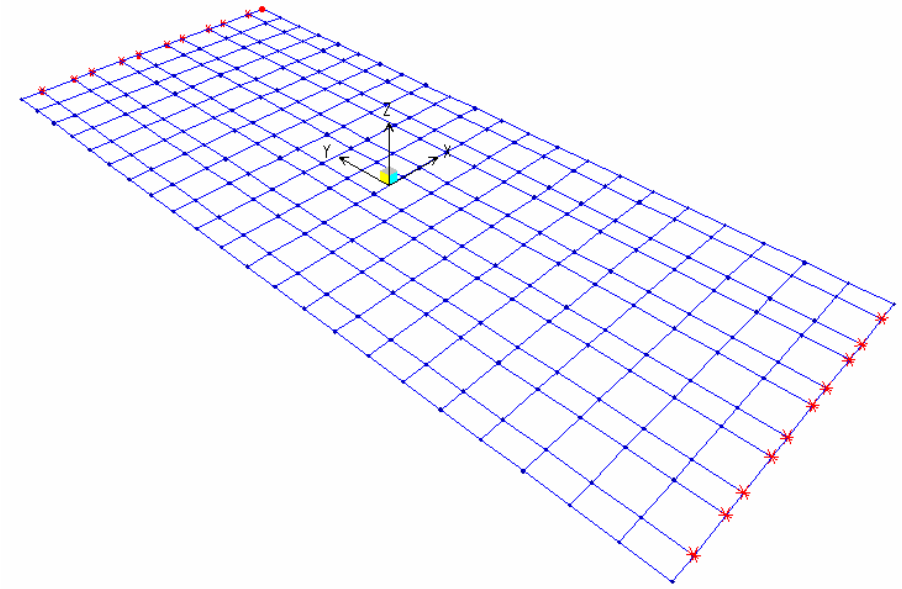


**Figure 5.3 Grillage Model No. 1.**

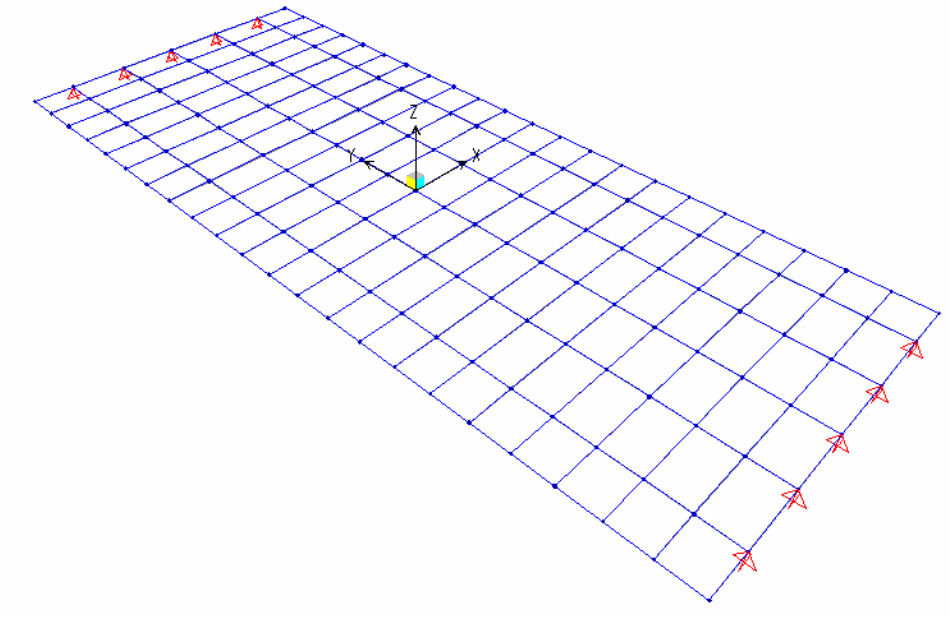


**Figure 5.4 Grillage Model No. 2.**

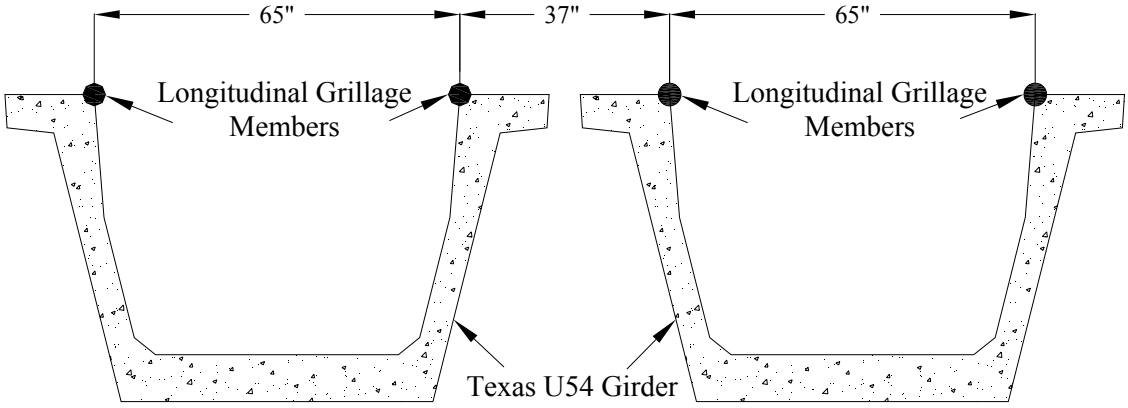


**Figure 5.5 Location of Longitudinal Member for Grillage Model No. 1.**

### 5.4.3 Comparison of Results (FE analysis vs Grillage Model)

The analysis results of Grillage Model No. 1 and No. 2 are compared with those of the FE analysis and are presented in Tables 5.4 and 5.5, respectively. The Grillage Model No. 1 yield results that are closer to the FE analysis results.

**Table 5.4 Comparison of FE Analysis Results with Respect to Grillage Model No. 1**

| Lanes Loaded | Moment (k-ft.) | | | |
|---|---|---|---|---|
| | Interior Girder | | Exterior Girder | |
| | FEA | Grillage | FEA | Grillage |
| One Lane Loaded | 381 | 396 | 557 | 513 |
| Two or More Lanes Loaded | 1116 | 1101 | 1246 | 1148 |

**Table 5.5 Comparison of FE Analysis Results with Respect to Grillage Model No. 2**

| Lanes Loaded | Moment (k-ft.) | | | |
|---|---|---|---|---|
| | Interior Girder | | Exterior Girder | |
| | FEA | Grillage | FEA | Grillage |
| One Lane Loaded | 381 | 412 | 557 | 496 |
| Two or More Lanes Loaded | 1116 | 1080 | 1246 | 1114 |

Grillage Model No. 1 is further calibrated for several conditions and all the analysis cases are described in Table 5.6. The results of grillage analyses for cases 1 through 4 and their comparison with the FE analysis results are presented in Tables 5.7 through 5.10. Its obvious that case 4 yields results closest to those of FE analysis for the interior girder and case 1 yields results that are closest to those of the FE analysis for the exterior girder. Case 4 is selected as the final grillage model as the focus of this study is only on the interior girders.

**Table 5.6 Various Cases Defined for Further Calibration on Grillage Model No. 1**

| Condition | Case 1 | Case 2 | Case 3 | Case 4 |
|---|---|---|---|---|
| Torsional Restraint Provided | no | yes | yes | yes |
| Section Properties of Intermediate and End Diaphragm Provided | no | no | yes | yes |
| Edge Longitudinal Members Provided | no | no | no | yes |

**Table 5.7 Comparison of Results for FEA with Respect to the Grillage Model No. 1 (Case No. 1)**

| Lanes Loaded | Moment (k-ft.) | | | |
|---|---|---|---|---|
| | Interior Girder | | Exterior Girder | |
| | FEA | Grillage | FEA | Grillage |
| One Lane Loaded | 381 | 441 | 557 | 567 |
| Two or More Lanes Loaded | 1116 | 1152 | 1246 | 1218 |

**Table 5.8 Comparison of Results for FEA with Respect to the Grillage Model No. 1 (Case No. 2)**

| Lanes Loaded | Moment (k-ft.) | | | |
|---|---|---|---|---|
| | Interior Girder | | Exterior Girder | |
| | FEA | Grillage | FEA | Grillage |
| One Lane Loaded | 381 | 431 | 557 | 548 |
| Two or More Lanes Loaded | 1116 | 1140 | 1246 | 1195 |

**Table 5.9 Comparison of Results for FEA with Respect to the Grillage Model No. 1 (Case No. 3)**

| Lanes Loaded | Moment (k-ft.) | | | |
|---|---|---|---|---|
| | Interior Girder | | Exterior Girder | |
| | FEA | Grillage | FEA | Grillage |
| One Lane Loaded | 381 | 429 | 557 | 513 |
| Two or More Lanes Loaded | 1116 | 1101 | 1246 | 1148 |

**Table 5.10 Comparison of Results for FEA with Respect to the Grillage Model No.1 (Case No. 4)**

| Lanes Loaded | Moment (k-ft.) | | | |
|---|---|---|---|---|
| | Interior Girder | | Exterior Girder | |
| | FEA | Grillage | FEA | Grillage |
| One Lane Loaded | 381 | 419 | 557 | 529 |
| Two or More Lanes Loaded | 1116 | 1127 | 1246 | 1182 |

## 5.5 GRILLAGE MODEL DEVELOPMENT

### 5.5.1 General

This section discusses the procedure of idealizing the physical bridge superstructure into an equivalent grillage model. The properties of longitudinal and transverse grid members are evaluated and support conditions are specified. The grillage model is developed based on the guidelines in the available literature such as Hambly (1991) and Zokaie et al. (1991). The grillage model was modeled and analyzed as a grid of beam elements by SAP2000, a structural analysis software (SAP2000 Version 8).

### 5.5.2 Grillage Model Geometry

The bridge cross-section shown in Figure 3.1 is modeled with a set of longitudinal and transverse beam elements. Figure 5.6 shows the placement of transverse and longitudinal grillage members adopted in this study. The grillage members are placed in the direction of principle strengths. Two longitudinal grillage members were placed for each U54 girder, i.e. representing each web of the girder. The longitudinal grillage members are aligned in the direction of skew because the deck will tend to span in the skew direction. The longitudinal members are skewed at 60 degrees with the support centerline. The transverse grillage members are oriented perpendicular to the longitudinal grillage members as shown in Figure 5.6.

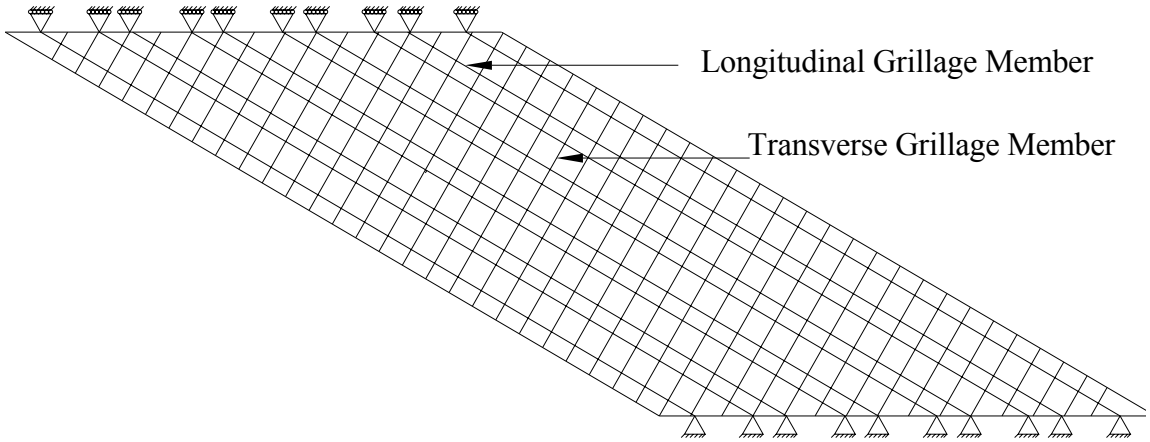


**Figure 5.6 Grillage Model (for 60 Degree Skew).**

### 5.5.3 Grillage Member Properties and Support Conditions

Grillage analysis requires the calculation of the moment of inertia, *I*, and torsional moment of inertia, *J,* for every grillage member. The following subsections discuss the equations used to find the torsional constant, and later, these two quantities are calculated for the various longitudinal and transverse grillage members.

#### *5.5.3.1 St. Venant's Torsional Stiffness Constant*

LRFD commentary C.4.6.2.2.1 allows the use of following relationships to determine the St. Venant's torsional inertia, *J*, instead of a more detailed evaluation.

1. For thin-walled open beams:

$$J = \frac{1}{3}\sum bt^3 \tag{5.1}$$

2. For stocky open sections (e.g., prestress I-beams and T-beams) and solid sections:

$$J = \frac{A^4}{40.0 I_p} \tag{5.2}$$

3. For closed thin-walled shapes:

$$J = \frac{4A_o^2}{\sum \frac{s}{t}} \tag{5.3}$$

where:

$b$ = Width of plate element (in.)

$t$ = Thickness of plate-like element (in.)

$A$ = Area of cross-section (in.$^2$)

$I_p$ = Polar moment of inertia (in.$^4$)

$A_o$ = Area enclosed by centerlines of elements (in.$^2$)

$s$ = Length of a side element (in.)

*5.5.3.2 Longitudinal Grillage Members*

Longitudinal grillage members distribute the live load in the longitudinal direction. Two longitudinal members are placed along each U54 beam, one along each web as recommended by Hambly (1991). The longitudinal girder moment of inertia is taken as the composite inertia of the girder with the contributing slab width for compositely designed U54 beams.

**Composite Texas U54 Bridge Girders**

The St. Venant's torsional stiffness constant for a composite U54 beam bridge girder cross-section can be calculated by Equation 5.3 as it corresponds to a closed thin-walled shape. The quantities $A_o$ and $\Sigma s/t$ for the composite section shown in Figure 5.7 are calculated and values are listed in Table 5.11. The torsional stiffness constant, $J$, and

the moment of inertia, $I$, are also calculated and listed in Table 5.11. Because two longitudinal grillage members were used for each U54 beam, both of inertia values are taken as half (i.e. $I$ = 503,500 in.$^4$ and $J$= 653,326.5 in.$^4$).

**Table 5.11 Composite Section Properties for U54 Girder**

| $A_o$ (in.$^2$) | $\Sigma s/t$ | $J$ (in.$^4$) | $I$ (in.$^4$) |
|---|---|---|---|
| 3453 | 36.5 | 1,306,653 | 1,007,000 |

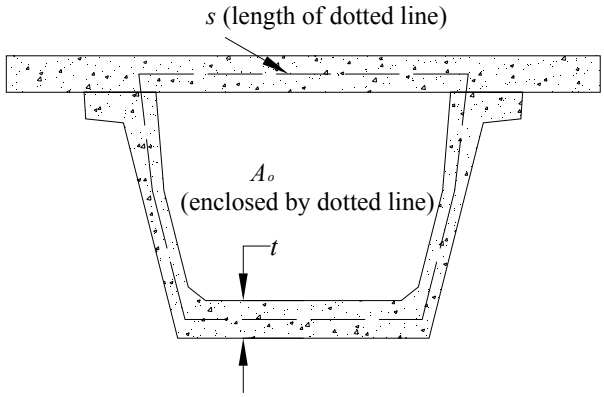


**Figure 5.7 Calculation of St. Venant's Torsional Stiffness Constant for Composite U54 Girder.**

**Edge Stiffening Elements**

The edge stiffening elements represent the T501 rails that were used in this study as per TxDOT practice. To simplify the calculations, the T501 rail is approximated as a combination of two rectangular sections joined together as shown in the Figure 5.8. The dimensions of the equivalent rectangular shape are selected such that the area is equal to the actual area of the T501 type barrier. Note that the effect of the edge stiffening elements was ignored during the development of the LRFD live load distribution factor formulas by Zokaie et al. (1991).

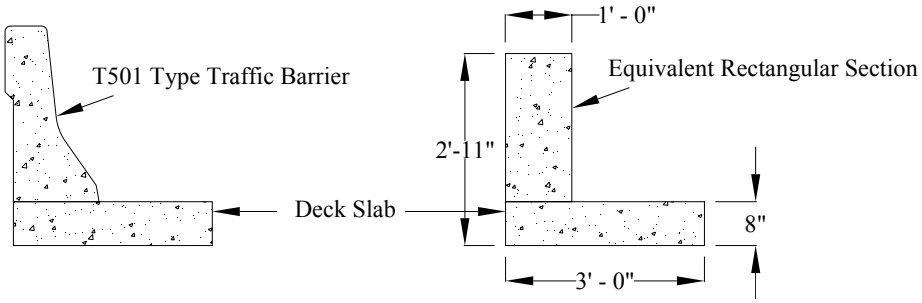


**Figure 5.8 T501 Type Traffic Barrier and Equivalent Rectangular Section.**

The St. Venant's torsional stiffness constant for the T501 rail or the equivalent rectangular section, which is the category of stocky open sections, was calculated by Equation 5.2. The torsional stiffness constant for the equivalent section is 28,088 in.$^4$ and the moment of inertia for the equivalent section is 67,913 in.$^4$

### *5.5.3.3 Transverse Grillage Members*

Transverse grillage members distribute the live load in the transverse direction. The number of transverse grillage members needed depends upon the type of results desired and the applied loading conditions. As the grillage mesh gets coarser, the load application becomes more approximate and a finer grillage mesh ensures not only a better result but also the load application tends to be more exact. In this study, the grillage members are spaced 5 ft. center-to-center, so that errors introduced in applying the loads to the nodal locations is minimized. Zokaie et al. (1991) recommended that transverse grillage spacing should be less than 1/10 of the effective span length and Hambly (1991) recommends lesser than 1/12 of the effective span length. The effective span length is the distance between the support center lines and transverse grillage spacing was taken as 1/28 of the effective span length for 140 ft. span length and 1/30 of the effective span length for 150 ft.

**Bridge Deck in Transverse Direction**

In the transverse direction where no diaphragms are present, the transverse grillage members are modeled as a rectangular section of the deck slab with a thickness of 8 in. and a tributary width of 60 in. The St. Venant's torsional stiffness constant for both diaphragm types, which can be treated as thin-walled open sections, is calculated by Equation 5.1. The resulting torsional stiffness constant and the moment of inertia for the general transverse grillage members is calculated to be 10,240 $in.^4$ and 5120 $in.^4$, respectively.

**End Diaphragms and Intermediate Diaphragms**

The TxDOT Bridge Design Manual (TxDOT 2001) requires intermediate and end diaphragms in a Texas U54 beam type bridge. The idealized composite cross-sections considered for the end and intermediate diaphragms are shown in the Figure 5.9.

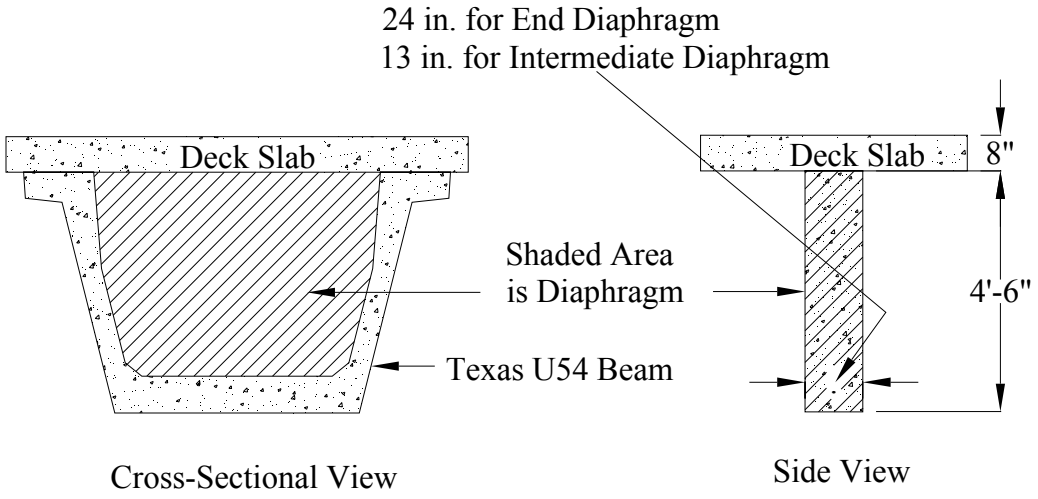


**Figure 5.9 Cross-Sections of End and Intermediate Diaphragms.**

The end diaphragm has a web thickness of 24 in., while the intermediate diaphragm has a web thickness of 13 in. Because the transverse grid members are spaced at 5 ft. center-to-center, the tributary width of the deck slab contributing to each diaphragm is taken to be 60 in. The St. Venant's torsional stiffness constant for both the

diaphragm types, which can be treated as stocky open sections, is calculated by Equation 5.2. The torsional stiffness constant and the moment of inertia for the end diaphragm is calculated to be 194,347 $in.^4$ and 1,073,566 $in.^4$, respectively. The torsional stiffness constant and the moment of inertia for the intermediate diaphragm is calculated to be 39,621 $in.^4$ and 1,077,768 $in.^4$, respectively.

#### *5.5.3.4 Support Conditions*

Because of the large transverse diaphragms at the supports, the torsional rotation of the longitudinal grillage members was fixed at the supports. Moreover, the translation was fixed in all three directions.

## 5.6 APPLICATION OF HL-93 DESIGN TRUCK LIVE LOAD

The HL-93 design live load truck was placed to produce the maximum response in the girders. In the case of bending moment, the resultant of the three axles of the HL-93 design truck was made coincident with the midspan location of the bridge. In the case of shear force calculations, the 32 kip axle of the HL-93 design truck was placed on the support location. In the transverse direction, first the HL-93 design truck is placed at 2 ft. from the edge of the barrier and all other trucks were placed at 4 ft. distance from each neighboring truck. The truck placement is shown in the Figures 5.10 and 5.11. Several lanes were loaded with the design truck and different combinations of the loaded lanes were considered and the maximum results were selected. After placement of the design truck, the wheel line load for each axle was distributed proportionally in the transverse direction to the adjacent longitudinal grillage members.

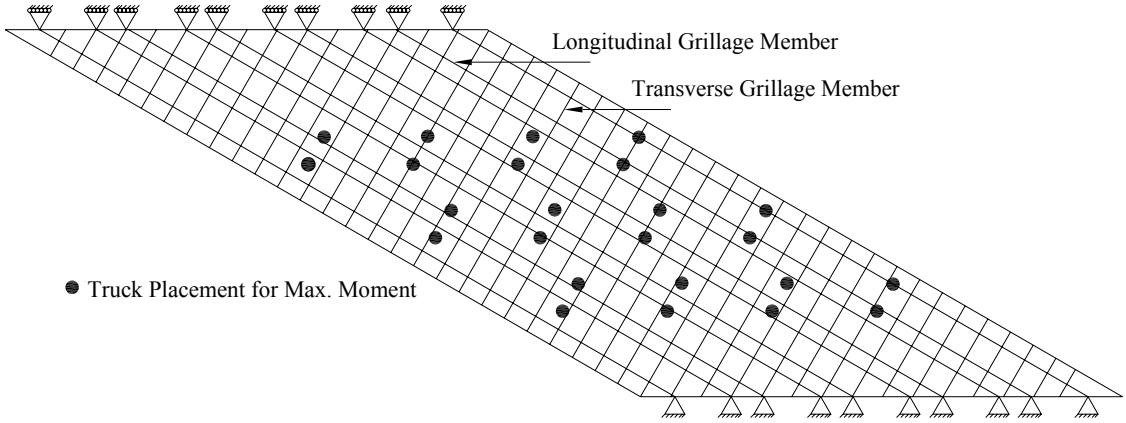


**Figure 5.10 Application of Design Truck Live Load for Maximum Moment on Grillage Model.**

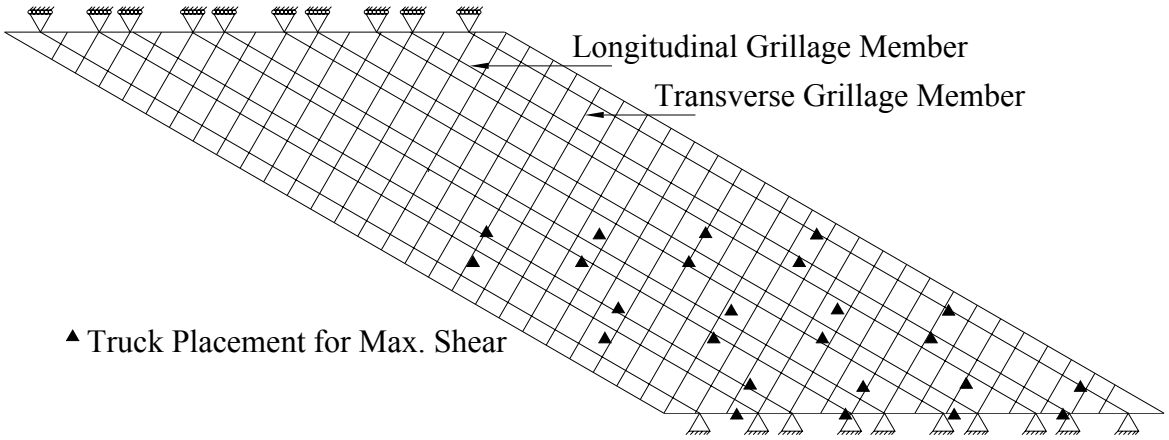


**Figure 5.11 Application of Design Truck Live Load for Maximum Shear on Grillage Model.**

## 5.7 GRILLAGE ANALYSIS AND POSTPROCESSING OF RESULTS

### *5.7.1.1 Multiple Presence Factors*

Multiple presence factors are intended to account for the probability of simultaneous lane occupation by the full HL-93 design live load. Table 5.12 summarizes the multiple presence factors that are recommended in LRFD Art. 3.6.1.1.2.

**Table 5.12 LRFD Multiple Presence Factors**

| No. of Lanes | Factors |
|---|---|
| One | 1.20 |
| Two | 1.00 |
| Three | 0.85 |
| More than Three | 0.65 |

### *5.7.1.2 Distribution Factors Based on Grillage Analysis*

The maximum girder moments and support shears are noted from the analysis of the grillage model for both the exterior and interior beams. After determining the moment and shear results from the grillage analysis, the moment and shear DFs are calculated to compare them with the LRFD DFs. The maximum distribution factor is the maximum force in a bridge girder divided by the maximum force produced by loading a simply supported beam with axle load of the HL-93 design truck in the longitudinal location. The design truck placement on a simply supported beam for moment and shear is shown in Figure 5.11. The DFs from the grillage analysis results are calculated by the following equation.

$$DF = \frac{N_{grillage}}{N_{SS}} \tag{5.4}$$

where:

$N_{grillage}$ = Maximum moment or shear calculated by the grillage analysis

$N_{SS}$ = Maximum moment or shear calculated by loading a simply supported beam in the same longitudinal direction with the same load placement as the grillage analysis.

The multiple presence factor is taken into account for cases of two or more lanes loaded by multiplying the DF, from Equation 5.4, by the appropriate multiple presence factor from Table 5.11.

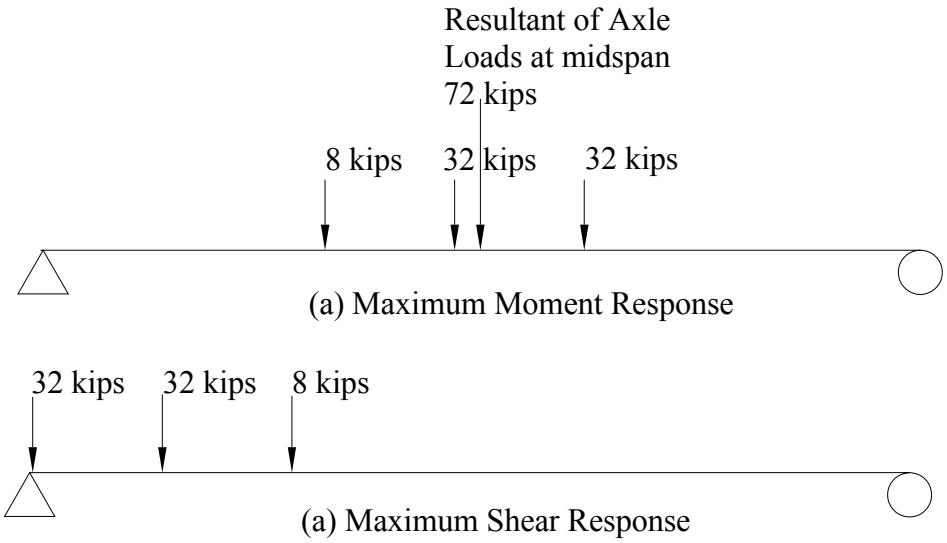


**Figure 5.12 Design Truck Load Placement on a Simply Supported Beam for Maximum Response.**

Based on the load placement shown in Figure 5.12, the maximum moments and shears for a simply supported beam are calculated for the two span lengths of 140 ft. and 150 ft., and are given in Table 5.13 below.

**Table 5.13 Maximum Moment and Shear Response on a Simply Supported Beam**

| Span Length (ft.) | Moment (k-ft.) | Shear (kips) |
|---|---|---|
| 140 | 2240 | 67.2 |
| 150 | 2420 | 67.5 |

## 5.8 LRFD LOAD DISTRIBUTION FACTORS

The live load DFs based on LRFD Art. 4.6.2.2. are calculated for the purpose of comparison with those found by the grillage analysis method. The DFs for interior and exterior girders, for one lane and two or more lanes loaded, and for shear and moments are summarized in Table 5.14. As recommended in LRFD Table 4.6.2.2.3b-1 and LRFD Table 4.6.2.2.2d-1, the DFs for exterior girders and one lane loaded case are relatively large because these are calculated by the lever rule method as per LRFD Specifications, which gives very conservative results. For comparison, the DF computed using the LRFD approximations are provided in parenthesis.

**Table 5.14 LRFD Live Load Moment and Shear Distribution Factors**

| Span Length (ft.) | No. of Lanes Loaded | Moment | | Shear | |
|---|---|---|---|---|---|
| | | Interior Girder | Exterior Girder | Interior Girder | Exterior Girder |
| 140 | One | 0.187 | 1.200 (0.357) | 0.643 | 2.220 (1.513) |
| | Two or More | 0.340 | 0.357 | 0.792 | 1.513 |
| 150 | One | 0.180 | 0.740 (0.350) | 0.639 | 2.260 (1.530) |
| | Two or More | 0.333 | 0.350 | 0.787 | 1.530 |

## 5.9 SUMMARY OF RESULTS AND CONCLUSION

Tables 5.15 and 5.16 summarize the findings of this section by comparing the live load DFs from the grillage analysis with those calculated by the LRFD Specifications for moment and shear, respectively. In general, the grillage analysis results are always conservative with respect to those of the LRFD Specifications. The difference for shear DFs for exterior girders is relatively large as compared to the difference for moment DFs and shear DFs for interior girders. This trend can be explained for two reasons: (1) for exterior girders with one lane loaded, the DFs are calculated by the lever rule method that gives very conservative results, and (2) for shear in exterior girders the LRFD Specifications specifies very large shear correction factors for skewed bridges.

**Table 5.15 Comparison of Moment DFs**

| Span Length (ft.) | No. of Lanes Loaded | Moment | | | |
|---|---|---|---|---|---|
| | | Interior Girder | | Exterior Girder | |
| | | LRFD DF | Grillage DF | LRFD DF | Grillage DF |
| 140 | One | 0.187 | 0.152 | 1.200 | 0.200 |
| | Two or More | 0.340 | 0.250 | 0.357 | 0.293 |
| 150 | One | 0.180 | 0.178 | 0.740 | 0.212 |
| | Two or More | 0.333 | 0.280 | 0.350 | 0.310 |

**Table 5.16 Comparison of Shear DFs**

| Span Length (ft.) | No. of Lanes Loaded | Shear | | | |
|---|---|---|---|---|---|
| | | Interior Girder | | Exterior Girder | |
| | | LRFD DF | Grillage DF | LRFD DF | Grillage DF |
| 140 | One | 0.643 | 0.450 | 2.220 (1.513) | 0.786 |
| | Two or More | 0.792 | 0.678 | 1.513 | 0.914 |
| 150 | One | 0.639 | 0.529 | 2.260 (1.530) | 0.790 |
| | Two or More | 0.787 | 0.750 | 1.530 | 0.950 |

Thus, based on the results of the grillage analysis it can be concluded that the LRFD distribution factor formulas are conservative. However, a more refined analysis such as a finite element analysis is recommended to validate the results of the grillage analysis results presented in this section.

# 6. SUMMARY, CONCLUSIONS AND RECOMMENDATIONS

## 6.1 SUMMARY

This thesis summarizes the details of one portion of TxDOT Research Project 0-4751 "Impact of AASHTO LRFD Specifications on the Design of Texas Bridges." The objectives of this portion of the study are to evaluate the impact of the current LRFD Specifications on typical Texas precast, pretensioned U54 bridge girders, to perform a critical review of the major changes when transitioning to LRFD design, and to recommend guidelines to assist TxDOT in implementing the LRFD Specifications. The research project objectives were accomplished by five tasks: (1) to review and synthesize the available literature, such that the background research relevant to the development of the AASHTO LRFD Bridge Design Specifications is documented; (2) to develop two detailed design examples, so that the application of *the AASHTO Standard Specifications for Highway Bridges, 17th edition* (2002) and *AASHTO LRFD Bridge Design Specifications, 3rd edition* (2004), for typical precast, pretensioned Texas U54 beam bridges can be illustrated; (3) to conduct a parametric study in order to perform an in-depth analysis of the differences between designs using the current Standard and LRFD Specifications (AASHTO 2002, 2004), with a focus on bridge types that are of most interest to TxDOT for future bridge structures; (4) to identify the crucial design issues for pretensioned concrete Texas U beams based on the parametric study supplemented by the literature review; and (5) to provide guidelines for revised design criteria as necessary.

The first task was accomplished through literature search of the background research relevant to the development of the LRFD Specifications. Various topics were covered in this task, such as history and development of the AASHTO LRFD Specifications, significant changes in the LRFD Specifications relative to the Standard

Specifications, reliability theory and LRFD code calibration, development of live load model and distribution factors, and debonding of prestressing strands. A literature review of refined analysis procedures used in this study was also performed.

Two detailed design examples, for Texas U54 beams, were prepared in the second task to assist TxDOT engineers to understand the design procedures of the LRFD Specifications by comparing with the design procedures of the Standard Specifications. In both the detailed design examples, the PSTRS14 (TxDOT 2004) method of determining prestress losses, initial and final concrete strengths, and debonding of strands by an iterative procedure was used. Camber was calculated by the Hyperbolic Functions Method (Sinno 1968). Based on TxDOT practice (TxDOT 2001), the modular ratio between beam and slab concrete was considered as unity for the service limit state design, in which the number of strands and optimum values of initial and final concrete strengths are determined. The actual value of modular ratio was used for all other limit states.

The third task, the parametric study, was accomplished by selecting appropriate parameters, as shown in Table 6.1, and for various combinations of these parameters the detailed designs calculations were performed for both specifications. Different design trends were determined and compared, graphically and in tabular format, for both specifications. In addition, the parametric study was used to identify the most critical limit states for the design of different bridge geometries. Significant observations were made with the comparisons of the shear design, number of strands, undistributed and distributed live load affects, and maximum possible span lengths.

**Table 6.1 Summary of Design Parameters for Parametric Study**

| Parameter | Description / Selected Values |
|---|---|
| Girder Spacing (ft.) | 8'-6", 10' -0", 11'-6", 14'-0" and 16'-8" |
| Spans | 90 ft. to maximum span at 10 ft. intervals |
| Strand Diameter (in.) | 0.5 and 0.6 |
| Concrete Strength at Release, $f'_{ci}$ | varied from 4,000 to 6,750 psi for design with optimum number of strands |
| Concrete Strength at Service, $f'_c$ | varied from 5,000 to 8,750 psi for design with optimum number of strands |
| Skew Angle (degrees) | 0, 15, 30 and 60 |

The fourth task was accomplished based on the information from the aforementioned three tasks, namely, literature review, development of detailed design examples, and parametric study, and the crucial design issues related to live load distribution factors, permanent dead load distribution, and debonding limits were identified. Other designs issues such as the appropriate value of the edge distance parameter, $d_e$, for the exterior girders and the effective flange width calculations were also identified. Three equations to calculate the nominal flexural strength of Texas U54 beam were derived based on the conditions of equilibrium and strain compatibility. The fifth task was accomplished by drawing conclusions and recommendations for all the design issues identified in the fourth task.

## 6.2 DESIGN ISSUES AND RECOMMENDATIONS

The following design issues associated with transitioning to the AASHTO LRFD Specifications were identified through the literature review and parametric study.

Recommendations are provided based on available information and findings as presented in previous sections and in the appendices.

### 6.2.1 Partial Debonding of Prestressing Strands

The research team has conducted a literature review to document the basis for the greater amounts of debonding used in TxDOT practice relative to the LRFD limits. The LRFD Specifications derive its debonding limits based on a FDOT study (Shahawy et al. 1992, 1993) where some specimen with 50 percent debonded strands (0.6 in. diameter) had inadequate shear capacity. Barnes, Burns and Kreger (1999) recommended that up to 75 percent of the strands can be debonded if (1) cracking is prevented in or near the transfer length, and (2) the AASHTO LRFD (1998) rules for terminating the tensile reinforcement are applied to the bonded length of prestressing strands. Abdalla, Ramirez and Lee (1993) recommended limiting debonding to 67 percent per section, while a debonding limit per row was not considered to be necessary. In the aforementioned research studies, none of the specimens failed in a shear mode. All the specimens failed in pure flexure, flexure with slip, and bond failure mechanisms. Krishnamurthy (1971) observed that the shear resistance of the section increased by increasing the number of debonded strands in the upper flange and it decreased when the number of debonded strands was increased in the bottom flange of the beam.

The current LRFD debonding provisions limit debonding of strands to 25 percent per section and 40 percent per row. These limits pose serious restrictions on the design of Texas U54 bridges relative to TxDOT's typical practice. This limitation would limit the span capability for designs using normal strength concretes.

Based on research by Barnes, Burns and Kreger (1999) and successful past practice by TxDOT, it is recommended that up to 75% of the strands may be debonded, if,

a) Cracking is prevented in or near the transfer length

b) AASHTO LRFD rules for terminating the tensile reinforcement are applied to the bonded length of prestressing strands.

c) The shear resistance at the regions where the strands are debonded is thoroughly investigated with due regard to the reduction in horizontal force available, as recommended in LRFD commentary 5.11.4.3

### 6.2.2 Effective Flange Width Calculation

According to the LRFD Specifications, C4.6.2.6.1, the effective flange width of the U54 beam was determined as though each web is an individual supporting element. Because the Standard Specifications do not give specific guidelines regarding the calculation of effective flange width for open box sections, the LRFD Specifications guideline of considering each web of the open box section as an individual supporting element was also used in the Standard designs. A reference vertical center-line was required for the LRFD and Standard Specifications provisions for the effective flange width calculations to be applicable. This reference vertical center-line was assumed to be passing through the top inside corner of the top flange of the Texas U54 beam. This procedure of determining the effective flange width is demonstrated in the detailed design examples in Appendix B. The effective flange widths calculated by the Standard and the LRFD Specifications were found to be the same for all girder spacings.

### 6.2.3 Limitations of AASHTO LRFD Approximate Method of Load Distribution

The formulas given in the LRFD Specifications for the approximate load distribution have certain limitations. The limitations are there because these formulas were developed based on a database of bridges within these limitations. Thus, it may not be a necessary conclusion that beyond these limitations, the LRFD distribution factor (DF) formulas will cease to give conservative estimates. However, it is important for the

engineer to understand these limitations and to be cautious if applying these formulas to cases falling outside the given range of applicability.

### *6.2.3.1 Span Length Limitation*

The use of the LRFD live load DF formulas is limited to spans no longer than 140 ft. The parametric study indicates that this limitation is slightly violated for the 8.5 ft. girder spacing with a 60 degree skew (corresponding maximum span = 144 ft.). The two cases noted in Table 6.2 were investigated using grillage analysis and the applicability of the LRFD live load DF formulas was found to be justified for the two cases noted in Table 6.2.

**Table 6.2 Parameters for Refined Analysis**

| Span (ft.) | Spacing (ft.) | Skew (degrees) | Total Number of Cases | LRFD Restrictions |
|---|---|---|---|---|
| 140, 150 | 8.5 | 60 | 2 | $L \leq 140$ ft. [1] |

1. This restriction is related to the LRFD Live Load Distribution Factor formulas to be applicable.

It was determined that for live load DF for moment in both interior and exterior girders, the LRFD approximate method is applicable and the limit can be increased up to 150 ft. span length. Also, a similar recommendation is made for the live load distribution factors for shear in interior girders only. Whereas, based on the results, it can be concluded that the LRFD approximate method of load distribution gives a conservative for live load DFs for shear in exterior girders.

Further research is recommended using a more rigorous analysis method such as finite element analysis, be conducted to validate the results of the grillage analysis. Based on the results of this research, it is expected that such a rigorous analysis might validate the use of LRFD approximate live load distribution and skew correction factors for shear in exterior beams.

#### *6.2.3.2 Number of Beams ($N_b$) Limitation*

The selected U54 girder spacings of 14 ft. and 16.67 ft. violate the LRFD provisions for uniform distribution of permanent dead loads [LRFD Art. 4.6.2.2], which among other requirements, requires the number of beams to be equal to or greater than four. For U54 girder spacings of 14 ft. and 16.67 ft., the possible number of girders that the standard bridge width, used in this study, can accommodate is three.

The permanent dead loads include self-weight of the girder, deck slab, diaphragm, wearing surface and the railing. According to design recommendations for Texas U54 beams in the TxDOT Bridge Design Manual (TxDOT 2001), two-thirds of the railing dead load should be distributed to the exterior girder and one-third to the adjacent interior girder. In the bridge superstructures, where there are only three girders, according to this TxDOT recommendation all the girders will be designed for two-thirds of the total rail dead load. As the railing is closer to the exterior girders, this TxDOT provision will cause the uniform distribution for permanent dead loads (especially considering the effect of barrier/rail load) to be unconservative for exterior beams and conservative for interior beams.

The implication of this violation of the number of beams limit is that to determine the actual distribution of the permanent dead loads the bridge designer will have to perform a refined analysis method to determine the appropriate distribution of permanent loads for the bridge (LRFD Art. 4.6.2.2.). The use of refined analysis methods such as the finite element method can be uneconomical, time consuming and cumbersome relative to the application of the aforementioned provision of the LRFD Art. 4.6.2.2.

It is recommended that a parametric study should be conducted for typical Texas U54 girder bridges, where the uniform distribution of permanent dead loads is validated for bridges with the number of beams equal to three by more rigorous refined analysis methods. Alternatively, as a conservative approach the exterior girder can be assumed to carry the entire barrier/rail dead load.

#### *6.2.3.3 Edge Distance Parameter ($d_e$) Limitation*

The edge distance parameter, $d_e$, is defined as the distance from the exterior web of exterior beam to the interior edge of curb or traffic barrier. The LRFD Specifications do not give any guidelines for the exact determination of $d_e$ for the case where the girders have inclined webs, as is the case with Texas U54 beams. Thus, based on the engineering judgment, a particular definition of $d_e$ was adopted as shown in Figure 6.1.

If the distribution of live load and permanent dead loads is to be determined according to the LRFD Art. 4.6.2.2., then among other requirements, the edge distance parameter, $d_e$, must be equal to or less than 3.0 ft. unless otherwise specified. For exterior girders that are spread box beams, such as Texas U54 girders, the edge distance parameter, $d_e$, is required to be equal to or less than 4.5 ft.

For Texas U54 girder design, the TxDOT Bridge Design Manual (TxDOT 2001) requires the standard overhang dimension to be equal to or less than 6 ft.-9 in. measured from the centerline of the bottom of the exterior U-beam to the edge of slab. So, for this standard overhang dimension, the distance from the edge of the bridge to the nominal face of the barrier to be 1 ft. and the definition of the edge distance parameter, $d_e$, as adopted by the research team (see Figure 6.1), $d_e$ will be 3.0 ft. This value is acceptable for using the LRFD Specifications approximate method for load distribution. If a greater overhang is desired, the aforementioned de limit will be exceeded and the designer will have to perform the refined analysis procedure to determine the appropriate load distribution.

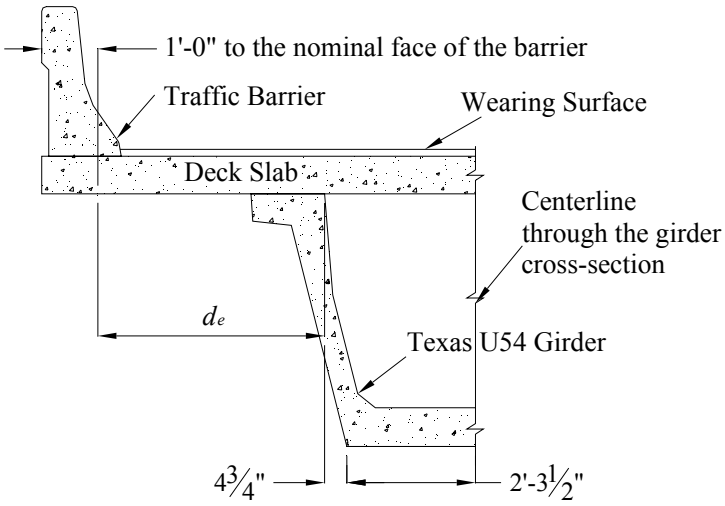


**Figure 6.1 Definition of Edge Distance Parameter, $d_e$.**

It is recommended that a parametric study should be conducted for typical Texas U54 girder bridges, where the load distribution is validated for bridges with $d_e \geq 3.0$ ft. by more rigorous refined analysis methods.

## 6.3 CONCLUSIONS

The following conclusions were derived based on the parametric study for Texas U54 girders. This study focused only on the service and ultimate limit states and additional limit states were not evaluated. The following observations compare the trends for LRFD designs versus Standard designs.

### 6.3.1 Live Load Moment

The live load DF for moment provided by the LRFD Specifications was significantly smaller relative to that of the Standard Specifications. This reduction increases with increasing span length, girder spacing, and skew angle (23.8 to 40.8 percent). The LRFD undistributed live load moments were much larger relative the

Standard values (47.1 to 70.8 percent). The LRFD dynamic load moment increased significantly up to a difference of 310 k-ft. (74 percent). This was due to the new heavier HL-93 live load model introduced in the LRFD Specifications. The LRFD distributed live load moments was larger (28.4 to 40.2 percent) for a 0 degree skew and for all spacings except 16.67 ft. For all other skew angles, the LRFD values were smaller (-4.7 to 16 percent) and this difference increased with an increase in skew angle.

### 6.3.2 Live Load Shear

The LRFD live load DF for shear were not very different than that of the Standard Specifications. For 8.5 ft., 14 ft., and 16.67 ft. spacings, the LRFD DFs for shear were smaller; while for 10 ft. and 11.5 ft. spacings, the DFs for both specifications were the same. In general, it increased by 0.036 (3.9 percent) and decreases by 0.156 (10.3 percent). The LRFD undistributed live load shears were much larger relative to that calculated by the Standard Specifications (35 to 55.6 percent). The LRFD dynamic load shear as provided by the LRFD Specifications increased significantly up to a difference of 8.0 kips (62 percent). This was due to the new heavier HL-93 live load model introduced in the LRFD Specifications. The LRFD distributed live load shears were significantly larger than that of the Standard designs (24.5 to 55.7 percent).

### 6.3.3 Maximum span lengths

Maximum differences in maximum span lengths for LRFD designs relative to the Standard designs are shown in Table 6.3. The trends vary with support skew, strand diameter, and girder spacing. In general, for 0.6 in. strands and girder spacings less than 11.5 ft., LRFD designs resulted in longer span lengths compared to that of the Standard Specifications by up to a difference of 10 ft. (7.4 percent). The LRFD designs resulted in longer span lengths compared to that of the Standard Specifications for girder spacing

less than 11.5 ft. by up to 18.5 ft. (18.8 percent). The same trends were found for 0.5 in. strand diameter; however, the differences are smaller.

Longer spans are explained because of the reduction in the distributed live load moment, and reduction in initial and final prestress losses in the LRFD Specifications for 30 and 60 degree skew cases relative to those of the Standard Specifications. For example, for the 60 degree skew, the distributed live load moment decreased up to a difference of 1526.3 k-ft (40.2 percent), the initial prestress losses decreased up to a difference of 3.0 ksi (19.4 percent), and the final prestress losses decreased up to a difference of 9.0 ksi (17.9 percent).

**Table 6.3 Maximum Differences in Maximum Span Lengths of LRFD Designs Relative to Standard Designs**

| Girder Spacing (ft.) | Strand Diameter = 0.5 in. | | Strand Diameter = 0.6 in. | |
|---|---|---|---|---|
| | Skew (degrees) | | Skew (degrees) | |
| | 0, 15, 30 | 60 | 0, 15, 30 | 60 |
| ≤ 11.5 | +3.5 ft. (2.8%) | +10 ft. (8.1%) | +4 ft. (3%) | +10 ft. (7.4%) |
| > 11.5 | +6.5 ft. (6.2%) | +12.5 ft. (12.0%) | +11.5 ft. (11.7%) | +18.5 ft. (18.8%) |

### 6.3.4 Number of Strands

For the 0, 15 and 30 degree skews and for girder spacings less than or equal to 11.5 ft., the LRFD designs required from 1 to 6 fewer strands. For girder spacings greater than 11.5 ft., the LRFD designs required from 1 to 10 fewer strands relative to the designs based on the Standard Specifications. There is a significant drop in the number of strands required by the LRFD designs relative to those of the Standard designs for the 60 degree skew because the flexural demand reduces significantly in this case. For the 60 degree skew and for girder spacings less than or equal to 11.5 ft., the LRFD designs required from 4 to 14 fewer strands; and for girder spacings greater than 11.5 ft., the LRFD designs required from 12 to 18 fewer strands relative to the Standard

designs. This significant difference can be attributed to mainly two reasons, (1) The effect of the 0.8 live load reduction factor included in the LRFD Service III limit state compared to the 1.0 live load reduction factor in the Standard Specifications, and (2) the reduction in live load moments.

### 6.3.5 Initial and Final Prestress Losses

For the 0, 15 and 30 degree skews, the designs based on the LRFD Specifications give a slightly larger estimate of initial and final losses as compared to those based on the Standard Specifications. This difference is significantly greater for the 60 degree skew cases. The initial relaxation loss increased up to a difference of 190.7 percent and the final relaxation loss increased up to a difference of 75.8 percent. The final relaxation loss increased with the span length and skew. The elastic shortening loss ranged –29.7 to 1.2 percent relative to the Standard designs and similarly, the creep loss decreased up to 47.5 percent. While the initial and final relaxation losses increased, the relative decrease in the elastic shortening and creep loss was greater.

### 6.3.6 Concrete Strength Required at Transfer

Relative to the Standard Specifications, the difference in the required concrete strength at transfer, $f'_{ci}$, for LRFD designs decreased with an increase in skew, girder spacing and span length. The maximum difference in $f'_{ci}$ was a decrease of 1480 psi (24.6 percent). This reduction is expected because the initial prestress losses and the number of strands decreased for LRFD designs. Moreover, the tensile stress limit in LRFD designs was increased slightly from $7.5\sqrt{(f'_{ci}\,(\text{psi}))}$ (Standard) to $0.24\sqrt{(f'_{ci}\,(\text{ksi}))}$ or $7.59\sqrt{(f'_{ci}(\text{psi}))}$ (LRFD).

### 6.3.7 Concrete Strength Required at Service

The designs based on the LRFD Specifications give a smaller (0 to 10.8 percent) estimate of the required concrete strength at service, $f'_c$, as compared to Standard designs. Skews did not affect the $f'_c$ values significantly. The difference in $f'_c$ required remained relatively constant for different girder spacings and span length. The reduction for the LRFD designs may be partially attributed to an increased compressive stress limit due to sustained loads from 0.4 $f'_c$ (Standard) to 0.45 $f'_c$ (LRFD). In addition, for most design cases the distributed live load moment decreased for LRFD designs relative to the Standard designs.

### 6.3.8 Factored Design Moment

The factored design moments based on Standard designs are always larger than for the same cases following the LRFD Specifications. The maximum difference is 3239 k-ft. (28.4 percent). The difference increases as the skew increases. This difference also increases with an increase in girder spacing. However, the difference between the factored design moments for the two specifications does not vary with changes in the span length for a particular spacing. The reason for this affect is that the Standard Specifications uses greater load factors in comparison to those of the LRFD Specifications and for most cases, the distributed live load moment is smaller for LRFD designs.

### 6.3.9 Factored Design Shear

Except for the shorter spans for 8.5 ft. and 16.67 ft. girder spacings, the factored design shear for LRFD designs slightly increased with respect to that for corresponding

Standard desings. While the Standard Specifications uses greater load factors, it also gives lower values for the distributed live load shear.

### 6.3.10 Transverse Shear Reinforcement Area

For all skews and both strand diameters, the transverse shear reinforcement area, $A_v$, values calculated for designs based on the LRFD Specifications are smaller compared to those of the designs based on Standard designs. In general, the difference increases with increasing girder spacing, while increasing span length has a very insignificant affect on this comparison. The $A_v$ requirement for LRFD designs decreased relative to Standard designs up to 0.47 in.$^2$/ft. (46.6 percent).

### 6.3.11 Interface Shear Reinforcement Area

For all skews and both strand diameters, the interface shear reinforcement area, $A_{vh}$, for LRFD designs are larger compared to the Standard designs. The difference increases with increasing girder spacing and span length. The $A_{vh}$ for LRFD designs increases relative to the Standard designs from 0.47 to 1.39 in$^2$ (148 to 443 percent).

### 6.3.12 Camber

The camber calculated for designs based on the Standard Specifications is larger when compared to the LRFD designs (6.2 to –45.2 percent). The difference increases for higher skew angles. This trend is because for the same set of parameters, the LRFD Specifications required a lesser number of strands.

## 6.4 RECOMMENDATIONS FOR FUTURE RESEARCH

The following recommendations are made for the future research based on the findings and limitations of this study.

1. The shear in exterior girders of a skewed bridge can significantly increase and thus, it is strongly recommended that the exterior girders should be designed for shear resistance based on the load distribution that takes into account the increased shear demand in obtuse corners of the bridge. Further study is also recommended to develop new, or verify the current formulas, for skew correction factors for shear in obtuse corners, for girder spacings greater than 11.5 ft.

2. The difference in the interface shear reinforcement area by the LRFD and Standard Specifications is very significant. New provisions currently under consideration for 2006 LRFD Specifications should be considered. The procedures for transverse shear design based on the Modified Compression Field Theory (MCFT) are relatively complex as compared to the previous procedures in the Standard Specifications. Hence, simplified design procedures for typical girder types and design situations may be useful.

# REFERENCES

AASHTO (1992), *Standard Specifications for Highway Bridges*, American Association of Highway and Transportation Officials (AASHTO), Washington, DC.

AASHTO (1994), *AASHTO LRFD Bridge Design Specifications*, 1st Ed., American Association of State Highway and Transportation Officials (AASHTO), Customary U.S. Units, Washington, DC.

AASHTO (1998), *AASHTO LRFD Bridge Design Specifications*, 2nd Ed., American Association of State Highway and Transportation Officials (AASHTO), Customary U.S. Units, Washington, DC.

AASHTO (2002), *Standard Specifications for Highway Bridges*, 17th Ed., American Association of Highway and Transportation Officials (AASHTO), Inc., Washington, DC.

AASHTO (2004), *AASHTO LRFD Bridge Design Specifications*, 3rd Ed., American Association of State Highway and Transportation Officials (AASHTO), Customary U.S. Units, Washington, DC.

Abdalla, O. A., Ramirez, J. A., and Lee, R. H. (1993). "Strand Debonding in Pretensioned Beams: Precast Prestressed Concrete Bridges with Debonded Strands. Simply Supported Tests [PART 2]," *FHWA/INDOT/JHRP-92/25,* FHWA & Indiana Department of Transportation.

Arya, A. S., Khachaturian, N. and Siess, C. P. (1960). "Lateral Distribution of Concentrated Loads on Multibeam Highway Bridges," Civil Engineering Studies, University of Illinois, Chicago, IL.

Bakht, B. and Jaeger, L. G. (1982). "Simplified Methods of Bridge Analysis for the Third Edition of OHBDC," *Canadian Journal of Civil Engineering*, 19, 551-559

Bakht, B. and Jaeger, L. G. (1985). *Bridge Analysis Simplified*, McGraw Hill, Inc., New York

Barnes, R. W., Burns, N. H., and Kreger, M. E. (1999). "Development Length of 0.6-inch Prestressing Strand in Standard I-Shaped Pretentioned Concrete Beams," *Research Report 1388-1*, Center for Transportation Research, The University of Texas at Austin.

Barr, J. P., Eberhard, O. M. and Stanton, F. J. (2001). "Live-Load Distribution Factors in Prestressed Concrete Girder Bridges," *ASCE Journal of Bridge Engineering*, 6 (5), 298-306.

Chen, Y., and Aswad, A. (1996). "Stretching Span Capability of Prestressed Concrete Bridges under AASHTO LRFD," *ASCE Journal of Bridge Engineering*, 1(3), 112-120.

Cheung, M. S., Bakht, B. and Jaeger, L. G. (1982). "Analysis of Box-Girder Bridges by Grillage and Orthotropic Plate Methods," *Canadian Journal of Civil Engineering*, 9, 595-601

Cusens, A. R. and Pama, R. P. (1975). *Bridge Deck Analysis*, John Wiley & Sons, Ltd., New York

Douglas, W. J., Vanhorn, D. A. (1966). "Lateral Distribution of Static Loads in Prestressed Concrete Box-Beam Bridge: Drehersville Bridge," *Fritz Engineering Laboratory Report No. 350.1,* Lehigh University, Bethlehem.

Eamon, C. D., and Nowak A. S. (2002). "Effects of Edge-Stiffening Elements and Diaphragms on Bridge Resistance and Load Distribution," *ASCE Journal of Bridge Engineering*, 7(5), 258-266.

Eby, C. C., Kulicki, J. M., and Kostem, C. N. (1973). "The Evaluation of St. Venant Torsional Constants for Prestressed Concrete I-Beams," *Fritz Engineering Laboratory Report No. 400.12*, Lehigh University, Bethlehem, PA.

Ellingwood, B., Galambos, T. V., MacGregor, J. G. and Cornell, C. A. (1980). "Development of a Probability Based Load Criterion for American National Standard A58," *NBS Special Publication 577*, National Bureau of Standards, Washington, DC.

Guilford, A. A., and Vanhorn, D. A. (1968). "Lateral Distribution of Vehicular Loads in a Prestressed Concrete Box-Beam Bridge – White Haven Bridge," *Fritz Engineering Laboratory Report No. 315.7*, Lehigh University, Bethlehem, PA.

Hambly, E. C. and Pennells, E. (1975). "Grillage Analysis Applied to Cellular Bridge Decks," *The Structural Engineer*, 53(7), 267-276

Hambly, E. C. (1991). *Bridge Deck Behavior*, Second Edition, Chapman & Hall Inc., New York.

Hueste, M. B. D. and Cuadros, G. (2003). "Evaluation of High Strength Concrete Prestressed Bridge Girder Design," *Project 0-2101-3 Final Report to Texas*

*Department of Transportation*, Texas Transportation Institute, College Station, TX.

Jaeger, L. G. and Bakht, B. (1982). "The Grillage Analogy in Bridge Analysis," *Canadian Journal of Civil Engineering*, 9, 224-235

Khaloo, A. R. and Mirzabozorg, H. (2003). "Load Distribution Factors In Simply Supported Skew Bridges," *ASCE Journal of Bridge Engineering,* 8(4), 241-244.

Lin, C. S., and Vanhorn, D. A. (1968). "The Effect of Midspan Diaphragms on Load Distribution in a Prestressed Concrete Box-Beam Bridge – Philadelphia Bridge," *Fritz Engineering Laboratory Report No. 315.6*, Lehigh University, Bethlehem, PA.

Motarjemi, D. and Vanhorn, D. A. (1969). "Theoretical Analysis of Load Distribution in Prestressed Concrete Box-Beam Bridges," *Fritz Engineering Laboratory Report No. 315.9*, Lehigh University, Bethlehem, PA.

Nowak, A. S., and Zhou, J. H. (1985). "Reliability Models for Bridge Analysis," *Report UMCE 85R3*, University of Michigan, Ann Arbor, MI

Nowak, A. S., Czernecki, J., Zhou, J. and Kayser, R. (1987). "Design Loads for Future Bridges," *Report UMCE 87-1*, University of Michigan, Ann Arbor, MI.

Nowak, A. S., Yamani, A. S., and Tabsh, S. W. (1994), "Probabilistic Models for Resistance of Concrete Bridge Girders," *ACI Structural Journal*, 91(3), 269-276.

Nowak, A. S. (1995). "Calibration of LRFD Bridge Code," *ASCE Journal of Structural Engineering*, 121(8)1245-1251.

Nowak, A.S., Szerszen, M.M. (1996). "Bridge Load and Resistance Models," Workshop on Structural Reliability in Bridge Engineering, The University of Colorado, Boulder, October 1996, pp. 30-41.

Nowak, A.S. and Saraf, V. K. (1996). "Target Safety Level for Bridges," Building an International Community of Structural Engineers, Proceedings of Structures Congress, 2, 696-703.

Nowak, A. S. (1999). "Calibration of LRFD Bridge Design Code," *NCHRP Report No. 368*, National Research Council, Washington, DC.

O'Brien, E. J. and Keogh, D. L. (1999). *Bridge Deck Analysis*, Taylor & Francis Group., New York.

PCI (2003). "Precast Prestressed Concrete Bridge Design Manual," Precast/Prestressed Concrete Institute. 2nd Edition.

Rackwitz, R. and Fiessler, B. (1978). "Structural Reliability under Combined Random Load Sequences," *Computer and Structures*, 9, 489-494.

Sanders, W. W. and Elleby, H. A. (1970). "Distribution of Wheel Loads on Highway Bridges," National Cooperative Highway Research Program Report 83, Transportation Research Board, Washington DC.

SAP2000 (Version 8). "Integrated Structural Analysis and Design Software," Computers and Structures, Inc., Berkeley, CA.

Scordelis, A. C. (1966) "Analysis of Simply Supported Box Girder Bridges," *Report No. SESM-66-17*, Division of Structural Engineering and Structural Mechanics, University of California, Berkeley, CA.

Shahawy, M. A., Issa, M. and Batchelor, deV B. (1992). "Strand Transfer Lengths in Full Scale AASHTO Prestressed Concrete Griders," *PCI Journal*, 84-96,

Shahawy, M., and Batchelor, deV B. (1992). "Bond and Shear Behavior of Prestressed AASHTO Type II Beams," Progress Report. Structural Research Center. Florida Department of Transportation, Tallahassee.

Shahawy, Robinson, M., B., and Batchelor, deV B. (1993). "An Investigation of Shear Strength of Prestressed Concrete AASHTO Type II Girders," Research Report. Structures Research Center. Florida Department of Transportation, Tallahassee.

Sinno, R. (1968). "The Time-Dependent Deflections of Prestressed Concrete Bridge Beams," PhD. Dissertation, Texas A&M University, College Station.

TxDOT (2001). "TxDOT Bridge Design Manual," Bridge Division, Texas Department of Transportation, Austin.

TxDOT (2004). "Prestressed Concrete Beam Design/Analysis Program," User Guide, Version 4.00, Bridge Division, Texas Department of Transportation, Austin.

Vanhorn, D. A. (1969). "Structural Behavior Characteristics of Prestressed Concrete Box-Beam Bridges," *Fritz Engineering Laboratory Report No. 315.8*, Lehigh University, Bethlehem.

Zellin, M., Kostem, C. N., and Vanhorn, D. A. (1973). "Structural Behavior of Beam-Slab Highway Bridges – A Summary of Completed Research and Bibliography," *Fritz Engineering Laboratory Report No. 387.1*, Lehigh University, Bethlehem.

Zokaie, T., Osterkamp, T. A., and Imbsen, R. A. (1991). "Distribution of Wheel Loads on Highway Bridges," *NHCRP Project Report 12-26*, Transportation Research Board, Washington DC.

Zokaie, T., (2000). "AASHTO-LRFD Live Load Distribution Specifications," *ASCE Journal of Bridge Engineering*, 5(2), 131-138.

# APPENDIX A

# PARAMETRIC STUDY RESULTS

## Table A.1 Comparison of Distribution Factors (All Skews) for U54 Interior Beams

| Spacing (ft.) | Span (ft.) | All Skews | Skew = 0 | | | Skew = 15 | | | Skew = 30 | | | Skew = 60 | | |
|---|---|---|---|---|---|---|---|---|---|---|---|---|---|---|
| | | DF | DF | Diff. | % Diff. w.r.t STD | DF | Diff. | % Diff. w.r.t STD | DF | Diff. | % Diff. w.r.t STD | DF | Diff. | % Diff. w.r.t STD |
| | | STD | LRFD | | | LRFD | | | LRFD | | | LRFD | | |
| 8.50 | 90 | 0.900 | 0.616 | -0.284 | -31.6 | 0.605 | -0.295 | -32.8 | 0.557 | -0.343 | -38.1 | 0.380 | -0.520 | -57.8 |
| | 100 | | 0.599 | -0.301 | -33.4 | 0.589 | -0.311 | -34.5 | 0.543 | -0.357 | -39.7 | 0.370 | -0.530 | -58.9 |
| | 110 | | 0.585 | -0.315 | -35.0 | 0.575 | -0.325 | -36.1 | 0.530 | -0.370 | -41.1 | 0.361 | -0.539 | -59.9 |
| | 120 | | 0.572 | -0.328 | -36.4 | 0.562 | -0.338 | -37.5 | 0.518 | -0.382 | -42.4 | 0.353 | -0.547 | -60.8 |
| | 130 | | 0.561 | -0.339 | -37.7 | 0.551 | -0.349 | -38.8 | 0.508 | -0.392 | -43.6 | 0.346 | -0.554 | -61.6 |
| | 140 | | 0.550 | -0.350 | -38.9 | 0.541 | -0.359 | -39.9 | 0.498 | -0.402 | -44.6 | 0.340 | -0.560 | -62.3 |
| 10.00 | 90 | 0.909 | 0.692 | -0.217 | -23.8 | 0.681 | -0.228 | -25.1 | 0.627 | -0.282 | -31.0 | 0.427 | -0.482 | -53.0 |
| | 100 | | 0.674 | -0.235 | -25.8 | 0.663 | -0.246 | -27.1 | 0.611 | -0.299 | -32.8 | 0.416 | -0.493 | -54.2 |
| | 110 | | 0.658 | -0.251 | -27.6 | 0.647 | -0.262 | -28.8 | 0.596 | -0.313 | -34.4 | 0.406 | -0.503 | -55.3 |
| | 120 | | 0.644 | -0.265 | -29.2 | 0.633 | -0.276 | -30.4 | 0.583 | -0.326 | -35.9 | 0.397 | -0.512 | -56.3 |
| | 130 | | 0.631 | -0.278 | -30.6 | 0.620 | -0.289 | -31.8 | 0.571 | -0.338 | -37.2 | 0.389 | -0.520 | -57.2 |
| | 140 | | 0.619 | -0.290 | -31.9 | 0.609 | -0.301 | -33.1 | 0.561 | -0.348 | -38.3 | 0.382 | -0.527 | -58.0 |
| 11.50 | 90 | 1.046 | 0.766 | -0.279 | -26.7 | 0.753 | -0.292 | -27.9 | 0.694 | -0.351 | -33.6 | 0.473 | -0.573 | -54.8 |
| | 100 | | 0.746 | -0.299 | -28.6 | 0.733 | -0.312 | -29.9 | 0.676 | -0.370 | -35.4 | 0.460 | -0.585 | -56.0 |
| | 110 | | 0.728 | -0.317 | -30.3 | 0.716 | -0.330 | -31.5 | 0.660 | -0.386 | -36.9 | 0.449 | -0.596 | -57.0 |
| | 120 | | 0.712 | -0.333 | -31.9 | 0.700 | -0.345 | -33.0 | 0.645 | -0.400 | -38.3 | 0.440 | -0.606 | -58.0 |
| | 130 | | 0.698 | -0.347 | -33.2 | 0.686 | -0.359 | -34.4 | 0.632 | -0.413 | -39.5 | 0.431 | -0.615 | -58.8 |
| | 140 | | 0.685 | -0.360 | -34.5 | 0.673 | -0.372 | -35.6 | 0.620 | -0.425 | -40.7 | 0.423 | -0.623 | -59.6 |
| 14.00 | 90 | 1.273 | 0.884 | -0.389 | -30.6 | 0.869 | -0.404 | -31.7 | 0.800 | -0.472 | -37.1 | 0.545 | -0.727 | -57.2 |
| | 100 | | 0.860 | -0.412 | -32.4 | 0.846 | -0.427 | -33.5 | 0.779 | -0.493 | -38.8 | 0.531 | -0.742 | -58.3 |
| | 110 | | 0.840 | -0.433 | -34.0 | 0.826 | -0.447 | -35.1 | 0.761 | -0.512 | -40.2 | 0.518 | -0.755 | -59.3 |
| | 120 | | 0.822 | -0.451 | -35.4 | 0.808 | -0.465 | -36.5 | 0.744 | -0.529 | -41.5 | 0.507 | -0.766 | -60.2 |
| | 130 | | 0.805 | -0.468 | -36.7 | 0.791 | -0.481 | -37.8 | 0.729 | -0.544 | -42.7 | 0.497 | -0.776 | -61.0 |
| | 140 | | 0.790 | -0.483 | -37.9 | 0.777 | -0.496 | -39.0 | 0.716 | -0.557 | -43.8 | 0.487 | -0.785 | -61.7 |
| 16.67 | 90 | 1.516 | 1.003 | -0.513 | -33.8 | 0.986 | -0.530 | -34.9 | 0.908 | -0.607 | -40.1 | 0.619 | -0.897 | -59.2 |
| | 100 | | 0.977 | -0.539 | -35.6 | 0.960 | -0.556 | -36.7 | 0.884 | -0.631 | -41.6 | 0.603 | -0.913 | -60.2 |
| | 110 | | 0.953 | -0.562 | -37.1 | 0.937 | -0.579 | -38.2 | 0.863 | -0.652 | -43.0 | 0.588 | -0.927 | -61.2 |
| | 120 | | 0.932 | -0.583 | -38.5 | 0.917 | -0.599 | -39.5 | 0.844 | -0.671 | -44.3 | 0.575 | -0.940 | -62.0 |
| | 130 | | 0.914 | -0.602 | -39.7 | 0.898 | -0.617 | -40.7 | 0.827 | -0.688 | -45.4 | 0.564 | -0.952 | -62.8 |
| | 140 | | 0.897 | -0.619 | -40.8 | 0.881 | -0.634 | -41.8 | 0.812 | -0.703 | -46.4 | 0.553 | -0.962 | -63.5 |

**Table A.2 Comparison of Distribution Factors and Undistributed Live Load Moments for U54 Interior Beams**

| Spacing (ft.) | Span (ft.) | Distribution Factors | | | | % Diff. w.r.t STD | Moment (LL+I) per Lane (k-ft) | | | | % Diff. w.r.t STD |
|---|---|---|---|---|---|---|---|---|---|---|---|
| | | STD | | LRFD | | | STD | | LRFD | | |
| | | DF | Impact | DF | Impact | | Truck (Controls) | Lane | Truck + Lane (Controls) | Tandem + Lane | |
| 8.50 | 90 | 0.900 | 0.233 | 0.613 | 0.33 | -26.5 | 1651.5 | 1053.0 | 2430.0 | 2077.8 | 47.1 |
| | 100 | | 0.222 | 0.597 | | -27.8 | 1857.6 | 1250.0 | 2821.4 | 2396.0 | 51.9 |
| | 110 | | 0.213 | 0.583 | | -29.0 | 2061.6 | 1463.0 | 3228.8 | 2730.3 | 56.6 |
| | 120 | | 0.204 | 0.570 | | -30.0 | 2263.5 | 1692.0 | 3652.2 | 3080.5 | 61.4 |
| | 130 | | 0.196 | 0.559 | | -30.9 | 2463.8 | 1937.0 | 4091.6 | 3446.8 | 66.1 |
| | 140 | | 0.189 | 0.549 | | -31.8 | 2662.5 | 2198.0 | 4547.0 | 3829.0 | 70.8 |
| 10.00 | 90 | 0.909 | 0.233 | 0.689 | 0.33 | -18.2 | 1651.5 | 1053.0 | 2430.0 | 2077.8 | 47.1 |
| | 100 | | 0.222 | 0.672 | | -19.6 | 1857.6 | 1250.0 | 2821.4 | 2396.0 | 51.9 |
| | 110 | | 0.213 | 0.656 | | -20.9 | 2061.6 | 1463.0 | 3228.8 | 2730.3 | 56.6 |
| | 120 | | 0.204 | 0.642 | | -22.0 | 2263.5 | 1692.0 | 3652.2 | 3080.5 | 61.4 |
| | 130 | | 0.196 | 0.629 | | -23.1 | 2463.8 | 1937.0 | 4091.6 | 3446.8 | 66.1 |
| | 140 | | 0.189 | 0.617 | | -24.0 | 2662.5 | 2198.0 | 4547.0 | 3829.0 | 70.8 |
| 11.50 | 90 | 1.046 | 0.233 | 0.763 | 0.33 | -21.3 | 1651.5 | 1053.0 | 2430.0 | 2077.8 | 47.1 |
| | 100 | | 0.222 | 0.743 | | -22.7 | 1857.6 | 1250.0 | 2821.4 | 2396.0 | 51.9 |
| | 110 | | 0.213 | 0.726 | | -23.9 | 2061.6 | 1463.0 | 3228.8 | 2730.3 | 56.6 |
| | 120 | | 0.204 | 0.710 | | -25.0 | 2263.5 | 1692.0 | 3652.2 | 3080.5 | 61.4 |
| | 130 | | 0.196 | 0.696 | | -26.0 | 2463.8 | 1937.0 | 4091.6 | 3446.8 | 66.1 |
| | 140 | | 0.189 | 0.683 | | -26.9 | 2662.5 | 2198.0 | 4547.0 | 3829.0 | 70.8 |
| 14.00 | 90 | 1.273 | 0.233 | 0.880 | 0.33 | -25.4 | 1651.5 | 1053.0 | 2430.0 | 2077.8 | 47.1 |
| | 100 | | 0.222 | 0.857 | | -26.7 | 1857.6 | 1250.0 | 2821.4 | 2396.0 | 51.9 |
| | 110 | | 0.213 | 0.837 | | -27.9 | 2061.6 | 1463.0 | 3228.8 | 2730.3 | 56.6 |
| | 120 | | 0.204 | 0.819 | | -28.9 | 2263.5 | 1692.0 | 3652.2 | 3080.5 | 61.4 |
| | 130 | | 0.196 | 0.803 | | -29.9 | 2463.8 | 1937.0 | 4091.6 | 3446.8 | 66.1 |
| | 140 | | 0.189 | 0.788 | | -30.7 | 2662.5 | 2198.0 | 4547.0 | 3829.0 | 70.8 |
| 16.67 | 90 | 1.516 | 0.233 | 0.999 | 0.33 | -28.9 | 1651.5 | 1053.0 | 2430.0 | 2077.8 | 47.1 |
| | 100 | | 0.222 | 0.973 | | -30.2 | 1857.6 | 1250.0 | 2821.4 | 2396.0 | 51.9 |
| | 110 | | 0.213 | 0.950 | | -31.3 | 2061.6 | 1463.0 | 3228.8 | 2730.3 | 56.6 |
| | 120 | | 0.204 | 0.929 | | -32.3 | 2263.5 | 1692.0 | 3652.2 | 3080.5 | 61.4 |
| | 130 | | 0.196 | 0.911 | | -33.2 | 2463.8 | 1937.0 | 4091.6 | 3446.8 | 66.1 |
| | 140 | | 0.189 | 0.894 | | -34.0 | 2662.5 | 2198.0 | 4547.0 | 3829.0 | 70.8 |

## Table A.3 Comparison of Distributed Live Load Moments for U54 Interior Beams

| Spacing (ft.) | Span (ft.) | All Skews | Skew = 0 | | | Skew = 15 | | | Skew = 30 | | | Skew = 60 | | |
|---|---|---|---|---|---|---|---|---|---|---|---|---|---|---|
| | | Moment (k-ft) | Skew Corr. Factor | Moment (k-ft) | % Diff. w.r.t STD | Skew Corr. Factor | Moment (k-ft) | % Diff. w.r.t STD | Skew Corr. Factor | Moment (k-ft) | % Diff. w.r.t STD | Skew Corr. Factor | Moment (k-ft) | % Diff. w.r.t STD |
| | | STD | | LRFD | | | LRFD | | | LRFD | | | LRFD | |
| 8.50 | 90 | 1486.3 | 1 | 1489.1 | 0.2 | 0.983 | 1463.8 | -1.5 | 0.906 | 1348.6 | -9.3 | 0.617 | 918.8 | -38.2 |
| | 100 | 1671.9 | | 1684.0 | 0.7 | | 1655.4 | -1.0 | | 1525.2 | -8.8 | | 1039.0 | -37.9 |
| | 110 | 1855.4 | | 1881.8 | 1.4 | | 1849.8 | -0.3 | | 1704.3 | -8.1 | | 1161.0 | -37.4 |
| | 120 | 2037.2 | | 2082.8 | 2.2 | | 2047.4 | 0.5 | | 1886.3 | -7.4 | | 1285.0 | -36.9 |
| | 130 | 2217.4 | | 2287.1 | 3.1 | | 2248.3 | 1.4 | | 2071.4 | -6.6 | | 1411.1 | -36.4 |
| | 140 | 2396.2 | | 2495.0 | 4.1 | | 2452.6 | 2.4 | | 2259.6 | -5.7 | | 1539.4 | -35.8 |
| 10.00 | 90 | 1501.3 | 1 | 1675.3 | 11.6 | 0.983 | 1646.9 | 9.7 | 0.906 | 1517.3 | 1.1 | 0.617 | 1033.7 | -31.2 |
| | 100 | 1688.8 | | 1894.6 | 12.2 | | 1862.4 | 10.3 | | 1715.9 | 1.6 | | 1168.9 | -30.8 |
| | 110 | 1874.1 | | 2117.1 | 13.0 | | 2081.2 | 11.0 | | 1917.4 | 2.3 | | 1306.2 | -30.3 |
| | 120 | 2057.8 | | 2343.2 | 13.9 | | 2303.4 | 11.9 | | 2122.2 | 3.1 | | 1445.7 | -29.7 |
| | 130 | 2239.8 | | 2573.1 | 14.9 | | 2529.4 | 12.9 | | 2330.4 | 4.0 | | 1587.6 | -29.1 |
| | 140 | 2420.5 | | 2807.0 | 16.0 | | 2759.3 | 14.0 | | 2542.2 | 5.0 | | 1731.9 | -28.4 |
| 11.50 | 90 | 1726.5 | 1 | 1854.0 | 7.4 | 0.983 | 1822.5 | 5.6 | 0.906 | 1679.1 | -2.7 | 0.617 | 1143.9 | -33.7 |
| | 100 | 1942.1 | | 2096.6 | 8.0 | | 2061.0 | 6.1 | | 1898.8 | -2.2 | | 1293.6 | -33.4 |
| | 110 | 2155.3 | | 2342.9 | 8.7 | | 2303.1 | 6.9 | | 2121.9 | -1.5 | | 1445.5 | -32.9 |
| | 120 | 2366.4 | | 2593.1 | 9.6 | | 2549.0 | 7.7 | | 2348.5 | -0.8 | | 1599.9 | -32.4 |
| | 130 | 2575.8 | | 2847.5 | 10.5 | | 2799.1 | 8.7 | | 2578.9 | 0.1 | | 1756.9 | -31.8 |
| | 140 | 2783.5 | | 3106.3 | 11.6 | | 3053.6 | 9.7 | | 2813.3 | 1.1 | | 1916.6 | -31.1 |
| 14.00 | 90 | 2101.9 | 1 | 2138.2 | 1.7 | 0.983 | 2101.9 | 0.0 | 0.906 | 1936.5 | -7.9 | 0.617 | 1319.2 | -37.2 |
| | 100 | 2364.3 | | 2418.0 | 2.3 | | 2377.0 | 0.5 | | 2189.9 | -7.4 | | 1491.9 | -36.9 |
| | 110 | 2623.8 | | 2702.0 | 3.0 | | 2656.1 | 1.2 | | 2447.1 | -6.7 | | 1667.1 | -36.5 |
| | 120 | 2880.9 | | 2990.6 | 3.8 | | 2939.8 | 2.0 | | 2708.4 | -6.0 | | 1845.1 | -36.0 |
| | 130 | 3135.7 | | 3284.0 | 4.7 | | 3228.2 | 2.9 | | 2974.2 | -5.2 | | 2026.2 | -35.4 |
| | 140 | 3388.6 | | 3582.5 | 5.7 | | 3521.6 | 3.9 | | 3244.5 | -4.3 | | 2210.4 | -34.8 |
| 16.67 | 90 | 2502.7 | 1 | 2426.6 | -3.0 | 0.983 | 2385.4 | -4.7 | 0.906 | 2197.7 | -12.2 | 0.617 | 1497.2 | -40.2 |
| | 100 | 2815.2 | | 2744.2 | -2.5 | | 2697.6 | -4.2 | | 2485.4 | -11.7 | | 1693.2 | -39.9 |
| | 110 | 3124.2 | | 3066.5 | -1.8 | | 3014.5 | -3.5 | | 2777.3 | -11.1 | | 1892.0 | -39.4 |
| | 120 | 3430.3 | | 3394.0 | -1.1 | | 3336.4 | -2.7 | | 3073.8 | -10.4 | | 2094.1 | -39.0 |
| | 130 | 3733.7 | | 3727.0 | -0.2 | | 3663.7 | -1.9 | | 3375.4 | -9.6 | | 2299.5 | -38.4 |
| | 140 | 4034.9 | | 4065.8 | 0.8 | | 3996.7 | -0.9 | | 3682.3 | -8.7 | | 2508.6 | -37.8 |

## Table A.4 Comparison of Undistributed and Distributed Shear Force at Respective Critical Sections (Strand Dia = 0.5 in. and Girder Spacing = 8.5 ft.)

| Skew | Shear (LL+I) per lane, (kips) | | | | | | % diff. w.r.t. STD | Shear (LL+I) per beam, (kips) | | | | % diff. w.r.t. STD |
|---|---|---|---|---|---|---|---|---|---|---|---|---|
| | LRFD | | | Standard | | | | LRFD | | Standard | | |
| | Span (ft.) | Truck + Lane (Controls) | Tandem + Lane | Span (ft.) | Truck (Controls) | Lane | | Span (ft.) | Shear (kips) | Span (ft.) | Shear (kips) | |
| 0 | 90.0 | 103.9 | 85.2 | 90 | 76.9 | 57.8 | 35.1 | 90.0 | 86.1 | 90 | 69.2 | 24.5 |
| | 100.0 | 109.0 | 89.2 | 100 | 77.4 | 60.8 | 40.7 | 100.0 | 89.5 | 100 | 69.7 | 28.3 |
| | 110.0 | 113.7 | 93.0 | 110 | 77.8 | 63.9 | 46.1 | 110.0 | 92.4 | 110 | 70.0 | 32.0 |
| | 120.0 | 117.9 | 96.4 | 120 | 78.1 | 66.9 | 51.0 | 120.0 | 94.9 | 120 | 70.3 | 35.1 |
| | 130.0 | 121.7 | 99.7 | 130 | 78.2 | 69.9 | 55.6 | 130.0 | 97.2 | 130 | 70.4 | 38.2 |
| | 136.5 | 124.2 | 101.9 | 135 | 78.3 | 71.5 | - | 136.5 | 98.8 | 135 | 71.5 | - |
| 15 | 90.0 | 103.9 | 85.2 | 90 | 76.9 | 57.8 | 35.1 | 90.0 | 86.1 | 90 | 69.2 | 24.5 |
| | 100.0 | 109.0 | 89.2 | 100 | 77.4 | 60.8 | 40.7 | 100.0 | 89.5 | 100 | 69.7 | 28.3 |
| | 110.0 | 113.7 | 93.0 | 110 | 77.8 | 63.9 | 46.1 | 110.0 | 92.4 | 110 | 70.0 | 32.0 |
| | 120.0 | 117.9 | 96.5 | 120 | 78.1 | 66.9 | 51.0 | 120.0 | 95.0 | 120 | 70.3 | 35.2 |
| | 130.0 | 121.7 | 99.7 | 130 | 78.2 | 69.9 | 55.6 | 130.0 | 97.2 | 130 | 70.4 | 38.2 |
| | 136.5 | 124.2 | 101.9 | 135 | 78.3 | 71.5 | - | 136.5 | 98.8 | 135 | 71.5 | - |
| 30 | 90.0 | 103.8 | 85.1 | 90 | 76.9 | 57.8 | 35.0 | 90.0 | 86.1 | 90 | 69.2 | 24.5 |
| | 100.0 | 108.9 | 89.1 | 100 | 77.4 | 60.8 | 40.6 | 100.0 | 89.4 | 100 | 69.7 | 28.2 |
| | 110.0 | 113.7 | 93.0 | 110 | 77.8 | 63.9 | 46.1 | 110.0 | 92.4 | 110 | 70.0 | 31.9 |
| | 120.0 | 117.9 | 96.4 | 120 | 78.1 | 66.9 | 51.0 | 120.0 | 94.9 | 120 | 70.3 | 35.1 |
| | 130.0 | 121.7 | 99.7 | 130 | 78.2 | 69.9 | 55.6 | 130.0 | 97.3 | 130 | 70.4 | 38.2 |
| | 138.5 | 125.1 | 102.6 | 135 | 78.3 | 71.5 | - | 138.5 | 99.3 | 135 | 71.5 | - |
| 60 | 90.0 | 103.8 | 85.1 | 90 | 76.9 | 57.8 | 35.0 | 90.0 | 86.1 | 90 | 69.2 | 24.4 |
| | 100.0 | 108.9 | 89.1 | 100 | 77.4 | 60.8 | 40.6 | 100.0 | 89.4 | 100 | 69.7 | 28.2 |
| | 110.0 | 113.7 | 93.0 | 110 | 77.8 | 63.9 | 46.1 | 110.0 | 92.4 | 110 | 70.0 | 31.9 |
| | 120.0 | 117.8 | 96.4 | 120 | 78.1 | 66.9 | 50.9 | 120.0 | 94.9 | 120 | 70.3 | 35.1 |
| | 130.0 | 121.7 | 99.7 | 130 | 78.2 | 69.9 | 55.6 | 130.0 | 97.2 | 130 | 70.4 | 38.1 |
| | 140.0 | 125.7 | 103.2 | 135 | 78.3 | 71.5 | - | 140.0 | 99.7 | 135 | 71.5 | - |
| | 145.0 | 127.8 | 105.0 | - | - | - | - | 145.0 | 101.0 | - | - | - |

## Table A.5 Comparison of Undistributed and Distributed Shear Force at Respective Critical Sections (Strand Dia = 0.5 in. and Girder Spacing = 10 ft.)

| Skew | Shear (LL+I) per lane, (kips) | | | | | | % diff. w.r.t. STD | Shear (LL+I) per beam, (kips) | | | | % diff. w.r.t. STD |
|---|---|---|---|---|---|---|---|---|---|---|---|---|
| | LRFD | | | Standard | | | | LRFD | | Standard | | |
| | Span (ft.) | Truck + Lane (Controls) | Tandem + Lane | Span (ft.) | Truck (Controls) | Lane | | Span (ft.) | Shear (kips) | Span (ft.) | Shear (kips) | |
| 0 | 90.0 | 104.2 | 85.4 | 90 | 76.9 | 57.8 | 35.5 | 90.0 | 98.4 | 90 | 69.9 | 40.8 |
| | 100.0 | 109.3 | 89.5 | 100 | 77.4 | 60.8 | 41.2 | 100.0 | 102.2 | 100 | 70.4 | 45.1 |
| | 110.0 | 113.9 | 93.2 | 110 | 77.8 | 63.9 | 46.4 | 110.0 | 105.4 | 110 | 70.7 | 49.1 |
| | 120.0 | 117.9 | 96.5 | 120 | 78.1 | 66.9 | 51.0 | 120.0 | 108.1 | 120 | 71.0 | 52.4 |
| | 130.0 | 121.7 | 99.7 | 130 | 78.2 | 69.9 | 55.6 | 130.0 | 110.7 | 130 | 71.1 | 55.7 |
| | 130.5 | 121.9 | 99.9 | - | - | - | - | 130.5 | 110.9 | - | - | - |
| 15 | 90.0 | 104.2 | 85.4 | 90 | 76.9 | 57.8 | 35.5 | 90.0 | 98.4 | 90 | 69.9 | 40.8 |
| | 100.0 | 109.3 | 89.4 | 100 | 77.4 | 60.8 | 41.2 | 100.0 | 102.2 | 100 | 70.4 | 45.1 |
| | 110.0 | 113.9 | 93.2 | 110 | 77.8 | 63.9 | 46.4 | 110.0 | 105.4 | 110 | 70.7 | 49.1 |
| | 120.0 | 117.9 | 96.5 | 120 | 78.1 | 66.9 | 51.1 | 120.0 | 108.2 | 120 | 71.0 | 52.5 |
| | 130.0 | 121.7 | 99.7 | 130 | 78.2 | 69.9 | 55.6 | 130.0 | 110.7 | 130 | 71.1 | 55.7 |
| | 131.0 | 122.2 | 100.1 | - | - | - | - | 131.0 | 111.1 | - | - | - |
| 30 | 90.0 | 104.2 | 85.4 | 90 | 76.9 | 57.8 | 35.5 | 90.0 | 98.4 | 90 | 69.9 | 40.8 |
| | 100.0 | 109.3 | 89.4 | 100 | 77.4 | 60.8 | 41.1 | 100.0 | 102.1 | 100 | 70.4 | 45.0 |
| | 110.0 | 113.9 | 93.1 | 110 | 77.8 | 63.9 | 46.3 | 110.0 | 105.4 | 110 | 70.7 | 49.0 |
| | 120.0 | 117.9 | 96.5 | 120 | 78.1 | 66.9 | 51.1 | 120.0 | 108.2 | 120 | 71.0 | 52.5 |
| | 130.0 | 121.7 | 99.7 | 130 | 78.2 | 69.9 | 55.6 | 130.0 | 110.7 | 130 | 71.1 | 55.7 |
| | 133.0 | 122.9 | 100.7 | - | - | - | - | 133.0 | 111.6 | - | - | - |
| 60 | 90.0 | 104.2 | 85.4 | 90 | 76.9 | 57.8 | 35.5 | 90.0 | 98.4 | 90 | 69.9 | 40.8 |
| | 100.0 | 109.3 | 89.4 | 100 | 77.4 | 60.8 | 41.1 | 100.0 | 102.1 | 100 | 70.4 | 45.1 |
| | 110.0 | 113.8 | 93.0 | 110 | 77.8 | 63.9 | 46.2 | 110.0 | 105.3 | 110 | 70.7 | 48.9 |
| | 120.0 | 117.9 | 96.5 | 120 | 78.1 | 66.9 | 51.0 | 120.0 | 108.2 | 120 | 71.0 | 52.4 |
| | 130.0 | 121.7 | 99.7 | 130 | 78.2 | 69.9 | 55.6 | 130.0 | 110.7 | 130 | 71.1 | 55.8 |
| | 139.0 | 125.3 | 102.9 | - | - | - | - | 139.0 | 113.3 | - | - | - |

**Table A.6 Comparison of Undistributed and Distributed Shear Force at Respective Critical Sections (Strand Dia = 0.5 in. and Girder Spacing = 11.5 ft.)**

| Skew | Shear (LL+I) per lane, (kips) | | | | | | % diff. w.r.t. STD | Shear (LL+I) per beam, (kips) | | | | % diff. w.r.t. STD |
|---|---|---|---|---|---|---|---|---|---|---|---|---|
| | LRFD | | | Standard | | | | LRFD | | Standard | | |
| | Span (ft.) | Truck + Lane (Controls) | Tandem + Lane | Span (ft.) | Truck (Controls) | Lane | | Span (ft.) | Shear (kips) | Span (ft.) | Shear (kips) | |
| 0 | 90.0 | 104.4 | 85.6 | 90 | 76.9 | 57.8 | 35.8 | 90.0 | 110.3 | 90 | 80.4 | 37.3 |
| | 100.0 | 109.6 | 89.6 | 100 | 77.4 | 60.8 | 41.5 | 100.0 | 114.5 | 100 | 81.0 | 41.4 |
| | 110.0 | 113.9 | 93.2 | 110 | 77.8 | 63.9 | 46.4 | 110.0 | 117.9 | 110 | 81.4 | 45.0 |
| | 120.0 | 118.0 | 96.5 | 120 | 78.1 | 66.9 | 51.1 | 120.0 | 121.0 | 120 | 81.6 | 48.3 |
| | 125.5 | 119.9 | 98.2 | 124 | 78.1 | 68.1 | - | 125.5 | 122.5 | 124 | 81.7 | - |
| 15 | 90.0 | 104.4 | 85.6 | 90 | 76.9 | 57.8 | 35.8 | 90.0 | 110.3 | 90 | 80.4 | 37.3 |
| | 100.0 | 109.6 | 89.6 | 100 | 77.4 | 60.8 | 41.5 | 100.0 | 114.5 | 100 | 81.0 | 41.4 |
| | 110.0 | 113.9 | 93.2 | 110 | 77.8 | 63.9 | 46.4 | 110.0 | 117.9 | 110 | 81.4 | 45.0 |
| | 120.0 | 118.0 | 96.5 | 120 | 78.1 | 66.9 | 51.1 | 120.0 | 121.0 | 120 | 81.6 | 48.3 |
| | 126.0 | 120.1 | 98.4 | 124 | 78.1 | 68.1 | - | 126.0 | 122.7 | 124 | 81.7 | - |
| 30 | 90.0 | 104.5 | 85.7 | 90 | 76.9 | 57.8 | 35.9 | 90.0 | 110.4 | 90 | 80.4 | 37.3 |
| | 100.0 | 109.6 | 89.6 | 100 | 77.4 | 60.8 | 41.5 | 100.0 | 114.5 | 100 | 81.0 | 41.4 |
| | 110.0 | 114.0 | 93.2 | 110 | 77.8 | 63.9 | 46.5 | 110.0 | 118.0 | 110 | 81.4 | 45.0 |
| | 120.0 | 117.9 | 96.5 | 120 | 78.1 | 66.9 | 51.0 | 120.0 | 120.9 | 120 | 81.6 | 48.2 |
| | 127.5 | 120.7 | 98.9 | 124 | 78.1 | 68.1 | - | 127.5 | 123.1 | 124 | 81.7 | - |
| 60 | 90.0 | 104.4 | 85.6 | 90 | 76.9 | 57.8 | 35.8 | 90.0 | 110.3 | 90 | 80.4 | 37.2 |
| | 100.0 | 109.5 | 89.6 | 100 | 77.4 | 60.8 | 41.4 | 100.0 | 114.5 | 100 | 81.0 | 41.4 |
| | 110.0 | 113.9 | 93.2 | 110 | 77.8 | 63.9 | 46.4 | 110.0 | 117.9 | 110 | 81.4 | 44.9 |
| | 120.0 | 118.0 | 96.5 | 120 | 78.1 | 66.9 | 51.1 | 120.0 | 121.0 | 120 | 81.6 | 48.3 |
| | 130.0 | 121.7 | 99.7 | 124 | 78.1 | 68.1 | - | 130.0 | 123.8 | 124 | 81.7 | - |
| | 134.0 | 123.3 | 101.1 | - | - | - | - | 134.0 | 125.1 | - | - | - |

**Table A.7 Comparison of Undistributed and Distributed Shear Force at Respective Critical Sections (Strand Dia = 0.5 in. and Girder Spacing = 14 ft.)**

| Skew | Shear (LL+I) per lane, (kips) | | | | | | % diff. w.r.t. STD | Shear (LL+I) per beam, (kips) | | | | % diff. w.r.t. STD |
|---|---|---|---|---|---|---|---|---|---|---|---|---|
| | LRFD | | | Standard | | | | LRFD | | Standard | | |
| | Span (ft.) | Truck + Lane (Controls) | Tandem + Lane | Span (ft.) | Truck (Controls) | Lane | | Span (ft.) | Shear (kips) | Span (ft.) | Shear (kips) | |
| 0 | 90.0 | 105.1 | 86.2 | 90 | 76.9 | 57.8 | 36.7 | 90.0 | 130.0 | 90 | 97.9 | 32.8 |
| | 100.0 | 110.0 | 90.0 | 100 | 77.4 | 60.8 | 42.1 | 100.0 | 134.6 | 100 | 98.6 | 36.6 |
| | 110.0 | 114.2 | 93.4 | 110 | 77.8 | 63.9 | 46.7 | 110.0 | 138.3 | 110 | 99.0 | 39.7 |
| | 115.5 | 116.3 | 95.1 | 113 | 77.9 | 64.8 | - | 115.5 | 140.2 | 113 | 99.1 | - |
| 15 | 90.0 | 105.1 | 86.2 | 90 | 76.9 | 57.8 | 36.7 | 90.0 | 130.0 | 90 | 97.9 | 32.8 |
| | 100.0 | 110.0 | 90.0 | 100 | 77.4 | 60.8 | 42.1 | 100.0 | 134.6 | 100 | 98.6 | 36.6 |
| | 110.0 | 114.2 | 93.4 | 110 | 77.8 | 63.9 | 46.7 | 110.0 | 138.3 | 110 | 99.0 | 39.7 |
| | 116.0 | 116.5 | 95.3 | 113 | 77.9 | 64.8 | - | 116.0 | 140.3 | 113 | 99.1 | - |
| 30 | 90.0 | 105.1 | 86.1 | 90 | 76.9 | 57.8 | 36.6 | 90.0 | 129.9 | 90 | 97.9 | 32.7 |
| | 100.0 | 110.0 | 90.0 | 100 | 77.4 | 60.8 | 42.1 | 100.0 | 134.6 | 100 | 98.6 | 36.6 |
| | 110.0 | 114.2 | 93.4 | 110 | 77.8 | 63.9 | 46.7 | 110.0 | 138.3 | 110 | 99.0 | 39.7 |
| | 118.0 | 117.2 | 95.9 | 113 | 77.9 | 64.8 | - | 118.0 | 141.0 | 113 | 99.1 | - |
| 60 | 90.0 | 105.0 | 86.1 | 90 | 76.9 | 57.8 | 36.6 | 90.0 | 129.8 | 90 | 97.9 | 32.7 |
| | 100.0 | 109.9 | 89.9 | 100 | 77.4 | 60.8 | 41.9 | 100.0 | 134.5 | 100 | 98.6 | 36.4 |
| | 110.0 | 114.1 | 93.3 | 110 | 77.8 | 63.9 | 46.7 | 110.0 | 138.3 | 110 | 99.0 | 39.6 |
| | 120.0 | 118.0 | 96.6 | 113 | 77.9 | 64.8 | - | 120.0 | 141.7 | 113 | 99.1 | - |
| | 123.5 | 119.3 | 97.7 | - | - | - | - | 123.5 | 142.8 | - | - | - |

**Table A.8 Comparison of Undistributed and Distributed Shear Force at Respective Critical Sections (Strand Dia = 0.5 in. and Girder Spacing = 16.67 ft.)**

| Skew | Shear (LL+I) per lane, (kips) | | | | | | % diff. w.r.t. STD | Shear (LL+I) per beam, (kips) | | | | % diff. w.r.t. STD |
|---|---|---|---|---|---|---|---|---|---|---|---|---|
| | LRFD | | | Standard | | | | LRFD | | Standard | | |
| | Span (ft.) | Truck + Lane (Controls) | Tandem + Lane | Span (ft.) | Truck (Controls) | Lane | | Span (ft.) | Shear (kips) | Span (ft.) | Shear (kips) | |
| 0 | 100.0 | 110.1 | 90.1 | 100.0 | 77.4 | 60.8 | 42.2 | 100.0 | 154.9 | 100.0 | 117.4 | 32.0 |
| | 109.0 | 113.8 | 93.1 | 104.5 | 77.6 | 62.2 | - | 109.0 | 158.7 | 104.5 | 117.6 | - |
| 15 | 100.0 | 110.1 | 90.1 | 100.0 | 77.4 | 60.8 | 42.2 | 100.0 | 154.9 | 100.0 | 117.4 | 32.0 |
| | 109.5 | 114.0 | 93.2 | 104.5 | 77.6 | 62.2 | - | 109.5 | 158.9 | 104.5 | 117.6 | - |
| 30 | 100.0 | 110.1 | 90.1 | 100.0 | 77.4 | 60.8 | 42.2 | 100.0 | 154.9 | 100.0 | 117.4 | 32.0 |
| | 110.0 | 114.2 | 93.4 | 104.5 | 77.6 | 62.2 | - | 110.0 | 159.1 | 104.5 | 117.6 | - |
| | 111.0 | 114.6 | 93.7 | - | - | - | - | 111.0 | 159.5 | - | - | - |
| 60 | 100.0 | 110.1 | 90.0 | 100.0 | 77.4 | 60.8 | 42.1 | 100.0 | 154.8 | 100.0 | 117.4 | 31.9 |
| | 110.0 | 114.2 | 93.4 | 104.5 | 77.6 | 62.2 | - | 110.0 | 159.1 | 104.5 | 117.6 | - |
| | 117.0 | 116.9 | 95.6 | - | - | - | - | 117.0 | 161.8 | - | - | - |

**Table A.9 Comparison of Undistributed and Distributed Shear Force at Respective Critical Sections (Strand Dia = 0.6 in. and Girder Spacing = 8.5 ft.)**

| Skew | Shear (LL+I) per lane, (kips) | | | | | | % diff. w.r.t. STD | Shear (LL+I) per beam, (kips) | | | | % diff. w.r.t. STD |
|---|---|---|---|---|---|---|---|---|---|---|---|---|
| | LRFD | | | Standard | | | | LRFD | | Standard | | |
| | Span (ft.) | Truck + Lane (Controls) | Tandem + Lane | Span (ft.) | Truck (Controls) | Lane | | Span (ft.) | Shear (kips) | Span (ft.) | Shear (kips) | |
| 0 | 90.0 | 103.8 | 85.1 | 90.0 | 76.9 | 57.8 | 35.0 | 90.0 | 86.1 | 90.0 | 69.2 | 24.4 |
| | 100.0 | 108.9 | 89.1 | 100.0 | 77.4 | 60.8 | 40.6 | 100.0 | 89.4 | 100.0 | 69.7 | 28.2 |
| | 110.0 | 113.7 | 93.0 | 110.0 | 77.8 | 63.9 | 46.1 | 110.0 | 92.4 | 110.0 | 70.0 | 32.0 |
| | 120.0 | 117.9 | 96.5 | 120.0 | 78.1 | 66.9 | 51.0 | 120.0 | 95.0 | 120.0 | 70.3 | 35.2 |
| | 130.0 | 121.7 | 99.7 | 130.0 | 78.2 | 69.9 | 55.6 | 130.0 | 97.2 | 130.0 | 70.4 | 38.2 |
| | 136.5 | 124.3 | 102.0 | 134.5 | 78.3 | 71.3 | - | 136.5 | 98.8 | 134.5 | 71.3 | - |
| 15 | 90.0 | 103.8 | 85.1 | 90.0 | 76.9 | 57.8 | 35.0 | 90.0 | 86.1 | 90.0 | 69.2 | 24.4 |
| | 100.0 | 108.9 | 89.1 | 100.0 | 77.4 | 60.8 | 40.6 | 100.0 | 89.4 | 100.0 | 69.7 | 28.2 |
| | 110.0 | 113.7 | 93.0 | 110.0 | 77.8 | 63.9 | 46.1 | 110.0 | 92.4 | 110.0 | 70.0 | 32.0 |
| | 120.0 | 117.9 | 96.5 | 120.0 | 78.1 | 66.9 | 51.0 | 120.0 | 95.0 | 120.0 | 70.3 | 35.2 |
| | 130.0 | 121.7 | 99.7 | 130.0 | 78.2 | 69.9 | 55.6 | 130.0 | 97.2 | 130.0 | 70.4 | 38.2 |
| | 137.0 | 124.5 | 102.1 | 134.5 | 78.3 | 71.3 | - | 137.0 | 98.9 | 134.5 | 71.3 | - |
| 30 | 90.0 | 103.8 | 85.1 | 90.0 | 76.9 | 57.8 | 35.0 | 90.0 | 86.1 | 90.0 | 69.2 | 24.4 |
| | 100.0 | 108.9 | 89.1 | 100.0 | 77.4 | 60.8 | 40.6 | 100.0 | 89.4 | 100.0 | 69.7 | 28.2 |
| | 110.0 | 113.7 | 93.0 | 110.0 | 77.8 | 63.9 | 46.1 | 110.0 | 92.4 | 110.0 | 70.0 | 32.0 |
| | 120.0 | 117.9 | 96.5 | 120.0 | 78.1 | 66.9 | 51.0 | 120.0 | 95.0 | 120.0 | 70.3 | 35.2 |
| | 130.0 | 121.8 | 99.8 | 130.0 | 78.2 | 69.9 | 55.7 | 130.0 | 97.3 | 130.0 | 70.4 | 38.3 |
| | 138.5 | 125.1 | 102.6 | 134.5 | 78.3 | 71.3 | - | 138.5 | 99.3 | 134.5 | 71.3 | - |
| 60 | 90.0 | 103.8 | 85.1 | 90.0 | 76.9 | 57.8 | 35.0 | 90.0 | 86.1 | 90.0 | 69.2 | 24.4 |
| | 100.0 | 108.9 | 89.1 | 100.0 | 77.4 | 60.8 | 40.6 | 100.0 | 89.4 | 100.0 | 69.7 | 28.2 |
| | 110.0 | 113.6 | 92.9 | 110.0 | 77.8 | 63.9 | 46.0 | 110.0 | 92.4 | 110.0 | 70.0 | 31.9 |
| | 120.0 | 117.8 | 96.4 | 120.0 | 78.1 | 66.9 | 50.9 | 120.0 | 94.9 | 120.0 | 70.3 | 35.1 |
| | 130.0 | 121.7 | 99.7 | 130.0 | 78.2 | 69.9 | 55.6 | 130.0 | 97.3 | 130.0 | 70.4 | 38.2 |
| | 140.0 | 125.7 | 103.2 | 134.5 | 78.3 | 71.3 | - | 140.0 | 99.7 | 134.5 | 71.3 | - |
| | 144.5 | 127.5 | 104.8 | - | - | - | - | 144.5 | 100.8 | - | - | - |

**Table A.10 Comparison of Undistributed and Distributed Shear Force at Respective Critical Sections (Strand Dia = 0.6 in. and Girder Spacing = 10 ft.)**

| Skew | Shear (LL+I) per lane, (kips) | | | | | | % diff. w.r.t. STD | Shear (LL+I) per beam, (kips) | | | | % diff. w.r.t. STD |
|---|---|---|---|---|---|---|---|---|---|---|---|---|
| | LRFD | | | Standard | | | | LRFD | | Standard | | |
| | Span (ft.) | Truck + Lane (Controls) | Tandem + Lane | Span (ft.) | Truck (Controls) | Lane | | Span (ft.) | Shear (kips) | Span (ft.) | Shear (kips) | |
| 0 | 90.0 | 104.2 | 85.4 | 90 | 76.9 | 57.8 | 35.5 | 90.0 | 98.4 | 90 | 69.9 | 40.8 |
| | 100.0 | 109.2 | 89.4 | 100 | 77.4 | 60.8 | 41.1 | 100.0 | 102.1 | 100 | 70.4 | 45.0 |
| | 110.0 | 113.9 | 93.2 | 110 | 77.8 | 63.9 | 46.4 | 110.0 | 105.4 | 110 | 70.7 | 49.0 |
| | 120.0 | 118.0 | 96.5 | 120 | 78.1 | 66.9 | 51.1 | 120.0 | 108.2 | 120 | 71.0 | 52.5 |
| | 130.0 | 121.8 | 99.8 | 130 | 78.2 | 69.9 | 55.8 | 130.0 | 110.9 | 130 | 71.1 | 55.9 |
| 15 | 90.0 | 104.2 | 85.4 | 90 | 76.9 | 57.8 | 35.5 | 90.0 | 98.4 | 90 | 69.9 | 40.8 |
| | 100.0 | 109.2 | 89.4 | 100 | 77.4 | 60.8 | 41.1 | 100.0 | 102.1 | 100 | 70.4 | 45.0 |
| | 110.0 | 113.9 | 93.2 | 110 | 77.8 | 63.9 | 46.4 | 110.0 | 105.4 | 110 | 70.7 | 49.0 |
| | 120.0 | 118.0 | 96.5 | 120 | 78.1 | 66.9 | 51.1 | 120.0 | 108.2 | 120 | 71.0 | 52.5 |
| | 130.0 | 121.8 | 99.8 | 130 | 78.2 | 69.9 | 55.7 | 130.0 | 110.9 | 130 | 71.1 | 55.9 |
| 30 | 90.0 | 104.1 | 85.4 | 90 | 76.9 | 57.8 | 35.4 | 90.0 | 98.4 | 90 | 69.9 | 40.7 |
| | 100.0 | 109.3 | 89.4 | 100 | 77.4 | 60.8 | 41.1 | 100.0 | 102.1 | 100 | 70.4 | 45.0 |
| | 110.0 | 113.9 | 93.2 | 110 | 77.8 | 63.9 | 46.4 | 110.0 | 105.4 | 110 | 70.7 | 49.1 |
| | 120.0 | 118.0 | 96.5 | 120 | 78.1 | 66.9 | 51.1 | 120.0 | 108.2 | 120 | 71.0 | 52.5 |
| | 130.0 | 121.7 | 99.7 | 130 | 78.2 | 69.9 | 55.6 | 130.0 | 110.8 | 130 | 71.1 | 55.8 |
| | 131.5 | 122.3 | 100.2 | - | - | - | - | 131.5 | 111.2 | - | - | - |
| 60 | 90.0 | 104.1 | 85.4 | 90 | 76.9 | 57.8 | 35.4 | 90.0 | 98.4 | 90 | 69.9 | 40.7 |
| | 100.0 | 109.2 | 89.3 | 100 | 77.4 | 60.8 | 41.0 | 100.0 | 102.0 | 100 | 70.4 | 44.9 |
| | 110.0 | 113.9 | 93.1 | 110 | 77.8 | 63.9 | 46.3 | 110.0 | 105.4 | 110 | 70.7 | 49.0 |
| | 120.0 | 117.9 | 96.5 | 120 | 78.1 | 66.9 | 51.1 | 120.0 | 108.2 | 120 | 71.0 | 52.5 |
| | 130.0 | 121.8 | 99.8 | 130 | 78.2 | 69.9 | 55.7 | 130.0 | 110.8 | 130 | 71.1 | 55.8 |
| | 138.0 | 124.8 | 102.5 | - | - | - | - | 138.0 | 112.9 | - | - | - |

**Table A.11 Comparison of Undistributed and Distributed Shear Force at Respective Critical Sections (Strand Dia = 0.6 in. and Girder Spacing = 11.5 ft.)**

| Skew | Shear (LL+I) per lane, (kips) | | | | | | % diff. w.r.t. STD | Shear (LL+I) per beam, (kips) | | | | % diff. w.r.t. STD |
|---|---|---|---|---|---|---|---|---|---|---|---|---|
| | LRFD | | | Standard | | | | LRFD | | Standard | | |
| | Span (ft.) | Truck + Lane (Controls) | Tandem + Lane | Span (ft.) | Truck (Controls) | Lane | | Span (ft.) | Shear (kips) | Span (ft.) | Shear (kips) | |
| 0 | 90 | 104.4 | 85.6 | 90 | 76.9 | 57.8 | 35.7 | 90 | 110.3 | 90 | 80.4 | 37.2 |
| | 100 | 109.5 | 89.6 | 100 | 77.4 | 60.8 | 41.4 | 100 | 114.5 | 100 | 81.0 | 41.4 |
| | 110 | 114.1 | 93.3 | 110 | 77.8 | 63.9 | 46.6 | 110 | 118.1 | 110 | 81.4 | 45.1 |
| | 120 | 118.0 | 96.6 | 120 | 78.1 | 66.9 | 51.2 | 120 | 121.1 | 120 | 81.6 | 48.4 |
| | 124 | 119.6 | 97.9 | 124 | 78.1 | 68.1 | 53.0 | 124 | 122.3 | 124 | 81.7 | 49.7 |
| 15 | 90 | 104.4 | 85.6 | 90 | 76.9 | 57.8 | 35.7 | 90 | 110.3 | 90 | 80.4 | 37.2 |
| | 100 | 109.5 | 89.6 | 100 | 77.4 | 60.8 | 41.4 | 100 | 114.5 | 100 | 81.0 | 41.4 |
| | 110 | 114.1 | 93.3 | 110 | 77.8 | 63.9 | 46.6 | 110 | 118.1 | 110 | 81.4 | 45.1 |
| | 120 | 118.0 | 96.6 | 120 | 78.1 | 66.9 | 51.2 | 120 | 121.1 | 120 | 81.6 | 48.4 |
| | 125 | 119.9 | 98.2 | 124 | 78.1 | 68.1 | - | 125 | 122.6 | 124 | 81.7 | - |
| 30 | 90 | 104.4 | 85.6 | 90 | 76.9 | 57.8 | 35.8 | 90 | 110.3 | 90 | 80.4 | 37.2 |
| | 100 | 109.5 | 89.6 | 100 | 77.4 | 60.8 | 41.4 | 100 | 114.5 | 100 | 81.0 | 41.4 |
| | 110 | 114.0 | 93.2 | 110 | 77.8 | 63.9 | 46.5 | 110 | 118.0 | 110 | 81.4 | 45.0 |
| | 120 | 118.0 | 96.5 | 120 | 78.1 | 66.9 | 51.1 | 120 | 121.0 | 120 | 81.6 | 48.3 |
| | 126 | 120.2 | 98.5 | 124 | 78.1 | 68.1 | - | 126 | 122.8 | 124 | 81.7 | - |
| 60 | 90 | 104.4 | 85.6 | 90 | 76.9 | 57.8 | 35.8 | 90 | 110.3 | 90 | 80.4 | 37.2 |
| | 100 | 109.4 | 89.5 | 100 | 77.4 | 60.8 | 41.3 | 100 | 114.4 | 100 | 81.0 | 41.3 |
| | 110 | 113.9 | 93.2 | 110 | 77.8 | 63.9 | 46.4 | 110 | 117.9 | 110 | 81.4 | 44.9 |
| | 120 | 118.0 | 96.6 | 120 | 78.1 | 66.9 | 51.2 | 120 | 121.1 | 120 | 81.6 | 48.3 |
| | 130 | 121.8 | 99.8 | 124 | 78.1 | 68.1 | - | 130 | 123.9 | 124 | 81.7 | - |
| | 133 | 122.9 | 100.8 | - | - | - | - | 133 | 124.8 | - | - | - |

**Table A.12 Comparison of Undistributed and Distributed Shear Force at Respective Critical Sections (Strand Dia = 0.6 in. and Girder Spacing = 14 ft.)**

| Skew | Shear (LL+I) per lane, (kips) | | | | | | % diff. w.r.t. STD | Shear (LL+I) per beam, (kips) | | | | % diff. w.r.t. STD |
|---|---|---|---|---|---|---|---|---|---|---|---|---|
| | LRFD | | | Standard | | | | LRFD | | Standard | | |
| | Span (ft.) | Truck + Lane (Controls) | Tandem + Lane | Span (ft.) | Truck (Controls) | Lane | | Span (ft.) | Shear (kips) | Span (ft.) | Shear (kips) | |
| 0 | 90.0 | 105.0 | 86.1 | 90 | 76.9 | 57.8 | 36.6 | 90.0 | 129.8 | 90 | 97.9 | 32.7 |
| | 100.0 | 110.0 | 90.0 | 100 | 77.4 | 60.8 | 42.0 | 100.0 | 134.6 | 100 | 98.6 | 36.5 |
| | 110.0 | 114.2 | 93.4 | 110 | 77.8 | 63.9 | 46.8 | 110.0 | 138.4 | 110 | 99.0 | 39.7 |
| | 115.5 | 116.4 | 95.2 | 112 | 77.9 | 64.5 | - | 115.5 | 140.3 | 112 | 99.1 | - |
| 15 | 90.0 | 105.0 | 86.1 | 90 | 76.9 | 57.8 | 36.6 | 90.0 | 129.8 | 90 | 97.9 | 32.7 |
| | 100.0 | 110.0 | 90.0 | 100 | 77.4 | 60.8 | 42.0 | 100.0 | 134.6 | 100 | 98.6 | 36.5 |
| | 110.0 | 114.2 | 93.4 | 110 | 77.8 | 63.9 | 46.8 | 110.0 | 138.4 | 110 | 99.0 | 39.7 |
| | 116.0 | 116.6 | 95.4 | 112 | 77.9 | 64.5 | - | 116.0 | 140.5 | 112 | 99.1 | - |
| 30 | 90.0 | 105.0 | 86.1 | 90 | 76.9 | 57.8 | 36.6 | 90.0 | 129.9 | 90 | 97.9 | 32.7 |
| | 100.0 | 110.0 | 90.0 | 100 | 77.4 | 60.8 | 42.0 | 100.0 | 134.5 | 100 | 98.6 | 36.5 |
| | 110.0 | 114.3 | 93.4 | 110 | 77.8 | 63.9 | 46.8 | 110.0 | 138.4 | 110 | 99.0 | 39.8 |
| | 117.0 | 117.0 | 95.7 | 112 | 77.9 | 64.5 | - | 117.0 | 140.8 | 112 | 99.1 | - |
| 60 | 90.0 | 105.0 | 86.1 | 90 | 76.9 | 57.8 | 36.5 | 90.0 | 129.8 | 90 | 97.9 | 32.7 |
| | 100.0 | 109.9 | 89.9 | 100 | 77.4 | 60.8 | 41.9 | 100.0 | 134.5 | 100 | 98.6 | 36.4 |
| | 110.0 | 114.2 | 93.4 | 110 | 77.8 | 63.9 | 46.7 | 110.0 | 138.3 | 110 | 99.0 | 39.6 |
| | 120.0 | 118.1 | 96.7 | 112 | 77.9 | 64.5 | - | 120.0 | 141.8 | 112 | 99.1 | - |
| | 123.5 | 119.5 | 97.8 | - | - | - | - | 123.5 | 143.1 | - | - | - |

**Table A.13 Comparison of Undistributed and Distributed Shear Force at Respective Critical Sections (Strand Dia = 0.6 in. and Girder Spacing = 16.67 ft.)**

| Skew | Shear (LL+I) per lane, (kips) | | | | | | % diff. w.r.t. STD | Shear (LL+I) per beam, (kips) | | | | % diff. w.r.t. STD |
|---|---|---|---|---|---|---|---|---|---|---|---|---|
| | LRFD | | | Standard | | | | LRFD | | Standard | | |
| | Span (ft.) | Truck + Lane (Controls) | Tandem + Lane | Span (ft.) | Truck (Controls) | Lane | | Span (ft.) | Shear (kips) | Span (ft.) | Shear (kips) | |
| 0 | 100 | 110.0779 | 90.0549 | 98.5 | 77.378 | 60.37 | - | 100 | 154.838 | 98.5 | 117.2629 | - |
| | 106 | 112.3561 | 91.8836 | - | - | - | - | 106 | 157.1101 | - | - | - |
| 15 | 100 | 110.0779 | 90.0549 | 98.5 | 77.378 | 60.37 | - | 100 | 154.838 | 98.5 | 117.2629 | - |
| | 107 | 113.0154 | 92.4207 | - | - | - | - | 107 | 157.8814 | - | - | - |
| 30 | 100 | 110.1253 | 90.0934 | 98.5 | 77.378 | 60.37 | - | 100 | 154.9047 | 98.5 | 117.2629 | - |
| | 110 | 114.309 | 93.4799 | - | - | - | - | 110 | 159.2412 | - | - | - |
| 60 | 100 | 110.0305 | 90.0164 | 98.5 | 77.378 | 60.37 | - | 100 | 154.7714 | 98.5 | 117.2629 | - |
| | 110 | 114.2792 | 93.4555 | - | - | - | - | 110 | 159.1996 | - | - | - |
| | 117 | 117.0224 | 95.7352 | - | - | - | - | 117 | 162.0043 | - | - | - |

**Table A.14 Comparison of Live Load Distribution Factors**

| Spacing | Span | Moment DF | | %diff. w.r.t STD | Shear DF | | %diff. w.r.t STD |
|---|---|---|---|---|---|---|---|
| | | LRFD | STD | | LRFD | STD | |
| 8.50 | 90 | 0.616 | 0.900 | -31.6 | 0.830 | 0.900 | -7.8 |
| | 100 | 0.599 | | -33.4 | 0.821 | | -8.8 |
| | 110 | 0.585 | | -35.0 | 0.813 | | -9.7 |
| | 120 | 0.572 | | -36.4 | 0.806 | | -10.5 |
| | 130 | 0.561 | | -37.7 | 0.799 | | -11.2 |
| | 140 | 0.550 | | -38.9 | 0.793 | | -11.9 |
| 10.00 | 90 | 0.692 | 0.909 | -23.8 | 0.945 | 0.909 | 3.9 |
| | 100 | 0.674 | | -25.8 | 0.935 | | 2.8 |
| | 110 | 0.658 | | -27.6 | 0.926 | | 1.8 |
| | 120 | 0.644 | | -29.2 | 0.917 | | 0.9 |
| | 130 | 0.631 | | -30.6 | 0.910 | | 0.1 |
| | 140 | 0.619 | | -31.9 | 0.903 | | -0.6 |
| 11.50 | 90 | 0.766 | 1.046 | -26.7 | 1.056 | 1.046 | 1.0 |
| | 100 | 0.746 | | -28.6 | 1.045 | | 0.0 |
| | 110 | 0.728 | | -30.3 | 1.035 | | -1.0 |
| | 120 | 0.712 | | -31.9 | 1.026 | | -1.9 |
| | 130 | 0.698 | | -33.2 | 1.018 | | -2.7 |
| | 140 | 0.685 | | -34.5 | 1.010 | | -3.4 |
| 14.00 | 90 | 0.884 | 1.273 | -30.6 | 1.237 | 1.273 | -2.8 |
| | 100 | 0.860 | | -32.4 | 1.223 | | -3.9 |
| | 110 | 0.840 | | -34.0 | 1.212 | | -4.8 |
| | 120 | 0.822 | | -35.4 | 1.201 | | -5.6 |
| | 130 | 0.805 | | -36.7 | 1.191 | | -6.4 |
| | 140 | 0.790 | | -37.9 | 1.182 | | -7.1 |
| 16.67 | 90 | 1.003 | 1.516 | -33.8 | 1.422 | 1.516 | -6.2 |
| | 100 | 0.977 | | -35.6 | 1.407 | | -7.2 |
| | 110 | 0.953 | | -37.1 | 1.393 | | -8.1 |
| | 120 | 0.932 | | -38.5 | 1.381 | | -8.9 |
| | 130 | 0.914 | | -39.7 | 1.370 | | -9.6 |
| | 140 | 0.897 | | -40.8 | 1.360 | | -10.3 |

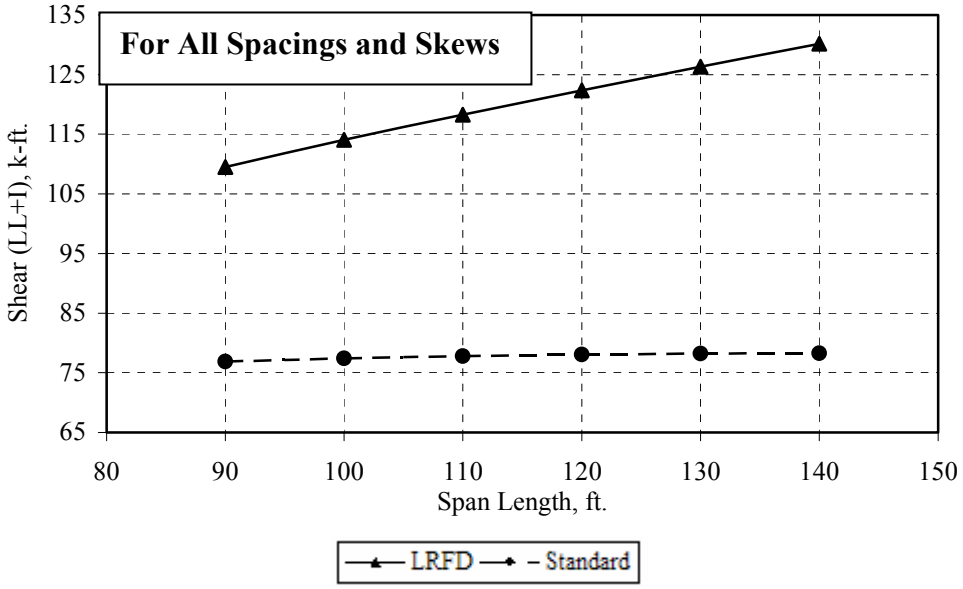


**Figure A.1 Comparison of Undistributed Live Load Shear Force at *H*/2.**

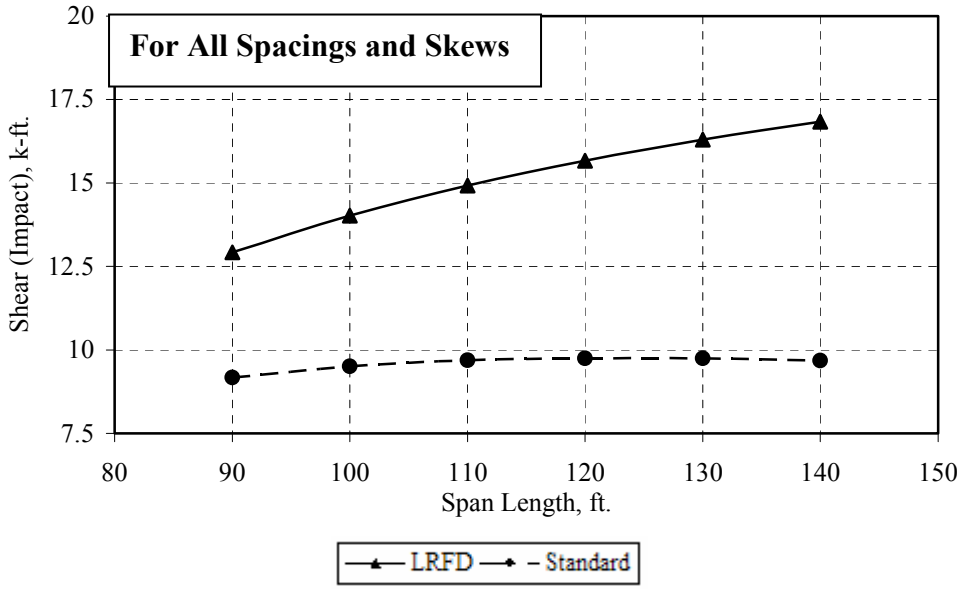


**Figure A.2 Comparison of Undistributed Dynamic Load Shear Force at *H*/2.**

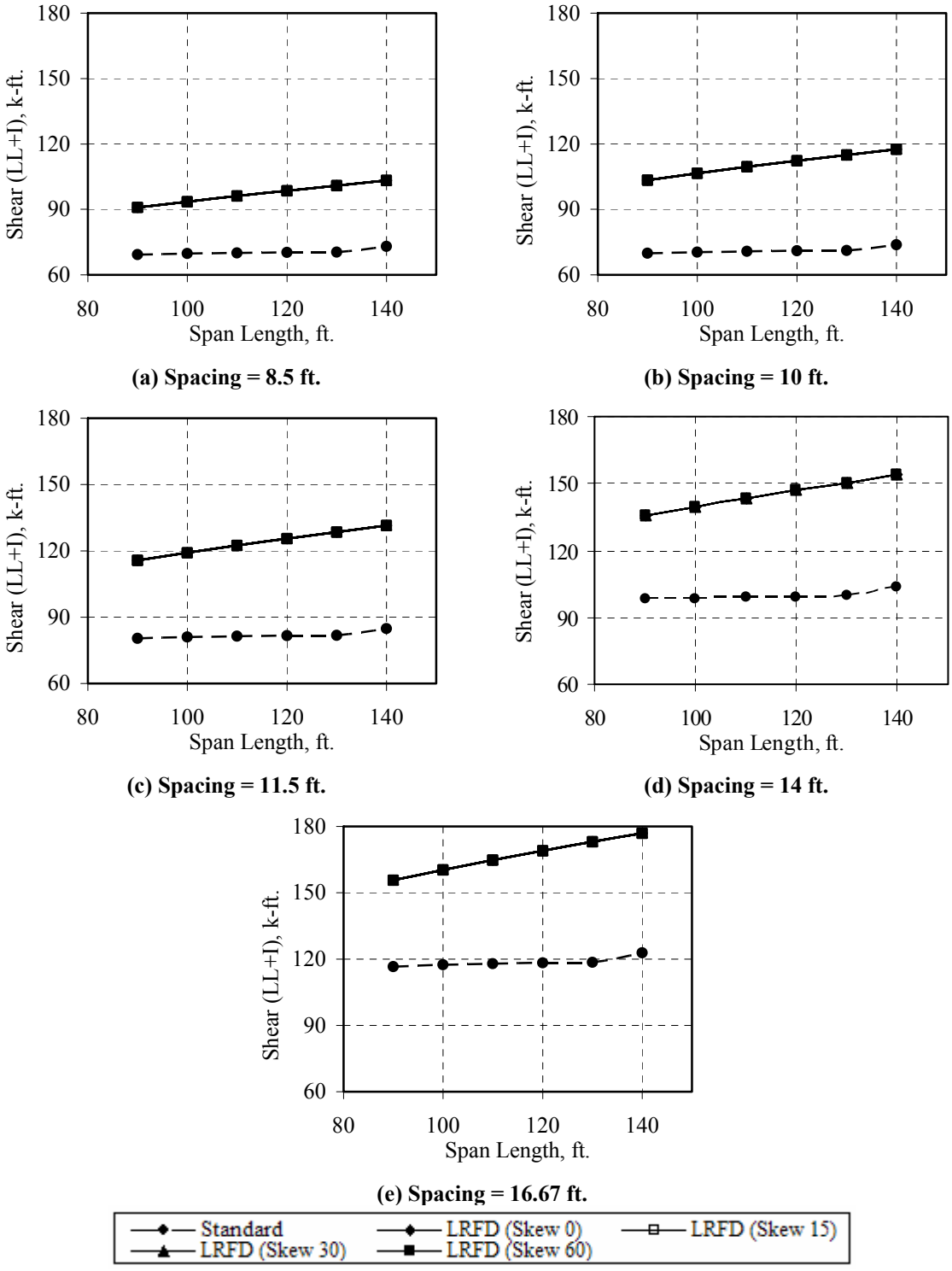


**Figure A.3 Comparison of Distributed Live Load Shear Force at *H/2***

**Table A.15 Comparison of Initial concrete Strength (Strand Dia = 0.5 in.)**

| Spacing (ft.) | Span (ft.) | All Skews | Skew = 0 | | | Skew = 15 | | | Skew = 30 | | | Skew = 60 | | |
|---|---|---|---|---|---|---|---|---|---|---|---|---|---|---|
| | | $f'_{ci}$ (psi) | $f'_{ci}$ (psi) | Diff. | % Diff. w.r.t STD | $f'_{ci}$ (psi) | Diff. | % Diff. w.r.t STD | $f'_{ci}$ (psi) | Diff. | % Diff. w.r.t STD | $f'_{ci}$ (psi) | Diff. | % Diff. w.r.t STD |
| | | STD | LRFD | | | LRFD | | | LRFD | | | LRFD | | |
| 8.50 | 90 | 4000 | 4000 | 0 | 0.0 | 4000 | 0 | 0.0 | 4000 | 0 | 0.0 | 4000 | 0 | 0.0 |
| 8.50 | 100 | 4000 | 4000 | 0 | 0.0 | 4000 | 0 | 0.0 | 4000 | 0 | 0.0 | 4000 | 0 | 0.0 |
| 8.50 | 110 | 4080 | 4000 | -80 | -2.0 | 4000 | -80 | -2.0 | 4000 | -80 | -2.0 | 4000 | -80 | -2.0 |
| 8.50 | 120 | 5072 | 4879 | -193 | -3.8 | 4719 | -353 | -7.0 | 4559 | -513 | -10.1 | 4077 | -995 | -19.6 |
| 8.50 | 130 | 6132 | 5929 | -203 | -3.3 | 5929 | -203 | -3.3 | 5771 | -361 | -5.9 | 4977 | -1155 | -18.8 |
| 10.00 | 90 | 4000 | 4000 | 0 | 0.0 | 4000 | 0 | 0.0 | 4000 | 0 | 0.0 | 4000 | 0 | 0.0 |
| 10.00 | 100 | 4000 | 4000 | 0 | 0.0 | 4000 | 0 | 0.0 | 4000 | 0 | 0.0 | 4000 | 0 | 0.0 |
| 10.00 | 110 | 4491 | 4464 | -27 | -0.6 | 4464 | -27 | -0.6 | 4303 | -188 | -4.2 | 4000 | -491 | -10.9 |
| 10.00 | 120 | 5555 | 5514 | -41 | -0.7 | 5356 | -199 | -3.6 | 5197 | -358 | -6.4 | 4559 | -996 | -17.9 |
| 10.00 | 130 | 6653 | 6598 | -55 | -0.8 | 6598 | -55 | -0.8 | 6460 | -193 | -2.9 | 5613 | -1040 | -15.6 |
| 11.50 | 90 | 4000 | 4000 | 0 | 0.0 | 4000 | 0 | 0.0 | 4000 | 0 | 0.0 | 4000 | 0 | 0.0 |
| 11.50 | 100 | 4152 | 4000 | -152 | -3.7 | 4000 | -152 | -3.7 | 4000 | -152 | -3.7 | 4000 | -152 | -3.7 |
| 11.50 | 110 | 5140 | 4944 | -196 | -3.8 | 4784 | -356 | -6.9 | 4624 | -516 | -10.0 | 4058 | -1082 | -21.1 |
| 11.50 | 120 | 6196 | 5988 | -208 | -3.4 | 5988 | -208 | -3.4 | 5830 | -366 | -5.9 | 5038 | -1158 | -18.7 |
| 14.00 | 90 | 4055 | 4029 | -26 | -0.6 | 4000 | -55 | -1.4 | 4000 | -55 | -1.4 | 4000 | -55 | -1.4 |
| 14.00 | 100 | 5050 | 4693 | -357 | -7.1 | 4693 | -357 | -7.1 | 4533 | -517 | -10.2 | 4000 | -1050 | -20.8 |
| 14.00 | 110 | 6342 | 5894 | -448 | -7.1 | 5894 | -448 | -7.1 | 5736 | -606 | -9.6 | 4943 | -1399 | -22.1 |
| 16.67 | 90 | 4498 | 4200 | -298 | -6.6 | 4200 | -298 | -6.6 | 4029 | -469 | -10.4 | 4000 | -498 | -11.1 |
| 16.67 | 100 | 6013 | 5488 | -525 | -8.7 | 5329 | -684 | -11.4 | 5171 | -842 | -14.0 | 4533 | -1480 | -24.6 |

**Table A.16 Comparison of Initial concrete Strength (Strand Dia = 0.6 in.)**

| Spacing (ft.) | Span (ft.) | All Skews | Skew = 0 | | | Skew = 15 | | | Skew = 30 | | | Skew = 60 | | |
|---|---|---|---|---|---|---|---|---|---|---|---|---|---|---|
| | | $f'_{ci}$ (psi) | $f'_{ci}$ (psi) | Diff. | % Diff. w.r.t STD | $f'_{ci}$ (psi) | Diff. | % Diff. w.r.t STD | $f'_{ci}$ (psi) | Diff. | % Diff. w.r.t STD | $f'_{ci}$ (psi) | Diff. | % Diff. w.r.t STD |
| | | STD | LRFD | | | LRFD | | | LRFD | | | LRFD | | |
| 8.50 | 90 | 4000 | 4000 | 0 | 0.0 | 4000 | 0 | 0.0 | 4000 | 0 | 0.0 | 4000 | 0 | 0.0 |
| 8.50 | 100 | 4000 | 4000 | 0 | 0.0 | 4000 | 0 | 0.0 | 4000 | 0 | 0.0 | 4000 | 0 | 0.0 |
| 8.50 | 110 | 4089 | 4000 | -89 | -2.2 | 4000 | -89 | -2.2 | 4000 | -89 | -2.2 | 4000 | -89 | -2.2 |
| 8.50 | 120 | 5240 | 4965 | -275 | -5.2 | 4725 | -515 | -9.8 | 4725 | -515 | -9.8 | 4243 | -997 | -19.0 |
| 8.50 | 130 | 6248 | 5857 | -391 | -6.3 | 5857 | -391 | -6.3 | 5620 | -628 | -10.1 | 5144 | -1104 | -17.7 |
| 10.00 | 90 | 4000 | 4000 | 0 | 0.0 | 4000 | 0 | 0.0 | 4000 | 0 | 0.0 | 4000 | 0 | 0.0 |
| 10.00 | 100 | 4000 | 4000 | 0 | 0.0 | 4000 | 0 | 0.0 | 4000 | 0 | 0.0 | 4000 | 0 | 0.0 |
| 10.00 | 110 | 4578 | 4549 | -29 | -0.6 | 4549 | -29 | -0.6 | 4308 | -270 | -5.9 | 4000 | -578 | -12.6 |
| 10.00 | 120 | 5481 | 5441 | -40 | -0.7 | 5441 | -40 | -0.7 | 5203 | -278 | -5.1 | 4725 | -756 | -13.8 |
| 10.00 | 130 | 6699 | 6642 | -57 | -0.9 | 6642 | -57 | -0.9 | 6420 | -279 | -4.2 | 5620 | -1079 | -16.1 |
| 11.50 | 90 | 4000 | 4000 | 0 | 0.0 | 4000 | 0 | 0.0 | 4000 | 0 | 0.0 | 4000 | 0 | 0.0 |
| 11.50 | 100 | 4161 | 4000 | -161 | -3.9 | 4000 | -161 | -3.9 | 4000 | -161 | -3.9 | 4000 | -161 | -3.9 |
| 11.50 | 110 | 5064 | 5028 | -36 | -0.7 | 5028 | -36 | -0.7 | 4789 | -275 | -5.4 | 4067 | -997 | -19.7 |
| 11.50 | 120 | 6309 | 6033 | -276 | -4.4 | 6033 | -276 | -4.4 | 5915 | -394 | -6.2 | 5203 | -1106 | -17.5 |
| 14.00 | 90 | 4000 | 4000 | 0 | 0.0 | 4000 | 0 | 0.0 | 4000 | 0 | 0.0 | 4000 | 0 | 0.0 |
| 14.00 | 100 | 5134 | 4856 | -278 | -5.4 | 4856 | -278 | -5.4 | 4617 | -517 | -10.1 | 4000 | -1134 | -22.1 |
| 14.00 | 110 | 6373 | 5976 | -397 | -6.2 | 5976 | -397 | -6.2 | 5740 | -633 | -9.9 | 5028 | -1345 | -21.1 |
| 16.67 | 90 | 4430 | 4207 | -223 | -5.0 | 4207 | -223 | -5.0 | 5000 | 570 | 12.9 | 5000 | 570 | 12.9 |

**Table A.17 Comparison of Final concrete Strength (Strand Dia = 0.5 in.)**

| Spacing (ft.) | Span (ft.) | All Skews | Skew = 0 | | | Skew = 15 | | | Skew = 30 | | | Skew = 60 | | |
|---|---|---|---|---|---|---|---|---|---|---|---|---|---|---|
| | | $f'_c$ (psi) | $f'_c$ (psi) | Diff. | % Diff. w.r.t STD | $f'_c$ (psi) | Diff. | % Diff. w.r.t STD | $f'_c$ (psi) | Diff. | % Diff. w.r.t STD | $f'_c$ (psi) | Diff. | % Diff. w.r.t STD |
| | | STD | LRFD | | | LRFD | | | LRFD | | | LRFD | | |
| 8.50 | 90 | 5000 | 5000 | 0 | 0.0 | 5000 | 0 | 0.0 | 5000 | 0 | 0.0 | 5000 | 0 | 0.0 |
| 8.50 | 100 | 5000 | 5000 | 0 | 0.0 | 5000 | 0 | 0.0 | 5000 | 0 | 0.0 | 5000 | 0 | 0.0 |
| 8.50 | 110 | 5431 | 5000 | -431 | -7.9 | 5000 | -431 | -7.9 | 5000 | -431 | -7.9 | 5000 | -431 | -7.9 |
| 8.50 | 120 | 6598 | 5919 | -679 | -10.3 | 5945 | -653 | -9.9 | 5970 | -628 | -9.5 | 6049 | -549 | -8.3 |
| 8.50 | 130 | 7893 | 7129 | -764 | -9.7 | 7129 | -764 | -9.7 | 7151 | -742 | -9.4 | 7211 | -682 | -8.6 |
| 10.00 | 90 | 5000 | 5000 | 0 | 0.0 | 5000 | 0 | 0.0 | 5000 | 0 | 0.0 | 5000 | 0 | 0.0 |
| 10.00 | 100 | 5000 | 5000 | 0 | 0.0 | 5000 | 0 | 0.0 | 5000 | 0 | 0.0 | 5000 | 0 | 0.0 |
| 10.00 | 110 | 5852 | 5231 | -621 | -10.6 | 5231 | -621 | -10.6 | 5257 | -595 | -10.2 | 5391 | -461 | -7.9 |
| 10.00 | 120 | 7117 | 6358 | -759 | -10.7 | 6381 | -736 | -10.3 | 6405 | -712 | -10.0 | 6505 | -612 | -8.6 |
| 10.00 | 130 | 8580 | 7660 | -920 | -10.7 | 7660 | -920 | -10.7 | 7652 | -928 | -10.8 | 7743 | -837 | -9.8 |
| 11.50 | 90 | 5000 | 5000 | 0 | 0.0 | 5000 | 0 | 0.0 | 5000 | 0 | 0.0 | 5000 | 0 | 0.0 |
| 11.50 | 100 | 5000 | 5000 | 0 | 0.0 | 5000 | 0 | 0.0 | 5000 | 0 | 0.0 | 5000 | 0 | 0.0 |
| 11.50 | 110 | 6223 | 5586 | -637 | -10.2 | 5611 | -612 | -9.8 | 5636 | -587 | -9.4 | 5736 | -487 | -7.8 |
| 11.50 | 120 | 7593 | 6804 | -789 | -10.4 | 6804 | -789 | -10.4 | 6826 | -767 | -10.1 | 6944 | -649 | -8.5 |
| 14.00 | 90 | 5000 | 5000 | 0 | 0.0 | 5000 | 0 | 0.0 | 5000 | 0 | 0.0 | 5000 | 0 | 0.0 |
| 14.00 | 100 | 5560 | 5022 | -538 | -9.7 | 5022 | -538 | -9.7 | 5047 | -513 | -9.2 | 5165 | -395 | -7.1 |
| 14.00 | 110 | 6916 | 6233 | -683 | -9.9 | 6233 | -683 | -9.9 | 6255 | -661 | -9.6 | 6374 | -542 | -7.8 |
| 16.67 | 90 | 5000 | 5000 | 0 | 0.0 | 5000 | 0 | 0.0 | 5000 | 0 | 0.0 | 5000 | 0 | 0.0 |
| 16.67 | 100 | 6119 | 5537 | -582 | -9.5 | 5560 | -559 | -9.1 | 5584 | -535 | -8.7 | 5684 | -435 | -7.1 |

**Table A.18 Comparison of Final concrete Strength (Strand Dia = 0.6 in.)**

| Spacing (ft.) | Span (ft.) | All Skews | Skew = 0 | | | Skew = 15 | | | Skew = 30 | | | Skew = 60 | | |
|---|---|---|---|---|---|---|---|---|---|---|---|---|---|---|
| | | $f'_c$ (psi) | $f'_c$ (psi) | Diff. | % Diff. w.r.t STD | $f'_c$ (psi) | Diff. | % Diff. w.r.t STD | $f'_c$ (psi) | Diff. | % Diff. w.r.t STD | $f'_c$ (psi) | Diff. | % Diff. w.r.t STD |
| | | STD | LRFD | | | LRFD | | | LRFD | | | LRFD | | |
| 8.50 | 90 | 5000 | 5000 | 0 | 0.0 | 5000 | 0 | 0.0 | 5000 | 0 | 0.0 | 5000 | 0 | 0.0 |
| 8.50 | 100 | 5000 | 5000 | 0 | 0.0 | 5000 | 0 | 0.0 | 5000 | 0 | 0.0 | 5000 | 0 | 0.0 |
| 8.50 | 110 | 5340 | 5000 | -340 | -6.4 | 5000 | -340 | -6.4 | 5000 | -340 | -6.4 | 5000 | -340 | -6.4 |
| 8.50 | 120 | 6378 | 5756 | -622 | -9.8 | 5812 | -566 | -8.9 | 5812 | -566 | -8.9 | 5928 | -450 | -7.1 |
| 8.50 | 130 | 7611 | 6854 | -757 | -9.9 | 6854 | -757 | -9.9 | 6905 | -706 | -9.3 | 7011 | -600 | -7.9 |
| 10.00 | 90 | 5000 | 5000 | 0 | 0.0 | 5000 | 0 | 0.0 | 5000 | 0 | 0.0 | 5000 | 0 | 0.0 |
| 10.00 | 100 | 5000 | 5000 | 0 | 0.0 | 5000 | 0 | 0.0 | 5000 | 0 | 0.0 | 5000 | 0 | 0.0 |
| 10.00 | 110 | 5852 | 5231 | -621 | -10.6 | 5231 | -621 | -10.6 | 5257 | -595 | -10.2 | 5391 | -461 | -7.9 |
| 10.00 | 120 | 7117 | 6358 | -759 | -10.7 | 6381 | -736 | -10.3 | 6405 | -712 | -10.0 | 6505 | -612 | -8.6 |
| 10.00 | 130 | 8580 | 7660 | -920 | -10.7 | 7660 | -920 | -10.7 | 7652 | -928 | -10.8 | 7743 | -837 | -9.8 |
| 11.50 | 90 | 5000 | 5000 | 0 | 0.0 | 5000 | 0 | 0.0 | 5000 | 0 | 0.0 | 5000 | 0 | 0.0 |
| 11.50 | 100 | 5000 | 5000 | 0 | 0.0 | 5000 | 0 | 0.0 | 5000 | 0 | 0.0 | 5000 | 0 | 0.0 |
| 11.50 | 110 | 6223 | 5586 | -637 | -10.2 | 5611 | -612 | -9.8 | 5636 | -587 | -9.4 | 5736 | -487 | -7.8 |
| 11.50 | 120 | 7593 | 6804 | -789 | -10.4 | 6804 | -789 | -10.4 | 6826 | -767 | -10.1 | 6944 | -649 | -8.5 |
| 14.00 | 90 | 5000 | 5000 | 0 | 0.0 | 5000 | 0 | 0.0 | 5000 | 0 | 0.0 | 5000 | 0 | 0.0 |
| 14.00 | 100 | 5560 | 5022 | -538 | -9.7 | 5022 | -538 | -9.7 | 5047 | -513 | -9.2 | 5165 | -395 | -7.1 |
| 14.00 | 110 | 6916 | 6233 | -683 | -9.9 | 6233 | -683 | -9.9 | 6255 | -661 | -9.6 | 6374 | -542 | -7.8 |
| 16.67 | 90 | 5000 | 5000 | 0 | 0.0 | 5000 | 0 | 0.0 | 5000 | 0 | 0.0 | 5000 | 0 | 0.0 |

## Table A.19 Comparison of Initial Prestress Loss (Strand Dia = 0.5 in.)

| Spacing (ft.) | Span (ft.) | All Skews | Skew = 0 | | | Skew = 15 | | | Skew = 30 | | | Skew = 60 | | |
|---|---|---|---|---|---|---|---|---|---|---|---|---|---|---|
| | | TIL (ksi) | TIL (ksi) | Diff. | % Diff. w.r.t STD | TIL (ksi) | Diff. | % Diff. w.r.t STD | TIL (ksi) | Diff. | % Diff. w.r.t STD | TIL (ksi) | Diff. | % Diff. w.r.t STD |
| | | STD | LRFD | | | LRFD | | | LRFD | | | LRFD | | |
| 8.50 | 90 | 10.6 | 9.7 | -0.9 | -8.7 | 9.7 | -0.9 | -8.7 | 9.7 | -0.9 | -8.7 | 8.2 | -2.4 | -22.6 |
| 8.50 | 100 | 12.2 | 12.2 | 0.0 | -0.2 | 12.2 | 0.0 | -0.2 | 11.5 | -0.7 | -6.0 | 10.1 | -2.2 | -17.8 |
| 8.50 | 110 | 14.2 | 14.4 | 0.3 | 1.9 | 14.4 | 0.3 | 1.9 | 13.8 | -0.4 | -2.9 | 12.4 | -1.8 | -12.5 |
| 8.50 | 120 | 15.3 | 16.0 | 0.7 | 4.4 | 15.6 | 0.3 | 2.1 | 15.3 | 0.0 | -0.3 | 14.1 | -1.2 | -8.0 |
| 8.50 | 130 | 16.4 | 17.3 | 0.9 | 5.4 | 17.3 | 0.9 | 5.4 | 16.9 | 0.6 | 3.4 | 15.2 | -1.2 | -7.0 |
| 10.00 | 90 | 11.5 | 12.1 | 0.6 | 5.2 | 12.1 | 0.6 | 5.2 | 11.0 | -0.5 | -4.2 | 9.9 | -1.6 | -14.0 |
| 10.00 | 100 | 13.7 | 14.5 | 0.8 | 5.7 | 14.5 | 0.8 | 5.7 | 13.5 | -0.2 | -1.4 | 11.5 | -2.2 | -15.9 |
| 10.00 | 110 | 15.3 | 16.3 | 1.0 | 6.5 | 16.3 | 1.0 | 6.5 | 15.7 | 0.4 | 2.8 | 14.2 | -1.0 | -6.8 |
| 10.00 | 120 | 16.2 | 17.3 | 1.1 | 7.0 | 17.3 | 1.1 | 7.0 | 16.8 | 0.6 | 3.9 | 15.7 | -0.5 | -2.8 |
| 10.00 | 130 | 17.4 | 18.8 | 1.3 | 7.7 | 18.8 | 1.3 | 7.7 | 18.3 | 0.9 | 5.4 | 16.7 | -0.7 | -3.9 |
| 11.50 | 90 | 12.6 | 12.6 | 0.0 | 0.0 | 12.6 | 0.0 | 0.0 | 11.9 | -0.7 | -5.5 | 10.4 | -2.1 | -17.0 |
| 11.50 | 100 | 15.1 | 15.6 | 0.5 | 3.2 | 15.6 | 0.5 | 3.2 | 14.9 | -0.2 | -1.4 | 12.9 | -2.2 | -14.8 |
| 11.50 | 110 | 16.2 | 17.0 | 0.8 | 5.0 | 16.7 | 0.5 | 2.9 | 16.3 | 0.1 | 0.8 | 15.0 | -1.2 | -7.3 |
| 11.50 | 120 | 17.2 | 18.2 | 1.0 | 5.9 | 18.2 | 1.0 | 5.9 | 17.9 | 0.7 | 4.2 | 16.3 | -0.9 | -5.1 |
| 14.00 | 90 | 15.6 | 16.6 | 1.0 | 6.5 | 16.0 | 0.4 | 2.5 | 16.0 | 0.4 | 2.5 | 12.6 | -3.0 | -19.4 |
| 14.00 | 100 | 16.7 | 17.3 | 0.6 | 3.4 | 17.3 | 0.6 | 3.4 | 14.6 | -2.1 | -12.5 | 15.6 | -1.1 | -6.7 |
| 14.00 | 110 | 18.1 | 18.9 | 0.7 | 3.9 | 18.9 | 0.7 | 3.9 | 18.6 | 0.4 | 2.3 | 17.0 | -1.1 | -6.2 |
| 16.67 | 90 | 17.5 | 17.0 | -0.5 | -2.9 | 17.0 | -0.5 | -2.9 | 16.6 | -0.9 | -5.1 | 14.6 | -2.9 | -16.6 |
| 16.67 | 100 | 18.3 | 18.8 | 0.6 | 3.2 | 18.5 | 0.3 | 1.6 | 18.2 | 0.0 | -0.1 | 17.0 | -1.3 | -7.0 |

**Table A.20 Comparison of Initial Prestress Loss (Strand Dia = 0.6 in.)**

| Spacing (ft.) | Span (ft.) | All Skews | Skew = 0 | | | Skew = 15 | | | Skew = 30 | | | Skew = 60 | | |
|---|---|---|---|---|---|---|---|---|---|---|---|---|---|---|
| | | TIL (ksi) | TIL (ksi) | Diff. | % Diff. w.r.t STD | TIL (ksi) | Diff. | % Diff. w.r.t STD | TIL (ksi) | Diff. | % Diff. w.r.t STD | TIL (ksi) | Diff. | % Diff. w.r.t STD |
| | | STD | LRFD | | | LRFD | | | LRFD | | | LRFD | | |
| 8.50 | 90 | 10.5 | 9.9 | -0.6 | -5.8 | 9.9 | -0.6 | -5.8 | 9.9 | -0.6 | -5.8 | 8.8 | -1.7 | -16.4 |
| 8.50 | 100 | 12.8 | 12.5 | -0.3 | -2.1 | 12.5 | -0.3 | -2.1 | 12.5 | -0.3 | -2.1 | 11.0 | -1.8 | -14.3 |
| 8.50 | 110 | 14.3 | 14.2 | 0.0 | 0.0 | 14.2 | 0.0 | 0.0 | 14.2 | 0.0 | 0.0 | 12.3 | -2.0 | -13.7 |
| 8.50 | 120 | 15.7 | 16.3 | 0.6 | 3.5 | 15.7 | 0.0 | 0.0 | 15.7 | 0.0 | 0.0 | 14.5 | -1.2 | -7.5 |
| 8.50 | 130 | 16.7 | 17.2 | 0.6 | 3.4 | 17.2 | 0.6 | 3.4 | 16.7 | 0.1 | 0.3 | 15.7 | -1.0 | -6.0 |
| 10.00 | 90 | 11.5 | 12.1 | 0.6 | 5.2 | 12.1 | 0.6 | 5.2 | 11.0 | -0.5 | -4.2 | 9.9 | -1.6 | -14.0 |
| 10.00 | 100 | 13.7 | 14.5 | 0.8 | 5.7 | 14.5 | 0.8 | 5.7 | 13.5 | -0.2 | -1.4 | 11.5 | -2.2 | -15.9 |
| 10.00 | 110 | 15.3 | 16.3 | 1.0 | 6.5 | 16.3 | 1.0 | 6.5 | 15.7 | 0.4 | 2.8 | 14.2 | -1.0 | -6.8 |
| 10.00 | 120 | 16.2 | 17.3 | 1.1 | 7.0 | 17.3 | 1.1 | 7.0 | 16.8 | 0.6 | 3.9 | 15.7 | -0.5 | -2.8 |
| 10.00 | 130 | 17.4 | 18.8 | 1.3 | 7.7 | 18.8 | 1.3 | 7.7 | 18.3 | 0.9 | 5.4 | 16.7 | -0.7 | -3.9 |
| 11.50 | 90 | 12.9 | 12.6 | -0.3 | -2.1 | 12.6 | -0.3 | -2.1 | 12.1 | -0.8 | -6.2 | 11.0 | -1.9 | -14.6 |
| 11.50 | 100 | 15.2 | 15.4 | 0.2 | 1.5 | 15.4 | 0.2 | 1.5 | 15.4 | 0.2 | 1.5 | 13.5 | -1.7 | -11.3 |
| 11.50 | 110 | 16.2 | 17.3 | 1.1 | 6.9 | 17.3 | 1.1 | 6.9 | 16.8 | 0.6 | 3.7 | 15.1 | -1.1 | -6.8 |
| 11.50 | 120 | 17.6 | 18.5 | 0.9 | 5.4 | 18.5 | 0.9 | 5.4 | 18.3 | 0.7 | 4.0 | 16.8 | -0.8 | -4.4 |
| 14.00 | 90 | 15.6 | 15.6 | 0.0 | 0.0 | 15.6 | 0.0 | 0.0 | 14.6 | -1.0 | -6.3 | 13.6 | -1.9 | -12.4 |
| 14.00 | 100 | 17.0 | 17.8 | 0.7 | 4.4 | 17.8 | 0.7 | 4.4 | 17.3 | 0.2 | 1.4 | 15.4 | -1.6 | -9.3 |
| 14.00 | 110 | 18.4 | 19.2 | 0.8 | 4.5 | 19.2 | 0.8 | 4.5 | 18.8 | 0.4 | 2.0 | 17.3 | -1.1 | -5.9 |
| 16.67 | 90 | 17.4 | 17.1 | -0.3 | -1.7 | 17.1 | -0.3 | -1.7 | 16.5 | -0.9 | -5.3 | 14.6 | -2.8 | -16.2 |

**Table A.20 Comparison of Final Prestress Loss (Strand Dia = 0.5 in.)**

| Spacing (ft.) | Span (ft.) | All Skews | Skew = 0 | | | Skew = 15 | | | Skew = 30 | | | Skew = 60 | | |
|---|---|---|---|---|---|---|---|---|---|---|---|---|---|---|
| | | TFL (ksi) | TFL (ksi) | Diff. | % Diff. w.r.t STD | TFL (ksi) | Diff. | % Diff. w.r.t STD | TFL (ksi) | Diff. | % Diff. w.r.t STD | TFL (ksi) | Diff. | % Diff. w.r.t STD |
| | | STD | LRFD | | | LRFD | | | LRFD | | | LRFD | | |
| 8.50 | 90 | 30.5 | 29.7 | -0.8 | -2.7 | 29.7 | -0.8 | -2.7 | 29.7 | -0.8 | -2.7 | 26.1 | -4.4 | -14.5 |
| 8.50 | 100 | 33.8 | 34.7 | 0.9 | 2.8 | 34.7 | 0.9 | 2.8 | 33.0 | -0.8 | -2.3 | 29.5 | -4.3 | -12.6 |
| 8.50 | 110 | 38.2 | 39.1 | 0.9 | 2.4 | 39.1 | 0.9 | 2.4 | 37.5 | -0.7 | -1.9 | 34.2 | -4.0 | -10.5 |
| 8.50 | 120 | 43.0 | 44.1 | 1.1 | 2.4 | 42.8 | -0.3 | -0.6 | 41.4 | -1.6 | -3.7 | 37.3 | -5.7 | -13.3 |
| 8.50 | 130 | 47.9 | 48.8 | 0.9 | 1.9 | 48.8 | 0.9 | 1.9 | 47.6 | -0.3 | -0.7 | 41.1 | -6.8 | -14.1 |
| 10.00 | 90 | 31.6 | 32.6 | 1.0 | 3.0 | 32.6 | 1.0 | 3.0 | 32.6 | 1.0 | 3.0 | 29.0 | -2.6 | -8.2 |
| 10.00 | 100 | 36.4 | 38.9 | 2.5 | 6.9 | 37.3 | 0.9 | 2.4 | 37.3 | 0.9 | 2.4 | 32.2 | -4.2 | -11.5 |
| 10.00 | 110 | 40.7 | 43.2 | 2.4 | 6.0 | 43.2 | 2.4 | 6.0 | 41.8 | 1.1 | 2.7 | 36.5 | -4.2 | -10.3 |
| 10.00 | 120 | 45.8 | 48.1 | 2.3 | 5.1 | 46.8 | 1.1 | 2.3 | 45.6 | -0.2 | -0.4 | 40.3 | -5.5 | -11.9 |
| 10.00 | 130 | 50.6 | 52.9 | 2.2 | 4.4 | 52.9 | 2.2 | 4.4 | 51.8 | 1.2 | 2.3 | 45.1 | -5.6 | -11.0 |
| 11.50 | 90 | 34.5 | 35.4 | 0.9 | 2.6 | 35.4 | 0.9 | 2.6 | 33.7 | -0.8 | -2.3 | 30.3 | -4.3 | -12.4 |
| 11.50 | 100 | 40.6 | 41.5 | 1.0 | 2.3 | 41.5 | 1.0 | 2.3 | 39.9 | -0.7 | -1.7 | 35.0 | -5.6 | -13.9 |
| 11.50 | 110 | 45.2 | 46.3 | 1.1 | 2.4 | 45.0 | -0.2 | -0.5 | 43.7 | -1.5 | -3.4 | 38.9 | -6.3 | -13.9 |
| 11.50 | 120 | 49.9 | 50.9 | 1.0 | 2.1 | 50.9 | 1.0 | 2.1 | 49.7 | -0.2 | -0.4 | 43.3 | -6.6 | -13.2 |
| 14.00 | 90 | 41.5 | 40.7 | -0.8 | -1.9 | 40.7 | -0.8 | -1.9 | 39.1 | -2.4 | -5.9 | 34.1 | -7.4 | -17.9 |
| 14.00 | 100 | 46.1 | 46.0 | -0.2 | -0.4 | 46.0 | -0.2 | -0.4 | 44.7 | -1.5 | -3.2 | 39.9 | -6.3 | -13.6 |
| 14.00 | 110 | 52.7 | 51.8 | -0.9 | -1.6 | 51.8 | -0.9 | -1.6 | 50.6 | -2.1 | -4.0 | 44.3 | -8.4 | -15.9 |
| 16.67 | 90 | 45.1 | 44.4 | -0.8 | -1.7 | 44.4 | -0.8 | -1.7 | 43.0 | -2.1 | -4.7 | 38.1 | -7.0 | -15.5 |
| 16.67 | 100 | 52.5 | 51.1 | -1.5 | -2.8 | 49.9 | -2.7 | -5.1 | 48.6 | -3.9 | -7.5 | 43.5 | -9.0 | -17.2 |

**Table A.21 Comparison of Final Prestress Loss (Strand Dia = 0.6 in.)**

| Spacing (ft.) | Span (ft.) | All Skews | Skew = 0 | | | Skew = 15 | | | Skew = 30 | | | Skew = 60 | | |
|---|---|---|---|---|---|---|---|---|---|---|---|---|---|---|
| | | TFL (ksi) | TFL (ksi) | Diff. | % Diff. w.r.t STD | TFL (ksi) | Diff. | % Diff. w.r.t STD | TFL (ksi) | Diff. | % Diff. w.r.t STD | TFL (ksi) | Diff. | % Diff. w.r.t STD |
| | | STD | LRFD | | | LRFD | | | LRFD | | | LRFD | | |
| 8.50 | 90 | 30.1 | 30.1 | 0.0 | 0.1 | 30.1 | 0.0 | 0.1 | 30.1 | 0.0 | 0.1 | 27.4 | -2.6 | -8.8 |
| 8.50 | 100 | 35.2 | 35.4 | 0.2 | 0.5 | 35.4 | 0.2 | 0.5 | 35.4 | 0.2 | 0.5 | 31.6 | -3.6 | -10.2 |
| 8.50 | 110 | 38.3 | 38.5 | 0.2 | 0.6 | 38.5 | 0.2 | 0.6 | 38.5 | 0.2 | 0.6 | 33.8 | -4.5 | -11.8 |
| 8.50 | 120 | 44.4 | 44.8 | 0.4 | 0.9 | 42.8 | -1.6 | -3.6 | 42.8 | -1.6 | -3.6 | 38.6 | -5.8 | -13.0 |
| 8.50 | 130 | 48.7 | 48.2 | -0.5 | -1.0 | 48.2 | -0.5 | -1.0 | 46.3 | -2.4 | -5.0 | 42.4 | -6.4 | -13.1 |
| 10.00 | 90 | 32.0 | 34.7 | 2.7 | 8.3 | 34.7 | 2.7 | 8.3 | 32.1 | 0.1 | 0.2 | 29.4 | -2.6 | -8.2 |
| 10.00 | 100 | 36.8 | 39.3 | 2.5 | 6.8 | 39.3 | 2.5 | 6.8 | 37.0 | 0.1 | 0.4 | 32.1 | -4.7 | -12.7 |
| 10.00 | 110 | 41.5 | 43.9 | 2.4 | 5.8 | 43.9 | 2.4 | 5.8 | 41.9 | 0.4 | 1.0 | 37.5 | -3.9 | -9.5 |
| 10.00 | 120 | 45.2 | 47.5 | 2.3 | 5.2 | 47.5 | 2.3 | 5.2 | 45.6 | 0.4 | 0.9 | 41.6 | -3.6 | -7.9 |
| 10.00 | 130 | 50.9 | 53.2 | 2.2 | 4.4 | 53.2 | 2.2 | 4.4 | 51.4 | 0.5 | 1.0 | 45.0 | -6.0 | -11.8 |
| 11.50 | 90 | 35.2 | 35.4 | 0.2 | 0.5 | 35.4 | 0.2 | 0.5 | 34.1 | -1.1 | -3.2 | 31.5 | -3.7 | -10.5 |
| 11.50 | 100 | 40.7 | 41.0 | 0.3 | 0.7 | 41.0 | 0.3 | 0.7 | 41.0 | 0.3 | 0.7 | 36.3 | -4.4 | -10.9 |
| 11.50 | 110 | 44.7 | 47.0 | 2.4 | 5.3 | 47.0 | 2.4 | 5.3 | 45.1 | 0.4 | 0.9 | 38.9 | -5.7 | -12.8 |
| 11.50 | 120 | 50.8 | 51.3 | 0.5 | 1.0 | 51.3 | 0.5 | 1.0 | 50.4 | -0.4 | -0.9 | 44.6 | -6.2 | -12.3 |
| 14.00 | 90 | 41.0 | 41.2 | 0.1 | 0.3 | 41.2 | 0.1 | 0.3 | 38.8 | -2.3 | -5.5 | 36.5 | -4.6 | -11.2 |
| 14.00 | 100 | 47.0 | 47.4 | 0.4 | 0.9 | 47.4 | 0.4 | 0.9 | 45.4 | -1.5 | -3.3 | 39.3 | -7.7 | -16.4 |
| 14.00 | 110 | 53.1 | 52.6 | -0.5 | -1.0 | 52.6 | -0.5 | -1.0 | 50.7 | -2.4 | -4.5 | 45.0 | -8.2 | -15.4 |
| 16.67 | 90 | 45.2 | 44.5 | -0.7 | -1.5 | 44.5 | -0.7 | -1.5 | 42.8 | -2.4 | -5.3 | 37.8 | -7.4 | -16.4 |

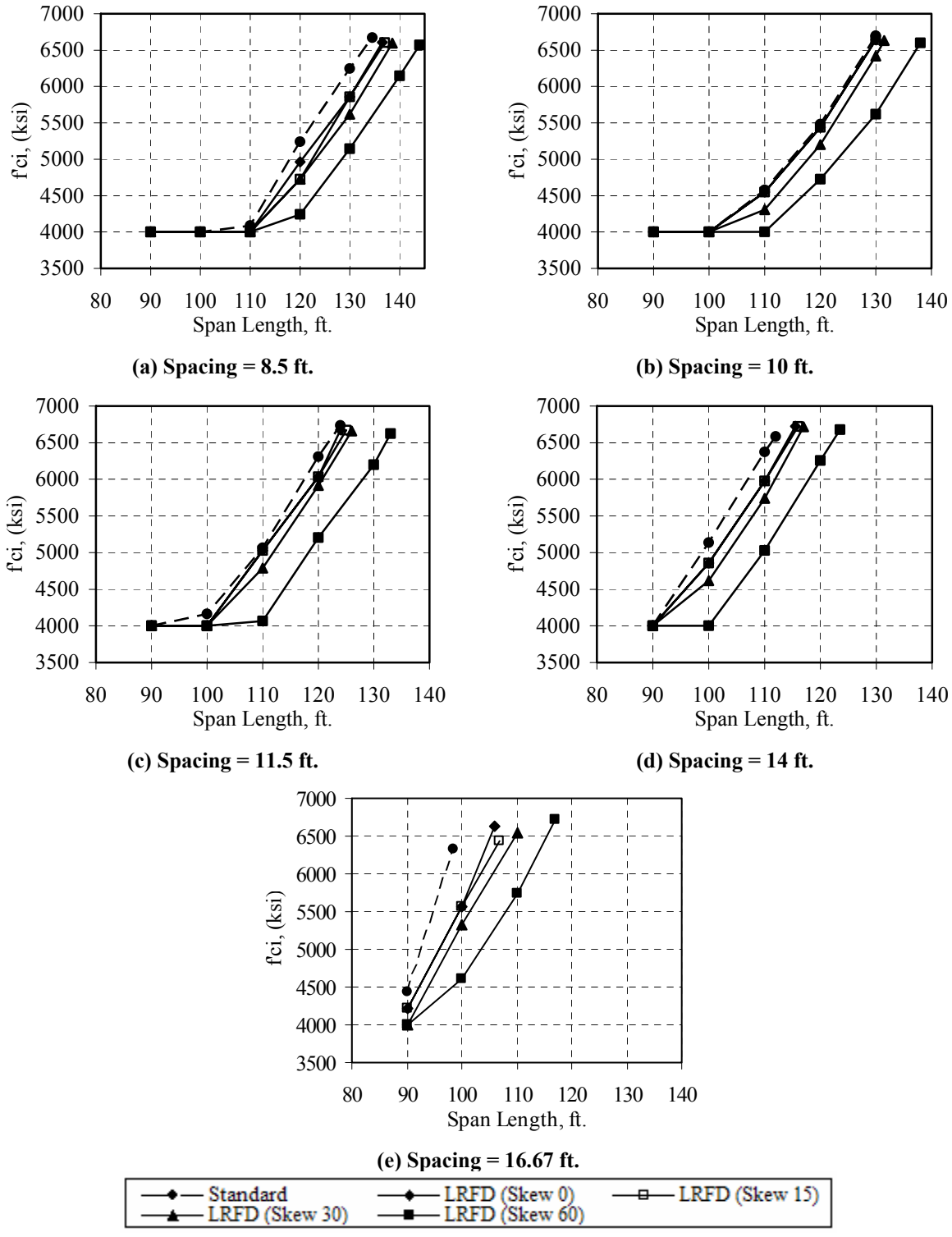


**Figure A.4 Comparison of Initial Concrete Strength (Strand Diameter 0.6 in.)**

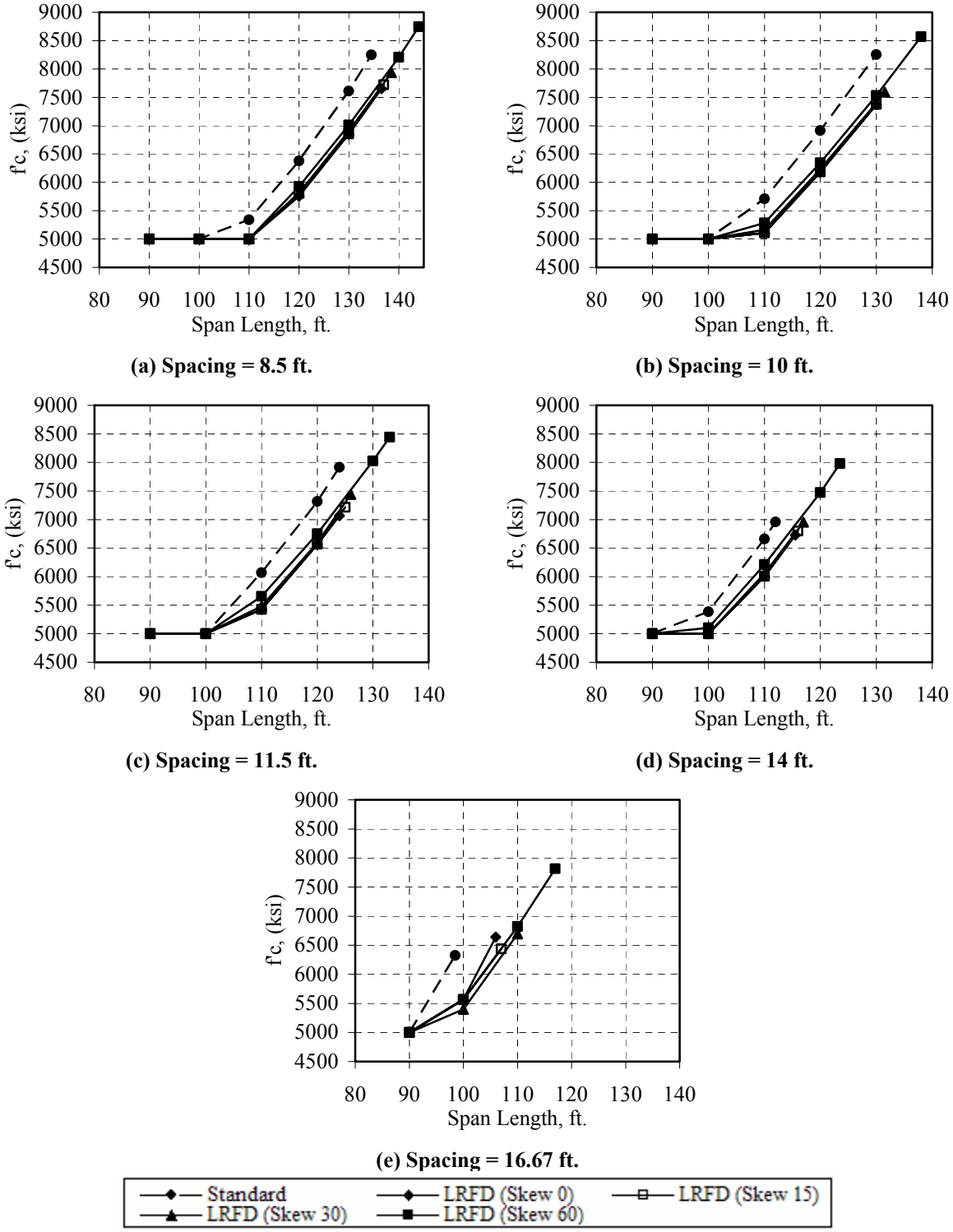


**(a) Spacing = 8.5 ft.**

**(b) Spacing = 10 ft.**

**(c) Spacing = 11.5 ft.**

**(d) Spacing = 14 ft.**

**(e) Spacing = 16.67 ft.**

**Figure A.5 Comparison of Final Concrete Strength (Strand Diameter 0.6 in.)**

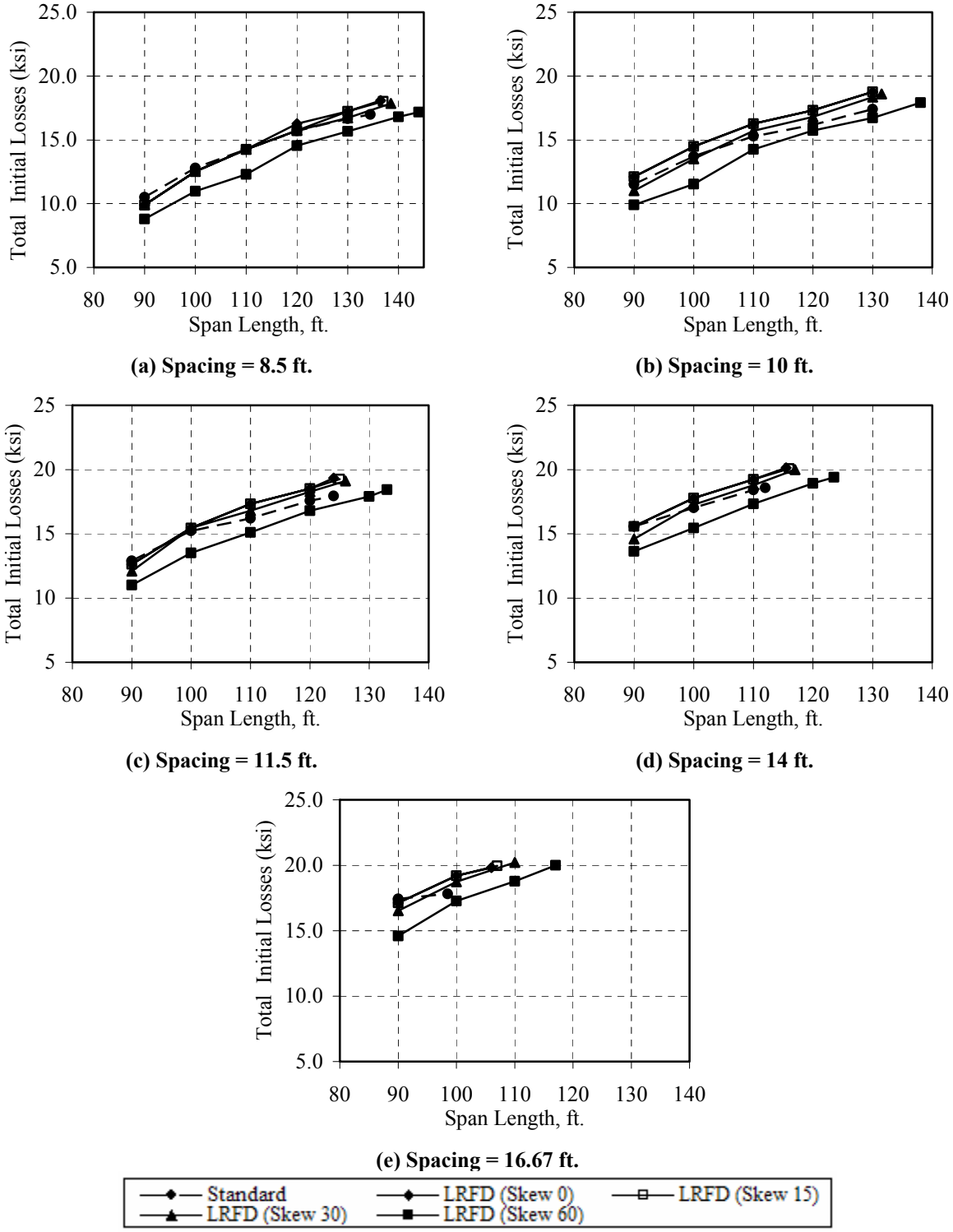


**Figure A.6 Comparison of Initial Prestress Loss (Strand Diameter 0.6 in.)**

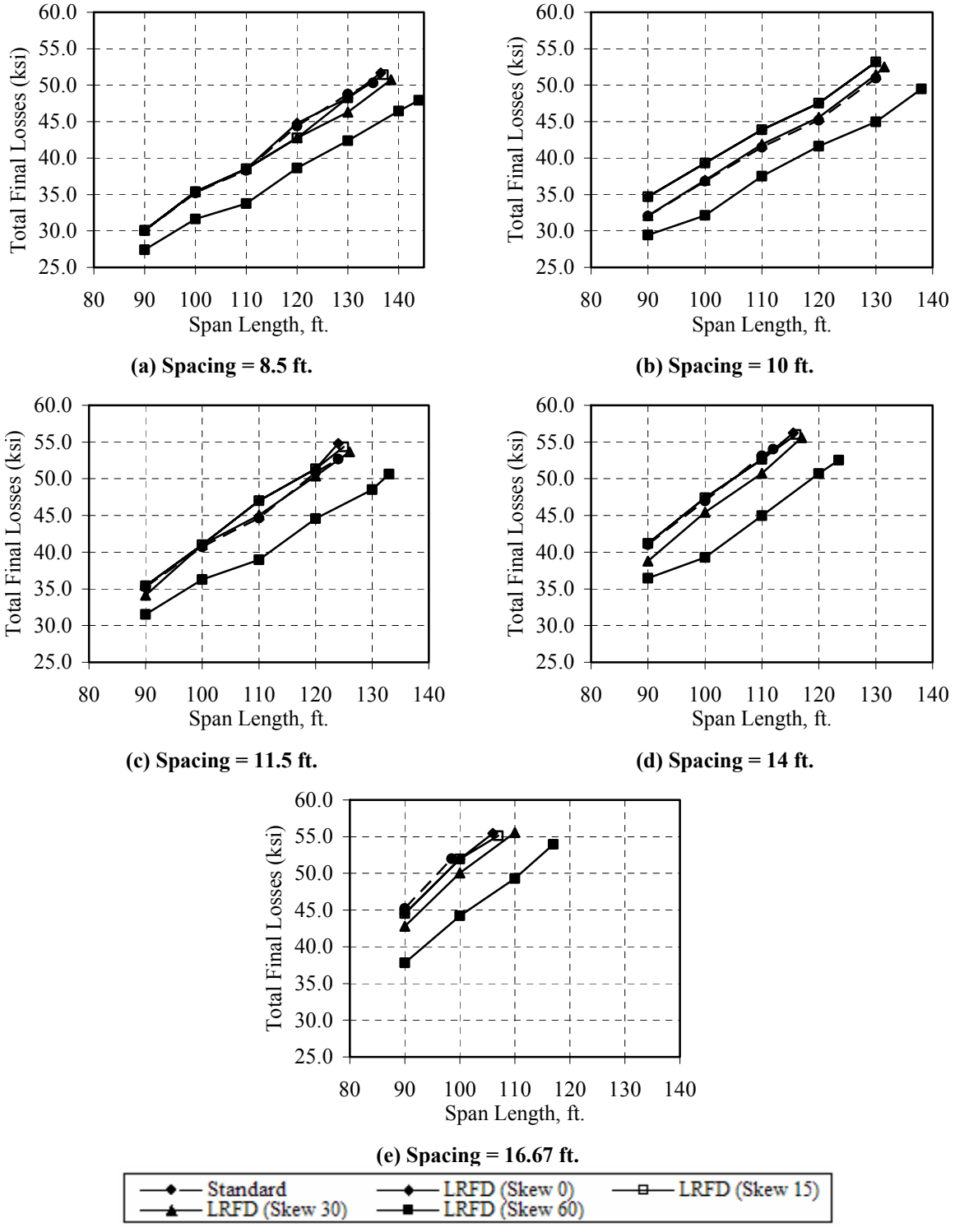


**(a) Spacing = 8.5 ft.**

**(b) Spacing = 10 ft.**

**(c) Spacing = 11.5 ft.**

**(d) Spacing = 14 ft.**

**(e) Spacing = 16.67 ft.**

**Figure A.7 Comparison of Final Prestress Loss (Strand Diameter 0.6 in.)**

**Table A.23 Comparison of Number of Strands (Strand Diameter = 0.6 in., Girder Spacing = 8.5 ft.)**

| Skew | Standard | | LRFD | | Difference in No. of Strands |
|---|---|---|---|---|---|
| | Span Length (ft.) | No. of Strands | Span Length (ft.) | No. of Strands | |
| 0 | 90.0 | 24 | 90.0 | 22 | -2 |
| | 100.0 | 31 | 100.0 | 29 | -2 |
| | 110.0 | 37 | 110.0 | 35 | -2 |
| | 120.0 | 47 | 120.0 | 45 | -2 |
| | 130.0 | 56 | 130.0 | 53 | -3 |
| | 134.5 | 60 | 136.5 | 60 | - |
| 15 | 90.0 | 24 | 90.0 | 22 | -2 |
| | 100.0 | 31 | 100.0 | 29 | -2 |
| | 110.0 | 37 | 110.0 | 35 | -2 |
| | 120.0 | 47 | 120.0 | 43 | -4 |
| | 130.0 | 56 | 130.0 | 53 | -3 |
| | 134.5 | 60 | 137.0 | 60 | - |
| 30 | 90.0 | 24 | 90.0 | 22 | -2 |
| | 100.0 | 31 | 100.0 | 29 | -2 |
| | 110.0 | 37 | 110.0 | 35 | -2 |
| | 120.0 | 47 | 120.0 | 43 | -4 |
| | 130.0 | 56 | 130.0 | 51 | -5 |
| | 134.5 | 60 | 138.5 | 60 | - |
| 60 | 90.0 | 24 | 90.0 | 20 | -4 |
| | 100.0 | 31 | 100.0 | 26 | -5 |
| | 110.0 | 37 | 110.0 | 31 | -6 |
| | 120.0 | 47 | 120.0 | 39 | -8 |
| | 130.0 | 56 | 130.0 | 47 | -9 |
| | 134.5 | 60 | 140.0 | 56 | -4 |
| | - | - | 144.5 | 60 | - |

**Table A.24 Comparison of Number of Strands**
**(Strand Diameter = 0.6 in., Girder Spacing = 10 ft.)**

| Skew | Standard | | LRFD | | Difference in No. of Strands |
|---|---|---|---|---|---|
| | Span Length (ft.) | No. of Strands | Span Length (ft.) | No. of Strands | |
| 0 | 90.0 | 26 | 90.0 | 26 | 0 |
| | 100.0 | 33 | 100.0 | 33 | 0 |
| | 110.0 | 41 | 110.0 | 41 | 0 |
| | 120.0 | 49 | 120.0 | 49 | 0 |
| | 130.0 | 60 | 130.0 | 60 | 0 |
| 15 | 90.0 | 26 | 90.0 | 26 | 0 |
| | 100.0 | 33 | 100.0 | 33 | 0 |
| | 110.0 | 41 | 110.0 | 41 | 0 |
| | 120.0 | 49 | 120.0 | 49 | 0 |
| | 130.0 | 60 | 130.0 | 60 | 0 |
| 30 | 90.0 | 26 | 90.0 | 24 | -2 |
| | 100.0 | 33 | 100.0 | 31 | -2 |
| | 110.0 | 41 | 110.0 | 39 | -2 |
| | 120.0 | 49 | 120.0 | 47 | -2 |
| | 130.0 | 60 | 130.0 | 58 | -2 |
| | - | - | 131.5 | 60 | - |
| 60 | 90.0 | 26 | 90.0 | 22 | -4 |
| | 100.0 | 33 | 100.0 | 27 | -6 |
| | 110.0 | 41 | 110.0 | 35 | -6 |
| | 120.0 | 49 | 120.0 | 43 | -6 |
| | 130.0 | 60 | 130.0 | 51 | -9 |
| | - | - | 138.0 | 60 | - |

**Table A.25 Comparison of Number of Strands**
**(Strand Diameter = 0.6 in., Girder Spacing = 11.5 ft.)**

| Skew | Standard | | LRFD | | Difference in No. of Strands |
|---|---|---|---|---|---|
| | Span Length (ft.) | No. of Strands | Span Length (ft.) | No. of Strands | |
| 0 | 90.0 | 29 | 90.0 | 27 | -2 |
| | 100.0 | 37 | 100.0 | 35 | -2 |
| | 110.0 | 45 | 110.0 | 45 | 0 |
| | 120.0 | 56 | 120.0 | 54 | -2 |
| | 124.0 | 60 | 124.0 | 60 | 0 |
| 15 | 90.0 | 29 | 90.0 | 27 | -2 |
| | 100.0 | 37 | 100.0 | 35 | -2 |
| | 110.0 | 45 | 110.0 | 45 | 0 |
| | 120.0 | 56 | 120.0 | 54 | -2 |
| | 124.0 | 60 | 125.0 | 60 | - |
| 30 | 90.0 | 29 | 90.0 | 26 | -3 |
| | 100.0 | 37 | 100.0 | 35 | -2 |
| | 110.0 | 45 | 110.0 | 43 | -2 |
| | 120.0 | 56 | 120.0 | 53 | -3 |
| | 124.0 | 60 | 126.0 | 60 | - |
| 60 | 90.0 | 29 | 90.0 | 24 | -5 |
| | 100.0 | 37 | 100.0 | 31 | -6 |
| | 110.0 | 45 | 110.0 | 37 | -8 |
| | 120.0 | 56 | 120.0 | 47 | -9 |
| | 124.0 | 60 | 130.0 | 56 | - |
| | - | - | 133.0 | 60 | - |

**Table A.26 Comparison of Number of Strands (Strand Diameter = 0.6 in., Girder Spacing = 14 ft.)**

| Skew | Standard | | LRFD | | Difference in No. of Strands |
|---|---|---|---|---|---|
| | Span Length (ft.) | No. of Strands | Span Length (ft.) | No. of Strands | |
| 0 | 90.0 | 35 | 90.0 | 33 | -2 |
| | 100.0 | 45 | 100.0 | 43 | -2 |
| | 110.0 | 56 | 110.0 | 53 | -3 |
| | 112.0 | 58 | 115.5 | 60 | - |
| 15 | 90.0 | 35 | 90.0 | 33 | -2 |
| | 100.0 | 45 | 100.0 | 43 | -2 |
| | 110.0 | 56 | 110.0 | 53 | -3 |
| | 112.0 | 58 | 116.0 | 60 | - |
| 30 | 90.0 | 35 | 90.0 | 31 | -4 |
| | 100.0 | 45 | 100.0 | 41 | -4 |
| | 110.0 | 56 | 110.0 | 51 | -5 |
| | 112.0 | 58 | 117.0 | 60 | - |
| 60 | 90.0 | 35 | 90.0 | 29 | -6 |
| | 100.0 | 45 | 100.0 | 35 | -10 |
| | 110.0 | 56 | 110.0 | 45 | -11 |
| | 112.0 | 58 | 120.0 | 56 | - |
| | - | - | 123.5 | 60 | - |

**Table A.27 Comparison of Number of Strands (Strand Diameter = 0.6 in., Girder Spacing = 16.67 ft.)**

| Skew | Standard | | LRFD | | Difference in No. of Strands |
|---|---|---|---|---|---|
| | Span Length (ft.) | No. of Strands | Span Length (ft.) | No. of Strands | |
| 0 | 90.0 | 41 | 90.0 | 37 | -4 |
| | 98.5 | 51 | 100.0 | 49 | - |
| | - | - | 106.0 | 56 | - |
| 15 | 90.0 | 41 | 90.0 | 37 | -4 |
| | 98.5 | 51 | 100.0 | 49 | - |
| | - | - | 107.0 | 56 | - |
| 30 | 90.0 | 41 | 90.0 | 35 | -6 |
| | 98.5 | 51 | 100.0 | 47 | - |
| | - | - | 110.0 | 58 | - |
| 60 | 90.0 | 41 | 90.0 | 31 | -10 |
| | 98.5 | 51 | 100.0 | 41 | - |
| | - | - | 110.0 | 51 | - |
| | - | - | 117.0 | 60 | - |

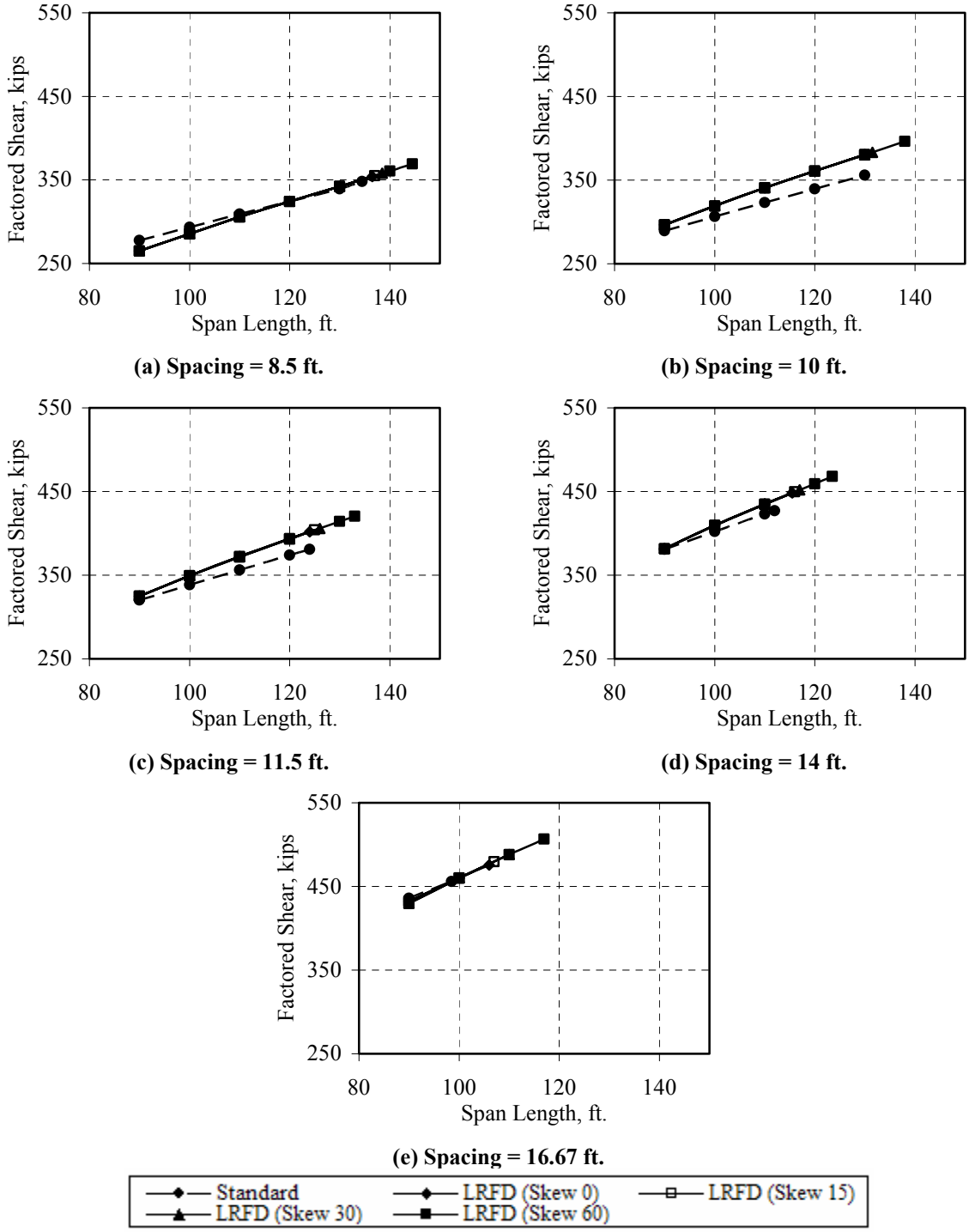


**(a) Spacing = 8.5 ft.**

**(b) Spacing = 10 ft.**

**(c) Spacing = 11.5 ft.**

**(d) Spacing = 14 ft.**

**(e) Spacing = 16.67 ft.**

**Figure A.8 Comparison of Factored Design Shear at Respective Critical Section Location (Strand Diameter 0.6 in.)**

## Table A.28 Comparison of Factored Design Moment

| Spacing (ft.) | Span (ft.) | All Skews | Skew = 0 | | | Skew = 15 | | | Skew = 30 | | | Skew = 60 | | |
|---|---|---|---|---|---|---|---|---|---|---|---|---|---|---|
| | | Moment (k-ft) | Span (ft.) | Moment (k-ft) | % Diff. w.r.t STD | Span (ft.) | Moment (k-ft) | % Diff. w.r.t STD | Span (ft.) | Moment (k-ft) | % Diff. w.r.t STD | Span (ft.) | Moment (k-ft) | % Diff. w.r.t STD |
| | | STD | LRFD | | | LRFD | | | LRFD | | | LRFD | | |
| 8.50 | 90.0 | 6197 | 90.0 | 5511 | -11.1 | 90.0 | 5466 | -11.8 | 90.0 | 5266 | -15.0 | 90.0 | 4530 | -26.9 |
| 8.50 | 100.0 | 7310 | 100.0 | 6541 | -10.5 | 100.0 | 6492 | -11.2 | 100.0 | 6270 | -14.2 | 100.0 | 5433 | -25.7 |
| 8.50 | 110.0 | 8493 | 110.0 | 7653 | -9.9 | 110.0 | 7597 | -10.5 | 110.0 | 7348 | -13.5 | 110.0 | 6410 | -24.5 |
| 8.50 | 120.0 | 9746 | 120.0 | 8839 | -9.3 | 120.0 | 8776 | -10.0 | 120.0 | 8500 | -12.8 | 120.0 | 7463 | -23.4 |
| 8.50 | 130.0 | 11070 | 130.0 | 10108 | -8.7 | 130.0 | 10038 | -9.3 | 130.0 | 9735 | -12.1 | 130.0 | 8594 | -22.4 |
| 8.50 | 135.0 | 11759 | 136.5 | 10972 | - | 136.5 | 10897 | - | 138.5 | 10844 | - | 140.0 | 9803 | - |
| 8.50 | - | - | - | - | - | - | - | - | - | - | - | 142.0 | 10047 | - |
| 10.00 | 90.0 | 6468 | 90.0 | 6067 | -6.2 | 90.0 | 6021 | -6.9 | 90.0 | 5797 | -10.4 | 90.0 | 4965 | -23.2 |
| 10.00 | 100.0 | 7642 | 100.0 | 7201 | -5.8 | 100.0 | 7147 | -6.5 | 100.0 | 6896 | -9.8 | 100.0 | 5953 | -22.1 |
| 10.00 | 110.0 | 8892 | 110.0 | 8418 | -5.3 | 110.0 | 8357 | -6.0 | 110.0 | 8074 | -9.2 | 110.0 | 7020 | -21.1 |
| 10.00 | 120.0 | 10219 | 120.0 | 9721 | -4.9 | 120.0 | 9652 | -5.5 | 120.0 | 9338 | -8.6 | 120.0 | 8170 | -20.1 |
| 10.00 | 130.0 | 11623 | 130.0 | 11107 | -4.4 | 130.0 | 11029 | -5.1 | 130.0 | 10684 | -8.1 | 130.0 | 9402 | -19.1 |
| 10.00 | - | - | 130.5 | 11176 | - | 131.0 | 11173 | - | 133.0 | 11107 | - | 139.0 | 10586 | - |
| 11.50 | 90.0 | 7155 | 90.0 | 6559 | -8.3 | 90.0 | 6505 | -9.1 | 90.0 | 6259 | -12.5 | 90.0 | 5340 | -25.4 |
| 11.50 | 100.0 | 8438 | 100.0 | 7777 | -7.8 | 100.0 | 7714 | -8.6 | 100.0 | 7438 | -11.9 | 100.0 | 6393 | -24.2 |
| 11.50 | 110.0 | 9801 | 110.0 | 9082 | -7.3 | 110.0 | 9016 | -8.0 | 110.0 | 8705 | -11.2 | 110.0 | 7536 | -23.1 |
| 11.50 | 120.0 | 11245 | 120.0 | 10478 | -6.8 | 120.0 | 10403 | -7.5 | 120.0 | 10057 | -10.6 | 120.0 | 8770 | -22.0 |
| 11.50 | 124.0 | 11846 | 125.5 | 11285 | - | 126.0 | 11283 | - | 127.5 | 11138 | - | 130.0 | 10086 | - |
| 11.50 | - | - | - | - | - | - | - | - | - | - | - | 134.0 | 10640 | - |
| 14.00 | 90.0 | 8466 | 90.0 | 7564 | -10.7 | 90.0 | 7481 | -11.6 | 90.0 | 7231 | -14.6 | 90.0 | 6171 | -27.1 |
| 14.00 | 100.0 | 9975 | 100.0 | 8987 | -9.9 | 100.0 | 8890 | -10.9 | 100.0 | 8551 | -14.3 | 100.0 | 7395 | -25.9 |
| 14.00 | 110.0 | 11578 | 110.0 | 10502 | -9.3 | 110.0 | 10392 | -10.2 | 110.0 | 10059 | -13.1 | 110.0 | 8717 | -24.7 |
| 14.00 | 113.0 | 12076 | 115.5 | 11381 | -5.8 | 116.0 | 11378 | -5.8 | 118.0 | 11309 | -6.4 | 120.0 | 10144 | -16.0 |
| 14.00 | - | - | - | - | - | - | - | - | - | - | - | 123.5 | 10664 | - |
| 16.67 | 90.0 | 9661 | 90.0 | 8391 | -13.1 | 90.0 | 8320 | -13.9 | 90.0 | 7999 | -17.2 | 90.0 | 6798 | -29.6 |
| 16.67 | 100.0 | 11387 | 100.0 | 9957 | -12.6 | 100.0 | 9874 | -13.3 | 100.0 | 9507 | -16.5 | 100.0 | 8148 | -28.4 |
| 16.67 | 104.5 | 12186 | 109.0 | 11446 | -6.1 | 109.5 | 11445 | -6.1 | 110.0 | 11120 | -8.7 | 110.0 | 9596 | -21.3 |
| 16.67 | - | - | - | - | - | - | - | - | 111.0 | 11293 | - | 117.0 | 10678 | - |

**Table A.29 Comparison of Factored Design Shear at Respective Critical Section Location (Strand Diameter 0.5 in.)**

| Spacing (ft.) | Span (ft.) | All Skews | Skew = 0 | | | Skew = 15 | | | Skew = 30 | | | Skew = 60 | | |
|---|---|---|---|---|---|---|---|---|---|---|---|---|---|---|
| | | Shear (k-ft) | Span (ft.) | Shear (k-ft) | % Diff. w.r.t STD | Span (ft.) | Shear (k-ft) | % Diff. w.r.t STD | Span (ft.) | Shear (k-ft) | % Diff. w.r.t STD | Span (ft.) | Shear (k-ft) | % Diff. w.r.t STD |
| | | STD | LRFD | | | LRFD | | | LRFD | | | LRFD | | |
| 8.50 | 90.0 | 277 | 90.0 | 265 | -4.5 | 90.0 | 265 | -4.5 | 90.0 | 265 | -4.5 | 90.0 | 265 | -4.5 |
| 8.50 | 100.0 | 293 | 100.0 | 286 | -2.6 | 100.0 | 286 | -2.6 | 100.0 | 286 | -2.7 | 100.0 | 286 | -2.7 |
| 8.50 | 110.0 | 309 | 110.0 | 306 | -1.0 | 110.0 | 306 | -1.0 | 110.0 | 306 | -1.0 | 110.0 | 306 | -1.1 |
| 8.50 | 120.0 | 324 | 120.0 | 324 | 0.0 | 120.0 | 324 | 0.0 | 120.0 | 324 | 0.0 | 120.0 | 324 | 0.0 |
| 8.50 | 130.0 | 339 | 130.0 | 342 | 0.8 | 130.0 | 342 | 0.8 | 130.0 | 342 | 0.8 | 130.0 | 342 | 0.8 |
| 8.50 | 135.0 | 349 | 136.5 | 354 | - | 136.5 | 354 | - | 138.5 | 358 | - | 140.0 | 361 | - |
| 8.50 | - | - | - | - | - | - | - | - | - | - | - | 142.0 | 371 | - |
| 10.00 | 90.0 | 289 | 90.0 | 297 | 2.5 | 90.0 | 297 | 2.5 | 90.0 | 296 | 2.5 | 90.0 | 296 | 2.5 |
| 10.00 | 100.0 | 306 | 100.0 | 319 | 4.3 | 100.0 | 319 | 4.2 | 100.0 | 319 | 4.2 | 100.0 | 319 | 4.2 |
| 10.00 | 110.0 | 323 | 110.0 | 341 | 5.5 | 110.0 | 341 | 5.5 | 110.0 | 341 | 5.4 | 110.0 | 340 | 5.3 |
| 10.00 | 120.0 | 340 | 120.0 | 360 | 6.1 | 120.0 | 361 | 6.2 | 120.0 | 361 | 6.2 | 120.0 | 361 | 6.2 |
| 10.00 | 130.0 | 356 | 130.0 | 380 | 6.7 | 130.0 | 380 | 6.7 | 130.0 | 380 | 6.7 | 130.0 | 380 | 6.7 |
| 10.00 | - | - | 130.5 | 381 | - | 131.0 | 382 | - | 133.0 | 386 | - | 139.0 | 398 | - |
| 11.50 | 90.0 | 320 | 90.0 | 325 | 1.6 | 90.0 | 325 | 1.6 | 90.0 | 325 | 1.6 | 90.0 | 325 | 1.5 |
| 11.50 | 100.0 | 338 | 100.0 | 350 | 3.3 | 100.0 | 350 | 3.3 | 100.0 | 350 | 3.3 | 100.0 | 349 | 3.3 |
| 11.50 | 110.0 | 356 | 110.0 | 372 | 4.4 | 110.0 | 372 | 4.4 | 110.0 | 372 | 4.4 | 110.0 | 372 | 4.4 |
| 11.50 | 120.0 | 374 | 120.0 | 393 | 5.2 | 120.0 | 393 | 5.2 | 120.0 | 393 | 5.1 | 120.0 | 393 | 5.2 |
| 11.50 | 124.0 | 381 | 125.5 | 404 | - | 126.0 | 405 | - | 127.5 | 408 | - | 130.0 | 414 | - |
| 11.50 | - | - | - | - | - | - | - | - | - | - | - | 134.0 | 423 | - |
| 14.00 | 90.0 | 381 | 90.0 | 382 | 0.3 | 90.0 | 382 | 0.3 | 90.0 | 382 | 0.2 | 90.0 | 382 | 0.2 |
| 14.00 | 100.0 | 402 | 100.0 | 410 | 1.9 | 100.0 | 410 | 1.9 | 100.0 | 410 | 1.9 | 100.0 | 409 | 1.8 |
| 14.00 | 110.0 | 423 | 110.0 | 435 | 2.8 | 110.0 | 435 | 2.8 | 110.0 | 435 | 2.8 | 110.0 | 435 | 2.7 |
| 14.00 | 113.0 | 429 | 115.5 | 448 | 4.3 | 116.0 | 449 | 4.6 | 118.0 | 454 | 5.8 | 120.0 | 459 | 6.9 |
| 14.00 | - | - | - | - | - | - | - | - | - | - | - | 123.5 | 467 | - |
| 16.67 | 90.0 | 436 | 90.0 | 430 | -1.2 | 90.0 | 430 | -1.2 | 90.0 | 430 | -1.2 | 90.0 | 430 | -1.3 |
| 16.67 | 100.0 | 459 | 100.0 | 460 | 0.3 | 100.0 | 460 | 0.2 | 100.0 | 460 | 0.2 | 100.0 | 460 | 0.2 |
| 16.67 | 104.5 | 469 | 109.0 | 485 | 3.3 | 109.5 | 486 | 3.5 | 110.0 | 487 | 3.8 | 110.0 | 487 | 3.8 |
| 16.67 | - | - | - | - | - | - | - | - | 111.0 | 490 | - | 117.0 | 506 | - |

**Table A.30 Comparison of Factored Design Shear at Respective Critical Section Location (Strand Diameter 0.6 in.)**

| Spacing (ft.) | Span (ft.) | All Skews | Skew = 0 | | | Skew = 15 | | | Skew = 30 | | | Skew = 60 | | |
|---|---|---|---|---|---|---|---|---|---|---|---|---|---|---|
| | | Shear (k-ft) | Span (ft.) | Shear (k-ft) | % Diff. w.r.t STD | Span (ft.) | Shear (k-ft) | % Diff. w.r.t STD | Span (ft.) | Shear (k-ft) | % Diff. w.r.t STD | Span (ft.) | Shear (k-ft) | % Diff. w.r.t STD |
| | | STD | LRFD | | | LRFD | | | LRFD | | | LRFD | | |
| 8.50 | 90.0 | 277 | 90.0 | 265 | -4.5 | 90.0 | 265 | -4.5 | 90.0 | 265 | -4.5 | 90.0 | 265 | -4.5 |
| 8.50 | 100.0 | 293 | 100.0 | 286 | -2.7 | 100.0 | 286 | -2.7 | 100.0 | 285 | -2.7 | 100.0 | 285 | -2.7 |
| 8.50 | 110.0 | 309 | 110.0 | 306 | -1.0 | 110.0 | 306 | -1.0 | 110.0 | 306 | -1.0 | 110.0 | 306 | -1.1 |
| 8.50 | 120.0 | 324 | 120.0 | 324 | 0.0 | 120.0 | 324 | 0.0 | 120.0 | 324 | 0.0 | 120.0 | 324 | 0.0 |
| 8.50 | 130.0 | 339 | 130.0 | 342 | 0.8 | 130.0 | 342 | 0.8 | 130.0 | 342 | 0.9 | 130.0 | 342 | 0.8 |
| 8.50 | 134.5 | 348 | 136.5 | 354 | - | 137.0 | 355 | - | 138.5 | 358 | - | 140.0 | 361 | - |
| 8.50 | - | - | - | - | - | - | - | - | - | - | - | 144.5 | 369 | - |
| 10.00 | 90.0 | 289 | 90.0 | 296 | 2.5 | 90.0 | 296 | 2.5 | 90.0 | 296 | 2.5 | 90.0 | 296 | 2.5 |
| 10.00 | 100.0 | 306 | 100.0 | 319 | 4.1 | 100.0 | 319 | 4.1 | 100.0 | 319 | 4.2 | 100.0 | 319 | 4.1 |
| 10.00 | 110.0 | 323 | 110.0 | 341 | 5.5 | 110.0 | 341 | 5.5 | 110.0 | 341 | 5.5 | 110.0 | 341 | 5.4 |
| 10.00 | 120.0 | 340 | 120.0 | 361 | 6.2 | 120.0 | 361 | 6.2 | 120.0 | 361 | 6.3 | 120.0 | 361 | 6.2 |
| 10.00 | 130.0 | 356 | 130.0 | 380 | 6.9 | 130.0 | 380 | 6.9 | 130.0 | 380 | 6.8 | 130.0 | 380 | 6.8 |
| 10.00 | - | - | - | - | - | - | - | - | 131.5 | 383 | - | 138.0 | 396 | - |
| 11.50 | 90.0 | 320 | 90.0 | 325 | 1.5 | 90.0 | 325 | 1.5 | 90.0 | 325 | 1.5 | 90.0 | 325 | 1.5 |
| 11.50 | 100.0 | 338 | 100.0 | 349 | 3.3 | 100.0 | 349 | 3.3 | 100.0 | 349 | 3.3 | 100.0 | 349 | 3.2 |
| 11.50 | 110.0 | 356 | 110.0 | 372 | 4.5 | 110.0 | 372 | 4.5 | 110.0 | 372 | 4.5 | 110.0 | 372 | 4.4 |
| 11.50 | 120.0 | 374 | 120.0 | 394 | 5.3 | 120.0 | 394 | 5.3 | 120.0 | 393 | 5.2 | 120.0 | 393 | 5.3 |
| 11.50 | 124.0 | 381 | 124.0 | 402 | - | 125.0 | 404 | - | 126.0 | 406 | - | 130.0 | 414 | - |
| 11.50 | - | - | - | - | - | - | - | - | - | - | - | 133.0 | 420 | - |
| 14.00 | 90.0 | 381 | 90.0 | 382 | 0.2 | 90.0 | 382 | 0.2 | 90.0 | 382 | 0.2 | 90.0 | 382 | 0.2 |
| 14.00 | 100.0 | 402 | 100.0 | 410 | 1.8 | 100.0 | 410 | 1.8 | 100.0 | 410 | 1.8 | 100.0 | 409 | 1.8 |
| 14.00 | 110.0 | 423 | 110.0 | 435 | 2.8 | 110.0 | 435 | 2.8 | 110.0 | 435 | 2.9 | 110.0 | 435 | 2.8 |
| 14.00 | 112.0 | 427 | 115.5 | 448 | 5.0 | 116.0 | 450 | 5.3 | 117.0 | 452 | 5.9 | 120.0 | 459 | 7.5 |
| 14.00 | - | - | - | - | - | - | - | - | - | - | - | 123.5 | 468 | - |
| 16.67 | 90.0 | 436 | 90.0 | 432 | -0.9 | 90.0 | 432 | -0.9 | 90.0 | 430 | -1.3 | 90.0 | 430 | -1.4 |
| 16.67 | 98.5 | 456 | 100.0 | 460 | 0.9 | 100.0 | 460 | 0.9 | 100.0 | 460 | 1.0 | 100.0 | 460 | 0.9 |
| 16.67 | - | - | 106.0 | 475 | - | 107.0 | 479 | - | 110.0 | 488 | - | 110.0 | 488 | - |
| 16.67 | - | - | - | - | - | - | - | - | - | - | - | 117.0 | 507 | - |

## Table A.31 Comparison of Nominal Moment Capacity (Strand Diameter 0.5 in.)

| Spacing (ft.) | Span (ft.) | All Skews | Skew = 0 | | | Skew = 15 | | | Skew = 30 | | | Skew = 60 | | |
|---|---|---|---|---|---|---|---|---|---|---|---|---|---|---|
| | | Mn (k-ft) | Span (ft.) | Mn (k-ft) | % Diff. w.r.t STD | Span (ft.) | Mn (k-ft) | % Diff. w.r.t STD | Span (ft.) | Mn (k-ft) | % Diff. w.r.t STD | Span (ft.) | Mn (k-ft) | % Diff. w.r.t STD |
| | | STD | LRFD | | | LRFD | | | LRFD | | | LRFD | | |
| 8.50 | 90.0 | 6707 | 90.0 | 6043 | -9.9 | 90.0 | 6043 | -9.9 | 90.0 | 6043 | -9.9 | 90.0 | 5322 | -20.7 |
| 8.50 | 100.0 | 8077 | 100.0 | 7805 | -3.4 | 100.0 | 7805 | -3.4 | 100.0 | 7457 | -7.7 | 100.0 | 6755 | -16.4 |
| 8.50 | 110.0 | 9729 | 110.0 | 9506 | -2.3 | 110.0 | 9506 | -2.3 | 110.0 | 9171 | -5.7 | 110.0 | 8492 | -12.7 |
| 8.50 | 120.0 | 11699 | 120.0 | 11608 | -0.8 | 120.0 | 11313 | -3.3 | 120.0 | 11013 | -5.9 | 120.0 | 10005 | -14.5 |
| 8.50 | 130.0 | 13690 | 130.0 | 13624 | -0.5 | 130.0 | 13624 | -0.5 | 130.0 | 13354 | -2.5 | 130.0 | 11943 | -12.8 |
| 8.50 | 135.0 | 14802 | 136.5 | 15013 | - | 136.5 | 15013 | - | 138.5 | 15037 | - | 140.0 | 13962 | - |
| 8.50 | - | - | - | - | - | - | - | - | - | - | - | 142.0 | 15129 | - |
| 10.00 | 90.0 | 7127 | 90.0 | 6814 | -4.4 | 90.0 | 6814 | -4.4 | 90.0 | 6814 | -4.4 | 90.0 | 6090 | -14.6 |
| 10.00 | 100.0 | 8862 | 100.0 | 8936 | 0.8 | 100.0 | 8587 | -3.1 | 100.0 | 8587 | -3.1 | 100.0 | 7529 | -15.0 |
| 10.00 | 110.0 | 10677 | 110.0 | 10789 | 1.0 | 110.0 | 10789 | 1.0 | 110.0 | 10465 | -2.0 | 110.0 | 9282 | -13.1 |
| 10.00 | 120.0 | 12830 | 120.0 | 13076 | 1.9 | 120.0 | 12777 | -0.4 | 120.0 | 12380 | -3.5 | 120.0 | 11111 | -13.4 |
| 10.00 | 130.0 | 14965 | 130.0 | 15203 | 1.6 | 130.0 | 15203 | 1.6 | 130.0 | 14955 | -0.1 | 130.0 | 13415 | -10.4 |
| 10.00 | - | - | 130.5 | 15437 | - | 131.0 | 15439 | - | 133.0 | 15675 | - | 139.0 | 15524 | - |
| 11.50 | 90.0 | 7894 | 90.0 | 7583 | -3.9 | 90.0 | 7583 | -3.9 | 90.0 | 7221 | -8.5 | 90.0 | 6492 | -17.8 |
| 11.50 | 100.0 | 9984 | 100.0 | 9717 | -2.7 | 100.0 | 9717 | -2.7 | 100.0 | 9365 | -6.2 | 100.0 | 8301 | -16.9 |
| 11.50 | 110.0 | 12086 | 110.0 | 11888 | -1.6 | 110.0 | 11562 | -4.3 | 110.0 | 11234 | -7.0 | 110.0 | 10066 | -16.7 |
| 11.50 | 120.0 | 14250 | 120.0 | 14123 | -0.9 | 120.0 | 14123 | -0.9 | 120.0 | 13809 | -3.1 | 120.0 | 12212 | -14.3 |
| 11.50 | 124.0 | 15244 | 125.5 | 15793 | - | 126.0 | 15796 | - | 127.5 | 15802 | - | 130.0 | 15027 | - |
| 11.50 | - | - | - | - | - | - | - | - | - | - | - | 134.0 | 15859 | - |
| 14.00 | 90.0 | 9763 | 90.0 | 9825 | 0.6 | 90.0 | 9466 | -3.0 | 90.0 | 8743 | -10.4 | 90.0 | 7648 | -21.7 |
| 14.00 | 100.0 | 11958 | 100.0 | 11382 | -4.8 | 100.0 | 11382 | -4.8 | 100.0 | 11043 | -7.7 | 100.0 | 9825 | -17.8 |
| 14.00 | 110.0 | 14697 | 110.0 | 14042 | -4.5 | 110.0 | 14042 | -4.5 | 110.0 | 13714 | -6.7 | 110.0 | 12056 | -18.0 |
| 14.00 | 113.0 | 15582 | 115.5 | 15763 | 1.2 | 116.0 | 15763 | 1.2 | 118.0 | 16041 | 2.9 | 120.0 | 14854 | -4.7 |
| 14.00 | - | - | - | - | - | - | - | - | - | - | - | 123.5 | 15763 | - |
| 16.67 | 90.0 | 11422 | 90.0 | 10271 | -10.1 | 90.0 | 10271 | -10.1 | 90.0 | 9907 | -13.3 | 90.0 | 8807 | -22.9 |
| 16.67 | 100.0 | 14100 | 100.0 | 13204 | -6.4 | 100.0 | 12864 | -8.8 | 100.0 | 12524 | -11.2 | 100.0 | 11147 | -20.9 |
| 16.67 | 104.5 | 15541 | 109.0 | 15988 | 2.9 | 109.5 | 15988 | 2.9 | 110.0 | 15686 | 0.9 | 110.0 | 13880 | -10.7 |
| 16.67 | - | - | - | - | - | - | - | - | 111.0 | 15988 | - | 117.0 | 15988 | - |

## Table A.32 Comparison of Nominal Moment Capacity (Strand Diameter 0.6 in.)

| Spacing (ft.) | Span (ft.) | All Skews | Skew = 0 | | | Skew = 15 | | | Skew = 30 | | | Skew = 60 | | |
|---|---|---|---|---|---|---|---|---|---|---|---|---|---|---|
| | | Mn (k-ft) | Span (ft.) | Mn (k-ft) | % Diff. w.r.t STD | Span (ft.) | Mn (k-ft) | % Diff. w.r.t STD | Span (ft.) | Mn (k-ft) | % Diff. w.r.t STD | Span (ft.) | Mn (k-ft) | % Diff. w.r.t STD |
| | | STD | LRFD | | | LRFD | | | LRFD | | | LRFD | | |
| 8.50 | 90.0 | 6587 | 90.0 | 6108 | -7.3 | 90.0 | 6108 | -7.3 | 90.0 | 6108 | -7.3 | 90.0 | 5579 | -15.3 |
| 8.50 | 100.0 | 8316 | 100.0 | 7904 | -5.0 | 100.0 | 7904 | -5.0 | 100.0 | 7904 | -5.0 | 100.0 | 7153 | -14.0 |
| 8.50 | 110.0 | 9721 | 110.0 | 9355 | -3.8 | 110.0 | 9355 | -3.8 | 110.0 | 9355 | -3.8 | 110.0 | 8392 | -13.7 |
| 8.50 | 120.0 | 11958 | 120.0 | 11717 | -2.0 | 120.0 | 11279 | -5.7 | 120.0 | 11279 | -5.7 | 120.0 | 10299 | -13.9 |
| 8.50 | 130.0 | 13837 | 130.0 | 13446 | -2.8 | 130.0 | 13446 | -2.8 | 130.0 | 13037 | -5.8 | 130.0 | 12195 | -11.9 |
| 8.50 | 134.5 | 14606 | 136.5 | 14811 | - | 137.0 | 14815 | - | 138.5 | 14824 | - | 140.0 | 14092 | - |
| 8.50 | - | - | - | - | - | - | - | - | - | - | - | 144.5 | 14901 | - |
| 10.00 | 90.0 | 7172 | 90.0 | 7217 | 0.6 | 90.0 | 7217 | 0.6 | 90.0 | 6688 | -6.7 | 90.0 | 6155 | -14.2 |
| 10.00 | 100.0 | 8905 | 100.0 | 8978 | 0.8 | 100.0 | 8978 | 0.8 | 100.0 | 8483 | -4.7 | 100.0 | 7480 | -16.0 |
| 10.00 | 110.0 | 10805 | 110.0 | 10918 | 1.0 | 110.0 | 10918 | 1.0 | 110.0 | 10439 | -3.4 | 110.0 | 9469 | -12.4 |
| 10.00 | 120.0 | 12633 | 120.0 | 12794 | 1.3 | 120.0 | 12794 | 1.3 | 120.0 | 12331 | -2.4 | 120.0 | 11393 | -9.8 |
| 10.00 | 130.0 | 14976 | 130.0 | 15213 | 1.6 | 130.0 | 15213 | 1.6 | 130.0 | 14821 | -1.0 | 130.0 | 13362 | -10.8 |
| 10.00 | - | - | - | - | - | - | - | - | 131.5 | 15221 | - | 138.0 | 15273 | - |
| 11.50 | 90.0 | 7994 | 90.0 | 7532 | -5.8 | 90.0 | 7532 | -5.8 | 90.0 | 7265 | -9.1 | 90.0 | 6729 | -15.8 |
| 11.50 | 100.0 | 9971 | 100.0 | 9554 | -4.2 | 100.0 | 9554 | -4.2 | 100.0 | 9554 | -4.2 | 100.0 | 8551 | -14.2 |
| 11.50 | 110.0 | 11884 | 110.0 | 12002 | 1.0 | 110.0 | 12002 | 1.0 | 110.0 | 11520 | -3.1 | 110.0 | 10051 | -15.4 |
| 11.50 | 120.0 | 14392 | 120.0 | 14130 | -1.8 | 120.0 | 14130 | -1.8 | 120.0 | 13897 | -3.4 | 120.0 | 12481 | -13.3 |
| 11.50 | 124.0 | 15244 | 124.0 | 15536 | - | 125.0 | 15541 | - | 126.0 | 15548 | - | 130.0 | 14575 | - |
| 11.50 | - | - | - | - | - | - | - | - | - | - | - | 133.0 | 15588 | - |
| 14.00 | 90.0 | 9599 | 90.0 | 9146 | -4.7 | 90.0 | 9146 | -4.7 | 90.0 | 8632 | -10.1 | 90.0 | 8115 | -15.5 |
| 14.00 | 100.0 | 12072 | 100.0 | 11673 | -3.3 | 100.0 | 11673 | -3.3 | 100.0 | 11173 | -7.4 | 100.0 | 9658 | -20.0 |
| 14.00 | 110.0 | 14677 | 110.0 | 14125 | -3.8 | 110.0 | 14125 | -3.8 | 110.0 | 13641 | -7.1 | 110.0 | 12169 | -17.1 |
| 14.00 | 112.0 | 15125 | 115.5 | 15742 | 4.1 | 116.0 | 15742 | 4.1 | 117.0 | 15742 | 4.1 | 120.0 | 14828 | -2.0 |
| 14.00 | - | - | - | - | - | - | - | - | - | - | - | 123.5 | 15742 | - |
| 16.67 | 90.0 | 11211 | 90.0 | 10252 | -8.6 | 90.0 | 10252 | -8.6 | 90.0 | 10252 | -8.6 | 90.0 | 8693 | -22.5 |
| 16.67 | 98.5 | 13694 | 100.0 | 13300 | -2.9 | 100.0 | 13300 | -2.9 | 100.0 | 12798 | -6.5 | 100.0 | 11278 | -17.6 |
| 16.67 | - | - | 106.0 | 15018 | - | 107.0 | 15018 | - | 110.0 | 15489 | - | 110.0 | 13799 | - |
| 16.67 | - | - | - | - | - | - | - | - | - | - | - | 117.0 | 15958 | - |

## Table A.33 Comparison of Camber (Strand Diameter 0.5 in.)

| Spacing (ft.) | Span (ft.) | All Skews | Skew = 0 | | | Skew = 15 | | | Skew = 30 | | | Skew = 60 | | |
|---|---|---|---|---|---|---|---|---|---|---|---|---|---|---|
| | | Camber (ft.) | Span (ft.) | Camber (ft.) | % Diff. w.r.t STD | Span (ft.) | Camber (ft.) | % Diff. w.r.t STD | Span (ft.) | Camber (ft.) | % Diff. w.r.t STD | Span (ft.) | Camber (ft.) | % Diff. w.r.t STD |
| | | STD | LRFD | | | LRFD | | | LRFD | | | LRFD | | |
| 8.50 | 90.0 | 0.102 | 90.0 | 0.079 | -22.5 | 90.0 | 0.079 | -22.5 | 90.0 | 0.079 | -22.5 | 90.0 | 0.056 | -45.1 |
| 8.50 | 100.0 | 0.145 | 100.0 | 0.131 | -9.7 | 100.0 | 0.131 | -9.7 | 100.0 | 0.118 | -18.6 | 100.0 | 0.09 | -37.9 |
| 8.50 | 110.0 | 0.208 | 110.0 | 0.192 | -7.7 | 110.0 | 0.192 | -7.7 | 110.0 | 0.176 | -15.4 | 110.0 | 0.144 | -30.8 |
| 8.50 | 120.0 | 0.293 | 120.0 | 0.276 | -5.8 | 120.0 | 0.261 | -10.9 | 120.0 | 0.245 | -16.4 | 120.0 | 0.196 | -33.1 |
| 8.50 | 130.0 | 0.396 | 130.0 | 0.376 | -5.1 | 130.0 | 0.376 | -5.1 | 130.0 | 0.359 | -9.3 | 130.0 | 0.268 | -32.3 |
| 8.50 | 135.0 | 0.452 | 136.5 | 0.447 | - | 136.5 | 0.447 | - | 138.5 | 0.442 | - | 140.0 | 0.365 | - |
| 8.50 | - | - | - | - | - | - | - | - | - | - | - | 142.0 | 0.418 | - |
| 10.00 | 90.0 | 0.113 | 90.0 | 0.102 | -9.7 | 90.0 | 0.102 | -9.7 | 90.0 | 0.102 | -9.7 | 90.0 | 0.079 | -30.1 |
| 10.00 | 100.0 | 0.171 | 100.0 | 0.17 | -0.6 | 100.0 | 0.157 | -8.2 | 100.0 | 0.157 | -8.2 | 100.0 | 0.118 | -31.0 |
| 10.00 | 110.0 | 0.243 | 110.0 | 0.241 | -0.8 | 110.0 | 0.241 | -0.8 | 110.0 | 0.228 | -6.2 | 110.0 | 0.176 | -27.6 |
| 10.00 | 120.0 | 0.339 | 120.0 | 0.338 | -0.3 | 120.0 | 0.323 | -4.7 | 120.0 | 0.307 | -9.4 | 120.0 | 0.245 | -27.7 |
| 10.00 | 130.0 | 0.447 | 130.0 | 0.445 | -0.4 | 130.0 | 0.445 | -0.4 | 130.0 | 0.432 | -3.4 | 130.0 | 0.341 | -23.7 |
| 10.00 | - | - | 130.5 | 0.455 | - | 131.0 | 0.454 | - | 133.0 | 0.461 | - | 139.0 | 0.441 | - |
| 11.50 | 90.0 | 0.134 | 90.0 | 0.123 | -8.2 | 90.0 | 0.123 | -8.2 | 90.0 | 0.113 | -15.7 | 90.0 | 0.091 | -32.1 |
| 11.50 | 100.0 | 0.209 | 100.0 | 0.196 | -6.2 | 100.0 | 0.196 | -6.2 | 100.0 | 0.183 | -12.4 | 100.0 | 0.144 | -31.1 |
| 11.50 | 110.0 | 0.295 | 110.0 | 0.281 | -4.7 | 110.0 | 0.268 | -9.2 | 110.0 | 0.255 | -13.6 | 110.0 | 0.207 | -29.8 |
| 11.50 | 120.0 | 0.399 | 120.0 | 0.382 | -4.3 | 120.0 | 0.382 | -4.3 | 120.0 | 0.367 | -8.0 | 120.0 | 0.292 | -26.8 |
| 11.50 | 124.0 | 0.446 | 125.5 | 0.454 | - | 126.0 | 0.455 | - | 127.5 | 0.455 | - | 130.0 | 0.417 | - |
| 11.50 | - | - | - | - | - | - | - | - | - | - | - | 134.0 | 0.451 | - |
| 14.00 | 90.0 | 0.186 | 90.0 | 0.185 | -0.5 | 90.0 | 0.175 | -5.9 | 90.0 | 0.155 | -16.7 | 90.0 | 0.123 | -33.9 |
| 14.00 | 100.0 | 0.269 | 100.0 | 0.247 | -8.2 | 100.0 | 0.247 | -8.2 | 100.0 | 0.236 | -12.3 | 100.0 | 0.196 | -27.1 |
| 14.00 | 110.0 | 0.388 | 110.0 | 0.356 | -8.2 | 110.0 | 0.356 | -8.2 | 110.0 | 0.344 | -11.3 | 110.0 | 0.281 | -27.6 |
| 14.00 | 113.0 | 0.426 | 115.5 | 0.43 | 0.9 | 116.0 | 0.431 | 1.2 | 118.0 | 0.444 | 4.2 | 120.0 | 0.404 | -5.2 |
| 14.00 | - | - | - | - | - | - | - | - | - | - | - | 123.5 | 0.444 | - |
| 16.67 | 90.0 | 0.227 | 90.0 | 0.195 | -14.1 | 90.0 | 0.195 | -14.1 | 90.0 | 0.185 | -18.5 | 90.0 | 0.155 | -31.7 |
| 16.67 | 100.0 | 0.33 | 100.0 | 0.299 | -9.4 | 100.0 | 0.289 | -12.4 | 100.0 | 0.278 | -15.8 | 100.0 | 0.236 | -28.5 |
| 16.67 | 104.5 | 0.389 | 109.0 | 0.411 | 5.7 | 109.5 | 0.413 | 6.2 | 110.0 | 0.406 | 4.4 | 110.0 | 0.344 | -11.6 |
| 16.67 | - | - | - | - | - | - | - | - | 111.0 | 0.418 | - | 117.0 | 0.434 | - |

## Table A.34 Comparison of Camber (Strand Diameter 0.6 in.)

| Spacing (ft.) | Span (ft.) | All Skews | Skew = 0 | | | Skew = 15 | | | Skew = 30 | | | Skew = 60 | | |
|---|---|---|---|---|---|---|---|---|---|---|---|---|---|---|
| | | Camber (ft.) | Span (ft.) | Camber (ft.) | % Diff. w.r.t STD | Span (ft.) | Camber (ft.) | % Diff. w.r.t STD | Span (ft.) | Camber (ft.) | % Diff. w.r.t STD | Span (ft.) | Camber (ft.) | % Diff. w.r.t STD |
| | | STD | LRFD | | | LRFD | | | LRFD | | | LRFD | | |
| 8.50 | 90.0 | 0.101 | 90.0 | 0.083 | -17.8 | 90.0 | 0.083 | -17.8 | 90.0 | 0.083 | -17.8 | 90.0 | 0.065 | -35.6 |
| 8.50 | 100.0 | 0.160 | 100.0 | 0.140 | -12.5 | 100.0 | 0.140 | -12.5 | 100.0 | 0.140 | -12.5 | 100.0 | 0.111 | -30.6 |
| 8.50 | 110.0 | 0.214 | 110.0 | 0.191 | -10.7 | 110.0 | 0.191 | -10.7 | 110.0 | 0.191 | -10.7 | 110.0 | 0.146 | -31.8 |
| 8.50 | 120.0 | 0.322 | 120.0 | 0.296 | -8.1 | 120.0 | 0.271 | -15.8 | 120.0 | 0.271 | -15.8 | 120.0 | 0.220 | -31.7 |
| 8.50 | 130.0 | 0.429 | 130.0 | 0.389 | -9.3 | 130.0 | 0.389 | -9.3 | 130.0 | 0.361 | -15.9 | 130.0 | 0.303 | -29.4 |
| 8.50 | 134.5 | 0.475 | 136.5 | 0.469 | - | 137.0 | 0.469 | - | 138.5 | 0.465 | - | 140.0 | 0.405 | - |
| 8.50 | - | - | - | - | - | - | - | - | - | - | - | 144.5 | 0.446 | - |
| 10.00 | 90.0 | 0.118 | 90.0 | 0.118 | 0.0 | 90.0 | 0.118 | 0.0 | 90.0 | 0.101 | -14.4 | 90.0 | 0.083 | -29.7 |
| 10.00 | 100.0 | 0.178 | 100.0 | 0.177 | -0.6 | 100.0 | 0.177 | -0.6 | 100.0 | 0.159 | -10.7 | 100.0 | 0.121 | -32.0 |
| 10.00 | 110.0 | 0.257 | 110.0 | 0.255 | -0.8 | 110.0 | 0.255 | -0.8 | 110.0 | 0.234 | -8.9 | 110.0 | 0.191 | -25.7 |
| 10.00 | 120.0 | 0.347 | 120.0 | 0.345 | -0.6 | 120.0 | 0.345 | -0.6 | 120.0 | 0.321 | -7.5 | 120.0 | 0.271 | -21.9 |
| 10.00 | 130.0 | 0.478 | 130.0 | 0.475 | -0.6 | 130.0 | 0.475 | -0.6 | 130.0 | 0.451 | -5.6 | 130.0 | 0.361 | -24.5 |
| 10.00 | - | - | - | - | - | - | - | - | 131.5 | 0.475 | - | 138.0 | 0.467 | - |
| 11.50 | 90.0 | 0.142 | 90.0 | 0.126 | -11.3 | 90.0 | 0.126 | -11.3 | 90.0 | 0.118 | -16.9 | 90.0 | 0.101 | -28.9 |
| 11.50 | 100.0 | 0.214 | 100.0 | 0.195 | -8.9 | 100.0 | 0.195 | -8.9 | 100.0 | 0.195 | -8.9 | 100.0 | 0.159 | -25.7 |
| 11.50 | 110.0 | 0.298 | 110.0 | 0.297 | -0.3 | 110.0 | 0.297 | -0.3 | 110.0 | 0.276 | -7.4 | 110.0 | 0.213 | -28.5 |
| 11.50 | 120.0 | 0.427 | 120.0 | 0.404 | -5.4 | 120.0 | 0.404 | -5.4 | 120.0 | 0.392 | -8.2 | 120.0 | 0.321 | -24.8 |
| 11.50 | 124.0 | 0.474 | 124.0 | 0.471 | - | 125.0 | 0.472 | - | 126.0 | 0.474 | - | 130.0 | 0.427 | - |
| 11.50 | - | - | - | - | - | - | - | - | - | - | - | 133.0 | 0.474 | - |
| 14.00 | 90.0 | 0.186 | 90.0 | 0.171 | -8.1 | 90.0 | 0.171 | -8.1 | 90.0 | 0.156 | -16.1 | 90.0 | 0.141 | -24.2 |
| 14.00 | 100.0 | 0.282 | 100.0 | 0.264 | -6.4 | 100.0 | 0.264 | -6.4 | 100.0 | 0.247 | -12.4 | 100.0 | 0.195 | -30.9 |
| 14.00 | 110.0 | 0.405 | 110.0 | 0.376 | -7.2 | 110.0 | 0.376 | -7.2 | 110.0 | 0.357 | -11.9 | 110.0 | 0.297 | -26.7 |
| 14.00 | 112.0 | 0.428 | 115.5 | 0.453 | 5.8 | 116.0 | 0.455 | 6.3 | 117.0 | 0.457 | 6.8 | 120.0 | 0.424 | -0.9 |
| 14.00 | - | - | - | - | - | - | - | - | - | - | - | 123.5 | 0.470 | - |
| 16.67 | 90.0 | 0.227 | 90.0 | 0.199 | -12.3 | 90.0 | 0.199 | -12.3 | 90.0 | 0.199 | -12.3 | 90.0 | 0.156 | -31.3 |
| 16.67 | 98.5 | 0.324 | 100.0 | 0.314 | -3.1 | 100.0 | 0.314 | -3.1 | 100.0 | 0.297 | -8.3 | 100.0 | 0.247 | -23.8 |
| 16.67 | - | - | 106.0 | 0.390 | - | 107.0 | 0.393 | - | 110.0 | 0.419 | - | 110.0 | 0.357 | - |
| 16.67 | - | - | - | - | - | - | - | - | - | - | - | 117.0 | 0.457 | - |

## Table A.35 Comparison of Transverse Shear Reinforcement Area (Strand Diameter 0.5 in.)

| Spacing (ft.) | Span (ft.) | All Skews | Skew = 0 | | | Skew = 15 | | | Skew = 30 | | | Skew = 60 | | |
|---|---|---|---|---|---|---|---|---|---|---|---|---|---|---|
| | | $A_v$ ($in^2$) | Span (ft.) | $A_v$ ($in^2$) | % Diff. w.r.t STD | Span (ft.) | $A_v$ ($in^2$) | % Diff. w.r.t STD | Span (ft.) | $A_v$ ($in^2$) | % Diff. w.r.t STD | Span (ft.) | $A_v$ ($in^2$) | % Diff. w.r.t STD |
| | | STD | LRFD | | | LRFD | | | LRFD | | | LRFD | | |
| 8.50 | 90.0 | 0.101 | 90.0 | 0.083 | -17.8 | 90.0 | 0.083 | -17.8 | 90.0 | 0.083 | -17.8 | 90.0 | 0.065 | -35.6 |
| 8.50 | 100.0 | 0.160 | 100.0 | 0.140 | -12.5 | 100.0 | 0.140 | -12.5 | 100.0 | 0.140 | -12.5 | 100.0 | 0.111 | -30.6 |
| 8.50 | 110.0 | 0.214 | 110.0 | 0.191 | -10.7 | 110.0 | 0.191 | -10.7 | 110.0 | 0.191 | -10.7 | 110.0 | 0.146 | -31.8 |
| 8.50 | 120.0 | 0.322 | 120.0 | 0.296 | -8.1 | 120.0 | 0.271 | -15.8 | 120.0 | 0.271 | -15.8 | 120.0 | 0.220 | -31.7 |
| 8.50 | 130.0 | 0.429 | 130.0 | 0.389 | -9.3 | 130.0 | 0.389 | -9.3 | 130.0 | 0.361 | -15.9 | 130.0 | 0.303 | -29.4 |
| 8.50 | 134.5 | 0.475 | 136.5 | 0.469 | - | 137.0 | 0.469 | - | 138.5 | 0.465 | - | 140.0 | 0.405 | - |
| 8.50 | - | - | - | - | - | - | - | - | - | - | - | 144.5 | 0.446 | - |
| 10.00 | 90.0 | 0.118 | 90.0 | 0.118 | 0.0 | 90.0 | 0.118 | 0.0 | 90.0 | 0.101 | -14.4 | 90.0 | 0.083 | -29.7 |
| 10.00 | 100.0 | 0.178 | 100.0 | 0.177 | -0.6 | 100.0 | 0.177 | -0.6 | 100.0 | 0.159 | -10.7 | 100.0 | 0.121 | -32.0 |
| 10.00 | 110.0 | 0.257 | 110.0 | 0.255 | -0.8 | 110.0 | 0.255 | -0.8 | 110.0 | 0.234 | -8.9 | 110.0 | 0.191 | -25.7 |
| 10.00 | 120.0 | 0.347 | 120.0 | 0.345 | -0.6 | 120.0 | 0.345 | -0.6 | 120.0 | 0.321 | -7.5 | 120.0 | 0.271 | -21.9 |
| 10.00 | 130.0 | 0.478 | 130.0 | 0.475 | -0.6 | 130.0 | 0.475 | -0.6 | 130.0 | 0.451 | -5.6 | 130.0 | 0.361 | -24.5 |
| 10.00 | - | - | - | - | - | - | - | - | 131.5 | 0.475 | - | 138.0 | 0.467 | - |
| 11.50 | 90.0 | 0.142 | 90.0 | 0.126 | -11.3 | 90.0 | 0.126 | -11.3 | 90.0 | 0.118 | -16.9 | 90.0 | 0.101 | -28.9 |
| 11.50 | 100.0 | 0.214 | 100.0 | 0.195 | -8.9 | 100.0 | 0.195 | -8.9 | 100.0 | 0.195 | -8.9 | 100.0 | 0.159 | -25.7 |
| 11.50 | 110.0 | 0.298 | 110.0 | 0.297 | -0.3 | 110.0 | 0.297 | -0.3 | 110.0 | 0.276 | -7.4 | 110.0 | 0.213 | -28.5 |
| 11.50 | 120.0 | 0.427 | 120.0 | 0.404 | -5.4 | 120.0 | 0.404 | -5.4 | 120.0 | 0.392 | -8.2 | 120.0 | 0.321 | -24.8 |
| 11.50 | 124.0 | 0.474 | 124.0 | 0.471 | - | 125.0 | 0.472 | - | 126.0 | 0.474 | - | 130.0 | 0.427 | - |
| 11.50 | - | - | - | - | - | - | - | - | - | - | - | 133.0 | 0.474 | - |
| 14.00 | 90.0 | 0.186 | 90.0 | 0.171 | -8.1 | 90.0 | 0.171 | -8.1 | 90.0 | 0.156 | -16.1 | 90.0 | 0.141 | -24.2 |
| 14.00 | 100.0 | 0.282 | 100.0 | 0.264 | -6.4 | 100.0 | 0.264 | -6.4 | 100.0 | 0.247 | -12.4 | 100.0 | 0.195 | -30.9 |
| 14.00 | 110.0 | 0.405 | 110.0 | 0.376 | -7.2 | 110.0 | 0.376 | -7.2 | 110.0 | 0.357 | -11.9 | 110.0 | 0.297 | -26.7 |
| 14.00 | 112.0 | 0.428 | 115.5 | 0.453 | 5.8 | 116.0 | 0.455 | 6.3 | 117.0 | 0.457 | 6.8 | 120.0 | 0.424 | -0.9 |
| 14.00 | - | - | - | - | - | - | - | - | - | - | - | 123.5 | 0.470 | - |
| 16.67 | 90.0 | 0.227 | 90.0 | 0.199 | -12.3 | 90.0 | 0.199 | -12.3 | 90.0 | 0.199 | -12.3 | 90.0 | 0.156 | -31.3 |
| 16.67 | 98.5 | 0.324 | 100.0 | 0.314 | -3.1 | 100.0 | 0.314 | -3.1 | 100.0 | 0.297 | -8.3 | 100.0 | 0.247 | -23.8 |
| 16.67 | - | - | 106.0 | 0.390 | - | 107.0 | 0.393 | - | 110.0 | 0.419 | - | 110.0 | 0.357 | - |
| 16.67 | - | - | - | - | - | - | - | - | - | - | - | 117.0 | 0.457 | - |

## Table A.36 Comparison of Transverse Shear Reinforcement Area (Strand Diameter 0.6 in.)

| Spacing (ft.) | Span (ft.) | All Skews | Skew = 0 | | | Skew = 15 | | | Skew = 30 | | | Skew = 60 | | |
|---|---|---|---|---|---|---|---|---|---|---|---|---|---|---|
| | | $A_v$ ($in^2$) | Span (ft.) | $A_v$ ($in^2$) | % Diff. w.r.t STD | Span (ft.) | $A_v$ ($in^2$) | % Diff. w.r.t STD | Span (ft.) | $A_v$ ($in^2$) | % Diff. w.r.t STD | Span (ft.) | $A_v$ ($in^2$) | % Diff. w.r.t STD |
| | | STD | LRFD | | | LRFD | | | LRFD | | | LRFD | | |
| 8.50 | 90.0 | 0.42 | 90.0 | 0.22 | -49.2 | 90.0 | 0.22 | -49.2 | 90.0 | 0.21 | -49.3 | 90.0 | 0.21 | -49.4 |
| 8.50 | 100.0 | 0.47 | 100.0 | 0.27 | -43.3 | 100.0 | 0.27 | -43.3 | 100.0 | 0.26 | -44.2 | 100.0 | 0.26 | -45.0 |
| 8.50 | 110.0 | 0.51 | 110.0 | 0.32 | -37.3 | 110.0 | 0.32 | -37.3 | 110.0 | 0.32 | -37.3 | 110.0 | 0.31 | -39.3 |
| 8.50 | 120.0 | 0.50 | 120.0 | 0.32 | -36.8 | 120.0 | 0.32 | -36.9 | 120.0 | 0.31 | -37.4 | 120.0 | 0.30 | -39.7 |
| 8.50 | 130.0 | 0.49 | 130.0 | 0.30 | -39.5 | 130.0 | 0.30 | -39.6 | 130.0 | 0.29 | -40.1 | 130.0 | 0.28 | -42.3 |
| 8.50 | 134.5 | 0.49 | 136.5 | 0.28 | - | 137.0 | 0.28 | - | 138.5 | 0.27 | - | 140.0 | 0.26 | - |
| 8.50 | - | - | - | - | - | - | - | - | - | - | - | 144.5 | 0.22 | - |
| 10.00 | 90.0 | 0.48 | 90.0 | 0.29 | -40.4 | 90.0 | 0.28 | -40.9 | 90.0 | 0.28 | -41.1 | 90.0 | 0.28 | -42.1 |
| 10.00 | 100.0 | 0.54 | 100.0 | 0.34 | -36.4 | 100.0 | 0.34 | -36.4 | 100.0 | 0.34 | -37.2 | 100.0 | 0.33 | -38.4 |
| 10.00 | 110.0 | 0.55 | 110.0 | 0.39 | -29.7 | 110.0 | 0.39 | -29.8 | 110.0 | 0.38 | -30.4 | 110.0 | 0.37 | -33.0 |
| 10.00 | 120.0 | 0.55 | 120.0 | 0.37 | -33.6 | 120.0 | 0.37 | -33.7 | 120.0 | 0.37 | -33.8 | 120.0 | 0.35 | -36.2 |
| 10.00 | 130.0 | 0.54 | 130.0 | 0.35 | -35.3 | 130.0 | 0.35 | -35.3 | 130.0 | 0.34 | -36.5 | 130.0 | 0.33 | -38.5 |
| 10.00 | - | - | - | - | - | - | | - | 131.5 | 0.34 | - | 138.0 | 0.29 | - |
| 11.50 | 90.0 | 0.61 | 90.0 | 0.35 | -43.1 | 90.0 | 0.35 | -43.2 | 90.0 | 0.35 | -43.1 | 90.0 | 0.34 | -43.9 |
| 11.50 | 100.0 | 0.67 | 100.0 | 0.41 | -38.6 | 100.0 | 0.41 | -38.6 | 100.0 | 0.41 | -38.7 | 100.0 | 0.40 | -40.3 |
| 11.50 | 110.0 | 0.67 | 110.0 | 0.43 | -35.5 | 110.0 | 0.43 | -35.5 | 110.0 | 0.43 | -36.1 | 110.0 | 0.42 | -38.0 |
| 11.50 | 120.0 | 0.67 | 120.0 | 0.41 | -38.6 | 120.0 | 0.41 | -38.7 | 120.0 | 0.41 | -39.6 | 120.0 | 0.40 | -41.4 |
| 11.50 | 124.0 | 0.67 | 124.0 | 0.41 | - | 125.0 | 0.40 | - | 126.0 | 0.40 | - | 130.0 | 0.37 | - |
| 11.50 | - | - | - | - | - | - | - | - | - | - | - | 133.0 | 0.37 | - |
| 14.00 | 90.0 | 0.85 | 90.0 | 0.48 | -43.8 | 90.0 | 0.48 | -43.8 | 90.0 | 0.48 | -43.9 | 90.0 | 0.46 | -45.3 |
| 14.00 | 100.0 | 0.90 | 100.0 | 0.55 | -38.9 | 100.0 | 0.55 | -39.0 | 100.0 | 0.55 | -39.5 | 100.0 | 0.54 | -40.6 |
| 14.00 | 110.0 | 0.92 | 110.0 | 0.53 | -41.9 | 110.0 | 0.53 | -41.9 | 110.0 | 0.53 | -42.3 | 110.0 | 0.51 | -44.5 |
| 14.00 | 112.0 | 0.91 | 115.5 | 0.52 | -43.0 | 116.0 | 0.52 | -43.2 | 117.0 | 0.51 | -43.8 | 120.0 | 0.49 | -46.5 |
| 14.00 | - | - | - | - | - | - | - | - | - | - | - | 123.5 | 0.48 | - |
| 16.67 | 90.0 | 1.07 | 90.0 | 0.60 | -44.2 | 90.0 | 0.60 | -44.2 | 90.0 | 0.59 | -44.8 | 90.0 | 0.58 | -45.5 |
| 16.67 | 98.5 | 1.09 | 100.0 | 0.62 | - | 100.0 | 0.64 | - | 100.0 | 0.63 | - | 100.0 | 0.61 | - |
| 16.67 | - | - | 106.0 | 0.58 | - | 107.0 | 0.60 | - | 110.0 | 0.60 | - | 110.0 | 0.58 | - |
| 16.67 | - | - | - | - | - | - | - | - | - | - | - | 117.0 | 0.56 | - |

## Table A.37 Comparison of Interface Shear Reinforcement Area (Strand Diameter 0.5 in.)

| Spacing (ft.) | Span (ft.) | All Skews | Skew = 0 | | | Skew = 15 | | | Skew = 30 | | | Skew = 60 | | |
|---|---|---|---|---|---|---|---|---|---|---|---|---|---|---|
| | | $A_{vh}$ ($in^2$) | Span (ft.) | $A_{vh}$ ($in^2$) | % Diff. w.r.t STD | Span (ft.) | $A_{vh}$ ($in^2$) | % Diff. w.r.t STD | Span (ft.) | $A_{vh}$ ($in^2$) | % Diff. w.r.t STD | Span (ft.) | $A_{vh}$ ($in^2$) | % Diff. w.r.t STD |
| | | STD | LRFD | | | LRFD | | | LRFD | | | LRFD | | |
| 8.50 | 90.0 | 0.315 | 90.0 | 0.79 | 150.7 | 90.0 | 0.79 | 150.4 | 90.0 | 0.79 | 150.4 | 90.0 | 0.78 | 147.5 |
| 8.50 | 100.0 | 0.315 | 100.0 | 0.86 | 172.2 | 100.0 | 0.86 | 172.1 | 100.0 | 0.85 | 170.9 | 100.0 | 0.85 | 168.4 |
| 8.50 | 110.0 | 0.315 | 110.0 | 0.92 | 192.1 | 110.0 | 0.92 | 192.1 | 110.0 | 0.92 | 192.0 | 110.0 | 0.91 | 188.6 |
| 8.50 | 120.0 | 0.315 | 120.0 | 0.98 | 211.1 | 120.0 | 0.98 | 211.1 | 120.0 | 0.98 | 209.8 | 120.0 | 0.96 | 204.1 |
| 8.50 | 130.0 | 0.315 | 130.0 | 1.04 | 229.7 | 130.0 | 1.04 | 228.7 | 130.0 | 1.03 | 227.6 | 130.0 | 1.01 | 222.0 |
| 8.50 | 135.0 | 0.315 | 136.5 | 1.08 | - | 136.5 | 1.08 | - | 138.5 | 1.09 | - | 140.0 | 1.07 | - |
| 8.50 | - | - | - | - | - | - | - | - | - | - | - | 142.0 | 1.11 | - |
| 10.00 | 90.0 | 0.315 | 90.0 | 0.94 | 199.8 | 90.0 | 0.94 | 199.8 | 90.0 | 0.94 | 198.4 | 90.0 | 0.94 | 197.0 |
| 10.00 | 100.0 | 0.315 | 100.0 | 1.02 | 223.1 | 100.0 | 1.02 | 223.1 | 100.0 | 1.02 | 223.1 | 100.0 | 1.01 | 219.5 |
| 10.00 | 110.0 | 0.315 | 110.0 | 1.09 | 246.6 | 110.0 | 1.09 | 246.6 | 110.0 | 1.09 | 244.9 | 110.0 | 1.07 | 240.2 |
| 10.00 | 120.0 | 0.315 | 120.0 | 1.16 | 267.3 | 120.0 | 1.15 | 266.1 | 120.0 | 1.15 | 264.9 | 120.0 | 1.14 | 260.7 |
| 10.00 | 130.0 | 0.315 | 130.0 | 1.22 | 288.8 | 130.0 | 1.22 | 288.8 | 130.0 | 1.21 | 285.7 | 130.0 | 1.20 | 280.4 |
| 10.00 | - | - | 130.5 | 1.23 | - | 131.0 | 1.24 | - | 133.0 | 1.24 | - | 139.0 | 1.26 | - |
| 11.50 | 90.0 | 0.315 | 90.0 | 1.08 | 243.3 | 90.0 | 1.08 | 243.2 | 90.0 | 1.08 | 242.1 | 90.0 | 1.07 | 239.1 |
| 11.50 | 100.0 | 0.315 | 100.0 | 1.16 | 268.9 | 100.0 | 1.16 | 268.0 | 100.0 | 1.16 | 267.9 | 100.0 | 1.15 | 264.5 |
| 11.50 | 110.0 | 0.315 | 110.0 | 1.24 | 293.0 | 110.0 | 1.24 | 293.0 | 110.0 | 1.23 | 291.6 | 110.0 | 1.21 | 284.9 |
| 11.50 | 120.0 | 0.315 | 120.0 | 1.31 | 314.5 | 120.0 | 1.31 | 314.5 | 120.0 | 1.30 | 313.1 | 120.0 | 1.28 | 307.0 |
| 11.50 | 124.0 | 0.315 | 125.5 | 1.35 | - | 126.0 | 1.36 | - | 127.5 | 1.36 | - | 130.0 | 1.35 | - |
| 11.50 | - | - | - | - | - | - | - | - | - | - | - | 134.0 | 1.39 | - |
| 14.00 | 90.0 | 0.315 | 90.0 | 1.37 | 333.5 | 90.0 | 1.37 | 333.5 | 90.0 | 1.36 | 332.5 | 90.0 | 1.35 | 328.4 |
| 14.00 | 100.0 | 0.315 | 100.0 | 1.47 | 365.7 | 100.0 | 1.47 | 365.7 | 100.0 | 1.46 | 364.0 | 100.0 | 1.44 | 358.4 |
| 14.00 | 110.0 | 0.315 | 110.0 | 1.56 | 393.7 | 110.0 | 1.56 | 393.7 | 110.0 | 1.55 | 392.2 | 110.0 | 1.53 | 385.0 |
| 14.00 | 113.0 | 0.315 | 115.5 | 1.61 | 410.9 | 116.0 | 1.61 | 411.7 | 118.0 | 1.63 | 417.1 | 120.0 | 1.61 | 412.2 |
| 14.00 | - | - | - | - | - | - | - | - | - | - | - | 123.5 | 1.65 | - |
| 16.67 | 90.0 | 0.315 | 90.0 | 1.59 | 406.0 | 90.0 | 1.59 | 406.0 | 90.0 | 1.59 | 405.0 | 90.0 | 1.58 | 401.5 |
| 16.67 | 100.0 | 0.315 | 100.0 | 1.71 | 442.2 | 100.0 | 1.70 | 440.6 | 100.0 | 1.70 | 439.1 | 100.0 | 1.68 | 432.4 |
| 16.67 | 104.5 | 0.315 | 109.0 | 1.80 | - | 109.5 | 1.80 | - | 110.0 | 1.80 | - | 110.0 | 1.77 | - |
| 16.67 | - | - | - | - | - | - | - | - | - | - | - | 117.0 | 0.457 | - |

## Table A.38 Comparison of Interface Shear Reinforcement Area (Strand Diameter 0.6 in.)

| Spacing (ft.) | Span (ft.) | All Skews | Skew = 0 | | | Skew = 15 | | | Skew = 30 | | | Skew = 60 | | |
|---|---|---|---|---|---|---|---|---|---|---|---|---|---|---|
| | | $A_{vh}$ ($in^2$) | Span (ft.) | $A_{vh}$ ($in^2$) | % Diff. w.r.t STD | Span (ft.) | $A_{vh}$ ($in^2$) | % Diff. w.r.t STD | Span (ft.) | $A_{vh}$ ($in^2$) | % Diff. w.r.t STD | Span (ft.) | $A_{vh}$ ($in^2$) | % Diff. w.r.t STD |
| | | STD | LRFD | | | LRFD | | | LRFD | | | LRFD | | |
| 8.50 | 90.0 | 0.315 | 90.0 | 0.78 | 148.9 | 90.0 | 0.78 | 148.9 | 90.0 | 0.78 | 148.8 | 90.0 | 0.78 | 148.0 |
| 8.50 | 100.0 | 0.315 | 100.0 | 0.85 | 168.9 | 100.0 | 0.85 | 168.9 | 100.0 | 0.84 | 166.9 | 100.0 | 0.84 | 165.3 |
| 8.50 | 110.0 | 0.315 | 110.0 | 0.91 | 189.9 | 110.0 | 0.91 | 189.9 | 110.0 | 0.91 | 188.4 | 110.0 | 0.90 | 184.8 |
| 8.50 | 120.0 | 0.315 | 120.0 | 0.97 | 207.0 | 120.0 | 0.97 | 207.0 | 120.0 | 0.96 | 205.5 | 120.0 | 0.95 | 202.3 |
| 8.50 | 130.0 | 0.315 | 130.0 | 1.02 | 222.5 | 130.0 | 1.02 | 222.5 | 130.0 | 1.01 | 221.3 | 130.0 | 1.00 | 218.5 |
| 8.50 | 134.5 | 0.315 | 136.5 | 1.05 | - | 137.0 | 1.06 | - | 138.5 | 1.06 | - | 140.0 | 1.06 | - |
| 8.50 | - | - | - | - | - | - | - | - | - | - | - | 144.5 | 1.08 | - |
| 10.00 | 90.0 | 0.315 | 90.0 | 0.94 | 197.5 | 90.0 | 0.93 | 196.5 | 90.0 | 0.93 | 196.5 | 90.0 | 0.93 | 195.3 |
| 10.00 | 100.0 | 0.315 | 100.0 | 1.01 | 220.7 | 100.0 | 1.01 | 220.7 | 100.0 | 1.00 | 218.8 | 100.0 | 0.99 | 215.0 |
| 10.00 | 110.0 | 0.315 | 110.0 | 1.08 | 243.0 | 110.0 | 1.08 | 243.0 | 110.0 | 1.08 | 241.4 | 110.0 | 1.06 | 237.7 |
| 10.00 | 120.0 | 0.315 | 120.0 | 1.14 | 260.4 | 120.0 | 1.14 | 260.4 | 120.0 | 1.14 | 260.3 | 120.0 | 1.12 | 255.9 |
| 10.00 | 130.0 | 0.315 | 130.0 | 1.20 | 280.6 | 130.0 | 1.20 | 280.6 | 130.0 | 1.19 | 278.7 | 130.0 | 1.18 | 274.5 |
| 10.00 | - | - | - | - | - | - | - | - | 131.5 | 1.20 | - | 138.0 | 1.23 | - |
| 11.50 | 90.0 | 0.315 | 90.0 | 1.07 | 238.4 | 90.0 | 1.07 | 238.4 | 90.0 | 1.06 | 238.1 | 90.0 | 1.06 | 236.9 |
| 11.50 | 100.0 | 0.315 | 100.0 | 1.15 | 264.7 | 100.0 | 1.15 | 264.7 | 100.0 | 1.15 | 264.6 | 100.0 | 1.14 | 260.8 |
| 11.50 | 110.0 | 0.315 | 110.0 | 1.22 | 288.0 | 110.0 | 1.22 | 288.0 | 110.0 | 1.22 | 286.5 | 110.0 | 1.21 | 283.1 |
| 11.50 | 120.0 | 0.315 | 120.0 | 1.28 | 306.9 | 120.0 | 1.28 | 306.9 | 120.0 | 1.28 | 305.9 | 120.0 | 1.27 | 301.8 |
| 11.50 | 124.0 | 0.315 | 124.0 | 1.31 | - | 125.0 | 1.32 | - | 126.0 | 1.32 | - | 130.0 | 1.33 | - |
| 11.50 | - | - | - | - | - | - | - | - | - | - | - | 133.0 | 1.35 | - |
| 14.00 | 90.0 | 0.315 | 90.0 | 1.35 | 328.9 | 90.0 | 1.35 | 328.9 | 90.0 | 1.35 | 327.2 | 90.0 | 1.33 | 322.6 |
| 14.00 | 100.0 | 0.315 | 100.0 | 1.45 | 360.7 | 100.0 | 1.45 | 360.7 | 100.0 | 1.45 | 359.1 | 100.0 | 1.43 | 355.5 |
| 14.00 | 110.0 | 0.315 | 110.0 | 1.53 | 385.1 | 110.0 | 1.53 | 385.1 | 110.0 | 1.52 | 383.8 | 110.0 | 1.51 | 378.9 |
| 14.00 | 112.0 | 0.315 | 115.5 | 1.58 | 400.7 | 116.0 | 1.58 | 401.5 | 117.0 | 1.58 | 403.0 | 120.0 | 1.59 | 403.8 |
| 14.00 | - | - | - | - | - | - | - | - | - | - | - | 123.5 | 1.62 | - |
| 16.67 | 90.0 | 0.315 | 90.0 | 1.59 | 403.4 | 90.0 | 1.59 | 403.4 | 90.0 | 1.57 | 399.5 | 90.0 | 1.56 | 395.6 |
| 16.67 | 98.5 | 0.315 | 100.0 | 1.68 | - | 100.0 | 1.68 | - | 100.0 | 1.68 | - | 100.0 | 1.66 | - |
| 16.67 | | | 106.0 | 1.73 | - | 107.0 | 1.74 | - | 110.0 | 1.76 | - | 110.0 | 1.74 | - |
| 16.67 | - | - | - | - | - | - | - | - | - | - | - | 117.0 | 1.81 | - |

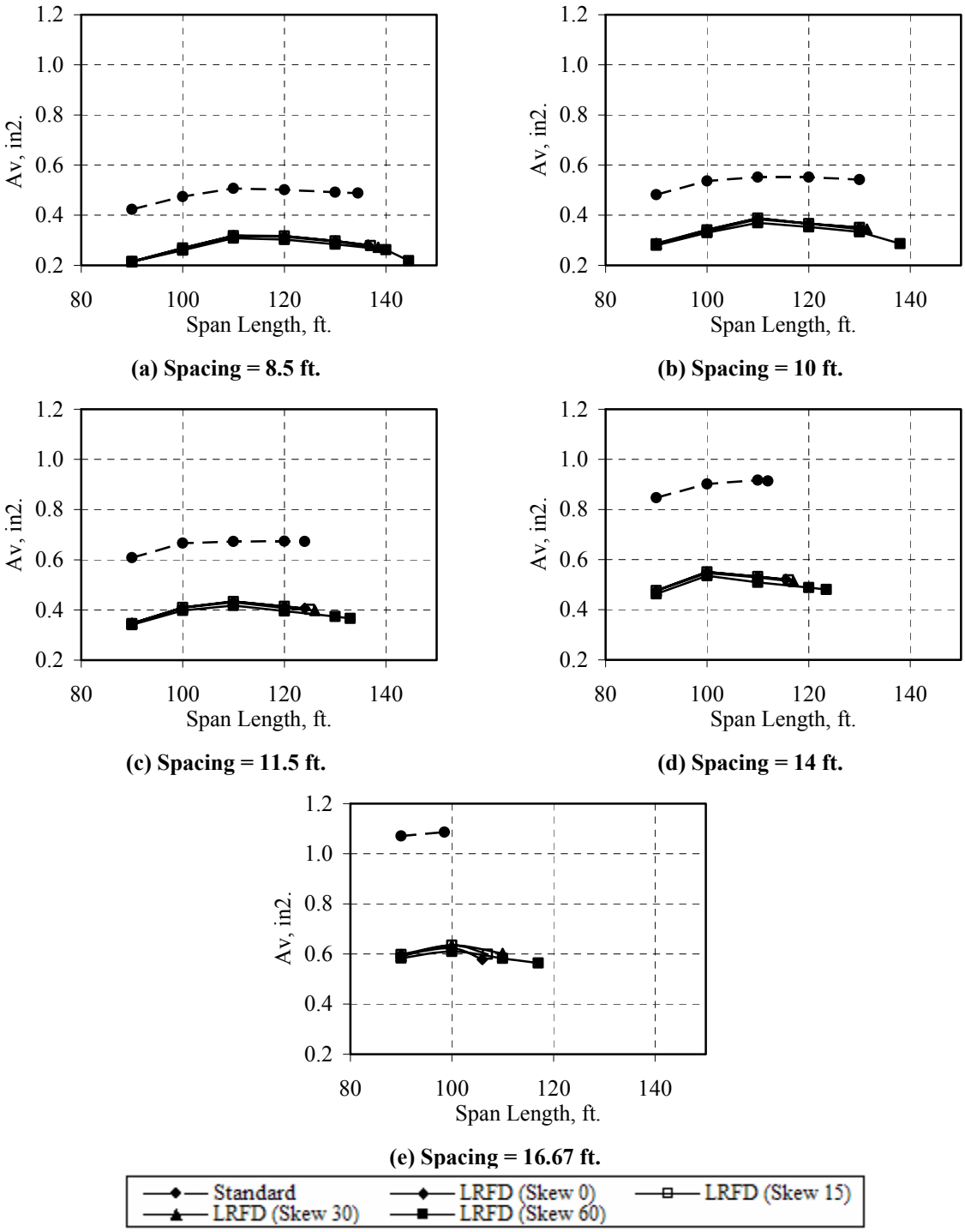


**Figure A.9 Comparison of Transverse Shear Reinforcement Area (Strand Diameter 0.6 in.)**

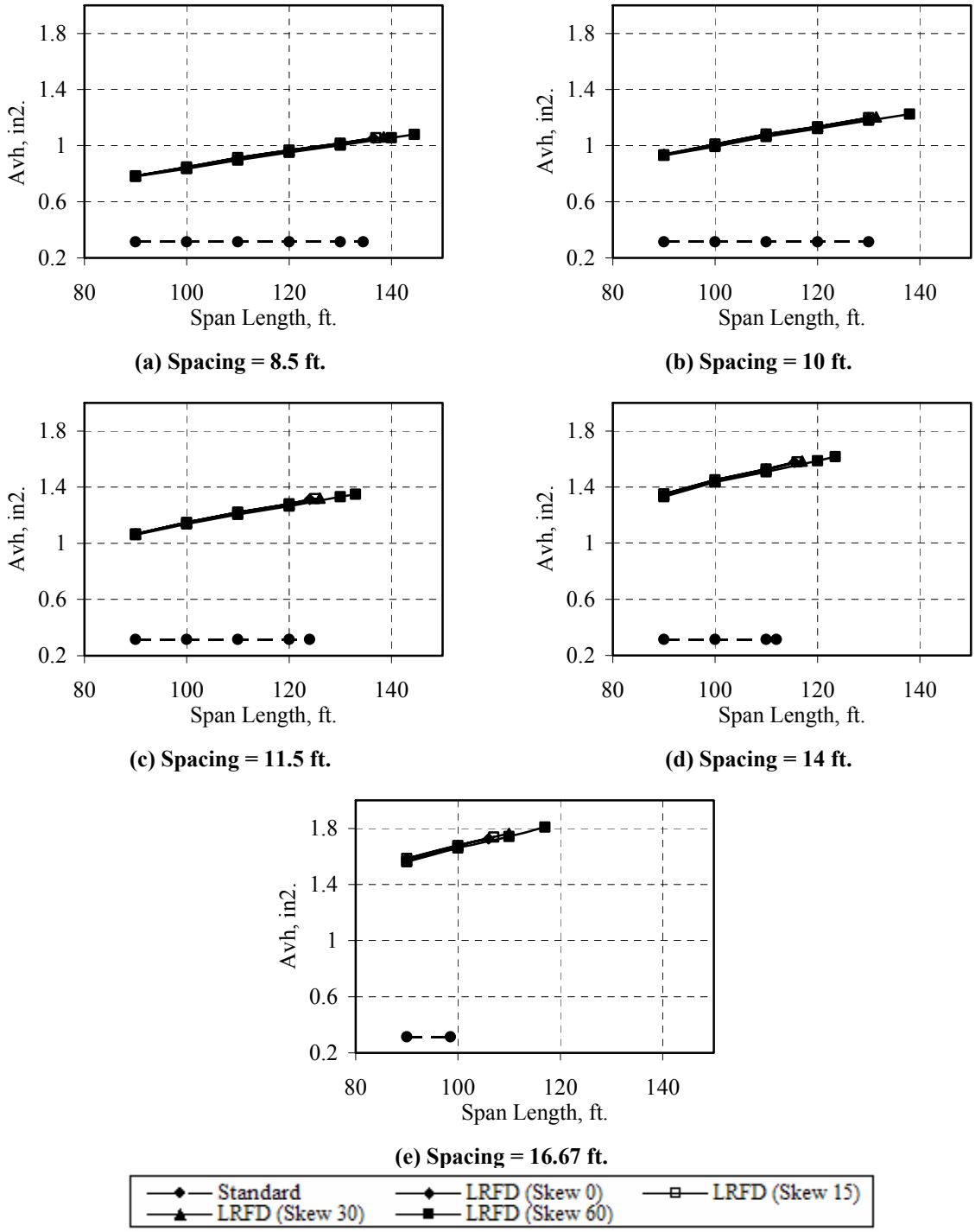


**Figure A.10 Comparison of Interface Shear Reinforcement Area (Strand Diameter 0.6 in.)**

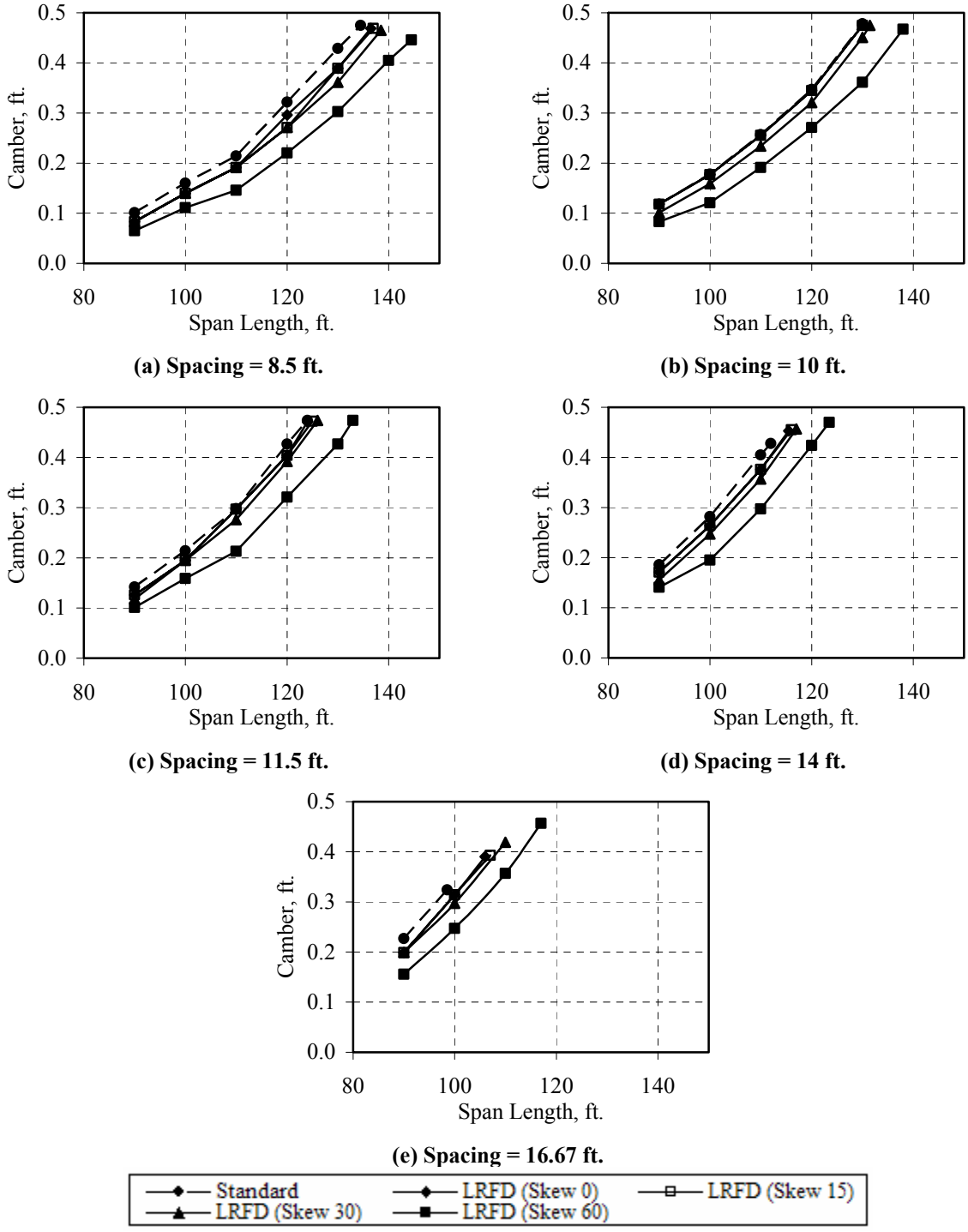


**(a) Spacing = 8.5 ft.**

**(b) Spacing = 10 ft.**

**(c) Spacing = 11.5 ft.**

**(d) Spacing = 14 ft.**

**(e) Spacing = 16.67 ft.**

**Figure A.11 Comparison of Camber (Strand Diameter 0.6 in.)**

# APPENDIX B

# DETAILED DESIGN EXAMPLES FOR INTERIOR TEXAS U54 PRESTRESSED CONCRETE BRIDGE GIRDER DESIGN USING AASHTO STANDARD AND LRFD SPECIFICATIONS

# Table of Contents

## B.1 Interior Texas U54 Prestressed Concrete Bridge Girder Design using AASHTO Standard Specifications

### *B.1.1 INTRODUCTION*

**Following is a detailed design example showing sample calculations for design of a typical interior Texas precast, prestressed concrete U54 girder supporting a single span bridge. The design is based on the *AASHTO Standard Specifications for Highway Bridges* 17th Edition 2002. The recommendations provided by the TxDOT Bridge Design Manual (TxDOT 2001) are considered in the design. The number of strands and concrete strength at release and at service are optimized using the TxDOT methodology.**

### *B.1.2 DESIGN PARAMETERS*

The bridge considered for design example has a span length of 110 ft. (c/c abutment distance), a total width of 46 ft. and total roadway width of 44 ft. The bridge superstructure consists of four Texas U54 girders spaced 11.5 ft. center-to-center designed to act compositely with an 8 in. thick cast-in-place (CIP) concrete deck as shown in Figure B.1.2.1. The wearing surface thickness is 1.5 in., which includes the thickness of any future wearing surface. T501 type rails are considered in the design. AASHTO HS20 is the design live load. The relative humidity (RH) of 60 percent is considered in the design. The bridge cross-section is shown in Figure B.1.2.1.

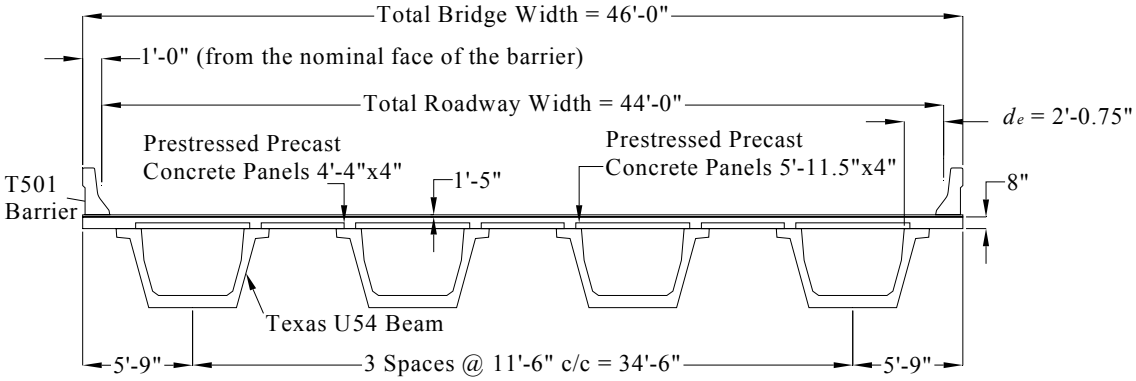


**Figure B.1.2.1 Bridge Cross-Section Details.**

The design span and overall girder length are based on the following calculations. Figure B.1.2.2 shows the girder end details for Texas U54 girders. It is clear that the distance between the centerline of the interior bent and end of the girder is 3 in.; and the distance between the centerline of the interior bent and the centerline of the bearings is 9.5 in.

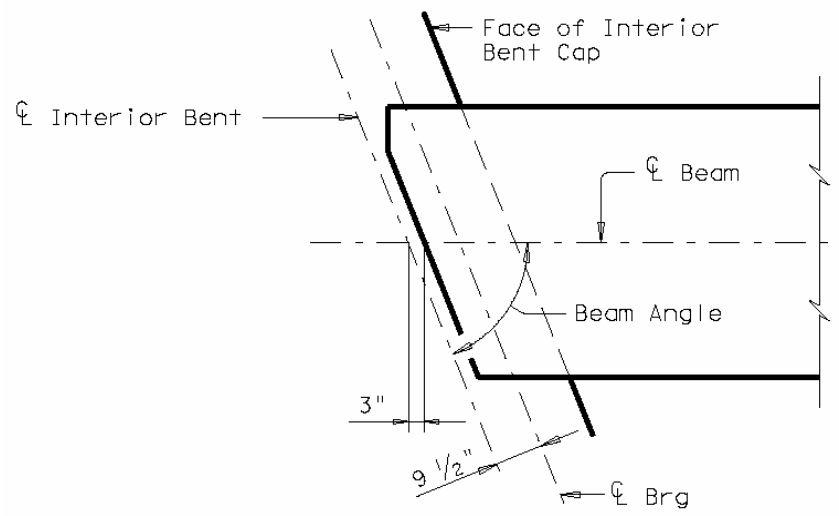


**Figure B.1.2.2 Girder End Detail for Texas U54 Girders (TxDOT 2001).**

Span length (c/c abutments) = 110 ft.–0 in.

From Figure B1.2.2.

Overall girder length = 110 ft. – 2(3 in.) = 109 ft.–6 in.

Design span = 110 ft. – 2(9.5 in.) = 108 ft.–5 in.

= 108.417 ft. (c/c of bearing)

## B.1.3 MATERIAL PROPERTIES

Cast-in-place slab:

Thickness $t_s$ = 8.0 in.

Concrete Strength at 28-days, $f_c'$ = 4000 psi

Unit weight of concrete = 150 pcf

*Wearing surface:*

Thickness of asphalt wearing surface (including any future wearing surfaces), $t_w$ = 1.5 in.

Unit weight of asphalt wearing surface = 140 pcf

[TxDOT recommendation]

Precast girders: Texas U54 girder

Concrete strength at release, $f'_{ci}$ = 4000 psi*

Concrete strength at 28 days, $f'_c$ = 5000 psi*

Concrete unit weight, $w_c$ = 150 pcf

(*This value is taken as an initial estimate and will be finalized based on most optimum design)

Prestressing strands: ½ in. diameter: seven wire low-relaxation

Area of one strand = 0.153 in.$^2$

Ultimate stress, $f'_s$ = 270,000 psi

Yield strength, $f_y$ = 0.9 $f'_s$ = 243,000 psi [STD Art. 9.1.2]

Initial pretensioning, $f_{si}$ = 0.75 $f'_s$

= 202,500 psi [STD Art. 9.15.1]

Modulus of elasticity, $E_s$ = 28,000 ksi [STD Art. 9.16.2.1.2]

Non-prestressed reinforcement:

Yield strength, $f_y$ = 60,000 psi

### *B.1.4 CROSS-SECTION PROPERTIES FOR A TYPICAL INTERIOR GIRDER*

Traffic barrier:

T501 type barrier weight = 326 plf /side

#### *B.1.4.1 Non-Composite Section*

The section properties of a Texas U54 girder as described in the TxDOT Bridge Design Manual (TxDOT 2001) are provided in Table B.1.2.1. The strand pattern and section geometry are shown in Figures B.1.2.3

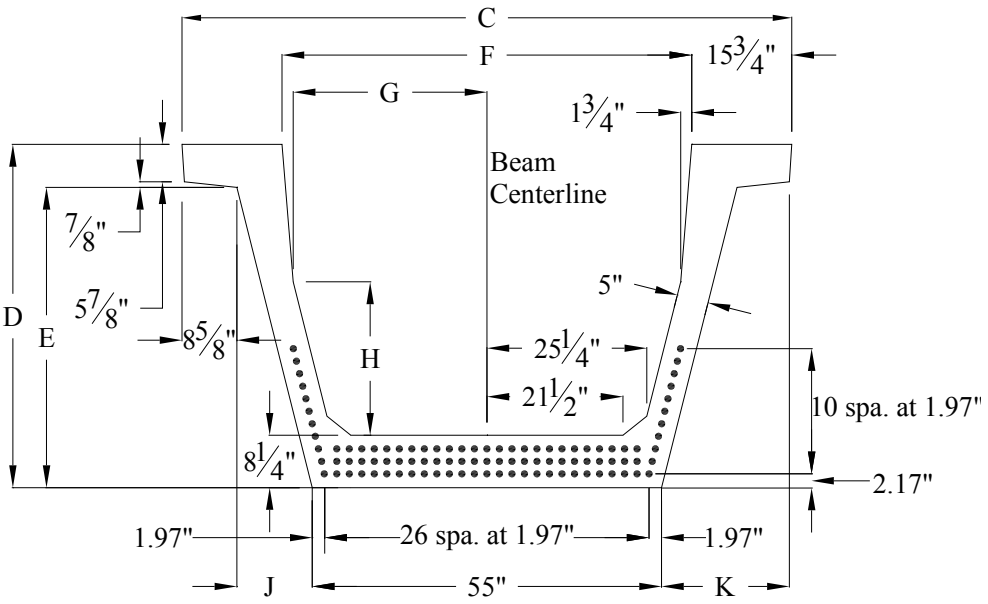


**Figure B.1.2.3 Typical Section and Strand Pattern of Texas U54 Girders (TxDOT 2001).**

**Table B.1.2.1 Section Properties of Texas U54 girders (Adapted from TxDOT Bridge Design Manual (TxDOT 2001)).**

| C | D | E | F | G | H | J | K | $y_t$ | $y_b$ | Area | $I$ | Weight |
|---|---|---|---|---|---|---|---|---|---|---|---|---|
| in. | in. | in. | in. | in. | in. | in. | in. | in. | in. | $in^2$. | $in^4$. | plf |
| 96 | 54 | 47.25 | 64.5 | 30.5 | 24.125 | 11.875 | 20.5 | 31.58 | 22.36 | 1120 | 403,020 | 1167 |

Note: Notations as used in Figure B.1.2.3.

where:

$I$ = Moment of inertia about the centroid of the non-composite precast girder, $in.^4$

$y_b$ = Distance from centroid to the extreme bottom fiber of the non-composite precast girder, in.

$y_t$ = Distance from centroid to the extreme top fiber of the non-composite precast girder, in.

$S_b$ = Section modulus referenced to the extreme bottom fiber of the non-composite precast girder, $in.^3$
$= I/ y_b = 403{,}020/22.36 = 18{,}024.15\ in.^3$

$S_t$ = Section modulus referenced to the extreme top fiber of the non-composite precast girder, in.$^3$
= $I/y_t$ = 403,020/31.58 = 12,761.88 in.$^3$

### B.1.4.2 Composite Section

[STD Art. 9.8.3]

### B.1.4.2.1 Effective Flange Width

The Standard Specifications do not give specific guidelines regarding the calculation of effective flange width for open box sections. Following the LRFD recommendations, the effective flange width is determined as though each web is an individual supporting element. Thus, the effective flange width will be calculated according to guidelines of the Standard Specifications Art. 9.8.3 as below and Figure B.1.4.1 shows the application of this assumption.

The effective web width of the precast girder is lesser of:

[STD Art. 9.8.3.1]

$b_e$ = Top flange width = 15.75 in.

or, $b_e$ = 6 × (flange thickness) + web thickness + fillets

= 6 × (5.875 in. + 0.875 in.) + 5.00 in. + 0 in. = 45.5 in.

The effective flange width is lesser of: [STD Art. 9.8.3.2]

- 1/4 effective girder span length = $\frac{108.417 \text{ ft. } (12 \text{ in./ft.})}{4}$
  = 325.25 in.
- 6 × (Slab thickness on each side of the effective web width) + effective girder web width = 6 × (8.0 in.+8.0 in.) + 15.75 in.
  = 111.75 in.
- One-half the clear distance on each side of the effective web width plus the effective web width:
  =0.5 × (4.0625 ft.+ 4.8125 ft.) + 1.3125 ft.

= 69 in. = 5.75 ft. (controls)

For the entire U-girder the effective flange width is 2 × (5.75 ft. × 12)
= 138 in. = 11.5 ft.

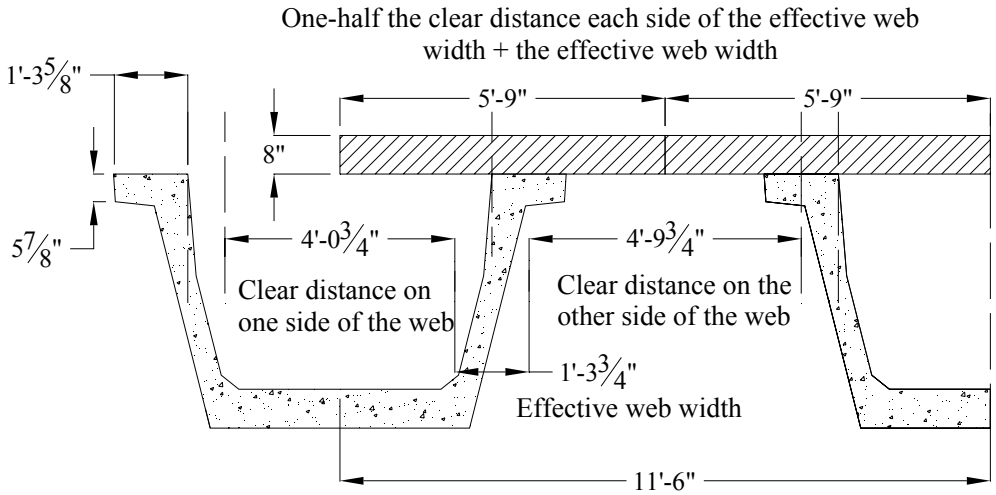


**Figure B.1.4.1 Effective Flange Width Calculation.**

***B.1.4.2.2 Modular Ratio Between Slab and Girder Concrete***

Following the TxDOT Design recommendation, the modular ratio between the slab and girder materials is taken as 1

$$n = \left( \frac{E_c \text{ for slab}}{E_c \text{ for beam}} \right) = 1$$

where:

$n$ = Modular ratio

$E_c$ = Modulus of elasticity of concrete (ksi)

***B.1.4.2.3 Transformed Section Properties***

Figure B.1.4.2 shows the composite section dimensions and Table B.1.2.2 shows the calculations for the transformed composite section.

Transformed flange width = $n$ × (effective flange width) = 1(138 in)

= 138 in.

Transformed Flange Area = $n$ × (effective flange width) ($t_s$)

= 1 (138 in.) (8 in.) = 1104 in.$^2$

**Table B.1.2.2 Properties of Composite Section.**

| | Transformed Area in.$^2$ | $y_b$ in. | $A\,y_b$ in. | $A(y_{bc} - y_b)^2$ in.$^4$ | I in.$^4$ | $I+A(y_{bc}- y_b)^2$ in.$^4$ |
|---|---|---|---|---|---|---|
| Girder | 1120 | 22.36 | 25,043.2 | 350,488.43 | 403,020 | 753,508.43 |
| Slab | 1104 | 58 | 64,032 | 355,711.56 | 5888 | 361,599.56 |
| ∑ | 2224 | | 89,075.2 | | | 1,115,107.99 |

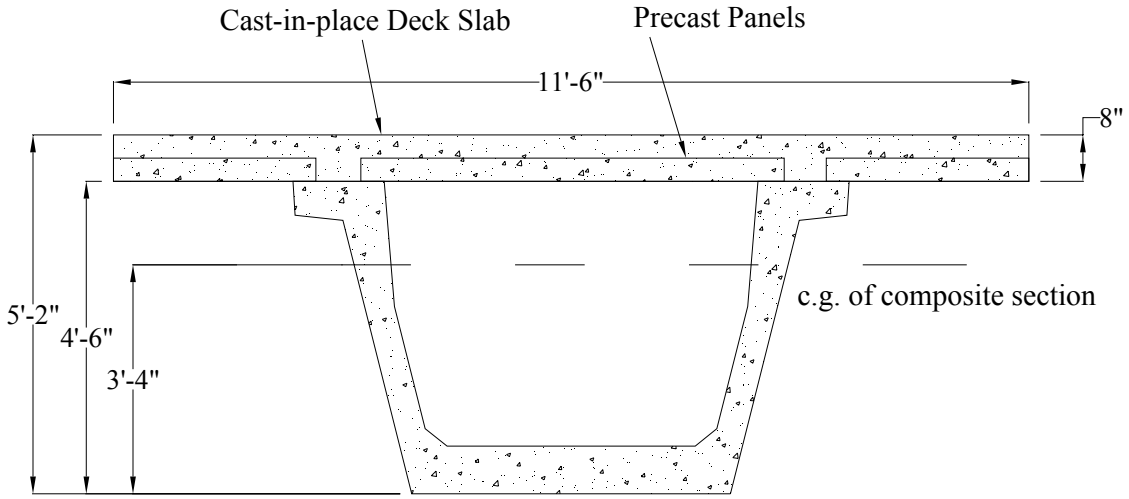


**Figure B.1.4.2 Composite Section.**

$A_c$ = Total area of composite section = 2224 in.$^2$

$h_c$ = Total height of composite section = 62 in.

$I_c$ = Moment of inertia about the centroid of the composite section = 1,115,107.99 in.$^4$

$y_{bc}$ = Distance from the centroid of the composite section to extreme bottom fiber of the precast girder = 89,075.2/ 2224 = 40.05 in.

$y_{tg}$ = Distance from the centroid of the composite section to extreme top fiber of the precast girder = 54 – 40.05 = 13.95 in.

$y_{tc}$ = Distance from the centroid of the composite section to extreme top fiber of the slab = 62 – 40.05 = 21.95 in.

$S_{bc}$ = Composite section modulus referenced to the extreme bottom fiber of the precast girder = $I_c/y_{bc}$ = 1,115,107.99 / 40.05 = 27,842.9in.$^3$

$S_{tg}$ = Composite section modulus referenced to the top fiber of the precast girder = $I_c/y_{tg}$ = 1,115,107.99 / 13.95 = 79,936.06 in.$^3$

$S_{tc}$ = Composite section modulus referenced to the top fiber of the slab = $I_c/y_{tc}$ = 1,115,107.99 / 21.95 = 50,802.19 in.$^3$

### B.1.5 SHEAR FORCES AND BENDING MOMENTS

#### B.1.5.1 Shear Forces and Bending Moments due to Dead Loads

##### B.1.5.1.1 Dead Loads

###### B.1.5.1.1.1 Due to Girder Self-weight

The self-weight of the girder and the weight of slab act on the non-composite simple span structure, while the weight of barriers, future wearing surface, and live load plus impact act on the composite simple span structure.

Self-weight of the girder = 1.167 kips/ft. [TxDOT Bridge Design Manual (TxDOT 2001)]

###### B.1.5.1.1.2 Due to Deck Slab

Weight of the CIP deck and precast panels on each girder

$$= (0.150 \text{ kcf})\left(\frac{8 \text{ in.}}{12 \text{ in./ft.}}\right)\left(\frac{138 \text{ in.}}{12 \text{ in./ft.}}\right)$$

$$= 1.15 \text{ kips/ft.}$$

###### B.1.5.1.1.3 Due to Diaphragm

The TxDOT Bridge Design Manual (TxDOT 2001) requires two interior diaphragms with U54 girders, located as close as 10 ft. from the midspan of the girder. Shear forces and bending moment values in the interior girder can be calculated using the following equations. The arrangement of diaphragms is shown in Figure B.1.5.1.

For $x = 0$ ft. – 44.21 ft.

$$V_x = 3 \text{ kips } M_x = 3x \text{ kips}$$

For $x = 44.21$ ft. – 54.21 ft.

$$V_x = 0 \text{ kips } M_x = 3x - 3(x - 44.21) \text{ kips}$$

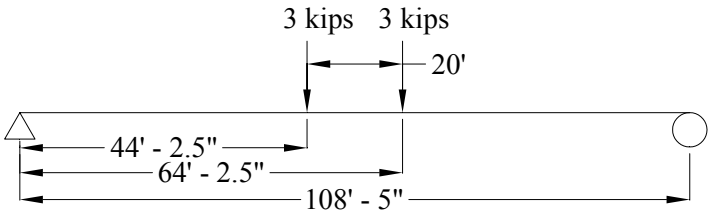


**Figure B.1.5.1 Location of Interior Diaphragms on a Simply Supported Bridge Girder.**

***B.1.5.1.1.4 Due to Haunch***

For U54 bridge girder design, TxDOT Bridge Design Manual (TxDOT 2001) accounts for haunches in designs that require special geometry and where the haunch will be large enough to have a significant impact on the overall girder. Because this study is for typical bridges, a haunch will not be included for U54 girders for composite properties of the section and additional dead load considerations.

***B.1.5.1.2 Superimposed Dead Load***

The TxDOT Bridge Design Manual (TxDOT 2001) recommends that 1/3 of the rail dead load should be used for an interior girder adjacent to the exterior girder.

Weight of T501 rails or barriers on each interior girder =

$$\left(\frac{326 \text{ plf}/1000}{3}\right)$$

= 0.109 kips/ft./interior girder

The dead loads placed on the composite structure are distributed equally among all girders [STD Art. 3.23.2.3.1.1 & TxDOT Bridge Design Manual (TxDOT 2001)].

$$\text{Weight of 1.5 in. wearing surface} = \frac{(0.140 \text{ pcf})\left(\frac{1.5 \text{ in.}}{12 \text{ in./ft.}}\right)(44 \text{ ft.})}{4 \text{ beams}}$$

= 0.193 kips/ft.

Total superimposed dead load = 0.109 + 0.193 = 0.302 kip/ft.

***B.1.5.1.3 Unfactored Shear Forces and Bending Moments***

Shear forces and bending moments in the girder due to dead loads, superimposed dead loads at every tenth of the span and at critical sections (midspan and $h/2$) are shown in this section. The bending moment ($M$) and shear force ($V$) due to dead loads and super imposed dead loads at any section at a distance $x$ are calculated using the following expressions.

$$M = 0.5\, w\, x\, (L - x)$$

$$V = w\, (0.5L - x)$$

Critical section for shear is located at a distance $h/2 = 62/2 = 31$ in.

= 2.583 ft.

The shear forces and bending moments due to dead loads and superimposed dead loads are shown in Tables B.1.5.1 and B.1.5.2.

**Table B.1.5.1 Shear Forces due to Dead Loads.**

| Distance | Section | Non-Composite Dead Load | | | Superimposed Dead Loads | | Total Dead Load Shear Force |
|---|---|---|---|---|---|---|---|
| | | Girder Weight | Slab Weight | Diaphram Weight | Barrier Weight | Wearing Surface Weight | |
| $x$ | $x/L$ | $V_g$ | $V_{slab}$ | $V_{dia}$ | $V_b$ | $V_{ws}$ | |
| ft. | | kips | kips | kips | kips | kips | kips |
| 0.000 | 0.000 | 63.26 | 62.34 | 3.00 | 5.91 | 10.46 | 144.97 |
| 2.583 | 0.024 | 60.25 | 59.37 | 3.00 | 5.63 | 9.96 | 138.21 |
| 10.842 | 0.100 | 50.61 | 49.87 | 3.00 | 4.73 | 8.37 | 116.58 |
| 21.683 | 0.200 | 37.96 | 37.40 | 3.00 | 3.55 | 6.28 | 88.19 |
| 32.525 | 0.300 | 25.30 | 24.94 | 3.00 | 2.36 | 4.18 | 59.78 |
| 43.367 | 0.400 | 12.65 | 12.47 | 3.00 | 1.18 | 2.09 | 31.39 |
| 54.209 | 0.500 | 0.00 | 0.00 | 0.00 | 0.00 | 0.00 | 0.00 |

**Table B.1.5.2 Bending Moments due to Dead loads.**

| Distance | Section | Non-Composite Dead Load | | | Superimposed Dead Loads | | Total Dead Load Bending Moment |
|---|---|---|---|---|---|---|---|
| | | Girder Weight | Slab Weight | Diaphram Weight | Barrier Weight | Wearing Surface Weight | |
| $x$ | $x/L$ | $M_g$ | $M_{slab}$ | $M_{dia}$ | $M_b$ | $M_{ws}$ | |
| ft. | | k-ft. | k-ft. | k-ft. | k-ft. | k-ft. | k-ft. |
| 0.000 | 0.000 | 0.00 | 0.00 | 0.00 | 0.00 | 0.00 | 0.00 |
| 2.583 | 0.024 | 159.51 | 157.19 | 7.75 | 14.90 | 26.38 | 365.73 |
| 10.842 | 0.100 | 617.29 | 608.30 | 32.53 | 57.66 | 102.09 | 1417.87 |
| 21.683 | 0.200 | 1097.36 | 1081.38 | 65.05 | 102.50 | 181.48 | 2527.77 |
| 32.525 | 0.300 | 1440.30 | 1419.32 | 97.58 | 134.53 | 238.20 | 3329.93 |
| 43.367 | 0.400 | 1646.07 | 1622.09 | 130.10 | 153.75 | 272.23 | 3824.24 |
| 54.209 | 0.500 | 1714.65 | 1689.67 | 132.63 | 160.15 | 283.57 | 3980.67 |

### *B.1.5.2 Shear Forces and Bending Moments due to Live Load*

#### *B.1.5.2.1 Due to Truck Load, $V_{LT}$ and $M_{LT}$*

[STD Art. 3.7.1.1]

The AASHTO Standard Specifications requires the live load to be taken as either HS20 truck loading or lane loading, whichever yields greater moments. The maximum shear force $V_T$ and bending moment $M_T$ due to

HS20 truck load on a per-lane-basis are calculated using the following equations as given in the *PCI Design Manual* (PCI 2003).

Maximum undistributed bending moment,
For $x/L = 0 – 0.333$

$$M_T = \frac{72(x)[(L - x) - 9.33]}{L}$$

For $x/L = 0.333 – 0.5$

$$M_T = \frac{72(x)[(L - x) - 4.67]}{L} - 112$$

Maximum undistributed shear force,
For $x/L = 0 – 0.5$

$$V_T = \frac{72[(L - x) - 9.33]}{L}$$

where:

$x$ = Distance from the center of the bearing to the section at which bending moment or shear force is calculated, ft.

$L$ = Design span length = 108.417 ft.

$M_T$ = Maximum undistributed bending moment due to HS-20 truck loading

$V_T$ = Maximum undistributed shear force due to HS-20 truck loading

The maximum undistributed bending moments and maximum undistributed shear forces due to HS-20 truck load are calculated at every tength of the span and at critical section for shear. The values are presented in Table B.1.5.3.

***B.1.5.2.2 Due to Lane Load, $V_L$ and $M_L$***

The maximum bending moments and shear forces due to uniformly distributed lane load of 0.64 kip/ft. are calculated using the following equations as given in the *PCI Design Manual* (PCI 2003).

Maximum undistributed bending moment,

$$M_L = \frac{P(x)(L - x)}{L} + 0.5(w)(x)(L - x)$$

Maximum undistributed Shear Force,

$$V_L = \frac{Q(L - x)}{L} + (w)(\frac{L}{2} - x)$$

where:

$x$ = Section at which bending moment or shear force is calculated

$L$ = Span length = 108.417 ft.

$P$ = Concentrated load for moment = 18 kips

$Q$ = Concentrated load for shear = 26 kips

$w$ = Uniform load per linear foot of load lane = 0.64 klf

The maximum undistributed bending moments and maximum undistributed shear forces due to HS-20 lane loading are calculated at every tenth of the span and at critical section for shear. The values are presented in Table B.1.5.3.

### *B1.5.3 Distributed Live Load Bending and Shear*

Distributed live load shear and bending moments are calculated by multiplying the distribution factor and the impact factor as follows

Distributed bending moment, $M_{LL+I}$

$$M_{LL+I} = (\text{bending moment per lane})\ (DF)\ (1+I)$$

Distributed Shear Force, $V_{LL+I}$

$$V_{LL+I} = (\text{shear force per lane})\ (DF)\ (1+I)$$

where:

$DF$ = Distribution factor

$I$ = Live load Impact factor

#### *B.1.5.3.1 Live Load Distribution Factor for a Typical Interior Girder*

As per recommendation of the TxDOT Bridge Design Manual (TxDOT 2001), the live load distribution factor for moment for a precast prestressed concrete U54 interior girder is given by the following expression.

$$DF_{mom} = \frac{S}{11} = \frac{11.5}{11} = 1.045 \text{ per truck/lane} \quad \text{[TxDOT 2001]}$$

where:

$S$ = Average interior girder spacing measured between girder centerlines (ft.)

The minimum value of $DF_{mom}$ is limited to 0.9.

For simplicity of calculation and because there is no significant difference, the distribution factor for moment is used also for shear as recommended by TxDOT Bridge Design Manual (TxDOT 2001)

The maximum distributed bending moments and maximum distributed shear forces due to HS-20 truck and HS-20 lane loading are calculated at every tenth of the span and at critical section for shear. The values are presented in Table B.1.5.3.

***B.1.5.3.2 Live Load Impact Factor***

The live load impact factor is given by the following expression

$$I = \frac{50}{L + 125}$$

where:

$I$ = Impact fraction to a maximum of 30 percent

$L$ = Span length (ft.) = 108.417 ft.

$$I = \frac{50}{108.417 + 125} = 0.214$$

Impact for shear varies along the span according to the location of the truck but the impact factor computed above is used for simplicity

**Table B.1.5.3 Shear Forces and Bending Moments due to Live loads.**

| Distance | Section | Live Load + Impact | | | | | | | |
|---|---|---|---|---|---|---|---|---|---|
| | | HS 20 Truck Loading (controls) | | | | HS20 Lane Loading | | | |
| | | Undistributed | | Distributed | | Undistributed | | Distributed | |
| $x$ | $x/L$ | Shear | Moment | Shear | Moment | Shear | Moment | Shear | Moment |
| ft. | | kips | k-ft. | kips | k-ft. | kips | k-ft. | kips | k-ft. |
| 0.000 | 0.000 | 65.80 | 0.00 | 83.52 | 0.00 | 34.69 | 0.00 | 36.27 | 0.00 |
| 2.583 | 0.024 | 64.09 | 165.54 | 81.34 | 210.10 | 33.06 | 87.48 | 34.56 | 91.45 |
| 10.842 | 0.100 | 58.60 | 635.38 | 74.38 | 806.41 | 28.10 | 338.53 | 29.38 | 353.92 |
| 21.683 | 0.200 | 51.40 | 1114.60 | 65.24 | 1414.62 | 22.20 | 601.81 | 23.21 | 629.16 |
| 32.525 | 0.300 | 44.20 | 1437.73 | 56.10 | 1824.74 | 17.00 | 789.88 | 17.77 | 825.78 |
| 43.370 | 0.400 | 37.00 | 1626.98 | 46.96 | 2064.93 | 12.49 | 902.73 | 13.06 | 943.76 |
| 54.210 | 0.500 | 29.80 | 1671.37 | 37.83 | 2121.27 | 8.67 | 940.34 | 9.07 | 983.08 |

### *B.1.5.4 Load Combinations*

[STD Art. 3.22]

[STD Table 3.22.1A]

For service load design (Group I): 1.00 $D$ + 1.00($L$+$I$)

where:

$D$ = Dead load

$L$ = Live load

$I$ = Impact factor

[STD Table 3.22.1A]

For load factor design (Group I): 1.3[1.00$D$ + 1.67($L$+$I$)]

## *B.1.6 ESTIMATION OF REQUIRED PRESTRESS*

### *B.1.6.1 Service load Stresses at Midspan*

The preliminary estimate of the required prestress and number of strands is based on the stresses at midspan.

Bottom tensile stresses at midspan due to applied loads

$$f_b = \frac{M_g + M_S}{S_b} + \frac{M_{SDL} + M_{LL+I}}{S_{bc}}$$

Top tensile stresses at midspan due to applied loads

$$f_t = \frac{M_g + M_S}{S_t} + \frac{M_{SDL} + M_{LL+I}}{S_{tg}}$$

where:

$f_b$ = Concrete stress at the bottom fiber of the girder (ksi).

$f_t$ = Concrete stress at the top fiber of the girder (ksi).

$M_g$ = Unfactored bending moment due to girder self-weight (k-ft.).

$M_S$ = Unfactored bending moment due to slab, diaphragm weight (k-ft.).

$M_{SDL}$ = Unfactored bending moment due to super imposed dead load (k-ft.).

$M_{LL+I}$ = Factored bending moment due to super imposed dead load (k-ft.).

Substituting the bending moments and section modulus values, bottom tensile stress at mid span is:

$$f_b = \frac{(1714.64 + 1689.66 + 132.63)(12)}{18024.15} + \frac{(443.72 + 2121.27)(12)}{27842.9}$$
$$= 3.46 \text{ ksi}$$

$$f_t = \frac{(1714.64 + 1689.66 + 132.63)(12)}{12761.88} + \frac{(443.72 + 2121.27)(12)}{79936.06}$$
$$= 3.71 \text{ ksi}$$

At service load conditions, allowable tensile stress is

### *B.1.6.2 Allowable Stress Limit*

$$F_b = 6\sqrt{f'_c} = 6\sqrt{5000}\left(\frac{1}{1000}\right) = 0.424 \text{ ksi} \qquad \text{[STD Art. 9.15.2.2]}$$

Required precompressive stress in the bottom fiber after losses:

Bottom tensile stress – allowable tensile stress at final = $f_b - F_b$
= 3.46 – 0.424 = 3.036 ksi

### *B.1.6.3 Required Number of Strands*

Assuming the distance from the center of gravity of strands to the bottom fiber of the girder is equal to $y_{bs}$ = 2 in.

Strand eccentricity at midspan:

$$e_c = y_b - y_{bs} = 22.36 - 2 = 20.36 \text{ in.}$$

Bottom fiber stress due to prestress after losses:

$$f_b = \frac{P_{se}}{A} + \frac{P_{se}\, e_c}{S_b}$$

where:

$P_{se}$ = Effective pretension force after all losses

$$3.036 = \frac{P_{se}}{1120} + \frac{20.36\, P_{se}}{18024.15}$$

Solving for $P_{se}$ we get,

$P_{se}$ = 1501.148 kips

Assuming final losses = 20 percent of $f_{si}$

Assumed final losses = 0.2(202.5 ksi) = 40.5 ksi

The prestress force per strand after losses:

$P_{se}$ = (cross-sectional area of one strand) [$f_{si}$ – losses]

$P_{se}$ = 0.153(202.5 – 40.5] = 24.786 kips

Number of strands required = 1500.159/24.786 = 60.56

Try 62 – ½ in. diameter, 270 ksi strands

Strand eccentricity at midspan after strand arrangement

$$e_c = 22.36 - \frac{27(2.17)+27(4.14)+8(6.11)}{62} = 18.934 \text{ in.}$$

$P_{se}$ = 62(24.786) = 1536.732 kips

$$f_b = \frac{1536.732}{1120} + \frac{18.934(1536.732)}{18024.15}$$

$$= 1.372 + 1.614 = 2.986 \text{ ksi} < f_b \text{ reqd.} = 3.034 \text{ ksi}$$

Try 64 – ½ in. diameter, 270 ksi strands

Strand eccentricity at midspan after strand arrangement

$$e_c = 22.36 - \frac{27(2.17)+27(4.14)+10(6.11)}{64} = 18.743 \text{ in.}$$

$P_{se}$ = 64(24.786) = 1586.304 kips

$$f_b = \frac{1586.304}{1120} + \frac{18.743(1586.304\ )}{18024.15}$$

$$= 1.416 + 1.650 = 3.066 \text{ ksi} > f_b \text{ reqd.} = 3.036 \text{ ksi}$$

Therefore, use 64 strands

| Number of Strands | Distance from bottom (in.) |
|---|---|
| 27 | 2.17 |
| 27 | 4.14 |
| 10 | 6.11 |

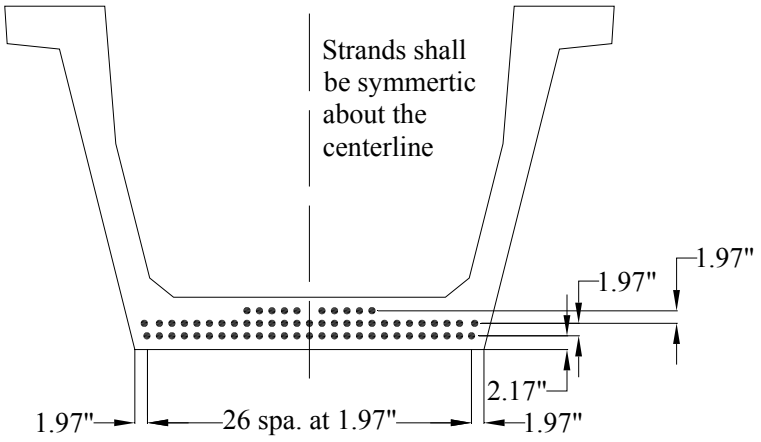


**Figure B.1.6.1 Initial Strand Pattern.**

## *B.1.7 PRESTRESS LOSSES*

[STD Art. 9.16.2]

Total prestress losses = $SH + ES + CR_C + CR_S$ [STD Eq. 9-3]

where:

$SH$ = Loss of prestress due to concrete shrinkage.

$EC$ = Loss of prestress due to elastic shortening.

$CR_C$ = Loss of prestress due to creep of concrete.

$CR_S$ = Loss of prestress due to relaxation of prestressing steel.

Number of strands = 64

A number of iterations will be performed to arrive at the optimum values of $f_c'$ and $f_{ci}'$

### B.1.7.1 Iteration 1

[STD Art. 9.16.2.1.1]

#### B.1.7.1.1 Shrinkage

$SH = 17{,}000 - 150\,RH$

where $RH$ is the relative humidity = 60 percent

$$SH = [17000 - 150(60)]\frac{1}{1000} = 8 \text{ ksi}$$

#### B.1.7.1.2 Elastic Shortening

$$ES = \frac{E_s}{E_{ci}} f_{cir}$$

where:

$f_{cir}$ = Average concrete stress at the center of gravity of the prestressing steel due to pretensioning force and dead load of girder immediately after transfer

$$= \frac{P_{si}}{A} + \frac{P_{si}\, e_c^{\,2}}{I} - \frac{(M_g\ )e_c}{I}$$

$P_{si}$ = Pretension force after allowing for the initial losses, assuming 8 percent initial losses = (number of strands)(area of each strand)[$0.92(0.75\, f_s')$]

= 64(0.153)(0.92)(0.75)(270) = 1824.25 kips

$M_g$ = Unfactored bending moment due to girder self weight

= 1714.64 k-ft.

$e_c$ = Eccentricity of the strand at the midspan = 18.743 in.

$$f_{cir} = \frac{1824.25}{1120} + \frac{1824.25\ (18.743)^2}{403020} - \frac{1714.64(12)(18.743)}{403020}$$

$$= 1.629 + 1.590 - 0.957 = 2.262 \text{ ksi}$$

Assuming $f_{ci}' = 4000$ psi

$$E_{ci} = (150)^{1.5}(33)\sqrt{4000}\ \ \frac{1}{1000} = 3834.254 \text{ ksi}$$ [STD Eq. 9-8]

$$ES = \frac{28000}{3834.254}\ (2.262) = 16.518 \text{ ksi}$$

#### B.1.7.1.3 Creep of Concrete

[STD Art. 9.16.2.1.3]

$CR_C = 12 f_{cir} - 7 f_{cds}$

where:

$f_{cds}$ = Concrete stress at the center of gravity of the prestressing steel due to all dead loads except the dead load present at the time the pretensioning force is applied (ksi)

$$= \frac{M_S\, e_c}{I} + \frac{M_{SDL}\,(y_{bc} - y_{bs})}{I_c}$$

where:

$M_S$ = Moment due to slab and diaphragm = 1822.29 k-ft.

$M_{SDL}$ = Superimposed dead load moment = 443.72 k-ft.

$y_{bc}$ = 40.05 in.

$y_{bs}$ = Distance from center of gravity of the strand at midspan to the bottom of the girder
= 22.36 – 18.743 = 3.617 in.

$I$ = Moment of inertia of the non-composite section
= 403,020 in.$^4$

$I_c$ = Moment of inertia of composite section
= 1,115,107.99 in.$^4$

$$f_{cds} = \frac{1822.29(12)(18.743)}{403020} + \frac{(443.72)(12)(40.05 - 3.617)}{1115107.99}$$

$$= 1.017 + 0.174 = 1.191 \text{ ksi}$$

$$CR_C = 12(2.262) - 7(1.191) = 18.807 \text{ ksi}$$

[STD Art. 9.16.2.1.4]

***B.1.7.1.4 Relaxation of Prestressing Steel***

For pretensioned members with 270 ksi low-relaxation strand

$CR_S = 5000 - 0.10\,ES - 0.05(SH + CR_C)$ [STD Eq. 9-10A]

$$= [5000 - 0.10(16518) - 0.05(8000 + 18807)]\left(\frac{1}{1000}\right)$$

$$= 2.008\text{ksi}$$

The PCI Bridge Design Manual (PCI 2003) considers only the elastic shortening loss in the calculation of total initial prestress loss. Whereas, the TxDOT Bridge Design Manual (TxDOT 2001)

recommends that 50 percent of the final steel relaxation loss shall also be considered for calculation of total initial prestress loss given as [elastic shortening loss + 0.50(total steel relaxation loss)]. Based on the TxDOT Bridge Design Manual (TxDOT 2001) recommendations, the initial prestress loss is calculated as follows.

$$\text{Initial prestress loss} = \frac{(ES + 0.5CRs)100}{0.75 f_s'}$$

$$= \frac{[16.518+0.5(2.008)]100}{0.75(270)}$$

= 8.653 percent > 8 percent (assumed initial prestress losses)

Therefore, next trial is required assuming 8.653 percent initial losses.

The change in initial prestress loss will not affect the prestress loss due to concrete shrinkage. Therefore, the next trials will involve updating the losses due to elastic shortening, steel relaxation and creep of concrete.

Loss in prestress due to elastic shortening

$$ES = \frac{E_s}{E_{ci}} f_{cir}$$

where:

$$f_{cir} = \frac{P_{si}}{A} + \frac{P_{si}\, e_c^2}{I} - \frac{(M_g)\, e_c}{I}$$

$P_{si}$ = Pretension force after allowing for the initial losses, assuming 8.653 percent initial losses = (number of strands)(area of each strand)[0.9135(0.75 $f_s'$ )]

= 64(0.153)(0.9135)(0.75)(270) = 1811.3 kips

$M_g$ = Unfactored bending moment due to girder self-weight = 1714.64 k-ft.

$e_c$ = Eccentricity of the strand at the midspan = 18.743 in.

$$f_{cir} = \frac{1811.3}{1120} + \frac{1811.3(18.743)^2}{403020} - \frac{1714.64(12)(18.743)}{403020}$$

= 1.617 + 1.579 – 0.957 = 2.239 ksi

Assuming $f_{ci}'$ = 4000 psi

$$E_{ci} = (150)^{1.5}(33)\sqrt{4000}\ \ \frac{1}{1000} = 3834.254 \text{ ksi}$$

$$ES = \frac{28000}{3834.254}(2.239) = 16.351 \text{ ksi}$$

Loss in prestress due to creep of concrete

$CR_C = 12f_{cir} - 7f_{cds}$

The value of $f_{cds}$ is independent of the initial prestressing force value and will be same as calculated B.1.7.1.3.

Therefore, $f_{cds} = 1.191$

$CR_C = 12(2.239) - 7(1.191) = 18.531$ ksi.

Loss in prestress due to relaxation of steel

$CR_S = 5000 - 0.10\,ES - 0.05(SH + CR_C)$

$$= [5000 - 0.10(16351) - 0.05(8000 + 18531)]\left(\frac{1}{1000}\right) = 2.038 \text{ ksi}$$

Initial prestress loss = $\dfrac{(ES + 0.5CRs)100}{0.75f_s'}$

$$= \frac{[16.351+0.5(2.038)]100}{0.75(270)}$$

= 8.578 percent < 8.653 percent (assumed initial prestress losses)

Therefore, next trial is required assuming 8.580 percent initial losses

Loss in prestress due to elastic shortening

$ES = \dfrac{E_s}{E_{ci}} f_{cir}$

where:

$$f_{cir} = \frac{P_{si}}{A} + \frac{P_{si}\,e_c^2}{I} - \frac{(M_g)\,e_c}{I}$$

$P_{si}$ = Pretension force after allowing for the initial losses, assuming 8.580 percent initial losses

= (number of strands)(area of each strand)[0.9142 (0.75 $f_s'$ )]

= 64(0.153)(0.9142)(0.75)(270) = 1812.75 kips

$$f_{cir} = \frac{1812.75}{1120} + \frac{1812.75(18.743)^2}{403020} - \frac{1714.64(12)(18.743)}{403020}$$

$= 1.619 + 1.580 - 0.957 = 2.242$ ksi

Assuming $f'_{ci} = 4000$ psi

$$E_{ci} = (150)^{1.5}(33)\sqrt{4000}\ \frac{1}{1000} = 3834.254 \text{ ksi}$$

$$ES = \frac{28000}{3834.254}\ (2.242) = 16.372 \text{ ksi}$$

Loss in prestress due to creep of concrete

$CR_C = 12f_{cir} - 7f_{cds}$

$f_{cds} = 1.191$

$CR_C = 12(2.242) - 7(1.191) = 18.567$ ksi.

Loss in prestress due to relaxation of steel

$CR_S = 5000 - 0.10\ ES - 0.05(SH + CR_C)$

$$= [5000 - 0.10(16372) - 0.05(8000 + 18567)]\left(\frac{1}{1000}\right) = 2.034 \text{ ksi}$$

Initial prestress loss = $\frac{(ES + 0.5CRs)100}{0.75f'_s}$

$= \frac{[16.372+0.5(2.034)]100}{0.75(270)} = 8.587$ percent ≈ 8.580 percent (assumed initial prestress losses)

***B.1.7.1.5 Total Losses at Transfer***

Total initial losses = $(ES + 0.5CR_S) = [16.372+0.5(2.034)] = 17.389$ ksi

$f_{si}$ = Effective initial prestress = 202.5 – 17.389 = 185.111 ksi

$P_{si}$ = Effective pretension force after allowing for the initial losses

= 64(0.153)(185.111) = 1812.607 kips

***B.1.7.1.6 Total Losses at Service Loads***

$SH$ = 8 ksi

$ES$ = 16.372 ksi

$CR_C$ = 18.587 ksi

$CR_S$ = 2.034 ksi

Total final losses = 8 + 16.372 + 18.587 + 2.034 = 44.973 ksi

or $\frac{44.973(100)}{0.75(270)}$ =22.21 percent

$f_{se}$ = Effective final prestress = 0.75(270) – 44.973 = 157.527 ksi

$P_{se}$ = 64(0.153)( 157.527) = 1542.504 kips

***B.1.7.1.7 Final Stresses at Midspan***

Final stress in the bottom fiber at midspan:

$$f_{bf} = \frac{P_{se}}{A} + \frac{P_{se}\, e_c}{S_b} - f_b$$

$$f_{bf} = \frac{1542.504}{1120} + \frac{18.743(1542.504)}{18024.15} - 3.458$$

= 1.334 + 1.554 - 3.458 = -0.57 ksi > -0.424 ksi

Therefore, try 66 strands

$$e_c = 22.36 - \frac{27(2.17) + 27(4.14) + 12(6.11)}{66} = 18.67 \text{ in.}$$

$P_{se}$ = 66(0.153)(157.527) = 1590.708 kips

$$f_{bf} = \frac{1590.708}{1120} + \frac{18.67(1590.708)}{18024.15} - 3.458$$

= 1.42 + 1.648 - 3.458 = -0.39 ksi < -0.424 ksi

Therefore, use 66 strands

Final concrete stress at the top fiber of the girder at midspan,

$$f_{tf} = \frac{P_{se}}{A} - \frac{P_{se}\, e_c}{S_t} + f_t = \frac{1590.708}{1120} - \frac{18.67(1590.708)}{12761.88} + 3.71$$

= 1.42 – 2.327 + 3.71 = 2. 803 ksi

***B.1.7.1.8 Initial Stresses at End***

Initial concrete stress at top fiber of the girder at girder end

$$f_{ti} = \frac{P_{si}}{A} - \frac{P_{si}\, e_c}{S_t} + \frac{M_g}{S_t}$$

where:

$P_{si}$ = 66(0.153)(185.111) = 1869.251 kips

$M_g$ = Moment due to girder self weight at girder end = 0 k-ft.

$$f_{ti} = \frac{1869.251}{1120} - \frac{18.67(1869.251)}{12761.88}$$

$$= 1.669 - 2.735 = -1.066 \text{ ksi}$$

Tension stress limit at transfer is $7.5\sqrt{f'_{ci}}$

Therefore, $f'_{ci\ \text{reqd.}} = \left(\frac{1066}{7.5}\right)^2 = 20{,}202$ psi

Initial concrete stress at bottom fiber of the girder at girder end

$$f_{bi} = \frac{P_{si}}{A} + \frac{P_{si}\, e_c}{S_b} - \frac{M_g}{S_b}$$

$$f_{bi} = \frac{1869.251}{1120} + \frac{18.67(1869.251)}{18024.15}$$

$$= 1.669 + 1.936 = 3.605 \text{ ksi}$$

Compression stress limit at transfer is $0.6\, f'_{ci}$

Therefore, $f'_{ci\ \text{reqd.}} = \frac{3605}{0.6} = 6009$ psi

***B.1.7.1.9 Debonding of Strands and Debonding Length***

The calculation for initial stresses at the girder end show that preliminary estimate of $f'_{ci} = 4000$ psi is not adequate to keep the tensile and compressive stresses at transfer within allowable stress limits as per STD Art. 9.15.2.1. Therefore, debonding of strands is required to keep the stresses within allowable stress limits.

In order to be consistent with the TxDOT design procedures, the debonding of strands is carried out in accordance with the procedure followed in PSTRS14 (TxDOT 2004). Two strands are debonded at a time at each section located at uniform increments of 3 ft. along the span length, beginning at the end of the girder. The debonding is started at the end of the girder because due to relatively higher initial stresses at the end, greater number of strands are required to be

debonded, and debonding requirement, in terms of number of strands, reduces as the section moves away from the end of the girder. In order to make the most efficient use of debonding due to greater eccentricities in the lower rows, the debonding at each section begins at the bottom most row and goes up. Debonding at a particular section will continue until the initial stresses are within the allowable stress limits or until a debonding limit is reached. When the debonding limit is reached, the initial concrete strength is increased and the design cycles to convergence. As per TxDOT Bridge Design Manual (TxDOT 2001) the limits of debonding for partially debonded strands are described as follows:

6. Maximum percentage of debonded strands per row and per section
    a. TxDOT Bridge Design Manual (TxDOT 2001) recommends a maximum percentage of debonded strands per row should not exceed 75 percent.
    b. TxDOT Bridge Design Manual (TxDOT 2001) recommends a maximum percentage of debonded strands per section should not exceed 75 percent.

7. Maximum Length of debonding
    a. TxDOT Bridge Design Manual (TxDOT 2001) recommends to use the maximum debonding length chosen to be lesser of the following:
        i. 15 ft.
        ii. 0.2 times the span length, or
        iii. half the span length minus the maximum development length as specified in the 1996 AASHTO Standard Specifications for Highway Bridges, Section 9.28.

#### *B.1.7.1.10 Maximum Debonding Length*

As per TxDOT Bridge Design Manual (TxDOT 2001), the maximum debonding length is the lesser of the following:

a. 15 ft.

b. 0.2 ($L$), or

c. 0.5 ($L$) - $l_d$

where, $l_d$ is the development length calculated based on AASHTO STD Art. 9.28.1 as follows:

$$l_d \geq \left( f_{su}^* - \frac{2}{3} f_{se} \right) D \qquad \text{[STD Eq. 9.42]}$$

where:

$l_d$ = Development length (in.)

$f_{se}$ = Effective stress in the prestressing steel after losses

= 157.527 (ksi)

$D$ = Nominal strand diameter = 0.5 in.

$f_{su}^*$ = Average stress in the prestressing steel at the ultimate load (ksi)

$$f_{su}^* = f_s' \left[ 1 - \left( \frac{\gamma^*}{\beta_1} \right) \left( \frac{\rho^* f_s'}{f_c'} \right) \right] \qquad \text{[STD Eq. 9.17]}$$

where:

$f_s'$ = Ultimate stress of prestressing steel (ksi)

$\gamma^*$ = Factor type of prestressing steel

= 0.28 for low-relaxation steel

$f_c'$ = Compressive strength of concrete at 28 days (psi)

$\rho^* = \frac{A_s^*}{bd}$ = ratio of prestressing steel

$$= \frac{0.153 \times 66}{138 \times 8.67 \times 12} = 0.00033$$

$\beta_1$ = Factor for concrete strength

$$\beta_1 = 0.85 - 0.05 \frac{(f_c' - 4000)}{1000} \qquad \text{[STD Art. 8.16.2.7]}$$

$$= 0.85 - 0.05 \frac{(5000 - 4000)}{1000} = 0.80$$

$$f_{su}^* = 270 \left[ 1 - \left( \frac{0.28}{0.80} \right) \left( \frac{0.00033 \times 270}{5} \right) \right] = 268.32 \text{ ksi}$$

The development length is calculated as,

$$l_d \geq \left( 268.32 - \frac{2}{3} 157.527 \right) \times 0.5$$

$l_d$ = 6.8 ft.

As per STD Art. 9.28.3, the development length calculated above should be doubled.

$l_d$ = 13.6 ft.

Hence, the debonding length is the lesser of the following,

a. 15 ft.

b. 0.2 × 108.417 = 21.68 ft.

c. 0.5 × 108.417 - 13.6 = 40.6 ft.

Hence, the maximum debonding length to which the strands can be debonded is 15 ft.

**Table B.1.7.1 Calculation of Initial Stresses at Extreme Fibers and Corresponding Required Initial Concrete Strengths.**

| | Location of the Debonding Section (ft. from end) | | | | | | |
|---|---|---|---|---|---|---|---|
| | End | 3 | 6 | 9 | 12 | 15 | Midspan |
| Row No. 1 (bottom row) | 27 | 27 | 27 | 27 | 27 | 27 | 27 |
| Row No. 2 | 27 | 27 | 27 | 27 | 27 | 27 | 27 |
| Row No. 3 | 12 | 12 | 12 | 12 | 12 | 12 | 12 |
| No. of Strands | 66 | 66 | 66 | 66 | 66 | 66 | 66 |
| $M_g$ (k-ft.) | 0 | 185 | 359 | 522 | 675 | 818 | 1715 |
| $P_{si}$ (kips) | 1869.25 | 1869.25 | 1869.25 | 1869.25 | 1869.25 | 1869.25 | 1869.25 |
| $e_c$ (in.) | 18.67 | 18.67 | 18.67 | 18.67 | 18.67 | 18.67 | 18.67 |
| Top Fiber Stresses (ksi) | -1.066 | -0.892 | -0.728 | -0.575 | -0.431 | -0.297 | 0.547 |
| Corresponding $f'_{ci\ reqd}$ (psi) | 20202 | 14145 | 9422 | 5878 | 3302 | 1568 | 912 |
| Bottom Fiber Stresses (ksi) | 3.605 | 3.482 | 3.366 | 3.258 | 3.156 | 3.061 | 2.464 |
| Corresponding $f'_{ci\ reqd}$ (psi) | 6009 | 5804 | 5611 | 5429 | 5260 | 5101 | 4106 |

In Table B.1.7.1, the calculation of initial stresses at the extreme fibers and corresponding requirement of $f'_{ci}$ suggests that the preliminary estimate of $f'_{ci}$ to be 4000 psi is inadequate. Since the strands can not be debonded beyond the section located at 15 ft. from the end of the girder, $f'_{ci}$ is increased from 4000 psi to 5101 psi and at all other sections where debonding can be done, the strands are debonded to bring the required $f'_{ci}$ below 5101 psi. Table B.1.7.2 shows the debonding schedule based on the procedure described earlier.

**Table B.1.7.2 Debonding of Strands at Each Section.**

| | Location of the Debonding Section (ft. from end) | | | | | | |
|---|---|---|---|---|---|---|---|
| | End | 3 | 6 | 9 | 12 | 15 | Midspan |
| Row No. 1 (bottom row) | 7 | 7 | 15 | 23 | 25 | 27 | 27 |
| Row No. 2 | 17 | 27 | 27 | 27 | 27 | 27 | 27 |
| Row No. 3 | 12 | 12 | 12 | 12 | 12 | 12 | 12 |
| No. of Strands | 36 | 46 | 54 | 62 | 64 | 66 | 66 |
| $M_g$ (k-ft.) | 0 | 185 | 359 | 522 | 675 | 818 | 1715 |
| $P_{si}$ (kips) | 1019.59 | 1302.81 | 1529.39 | 1755.96 | 1812.61 | 1869.25 | 1869.25 |
| $e_c$ (in.) | 17.95 | 18.01 | 18.33 | 18.57 | 18.62 | 18.67 | 18.67 |
| Top Fiber Stresses (ksi) | -0.524 | -0.502 | -0.494 | -0.496 | -0.391 | -0.297 | 0.547 |
| Corresponding $f'_{ci\ reqd}$ (psi) | 4881 | 4480 | 4338 | 4374 | 2718 | 1568 | 912 |
| Bottom Fiber Stresses (ksi) | 1.926 | 2.342 | 2.682 | 3.029 | 3.041 | 3.061 | 2.464 |
| Corresponding $f'_{ci\ reqd}$ (psi) | 3210 | 3904 | 4470 | 5049 | 5069 | 5101 | 4106 |

### *B.1.7.2 Iteration 2*

Following the procedure in iteration 1 another iteration is required to calculate prestress losses based on the new value of $f'_{ci}$= 5101 psi. The results of this second iteration are shown in Table B.1.7.3.

**Table B.1.7.3 Results of Iteration No. 2.**

| | Trial #1 | Trial # 2 | Units |
|---|---|---|---|
| No. of Strands | 66 | 66 | |
| $e_c$ | 18.67 | 18.67 | in. |
| $SR$ | 8 | 8 | ksi |
| Assumed Initial Prestress Loss | 8.587 | 7.967 | percent |
| $P_{si}$ | 1869.19 | 1881.87 | kips |
| $M_g$ | 1714.65 | 1714.65 | k - ft. |
| $f_{cir}$ | 2.332 | 2.354 | ksi |
| $f_{ci}$ | 5101 | 5101 | psi |
| $E_{ci}$ | 4329.91 | 4329.91 | ksi |
| $ES$ | 15.08 | 15.22 | ksi |
| $f_{cds}$ | 1.187 | 1.187 | ksi |
| $CRc$ | 19.68 | 19.94 | ksi |
| $CRs$ | 2.11 | 2.08 | ksi |
| Calculated Initial Prestress Loss | 7.967 | 8.025 | percent |
| Total Prestress Loss | 44.86 | 45.24 | ksi |

### *B.1.7.2.1 Total Losses at Transfer*

Total Initial losses = $(ES + 0.5CRs)$ = [15.21 + 0.5(2.08)]= 16.25 ksi

$f_{si}$ = Effective initial prestress = 202.5 – 16.25 = 186.248 ksi

$P_{si}$ = Effective pretension force after allowing for the initial losses

$P_{si}$ = 66(0.153)(186.248) = 1880.732 kips

***B.1.7.2.2 Total Losses at Service Loads***

$SH$ = 8 ksi

$ES$ = 15.21 ksi

$CR_C$ = 19.92 ksi

$CR_S$ = 2.08 ksi

Total final losses = 8 + 15.21 + 19.92 + 2.08 = 45.21 ksi

or $\frac{45.21(100)}{0.75(270)}$ =22.32 percent

$f_{se}$ = Effective final prestress = 0.75(270) – 45.21 = 157.29 ksi

$P_{se}$ = 66(0.153)(157.29) = 1588.34 kips

***B.1.7.2.3 Final Stresses at Midspan***

Top fiber stress in concrete at midspan at service loads

$$f_{tf} = \frac{P_{se}}{A} - \frac{P_{se}\, e_c}{S_t} + f_t = \frac{1588.34}{1120} - \frac{18.67(1588.34)}{12761.88} + 3.71$$

$$= 1.418 - 2.323 + 3.71 = 2.805 \text{ ksi}$$

Allowable compression stress limit for all load combinations = 0.6 $f'_c$

$f'_{c\ reqd}$ = 2805/0.6 = 4675 psi

Top fiber stress in concrete at midspan due to effective prestress + permanent dead loads

$$f_{tf} = \frac{P_{se}}{A} - \frac{P_{se}\, e_c}{S_t} + \frac{M_g + M_S}{S_t} + \frac{M_{SDL}}{S_{tg}}$$

$$= \frac{1588.34}{1120} - \frac{18.67(1588.34)}{12761.88} + \frac{(1714.64 + 1822.29)(12)}{12761.88} + \frac{443.72(12)}{79936.06}$$

$$= 1.418 - 2.323 + 3.326 + 0.067 = 2.49 \text{ ksi}$$

Allowable compression stress limit for effective pretension force + permanent dead loads = 0.4 $f'_c$

$f'_{c\ reqd}$ = 2490/0.4 = 6225 psi (controls)

Top fiber stress in concrete at midspan due to live load

+ 0.5 (effective prestress + dead loads)

$$f_{tf} = \frac{M_{LL+I}}{S_{tg}} + 0.5\left(\frac{P_{se}}{A} - \frac{P_{se}\, e_c}{S_t} + \frac{M_g + M_S}{S_t} + \frac{M_{SDL}}{S_{tg}}\right)$$

$$= \frac{2121.27(12)}{79936.06} + 0.5\left(\frac{1588.34}{1120} - \frac{18.67(1588.34)}{12761.88} + \frac{(1714.64 + 1822.29)(12)}{12761.88} + \frac{443.72(12)}{79936.06}\right)$$

= 0.318 + 0.5(1.418 – 2.323 + 3.326 + 0.067) = 1.629 ksi

Allowable compression stress limit for effective pretension force + permanent dead loads = 0.4 $f'_c$

$f'_{c\ reqd}$ = 1562/0.4 = 3905 psi

Bottom fiber stress in concrete at midspan at service load

$$f_{bf} = \frac{P_{se}}{A} + \frac{P_{se}\, e_c}{S_b} - f_b$$

$$f_{bf} = \frac{1588.34}{1120} + \frac{18.67(1588.34)}{18024.15} - 3.46$$

= 1.418 + 1.633 – 3.46 = -0.397 ksi

Allowable tension in concrete = $6\sqrt{f'_c}$

$$f'_{c\ reqd} = \left(\frac{3970}{6}\right)^2 = 4366 \text{ psi}$$

***B.1.7.2.4 Initial Stresses at Debonding Locations***

With the same number of debonded strands as was determined in the previous iteration, the top and bottom fiber stresses with their corresponding initial concrete strengths are calculated. It can be observed that at 15 ft. location, the $f'_{ci}$ value is updated to 5138 psi. The results are shown in Table B.1.7.4.

**Table B.1.7.4 Debonding of Strands at Each Section.**

| | Location of the Debonding Section (ft. from end) | | | | | | |
|---|---|---|---|---|---|---|---|
| | 0 | 3 | 6 | 9 | 12 | 15 | 54.2 |
| Row No. 1 (bottom row) | 7 | 7 | 15 | 23 | 25 | 27 | 27 |
| Row No. 2 | 17 | 27 | 27 | 27 | 27 | 27 | 27 |
| Row No. 3 | 12 | 12 | 12 | 12 | 12 | 12 | 12 |
| No. of Strands | 36 | 46 | 54 | 62 | 64 | 66 | 66 |
| $M_g$ (k-ft.) | 0 | 185 | 359 | 522 | 675 | 818 | 1715 |
| $P_{si}$ (kips) | 1025.85 | 1310.81 | 1538.78 | 1766.75 | 1823.74 | 1880.73 | 1880.73 |
| $e_c$ (in.) | 17.95 | 18.01 | 18.33 | 18.57 | 18.62 | 18.67 | 18.67 |
| Top Fiber Stresses (ksi) | -0.527 | -0.506 | -0.499 | -0.502 | -0.398 | -0.303 | 0.540 |
| Corresponding $f'_{ci\ reqd}$ (psi) | 4937 | 4552 | 4427 | 4480 | 2816 | 1632 | 900 |
| Bottom Fiber Stresses (ksi) | 1.938 | 2.357 | 2.700 | 3.050 | 3.063 | 3.083 | 2.486 |
| Corresponding $f'_{ci\ reqd}$ (psi) | 3229 | 3929 | 4500 | 5084 | 5105 | 5138 | 4143 |

### *B.1.7.3 Iteration 3*

Following the procedure in iteration 1, a third iteration is required to calculate prestress losses based on the new value of $f'_{ci}$ = 5138 psi. The results of this second iteration are shown in Table B.1.7.5

**Table B.1.7.5 Results of Iteration No. 3.**

| | Trial #1 | Trial # 2 | Units |
|---|---|---|---|
| No. of Strands | 66 | 66 | |
| $e_c$ | 18.67 | 18.67 | in. |
| $SR$ | 8 | 8 | ksi |
| Assumed Initial Prestress Loss | 8.025 | 8.000 | percent |
| $P_{si}$ | 1880.85 | 1881.26 | kips |
| $M_g$ | 1714.65 | 1714.65 | k - ft. |
| $f_{cir}$ | 2.352 | 2.354 | ksi |
| $f_{ci}$ | 5138 | 5138 | psi |
| $E_{ci}$ | 4346 | 4346 | ksi |
| $ES$ | 15.16 | 15.17 | ksi |
| $f_{cds}$ | 1.187 | 1.187 | ksi |
| $CRc$ | 19.92 | 19.94 | ksi |
| $CRs$ | 2.09 | 2.09 | ksi |
| Calculated Initial Prestress Loss | 8.000 | 8.005 | percent |
| Total Prestress Loss | 45.16 | 45.19 | ksi |

### *B.1.7.3.1 Total Losses at Transfer*

Total initial losses = $(ES + 0.5CRs)$ = [15.17+0.5(2.09)]= 16.211 ksi

$f_{si}$ = Effective initial prestress = 202.5 – 16.211 = 186.289 ksi

$P_{si}$ = Effective pretension force after allowing for the initial losses

= 66(0.153)(186.289) = 1881.146 kips

***B.1.7.3.2 Total Losses at Service Loads***

$SH$ = 8 ksi

$ES$ = 15.17 ksi

$CR_C$ = 19.94 ksi

$CR_S$ = 2.09 ksi

Total final losses = 8 + 15.17 + 19.94 + 2.09 = 45.193 ksi

or $\frac{45.193\ (100)}{0.75(270)}$ =22.32 percent

$f_{se}$ = Effective final prestress = 0.75(270) – 45.193 = 157.307 ksi

$P_{se}$ = 66(0.153)( 157.307) = 1588.486 kips

***B.1.7.3.3 Final Stresses at Midspan***

Top fiber stress in concrete at midspan at service loads

$$f_{tf} = \frac{P_{se}}{A} - \frac{P_{se}\ e_c}{S_t} + f_t = \frac{1588.486}{1120} - \frac{18.67(1588.486)}{12761.88} + 3.71$$

= 1.418 – 2.323 + 3.71 = 2.805 ksi

Allowable compression stress limit for all load combinations = 0.6 $f'_c$

$f'_{c\ reqd.}$ = 2805/0.6 = 4675 psi

Top fiber stress in concrete at midspan due to effective prestress + permanent dead loads

$$f_{tf} = \frac{P_{se}}{A} - \frac{P_{se}\ e_c}{S_t} + \frac{M_g\ +\ M_S}{S_t} + \frac{M_{SDL}}{S_{tg}}$$

$$= \frac{1588.486}{1120} - \frac{18.67(1588.486)}{12761.88} + \frac{(1714.64 + 1822.29)(12)}{12761.88} + \frac{443.72(12)}{79936.06}$$

= 1.418 – 2.323 + 3.326 + 0.067 = 2.49 ksi

Allowable compression stress limit for effective pretension force + permanent dead loads = 0.4 $f'_c$

$f'_{c\ reqd}$ = 2490/0.4 = 6225 psi (controls)

Top fiber stress in concrete at midspan due to live load + 0.5(effective prestress + dead loads)

$$f_{tf} = \frac{M_{LL+I}}{S_{tg}} + 0.5\left(\frac{P_{se}}{A} - \frac{P_{se}\, e_c}{S_t} + \frac{M_g + M_S}{S_t} + \frac{M_{SDL}}{S_{tg}}\right)$$

$$= \frac{2121.27(12)}{79936.06} + 0.5\left(\frac{1588.486}{1120} - \frac{18.67(1588.486)}{12761.88} + \frac{(1714.64 + 1822.29)(12)}{12761.88} + \frac{443.72(12)}{79936.06}\right)$$

$= 0.318 + 0.5(1.418 – 2.323 + 3.326 + 0.067) = 1.562$ ksi

Allowable compression stress limit for effective pretension force + permanent dead loads = $0.4\, f'_c$

$f'_{c\ reqd.} = 1562/0.4 = 3905$ psi

Bottom fiber stress in concrete at midspan at service load

$$f_{bf} = \frac{P_{se}}{A} + \frac{P_{se}\, e_c}{S_b} - f_b$$

$$f_{bf} = \frac{1588.486}{1120} + \frac{18.67(1588.486)}{18024.15} - 3.458$$

$= 1.418 + 1.645 – 3.46 = -0.397$ ksi

Allowable tension in concrete = $6\sqrt{f'_c}$

$$f'_{c\ reqd.} = \left(\frac{3970}{6}\right)^2 = 4366 \text{ psi}$$

***B.1.7.3.4 Initial Stresses at Debonding Location***

With the same number of debonded strands, as was determined in the previous iteration, the top and bottom fiber stresses with their corresponding initial concrete strengths are calculated. It can be observed that at 15 ft. location, the $f'_{ci}$ value is updated to 5140 psi. The results are shown in Table B.1.7.6.

**Table B.1.7.6 Debonding of Strands at Each Section.**

| | Location of the Debonding Section (ft. from end) | | | | | | |
|---|---|---|---|---|---|---|---|
| | 0 | 3 | 6 | 9 | 12 | 15 | 54.2 |
| Row No. 1 (bottom row) | 7 | 7 | 15 | 23 | 25 | 27 | 27 |
| Row No. 2 | 17 | 27 | 27 | 27 | 27 | 27 | 27 |
| Row No. 3 | 12 | 12 | 12 | 12 | 12 | 12 | 12 |
| No. of Strands | 36 | 46 | 54 | 62 | 64 | 66 | 66 |
| $M_g$ (k-ft.) | 0 | 185 | 359 | 522 | 675 | 818 | 1,715 |
| $P_{si}$ (kips) | 1026.08 | 1311.10 | 1539.12 | 1767.14 | 1824.14 | 1881.15 | 1881.15 |
| $e_c$ (in.) | 17.95 | 18.01 | 18.33 | 18.57 | 18.62 | 18.67 | 18.67 |
| Top Fiber Stresses (ksi) | -0.527 | -0.506 | -0.499 | -0.503 | -0.398 | -0.304 | 0.540 |
| Corresponding $f'_{ci\ reqd}$ (psi) | 4937 | 4552 | 4427 | 4498 | 2816 | 1643 | 900 |
| Bottom Fiber Stresses (ksi) | 1.938 | 2.358 | 2.701 | 3.051 | 3.064 | 3.084 | 2.487 |
| Corresponding $f'_{ci\ reqd}$ (psi) | 3230 | 3930 | 4501 | 5085 | 5106 | 5140 | 4144 |

Since actual initial losses are 8.005, percent as compared to previously assumed 8.0 percent, and $f'_{ci}$ = 5140 psi, as compared to previously calculated $f'_{ci}$ = 5138 psi. These values are sufficiently converged, so no further iteration will be required. The optimized value of $f'_c$ required is 6225 psi. AASHTO Standard Article 9.23 requires $f'_{ci}$ to be at least 4000 for pretensioned members.

Use $f'_c$ = 6225 psi and $f'_{ci}$ = 5140 psi.

### B.1.8 STRESS SUMMARY

### B.1.8.1 Concrete Stresses at Transfer

[STD Art. 9.15.2.1]

#### B.1.8.1.1 Allowable Stress Limits

Compression: 0.6 $f'_{ci}$ = 0.6(5140) = +3084 psi = 3.084 ksi (compression)

Tension: The maximum allowable tensile stress is smaller of

$3\sqrt{f'_{ci}} = 3\sqrt{5140} = 215.1$ psi and 200 psi (controls)

$7.5\sqrt{f'_{ci}} = 7.5\sqrt{5140} = 537.71$ psi (tension) > 200 psi, bonded reinforcement should be provided to resist the total tension force in the concrete computed on the assumption of an uncracked section to allow 537.71 psi tensile stress in concrete.

#### B.1.8.1.2 Stresses at Girder End and at Transfer Length Section

##### B.1.8.1.2.1 Stresses at Transfer Length Section

The stresses at the girder end and at the transfer length section need only be checked at release, because losses with time will reduce the concrete stresses making them less critical.

Transfer length = 50 (strand diameter)
= 50 (0.5) = 25 in. = 2.083 ft. [STD Art. 9.20.2.4]

Transfer length section is located at a distance of 2.083 ft. from end of the girder. Overall girder length of 109.5 ft. is considered for the calculation of bending moment at transfer length. As shown in Table B.1.7.6, the number of strands at this location, after debonding of strands, is 36.

Moment due to girder self weight

$M_g$ = 0.5(1.167)(2.083)(109.5 – 2.083)

= 130.558 k –ft.

Concrete stress at top fiber of the girder

$$f_t = \frac{P_{si}}{A} - \frac{P_{si}\, e_t}{S_t} + \frac{M_g}{S_t}$$

$P_{si}$ = 36(0.153)(185.946) = 1024.19 kips

Strand eccentricity at transfer section, $e_c$ = 17.95 in.

$$f_t = \frac{1024.19}{1120} - \frac{17.95\,(1024.19)}{12761.88} + \frac{130.558(12)}{12761.88}$$

$$= 0.915 - 1.44 + 0.123 = -0.403 \text{ ksi}$$

Allowable tension (with bonded reinforcement) = 537.71 psi > 403 psi (O.K.)

Compute stress limit for concrete at the bottom fiber of the girder

Concrete stress at the bottom fiber of the girder

$$f_b = \frac{P_{si}}{A} + \frac{P_{si}\, e_c}{S_b} - \frac{M_g}{S_b}$$

$$f_{bi} = \frac{1024.19}{1120} + \frac{17.95\,(1024.19)}{18024.15} - \frac{130.558(12)}{18024.15}$$

$$= 0.915 + 1.02 - 0.087 = 1.848 \text{ ksi}$$

Allowable compression = 3.084 ksi < 1.848 ksi (reqd.)

***B.1.8.1.2.2 Stresses at Girder End***

Strand eccentricity at end of girder is:

$$e_c = 22.36 - \frac{7(2.17)+17(4.14)+12(6.11)}{36} = 17.95 \text{ in.}$$

$P_{si}$ = 36 (0.153) (185.946) = 1024.19 kips

Concrete stress at the top fiber of the girder

$$f_t = \frac{1024.19}{1120} - \frac{17.95\,(1024.19)}{12761.88} = 0.915 - 1.44 = -0.526 \text{ ksi}$$

Allowable tension (with bonded reinforcement) = 537.71 psi > 526 psi (O.K.)

Concrete stress at the bottom fiber of the girder

$$f_b = \frac{P_{si}}{A} + \frac{P_{si}\, e_c}{S_b} - \frac{M_g}{S_b}$$

$$f_b = \frac{1021.701}{1120} + \frac{17.95\,(1021.701)}{18024.15} = 0.915 + 1.02 = 1.935 \text{ ksi}$$

Allowable compression = 3.084 ksi > 1.935 ksi (reqd.)

***B.1.8.1.3 Stresses at Midspan***

Bending moment at midspan due to girder self –weight based on overall length.

$M_g = 0.5(1.167)(54.21)(109.5 - 54.21) = 1748.908$ k-ft.

Concrete stress at top fiber of the girder at midspan

$$f_t = \frac{P_{si}}{A} - \frac{P_{si}\, e_c}{S_t} + \frac{M_g}{S_t}$$

$$f_t = \frac{1881.15}{1120} - \frac{17.95\,(1881.15)}{12761.88} + \frac{1748.908\,(12)}{12761.88}$$

$= 1.68 - 2.64 + 1.644 = 0.684$ ksi

Allowable compression: 3.084 ksi >> 0.684 ksi (reqd.)

Concrete stresses in bottom fiber of the girder at midspan

$$f_b = \frac{P_{si}}{A} + \frac{P_{si}\, e_c}{S_b} - \frac{M_g}{S_b}$$

$$f_b = \frac{1881.15}{1120} + \frac{17.95(1881.15)}{18024.15} - \frac{1748.908(12)}{18024.15}$$

$= 1.68 + 1.87 - 1.164 = 2.386$ ksi

Allowable compression: 3.084 ksi > 2.386 ksi (reqd.)

***B.1.8.1.4 Stress Summary at Transfer***

| | Top of girder $f_t$ (ksi) | Bottom of girder $f_b$ (ksi) |
|---|---|---|
| At End | -0.526 | +1.935 |
| At transfer length section from End | -0.403 | +1.848 |
| At Midspan | +0.684 | +2.386 |

### *B.1.8.2 Concrete Stresses at Service Loads*

[STD Art. 9.15.2.2]

#### *B.1.8.2.1 Allowable Stress Limits*

Compression

Case (I): for all load combinations

$0.60\,f_c'$ = 0.60(6225)/1000 = +3.74 ksi (for precast girder)

$0.60\,f_c'$ = 0.60(4000)/1000 = +2.4 ksi (for slab)

Case (II): for effective pretension force + permanent dead loads

$0.40\,f_c'$ = 0.40(6225)/1000 = +2.493 ksi (for precast girder)

$0.40\,f_c'$ = 0.40(4000)/1000 = +1.6 ksi (for slab)

Case (III): for live load +0.5(effective pretension force + dead loads)

$0.40\,f_c'$ = 0.40(6225)/1000 = +2.493 ksi (for precast girder)

$0.40\,f_c'$ = 0.40(4000)/1000 = +1.6 ksi (for slab)

Tension: $6\sqrt{f_c'} = 6\sqrt{6225}\left(\frac{1}{1000}\right)$ = -0.4737 ksi

#### *B.1.8.2.2 Stresses at Midspan*

$P_{se}$ = 66(0.153)(157.307) = 1588.49 kips

Concrete stresses at top fiber of the girder at service loads

$$f_t = \frac{P_{se}}{A} - \frac{P_{se}\,e_c}{S_t} + \frac{M_g + M_S}{S_t} + \frac{M_{SDL} + M_{LL+I}}{S_{tg}}$$

Case (I):

$$f_t = \left( \begin{array}{l} \frac{1588.49}{1120} - \frac{18.67(1588.49)}{12761.88} \\ + \frac{(1714.64+1822.29)(12)}{12761.88} + \frac{(443.72+2121.278)(12)}{79936.06} \end{array} \right)$$

$f_t$ = 1.418 – 2.323 + 3.326 + 0.385 = 2.805 ksi (O.K.)

Allowable compression: +3.84 ksi > +2.805 ksi (reqd.) (O.K.)

Case (II): Effective pretension force + permanent dead loads

$$f_t = \frac{P_{se}}{A} - \frac{P_{se}\, e_c}{S_t} + \frac{M_g + M_S}{S_t} + \frac{M_{SDL}}{S_{tg}}$$

$$f_t = \frac{1588.49}{1120} - \frac{18.67(1588.49)}{12761.88} + \frac{(1714.64+1822.29)(12)}{12761.88} + \frac{(443.72)(12)}{79936.06}$$

$f_t$ =1.418 – 2.323 + 3.326 + 0.067 = 2.49 ksi

Allowable compression: +2.493 ksi > +2.49 ksi (reqd.)

Case (III): Live load + ½(Pretensioning force + dead loads)

$$f_t = \frac{M_{LL+I}}{S_{tg}} + 0.5\left(\frac{P_{se}}{A} - \frac{P_{se}\, e_c}{S_t} + \frac{M_g + M_S}{S_t} + \frac{M_{SDL}}{S_{tg}}\right)$$

$$= \frac{2121.27(12)}{79936.06} + 0.5\left(\frac{1588.49}{1120} - \frac{18.67(1588.49)}{12761.88} + \frac{(1714.64+1822.29)(12)}{12761.88} + \frac{(443.72)(12)}{79936.06}\right)$$

$f_t$ = 0.318 + 0.5(1.418 – 2.323 + 3.326 + 0.067) = 1.563 ksi

Allowable compression: +2.493 ksi > +1.563 ksi (reqd.)

Concrete stresses at bottom fiber of the girder:

$$f_b = \frac{P_{se}}{A} + \frac{P_{se}\, e_c}{S_b} - \frac{M_g + M_S}{S_b} - \frac{M_{SDL} + M_{LL+I}}{S_{bc}}$$

$$f_b = \left( \frac{1588.49}{1120} - \frac{18.67(1588.49)}{18024.15} - \frac{(1714.64+1822.29)(12)}{18024.15} - \frac{(443.72+2121.27)(12)}{27842.9} \right)$$

$f_b$ = 1.418 + 1.645 – 2.36 – 1.098 = – 0.397 ksi

Allowable Tension: 473.7 ksi > 397 psi

Stresses at the top of the slab

Case (I):

$$f_t = \frac{M_{SDL} + M_{LL+I}}{S_{tc}} = \frac{(443.72+2121.27)(12)}{50802.19} = +0.604 \text{ ksi}$$

Allowable compression: +2.4 ksi > +0.604 ksi (reqd.)

Case (II):

$$f_t = \frac{M_{SDL}}{S_{tc}} = \frac{(443.72)(12)}{50802.19} = 0.103 \text{ ksi}$$

Allowable compression: +1.6 ksi > +0.103 ksi (reqd.)

Case (III):

$$f_t = \frac{M_{LL+I} + 0.5(M_{SDL})}{S_{tc}} = \frac{(2121.27)(12) + 0.5(443.72)(12)}{50802.19}$$

= 0.553 ksi

Allowable compression: +1.6 ksi > +0.553 ksi (reqd.)

### *B.1.8.2.3 Summary of Stresses at Service Loads*

| | | Top of Slab | Top of Girder | Bottom of Girder |
|---|---|---|---|---|
| | | $f_t$ (ksi) | $f_t$ (ksi) | $f_b$ (ksi) |
| At Midspan | CASE I | +0.604 | +2.805 | -0.397 |
| | CASE II | +0.103 | +2.490 | |
| | CASE III | +0.553 | +1.563 | |

### *B.1.8.3 Actual Modular Ratio and Transformed Section Properties for Strength Limit State and Deflection Calculations*

Till this point, a modular ratio equal to 1 has been used for the Service Limit State design. For the evaluation of Strength Limit State and Deflection calculations, actual modular ratio will be calculated and the transformed section properties will be used.

$$n = \frac{E_c \text{ for slab}}{E_c \text{ for beam}} = \left(\frac{3834.25}{4531.48}\right) = 0.883$$

Transformed flange width = $n$ (effective flange width)

= 0.883(138 in.) = 121.85 in.

Transformed Flange Area = $n$ (effective flange width) ($t_s$)

= 1(121.85 in.)(8 in.) = 974.8 in.$^2$

*Table B.1.8.1 Properties of Composite Section*

| | Transformed Area in.$^2$ | $y_b$ in. | $A\,y_b$ in. | $A(y_{bc} - y_b)^2$ | $I$ in.$^4$ | $I+A(y_{bc}- y_b)^2$ in.$^4$ |
|---|---|---|---|---|---|---|
| Girder | 1120 | 22.36 | 25,043.20 | 307,883.97 | 403,020 | 710,903.97 |
| Slab | 974.8 | 58 | 56,538.40 | 354,128.85 | 41,591 | 395,720.32 |
| ∑ | 2094.8 | | 81,581.60 | | | 1,106,624.29 |

$A_c$ = Total area of composite section = 2094.8 in.$^2$

$h_c$ = Total height of composite section = 62 in.

$I_c$ = Moment of inertia of composite section = 1,106,624.29 in.$^4$

$y_{bc}$ = Distance from the centroid of the composite section to extreme bottom fiber of the precast girder = 81,581.6 / 2094.8 = 38.94 in.

$y_{tg}$ = Distance from the centroid of the composite section to extreme top fiber of the precast girder = 54 – 38.94 = 15.06 in.

$y_{tc}$ = Distance from the centroid of the composite section to extreme top fiber of the slab = 62 – 38.94 = 23.06 in.

$S_{bc}$ = Composite section modulus with reference to the extreme bottom fiber of the precast girder = $I_c/y_{bc}$
= 1,106,624.29 / 38.94 = 28,418.7 in.$^3$

$S_{tg}$ = Composite section modulus with reference to the top fiber of the precast girder = $I_c/y_{tg}$ = 1,106,624.29 / 15.06 = 73,418.03 in.$^3$

$S_{tc}$ = Composite section modulus with reference to the top fiber of the slab
= $I_c/y_{tc}$ = 1,106,624.29 / 23.06 = 47,988.91 in.$^3$

### B.1.9 FLEXURAL STRENGTH

Group I load factor design loading combination

$M_u = 1.3[M_g + M_s + M_{SDL} + 1.67(M_{LL+I})]$

$= 1.3[1714.64 + 1822.29 + 443.72 + 1.67(2121.27)] = 9780.12$ k-ft.

Average stress in pretensioning steel at ultimate load

$$f_{su}^* = f_s'\left(1 - \frac{\gamma^*}{\beta_1}\rho^*\frac{f_s'}{f_c'}\right)$$

where:

$f_{su}^*$ = Average stress in prestressing steel at ultimate load

$\gamma^*$ = 0.28 for low-relaxation strand

$$\beta_1 = 0.85 - 0.05\frac{(f_c' - 4000)}{1000}$$

$$= 0.85 - 0.05\frac{(4000 - 4000)}{1000} = 0.85$$

$$\rho^* = \frac{A_s^*}{bd}$$

where:

$A_s^*$ = Area of pretensioned reinforcement = 66(0.153) = 10.1 in.$^2$

$b$ = Transformed effective flange width = 121.85 in.

$y_{bs}$ = Distance from center of gravity of the strands to the bottom fiber of the girder = 22.36 – 18.67 = 3.69 in.

$d$ = Distance from top of slab to centroid of pretensioning strands

= Girder depth ($h$) + slab thickness – $y_{bs}$

= 54 + 8 – 3.69 = 58.31 in.

$$\rho^* = \frac{10.1}{121.85(58.31)} = 0.00142$$

$$f_{su}^* = 270\left[1 - \left(\frac{0.28}{0.85}\right)(0.00142)\left(\frac{270}{4}\right)\right] = 261.48 \text{ ksi}$$

Depth of compression block

$$a = \frac{A_s^* f_{su}^*}{0.85 f_c' b} = \frac{10.1(261.48)}{0.85(4)(121.85)} = 6.375 \text{ in.} < 8.0 \text{ in.}$$

The depth of compression block is less than flange thickness hence the section is designed as rectangular section

Design flexural strength:

$$\phi M_n = \phi A_s^* f_{su}^* d\left(1 - 0.6\frac{\rho^* f_{su}^*}{f_c'}\right) \qquad \text{[STD Eq. 9-13]}$$

where:

$\phi$ = Strength reduction factor = 1.0 [STD Art. 9.14]

$M_n$ = Nominal moment strength of a section

$$\phi M_n = 1.0(10.1)(261.48)\frac{(58.31)}{12}\left(1 - 0.6\frac{0.00142(261.48)}{4}\right)$$

= 12118.1 k-ft. > 9780.12 k-ft. (O.K.)

### B.1.10 DUCTILITY LIMITS

### B.1.10.1 Maximum Reinforcement

Reinforcement index for rectangular section:

$$\frac{\rho^* f_{su}^*}{f_c'} < 0.36\beta_1 = 0.00142\left(\frac{261.48}{4}\right) = 0.093 < 0.36(0.85) = 0.306$$

### B.1.10.2 Minimum Reinforcement

[STD Art. 9.18.2]

The ultimate moment at the critical section developed by the pretensioned and non-pretensioned reinforcement shall be at least 1.2 times the cracking moment, $M_{cr}$

[STD Art. 9.18.2.1]

$$\phi M_n \geq 1.2\, M_{cr}$$

Cracking moment $M_{cr} = (f_r + f_{pe})\, S_{bc} - M_{d\text{-}nc}\left(\frac{S_{bc}}{S_b} - 1\right)$

where:

$f_r$ = Modulus of rupture (ksi)

$$= 7.5\sqrt{f_c'} = 7.5\sqrt{6225}\left(\frac{1}{1000}\right) = 0.592 \text{ ksi}$$

$f_{pe}$ = Compressive stress in concrete due to effective prestress forces at extreme fiber of section where tensile stress is caused by externally applied loads (ksi)

$$f_{pe} = \frac{P_{se}}{A} + \frac{P_{se}\, e_c}{S_b}$$

where:

$P_{se}$ = Effective prestress force after losses = 1583.791 kips

$e_c$ = 18.67 in.

$$f_{pe} = \frac{1588.49}{1120} + \frac{1588.49\ (18.67)}{18024.15} = 1.418 + 1.641 = 3.055 \text{ ksi}$$

$M_{d\text{-}nc}$ = Non-composite dead load moment at midspan due to self-weight of girder and weight of slab

= 1714.64 + 1822.29 = 3536.93 k-ft.

$$M_{cr} = (0.592 + 3.055)(28418.7)\left(\frac{1}{12}\right) - 3536.93\left(\frac{28418.7}{18024.15} - 1\right)$$

= 8636.92 – 2039.75 = 6597.165 k-ft.

$1.2\ M_{cr}$ = 1.2(6597.165) = 7916.6 k-ft. < $\phi Mn$ = 12,118.1 k-ft. (O.K.)

### *B.1.11 TRANSVERSE SHEAR DESIGN*

[STD Art. 9.20]

Members subject to shear shall be designed so that

$V_u < \phi\,(V_c + V_s)$

where:

$V_u$ = the factored shear force at the section considered

$V_c$ = the nominal shear strength provided by concrete

$V_s$ = the nominal shear strength provided by web reinforcement

$\phi$ = strength reduction factor = 0.90

The critical section for shear is located at a distance $h/2$ from the face of the support, however the critical section for shear is conservatively calculated from the centerline of the support

$h/2 = \dfrac{62}{2(12)} = 2.583$ ft.

From Tables B.1.5.1 and Table B.1.5.2 the shear forces at critical section are as follows,

$V_d$ = Shear force due to total dead loads at section considered
= 144.75 kips

$V_{LL+I}$ = Shear force due to live load and impact at critical section
= 81.34 kips

$V_u$ = $1.3(V_d + 1.67V_{LL+I}) = 1.3(144.75 + 1.67(81.34) = 364.764$ kips

Computation of $V_{ci}$

$$V_{ci} = 0.6\sqrt{f_c'}b'd + V_d + \frac{V_i M_{cr}}{M_{\max}}$$

where ,

$b'$ = Width of web of a flanged member = 5 in.

$f_c'$ = Compressive strength of girder concrete at 28 days = 6225 psi.

$M_d$ = Bending moment at section due to unfactored dead load
= 365.18 k-ft.

$M_{LL+I}$ = Factored bending moment at section due to live load and impact
= 210.1 k-ft.

$M_u$ = Factored bending moment at the section.
= $1.3(M_d + 1.67M_{LL+I}) = 1.3[365.18 + 1.67(210.1)] = 930.861$ k-ft.

$V_{mu}$ = Factored shear force occurring simultaneously with $M_u$ conservatively taken as maximum shear load at the section
= 364.764 kips.

$M_{max}$ = Maximum factored moment at the section due to externally applied loads = $M_u - M_d = 930.861 - 365.18 = 565.681$ k-ft.

$V_i$ = Factored shear force at the section due to externally applied loads occurring simultaneously with $M_{max}$

= $V_{mu}$-$V_d = 364.764 - 144.75 = 220.014$ kips

$f_{pe}$ = Compressive stress in concrete due to effective pretension forces at extreme fiber of section where tensile stress is caused by externally applied loads i.e. bottom of the girder in present case

$$f_{pe} = \frac{P_{se}}{A} + \frac{P_{se}\,e}{S_b}$$

eccentricity of the strands at $h_c/2$

$e_{h/2}$ = 18.046 in.

$P_{se}$ = 36(0.153)(157.307) = 866.45 kips

$$f_{pe} = \frac{866.45}{1120} + \frac{866.45(17.95)}{18024.15} = 0.77 + 0.86 = 1.63 \text{ ksi}$$

$f_d$ = Stress due to unfactored dead load, at extreme fiber of section

where tensile stress is caused by externally applied loads

$$= \left[ \frac{M_g + M_S}{S_b} + \frac{M_{SDL}}{S_{bc}} \right]$$

$$= \left[ \frac{(159.51 + 157.19 + 7.75)(12)}{18024.15} + \frac{41.28(12)}{28418.70} \right] = 0.234 \text{ ksi}$$

$M_{cr}$ = Moment causing flexural cracking of section due to externally applied loads = $(6\sqrt{f'_c} + f_{pe} - f_d)\, S_{bc}$

$$= \left( \frac{6\sqrt{6225}}{1000} + 1.631 - 0.234 \right) \frac{28418.70}{12} = 4429.5 \text{ k-ft.}$$

$d$ = Distance from extreme compressive fiber to centroid of pretensioned reinforcement, but not less than $0.8h_c$ = 49.6 in.
= 62 – 4.41 = 57.59 in. > 49.96 in.

Therefore, use = 57.59 in.

$$V_{ci} = 0.6\sqrt{f'_c}\, b'd + V_d + \frac{V_i M_{cr}}{M_{\max}}$$

$$= \frac{0.6\sqrt{6225}(2 \times 5)(57.59)}{1000} + 144.75 + \frac{220.014(4429.5)}{565.681} = 1894.81 \text{ kips}$$

This value should not be less than

Minimum $V_{ci} = 1.7\sqrt{f'_c}\, b'd$

$$= \frac{1.7\sqrt{6225}(2 \times 5)(57.59)}{1000} = 77.24 \text{ kips} < V_{ci} = 1894.81 \text{ kips}$$

Computation of $V_{cw}$

$V_{cw} = (3.5\sqrt{f'_c} + 0.3 f_{pc})\, b'd + V_p$

where:

$f_{pc}$ = Compressive stress in concrete at centroid of cross-section (Since the centroid of the composite section does not lie within the flange of the cross-section) resisting externally applied loads. For a non-composite section

$$f_{pc} = \frac{P_{se}}{A} - \frac{P_{se}\, e(y_{bc} - y_b)}{I} + \frac{M_D(y_{bc} - y_b)}{I}$$

$M_D$ = Moment due to unfactored non-composite dead loads
= 324.45 k-ft.

$$f_{pc} = \left( \frac{863.89}{1120} - \frac{863.89\ (17.95)(38.94\text{-}22.36)}{403020} + \frac{324.45(12)(38.94\text{-}22.36)}{403020} \right)$$

$= 0.771 - 0.638 + 0.160 = 0.293$ psi

$V_p = 0$

$$V_{cw} = \left( \frac{3.5\sqrt{6225}}{1000} + 0.3(0.293) \right)(2\times 5)(57.59) = 209.65 \text{ kips (controls)}$$

The allowable nominal shear strength provided by concrete should be lesser of $V_{ci}$ = 1894.81 kips and $V_{cw}$ = 209.65 kips

Therefore, $V_c$ = 209.65 kips

$V_u < \phi\,(V_c + V_s)$

where: $\phi$ = Strength reduction factor for shear = 0.90

Required $V_s = \frac{V_u}{\phi} - V_c = \frac{364.764}{0.9} - 209.65 = 195.643$ kips

Maximum shear force that can be carried by reinforcement

$V_{s\,max} = 8\sqrt{f'_c}\ b'd$ [STD Art. 9.20.3.1]

$$= 8\sqrt{6225}\ \frac{(2\times 5)(57.59)}{1000}$$

= 363.502 kips > required $V_s$ = 195.643 kips (O.K.)

Area of shear steel required [STD Art. 9.20.3.1]

$$V_s = \frac{A_v f_y d}{s} \quad \text{[STD Eq. 9-30]}$$

or $A_v = \frac{V_s s}{f_y d}$

where:

$A_v$ = Area of web reinforcement, in.$^2$

$s$ = Longitudinal spacing of the web reinforcement, in.

Setting s = 12 in. to have units of in.$^2$/ft. for $A_v$

$$A_v = \frac{(195.643)(12)}{(60)(57.59)} = 0.6794 \text{ in.}^2/\text{ft.}$$

Minimum shear reinforcement [STD Art. 9.20.3.3]

$$A_{v-min} = \frac{50\, b'\, s}{f_y} = \frac{(50)(2\times 5)(12)}{60000} = 0.1 \text{ in.}^2/\text{ft.} \quad \text{[STD Eq. 9-31]}$$

The required shear reinforcement is the maximum of $A_v$ = 0.378 in.$^2$/ft. and $A_{v-min}$ = 0.054 in.$^2$/ft.

[STD Art. 9.20.3.2]

Maximum spacing of web reinforcement is 0.75 $h_c$ or 24 in., unless

$$V_s = 195.643 \text{ kips} > 4\sqrt{f_c'}\, b'\, d = 4\sqrt{6225}\, \frac{(2\times 5)(57.59)}{1000} = 181.751 \text{ kips}$$

Use 1 # 4 double legged with $A_v$ = 0.392 in.$^2$ / ft., the required spacing can be calculated as,

$$s = \frac{f_y\, d\, A_v}{V_s} = \frac{60\times 57.59\times 0.392}{195.643} = 6.92 \text{ in.}$$

Since, $V_s$ is less than the limit,

Maximum spacing = 0.75 $h$ = 0.75(54 + 8 + 1.5) = 47.63 in.

or = 24 in.

Therefore, maximum $s$ = 24 in.

Use # 4, two legged stirrups at 6.5 in. spacing.

### B.1.12 HORIZONTAL SHEAR DESIGN

The critical section for horizontal shear is at a distance of $h_c/2$ from the centerline of the support

$V_u$ = 364.764 kips

$V_u \leq V_{nh}$

where

$V_{nh}$ = Nominal horizontal shear strength, kips

$$V_{nh} \geq \frac{V_u}{\phi} = \frac{364.764}{0.9} = 405.293 \text{ kips}$$

Case (a & b): Contact surface is roughened, or when minimum ties are used.

Allowable shear force:

$V_{nh} = 80 b_v d$

where:

$b_v$ = Width of cross-section at the contact surface being investigated = $2 \times 15.75 = 31.5$ in.

$d$ = Distance from extreme compressive fiber to centroid of the pretensioning force = 54 –4.41 = 49.59 in.

$$V_{nh} = \frac{80(31.5)(49.59)}{1000} = 124.97 \text{ kips} < 405.293 \text{ kips}$$

Case(c): Minimum ties provided, and contact surface roughened

Allowable shear force:

$V_{nh} = 350 b_v d$

$$= \frac{350(31.5)(49.59)}{1000} = 546.73 \text{ kips} > 405.293 \text{ kips}$$

Required number of stirrups for horizontal shear

Minimum $A_{vh} = 50\dfrac{b_v\, s}{f_y} = 50\dfrac{(31.5)(6.5)}{60000} = 0.171$ in.$^2$/ft.

Therefore, extend every alternate web reinforcement into the cast-in-place slab to satisfy the horizontal shear requirements.

Maximum spacing = $4b = 4(2\times 15.75) = 126$ in. [STD Art. 9.20.4.5.a]

or = 24.00 in.

Maximum spacing = 24 in. > ($s_{\text{provided}}$ = 13.00 in.)

## *B.1.13 PRETENSIONED ANCHORAGE ZONE*

### *B.1.13.1 Minimum Vertical Reinforcement*

[STD Art. 9.22]

In a pretensioned girder, vertical stirrups acting at a unit stress of 20,000 psi to resist at least 4 percent of the total pretensioning force must be placed within the distance of $d/4$ of the girder end.

[STD Art. 9.22.1]

Minimum stirrups at the each end of the girder:

$P_s$ = Prestress force before initial losses

= 36(0.153)[(0.75)(270)] = 1,115.37 kips

4 percent of $P_s$ = 0.04(1115.37) = 44.62 kips

Required $A_v = \dfrac{44.62}{20} = 2.231$ in.$^2$

$\dfrac{d}{4} = \dfrac{57.59}{4} = 14.4$ in.

Use 5 pairs of #5 @ 2.5 in. spacing at each end of the girder
(provided $A_v$ = 3.1 in.$^2$)

[STD Art. 9.22.2]

Provide nominal reinforcement to enclose the pretensioning steel for a distance from the end of the girder equal to the depth of the girder

## B.1.14 DEFLECTION AND CAMBER

### B.1.14.1 Maximum Camber Calculations Using Hyperbolic Functions Method

TxDOT's prestressed bridge design software, PSTRS14 uses the Hyperbolic Functions Method proposed by Sinno (1968) for the calculation of maximum camber. This design example illustrates the PSTRS14 methodology for calculation of maximum camber.

Step 1: Total prestress after release

$$P = \frac{P_{si}}{\left(1 + pn + \frac{e_c^2 A_s n}{I}\right)} + \frac{M_D e_c A_s n}{I\left(1 + pn + \frac{e_c^2 A_s n}{I}\right)}$$

where:

$P_{si}$ = Total prestressing force = 1881.146 kips

$I$ = Moment of inertia of non-composite section = 403,020 in.$^4$

$e_c$ = Eccentricity of pretensioning force at the midspan = 18.67 in.

$M_D$ = Moment due to self weight of the girder at midspan

= 1714.64 k-ft.

$A_s$ = Area of strands = number of strands (area of each strand)

$\rho$ = $A_s/A$

where:

$A$ = Area of cross-section of girder = 1120 in.$^2$

$\rho$ = 10.098/1120 = 0.009016

$E_c$ = Modulus of elasticity of the girder concrete at release, ksi

$= 33(w_c)^{3/2}\sqrt{f_c'}$ [STD Eq. 9-8]

$= 33(150)^{1.5}\sqrt{5140}\ \frac{1}{1000} = 4346.43$ ksi

$E_s$ = Modulus of elasticity of prestressing strands = 28000 ksi

$n$ = $E_s/E_c$ = 28000/4346.43 = 6.45

$$\left(1 + pn + \frac{e_c^2 A_s n}{I}\right) = 1 + (0.009016)(6.45) + \frac{(18.67^2)(10.098)(6.45)}{403020}$$

$$= 1.115$$

$$P = \frac{P_{si}}{\left(1 + pn + \frac{e_c^2 A_s n}{I}\right)} + \frac{M_D e_c A_s n}{I\left(1 + pn + \frac{e_c^2 A_s n}{I}\right)}$$

$$= \frac{1881.15}{1.115} + \frac{(1714.64)(12 \text{ in./ft.})(18.67)(10.098)(6.45)}{403020(1.115)}$$

$$= 1687.13 + 55.68 = 1742.81 \text{ kips}$$

Concrete stress at steel level immediately after transfer

$$f_{ci}^{s} = P\left(\frac{1}{A} + \frac{e_c^2}{I}\right) - f_c^s$$

where:

$f_c^s$ = Concrete stress at steel level due to dead loads

$$= \frac{M_D e_c}{I} = \frac{(1714.64)(12 \text{ in./ft.})(18.67)}{403020} = 0.953 \text{ ksi}$$

$$f_{ci}^{s} = 1742.81 \left(\frac{1}{1120} + \frac{18.67^2}{403020}\right) - 0.953 = 2.105 \text{ ksi}$$

Step 2: Ultimate time-dependent strain at steel level

$$\varepsilon_{c1}^{s} = \varepsilon_{cr}^{\infty} f_{ci}^{s} + \varepsilon_{sh}^{\infty}$$

where:

$\varepsilon_{cr}^{\infty}$ = Ultimate unit creep strain = 0.00034 in./in. (this value is prescribed by Sinno (1968)

$\varepsilon_{sh}^{\infty}$ = Ultimate unit creep strain = 0.000175 in./in. (this value is prescribed by Sinno (1968))

$\varepsilon_{c1}^{\infty}$ = 0.00034(2.105) + 0.000175 = 0.0008907 in./in.

Step 3: Adjustment of total strain in step 2

$$\varepsilon_{c2}^{s} = \varepsilon_{c1}^{s} - \varepsilon_{c1}^{s} E_{ps} \frac{A_s}{E_{ci}}\left(\frac{1}{A_n} + \frac{e_c^2}{I}\right)$$

$$= 0.0008907 - 0.0008907\ (28000)\frac{10.098}{4346.43}\left(\frac{1}{1120} + \frac{18.67^2}{403020}\right)$$

$$= 0.000993 \text{ in./in.}$$

Step 4: Change in concrete stress at steel level

$$\Delta f_c^s = \varepsilon_{c2}^{s} E_{ps} A_s \left(\frac{1}{A_n} + \frac{e_c^2}{I}\right)$$

$$= 0.000993\ (28000)(10.098)\left(\frac{1}{1120} + \frac{18.67^2}{403020}\right)$$

$\Delta f_c^s = 0.494$ ksi

Step 5: Correction of the total strain from step2

$$\varepsilon_{c4}^s = \varepsilon_{\text{cr}}^{\infty} + \left(f_{ci}^s - \frac{\Delta f_c^s}{2}\right) + \varepsilon_{\text{sh}}^{\infty}$$

$$\varepsilon_{\text{c4}}^s = 0.00034\left(2.105 - \frac{0.494}{2}\right) + 0.000175 = 0.000807 \text{ in./in.}$$

Step 6: Adjustment in total strain from step 5

$$\varepsilon_{c5}^s = \varepsilon_{c4}^s - \varepsilon_{c4}^s E_{ps} \frac{A_s}{E_c}\left(\frac{1}{A_n} + \frac{e_c^2}{I}\right)$$

$$= 0.000807 - 0.000807(28000)\frac{10.098}{4346.43}\left(\frac{1}{1120} + \frac{18.67^2}{403020}\right) = 0.000715$$

in./in.

Step 7: Change in concrete stress at steel level

$$\Delta f_{c1}^s = \varepsilon_{c5}^s E_{ps} A_s \left(\frac{1}{A_n} + \frac{e_c^2}{I}\right) = 0.000715\ (28000)(10.098)$$

$$\left(\frac{1}{1120} + \frac{18.67^2}{403020}\right)$$

$\Delta f_{c1}^s = 0.36$ ksi

Step 8: Correction of the total strain from step 5

$$\varepsilon_{\text{c6}}^s = \varepsilon_{\text{cr}}^{\infty} + \left(f_{ci}^s - \frac{\Delta f_{c1}^s}{2}\right) + \varepsilon_{\text{sh}}^{\infty}$$

$$\varepsilon_{\text{c6}}^s = 0.00034\left(2.105 - \frac{0.36}{2}\right) + 0.000175 = 0.00083 \text{ in./in.}$$

Step 9: Adjustment in total strain from step 8

$$\varepsilon_{c7}^{s} = \varepsilon_{c6}^{s} - \varepsilon_{c6}^{s} E_{ps} \frac{A_s}{E_{ci}} \left( \frac{1}{A_n} + \frac{e_c^2}{I} \right)$$

$$= 0.00083 - 0.00083\,(28000)\,\frac{10.098}{4346.43} \left( \frac{1}{1120} + \frac{18.67^2}{403020} \right)$$

$$= 0.000735 \text{ in./in.}$$

Step 10: Computation of initial prestress loss

$$PL_i = \frac{P_{si} - P}{P_{si}} = \frac{1877.68 - 1742.81}{1877.68} = 0.0735$$

Step 11: Computation of Final Prestress loss

$$PL^{\infty} = \frac{\varepsilon_{c7}^{\infty} E_{ps} A_s}{P_{si}} = \frac{0.000735(28000)(10.098)}{1877.68} = 0.111$$

Total Prestress loss

$PL = PL_i + PL^{\infty} = 100(0.0735 + 0.111) = 18.45$ percent

Step 12: Initial deflection due to dead load

$$C_{DL} = \frac{5\, w\, L^4}{384\, E_c\, I}$$

where:

$w$ = Weight of girder = 1.167 kips/ft.

$L$ = Span length = 108.417 ft.

$$C_{DL} = \frac{5\left( \frac{1.167}{12 \text{ in./ft.}} \right)[(108.417)(12 \text{ in./ft.})]^4}{384(4346.43)(403020)} = 2.073 \text{ in.}$$

Step 13: Initial Camber due to prestress

The *M/EI* diagram is drawn for the moment caused by the initial prestressing, is shown in Figure B.1.14.1. Due to debonding of strands, the number of strands vary at each debonding section location. Strands that are bonded, achieve their effective prestress level at the end of transfer length. Points 1 through 6 show the end of transfer length for the preceding section. The *M/EI* values are calculated as,

$$\frac{M}{EI} = \frac{P_{si} \times ec}{E_c I}$$

The *M/EI* values are calculated for each point 1 through 6 and are shown in Table B.1.14.1. The initial camber due to prestress, $C_{pi}$, can be calculated by Moment Area Method, by taking the moment of the *M/EI* diagram about the end of the girder.

$C_{pi}$ = 4.06 in.

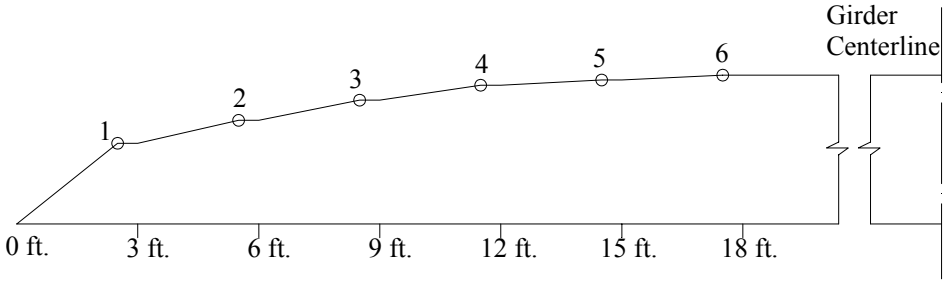


**Figure B.1.14.1 M/EI Diagram to Calculate the Initial Camber due to Prestress.**

**Table B.1.14.1 M/EI Values at the End of Transfer Length.**

| Identifier for the End of Transfer Length | $P_{si}$ (kips) | $e_c$ (in.) | *M/EI* (in.$^3$) |
|---|---|---|---|
| 1 | 1024.19 | 17.95 | 1.026E-08 |
| 2 | 1308.69 | 18.01 | 1.029E-08 |
| 3 | 1536.29 | 18.33 | 1.048E-08 |
| 4 | 1763.88 | 18.57 | 1.061E-08 |
| 5 | 1820.78 | 18.62 | 1.064E-08 |
| 6 | 1877.68 | 18.67 | 1.067E-08 |

Step 14: Initial Camber

$C_i = C_{pi} - C_{DL}$ = 4.06 – 2.073 = 1.987 in.

Step 15: Ultimate Time Dependent Camber

Ultimate strain $\varepsilon_e^s = \frac{f_{ci}^s}{E_c}$ = 2.105/4346.43 = 0.00049 in./in.

$$\text{Ultimate camber } C_t = C_i\left(1 - PL^{\infty}\right)\frac{\varepsilon_{cr}^{\infty}\left(f_{ci}^{s} - \frac{\Delta f_{c1}^{s}}{2}\right) + \varepsilon_e^s}{\varepsilon_e^s}$$

$$= 1.987(1 - 0.111)\frac{0.00034\left(2.105 - \frac{0.494}{2}\right) + 0.00049}{0.00049}$$

$C_t = 4.044$ in. = 0.34 ft.↑

***B.1.14.2 Deflection due to Girder Self-Weight***

$$\Delta_{girder} = \frac{5w_g L^4}{384E_{ci}I}$$

where:

$w_g$ = Girder weight = 1.167 kips/ft.

Deflection due to girder self weight at transfer

$$\Delta_{girder} = \frac{5(1.167/12)[(109.5)(12)]^4}{384(4346.43)(403020)} = 2.16 \text{ in.}\downarrow$$

Deflection due to girder self-weight used to compute deflection at erection

$$\Delta_{girder} = \frac{5(1.167/12)[(108.4167)(12)]^4}{384(4783.22)(403020)} = 1.88 \text{ in.}\downarrow$$

***B.1.14.3 Deflection due to Slab and Diaphragm Weight***

$$\Delta_{slab} = \frac{5w_s L^4}{384E_c I} + \frac{w_{dia} b}{24E_c I}\left(3l^2 - 4b^2\right)$$

where:

$w_s$ = Slab weight = 1.15 kips/ft.

$E_c$ = Modulus of elasticity of girder concrete at service = 4783.22 ksi

$$\Delta_{slab} = \left(\frac{5(1.15/12)[(108.4167)(12)]^4}{384(4783.22)(403020)} + \frac{(3)(44.2083\times12)}{(24\times4783.22\times403020)}\left(3(108.4167\times12)^2 - 4(44.2083\times12)^2\right)\right)$$

$= 1.99$ in.↓

### B.1.14.4 Deflection due to Superimposed Loads

$$\Delta_{SDL} = \frac{5w_{SDL}L^4}{384E_c I_c}$$

where:

$w_{SDL}$ = Super imposed dead load = 0.31 kips/ft.

$I_c$ = Moment of inertia of composite section = 1,106,624.29 in.$^4$

$$\Delta_{SDL} = \frac{5(0.302/12)[(108.4167)(12)]^4}{384(4783.22)(1106624.29)} = 0.18 \text{ in.}\downarrow$$

Total deflection at service due to all dead loads = 1.88 + 1.99 + 0.18

### B.1.14.5 Deflection due to Live Loads

The deflections due to live loads are not calculated in this example as they are not a design factor for TxDOT bridges.

### B.1.15 COMPARISON OF RESULTS

To measure the level of accuracy in this detailed design example, the results are compared with that of PSTRS14 (TxDOT 2004). The summary of comparison is shown in Table B.1.15. In the service limit state design, the results of this example matches those of PSTRS14 with very insignificant differences. A difference of 26 percent in transverse shear stirrup spacing is observed. This difference can be because PSTRS14 calculates the spacing according to the AASHTO Standard Specifications 1989 edition (AASHTO 1989) and in this detailed design example, all the calculations were performed according to the AASHTO Standard Specifications 2002 edition (AASHTO 2002). There is a difference of 15.3 percent in camber calculation, which may be because PSTRS14 uses a single step hyperbolic functions method, whereas a multi step approach is used in this detailed design example.

**Table B.1.15.1 Comparison of Results for the AASHTO Standard Specifications (PSTRS14 vs Detailed Design Example).**

| Design Parameters | | PSTRS14 | Detailed Design Example | Percent Piff. PSTRS14 |
|---|---|---|---|---|
| Prestress Losses, (percent) | Initial | 8.00 | 8.01 | -0.1 |
| | Final | 22.32 | 22.32 | 0.0 |
| Required Concrete Strengths, (psi) | $f'_{ci}$ | 5140 | 5140 | 0.0 |
| | $f'_c$ | 6223 | 6225 | 0.0 |
| At Transfer (ends), (psi) | Top | -530 | -526 | 0.8 |
| | Bottom | 1938 | 1935 | 0.2 |
| At Service (midspan), (psi) | Top | -402 | -397 | 1.2 |
| | Bottom | 2810 | 2805 | 0.2 |
| Number of Strands | | 66 | 66 | 0.0 |
| Number of Debonded Strands | | (20+10) | (20+10) | 0.0 |
| $M_u$, (kip–ft.) | | 9801 | 9780 | 0.3 |
| $\phi M_n$, (kip–ft.) | | 12,086 | 12,118.1 | -0.3 |
| Transverse Shear Stirrup (#4 bar) Spacing, (in.) | | 8.8 | 6.5 | 26.1 |
| Maximum Camber, (ft.) | | 0.295 | 0.34 | -15.3 |

## B.1.16 REFERENCES


AASHTO (2002), *Standard Specifications for Highway Bridges*, 17th Ed., American Association of Highway and Transportation Officials (AASHTO), Inc., Washington, DC.

AASHTO (2004), *AASHTO LRFD Bridge Design Specifications*, 3rd Ed., American Association of State Highway and Transportation Officials (AASHTO), Customary U.S. Units, Washington, DC.

PCI (2003). "Precast Prestressed Concrete Bridge Design Manual," Precast/Prestressed Concrete Institute. 2nd edition.

Sinno, R. (1968). "The time-dependent deflections of prestressed concrete bridge beams," PhD. Dissertation, Texas A&M University.

TxDOT (2001). "TxDOT Bridge Design Manual," Bridge Division, Texas Department of Transportation.

TxDOT (2004). "Prestressed Concrete Beam Design/Analysis Program," User Guide, Version 4.00, Bridge Division, Texas Department of Transportation.

# Table of Contents

## B.2 Interior Texas U54 Prestressed Concrete Bridge Girder Design Using AASHTO LRFD Specifications

### *B.2.1 INTRODUCTION*

**Following is a detailed design example showing sample calculations for design of a typical interior Texas precast, prestressed concrete U54 girder supporting a single span bridge. The design is based on the *AASHTO LRFD Bridge Design Specifications, U.S.*, 3rd Edition 2004. The recommendations provided by the TxDOT Bridge Design Manual (TxDOT 2001) are considered in the design. The number of strands and concrete strength at release and at service are optimized using the TxDOT methodology.**

### *B.2.2 DESIGN PARAMETERS*

The bridge considered for design has a span length of 110 ft. (c/c abutment distance), a total width of 46 ft. and total roadway width of 44 ft. The bridge superstructure consists of four Texas U54 girders spaced 11.5 ft. center-to-center designed to act compositely with an 8 in. thick cast-in-place (CIP) concrete deck as shown in Figure B.2.2.1. The wearing surface thickness is 1.5 in., which includes the thickness of any future wearing surface. T501 type rails are considered in the design. AASHTO LRFD HL93 is the design live load. A relative humidity (RH) of 60 percent is considered in the design. The bridge cross-section is shown in Figure B.2.2.1.

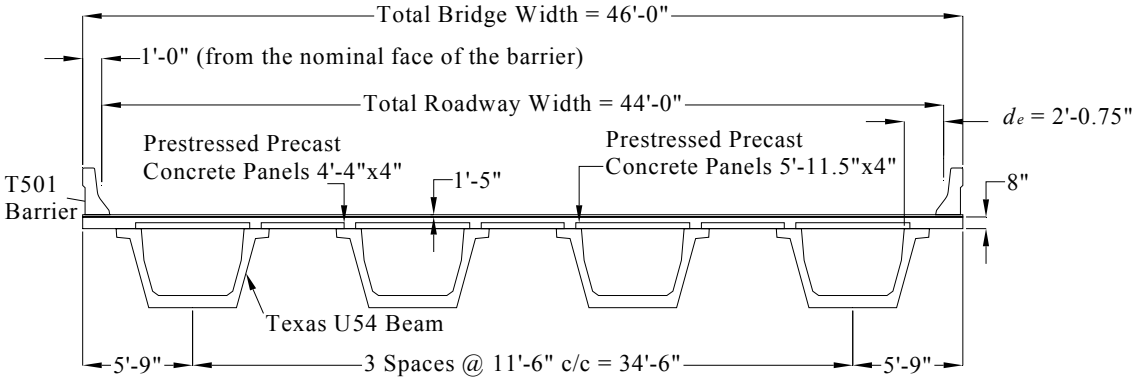


Figure B.2.2.1 Bridge Cross-Section Details.

The design span and overall girder length are based on the following calculations. Figure B.2.2.2 shows the girder end details for Texas U54 girders. It is clear that the distance between the centerline of the interior bent and end of the girder is 3 in.; and the distance between the centerline of the interior bent and the centerline of the bearings is 9.5 in.

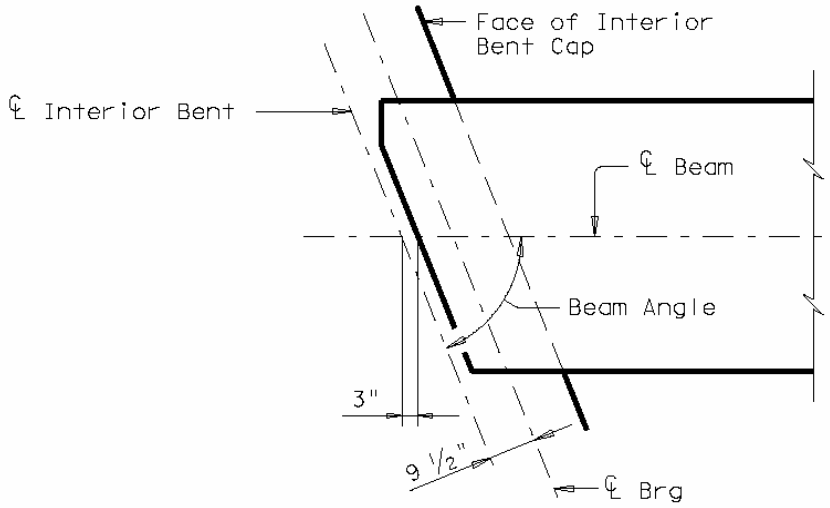


**Figure B.2.2.2 Girder End Detail for Texas U54 Girders (TxDOT Standard Drawing 2001).**

Span length (c/c interior bents) = 110 ft. – 0 in.

From Figure B.2.2.2.

Overall girder length = 110 ft. – 2(3 in.) = 109 ft. – 6 in.

Design span = 110 ft. – 2(9.5 in.) = 108 ft. – 5 in.

= 108.417 ft. (c/c of bearing)

## B.2.3 MATERIAL PROPERTIES

Cast-in-place slab:

Thickness $t_s$ = 8.0 in.

Concrete Strength at 28-days, $f'_c$ = 4000 psi

Unit weight of concrete = 150 pcf

Wearing surface:

Thickness of asphalt wearing surface (including any future wearing surfaces), $t_w$ = 1.5 in.

Unit weight of asphalt wearing surface = 140 pcf

Precast girders: Texas U54 girder

Concrete Strength at release, $f'_{ci}$ = 4000 psi*

Concrete strength at 28 days, $f'_c$ = 5000 psi*

Concrete unit weight = 150 pcf

(*This value is taken as an initial estimate and will be updated based on most optimum design)

Prestressing strands: 0.5 in. diameter, seven wire low-relaxation

Area of one strand = 0.153 in.$^2$

Ultimate tensile strength, $f_{pu}$ = 270,000 psi [LRFD Table 5.4.4.1-1]

Yield strength, $f_{py} = 0.9\ f_{pu}$ = 243,000 psi [LRFD Table 5.4.4.1-1]

Modulus of elasticity, $E_s$ = 28,500 ksi [LRFD Art. 5.4.4.2]

Stress limits for prestressing strands: [LRFD Table 5.9.3-1]

before transfer, $f_{pi} \leq 0.75\ f_{pu}$ = 202,500 psi

at service limit state (after all losses)

$f_{pe} \leq 0.80\ f_{py}$ = 194,400 psi

Non-prestressed reinforcement:

Yield strength, $f_y$ = 60,000 psi

Modulus of elasticity, $E_s$ = 29,000 ksi [LRFD Art. 5.4.3.2]

Traffic barrier:

T501 type barrier weight = 326 plf /side

## *B.2.4 CROSS-SECTION PROPERTIES FOR A TYPICAL INTERIOR GIRDER*

### *B.2.4.1 Non-Composite Section*

The section properties of a Texas U54 girder as described in the TxDOT Bridge Design Manual (TxDOT 2001) are provided in Table B.2.4.1. The strand pattern and section geometry are shown in Figure B.2.4.1.

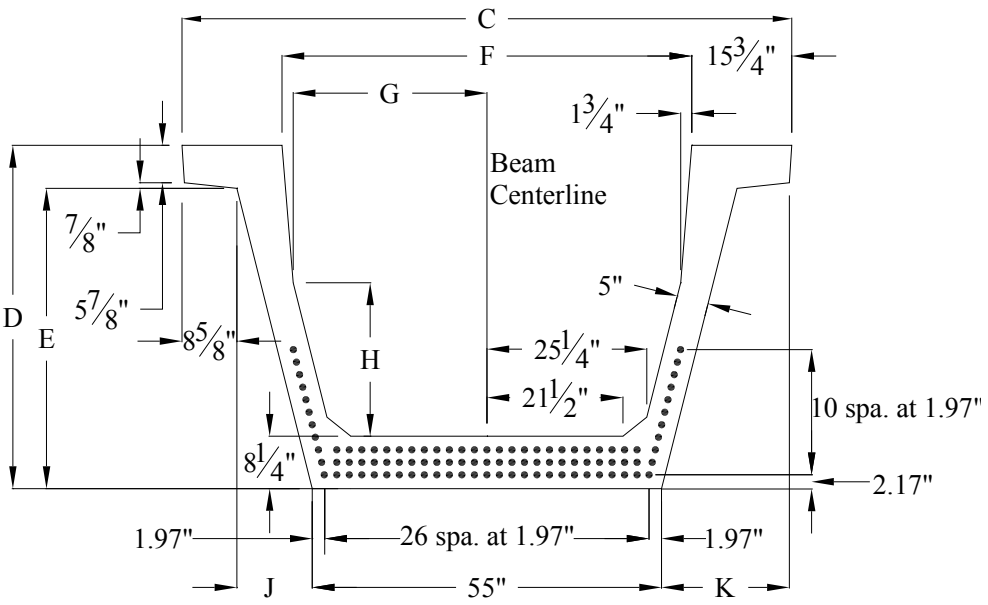


**Figure B.2.4.1 Typical Section and Strand Pattern of Texas U54 Girders (TxDOT 2001).**

**Table B.2.4.1 Section Properties of Texas U54 girders (Adapted from TxDOT Bridge Design Manual (TxDOT 2001)).**

| C | D | E | F | G | H | J | K | $y_t$ | $y_b$ | Area | $I$ | Weight |
|---|---|---|---|---|---|---|---|---|---|---|---|---|
| in. | in. | in. | in. | in. | in. | in. | in. | in. | in. | in.$^2$ | in.$^4$ | plf |
| 96 | 54 | 47.25 | 64.5 | 30.5 | 24.125 | 11.875 | 20.5 | 31.58 | 22.36 | 1120 | 403,020 | 1167 |

Note: notations as used in Figure B.4.1.

where:

$I$ = Moment of inertia about the centroid of the non-composite precast girder, in$^4$.

$y_b$ = Distance from centroid to the extreme bottom fiber of the non-composite precast girder, in.

$y_t$ = Distance from centroid to the extreme top fiber of the non-compositeprecast girder, in.

$S_b$ = Section modulus referenced to the extreme bottom fiber of the non-composite precast girder, in$^3$.
$= I/ y_b = 403{,}020/22.36 = 18{,}024.15$ in.$^3$

$S_t$ = Section modulus referenced to the extreme top fiber of the non-composite precast girder, in$^3$.
= $I/ y_t$ = 403,020/31.58 = 12,761.88 in.$^3$

### *B.2.4.2 Composite Section*
### *B.2.4.2.1 Effective Flange Width*

According to the LRFD Specifications, C4.6.2.6.1, the effective flange width of the U54 girder is determined as though each web is an individual supporting element. Figure B.2.4.2 shows the application of this assumption and the cross-hatched area of the deck slab shows the combined effective flange width for the two individual webs of adjacent U54 girders.

The effective flange width of each web may be taken as the least of

[LRFD Art. 4.6.2.6.1]

- 1/4×(effective girder span length):
$$= \frac{108.417 \text{ ft. } (12 \text{ in./ft.})}{4} = 325.25 \text{ in.}$$

- 12×(Average depth of slab) + greater of (web thickness or one-half the width of the top flange of the girder (web, in this case)) = 12× (8.0 in.) + greater of (5 in. or 15.75 in./2)
= 103.875 in.

- The average spacing of the adjacent girders (webs, in this case) = 69 in. = 5.75 ft. (controls)

For the entire U-girder the effective flange width is

= 2×(5.75 ft. ×12) = 138 in.

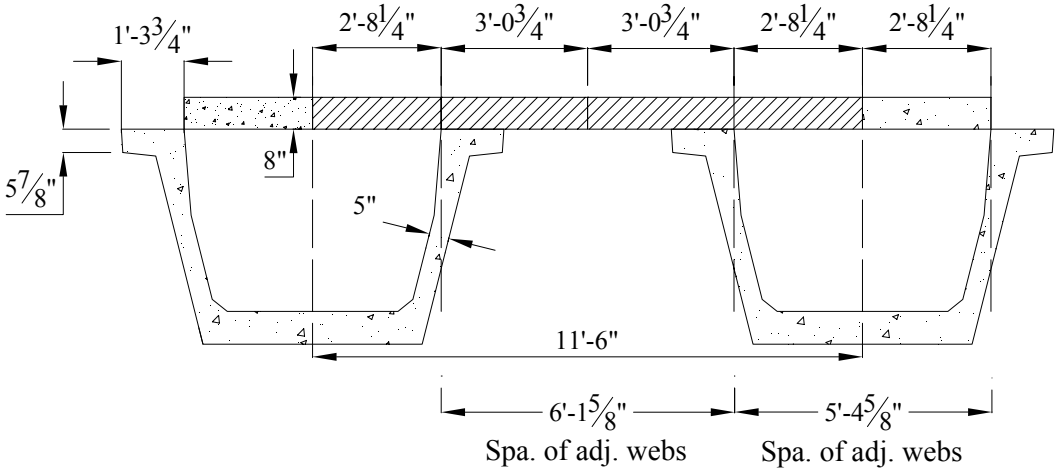


*Figure B.2.4.2 Effective Flange Width Calculations.*

### B.2.4.2.2 Modular Ratio Between Slab and Girder Concrete

Following the TxDOT Bridge Design Manual (TxDOT 2001) recommendation, the modular ratio between the slab and girder concrete is taken as 1. This assumption is used for service load design calculations. For the flexural strength limit design, shear design, and deflection calculations, the actual modular ratio based on optimized concrete strengths is used.

$$n = \left( \frac{E_c \text{ for slab}}{E_c \text{ for beam}} \right) = 1$$

where:

$n$ = Modular ratio
$E_c$ = Modulus of elasticity, ksi

Figure B.2.4.3 shows the composite section dimensions and Table B.2.4.2 shows the calculations for the transformed composite section.

### B.2.4.2.3 Transformed Section Properties

Transformed flange width = $n$ × (effective flange width)
= 1 (138 in.) = 138 in.

Transformed Flange Area = $n$ × (effective flange width) ($t_s$)
= 1 (138 in.) (8 in.) = 1104 in.$^2$

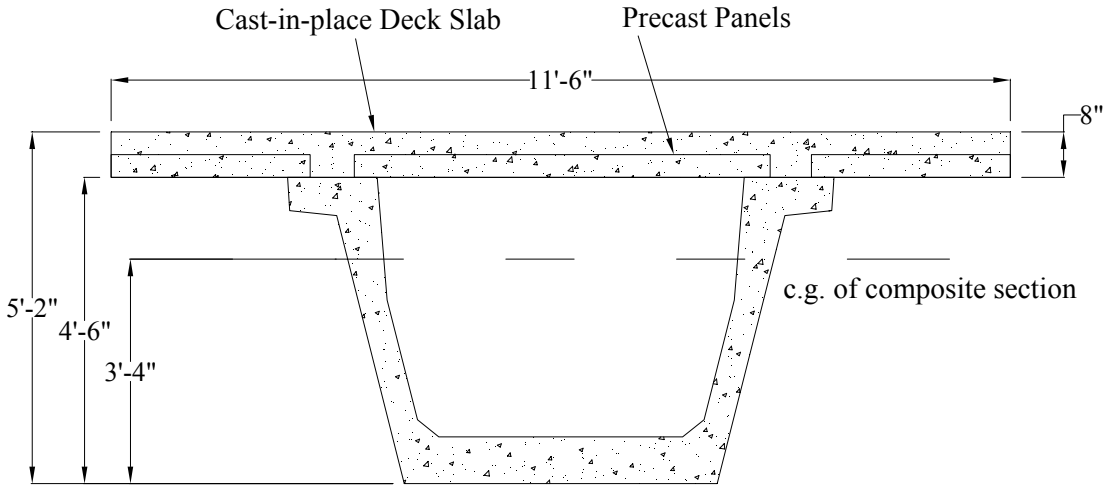


**Figure B.2.4.3 Composite Section.**

**Table B.2.4.2 Properties of Composite Section.**

| | Transformed Area in.$^2$ | $y_b$ in. | $A\,y_b$ in. | $A(y_{bc} - y_b)^2$ in.$^4$ | $I$ in.$^4$ | $I+A(y_{bc}- y_b)^2$ in.$^4$ |
|---|---|---|---|---|---|---|
| Girder | 1120 | 22.36 | 25,043.2 | 350,488.43 | 403,020 | 753,508.43 |
| Slab | 1104 | 58 | 64,032 | 355,711.62 | 5888 | 361,599.56 |
| ∑ | 2224 | | 89,075.2 | | | 1,115,107.99 |

$A_c$ = Total area of composite section = 2224 in.$^2$

$h_c$ = Total height of composite section = 62 in.

$I_c$ = Moment of inertia about the centroid of the composite section = 1,115,107.99 in.$^4$

$y_{bc}$ = Distance from the centroid of the composite section to extreme bottom fiber of the precast girder = 89,075.2 / 2224 = 40.05 in.

$y_{tg}$ = Distance from the centroid of the composite section to extreme top fiber of the precast girder = 54 – 40.05 = 13.95 in.

$y_{tc}$ = Distance from the centroid of the composite section to extreme top fiber of the slab = 62 – 40.05 = 21.95 in.

$S_{bc}$ = Composite section modulus for extreme bottom fiber of the precast girder = $I_c/y_{bc}$ = 1,115,107.99 / 40.05 = 27,842.9 in.$^3$

$S_{tg}$ = Composite section modulus for top fiber of the precast girder = $I_c/y_{tg}$ = 1,115,107.99 / 13.95 = 79,936.06 in.$^3$

$S_{tc}$ = Composite section modulus for top fiber of the slab = $I_c/y_{tc}$ = 1,115,107.99 / 21.95 = 50,802.19 in.$^3$

## *B.2.5 SHEAR FORCES AND BENDING MOMENTS*

### *B.2.5.1 Shear Forces and Bending Moments Due to Dead Loads*

#### *B.2.5.1.1 Dead Loads*

Self-weight of the girder = 1.167 kips/ft.

[TxDOT Bridge Design Manual (TxDOT 2001)]

Weight of CIP deck and precast panels on each girder

$$= (0.150 \text{ pcf})\left(\frac{8 \text{ in.}}{12 \text{ in./ft.}}\right)\left(\frac{138 \text{ in.}}{12 \text{ in./ft.}}\right)$$

$$= 1.15 \text{ kips/ft.}$$

#### *B.2.5.1.2 Superimposed Dead Loads*

Superimposed dead loads are the dead loads assumed to act after the composite action between girders and deck slab is developed. The LRFD specifications, Art. 4.6.2.2.1, states that permanent loads (rail, sidewalks and future wearing surface) may be distributed uniformly among all girders if the following conditions are met:

1. Width of the deck is constant (O.K.)

2. Number of girders, $N_b$, is not less than four ($N_b = 4$) (O.K.)
3. The roadway part of the overhang, $d_e \leq 3.0$ ft.
   $d_e = 5.75 - 1.0 - 27.5/12 - 4.75/12 = 2.063$ ft. (O.K.)

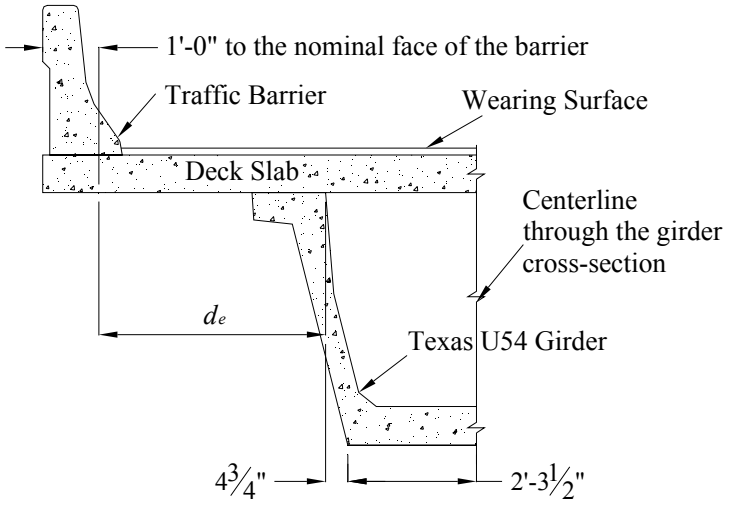


*Figure B.2.5.1 Illustration of $d_e$ Calculation.*

4. Curvature in plan is less than 4 degrees (curvature is 0 degree) (O.K.)
5. Cross-section of the bridge is consistent with one of the cross-sections given in Table 4.6.2.2.1-1 in LRFD Specifications, the girder type is (c) – spread box beams (O.K.)

Since these criteria are satisfied, the barrier and wearing surface loads are equally distributed among the four girders.

***B.2.5.1.2.1 Due to Diaphragm***

TxDOT Bridge Design Manual (TxDOT 2001) requires two interior diaphragms with U54 girder, located as close as 10 ft. from the midspan of the girder. Shear forces and bending moment values in the interior girder can be calculated using the following equations. The placement of the diaphragms is shown in Figure 2.5.2.

For $x = 0$ ft. – 44.21 ft.

$V_x = 3$ kips $\qquad M_x = 3x$ kips

For $x = 44.21$ ft. – 54.21 ft.

$V_x = 0$ kips $\qquad M_x = 3x - 3(x - 44.21)$ kips

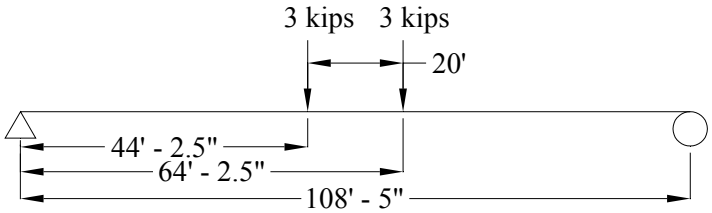


**Figure B.2.5.2 Location of Interior Diaphragms on a Simply Supported Bridge Girder.**

***B.2.5.1.2.2 Due to Haunch***

For a U54 girder bridge design, TxDOT accounts for haunches in designs that require special geometry and where the haunch will be large enough to have a significant impact on the overall girder. Because this study is for typical bridges, a haunch will not be included for U54 girders for composite properties of the section and additional dead load considerations.

***B.2.5.1.2.3 Due to T501 Rail***

The TxDOT Bridge Design Manual recommends (TxDOT 2001, Chap. 7 Sec. 24) that 1/3 of the rail dead load should be used for an interior girder adjacent to the exterior girder.

$$\text{Weight of T501 rails or barriers on each interior girder} = \left(\frac{326 \text{ plf}/1000}{3}\right)$$

$$= 0.109 \text{ kips/ft./interior girder}$$

***B.2.5.1.2.4 Due to Wearing Surface***

$$\text{Weight of 1.5 in. wearing surface} = \frac{(0.140 \text{ pcf})\left(\frac{1.5 \text{ in.}}{12 \text{ in./ft.}}\right)(44 \text{ ft.})}{4 \text{ beams}}$$

$$= 0.193 \text{ kips/ft.}$$

Total superimposed dead load = 0.109 + 0.193 = 0.302 kips/ft.

***B.2.5.1.3 Unfactored Shear Forces and Bending Moments***

Shear forces and bending moments in the girder due to dead loads, superimposed dead loads at every tenth of the design span, and at critical sections (midspan and critical section for shear) are provided in this section. The critical section for shear design is determined by an iterative procedure later in the example. The bending moment ($M$) and shear force ($V$) due to uniform dead loads and uniform superimposed dead loads at any section at a distance $x$ are calculated using the following expressions, where the uniform dead load is denoted as $w$.

$$M = 0.5wx\,(L - x)$$

$$V = w\,(0.5L - x)$$

The shear forces and bending moments due to dead loads and superimposed dead loads are shown in Tables B.2.5.1 and B.2.5.2. respectively.

**Table B.2.5.1 Shear Forces due to Dead Loads.**

| Distance | Section | Non-Composite Dead Loads | | | Superimposed Dead Loads | | Total Dead Load Shear Force |
|---|---|---|---|---|---|---|---|
| $x$ | $x/L$ | Girder Weight $V_g$ | Slab Weight $V_{slab}$ | Diaphram Weight $V_{dia}$ | Barrier Weight $V_b$ | Wearing Surface Weight $V_{ws}$ | |
| ft. | | kips | kips | kips | kips | kips | kips |
| 0.375 | 0.003 | 62.82 | 61.91 | 3.00 | 5.87 | 10.39 | 143.99 |
| 5.503 | 0.051 | 56.84 | 56.01 | 3.00 | 5.31 | 9.40 | 130.56 |
| 10.842 | 0.100 | 50.61 | 49.87 | 3.00 | 4.73 | 8.37 | 116.58 |
| 21.683 | 0.200 | 37.96 | 37.40 | 3.00 | 3.55 | 6.28 | 88.19 |
| 32.525 | 0.300 | 25.30 | 24.94 | 3.00 | 2.36 | 4.18 | 59.78 |
| 43.367 | 0.400 | 12.65 | 12.47 | 3.00 | 1.18 | 2.09 | 31.39 |
| 54.209 | 0.500 | 0.00 | 0.00 | 0.00 | 0.00 | 0.00 | 0.00 |

**Table B.2.5.2 Bending Moments due to Dead Loads.**

| Distance | Section | Non-Composite Dead Loads | | | Superimposed Dead Loads | | Total Dead Load Moment |
|---|---|---|---|---|---|---|---|
| $x$ | $x/L$ | Girder Weight $M_g$ | Slab Weight $M_{slab}$ | Diaphram Weight $M_{dia}$ | Barrier Weight $M_b$ | Wearing Surface Weight $M_{ws}$ | |
| ft. | | k-ft. | k-ft. | k-ft. | k-ft. | k-ft. | k-ft. |
| 0.375 | 0.003 | 23.64 | 23.30 | 1.13 | 2.21 | 3.91 | 54.19 |
| 5.503 | 0.051 | 330.46 | 325.64 | 16.51 | 30.87 | 54.65 | 758.13 |
| 10.842 | 0.100 | 617.29 | 608.30 | 32.53 | 57.66 | 102.09 | 1417.87 |
| 21.683 | 0.200 | 1097.36 | 1081.38 | 65.05 | 102.50 | 181.48 | 2527.77 |
| 32.525 | 0.300 | 1440.30 | 1419.32 | 97.58 | 134.53 | 238.20 | 3329.93 |
| 43.367 | 0.400 | 1646.07 | 1622.09 | 130.10 | 153.75 | 272.23 | 3824.24 |
| 54.209 | 0.500 | 1714.65 | 1689.67 | 132.63 | 160.15 | 283.57 | 3980.67 |

### *B.2.5.2 Shear Forces and Bending Moments due to Live Load*

#### *B.2.5.2.1 Live Load*

[LRFD Art. 3.6.1.2.1]

The LRFD Specifications specify a significantly different live load as compared to the Standard Specifications. The LRFD design live load is designated as HL-93, which consists of a combination of:

- Design truck with dynamic allowance or design tandem with dynamic allowance, whichever produces greater moments and shears, and
- Design lane load without dynamic allowance

[LRFD Art. 3.6.1.2.2]

The design truck consists of an 8 kips front axle and two 32 kip rear axles. The distance between the axles is constant at 14 ft.

[LRFD Art. 3.6.1.2.3]

The design tandem consists of a pair of 25 kip axles spaced 4.0 ft. apart. However, the tandem loading governs for shorter spans (i.e. spans lesser than 40 ft.)

[LRFD Art. 3.6.1.2.4]

The lane load consists of a load of 0.64 klf uniformly distributed in the longitudinal direction.

#### *B.2.5.2.2 Live Load Distribution Factor for Typical Interior Girder*

[LRFD Art. 4.6.2.2]

The bending moments and shear forces due to vehicular live load can be distributed to individual girders using the simplified approximate distribution factor formulas specified by the LRFD Specifications. However, the simplified live load distribution factor formulas can be used only if the following conditions are met:

1. Width of the slab is constant (O.K.)
2. Number of girders, $N_b$, is not less than four ($N_b = 4$) (O.K.)
3. Girders are parallel and of the same stiffness (O.K.)
4. The roadway part of the overhang, $d_e \leq 3.0$ ft.
   $d_e = 5.75 - 1.0 - 27.5/12 - 4.75/12 = 2.063$ ft. (O.K.)
5. Curvature in plan is less than 4 degrees (curvature is 0 degrees) (O.K.)
6. Cross-section of the bridge girder is consistent with one of the cross-sections given in [LRFD Table 4.6.2.2.1-1], the girder type is (c) – spread box beams (O.K.)

The number of design lanes is computed as:

Number of design lanes = the integer part of the ratio of ($w$/12), where $w$ is the clear roadway width, in ft., between curbs/or barriers

[LRFD Art. 3.6.1.1.1]

$w$ = 44 ft.

Number of design lanes = integer part of (44 ft./12) = 3 lanes

The LRFD Table 4.6.2.2.2b-1 specifies the approximate vehicular live load moment distribution factors for interior girders.

For two or more design lanes loaded:

***B.2.5.2.3 Distribution Factor for Bending Moment***

$$DFM = \left(\frac{S}{6.3}\right)^{0.6}\left(\frac{Sd}{12.0L^2}\right)^{0.125}$$ [LRFD Table 4.6.2.2.2b-1]

Provided that:

| | | |
|---|---|---|
| $6.0 \le S \le 18.0$; | $S$ = 11.5 ft. | (O.K.) |
| $20 \le L \le 140$; | $L$ = 108.417 ft. | (O.K.) |
| $18 \le d \le 65$; | $d$ = 54 in. | (O.K.) |
| $N_b \ge 3$; | $N_b$ = 4 | (O.K.) |

where:

$DFM$ = Live load moment distribution factor for interior girder

$S$ = Girder spacing, ft.

$L$ = Girder span, ft.

$D$ = Depth of the girder, ft.

$N_b$ = Number of girders

$$DFM = \left(\frac{11.5}{6.3}\right)^{0.6}\left(\frac{11.5\times 54}{12.0\times(108.417)^2}\right)^{0.125} = 0.728 \text{ lanes/girder}$$

For one design lane loaded:

$$DFM = \left(\frac{S}{3.0}\right)^{0.35}\left(\frac{Sd}{12.0L^2}\right)^{0.25}$$ [LRFD Table 4.6.2.2.2b-1]

$$DFM = \left(\frac{11.5}{3.0}\right)^{0.35}\left(\frac{11.5\times 54}{12.0\times(108.417)^2}\right)^{0.25} = 0.412 \text{ lanes/girder}$$

Thus, the case for two or more lanes loaded controls and
$DFM = 0.728$ lanes/girder.

***B.2.5.2.4 Distribution Factor for Shear Force***

The LRFD Table 4.6.2.2.3a-1 specifies the approximate vehicular live load shear distribution factors for interior girders.

For two or more design lanes loaded:

$$DFV = \left(\frac{S}{7.4}\right)^{0.8}\left(\frac{d}{12.0L}\right)^{0.1} \qquad \text{[LRFD Table 4.6.2.2.3a-1]}$$

Provided that:

| | | |
|---|---|---|
| $6.0 \le S \le 18.0$; | $S = 11.5$ ft. | (O.K.) |
| $20 \le L \le 140$; | $L = 108.417$ ft. | (O.K.) |
| $18 \le d \le 65$; | $d = 54$ in. | (O.K.) |
| $N_b \ge 3$; | $N_b = 4$ | (O.K.) |

where:

$DFV$ = Live load shear distribution factor for interior girder
$S$ = Girder spacing, ft.
$L$ = Girder span, ft.
$D$ = Depth of the girder, ft.
$N_b$ = Number of girders

$$DFV = \left(\frac{11.5}{7.4}\right)^{0.8}\left(\frac{54}{12.0\times 108.417}\right)^{0.1} = 1.035 \text{ lanes/girder}$$

For one design lane loaded:

$$DFV = \left(\frac{S}{10}\right)^{0.6}\left(\frac{d}{12.0L}\right)^{0.1} \qquad \text{[LRFD Table 4.6.2.2.3a-1]}$$

$$DFV = \left(\frac{11.5}{10}\right)^{0.6}\left(\frac{54}{12.0\times 108.417}\right)^{0.1} = 0.791 \text{ lanes/girder}$$

Thus, the case for two or more lanes loaded controls and
$DFV = 1.035$ lanes/girder

### B.2.5.2.6 Skew Correction

LRFD Article 4.6.2.2.2e specifies the skew correction factors for load distribution factors for bending moment in longitudinal girders on skewed supports. LRFD Table 4.6.2.2.2e-1 presents the skew correction factor formulas for type c girders (spread box beams).

For type c girders the skew correction factor is given by the following formula:

For $0^\circ \leq \theta \geq 60^\circ$,

$$\text{Skew Correction} = 1.05 - 0.25 \tan\theta \leq 1.0$$

If $\theta > 60^\circ$, use $\theta = 60^\circ$

The LRFD Specifications specify the skew correction for shear in the obtuse corner of the skewed bridge plan. This design example considers only the interior girders, which are not in the obtuse corner of a skewed bridge. Therefore, the distribution factors for shear are not reduced for skew.

### B.2.5.2.7 Dynamic Allowance

The LRFD Specifications specify the dynamic load effects as a percentage of the static live load effects. LRFD Table 3.6.2.1.-1 specifies the dynamic allowance to be taken as 33 percent of the static load effects for all limit states except the fatigue limit state, and 15 percent for the fatigue limit state. The factor to be applied to the static load shall be taken as:

$$(1 + IM/100)$$

where:

$IM$ = dynamic load allowance, applied to truck load only

$IM$ = 33 percent

### B.2.5.2.8 Undistributed Shear Forces and Bending Moments

The maximum shear force $V_T$ and bending moment $M_T$ due to the HS-20 truck loading for all limit states, except for the fatigue limit state, on a per-lane-basis are calculated using the following equations given in the *PCI Bridge Design Manual* (PCI 2003):

#### B.2.5.2.8.1 Due to Truck Load, $V_{LT}$ and $M_{LT}$

Maximum undistributed bending moment,

For $x/L = 0 - 0.333$

$$M_T = \frac{72(x)[(L - x) - 9.33]}{L}$$

For $x/L = 0.333 - 0.5$

$$M_T = \frac{72(x)[(L - x) - 4.67]}{L} - 112$$

Maximum undistributed shear force,

For $x/L = 0 - 0.5$

$$V_T = \frac{72[(L - x) - 9.33]}{L}$$

where:

$x$ = Distance from the center of the bearing to the section at which bending moment or shear force is calculated, ft.

$L$ = Design span length = 108.417 ft.

$M_T$ = Maximum undistributed bending moment due to HS-20 truck loading

$V_T$ = Maximum undistributed shear force due to HS-20 truck loading

Distributed bending moment due to truck load including dynamic load allowance ($M_{LT}$) is calculated as follows:

$$M_{LT} = (M_T)\ (DFM)\ (1+IM/100)$$
$$= (M_T)\ (0.728)\ (1+0.33)$$
$$= (M_T)\ (0.968) \text{ k-ft.}$$

Distributed shear force due to truck load including dynamic load allowance ($V_{LT}$) is calculated as follows:

$$V_{LT} = (V_T)\ (DFV)\ (1+IM/100)$$
$$= (V_T)\ (1.035)\ (1+0.33)$$
$$= (V_T)\ (1.378) \text{ kips}$$

where:

*DFM* = Live load moment distribution factor for interior girders

*DFV* = Live load shear distribution factor for interior girders

The maximum bending moments and shear forces due to HS-20 truck load are calculated at every tenth of the span and at critical section for shear. The values are presented in Table B.2.5.

***B.2.5.2.8.2 Due to Tandem Load, $V_{TA}$ and $M_{TA}$***

The maximum shear forces $V_{TA}$ and bending moments $M_{TA}$ due to design tandem loading for all limit states, except for the fatigue limit state, on a per-lane-basis due to HL93 tandem loadings are calculated using the following equations:

Maximum undistributed bending moment,
For $x/L = 0 – 0.5$

$$M_{TA} = 50(x)\left(\frac{L-x-2}{L}\right)$$

Maximum undistributed shear force,
For $x/L = 0 - 0.5$

$$V_{TA} = 50\left(\frac{L-x-2}{L}\right)$$

The distributed bending moment $M_{TA}$ and distributed shear forces $V_{TA}$ are calculated in the same way as for the HL93 truck loading, as shown in section B.2.5.2.7.1.

***B.2.5.2.8.3 Due to Lane Load, $V_L$ and $M_L$***

The maximum bending moments $M_L$ and maximum shear forces $V_L$ due to uniformly distributed lane load of 0.64 kip/ft. are calculated using the following equations given in *PCI Bridge Design Manual* (PCI 2003):

Maximum undistributed bending moment, $M_L = 0.5(w)(x)(L-x)$

Maximum undistributed shear force, $V_L = \dfrac{0.32\times(L-x)^2}{L}$ *for* $x \le 0.5L$

where:

$M_L$ = Maximum undistributed bending moment due to HL-93 lane loading (k-ft.)

$V_L$ = Maximum undistributed shear force due to HL-93 lane loading (kips)

$w$ = Uniform load per linear foot of load lane = 0.64 klf

Note that maximum shear force at a section is calculated at a section by placing the uniform load on the right of the section considered, as given in *PCI Bridge Design Manual* (PCI 2003). This method yields a conservative estimate of the shear force as compared to the shear force at a section under uniform load placed on the entire span length. The critical load placement for shear due to lane loading is shown in Figure B.2.5.3.

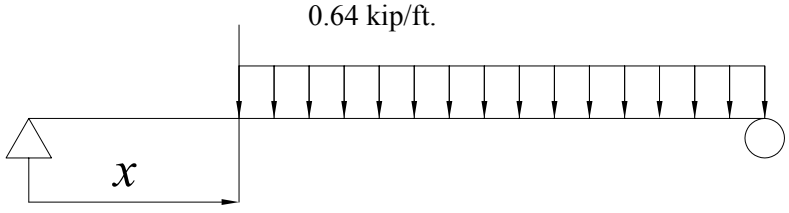


**Figure B.2.5.3 Design Lane Loading for Calculation of the Undistributed Shear.**

Distributed bending moment due to lane load ($M_{LL}$) is calculated as follows:

$$M_{LL} = (M_L)\ (DFM)$$
$$= (M_L)\ (0.728) \text{ k-ft.}$$

Distributed shear force due to lane load ($V_{LL}$) is calculated as follows:

$$V_{LL} = (V_L)\ (DFV)$$
$$= (V_L)\ (1.035) \text{ kips}$$

The maximum bending moments and maximum shear forces due to HL-93 lane loading are calculated at every tenth of the span and at critical section for shear. The values are presented in Table B.2.5.3.

**Table B.2.5.3 Shear forces and Bending Moments due to Live Loads.**

| Distance from Bearing Centerline | Section | HS-20 Truck Load with Impact (controls) | | Lane Load | | Tandem Load with Impact | |
|---|---|---|---|---|---|---|---|
| | | $V_{LT}$ | $M_{LT}$ | $V_L$ | $M_L$ | $V_{TA}$ | $M_{TA}$ |
| $x$ | $x/L$ | Shear | Moment | Shear | Moment | Shear | Moment |
| ft. | | kips | k-ft. | kips | k-ft. | kips | k-ft. |
| 0.375 | 0.000 | 90.24 | 23.81 | 35.66 | 9.44 | 67.32 | 17.76 |
| 6.000 | 0.055 | 85.10 | 359.14 | 32.04 | 143.15 | 64.06 | 247.97 |
| 10.842 | 0.100 | 80.67 | 615.45 | 29.08 | 246.55 | 60.67 | 462.71 |
| 21.683 | 0.200 | 70.76 | 1079.64 | 22.98 | 438.30 | 53.79 | 820.41 |
| 32.525 | 0.300 | 60.85 | 1392.64 | 17.59 | 575.27 | 46.91 | 1073.17 |
| 43.370 | 0.400 | 50.93 | 1575.96 | 12.93 | 657.47 | 40.03 | 1220.96 |
| 54.210 | 0.500 | 41.03 | 1618.96 | 8.98 | 684.85 | 33.14 | 1263.76 |

### *B.2.5.3 Load Combinations*

LRFD Art. 3.4.1 specifies load factors and load combinations. The total factored load effect is specified to be taken as:

$$Q = \sum \eta_i \gamma_i Q_i \qquad \text{[LRFD Eq. 3.4.1-1]}$$

where:

$Q$ = Factored force effects.

$Q_i$ = Unfactored force effects.

$\gamma_i$ = Load factor, a statistically determined multiplier applied to force effects specified by LRFD Table 3.4.1-1.

$\eta_i$ = Load modifier, a factor relating to ductility, redundancy and operational importrance.

= $\eta_D \eta_R \eta_I \geq 0.95$, for loads for which a maximum value of $\gamma_i$ is appropriate. [LRFD Eq. 1.3.2.1-2]

= $1/(\eta_D \eta_R \eta_I) \leq 1.0$, for loads for which a minimum value of $\gamma_i$ is appropriate. [LRFD Eq. 1.3.2.1-3]

$\eta_D$ = A factor relating to ductility.
= 1.00 for all limit states except strength limit state.

For the strength limit state:

$\eta_D$ $\geq$ 1.05 for non ductile components and connections.
$\eta_D$ = 1.00 for conventional design and details complying with the LRFD Specifications.
$\eta_D$ $\leq$ 0.95 for components and connections for which additional ductility-enhancing measures have been specified beyond those required by the LRFD Specifications.

$\eta_D$ = 1.00 is used in this example for strength and service limit states as this design is considered to be conventional and complying with the LRFD Specifications.

$\eta_R$ = A factor relating to redundancy.
= 1.00 for all limit states except strength limit state.

For the strength limit state:

$\eta_R$ $\geq$ 1.05 for nonredundant members.
$\eta_R$ = 1.00 for conventional levels of redundancy.
$\eta_R$ $\leq$ 0.95 for exceptional levels of redundancy.

$\eta_R$ = 1.00 is used in this example for strength and service limit states as this design is considered to be conventional level of redundancy to the structure.

$\eta_D$ = A factor relating to operational importance.
= 1.00 for all limit states except strength limit state.

For the strength limit state:

$\eta_I$ $\geq$ 1.05 for important bridges.
$\eta_I$ = 1.00 for typical bridges.
$\eta_I$ $\leq$ 0.95 for relatively less important bridges.

$\eta_I$ = 1.00 is used in this example for strength and service limit states as this example illustrates the design of a typical bridge.

$\eta_i$ = $\eta_D \eta_R \eta_I$ = 1.00 for this example

The LRFD Art. 3.4.1 specifies load combinations for various limit states. The load combinations pertinent to this design example are shown in the following.

Service I: Check compressive stresses in prestressed concrete components:
$Q = 1.00(DC + DW) + 1.00(LL + IM)$ [LRFD Table 3.4.1-1]

Service III: Check tensile stresses in prestressed concrete components:
$Q = 1.00(DC + DW) + 0.80(LL + IM)$ [LRFD Table 3.4.1-1]

Strength I: Check ultimate strength: [LRFD Table 3.4.1-1 & 2]
Maximum $Q = 1.25(DC) + 1.50(DW) + 1.75(LL + IM)$

Minimum $Q = 0.90(DC) + 0.65(DW) + 1.75(LL + IM)$

where:

$DC$ = Dead load of structural components and non-structural attachments.

$DW$ = Dead load of wearing surface and utilities.

$LL$ = Vehicular live load.

$IM$ = Vehicular dynamic load allowance.

## B.2.6 ESTIMATION OF REQUIRED PRESTRESS

The preliminary estimate of the required prestress and number of strands is based on the stresses at midspan

### B.2.6.1 Service Load Stresses at Midspan

Bottom tensile stresses (SERVICE III) at midspan due to applied loads

$$f_b = \frac{M_g + M_S}{S_b} + \frac{M_b + M_{ws} + 0.8(M_{LT} + M_{LL})}{S_{bc}}$$

Top compressive stresses (SERVICE I) at midspan due to applied loads

$$f_t = \frac{M_g + M_S}{S_t} + \frac{M_b + M_{ws} + M_{LT} + M_{LL}}{S_{tg}}$$

where:

$f_b$ = Concrete stress at the bottom fiber of the girder, ksi

$f_t$ = Concrete stress at the top fiber of the girder, ksi

$M_g$ = Unfactored bending moment due to girder self-weight, k-ft.

$M_S$ = Unfactored bending moment due to slab and diaphragm weight, k-ft.

$M_b$ = Unfactored bending moment due to barrier weight, k-ft.

$M_{ws}$ = Unfactored bending moment due to wearing surface, k-ft.

$M_{LT}$ = Factored bending moment due to truck load, k-ft.

$M_{LL}$ = Factored bending moment due to lane load, k-ft.

Substituting the bending moments and section modulus values, bottom tensile stress at midspan is:

$$f_b = \left( \frac{(1714.65+1689.67+132.63)(12)}{18,024.15} + \frac{(160.15+283.57+0.8\times(1618.3+684.57))(12)}{27,842.9} \right) = 3.34 \text{ ksi}$$

$$f_t = \left( \frac{(1714.65+1689.67+132.63)(12)}{12,761.88} + \frac{(160.15+283.57+1618.3+684.57)(12)}{79,936.06} \right) = 3.738 \text{ ksi}$$

***B.2.6.2 Allowable Stress Limit***

At service load conditions, allowable tensile stress is

$f_c'$ = specified 28-day concrete strength of girder (initial guess), 5,000 psi

$F_b = 0.19\sqrt{f_c'(ksi)} = 0.19\sqrt{5} = 0.425$ ksi [LRFD Table. 5.9.4.2.2-1]

***B.2.6.3 Required Number of Strands***

Required precompressive stress in the bottom fiber after losses:

Bottom tensile stress – allowable tensile stress at final = $f_b - F_b$

= 3.34 – 0.425 = 2.915 ksi

Assuming the distance from the center of gravity of strands to the bottom fiber of the girder is equal to $y_{bs}$ = 2 in.

Strand eccentricity at midspan:

$e_c = y_b - y_{bs}$ = 22.36 – 2 = 20.36 in.

Bottom fiber stress due to prestress after losses:

$$f_b = \frac{P_{se}}{A} + \frac{P_{se}\ e_c}{S_b}$$

where, $P_{se}$ = effective pretension force after all losses

$$2.915 = \frac{P_{se}}{1120} + \frac{20.36\ P_{se}}{18024.15}$$

Solving for $P_{se}$ we get,

$P_{se}$ = 1441.319 kips

Assuming final losses = 20 percent of $f_{pi}$

Assumed final losses = 0.2(202.5 ksi) = 40.5 ksi

The prestress force per strand after losses

= (cross-sectional area of one strand) ($f_{pe}$ )

= 0.153 × (202.5-40.5) = 24.786 kips

Number of strands required = 1441.319 /24.786 = 58.151

Try 60 – ½ in. diameter, 270 ksi strands

Strand eccentricity at midspan after strand arrangement

$$e_c = 22.36 - \frac{27(2.17)+27(4.14)+6(6.11)}{60} = 18.91 \text{ in.}$$

$P_{se}$ = 60(24.786) = 1487.16 kips

$$f_b = \frac{1487.16}{1120} + \frac{18.91(1487.16)}{18024.15}$$

$$= 1.328 + 1.56 = 2.888 \text{ ksi} < 2.915 \text{ ksi} \qquad \text{(N.G.)}$$

Try 62 – ½ in. diameter, 270 ksi strands

Strand eccentricity at midspan after strand arrangement

$$e_c = 22.36 - \frac{27(2.17)+27(4.14)+8(6.11)}{62} = 18.824 \text{ in.}$$

$P_{se}$ = 62(24.786) = 1536.732 kips

$$f_b = \frac{1536.732}{1120} + \frac{18.824(1536.732)}{18024.15}$$

$$= 1.372 + 1.605 = 2.977 \text{ ksi} > 2.915 \text{ ksi}$$

Therefore, use 62 strands

| Number of Strands | Distance from bottom (in.) |
|---|---|
| 27 | 2.17 |
| 27 | 4.14 |
| 8 | 6.11 |

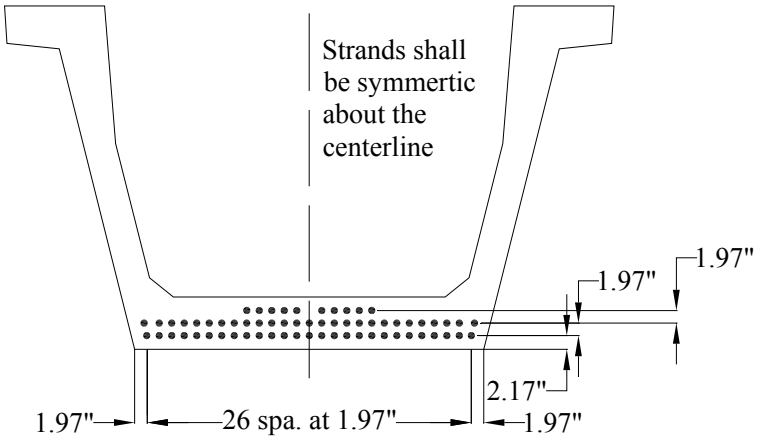


**Figure B.2.6.1 Initial Strand Pattern.**

### *B.2.7 PRESTRESS LOSSES*

Total prestress losses = $\Delta f_{pES} + \Delta f_{pSR} + \Delta f_{pCR} + \Delta f_{pR2}$ [LRFD Eq. 5.9.5.1-1]

where:

$\Delta f_{pSR}$ = Loss of prestress due to concrete shrinkage

$\Delta f_{pES}$ = Loss of prestress due to elastic shortening

$\Delta f_{pCR}$ = Loss of prestress due to creep of concrete

$\Delta f_{pR2}$ = Loss of prestress due to relaxation of Prestressing steel after transfer

Number of strands = 62

A number of iterations will be performed to arrive at the optimum $f'_c$ and $f'_{ci}$

### B.2.7.1 Iteration 1

### B.2.7.1.1 Concrete Shrinkage

$$\Delta f_{pSR} = (17.0 - 0.15\,H) \qquad \text{[LRFD Eq. 5.9.5.4.2-1]}$$

where:

$H$ = Relative humidity = 60 percent

$$\Delta f_{pSR} = [17.0 - 0.150(60)]\frac{1}{1000} = 8 \text{ ksi}$$

### B.2.7.1.2 Elastic Shortening

$$\Delta f_{pES} = \frac{E_p}{E_{ci}} f_{cgp} \qquad \text{[LRFD Eq. 5.9.5.2.3a-1]}$$

where:

$$f_{cgp} = \frac{P_{si}}{A} + \frac{P_{si}\,e_c^{\,2}}{I} - \frac{(M_g)e_c}{I}$$

The LRFD Specifications, Art. 5.9.5.2.3a, states that $f_{cgp}$ can be calculated on the basis of prestressing steel stress assumed to be $0.7f_{pu}$ for low-relaxation strands. However, we will assume the initial losses as a percentage of initial prestressing stress before release, $f_{pi}$. The assumed initial losses shall be be checked and if different from the assumed value, a second iteration will be carried on. Moreover, iterations may also be required if the $f'_{ci}$ value doesn't match that calculated in a previous step.

where:

$f_{cgp}$ = Sum of the concrete stresses at the center of gravity of the prestressing tendons due to prestressing force and the self-weight of the member at the sections of the maximum moment (ksi)

$P_{si}$ = Pretension force after allowing for the initial losses,

As the initial losses are unknown at this point, 8 percent initial loss in prestress is assumed as a first estimate.

$P_{si}$ = (number of strands)(area of each strand)[0.92(0.75 $f_{pu}$)]

= 62(0.153)(0.92)(0.75)(270) = 1767.242 kips

$M_g$ = Unfactored bending moment due to girder self-weight

= 1714.64 k-ft.

$e_c$ = Eccentricity of the strand at the midspan = 18.824 in.

$$f_{cgp} = \frac{1767.242}{1120} + \frac{1767.242(18.824)^2}{403020} - \frac{1714.64(12)(18.824)}{403020}$$

$= 1.578 + 1.554 - 0.961 = 2.171$ ksi

Initial estimate for concrete strength at release, $f'_{ci} = 4000$ psi

$$E_{ci} = (150)^{1.5}(33)\sqrt{4000}\ \frac{1}{1000} = 3834.254 \text{ ksi}$$

$$\Delta f_{pES} = \frac{28500}{3834.254}(2.171) = 16.137 \text{ ksi}$$

***B.2.7.1.3 Creep of Concrete***

$$\Delta f_{pCR} = 12 f_{cgp} - 7\Delta f_{cdp} \qquad \text{[LRFD Eq. 5.9.5.4.3-1]}$$

where:

$\Delta f_{cdp}$ = Change in the concrete stress at center of gravity of prestressing steel due to permanent loads, with the exception of the load acting at the time the prestressing force is applied. Values of $\Delta f_{cdp}$ should be calculated at the same section or at sections for which $f_{cgp}$ is calculated. (ksi)

$$\Delta f_{cdp} = \frac{(M_{slab} + M_{dia})e_c}{I} + \frac{(M_b + M_{ws})(y_{bc} - y_{bs})}{I_c}$$

where:

$y_{bc}$ = 40.05 in.

$y_{bs}$ = The distance from center of gravity of the strand at midspan to the bottom of the girder = 22.36 – 18.824 = 3.536 in.

$I$ = Moment of inertia of the non-composite section = 403,020 in.$^4$

$I_c$ = Moment of inertia of composite section = 1,115,107.99 in.$^4$

$$f_{cdp} = \frac{(1689.67+132.63)(12)(18.824)}{403020} + \frac{(160.15+283.57)(12)(37.54 - 3.536)}{1115107.99}$$

$= 1.021 + 0.174 = 1.195$ ksi

$\Delta f_{pCR} = 12(2.171) - 7(1.195) = 17.687$ ksi.

***B.2.7.1.4 Relaxation of Prestressing Steel***

For pretensioned members with 270 ksi low-relaxation strand conforming to AASHTO M 203 [LRFD Art. 5.9.5.4.4c]

Relaxation loss after Transfer,

$\Delta f_{pR2} = 0.3\ [20.0 - 0.4\ \Delta f_{pES} - 0.2(\Delta f_{pSR} + \Delta f_{pCR})]$ [LRFD Eq. 5.9.5.4.4c-1]

$= 0.3\ [20.0 - 0.4(16.137) - 0.2(8 + 17.687)] = 2.522$ ksi

Relaxation loss before Transfer,

Initial relaxation loss, $\Delta f_{pR1}$, is generally determined and accounted for by the Fabricator. However, $\Delta f_{pR1}$ is calculated and included in the losses calculations for demonstration purpose and alternatively, it can be assumed to be zero. A total of 0.5 day time period is assumed between stressing of strands and initial transfer of prestress force. As per LRFD Commentary C.5.9.5.4.4, $f_{pj}$ is assumed to be $0.8 \times f_{pu}$ for this example.

$$\Delta f_{pR1} = \frac{\log(24.0 \times t)}{40.0}\left[\frac{f_{pj}}{f_{py}} - 0.55\right] f_{pj} \qquad \text{[LRFD Eq. 5.9.5.4.4b-2]}$$

$$= \frac{\log(24.0 \times 0.5\ \text{day})}{40.0}\left[\frac{216}{243} - 0.55\right] 216 = 1.975\ \text{ksi}$$

$\Delta f_{pR1}$ will remain constant for all the iterations and $\Delta f_{pR1} = 1.975$ ksi will be used throughout the losses calculation procedure.

Total initial prestress loss = $\Delta f_{pES} + \Delta f_{pR1} = 16.137 + 1.975 = 18.663$ ksi

$$\text{Initial Prestress loss} = \frac{\left(\Delta f_{ES} + \Delta f_{pR1}\right) \times 100}{0.75 f_{pu}} = \frac{[16.137+1.975]100}{0.75(270)}$$

$= 8.944$ percent > 8 percent (assumed initial prestress losses)

Therefore, next trial is required assuming 8.944 percent initial losses

$\Delta f_{pES} = 8$ ksi [LRFD Eq. 5.9.5.4.2-1]

$$\Delta f_{pES} = \frac{E_p}{E_{ci}} f_{cgp} \qquad \text{[LRFD Eq. 5.9.5.2.3a-1]}$$

where:

$$f_{cgp} = \frac{P_{si}}{A} + \frac{P_{si}\, e_c^2}{I} - \frac{(M_g)e_c}{I}$$

$P_{si}$ = Pretension force after allowing for the initial losses, assuming 8.944 percent initial losses = (number of strands)(area of each strand)[0.9106(0.75 $f_{pu}$ )]

= 62(0.153)(0.9106)(0.75)(270) = 1749.185 kips

$$f_{cgp} = \frac{1749.185}{1120} + \frac{1749.185\ (18.824)^2}{403020} - \frac{1714.65(12)(18.824)}{403020}$$

= 1.562 + 1.538 – 0.961 = 2.139 ksi

Assuming $f'_{ci}$ = 4000 psi

$$E_{ci} = (150)^{1.5}(33)\sqrt{4000}\ \ \frac{1}{1000} = 3834.254 \text{ ksi}$$

$$\Delta f_{pES} = \frac{28500}{3834.254}\ (2.139) = 15.899 \text{ ksi}$$

$\Delta f_{pCR} = 12\, f_{cgp} - 7\Delta f_{cdp}$ [LRFD Eq. 5.9.5.4.3-1]

$\Delta f_{cdp}$ is same as calculated in the previous trial.

$\Delta f_{cdp}$ = 1.195 ksi

$\Delta f_{pCR}$ = 12(2.139) – 7(1.195) = 17.303 ksi.

For pretensioned members with 270 ksi low-relaxation strand conforming to AASHTO M 203
[LRFD Art. 5.9.5.4.4c]

$\Delta f_{pR2} = 0.3\ [20.0 - 0.4\ \Delta f_{pES} - 0.2(\Delta f_{pSR} + \Delta f_{pCR})$

= 0.3 [20.0 – 0.4(15.899) – 0.2(8 + 17.303)] = 2.574 ksi

Total initial prestress loss = $\Delta f_{pES} + \Delta f_{pR1}$ = 15.899 + 1.975= 17.874 ksi

Initial Prestress loss = $\frac{\left(\Delta f_{ES} + \Delta f_{pR1}\right)\times 100}{0.75 f_{pu}} = \frac{[15.899 + 1.975]100}{0.75(270)}$

= 8.827 percent < 8.944 percent (assumed initial prestress losses)

Therefore, next trial is required assuming 8.827 percent initial losses

$\Delta f_{pES}$ = 8 ksi [LRFD Eq. 5.9.5.4.2-1]

$$\Delta f_{pES} = \frac{E_p}{E_{ci}} f_{cgp}$$ [LRFD Eq. 5.9.5.2.3a-1]

where:

$$f_{cgp} = \frac{P_{si}}{A} + \frac{P_{si}\, e_c^2}{I} - \frac{(M_g)\, e_c}{I}$$

$P_{si}$ = Pretension force after allowing for the initial losses, assuming 8.827 percent initial losses

= (number of strands)(area of each strand)[0.9117(0.75 $f_{pu}$ )]

= 62(0.153)(0.9117)(0.75)(270) = 1,751.298 kips

$$f_{cgp} = \frac{1751.298}{1120} + \frac{1751.298(18.824)^2}{403020} - \frac{1714.65(12)(18.824)}{403020}$$

= 1.564+ 1.54– 0.961 = 2.143 ksi

Assuming $f'_{ci}$ = 4000 psi

$$E_{ci} = (150)^{1.5}(33)\sqrt{4000}\ \frac{1}{1000} = 3834.254 \text{ ksi}$$

$$\Delta f_{pES} = \frac{28500}{3834.254}\ (2.143) = 15.929 \text{ ksi}$$

$\Delta f_{pCR} = 12\, f_{cgp} - 7\Delta f_{cdp}$ [LRFD Eq. 5.9.5.4.3-1]

$\Delta f_{cdp}$ is same as calculated in the previous trial.

$\Delta f_{cdp}$ = 1.193 ksi

$\Delta f_{pCR}$ = 12(2.143) – 7(1.193) = 17.351 ksi.

For pretensioned members with 270 ksi low-relaxation strand conforming to AASHTO M 203 [LRFD Art. 5.9.5.4.4c]

$\Delta f_{pR2}$ = 30 percent[20.0 – 0.4 $\Delta f_{pES}$ – 0.2($\Delta f_{pSR}$ + $\Delta f_{pCR}$)

= 0.3[20.0 – 0.4(15.929) – 0.2(8 + 17.351)] = 2.567 ksi

***B.2.7.1.5 Total Losses at Transfer***

Total initial prestress loss = $\Delta f_{pES} + \Delta f_{pR1}$ = 15.929 + 1.975= 17.904 ksi

Initial prestress loss = $\dfrac{\left(\Delta f_{ES} + \Delta f_{pR1}\right)\times 100}{0.75 f_{pu}} = \dfrac{[15.929+2.526]100}{0.75(270)}$

= 8.841 percent ≈ 8.827 percent (assumed initial prestress losses)

***B.2.7.1.6 Total Losses at Service Loads***

Total initial losses = $\Delta f_{ES}$ = 15.929 + 1.975= 17.904 ksi

$f_{si}$ = effective initial prestress = 202.5 – 17.904 = 184.596 ksi

$P_{si}$ = effective pretension force after allowing for the initial losses

= 62(0.153)( 184.596) = 1751.078 kips

***B.2.7.1.7 Final Stresses at Midspan***

$\Delta f_{SR}$ = 8 ksi

$\Delta f_{ES}$ = 15.929 ksi

$\Delta f_{R2}$ = 2.567 ksi

$\Delta f_{CR}$ = 17.351 ksi

Total final losses = 8 + 15.929 + 2.567 + 17.351 = 45.822 ksi

or $\dfrac{45.822\ (100)}{0.75(270)}$ =22.63 percent

$f_{se}$ = effective final prestress = 0.75(270) – 45.822 = 156.678 ksi

$P_{se}$ = 62(0.153)( 156.678) = 1486.248 kips

Bottom fiber stress in concrete at midspan at service load

$f_{bf} = \dfrac{P_{se}}{A} + \dfrac{P_{se}\ e_c}{S_b} - f_b$

$$f_{bf} = \frac{1486.248}{1120} + \frac{18.824(1486.248)}{18024.15} - 3.34 = 1.327 + 1.552 - 3.34$$

$= -0.461$ ksi $>$ $-0.425$ ksi (allowable) (N.G.)

This shows that 62 strands are not adequate. Therefore, try 64 strands

$$e_c = 22.36 - \frac{27(2.17)+27(4.14)+10(6.11)}{62} = 18.743 \text{ in}$$

$P_{se} = 64(0.153)(156.678) = 1534.191$ kips

$$f_{bf} = \frac{1534.191}{1120} + \frac{18.743(1534.191)}{18024.15} - 3.34 = 1.370 + 1.595 - 3.34$$

$= -0.375$ ksi $<$ $-0.425$ ksi (allowable) (O.K.)

Therefore, use 64 strands.

Allowable tension in concrete = $0.19\sqrt{f'_c(ksi)}$

$$f'_{c\ reqd.} = \left(\frac{0.375}{0.19}\right)^2 \times 1000 = 3896 \text{ psi}$$

Top fiber stress in concrete at midspan at service loads

$$f_{tf} = \frac{P_{se}}{A} - \frac{P_{se}\ e_c}{S_t} + f_t = \frac{1534.191}{1120} - \frac{18.743(1534.191)}{12761.88} + 3.737$$

$= 1.370 - 2.253 + 3.737 = 2.854$ ksi

Allowable compression stress limit for all load combinations = $0.6\ f'_c$

$f'_{c\ reqd} = 2854/0.6 = 4757$ psi

Top fiber stress in concrete at midspan due to effective prestress + permanent dead loads

$$f_{tf} = \frac{P_{se}}{A} - \frac{P_{se}\, e_c}{S_t} + \frac{M_g + M_b + M_{dia}}{S_t} + \frac{M_b + M_{ws}}{S_{tg}}$$

$$= \frac{1534.191}{1120} - \frac{18.743(1534.191)}{12761.88} + \frac{(1714.65 + 1689.67 + 132.63)(12)}{12761.88} + \frac{(160.15 + 283.57)(12)}{79936.06}$$

$$= 1.370 - 2.253 + 3.326 + 0.067 = 2.510 \text{ ksi}$$

Allowable compression stress limit for effective pretension force + permanent dead loads = 0.45 $f'_c$

$$f'_{c\ reqd.} = 2510/0.45 = 5578 \text{ psi} \qquad \text{(controls)}$$

Top fiber stress in concrete at midspan due to live load + 0.5 (effective prestress + dead loads)

$$f_{tf} = \frac{M_{LL+I}}{S_{tg}} + 0.5\left(\frac{P_{se}}{A} - \frac{P_{se}\, e_c}{S_t} + \frac{M_g + M_b + M_{dia}}{S_t} + \frac{M_b + M_{ws}}{S_{tg}}\right)$$

$$= \frac{(1618.3 + 684.57)(12)}{79936.06} + 0.5\left(\begin{array}{l} \dfrac{1534.191}{1120} - \dfrac{18.743(1534.191)}{12761.88} \\ + \dfrac{(1714.65 + 1689.67 + 132.63)(12)}{12761.88} \\ + \dfrac{(160.15 + 283.57)(12)}{79936.06} \end{array}\right)$$

$$= 0.346 + 0.5(1.370 - 2.253 + 3.326 + 0.067) = 1.601 \text{ ksi}$$

Allowable compression stress limit for effective pretension force + permanent dead loads = 0.4 $f'_c$

$$f'_{c\ \text{reqd.}} = 1601/0.4 = 4003 \text{ psi}$$

***B.2.7.1.8 Initial Stresses at End***

Since $P_{si} = 64\ (0.153)\ (184.596) = 1807.564$ kips

Initial concrete stress at top fiber of the girder at midspan

$$f_{ti} = \frac{P_{si}}{A} - \frac{P_{si}\, e_c}{S_t} + \frac{M_g}{S_t}$$

where, $M_g$ = moment due to girder self-weight at girder end = 0 k-ft.

$$f_{ti} = \frac{1807.564}{1120} - \frac{18.743(1807.564)}{12761.88} = 1.614 - 2.655 = -1.041 \text{ ksi}$$

Tension stress limit at transfer = $0.24\sqrt{f'_{ci}(ksi)}$

Therefore, $f'_{ci\ \text{reqd.}} = \left(\frac{1.041}{0.24}\right)^2 \times 1000$ = 18,814 psi

$$f_{bi} = \frac{P_{si}}{A} + \frac{P_{si}\ e_c}{S_b} - \frac{M_g}{S_b}$$

$$f_{bi} = \frac{1807.564}{1120} + \frac{18.743(1807.564)}{18024.15}$$

$$= 1.614 + 1.88 = 3.494 \text{ ksi}$$

Compression stress limit at transfer = 0.6 $f'_{ci}$

Therefore, $f'_{ci\ \text{reqd.}} = \frac{3494}{0.6}$ = 5,823 psi

The calculation for initial stresses at the girder end show that preliminary estimate of $f'_{ci} = 4{,}000$ psi is not adequate to keep the tensile and compressive stresses at transfer within allowable stress limits as per LRFD Art. 5.9.4.1. Therefore, debonding of strands is required to keep the stresses within allowable stress limits.

***B.2.7.1.9 Debonding of Strands and Debonding Length***

In order to be consistent with the TxDOT design procedures, the debonding of strands is carried out in accordance with the procedure followed in PSTRS14 (TxDOT 2004).

Two strands are debonded at a time at each section located at uniform increments of 3 ft. along the span length, beginning at the end of the girder. The debonding is started at the end of the girder because due to relatively higher initial stresses at the end, greater number of strands are required to be debonded, and debonding requirement, in terms of number of strands, reduces as the section moves away from the end of the girder. In order to make the most efficient use of debonding due to greater eccentricities in the lower rows, the debonding at each section begins at the bottom most row and goes up. Debonding at a particular section will continue until the initial stresses are within the allowable stress limits or until a debonding limit is reached. When the debonding limit is reached, the initial concrete strength is increased and the design cycles to convergence. As per TxDOT Bridge Design Manual (TxDOT 2001) and AASHTO LRFD Art. 5.11.4.3, the limits of debonding for partially debonded strands are described as follows:

1. Maximum percentage of debonded strands per row

    b. TxDOT Bridge Design Manual (TxDOT 2001) recommends a maximum percentage of debonded strands per row should not exceed 75 percent.

    c. AASHTO LRFD recommends a maximum percentage of debonded strands per row should not exceed 40 percent.

2. Maximum percentage of debonded strands per section

    d. TxDOT Bridge Design Manual (TxDOT 2001) recommends a maximum percentage of debonded strands per section should not exceed 75 percent.

    e. AASHTO LRFD recommends a maximum percentage of debonded strands per section should not exceed 25 percent.

3. LRFD requires that not more than 40 percent of the debonded strands or four strands, whichever is greater, shall have debonding terminated at any section.

4. Maximum length of debonding

    f. TxDOT Bridge Design Manual (TxDOT 2001) recommends to use the maximum debonding length chosen to be lesser of the following:
        i. 15 ft.
        ii. 0.2 times the span length, or
        iii. Half the span length minus the maximum development length as specified in the 1996 AASHTO Standard Specifications for Highway Bridges, Section 9.28. However, for the purpose of demonstration, the maximum development length will be calculated as specified in AASHTO LRFD Art. 5.11.4.2 and Art. 5.11.4.3.

    g. AASHTO LRFD recommends, “the length of debonding of any strand shall be such that all limit states are satisfied with consideration of the total developed resistance at any section being investigated.

5. AASHTO LRFD further recommends, "debonded strands shall be symmetrically distributed about the center line of the member. Debonded lengths of pairs of strands that are symmetrically positioned about the centerline of the member shall be equal. Exterior strands in each horizontal row shall be fully bonded."

The recommendations of TxDOT Bridge Design Manual regarding the debonding percentage per section per row and maximum debonding length as described above are followed in this detailed design example.

### *B.2.7.1.10 Maximum Debonding Length*

As per TxDOT Bridge Design Manual (TxDOT 2001), the maximum debonding length is the lesser of the following:

d. 15 ft.

e. 0.2 ($L$), or

f. 0.5 ($L$) - $l_d$

where:

$l_d$ = Development length calculated based on AASHTO LRFD Art. 5.11.4.2 and Art. 5.11.4.3. as follows:

$$l_d \geq \kappa\left( f_{ps} - \frac{2}{3} f_{pe} \right) d_b \quad \text{[LRFD Eq. 5.11.4.2-1]}$$

where:

$l_d$ = Development length (in.)

$\kappa$ = 2.0 for pretensioned strands [LRFD Art. 5.11.4.3]

$f_{pe}$ = Effective stress in the prestressing steel after losses
= 156.276 (ksi)

$d_b$ = Nominal strand diameter = 0.5 in.

$f_{ps}$ = Average stress in the prestressing steel at the time for which the nominal resistance of the member is required, calculated in the following (ksi)

$$f_{ps} = f_{pu}\left(1 - k\frac{c}{d_p}\right)$$ [LRFD Eq. 5.7.3.1.1-1]

$k$ = 0.28 for low-relaxation strand [LRFD Table C5.7.3.1.1-1]

For Rectangular Section Behavior,

$$c = \frac{A_{ps}f_{pu} + A_s f_y - A'_s f'_y}{0.85 f'_c \beta_1 b + kA_{ps}\frac{f_{pu}}{d_p}}$$ [LRFD Eq. 5.7.3.1.1-4]

$d_p = h - y_{bs}$ = 62 – 3.617= 58.383 in.

$\beta_1$ = 0.85 for f'c $f'_c \le 4.0$ ksi [LRFD Art. 5.7.2.2]

= $0.85 - 0.05(f'_c - 4.0) \le 0.65$ for $f'_c \ge 4.0$ ksi

= 0.85

$k$ = 0.28

For Rectangular Section Behavior

$$c = \frac{64(0.153)(270)}{0.85(4)(0.85)(138) + (0.28)64(0.153)\frac{270}{(58.383)}} = 6.425 \text{ inches}$$

$a = 0.85 \times 6.425 = 5.461$ inches < 8 inches

Thus, its a rectangular section behavior.

$$f_{ps} = 270\left(1 - 0.28\frac{6.425}{(58.383)}\right) = 261.68 \text{ ksi}$$

The development length is calculated as,

$$l_d \ge 2.0\left(261.68 - \frac{2}{3}156.28\right)0.5 = 157.5 \text{ in.}$$

$l_d$ = 13.12 ft.

Hence, the debonding length is the lesser of the following,

d. 15 ft.

e. 0.2 × 108.417 = 21.68 ft.

f. 0.5 × 108.417 - 13.12 = 41 ft.

Hence, the maximum debonding length to which the strands can be debonded is 15 ft.

**Table B.2.7.1 Calculation of Initial Stresses at Extreme Fibers and Corresponding Required Initial Concrete Strengths.**

| | Location of the Debonding Section (ft. from end) | | | | | | |
|---|---|---|---|---|---|---|---|
| | End | 3 | 6 | 9 | 12 | 15 | Midspan |
| Row No. 1 (bottom row) | 27 | 27 | 27 | 27 | 27 | 27 | 27 |
| Row No. 2 | 27 | 27 | 27 | 27 | 27 | 27 | 27 |
| Row No. 3 | 10 | 10 | 10 | 10 | 10 | 10 | 10 |
| No. of Strands | 64 | 64 | 64 | 64 | 64 | 64 | 64 |
| $M_g$ (k-ft.) | 0 | 185 | 359 | 522 | 675 | 818 | 1715 |
| $P_{si}$ (kips) | 1807.56 | 1807.56 | 1807.56 | 1807.56 | 1807.56 | 1807.56 | 1807.56 |
| $e_c$ (in.) | 18.743 | 18.743 | 18.743 | 18.743 | 18.743 | 18.743 | 18.743 |
| Top Fiber Stresses (ksi) | -1.041 | -0.867 | -0.704 | -0.550 | -0.406 | -0.272 | 0.571 |
| Corresponding $f'_{ci\ reqd}$ (psi) | 18814 | 13050 | 8604 | 5252 | 2862 | 1284 | 5660 |
| Bottom Fiber Stresses (ksi) | 3.494 | 3.371 | 3.255 | 3.146 | 3.044 | 2.949 | 2.352 |
| Corresponding $f'_{ci\ reqd}$ (psi) | 5823 | 5618 | 5425 | 5243 | 5074 | 4915 | 3920 |

In Table B.2.7.1, the calculation of initial stresses at the extreme fibers and corresponding requirement of $f'_{ci}$ suggests that the preliminary estimate of $f'_{ci}$ to be 4000 psi is inadequate. Since strand can not be debonded beyond the section located at 15 ft. from the end of the girder, so, $f'_{ci}$ is increased from 4000 psi to 4,915 psi and at all other section, where debonding can be done, the strands are debonded to bring the required $f'_{ci}$ below 4915 psi. Table B.2.7.2 shows the debonding schedule based on the procedure described earlier.

**Table B.2.7.2 Debonding of Strands at Each Section.**

| | Location of the Debonding Section (ft. from end) | | | | | | |
|---|---|---|---|---|---|---|---|
| | End | 3 | 6 | 9 | 12 | 15 | Midspan |
| Row No. 1 (bottom row) | 7 | 9 | 17 | 23 | 25 | 27 | 27 |
| Row No. 2 | 19 | 27 | 27 | 27 | 27 | 27 | 27 |
| Row No. 3 | 10 | 10 | 10 | 10 | 10 | 10 | 10 |
| No. of Strands | 36 | 46 | 54 | 60 | 62 | 64 | 64 |
| $M_g$ (k-ft.) | 0 | 185 | 359 | 522 | 675 | 818 | 1715 |
| $P_{si}$ (kips) | 1016.76 | 1299.19 | 1525.13 | 1694.591 | 1751.08 | 1807.56 | 1807.56 |
| $e_c$ (in.) | 18.056 | 18.177 | 18.475 | 18.647 | 18.697 | 18.743 | 18.743 |
| Top Fiber Stresses (ksi) | -0.531 | -0.517 | -0.509 | -0.472 | -0.367 | -0.272 | 0.571 |
| Corresponding $f'_{ci\ reqd}$ (psi) | 4895 | 4640 | 4498 | 3868 | 2338 | 1284 | 5660 |
| Bottom Fiber Stresses (ksi) | 1.926 | 2.347 | 2.686 | 2.919 | 2.930 | 2.949 | 2.352 |
| Corresponding $f'_{ci\ reqd}$ (psi) | 3211 | 3912 | 4477 | 4864 | 4884 | 4915 | 3920 |

### B.2.7.2 Iteration 2

Following the procedure in iteration 1 another iteration is required to calculate prestress losses based on the new value of $f'_{ci}$ = 4915 psi. The results of this second iteration are shown in Table B.2.7.3

**Table B.2.7.3 Results of Iteration No. 2.**

| | Trial #1 | Trial # 2 | Trial # 3 | Units |
|---|---|---|---|---|
| No. of Strands | 64 | 64 | 64 | |
| $ec$ | 18.743 | 18.743 | 18.743 | in |
| $\Delta f_{pSR}$ | 8 | 8 | 8 | ksi |
| Assumed Initial Prestress Loss | 8.841 | 8.369 | 8.423 | percent |
| $P_{si}$ | 1807.59 | 1816.91 | 1815.92 | kips |
| $M_g$ | 1714.65 | 1714.65 | 1714.65 | k - ft. |
| $f_{cgp}$ | 2.233 | 2.249 | 2.247 | ksi |
| $f_{ci}$ | 4915 | 4915 | 4915 | psi |
| $E_{ci}$ | 4250 | 4250 | 4250 | ksi |
| $\Delta f_{pES}$ | 14.973 | 15.081 | 15.067 | ksi |
| $f_{cdp}$ | 1.191 | 1.191 | 1.191 | ksi |
| $\Delta f_{pCR}$ | 18.459 | 18.651 | 18.627 | ksi |
| $\Delta f_{pR1}$ | 1.975 | 1.975 | 1.975 | ksi |
| $\Delta f_{pR2}$ | 2.616 | 2.591 | 2.594 | ksi |
| Calculated Initial Prestress Loss | 8.369 | 8.423 | 8.416 | percent |
| Total Prestress Loss | 46.023 | 46.298 | 46.263 | ksi |

#### B.2.7.2.1 Total Losses at Transfer

Total Initial losses = $\Delta f_{ES} + \Delta f_{R1}$ = 15.067 + 1.975 = 17.042 ksi

$f_{si}$ = Effective initial prestress = 202.5 – 17.042 = 185.458 ksi

$P_{si}$ = Effective pretension force after allowing for the initial losses

= 64(0.153)( 185.458) = 1816.005 kips

#### B.2.7.2.2 Total Losses at Service Loads

$\Delta f_{SH}$ = 8 ksi

$\Delta f_{ES}$ = 15.067 ksi

$\Delta f_{R2}$ = 2.594 ksi

$\Delta f_{R1}$ = 1.975 ksi

$\Delta f_{CR}$ = 18.519 ksi

Total final losses = 8 + 15.067 + 2.594 + 1.975 + 18.627 = 46.263 ksi

or $\dfrac{46.263(100)}{0.75(270)}$ =22.85 percent

$f_{se}$ = Effective final prestress = 0.75(270) – 46.263 = 156.237 ksi

$P_{se}$ = 64 (0.153) (156.237) = 1529.873 kips

***B.2.7.2.3 Final Stresses at Midspan***

Top fiber stress in concrete at midspan at service loads

$$f_{tf} = \frac{P_{se}}{A} - \frac{P_{se}\, e_c}{S_t} + f_t = \frac{1529.873}{1120} - \frac{18.743(1529.873)}{12761.88} + 3.737$$

$$= 1.366 - 2.247 + 3.737 = 2.856 \text{ ksi}$$

Allowable compression stress limit for all load combinations = 0.6 $f'_c$

$f'_{c\ reqd.} = 2856/0.6 = 4760$ psi

Top fiber stress in concrete at midspan due to effective prestress + permanent dead loads

$$f_{tf} = \frac{P_{se}}{A} - \frac{P_{se}\, e_c}{S_t} + \frac{M_g + M_b + M_{dia}}{S_t} + \frac{M_b + M_{ws}}{S_{tg}}$$

$$= \left( \frac{1529.873}{1120} - \frac{18.743(1529.873)}{12761.88} + \frac{(1714.65 + 1689.67 + 132.63)(12)}{12761.88} + \frac{(160.15 + 283.57)(12)}{79936.06} \right)$$

$$= 1.366 - 2.247 + 3.326 + 0.067 = 2.512 \text{ ksi}$$

Allowable compression stress limit for effective pretension force + permanent dead loads = 0.45 $f'_c$

$f'_{c\ reqd.} = 2512/0.45 = 5582$ psi (controls)

Top fiber stress in concrete at midspan due to live load + 0.5(effective prestress + dead loads)

$$f_{tf} = \frac{(M_{LT} + M_{LL})}{S_{tg}} + 0.5\left( \frac{P_{se}}{A} - \frac{P_{se}\, e_c}{S_t} + \frac{M_g + M_b + M_{dia}}{S_t} + \frac{M_b + M_{ws}}{S_{tg}} \right)$$

$$= \frac{(1618.3 + 684.57)(12)}{79936.06} + 0.5\left( \frac{1529.873}{1120} - \frac{18.743(1529.873)}{12761.88} + \frac{(1714.65 + 1689.67 + 132.63)(12)}{12761.88} + \frac{(160.15 + 283.57)(12)}{79936.06} \right)$$

$$= 0.346 + 0.5(1.366 - 2.247 + 3.326 + 0.067) = 1.602 \text{ ksi}$$

Allowable compression stress limit for effective pretension force + permanent dead loads = 0.4 $f'_c$

$f'_{c\ reqd.}$ = 1602/0.4 = 4,005 psi

Bottom fiber stress in concrete at midspan at service load

$$f_{bf} = \frac{P_{se}}{A} + \frac{P_{se}\ e_c}{S_b} - f_b$$

$$f_{bf} = \frac{1529.873}{1120} + \frac{18.743(1529.873)}{18024.15} - 3.34$$

$$= 1.366 + 1.591 - 3.34 = -0.383 \text{ ksi}$$

Allowable tension in concrete = $0.19\sqrt{f'_c(ksi)}$

$$f'_{c\ reqd.} = \left(\frac{383}{0.19}\right)^2 \times 1000 = 4063 \text{ psi}$$

***B.2.7.2.4 Initial Stresses at Debonding Locations***

With the same number of debonded strands, as was determined in the previous iteration, the top and bottom fiber stresses with their corresponding initial concrete strengths are calculated and results are presented in Table B.2.7.4. It can be observed that at 15 ft. location, the $f'_{ci}$ value is updated to 4943 psi.

**Table B.2.7.4 Debonding of Strands at Each Section.**

| | Location of the Debonding Section (ft. from end) | | | | | | |
|---|---|---|---|---|---|---|---|
| | 0 | 3 | 6 | 9 | 12 | 15 | 54.2 |
| Row No. 1 (bottom row) | 7 | 9 | 17 | 23 | 25 | 27 | 27 |
| Row No. 2 | 19 | 27 | 27 | 27 | 27 | 27 | 27 |
| Row No. 3 | 10 | 10 | 10 | 10 | 10 | 10 | 10 |
| No. of Strands | 36 | 46 | 54 | 60 | 62 | 64 | 64 |
| $M_g$ (k-ft.) | 0 | 185 | 359 | 522 | 675 | 818 | 1715 |
| $P_{si}$ (kips) | 1021.50 | 1305.25 | 1532.25 | 1702.50 | 1759.26 | 1816.01 | 1816.01 |
| $e_c$ (in.) | 18.056 | 18.177 | 18.475 | 18.647 | 18.697 | 18.743 | 18.743 |
| Top Fiber Stresses (ksi) | -0.533 | -0.520 | -0.513 | -0.477 | -0.372 | -0.277 | 0.567 |
| Corresponding $f'_{ci\ reqd}$ (psi) | 4932 | 4694 | 4569 | 3950 | 2403 | 1332 | 5581 |
| Bottom Fiber Stresses (ksi) | 1.935 | 2.359 | 2.700 | 2.934 | 2.946 | 2.966 | 2.368 |
| Corresponding $f'_{ci\ reqd}$ (psi) | 3226 | 3931 | 4500 | 4890 | 4910 | 4943 | 3947 |

***B.2.7.3 Iteration 3***

Following the procedure in iteration 1, a third iteration is required to calculate prestress losses based on the new value of $f'_{ci}$ = 4943 psi.

The results of this second iteration are shown in Table B.2.7.5.

**Table B.2.7.5 Results of Iteration No. 3.**

| | Trial #1 | Trial #2 | Units |
|---|---|---|---|
| No. of Strands | 64 | 64 | |
| $e_c$ | 18.743 | 18.743 | in. |
| $\Delta f_{pSR}$ | 8 | 8 | ksi |
| Assumed Initial Prestress Loss | 8.416 | 8.395 | percent |
| $P_{si}$ | 1815 | 1816 | kips |
| $M_g$ | 1714.65 | 1714.65 | k - ft. |
| $f_{cgp}$ | 2.247 | 2.248 | ksi |
| $f_{ci}$ | 4943 | 4943 | psi |
| $E_{ci}$ | 4262 | 4262 | ksi |
| $\Delta f_{pES}$ | 15.025 | 15.031 | ksi |
| $f_{cdp}$ | 1.191 | 1.191 | ksi |
| $\Delta f_{pCR}$ | 18.627 | 18.639 | ksi |
| $\Delta f_{pR1}$ | 1.975 | 1.975 | ksi |
| $\Delta f_{pR2}$ | 2.599 | 2.598 | ksi |
| Corresponding Initial Prestress Loss | 8.395 | 8.398 | percent |
| Total Prestress Loss | 46.226 | 46.243 | ksi |

***B.2.7.3.1 Total Losses at Transfer***

Total Initial losses = $\Delta f_{ES} + \Delta f_{R1}$ = 15.031 + 1.975 = 17.006 ksi

$f_{si}$ = Effective initial prestress = 202.5 – 17.006= 185.494 ksi

$P_{si}$ = Effective pretension force after allowing for the initial losses

= 64(0.153)( 185.494) = 1816.357 kips

***B.2.7.3.2 Total Losses at Service Loads***

$\Delta f_{SH}$ = 8 ksi

$\Delta f_{ES}$ = 15.031 ksi

$\Delta f_{R2}$ = 2.598 ksi

$\Delta f_{R1}$ = 1.975 ksi

$\Delta f_{CR}$ = 18.639 ksi

Total final losses = 8 + 15.031 + 2.598 + 1.975 + 18.639 = 46.243 ksi

or $\dfrac{46.243\ (100)}{0.75(270)}$ = 22.84 percent

$f_{se}$ = Effective final prestress = 0.75(270) – 46.243 = 156.257 ksi

$P_{se}$ = 64(0.153)( 156.257) = 1,530.069 kips

***B.2.7.3.3 Final Stresses at Midspan***

Top fiber stress in concrete at midspan at service loads

$$f_{tf} = \frac{P_{se}}{A} - \frac{P_{se}\, e_c}{S_t} + f_t = \frac{1530.069}{1120} - \frac{18.743(1530.069)}{12761.88} + 3.737$$

$$= 1.366 - 2.247 + 3.737 = 2.856 \text{ ksi}$$

Allowable compression stress limit for all load combinations = 0.6 $f'_c$

$f'_{c\ reqd.} = 2856/0.6 = 4{,}760$ psi

Top fiber stress in concrete at midspan due to effective prestress + permanent dead loads

$$f_{tf} = \frac{P_{se}}{A} - \frac{P_{se}\, e_c}{S_t} + \frac{M_g + M_b + M_{dia}}{S_t} + \frac{M_b + M_{ws}}{S_{tg}}$$

$$= \left( \frac{1530.069}{1120} - \frac{18.743(1530.069)}{12761.88} + \frac{(1714.65 + 1689.67 + 132.63)(12)}{12761.88} + \frac{(160.15 + 283.57)(12)}{79936.06} \right)$$

$$= 1.366 - 2.247 + 3.326 + 0.067 = 2.512 \text{ ksi}$$

Allowable compression stress limit for effective pretension force + permanent dead loads = 0.45 $f'_c$

$f'_{c\ reqd.} = 2512/0.45 = 5{,}582$ psi (controls)

Top fiber stress in concrete at midspan due to live load + 0.5(effective prestress + dead loads)

$$f_{tf} = \frac{(M_{LT} + M_{LL})}{S_{tg}} + 0.5\left( \frac{P_{se}}{A} - \frac{P_{se}\, e_c}{S_t} + \frac{M_g + M_b + M_{dia}}{S_t} + \frac{M_b + M_{ws}}{S_{tg}} \right)$$

$$= \frac{(1618.3 + 684.57)(12)}{79936.06} + 0.5\left( \frac{1530.069}{1120} - \frac{18.743(1530.069)}{12761.88} + \frac{(1714.65 + 1689.67 + 132.63)(12)}{12761.88} + \frac{(160.15 + 283.57)(12)}{79936.06} \right)$$

$$= 0.346 + 0.5(1.366 - 2.247 + 3.326 + 0.067) = 1.602 \text{ ksi}$$

Allowable compression stress limit for effective pretension force + permanent dead loads = 0.4 $f'_c$

$f'_{c\ reqd.} = 1602/0.4 = 4{,}005$ psi

Bottom fiber stress in concrete at midspan at service load

$$f_{bf} = \frac{P_{se}}{A} + \frac{P_{se}\ e_c}{S_b} - f_b$$

$$f_{bf} = \frac{1530.069}{1120} + \frac{18.743(1530.069)}{18024.15} - 3.34 = 1.366 + 1.591 - 3.34$$

$$= -0.383 \text{ ksi}$$

Allowable tension in concrete = $0.19\sqrt{f'_c(ksi)}$

$$f'_{c\ reqd.} = \left(\frac{383}{0.19}\right)^2 \times 1000 = 4063 \text{ psi}$$

***B.2.7.3.4 Initial Stresses at Debonding Location***

With the same number of debonded strands, as was determined in the previous iteration, the top and bottom fiber stresses with their corresponding initial concrete strengths are calculated and results are presented in Table B.2.7.6. It can be observed that at 15 ft. location, the $f'_{ci}$ value is updated to 4944 psi.

**Table B.2.7.6 Debonding of Strands at Each Section.**

| | Location of the Debonding Section (ft. from end) | | | | | | |
|---|---|---|---|---|---|---|---|
| | 0 | 3 | 6 | 9 | 12 | 15 | 54.2 |
| Row No. 1 (bottom row) | 7 | 9 | 17 | 23 | 25 | 27 | 27 |
| Row No. 2 | 19 | 27 | 27 | 27 | 27 | 27 | 27 |
| Row No. 3 | 10 | 10 | 10 | 10 | 10 | 10 | 10 |
| No. of Strands | 36 | 46 | 54 | 60 | 62 | 64 | 64 |
| $M_g$ (k-ft.) | 0 | 185 | 359 | 522 | 675 | 818 | 1715 |
| $P_{si}$ (kips) | 1021.70 | 1305.51 | 1532.55 | 1702.84 | 1759.60 | 1816.36 | 1816.36 |
| $e_c$ (in.) | 18.056 | 18.177 | 18.475 | 18.647 | 18.697 | 18.743 | 18.743 |
| Top Fiber Stresses (ksi) | -0.533 | -0.520 | -0.513 | -0.477 | -0.372 | -0.277 | 0.566 |
| Corresponding $f'_{ci\ reqd}$ (psi) | 4932 | 4694 | 4569 | 3950 | 2403 | 1332 | 5562 |
| Bottom Fiber Stresses (ksi) | 1.936 | 2.359 | 2.701 | 2.934 | 2.947 | 2.966 | 2.369 |
| Corresponding $f'_{ci\ reqd}$ (psi) | 3226 | 3932 | 4501 | 4891 | 4911 | 4944 | 3948 |

Since in the last iteration, actual initial losses are 8.398 percent as compared to previously assumed 8.395 percent and $f'_{ci}$ = 4944 psi as compared to previously assumed $f'_{ci}$ = 4943 psi. These values are close enough, so no further iteration will be required. Use $f'_c$ = 5582 psi, $f'_{ci}$ = 4944 psi

### B.2.8 STRESS SUMMARY

Compression: 0.6 $f'_{ci}$ = 0.6(4944) = +2,966.4 psi
= 2.966 ksi (compression)

Tension:
The maximum allowable tensile stress for bonded reinforcement (precompressed tensile zone) is

$0.24\sqrt{f'_{ci}}$ = [$0.24\sqrt{4.944(\text{ksi})}$ ]×1000 = 534 psi

### B.2.8.1 Concrete Stresses at Transfer

### B.2.8.1.1 Allowable Stress Limits

The maximum allowable tensile stress for without bonded reinforcement (non-precompressed tensile zone) is

$0.0948\sqrt{f'_{ci}}$ =[$0.0948\times\sqrt{4.944(\text{ksi})}$ ]×1000 = 210.789 ksi ≥ 0.2 ksi

### B.2.8.1.2 Stresses at Girder End and at Transfer Length Section

Stresses at girder end and transfer length section need only be checked at release, because losses with time will reduce the concrete stresses making them less critical.

Transfer length = 60 (strand diameter) [LRFD Art. 5.8.2.3]
= 60 (0.5) = 30 in. = 2.5 ft.

### B.2.8.1.2.1 Stresses at Transfer Length Section

Transfer length section is located at a distance of 2.5 ft. from end of the girder. Overall girder length of 109.5 ft. is considered for the calculation of bending moment at transfer length. As shown in Table B.2.7.6, the number of strands at this location, after debonding of strands, is 36.

Moment due to girder self-weight and diaphragm,

$M_g$ = 0.5(1.167) (2.5) (109.5 – 2.5) = 156.086 k –ft.

$M_{dia}$ = 3(2.5) = 7.5 k–ft.

Concrete stress at top fiber of the girder

$$f_t = \frac{P_{si}}{A} - \frac{P_{si}\, e_t}{S_t} + \frac{M_g + M_{dia}}{S_t}$$

$P_{si}$ = 36 (0.153) (185.494) = 1021.701 kips

Strand eccentricity at transfer section, $e_c$ = 18.056 in.

$$f_t = \frac{1021.701}{1120} - \frac{18.056(1021.701)}{12761.88} + \frac{(156.086+7.5)(12)}{12761.88}$$

= 0.912 – 1.445 + 0.154 = -0.379 ksi

Allowable tension (with bonded reinforcement) = 534 psi > 379 psi (O.K.)

Concrete stress at the bottom fiber of the girder

$$f_b = \frac{P_{si}}{A} + \frac{P_{si}\, e_c}{S_b} - \frac{M_g + M_{dia}}{S_b}$$

$$f_{bi} = \frac{1021.701}{1120} + \frac{18.056(1021.701)}{18024.15} - \frac{(156.086+7.5)(12)}{18024.15}$$

$= 0.912 + 1.024 – 0.109 = 1.827$ ksi

Allowable compression = 2.966 ksi > 1.827 ksi (reqd.) (O.K.)

***B.2.8.1.2.2 Stresses at Girder End***

And the strand eccentricity at end of girder is:

$$e_c = 22.36 - \frac{7(2.17)+17(4.14)+8(6.11)}{36} = 18.056 \text{ in.}$$

$P_{si} = 36\ (0.153)\ (185.494) = 1021.701$ kips

Concrete stress at the top fiber of the girder

$$f_t = \frac{1021.701}{1120} - \frac{18.056(1021.701)}{12761.88} = 0.912 – 1.445 = -0.533 \text{ ksi}$$

Allowable tension (with bonded reinforcement) = -0.534 psi > -0.533 psi (O.K.)

Concrete stress at the bottom fiber of the girder

$$f_b = \frac{P_{si}}{A} + \frac{P_{si}\, e_c}{S_b} - \frac{M_g}{S_b}$$

$$f_{bi} = \frac{1021.701}{1120} + \frac{18.056(1021.701)}{18024.15} = 0.912 + 1.024 = 1.936 \text{ ksi}$$

Allowable compression = 2.966 ksi > 1.936 ksi (reqd.) (O.K.)

***B.2.8.1.3 Stresses at Midspan***

Bending moment at midspan due to girder self –weight based on overall length

$M_g = 0.5(1.167)(54.21)(109.5 – 54.21) = 1749.078$ K-ft.

$P_{si} = 64\ (0.153)\ (185.494) = 1816.357$ kips

Concrete stress at top fiber of the girder at midspan

$$f_t = \frac{P_{si}}{A} - \frac{P_{si}\, e_c}{S_t} + \frac{M_g}{S_t}$$

$$f_t = \frac{1816.357}{1120} - \frac{18.743(1816.357)}{12761.88} + \frac{1749.078(12)}{12761.88}$$

$$= 1.622 - 2.668 + 1.769 = 0.723 \text{ ksi}$$

Allowable compression: 2.966 ksi >> 0.723 ksi (reqd.) (O.K.)

Concrete stresses in bottom fibers of the girder at midspan

$$f_b = \frac{P_{si}}{A} + \frac{P_{si}\, e_c}{S_b} - \frac{M_g}{S_b}$$

$$f_b = \frac{1816.357}{1120} + \frac{18.743(1816.357)}{18024.15} - \frac{1749.078\,(12)}{18024.15}$$

$$= 1.622 + 1.889 - 1.253 = 2.258 \text{ ksi}$$

Allowable compression: 2.966 ksi > 2.258 ksi (reqd.) (O.K.)

***B.2.8.1.4 Stress Summary at Transfer***

| | Top of girder $f_t$ (ksi) | Bottom of girder $f_b$ (ksi) |
|---|---|---|
| At End | -0.533 | +1.936 |
| At transfer length section | -0.379 | +1.827 |
| At Midspan | +0.723 | +2.258 |

***B.2.8.2 Concrete Stresses at Service Loads***

***B.2.8.2.1 Allowable Stress Limits***

Compression:

Case (I): for all load combinations

$0.60\, f_c' = 0.60(5582)/1000 = +3.349$ ksi (for precast girder)

$0.60\, f_c' = 0.60(4000)/1000 = +2.4$ ksi (for slab)

Case (II): for effective pretension force + permanent dead loads

$0.45\, f_c' = 0.45(5582)/1000 = +2.512$ ksi (for precast girder)

$0.45\, f_c' = 0.45(4000)/1000 = +1.8$ ksi (for slab)

Case (III): for live load +0.5 (effective pretension force + dead loads)

$0.40\, f_c' = 0.40(5582)/1000 = +2.233$ ksi (for precast girder)

$0.40\, f_c' = 0.40(4000)/1000 = +1.6$ ksi (for slab)

Tension: $0.19\sqrt{f'_c} = 0.19\sqrt{5.582(\text{ksi})} \times 1000 = -448.9$ ksi

$P_{se} = 64(0.153)(156.257) = 1530.069$ kips

***B.2.8.2.2 Stresses at Midspan***

Case (I): Concrete stresses at top fiber of the girder at service loads

$$f_{tf} = \frac{P_{se}}{A} - \frac{P_{se}\, e_c}{S_t} + f_t = \frac{1530.069}{1120} - \frac{18.743(1530.069)}{12761.88} + 3.737$$

$$= 1.366 - 2.247 + 3.737 = 2.856 \text{ ksi}$$

Allowable compression: +3.349 ksi > +2.856 ksi (reqd.) (O.K.)

Case (II): Effective pretension force + permanent dead loads

$$f_{tf} = \frac{P_{se}}{A} - \frac{P_{se}\, e_c}{S_t} + \frac{M_g + M_b + M_{dia}}{S_t} + \frac{M_b + M_{ws}}{S_{tg}}$$

$$= \left( \frac{1530.069}{1120} - \frac{18.743(1530.069)}{12761.88} + \frac{(1714.65 + 1689.67 + 132.63)(12)}{12761.88} + \frac{(160.15 + 283.57)(12)}{79936.06} \right)$$

$$= 1.366 - 2.247 + 2.326 + 0.067 = 1.512 \text{ ksi}$$

Allowable compression: +2.512 ksi > +1.512 ksi (reqd.) (O.K.)

Case (III): Live load + ½(Pretensioning force + dead loads)

$$f_{tf} = \frac{(M_{LT} + M_{LL})}{S_{tg}} + 0.5\left( \frac{P_{se}}{A} - \frac{P_{se}\, e_c}{S_t} + \frac{M_g + M_b + M_{dia}}{S_t} + \frac{M_b + M_{ws}}{S_{tg}} \right)$$

$$= \frac{(1618.3 + 684.57)(12)}{79936.06} + 0.5\left( \frac{1525.956}{1120} - \frac{18.743(1525.956)}{12761.88} + \frac{(1714.65 + 1689.67 + 132.63)(12)}{12761.88} + \frac{(160.15 + 283.57)(12)}{79936.06} \right)$$

$$= 0.346 + 0.5(1.366 - 2.247 + 2.326 + 0.067) = 1.602 \text{ ksi}$$

Allowable compression: +2.233 ksi > +1.602 ksi (reqd.) (O.K.)

Concrete stresses at bottom fiber of the girder:

$$f_{bf} = \frac{P_{se}}{A} + \frac{P_{se}\, e_c}{S_b} - f_b$$

$$f_{bf} = \frac{1530.069}{1120} + \frac{18.743(1530.069)}{18024.15} - 3.34 = 1.366 + 1.591 - 3.338$$

$$= -0.383 \text{ ksi}$$

Allowable Tension: -0.449 ksi (O.K.)

***B.2.8.2.3 Stresses at the Top of the Deck Slab***

Stresses at the top of the slab

Case (I):

$$f_t = \frac{M_b + M_{ws} + M_{LT}M_{LL}}{S_{tc}} = \frac{(1618.3+684.57+160.15+283.57)(12)}{50802.19}$$

$$= +0.649 \text{ ksi}$$

Allowable compression: +2.4 ksi > +0.649 ksi (reqd.) (O.K.)

Case (II):

$$f_t = \frac{M_b + M_{ws}}{S_{tc}} = \frac{(160.15+283.57)(12)}{50802.19} = 0.105 \text{ ksi}$$

Allowable compression: +1.8 ksi > +0.105 ksi (reqd.) (O.K.)

Case (III):

$$f_t = \frac{0.5(M_b + M_{ws}) + M_{LT}M_{LL}}{S_{tc}} = \frac{(1618.3+684.57+0.5(160.15+283.57))(12)}{50802.19}$$

$$= 0.596 \text{ ksi}$$

Allowable compression: +1.6 ksi > +0.596 ksi (reqd.) (O.K.)

***B.2.8.2.4 Summary of Stresses at Service Loads***

| | | Top of Slab $f_t$ (ksi) | Top of Girder $f_t$ (ksi) | Bottom of Girder $f_b$ (ksi) |
|---|---|---|---|---|
| At Midspan | CASE I | + 0.649 | +2.856 | -0.383 |
| | CASE II | + 0.105 | +1.512 | |
| | CASE III | +0.596 | +1.602 | |

***B.2.8.3 Fatigue Stress Limit***

According to LRFD Art. 5.5.3, the fatigue of the reinforcement need not be checked for fully prestressed components designed to have extreme fiber tensile stress due to Service III Limit State within the tensile stress limit. Since, in this detailed design example the U54 girder is being designed as a fully prestressed component and the extreme fiber tensile stress due to Service III Limit State is within the allowable tensile stress limits, no fatigue check is required.

### *B.2.8.4 Actual Modular Ratio and Transformed Section Properties for Strength Limit State and Deflection Calculations*

Till this point, a modular ratio equal to 1 has been used for the Service Limit State design. For the evaluation of Strength Limit State and Deflection calculations, actual modular ratio will be calculated and the transformed section properties will be used.

$$n = \frac{E_c \text{ for slab}}{E_c \text{ for beam}} = \left(\frac{3834.25}{4341.78}\right) = 0.846$$

Transformed flange width = $n$ (effective flange width)
= 0.846(138 in.) = 116.75 in.

Transformed Flange Area = $n$ (effective flange width) ($t_s$)
= 1(116.75 in.)(8 in.) = 934 in.$^2$

**Table B.2.8.1 Properties of Composite Section.**

| | Transformed Area in.$^2$ | $y_b$ in. | $A\,y_b$ in. | $A(y_{bc} - y_b)^2$ | $I$ in.$^4$ | $I+A(y_{bc}- y_b)^2$ in.$^4$ |
|---|---|---|---|---|---|---|
| Girder | 1120 | 22.36 | 25,043.20 | 294,295.79 | 403,020 | 697,315.79 |
| Slab | 934 | 58 | 54,172.00 | 352,608.26 | 4981 | 357,589.59 |
| ∑ | 2054 | | 79,215.20 | | | 1,054,905.38 |

where:

$A_c$ = Total area of composite section = 2054 in.$^2$

$h_c$ = Total height of composite section = 62 in.

$I_c$ = Moment of inertia of composite section = 1,054,905.38 in.$^4$

$y_{bc}$ = Distance from the centroid of the composite section to extreme bottom fiber of the precast girder = 79,215.20 / 2054
= 38.57 in.

$y_{tg}$ = Distance from the centroid of the composite section to extreme top fiber of the precast girder = 54 – 38.57 = 15.43 in.

$y_{tc}$ = Distance from the centroid of the composite section to extreme top fiber of the slab = 62 – 38.57 = 23.43 in.

$S_{bc}$ = Composite section modulus for extreme bottom fiber of the precast girder = $I_c/y_{bc}$ = 1,054,905.38 / 38.57 = 27,350.41 in.$^3$

$S_{tg}$ = Composite section modulus for top fiber of the precast girder = $I_c/y_{tg}$ = 1,054,905.38 / 15.43 = 68,367.17 in.$^3$

$S_{tc}$ = Composite section modulus for top fiber of the slab = $I_c/y_{tc}$ = 1,054,905.38 / 23.43 = 45,023.7 in.$^3$

### B.2.9 STRENGTH LIMIT STATE

Total ultimate moment from strength I is:

$$M_u = 1.25(DC) + 1.5(DW) + 1.75(LL + IM)$$

$$M_u = 1.25(1714.65 + 1689.67 + 132.63 + 160.15) + 1.5(283.57) + 1.75(1618.3 + 684.57) = 9076.73 \text{ k - ft}$$

Average stress in prestressing steel when

$f_{pe} \geq 0.5 f_{pu}$ = (156.257 > 0.5(270)= 135 ksi)

$$f_{ps} = f_{pu}\left(1 - k\frac{c}{d_p}\right) \qquad \text{[LRFD Eq. 5.7.3.1.1-1]}$$

$k$ = 0.28 for low-relaxation strand [LRFD Table C5.7.3.1.1-1]

For Rectangular Section Behavior

$$c = \frac{A_{ps} f_{pu} + A_s f_y - A_s' f_y'}{0.85 f_c' \beta_1 b + k A_{ps} \frac{f_{pu}}{d_p}} \qquad \text{[LRFD Eq. 5.7.3.1.1-4]}$$

$d_p = h - y_{bs}$ = 62 – 3.617= 58.383 in.

$\beta_1$ = 0.85 for $f_c' \leq 4.0$ ksi [LRFD Art. 5.7.2.2]

= $0.85 - 0.05(f_c' - 4.0) \leq 0.65$ for $f_c' \geq 4.0$ ksi

= 0.85

$k$ = 0.28

For rectangular section behavior

$$c = \frac{64(0.153)(270)}{0.85(5.587)(0.85)(116.75) + (0.28)64(0.153)\frac{270}{(58.383)}} = 5.463 \text{ in.}$$

$a$ = 0.85 × 5.463 = 4.64 in. < 8 in.

Thus, its a rectangular section behavior.

$$f_{ps} = 270\left(1 - 0.28\frac{5.463}{(58.383)}\right) = 262.93 \text{ ksi}$$

Nominal flexural resistance, [LRFD Art. 5.7.3.2.3]

$$M_n = A_{ps} f_{ps}\left(d_p - \frac{a}{2}\right) \qquad \text{[LRFD Eq. 5.7.3.2.2-1]}$$

The equation above is a simplified form of LRFD Equation 5.7.3.2.2-1 because no compression reinforcement or mild tension reinforcement is considered and the section behaves as a rectangular section.

Factored flexural resistance:

$M_r = \phi M_n$ [LRFD Eq. 5.7.3.2.1-1]

where:

$\phi$ = resistance factor [LRFD Eq. 5.5.4.2.1]

=1.00, for flexure and tension of prestress concrete

$M_r$ = 12,028.37 k – ft. > $M_u$ = 9076.73 k – ft. (O.K.)

***B.2.9.1 LIMITS OF REINFORCEMENT***

[LRFD Eq. 5.7.3.3]

The amount of prestressed and non-prestressed reinforcement should be such that

***B.2.9.1.1 Maximum Reinforcement***

$$\frac{c}{d_e} \le 0.42 \qquad \text{[LRFD Eq. 5.7.3.3.1-1]}$$

$$\text{where, } d_e = \frac{A_{ps} f_{ps} d_p + A_s f_y d_s}{A_{ps} f_{ps} + A_s f_y} \qquad \text{[LRFD Eq. 5.7.3.3.1-2]}$$

Since $A_s = 0$, $d_e = d_p = 58.383$ in.

$$\frac{c}{d_e} = \frac{5.463}{58.383} = 0.094 \le 0.42 \qquad \text{O.K.}$$

[LRFD Art. 5.7.3.3.2]

***B.2.9.1.2 Minimum Reinforcement***

At any section, the amount of prestressed and nonprestressed tensile reinforcement should be adequate to develop a factored flexural resistant, $M_r$, equal to the lesser of:

- 1.2 times the cracking strength determined on the basis of elastic stress distribution and the modulus of rupture, and,
- 1.33 times the factored moment required by the applicable strength load combination.

Check at the midspan:

$$M_{cr} = S_c (f_r + f_{cpe}) - M_{dnc} \left( \frac{S_c}{S_{nc}} - 1 \right) \le S_c f_r \qquad \text{[LRFD Eq. 5.7.3.3.2-1]}$$

$f_{cpe}$ = Compressive stress in concrete due to effective prestress forces only (after allowance for all prestress losses) at extreme fiber of section where tensile stress is caused by externally applied loads (ksi)

$$f_{cpe} = \frac{P_{se}}{A} + \frac{P_{se}e_c}{S_b} = \frac{1530.069}{1120} + \frac{1530.069(18.743)}{18024.15}$$
$$= 1.366 + 1.591 = 2.957 \; ksi$$

$M_{dnc}$ = Total unfactored dead load moment acting on the monolithic or noncomposite section (kip-ft.)
$= M_g + M_{slab} + M_{dia}$ = 1714.65+1689.67+132.63 = 3536.95 kip-ft.

$S_c = S_{bc}$

$S_{nc} = S_b$

$f_r = \; f_r = 0.24\sqrt{f_c'(ksi)} = 0.24(\sqrt{5.587}) = 0.567 \; ksi$ [LRFD Art. 5.4.6.2]

$$M_{cr} = \frac{27350.41}{12}(0.567 + 2.957) - 3536.95\left(\frac{27350.41}{18024.15} - 1\right) \le \frac{27350.41}{12}(0.567)$$

$M_{cr} = 6183.54 \le 1292.31$

so use $M_{cr} = 1292.31$ k-ft

$1.2M_{cr} = 1550.772$ k-ft

where, $M_u = 9076.73$ k-ft

$1.33M_u = 12,097.684$ k-ft

Since $1.2M_{cr} < 1.33\ M_u$, the $1.2\ M_{cr}$ requirement controls.

$M_r = 12{,}028.37$ k – ft. $> 1.2M_{cr}$ = 1550.772 k-ft. (O.K.)

Art. 5.7.3.3.2 LRFD Specifications require that this criterion be met at every section.

### *B.2.10 TRANSVERSE SHEAR DESIGN*

The area and spacing of shear reinforcement must be determined at regular intervals along the entire length of the girder. In this design example, transverse shear design procedures are demonstrated below by determining these values at the critical section near the supports.

Transverse shear reinforcement is provided when:

$V_u < 0.5\ \phi\ (V_c + V_p)$ [LRFD Art. 5.8.2.4-1]

where:

$V_u$ = Factored shear force at the section considered

$V_c$ = Nominal shear strength provided by concrete
$V_s$ = Nominal shear strength provided by web reinforcement

$\phi$ = Strength reduction factor = 0.90 [LRFD Art. 5.5.4.2.1]

***B.2.10.1 Critical Section***

Critical section near the supports is the greater of: [LRFD Art. 5.8.3.2]

$0.5d_v\cot\theta$ or $d_v$

where:

$d_v$ = Effective shear depth [LRFD Art. 5.8.2.9]
= Distance between resultants of tensile and compressive forces, ($d_e$ - $a/2$), but not less than the greater of ($0.9d_e$) or ($0.72h$)

***B.2.10.1.1 Angle of Diagonal Compressive Stresses***

$\theta$ = Angle of inclination of diagonal compressive stresses, assume θ is 23° (slope of compression field)

The shear design at any section depends on the angle of diagonal compressive stresses at the section. Shear design is an iterative process that begins with assuming a value for $\theta$.

***B.2.10.1.2 Effective Shear Depth***

$d_v$ = $d_e - a/2$ = 58.383 – 4.64/2 = 56.063 in. (controls)
$0.9\,d_e$ = 0.9 (58. 383) = 52.545 in.
$0.72h$ = 0.72×62 = 44.64 in.

***B.2.10.1.3 Calculation of Critical Section***

The critical section near the support is greater of:
$d_v$ = 56.063 in. and
$0.5d_v\cot\theta$ = 0.5×(56.063)×cot(23) = 66.04 in. = 5.503 ft. (controls)

***B.2.10.2 Contribution of Concrete to Nominal Shear Resistance***

The contribution of the concrete to the nominal shear resistance is:

$$V_c = 0.0316\beta\sqrt{f_c'(ksi)}\,b_v d_v \qquad \text{[LRFD Eq. 5.8.3.3-3]}$$

***B.2.10.2.1 Strain in Flexural Tension Reinforcement***

Calculate the strain in the reinforcement on the flexural tension side. Assuming that the section contains at least the minimum transverse reinforcement as specified in LRFD Specifications Article 5.8.2.5:

$$\varepsilon_x = \frac{\frac{M_u}{d_v} + 0.5N_u + 0.5(V_u - V_p)\cot\theta - A_{ps}f_{po}}{2(E_sA_s + E_pA_{ps})} \le 0.001 \quad \text{[LRFD Eq. 5.8.3.3-1]}$$

If LRFD Eq. 5.8.3.3-1 yield a negative value, then, LRFD Eq. 5.8.3.3-3

should be used given as below:

$$\varepsilon_x = \frac{\frac{M_u}{d_v} + 0.5N_u + 0.5(V_u - V_p)\cot\theta - A_{ps}f_{po}}{2(E_cA_c + E_sA_s + E_pA_{ps})} \quad \text{[LRFD Eq. 5.8.3.3-3]}$$

where:

$V_u$ = Factored shear force at the critical section, taken as positive quantity

= 1.25(56.84+56.01+3.00+5.31)+1.50(9.40)+1.75(85.55+32.36)

= 371.893 kips

$M_u$ = 1.25(330.46+325.64+16.51+30.87)+1.5(54.65)+1.75(331.15+131.93)

$M_u$ = Factored moment, taken as positive quantity

$M_u$ = 1771.715 k-ft. > $V_u d_v$ (kip-in.)

= 1771.715 k – ft. > 371.893×56.063/12 = 1737.45 kip – ft. (O.K.)

$V_p$ = Component of the effective prestressing force in the direction of the applied shear = 0 (because no harped strands are used)

$N_u$ = Applied factored normal force at the specified section = 0

$A_c$ = Area of the concrete (in.$^2$) on the flexural tension side below $h$/2

= 714 in.$^2$

$$v_u = \frac{V_u - \phi V_p}{\phi b_v d_v} = \frac{371.893}{0.9\times 10\times 56.063} = 0.737 \text{ ksi} \quad \text{[LRFD Eq. 5.8.2.9-1]}$$

$v_u / f'_c$ = 0.737 / 5.587 = 0.132

As per LRFD Art. 5.8.3.4.2, if the section is within the transfer length of any strands, then calculate the effective value of $f_{po}$, else assume $f_{po} = 0.7f_{pu}$ Since, transfer length of the bonded strands at the section located at 3 ft. from the end of the girder extends from 3 ft. to 5.5 ft. from the end of the girder, whereas the critical section for shear is 5.47 ft. from the support center line. The support center line is 6.5 in. away from the end of the girder. The critical section for shear will be 5.47 + 6.5/12 = 6.00 ft. from the end of the girder, so the critical section does not fall within the transfer length of the strands that are bonded from the section located at 3 ft. from

the end of the girder, thus, we do not need to perform detailed calculations for $f_{po}$.

$f_{po}$ = A parameter taken as modulus of elasticity of prestressing tendons multiplifed by the locked-in difference in strain between the prestressing tendons and the surrounding concrete (ksi).

= Approximately equal to $0.7 f_{pu}$ [LRFD Fig. C5.8.3.4.2-5]

$= 0.70 f_{pu} = 0.70 \times 270 = 189$ ksi

Or it can be conservatively taken as the effective stress in the prestressing steel, $f_{pe}$

$$f_{po} = f_{pe} + f_{pc}\left(\frac{E_{ps}}{E_c}\right)$$

where:

$f_{pc}$ = Compressive stress in concrete after all prestress losses have occurred either at the centroid of the cross-section resisting live load or at the junction of the web and flange when the centroid lies in the flange (ksi); in a composite section, it is the resultant compressive stress at the centroid of the composite section or at the junction of the web and flange when the centroid lies within the flange, that results from both prestress and the bending moments resisted by the precast member acting alone (ksi).

$$f_{pc} = \frac{P_{se}}{A_n} - \frac{P_{se}ec\left(y_{bc} - y_b\right)}{I} + \frac{\left(M_g + M_{slab}\right)\left(y_{bc} - y_b\right)}{I}$$

The number of strands at the critical section location is 46 and the corresponding eccentricity is 18.177 in., as calculated in Table B.2.11.

$$P_{se} = 46 \times 0.153 \times 155.837 = 1096.781 \text{ ksi}$$

$$f_{pc} = \left(\frac{1096.781}{1120} - \frac{1096.781 \times 18.177\left(40.05 - 22.36\right)}{403020} + \frac{12 \times \left(328.58 + 323.79\right)\left(40.05 - 22.36\right)}{403020}\right) = 0.492 \text{ ksi}$$

$$f_{po} = 155.837 + 0.492\left(\frac{28500}{4531.48}\right) = 158.93 \text{ ksi}$$

$$\varepsilon_x = \frac{\frac{1771.715\times12}{56.063} + 0.5(0.0) + 0.5(371.893 - 0.0)\cot 23^o - 46\times0.153\times158.93}{2(28000\times0.0 + 28500\times46\times0.153)} \le 0.001$$

$\varepsilon_x$ = -7.51 x $10^{-04}$ $\le 0.001$

Since this value is negative LRFD Eq. 5.8.3.4.2-3 should be used to calculate $\varepsilon_x$

$$\varepsilon_x = \frac{\frac{1771.715\times12}{56.063} + 0.5(0.0) + 0.5(371.893 - 0.0)\cot 23^o - 46\times0.153\times158.93}{2((4531.48)(714) + ((28500)(46)(0.153))}$$

$\varepsilon_x$ = -4.384 x $10^{-05}$

$b_v$ = 2×5 in. = 10 in. [LRFD Art. 5.8.2.9]

***B.2.10.2.2 Values of β and θ***

Choose the values of $\beta$ and θ from LRFD Table 5.8.3.4.2-1 and after interpolation we get the final values of $\beta$ and θ, as shown in Table B.2.10.1. Since θ = 23.3 degrees value is close to the 23 degrees assumed, no further iterations are required.

**Table B.2.10.1 Interpolation for β and θ.**

| $v_u/f'_c$ | $\varepsilon_x$ x 1000 | | |
|---|---|---|---|
| | -0.05 | **-0.04384** | 0 |
| 0.15 | 24.2 | | 25 |
| | 2.776 | | 2.72 |
| **0.132** | 23.19 | **θ = 23.3** | 24.06 |
| | 2.895 | ***β* = 2.89** | 2.83 |
| 0.125 | 22.8 | | 23.7 |
| | 2.941 | | 2.87 |

***B.2.10.2.3 Concrete Contribution***

The nominal shear resisted by the concrete is:

$$V_c = 0.0316\beta\sqrt{f_c'(ksi)}b_v d_v \qquad \text{[LRFD Eq. 5.8.3.3-3]}$$

$$V_c = 0.0316(2.89)\sqrt{5.587}(56.063)(10) = 121.02 \text{ kips}$$

***B.2.10.3 Contribution of Reinforcement to Nominal Shear Resistance***

Check if $V_u > 0.5\ \phi(V_c + V_p)$ [LRFD Eq. 5.8.2.4-1]

$V_u$ = 371.893 > 0.5×0.9×(121.02+0) = 54.46 kips

Therefore, transverse shear reinforcement should be provided.

***B.2.10.3.1 Requirement for Reinforcement***

$$\frac{V_u}{\phi} \le V_n = (V_c + V_s + V_p) \qquad \text{[LRFD Eq. 5.8.3.3-1]}$$

$V_s$ = shear force carried by transverse reinforcement

$$= \frac{V_u}{\phi} - V_c - V_p = \left(\frac{371.893}{0.9} - 121.02 - 0\right) = 292.19 \text{ kips}$$

***B.2.10.3.2 Required Area of Reinforcement***

$$V_s = \frac{A_v f_y d_v (\cot\theta + \cot\alpha)\sin\alpha}{s} \qquad \text{[LRFD Eq. 5.8.3.3-4]}$$

where:

$s$ = Spacing of stirrups, in.

$\alpha$ = Angle of inclination of transverse reinforcement to longitudinal axis = 90 degrees

Therefore, area of shear reinforcement within a spacing $s$ is:

reqd $A_v = (s\ V_s)/(f_y d_v \cot\theta)$

$= (s \times 292.19)/(60 \times 56.063 \times \cot(23)) = 0.0369 \times s$

If $s$ = 12 in., then $A_v$ = 0.443 in.$^2$ / ft.

***B.2.10.3.3 Spacing of Reinforcement***

Maximum spacing of transverse reinforcement may not exceed the following: [LRFD Art.. 5.8.2.7]

Since $v_u$ =0.737 > 0.125× $f_c'$ = 0.125×5.587 = 0.689

So, $s_{max}$ = 0.4× 56.063 = 22.43 in. < 24.0 in. use $s_{max}$ = 22.43 in.

Use 1 # 4 double legged with $A_v$ = 0.392 in.$^2$ / ft., the required spacing can be calculated as,

$$s = \frac{A_v}{0.0369} = \frac{0.392}{0.0369} = 10.6 \text{ in.}$$

$$V_s = \frac{0.392(60)(56.063)(\cot 23)}{10}$$

$$= 310.643 \text{ kips} > V_s(\text{reqd.}) = 292.19 \text{ kips}$$

[LRFD Art.. 5.8.2.5]

***B.2.10.3.4 Minimum Reinforcement Requirement***

The area of transverse reinforcement should be less than:

$$A_s \geq 0.0316\sqrt{f'_c(ksi)}\,\frac{b_v s}{f_y} \qquad \text{[LRFD Eq. 5.8.2.5-1]}$$

$$A_s \geq 0.0316\sqrt{5.587}\,\frac{10\times 10}{60} = 0.125 \text{ in.}^2 \qquad \text{(O.K.)}$$

***B.2.10.3.5 Maximum Nominal Shear Reinforcement***

In order to assure that the concrete in the web of the girder will not crush prior to yield of the transverse reinforcement, the LRFD Specifications give an upper limit for $V_n$ as follows:

$$V_n = 0.25 f'_c b_v d_v + V_p \qquad \text{[LRFD Eq. 5.8.3.3-2]}$$

$$V_c + V_s \leq 0.25 f'_c b_v d_v + V_p$$

$$(121.02 + 310.643) \; < \; (0.25\times 5.587\times 10\times 56.063 + 0)$$

431.663 kips < 783.06 kips O.K.

***B.2.10.4 Minimum Longitudinal Reinforcement Requirement***

Longitudinal reinforcement should be proportioned so that at each section the following LRFD Equation 5.8.3.5-1 is satisfied:

$$A_s f_y + A_{ps} f_{ps} \geq \frac{M_u}{d_v \phi_f} + 0.5\frac{N_u}{\phi_c} + \left(\frac{V_u}{\phi_v} + 0.5V_s - V_p\right)\cot\theta$$

Using load combination Strength I, the factored shear force and bending moment at the face of bearing:

$V_u$ = 1.25(62.82+61.91+3+5.87)+1.5(10.39)+1.75(90.24+35.66)
= 402.91 kips

$M_u$ = 1.25(23.64+23.3+1.13+2.2)+1.5(3.91)+1.75(23.81+9.44)

= 126.885 k -ft.

$$46\times 0.153\times 262.93 \geq \frac{126.885\times 12}{56.063\times 1.0} + 0.0 + \left(\frac{402.91}{0.9} + 0.5\times 310.643 - 0.0\right)\cot 23$$

1850.5 ≥ 1448.074 (O.K.)

### B.2.11 INTERFACE SHEAR TRANSFER

[LRFD Art. 5.8.4]

According to the guidance given by the LRFD Specifications for computing the factored horizontal shear.

$$V_h = \frac{V_u}{d_e} \qquad \text{[LRFD Eq. C5.8.4.1-1]}$$

### B.2.11.1 Factored Horizontal Shear

$V_h$ = Horizontal shear per unit length of girder, kips

$V_u$ = The factored vertical shear, kips

$d_e$ = The distance between the centroid of the steel in the tension side of the girder to the center of the compression blocks in the deck ($d_e$ - $a/2$), (in.)

The LRFD Specifications do not identify the location of the critical section. For convenience, it will be assumed here to be the same location as the critical section for vertical shear, i.e. 5.503 ft. from the support center line.

$V_u$ = 1.25(5.31)+1.50(9.40)+1.75(85.55+32.36) = 227.08 kips

$d_e$ = 58.383 – 4.64/2 = 56.063 in.

$$V_h = \frac{227.08}{56.063} = 4.05 \text{ kips/in.}$$

$V_n = V_h / \phi$ = 4.05 / 0.9 = 4.5 kip / in.

### B.2.11.2 Required Nominal Resistance

The nominal shear resistance of the interface surface is:

$$V_n = cA_{cv} + \mu\left[A_{vf} f_y + P_c\right] \qquad \text{[LRFD Eq. 5.8.4.1-1]}$$

### B.2.11.3 Required Interface Shear Reinforcement

$c$ = Cohesion factor [LRFD Art. 5.8.4.2]

$\mu$ = Friction factor [LRFD Art. 5.8.4.2]

$A_{cv}$ = Area of concrete engaged in shear transfer, in.$^2$.

$A_{vf}$ = Area of shear reinforcement crossing the shear plane, in.$^2$

$P_c$ = Permanent net compressive force normal to the shear plane, kips

$f_y$ = Shear reinforcement yield strength, ksi

[LRFD Art. 5.8.4.2]

For concrete placed against clean, hardened concrete and free of laitance, but not an intentionally roughened surface:

$c$ = 0.075 ksi

$\mu = 0.6\lambda$, where $\lambda = 1.0$ for normal weight concrete, and therefore,

$\mu = 0.6$

The actual contact width, $b_v$, between the slab and the girder = 2(15.75)

= 31.5 in.

$A_{cv}$ = (31.5in.)(1in.) = 31.5 in.$^2$

The LRFD Eq. 5.8.4.1-1 can be solved for $A_{vf}$ as follows:

$$4.5 = 0.075 \times 31.5 + 0.6\left[ A_{vf}(60) + 0.0 \right]$$

Solving for $A_{vf}$ = 0.0594 in.$^2$/in. = 0.713 in.$^2$ / ft.

Use 1 # 4 double legged. For the required $A_{vf}$ = 0.713 in.$^2$ / ft., the required spacing can be calculated as,

$$s = \frac{A_v \times 12}{A_{vf}} = \frac{0.392 \times 12}{0.713} = 6.6 \text{ in.}$$

Ultimate horizontal shear stress between slab and top of girder can be calculated,

$$V_{ult} = \frac{V_n \times 1000}{b_f} = \frac{4.5 \times 1000}{31.5} = 143.86 \text{ psi}$$

[LRFD Art. 5.10.10.1]

### B.2.12 PRETENSIONED ANCHORAGE ZONE

Design of the anchorage zone reinforcement is computed using the force in the strands just at transfer:

Force in the strands at transfer = $F_{pi}$ = 64 (0.153)(202.5) = 1982.88 kips

### B.2.12.1 Anchorage Zone Reinforcement

The bursting resistance, $P_r$, should not be less than 4 percent of $F_{pi}$

$$P_r = f_s A_s \geq 0.04 F_{pi} = 0.04(1982.88) = 79.32 kips$$

where:

$A_s$ = Total area of vertical reinforcement located within a distance of h/4 from the end of the girder, in $^2$.

$f_s$ = Stress in steel not exceeding 20 ksi.

Solving for required area of steel $A_s$= 79.32 /20 = 3.97 in.$^2$

Atleast 3.97 in.$^2$ of vertical transverse reinforcement should be provided within a distance of (h/4 = 62 / 4 = 15.5 in.). from the end of the girder. Use (7) #5 double leg bars at 2.0 in. spacing starting at 2 in. from the end of the girder. The provided $A_s$ = 7(2)0.31 = 4.34 in.$^2$ > 3.97 in.$^2$ (O.K.)

[LRFD Art. 5.10.10.2]

### B.2.12.2 Confinement Reinforcement

Transverse reinforcement shall be provided and anchored by extending the leg of stirrup into the web of the girder.

### B.2.13 DEFLECTION AND CAMBER

#### B.2.13.1 Maximum Camber Calculations Using Hyperbolic Functions Method

TxDOT's prestressed bridge design software, PSTRS14 uses the Hyperbolic Functions Method proposed by Sinno (1968) for the calculation of maximum camber. This design example illustrates the PSTRS14 methodology for calculation of maximum camber.

Step 1: Total Prestress after release

$$P = \frac{P_{si}}{\left(1 + p\,n + \frac{e_c^2 A_s n}{I}\right)} + \frac{M_D\, e_c A_s n}{I\left(1 + p\,n + \frac{e_c^2 A_s n}{I}\right)}$$

where:

$P_{si}$ = Total prestressing force = 1,811.295 kips

$I$ = Moment of inertia of non-composite section = 403,020 in.$^4$

$e_c$ = Eccentricity of pretensioning force at the midspan = 18.743 in.

$M_D$ = Moment due to self-weight of the girder at midspan = 1714.65 k-ft.

$A_s$ = Area of strands = number of strands (area of each strand)

= 64(0.153) = 9.792 in.$^2$

$\rho = A_s / A_n$

where:

$A_n$ = Area of cross-section of girder = 1120 in.$^2$

$\rho$ = 9.972/1120 = 0.009

PSTRS14 uses final concrete strength to calculate $E_c$,

$E_c$ = Modulus of elasticity of the girder concrete, ksi

$$= 33(w_c)^{3/2}\sqrt{f'_c} = 33(150)^{1.5}\sqrt{5587}\ \frac{1}{1000} = 4531.48 \text{ ksi}$$

$E_{ps}$ = Modulus of elasticity of prestressing strands = 28,500 ksi

$n = E_{ps}/E_c$ = 28500/4531.48= 6.29

$$\left(1 + pn + \frac{e_c^2 A_s n}{I}\right) = 1 + (0.009)(6.29) + \frac{(18.743^2)(9.792)(6.29)}{403020}$$

$$= 1.109$$

$$P = \frac{P_{si}}{\left(1 + p\,n + \frac{e_c^2 A_s n}{I}\right)} + \frac{M_D\, e_c A_s n}{I\left(1 + p\,n + \frac{e_c^2 A_s n}{I}\right)}$$

$$= \frac{1811.295}{1.109} + \frac{(1714.65)(12 \text{ in./ft.})(18.743)(9.792)(6.29)}{403020(1.109)}$$

$$= 1632.68 + 53.13 = 1685.81 \text{ kips}$$

Concrete Stress at steel level immediately after transfer

$$f_{ci}^{s} = P\left(\frac{1}{A} + \frac{e_c^2}{I}\right) - f_c^s$$

where:

$f_c^s$ = Concrete stress at steel level due to dead loads

$$= \frac{M_D e_c}{I} = \frac{(1714.65)(12 \text{ in./ft.})(18.743)}{403020} = 0.957 \text{ ksi}$$

$$f_{ci}^{s} = 1685.81\left(\frac{1}{1120} + \frac{18.743^2}{403020}\right) - 0.957 = 2.018 \text{ ksi}$$

Step 2: Ultimate time-dependent strain at steel level

$$\varepsilon_{c1}^{s} = \varepsilon_{cr}^{\infty} f_{ci}^{s} + \varepsilon_{sh}^{\infty}$$

where:

$\varepsilon_{cr}^{\infty}$ = Ultimate unit creep strain = 0.00034 in./in. (this value is prescribed by Sinno (1968)

$\varepsilon_{sh}^{\infty}$ = Ultimate unit creep strain = 0.000175 in./in. (this value is prescribed by Sinno (1968))

$\varepsilon_{c1}^{\infty}$ = 0.00034(2.018) + 0.000175 = 0.0008611 in./in.

Step 3: Adjustment of total strain in step 2

$$\varepsilon_{c2}^{s} = \varepsilon_{c1}^{s} - \varepsilon_{c1}^{s} E_{ps} \frac{A_s}{E_{ci}}\left(\frac{1}{A_n} + \frac{e_c^2}{I}\right)$$

$$= 0.0008611 - 0.0008611\,(28500)\frac{9.792}{4531.48}\left(\frac{1}{1120} + \frac{18.743^2}{403020}\right)$$

$$= 0.000768 \text{ in./in.}$$

Step 4: Change in concrete stress at steel level

$$\Delta f_c^s = \varepsilon_{c2}^s E_{ps} A_s \left( \frac{1}{A_n} + \frac{e_c^2}{I} \right)$$

$$= 0.000768\ (28500)(9.792)\left( \frac{1}{1120} + \frac{18.743^2}{403020} \right)$$

$\Delta f_c^s = 0.375$ ksi

Step 5: Correction of the total strain from step2

$$\varepsilon_{c4}^s = \varepsilon_{cr}^{\infty} + \left( f_{ci}^s - \frac{\Delta f_c^s}{2} \right) + \varepsilon_{sh}^{\infty}$$

$$\varepsilon_{c4}^s = 0.00034\left( 2.018 - \frac{0.375}{2} \right) + 0.000175 = 0.0007974 \text{ in./in.}$$

Step 6: Adjustment in total strain from step 5

$$\varepsilon_{c5}^s = \varepsilon_{c4}^s - \varepsilon_{c4}^s E_{ps} \frac{A_s}{E_c} \left( \frac{1}{A_n} + \frac{e_c^2}{I} \right)$$

$$= 0.0007974 - 0.0007974\ (28500)\ \frac{9.792}{4531.48}\left( \frac{1}{1120} + \frac{18.743^2}{403020} \right)$$

$= 0.000711$ in./in.

Step 7: Change in concrete stress at steel level

$$\Delta f_{c1}^s = \varepsilon_{c5}^s E_{ps} A_s \left( \frac{1}{A_n} + \frac{e_c^2}{I} \right)$$

$$= 0.000711(28500)(9.792)\left( \frac{1}{1120} + \frac{18.743^2}{403020} \right)$$

$\Delta f_{c1}^s = 0.350$ ksi

Step 8: Correction of the total strain from step 5

$$\varepsilon_{c6}^s = \varepsilon_{cr}^{\infty} + \left( f_{ci}^s - \frac{\Delta f_{c1}^s}{2} \right) + \varepsilon_{sh}^{\infty}$$

$$\varepsilon_{c6}^s = 0.00034\left( 2.018 - \frac{0.350}{2} \right) + 0.000175 = 0.000802 \text{ in./in.}$$

Step 9: Adjustment in total strain from step 8

$$\varepsilon_{c7}^{s} = \varepsilon_{c6}^{s} - \varepsilon_{c6}^{s} E_{ps} \frac{A_s}{E_{ci}} \left( \frac{1}{A_n} + \frac{e_c^2}{I} \right)$$

$$= 0.000802 - 0.000802\ (28500)\ \frac{9.792}{4531.48} \left( \frac{1}{1120} + \frac{18.743^2}{403020} \right)$$

$$= 0.000715 \text{ in./in.}$$

Step 10: Computation of initial prestress loss

$$PL_i = \frac{Psi - P}{Psi} = \frac{1811.295 - 1685.81}{1811.295} = 0.0693$$

Step 11: Computation of Final Prestress loss

$$PL^{\infty} = \frac{\varepsilon_{c7}^{\infty} E_{ps} A_s}{P_{si}} = \frac{0.000715(28500)(9.792)}{1811.295} = 0.109$$

Total Prestress loss

$PL = PL_i + PL^{\infty} = 100(0.0693 + 0.109) = 17.83$ percent

Step 12: Initial deflection due to dead load

$$C_{DL} = \frac{5\ w\ L^4}{384\ E_c\ I}$$

where:

$w$ = Weight of girder = 1.167 kips/ft.

$L$ = Span length = 108.417 ft.

$$C_{DL} = \frac{5\left( \frac{1.167}{12 \text{ in./ft.}} \right)[(108.417)(12 \text{ in./ft.})]^4}{384(4531.48)(403020)} = 1.986 \text{ in.}$$

Step 13: Initial Camber due to prestress

*M/EI* diagram is drawn for the moment caused by the initial prestressing, is shown in Figure B.2.13.1. Due to debonding of strands, the number of strands vary at each debonding section location. Strands that are bonded, achieve their effective prestress level at the end of transfer length. Points 1

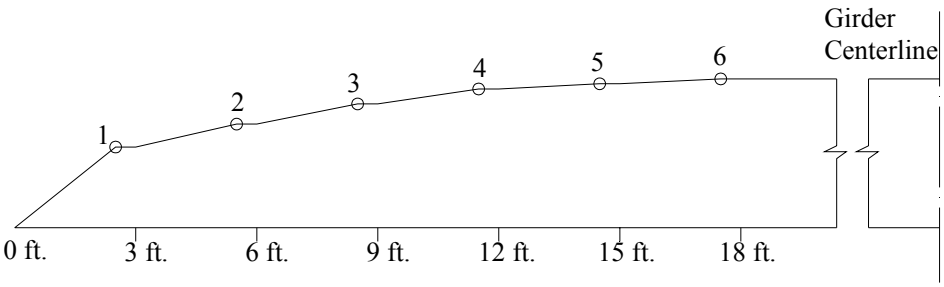


*Figure B.2.13.1 M/EI Diagram to Calculate the Initial Camber due to Prestress.*

through 6 show the end of transfer length for the preceding section. The *M/EI* values are calculated as,

$$\frac{M}{EI} = \frac{P_{si} \times ec}{E_c I}$$

The *M/EI* values are calculated for each point 1 through 6 and are shown in Table B.2.13.1. The initial camber due to prestress, $C_{pi}$, can be calculated by Moment Area Method, by taking the moment of the *M/EI* diagram about the end of the girder.

$C_{pi}$ = 3.88 in.

**Table B.2.13.1 M/EI Values at the End of Transfer Length.**

| Identifier for the End of Transfer Length | $P_{si}$ (kips) | $e_c$ (in.) | M/EI (in.$^3$) |
|---|---|---|---|
| 1 | 1018.864 | 18.056 | 1.01E-05 |
| 2 | 1301.882 | 18.177 | 1.30E-05 |
| 3 | 1528.296 | 18.475 | 1.55E-05 |
| 4 | 1698.107 | 18.647 | 1.73E-05 |
| 5 | 1754.711 | 18.697 | 1.80E-05 |
| 6 | 1811.314 | 18.743 | 1.86E-05 |

Step 14: Initial Camber

$C_i = C_{pi} - C_{DL}$ = 3.88 – 1.986 = 1.894 in.

Step 15: Ultimate Time Dependent Camber

Ultimate strain $\varepsilon_e^s = \frac{f_{ci}^s}{E_c}$ = 2.018/4531.48 = 0.000445 in./in.

Ultimate camber $C_t = C_i\left(1 - PL^{\infty}\right)\dfrac{\varepsilon_{cr}^{\infty}\left(f_{ci}^{s} - \dfrac{\Delta f_{c1}^{s}}{2}\right) + \varepsilon_{e}^{s}}{\varepsilon_{e}^{s}}$

$$= 1.894(1 - 0.109)\frac{0.00034\left(2.018 - \dfrac{0.347}{2}\right) + 0.000445}{0.000445}$$

$C_t = 4.06$ in. $= 0.34$ ft.$\uparrow$

***B.2.13.2 Deflection Due to Girder Self-Weight***

$$\Delta_{girder} = \frac{5w_g L^4}{384E_{ci}I}$$

where, $w_g$ = girder weight = 1.167 kips/ft.

Deflection due to girder self-weight at transfer

$$\Delta_{girder} = \frac{5(1.167/12)[(109.5)(12)]^4}{384(4262.75)(403020)} = 0.186 \text{ ft.}\downarrow$$

Deflection due to girder self-weight used to compute deflection at erection

$$\Delta_{girder} = \frac{5(1.167/12)[(108.417)(12)]^4}{384(4262.75)(403020)} = 0.165 \text{ ft.}\downarrow$$

***B.2.13.3 Deflection Due to Slab and Diaphragm Weight***

$$\Delta_{slab} = \frac{5w_s L^4}{384E_c I} + \frac{w_{dia} b}{24E_c I}\left(3l^2 - 4b^2\right)$$

where:

$w_s$ = Slab weight = 1.15 kips/ft.

$E_c$ = Modulus of elasticity of girder concrete at service = 4529.45 ksi

$$\Delta_{slab} = \frac{5(1.15/12)[(108.417)(12)]^4}{384(4529.45)(403020)} + \frac{(3)(44.21\times12)}{(24\times4529.45\times403020)}\left(3(108.417\times12)^2 - 4(44.21\times12)^2\right) = 0.163 \text{ ft.}\downarrow$$

***B.2.13.4 Deflection Due to Superimposed Loads***

$$\Delta_{SDL} = \frac{5w_{SDL}L^4}{384E_c I_c}$$

where:

$w_{SDL}$ = Superimposed dead load = 0.302 kips/ft.

$I_c$ = Moment of inertia of composite section = 1,054,905.38 in.$^4$

$$\Delta_{SDL} = \frac{5(0.302/12)[(108.417)(12)]^4}{384(4529.45)(1054905.38)} = 0.0155 \text{ ft.}\downarrow$$

Total deflection at service for all dead loads = 0.165 + 0.163 + 0.0155
= 0.34 ft. ↓

### *B.2.13.5 Deflection Due to Live Load and Impact*

The deflections due to live loads are not calculated in this example as they are not a design factor for TxDOT bridges.

### *B.2.14 COMPARISON OF RESULTS*

In order to measure the level of accuracy in this detailed design example, the results are compared with that of PSTRS14 (TxDOT 2004). The summary of comparison is shown in Table B.2.15. In the service limit state design, the results of this example matches those of PSTRS14 with very insignificant differences. A difference up to 5.9 percent can be noticed for the top and bottom fiber stress calculation at transfer, and this is due to the difference in top fiber section modulus values and the number of debonded strands in the end zone, respectively. There is a huge difference of 24.5 percent in camber calculation, which can be due to the fact that PSTRS14 uses a single step hyperbolic functions method, whereas, a multi step approach is used in this detailed design example.

**Table B.2.14.1 Comparison of Results for the AASHTO LRFD Specifications (PSTRS vs Detailed Design Example).**

| Design Parameters | | PSTRS14 | Detailed Design Example | Percent Diff. w.r.t. PSTRS14 |
|---|---|---|---|---|
| Prestress Losses, (percent) | Initial | 8.41 | 8.398 | 0.1 |
| | Final | 22.85 | 22.84 | 0.0 |
| Required Concrete Strengths, (psi) | $f'_{ci}$ | 4944 | 4944 | 0.0 |
| | $f'_c$ | 5586 | 5582 | 0.1 |
| At Transfer (ends), (psi) | Top | -506 | -533 | -5.4 |
| | Bottom | 1828 | 1936 | -5.9 |
| At Service (midspan), (psi) | Top | 2860 | 2856 | 0.1 |
| | Bottom | -384 | -383 | 0.3 |
| Number of Strands | | 64 | 64 | 0.0 |
| Number of Debonded Strands | | (20+10) | (20+8) | 2 |
| $M_u$, (kip–ft.) | | 9082 | 9077 | -0.1 |
| $\phi M_n$, (kip–ft.) | | 11,888 | 12,028 | -1.2 |
| Ultimate Horizontal Shear Stress @ critical section, (psi) | | 143.3 | 143.9 | 0.0 |
| Transverse Shear Stirrup (#4 bar) Spacing, (in.) | | 10.3 | 10 | 2.9 |
| Maximum Camber, (ft.) | | 0.281 | 0.35 | -24.6 |

### *B.2.16 REFERENCES*

AASHTO (2002), *Standard Specifications for Highway Bridges*, 17th Ed., American Association of Highway and Transportation Officials (AASHTO), Inc., Washington, DC.

AASHTO (2004), *AASHTO LRFD Bridge Design Specifications*, 3rd Ed., American Association of State Highway and Transportation Officials (AASHTO), Customary U.S. Units, Washington, DC.

PCI (2003). "Precast Prestressed Concrete Bridge Design Manual," Precast/Prestressed Concrete Institute. 2nd edition.

Sinno, R. (1968). "The time-dependent deflections of prestressed concrete bridge beams," PhD. Dissertation, Texas A&M University.

TxDOT (2001). "TxDOT Bridge Design Manual," Bridge Division, Texas Department of Transportation.

TxDOT (2004). "Prestressed Concrete Beam Design/Analysis Program," User Guide, Version 4.00, Bridge Division, Texas Department of Transportation.

# APPENDIX C

# ILLUSTRATIONS OF DERHERSVILLE BRIDGE USED FOR THE VERIFICATION OF FINITE ELEMENT ANALYSIS MODEL IN SECTION 5

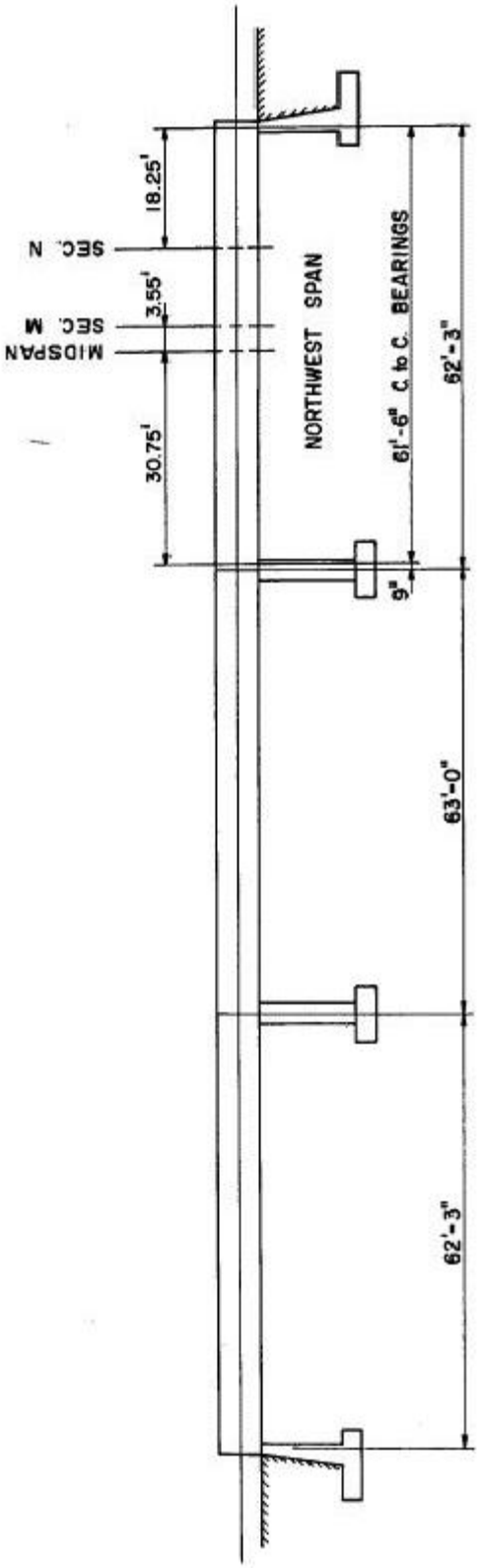


**Figure C.1 Elevation of Derhersville Bridge (Douglas 1966)**

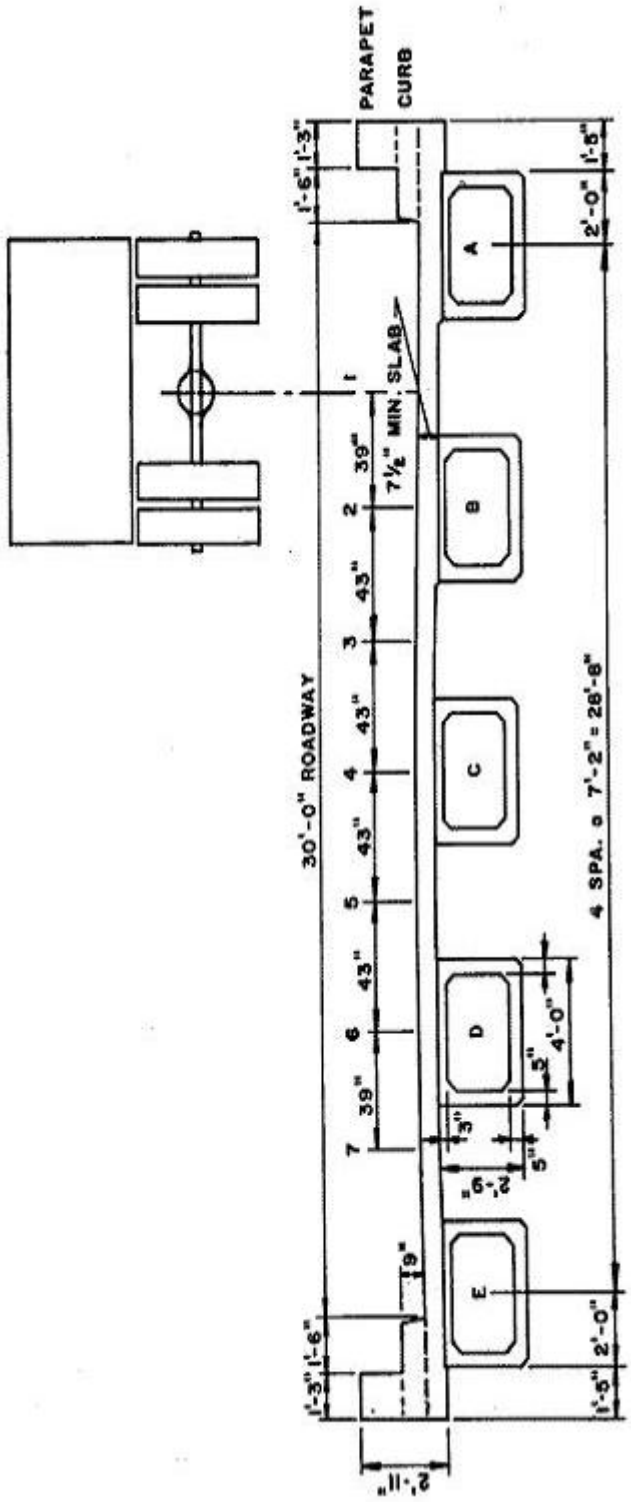


**Figure C.2 Cross-section of Derhersville Bridge and Centerlines of Loading Lanes (Douglas 1966)**

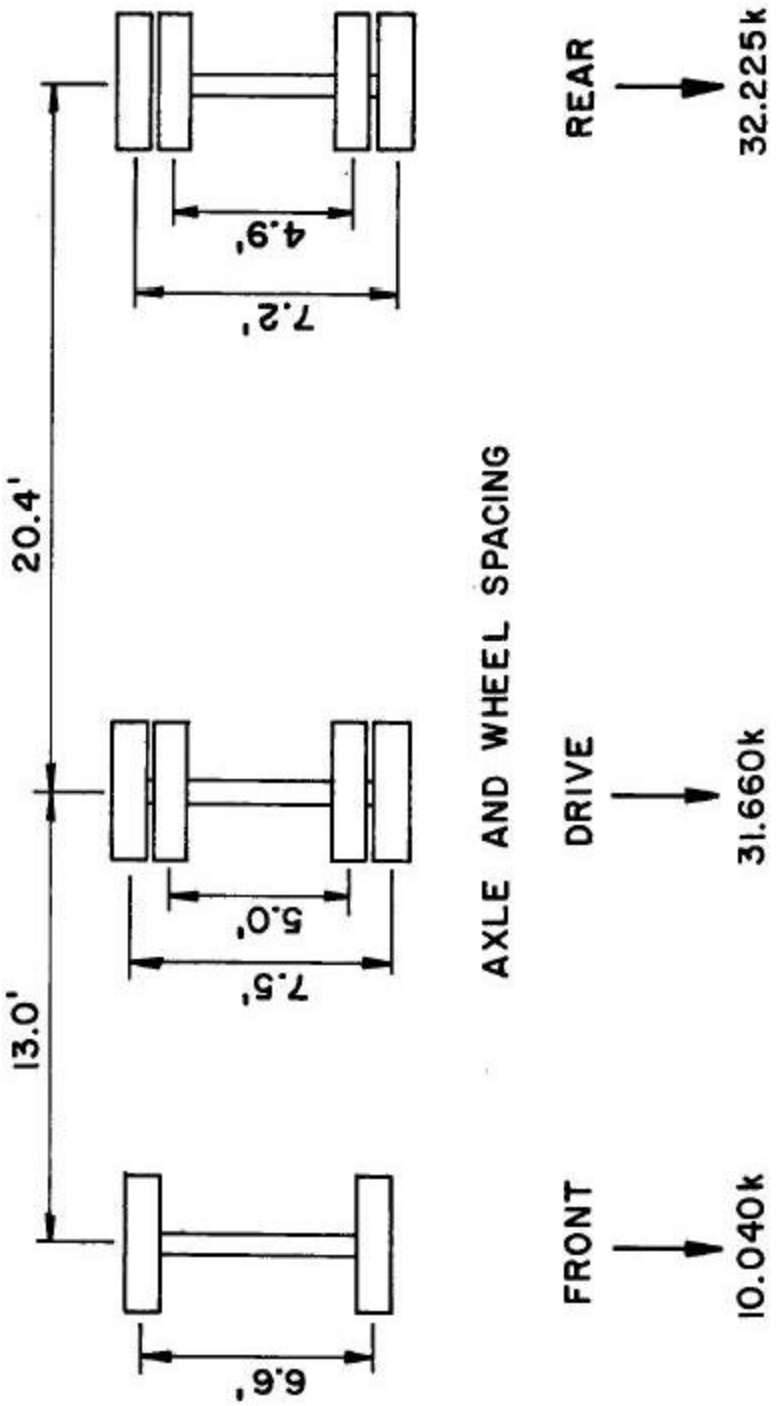


**Figure C.3 Axle Loads of the Test Vehicle Used in the Verification of Finite Element Model (Douglas 1966)**

# VITA

Mohsin Adnan was born in Peshawar, Pakistan. He studied in NWFP University of Engineering and Technology, Pakistan, where he received his degree of Bachelor of Science degree in civil engineering in 2001. He worked in two different consulting firms as a design engineer for two years and as a lecturer in NWFP University for four months before moving to Texas A&M University. At Texas A&M University he enrolled as a master's student in civil engineering (structures emphasis). He has been working as a research assistant with Dr. Mary Beth Hueste and Dr. Peter Keating. His research focused on evaluating the impact of AASHTO LRFD Specifications on prestressed concrete bridges in Texas. He can be contacted through the following address:

Mohsin Adnan
5 Exeter Drive,
Marlboro, New Jersey 07746

E-mail: mohsinadnan@tamu.edu